University of California,
Irvine

Total Synthesis of Paxilline Indole Diterpenes

and

Development of New Chemical Methods Utilizing Cobalt Catalysis

Dissertation

submitted in partial satisfaction of the requirements
for the degree of

Doctor of Philosophy

in Chemistry

by

David Thomas George

Dissertation Committee:
Assistant Professor Sergey V. Pronin, Chair
Professor Christopher D. Vanderwal
Distinguished Professor Larry E. Overman

2018

Dedication

To

my parents, family, and friends

in recognition of their encouragement and support.

Table of Contents

List of Figures

List of Schemes

List of Tables

Acknowledgements

I would like to express the deepest appreciation to my committee chair, Professor Sergey V. Pronin, for his mentorship, boundless enthusiasm, work ethic, and genius. During the early stages of graduate school you took a risk on me and decided to let me help initiate your research program. For that decision I am forever grateful, as it will have a long-lasting impact on my life. I look forward to following your successes.

I would like to thank my committee members, Professor Christopher D. Vanderwal and Distinguished Professor Larry E. Overman, for their words of advice and encouragement over the course of my graduate studies. You both embody what I hope to be as a scientist with your thoughtful approach to science, commitment to tackling impactful research, and humility in the face of high-level success.

I would like to thank my undergraduate mentors, Wayland E Noland Distinguished Chair of Chemistry/Associate Professor Daniel J. Weix (University of Wisconsin, Madison) and Assistant Professor Daniel A. Everson (California State University, Chico) for opening the world of organic chemistry to me. Early in my time at the University of Rochester, I was not the best student, but they each saw potential in me and allowed me to grow and develop academically. I can say with confidence that I would not be in the position that I am in today if it were not for the two of you.

I would like to thank each of my colleagues in the Pronin lab. I know from experience how difficult it is to work in a young research group and appreciate that we were able to maintain an excellent culture within our group. I look forward to following each of your careers and know that great things lie ahead during the remainder of your time in graduate school and later in life.

I would like to thank my parents for their support and for teaching me the value of education. I hope that I have made them proud and look forward to spending more time with them as I begin my career.

To my friends: Thank you for giving me an outlet to temporarily forget about the challenges of graduate school.

Lastly, I would like to Valentina Barrera for her support, companionship, and love during graduate school. You made life enjoyable and provided me an escape from the challenges associated with my studies. I am so proud of all that you have accomplished throughout your own graduate school experience and cannot wait to continue our lives together.

Curriculum Vitae

David T. George

Research Investigator II
Chemical and Synthetic Devlopment
Bristol-Myers Squibb

Email: dgeorge492@gmail.com
(732)-865-3050

Education:

2013 – 2018	Ph.D candidate *Advisor*: Sergey V. Pronin University of California, Irvine, CA
2009 – 2013	B.S. with distinction in Chemistry *Advisor*: Daniel J. Weix University of Rochester, Rochester, NY

Relevant experience, technical skills, and attributes

- Extensive experience with the total synthesis of paxilline indole diterpenes and the development of transition metal-catalyzed reactions
- Experience with multiple reaction types and synthetic approaches
- Able to perform under tight deadlines and manage time efficiently
- Proven ability to excel in a collaborative environment or act as a project leader
- Proficiency with standard analytical techniques (NMR, Mass spectrometry, GC, IR, HPLC)
- Enthusiastic and willing to take on a challenge

Awards:

- Eli Lilly Graduate Student Fellow (2016)
- President's Choice Award in the Natural Sciences and Mathematics (2013)

Publications:

1. George, D. T.; Kuenstner, E. J.; Pronin, S. V. Synthesis of Emindole SB. *Synlett* **2016**, *28*, 12.
2. George, D. T.; Kuenstner, E. J.; Pronin, S. V. A Concise Approach to Paxilline Indole Diterpenes. *J. Am. Chem. Soc.* **2015**, *137*, 15410.
3. Everson, D. A.; George, D. T.; Weix, D. J. Nickel-Catalyzed Cross-Coupling of Aryl Halides with Alkyl Halides: Ethyl 4-(4-(4-methylphenylsulfonamido)phenyl)butanoate. *Org. Synth.* **2013**, *90*, 200.

Research Presentations:

1. University of Rochester Undergraduate Research Symposium (April 2013)
2. Division of Organic Chemistry Graduate Research Symposium (July 2017)

Poster Presentations:

1. 17th Biennial Lilly Grantee Symposium (March 2016)

2. Northeast Regional Meeting of the American Chemical Society (October 2012)
3. University of Rochester Undergraduate Research Symposium (April 2012)
4. National Science Foundation Research Experience for Undergraduates (August 2011)

Abstract of the Dissertation

Total Synthesis of Paxilline Indole Diterpenes

and

Development of New Chemical Methods Utilizing Cobalt Catalysis

By

David Thomas George

Doctor of Philosophy in Chemistry

University of California, Irvine, 2018

Professor Sergey V. Pronin, Chair

In Chapter One a review of the paxilline indole diterpene (PID) class of secondary metabolites is provided. The review introduces the paxilline indole diterpenes and describes defining structural and biosynthetic features. Thorough analysis of the prior synthetic art offers perspective that will contextualize the synthetic efforts described by our own lab in subsequent Chapters.

In Chapter Two a structure-goal and transform-based strategy to the paxilline indole diterpenes family of secondary metabolites is described. The pursuit of a tricarbocyclic subtarget led to the development of a new regioselective alkenylation of enoxysilanes and a radical-polar crossover polycyclization cascade. Our initial efforts in this area guided the application of a tether-controlled radical conjugate addition/aldol sequence to access the common pentacyclic core of the family. Realization of our strategy resulted in an 11-step synthesis of emindole SB, which is the simplest congener of the family.

In Chapter Three efforts focused on the extension of our strategy to the paxilline indole diterpenes are described. The insight provided by previous work from our lab guided the pursuit of a radical-polar crossover polycyclization cascade that enabled the preparation of a precursor to the tetracyclic terpenoid core of 11-ketopaspaline. A diastereoselective late-stage reduction of a ketal moiety delivered an undesired epimeric terpenoid core and thwarted a potential 14-step total synthesis of 11-ketopaspaline.

In Chapter Four a brief review of cobalt-catalyzed hydrofunctionalization of alkenes utilizing a radical-polar crossover reaction manifold initiated by a chemoselective hydrogen atom transfer is described. This body of research served as inspiration for the unexpected development of a chemoselective Ritter reaction. The formation of *tert*-alkyl acetamides from simple alkenes is achieved under mild conditions and in the presence of acid-sensitive functional groups. Efforts toward the hydrofunctionalization of monosubstituted alkenes via discreet organocobalt(III) and cationic organocobalt(IV) complexes is also described. Experiments aimed at elucidating the reaction mechanism indicated that radical intermediates are short-lived and relevant secondary organocobalt(III) complexes are plausible intermediates.

Chapter 1: Paxilline Indole Diterpenes

1.1 Paxilline Indole Diterpenes

1.1.1 Introduction to and Isolation of the Paxilline Indole Diterpenes

The paxilline indole diterpenes (PIDs) are a family of secondary metabolites that possess a diverse array of structural architectures and bioactivities (*vide infra*). As such, the PIDs have garnered considerable interest from the scientific community and aligned the focus of scientists from many disciplines. These efforts have yielded a rich deposit of information and produced results ranging from the isolation of numerous (>100) congeners, insight into the biosynthesis of PIDs, the identification of interesting bioactivities, and synthetic efforts toward various PIDs.

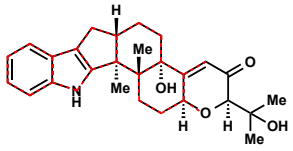

paxilline (**1.1**)

Figure 1.1. Structure of Paxilline.

Benjamin J. and Christina H. Wilson presented the PIDs to the scientific community in 1964 via the isolation of the tremorgenic toxin alfatrem.[1] In the years that followed, various other congeners of the family were isolated, but an unambiguous structural assignment remained elusive.[2–5] However, Clardy and co-workers in 1975 obtained a crystal suitable for X-ray crystallographic analysis, which delivered the unambiguous identity of paxilline (**1.1**; Figure 1.1) and confirmed the tentatively assigned structures from preceding isolations.[6,7] Interesting structural features of the PIDs include a pentacyclic core (Figure 1.1, highlighted in red) containing an indole annulated with a tricarbocyclic terpenoid motif that possesses a *trans*-fused 5-6 ring system and *trans*-oriented vicinal quaternary stereocenters bearing axial methyl groups. To date, over 100 congeners have been isolated and subject to structural elucidation; these reports have led to the identification of sub-classes within the family and include the:

janthitrems,[8] lolicines/lolitrems[9] nodulisporic acids,[10] penitrems,[3,4,11] shearinines,[12] and terpendoles.[13] In addition to the above sub-classes, various other congeners have been isolated (Figure 1.2).[14]

early isolates:

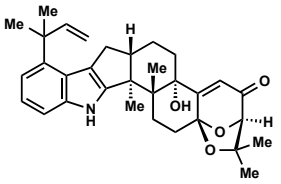

alfatrem (**1.2**)

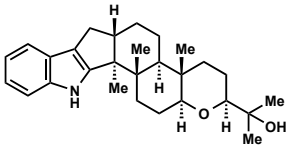

paspaline (**1.3**)

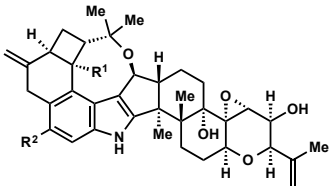

penitrem A (**1.4**) R^1 = OH, R^2 = Cl
penitrem B (**1.5**) $R^1 = R^2$ = H
penitrem C (**1.6**) R^1 = H, R^2 = Cl

janthitrems:

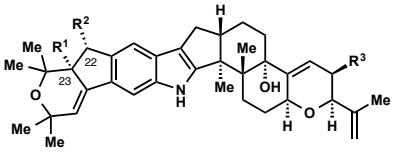

janthitrem B (**1.7**) R^1 = H, $R^2 = R^3$ = OH
janthitrem C* (**1.8**) $R^1 = R^2$ = H, R^3 = OH
janthitrem D (**1.9**) tentatively isolated, no additional data
JBIR-137 (**1.10**) $R^1 = R^2 = \Delta^{22,23}$, R^3 = OH
*stereochemistry at C23 undefined

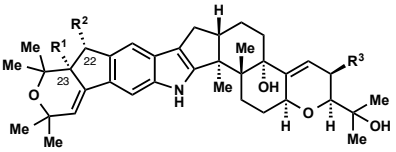

janthitrem A (**1.11**) $C_{37}H_{47}NO_6$ - structure unknown
janthitrem E* (**1.12**) R^1 = H, $R^2 = R^3$ = OH
janthitrem F* (**1.13**) R^1 = H, $R^2 = R^3$ = OAc
janthitrem G* (**1.14**) $R^1 = R^2$ = H, R^3 = OAc
*stereochemistry at C22 and C23 undefined

lolicines and related isolates:

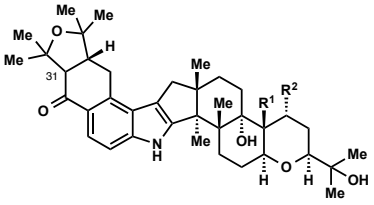

lolicine A (**1.15**) R^1 = Me, R^2 = OH
lolicine A 11-*O*-propionate (**1.16**) R^1 = Me, R^2 = OC(O)Et
lolicine B (**1.17**) R^1 = CHO, R^2 = OH
lolicine B 11-*O*-propionate (**1.18**) R^1 = CHO, R^2 = OC(O)Et
*Stereochemistry at C31 undefined

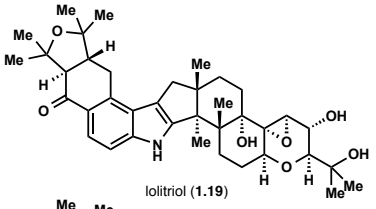

lolitriol (**1.19**)

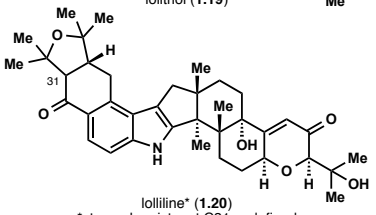

lolliline* (**1.20**)
*stereochemistry at C31 undefined

lolitrems:

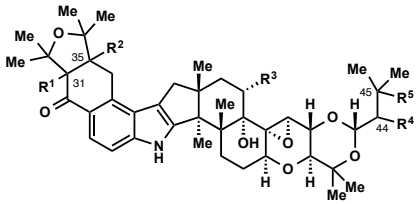

lolitrem A* (**1.21**) R^1 = α–H, R^2 = β-H, R^3 = H, $R^4 = R^5$ = epoxide
lolitrem B (**1.22**) R^1 = α–H, R^2 = β-H, R^3 = H, $R^4 = R^5 = \Delta^{44,45}$
lolitrem C (**1.23**) R^1 = α–H, R^2 = β-H, $R^3 = R^4 = R^5$ = H
lolitrem D (**1.24**) tentatively isolated
lolitrem F (**1.25**) $R^1 = R^2$ = α-H, R^3 = H, $R^4 = R^5 = \Delta^{44,45}$
lolitrem H** (**1.26**) $R^1 = R^2$ = H, R^3 = OH, $R^4 = R^5 = \Delta^{44,45}$
*stereochemistry at C44 undefined
**stereochemistry at C31 and C35 undefined

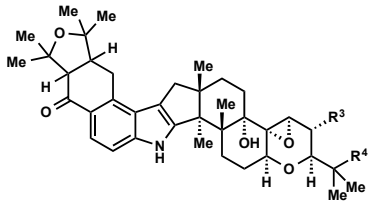

lolitrem E (**1.27**) R^1 = α–H, R^2 = β-H, R^3 = OH, $R^4 = OCH_2CHCMe_2$
lolitrem N (**1.28**) $R^1 = R^2$ = α-H, $R^3 = R^4$ = OH
lolitrem N 10-*O*-propionate (**1.29**) $R^1 = R^2$ = α-H, R^3 = OH, R^4 = OC(O)Et
31-epi-lolitrem N (**1.30**) R^1 = β-H, R^2 = α-H, $R^3 = R^4$ = OH
31-epi-lolitrem N 10-*O*-acetate (**1.31**) R^1 = β-H, R^2 = α-H, R^3 = OAc, R^4 = OH

nodulisporic acids:

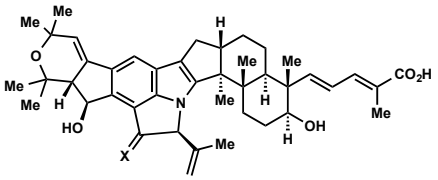

nodulisporic acid A (**1.32**) X = O
nodulisporic acid B (**1.33**) X = H_2

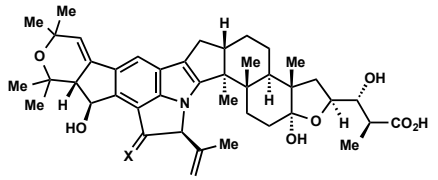

nodulisporic acid A_2 (**1.36**) X = O
nodulisporic acid B_2 (**1.37**) X = H_2

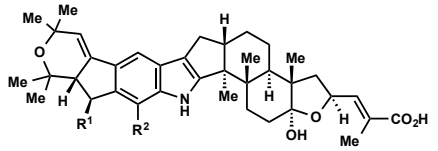

nodulisporic acid C_1 (**1.40**) R^1 = OH; R^2 = CH_2CHCMe_2
nodulisporic acid D_1 (**1.41**) R^1 = R^2 = H

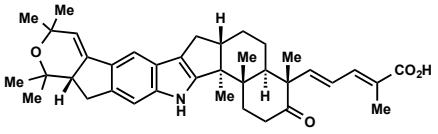

nodulisporic acid D_3 (**1.44**)

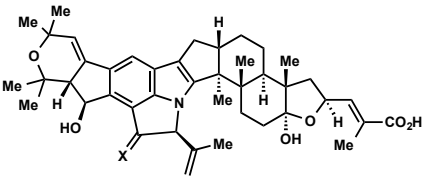

nodulisporic acid A_1 (**1.34**) X = O
nodulisporic acid B_1 (**1.35**) X = H_2

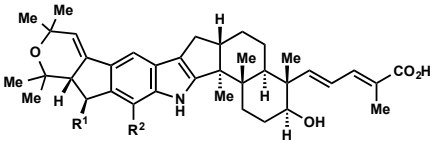

nodulisporic acid C (**1.38**) R^1 = OH; R^2 = CH_2CHCMe_2
nodulisporic acid D (**1.39**) R^1 = R^2 = H

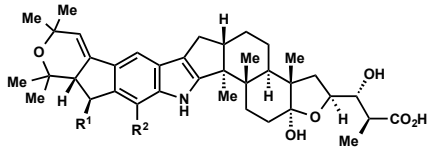

nodulisporic acid C_2 (**1.42**) R^1 = OH; R^2 = CH_2CHCMe_2
nodulisporic acid D_2 (**1.43**) R^1 = R^2 = H

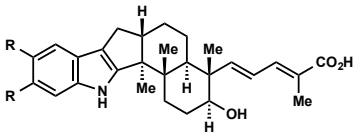

nodulisporic acid E (**1.45**) R = CH_2CHCMe_2
nodulisporic acid F (**1.46**) R = H

penitrems and related isolates:

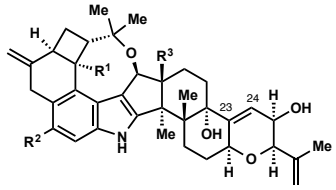

penitrem A (**1.4**) R^1 = OH, R^2 = Cl, R^3 = H, C23–C24 α-epoxide
penitrem B (**1.5**) R^1 = R^2 = R^3 = H, C23–C24 α-epoxide
penitrem C (**1.6**) R^1 = H, R^2 = Cl, R^3 = H
penitrem D (**1.47**) R^1 = R^2 = R^3 = H
penitrem E (**1.48**) R^1 = OH, R^2 = R^3 = H, C23–C24 α-epoxide
penitrem F (**1.49**) R^1 = H, R^2 = Cl, R^3 = H, C23–C24 α-epoxide
penitrem G (**1.50**) R^1 = R^2 = H, R^3 = OH
penitrem H (**1.51**) R^1 = OH, R^2 = Cl, R^3 = OMe, C23–C24 α-epoxide
19-hydroxy penitrem A (**1.52**) R^1 = OH, R^2 = Cl, R^3 = OH, C23–C24 α-epoxide
19-hydroxy penitrem E (**1.53**) R^1 = OH, R^2 = R^3 = OH, C23–C24 α-epoxide
6-bromopenitrem E (**1.54**) R^1 = OH, R^2 = Br, R^3 = H, C23–C24 α-epoxide

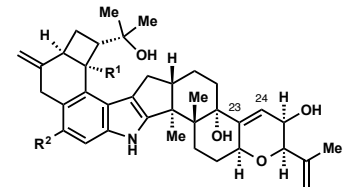

secopenitrem B (**1.55**) R^1 = R^2 = H, C23–C24 α-epoxide
secopenitrem D (**1.56**) R^1 = R^2 = H
thomitrem A (**1.57**) R^1 = OH, R^2 = Cl, C23–C24 α-epoxide
thomitrem E (**1.58**) R^1 = OH, R^2 = H, C23–C24 α-epoxide

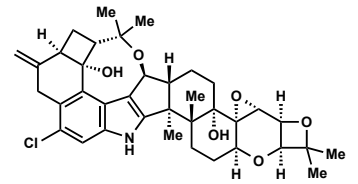

pennigritrem (**1.59**)

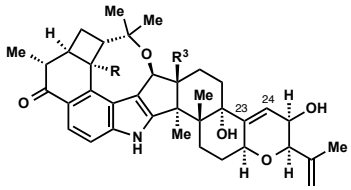

penitrenome A (**1.60**) R = H, C23–C24 α-epoxide
penitrenome B (**1.61** R = OH, C23–C24 α-epoxide
pentrenome C (**1.62**) R = H
10-oxo-11,33-dihydropenitrem B (**1.63**) R = H, C23–C24 α-epoxide

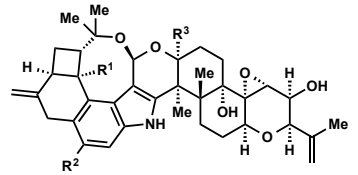

rhizovarin A (**1.66**) R^1 = OH, R^2 = Cl, R^3 = OH
rhizovarin B (**1.67**) R^1 = OH, R^2 = Cl, R^3 = OMe
rhizovarin C (**1.68**) R^1 = OH, R^2 = H, R^3 = OMe

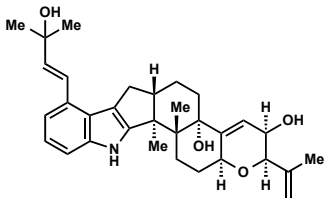

PC-M4 (**1.64**)

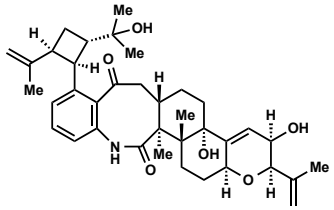

rhizovarin D (**1.69**)

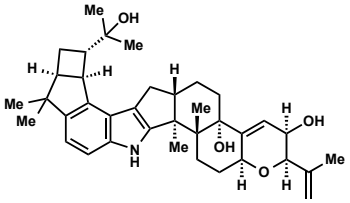

PC-M5 (**1.65**)

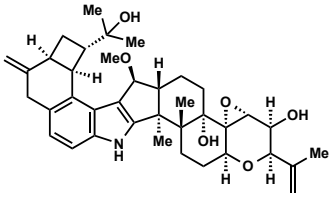

rhizovarin E (**1.70**)

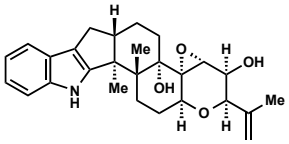

rhizovarin F (**1.71**)

shearinines:

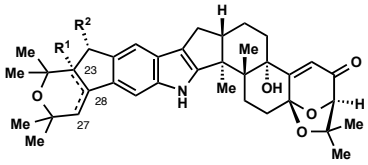

shearinine A (**1.72**) $R^1 = R^2 = H$, $\Delta^{27,28}$
shearinine D (**1.73**) $R^1 = H$, $R^2 = OH$, $\Delta^{27,28}$
shearinine E (**1.74**) $R^1 = H$, $R^2 = OMe$, $\Delta^{27,28}$
shearinine F (**1.75**) $R^2 = OMe$, $\Delta^{23,28}$
shearinine G (**1.76**) $R^2 = oxo$, $\Delta^{23,28}$

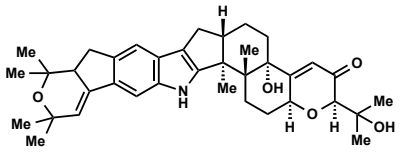

shearinine B (**1.77**)

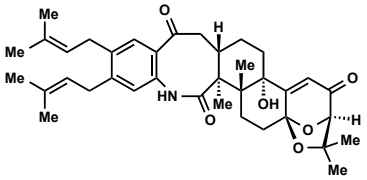

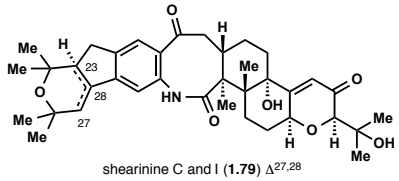

shearinine C and I (**1.79**) $\Delta^{27,28}$
shearinine H (**1.80**) $\Delta^{23,28}$

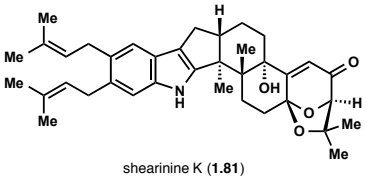

shearinine K (**1.81**)

terpendoles:

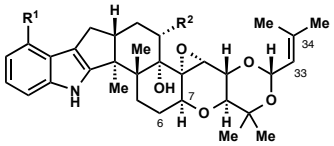

terpendole A* (**1.82**) $R^1 = R^2 = H$, C33 and C34 epoxide
terpendole C (**1.83**) $R^1 = R^2 = H$
terpendole K (**1.84**) $R^1 = R^2 = H$, $\Delta^{6,7}$
terpendole L (**1.85**) $R^1 = CH_2CHCMe_2$, $R^2 = H$
terpendole M (**1.86**) $R^1 = H$, $R^2 = OH$
*stereochemistry at C33 undefined

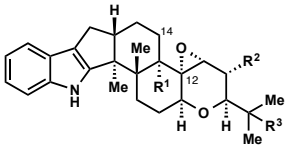

terpendole B (**1.87**) $R^1 = R^2 = H$, $R^3 = OH$
terpendole D (**1.88**) $R^1 = H$, $R^2 = OH$, $R^3 = OCH_2CHCMe_2$
terpendole H* (**1.89**) $R^2 = R^3 = OH$, C13 and C14 epoxide
terpendole I (**1.90**) $R^1 = R^2 = R^3 = OH$
terpendole J (**1.91**) $R^1 = R^2 = OH$, $R^3 = OCH_2CHCMe_2$
*stereochemistry at C13 and C14 undefined

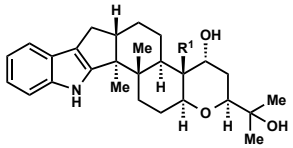

terpendole E (**1.92**) $R^1 = Me$
terpendole F (**1.93**) $R^1 = CH_2OH$
terpendole G (**1.94**) $R^1 = CHO$

additional congeners:

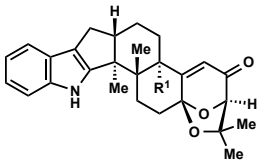

paspalicine (**1.95**) R^1 = H
paspalinine (**1.96**) R^1 = OH

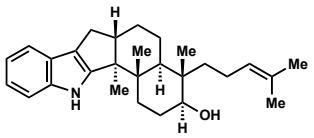

emindole SB (**1.97**)

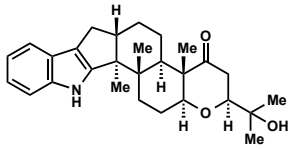

11-ketopaspaline (**1.98**)

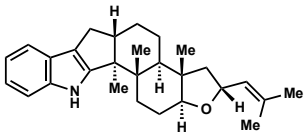

JBIR-03 (**1.99**)

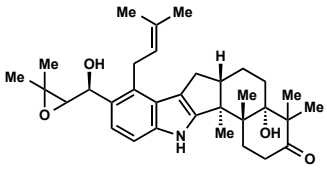

sespendole* (**1.100**)
stereochemistry at epoxide undefined

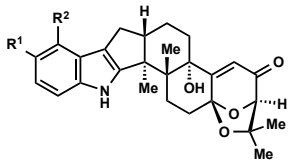

paspalitrem A (**1.101**) R^1 = CH_2CHCMe_2, R^2 = H
paspalitrem B (**1.102**) R^1 = (*E*)-$CHCHCMe_2OH$
paspalitrem C (**1.103**) R^1 = H, R^2 = CH_2CHCMe_2

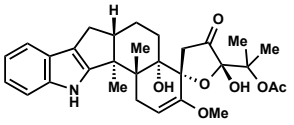

thiesinine A (**1.104**)

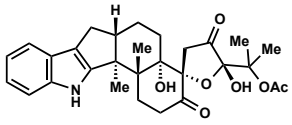

thiesinine B (**1.105**)

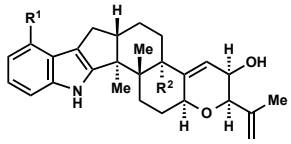

penijanthine A (**1.106**) R^1 = H, R^2 = OH
penijanthine B (**1.107**) R^1 = CH_2CHCMe_2, R^2 = OH
4b-deoxypenijanthine A (**1.108**) R^1 = R^2 = H

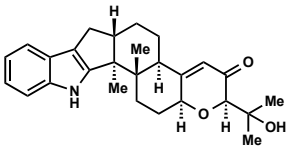

13-deoxypaxilline (**1.109**)

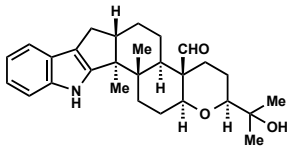

paspaline B (**1.110**)

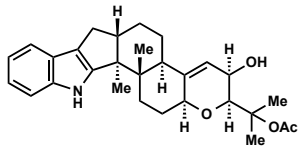

4b-deoxy-1'-*O*-acetylpaxilline (**1.111**)

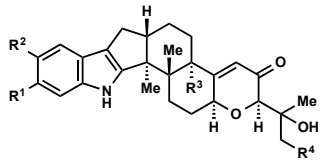

21-isopentenylpaxilline (**1.112**) R^1 = H, R^2 = CH_2CHCMe_2, R^3 = OH, R^4 = H
2'-hydroxypaxilline (**1.113**) R^1 = R^2 = H, R^3 = R^4 = OH
9,10-diisopentenylpaxilline (**1.114**) R^1 = R^2 = CH_2CHCMe_2, R^3 = OH, R^4 = H

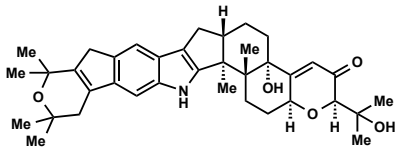

pyrapaxilline (**1.115**)

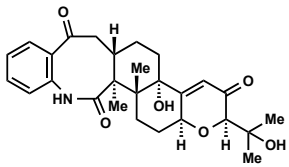

2,18-dioxo-2,18-seco-paxilline (**1.116**)

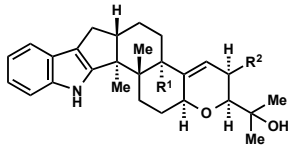

PC-M5' (**1.117**) R^1 = OH, R^2 = OAc
PC-M6 (**1.118**) R^1 = H, R^2 = OH

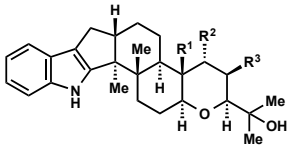

4a-demethylpaspaline-4-a-carboxylic acid (**1.119**) R^1 = CO_2H, R^2 = R^3 = H
4a-demethylpaspaline, 3,4,4a-triol (**1.120**) R^1 = R^2 = R^3 = OH

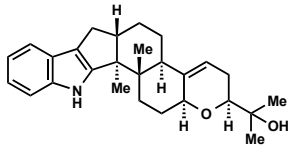

3-deoxo-4b-deoxypaxilline (**1.121**)

Figure 1.2. The Chemical Structures of Isolated Paxilline Indole Diterpenes.

1.1.2 Biosynthesis of the Paxilline Indole Diterpenes

Analysis of the diverse structural architectures found among the congeners of the family reveals various levels of oxidation of the terpenoid core in addition to oxidation, prenylation, and annulation patterns decorated on the indole. In nature, these remarkable structural features arise from an unusual polyene cyclization of 3-geranylgeranylindole and subsequent skeletal modifications mediated by diversity generating gene clusters. The structural diversity, interesting connectivity patterns, and unique *trans*-hexahydroindane possessing vicinal quaternary stereocenters bearing axial methyl groups, have served as an impetus for research related to their biosynthetic origins.

Scheme 1.1. Initial Labeling Study and Original Proposed Biosynthesis of Paspaline.

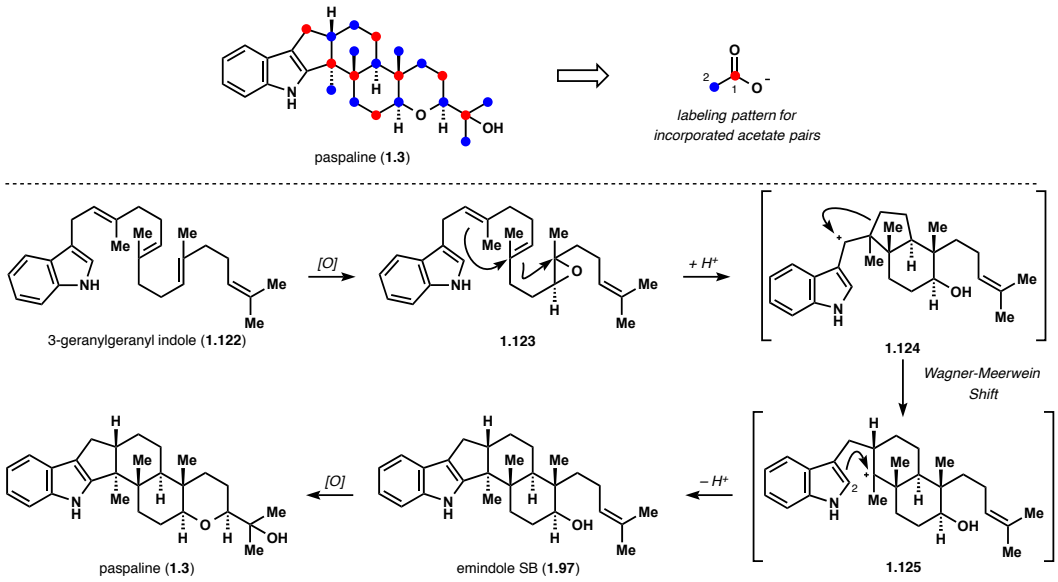

Pioneering research in this area focused on the origin of the pentacyclic core. As such, labeling studies using ^{13}C-isotopes of acetate revealed each pair of carbon atoms throughout the pentacyclic core of paspaline **1.3**, which led to the first proposed biosynthesis of any PID (Scheme 1.1).[15] In this seminal work, a polyene cyclization was proposed to initiate with epoxide **1.123**, which was derived from 3-geranylgeranyl indole (**1.122**). An ensuing and unusual polyene cyclization cascade, involving an anti-Markovnikov cyclization pattern, resulted in the formation

of an unstable and fleeting secondary carbocation that participated in a Wagner-Meerwein shift to form tertiary carbocation **1.125**. Finally, attack by the indole at the C2 position and loss of a proton delivered emindole SB (**1.97**)[16] en route to paspaline (**1.3**). Continued efforts by chemists in this area led the generation of speculative biosynthetic grids that were used to describe the relationship of select congeners.[17]

In the 21st century, major advances in molecular cloning have enabled gene deletion studies that have provided a more refined approach toward the elucidation of the biosynthetic machinery responsible for the formation of secondary metabolites. As such, research groups that utilize these new techniques have isolated and determined some of the gene clusters that facilitate the formation of various structural architectures observed among the PIDs.

Scheme 1.2. Biosynthetic Conversion of Paspaline to Paxilline.

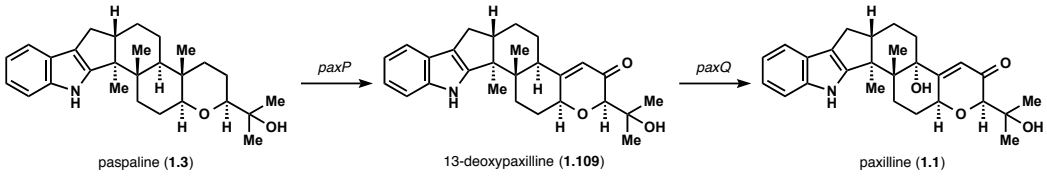

The first utilization of this approach identified seven gene clusters that were required for paxilline (**1.1**) biosynthesis: a geranylgeranyl pyrophosphate (GGPP) synthase (*paxG*), two flavin adenine dinucleotide (FAD) dependent monooxygenases (*paxM* and *N*), two cytochrome P450 monooxygenases (*paxP* and *Q*), a dimethallyltryptophan (DMAT) synthase (*pax*D), and two possible transcription factors (*paxR* and *S*).[18] Similar studies identified the gene clusters that were responsible for production of lolitrem B (**1.22**),[19] paspaline (**1.3**),[20] alfatrem (**1.2**),[21] and terpendole E (**1.92**).[22] The identified clusters for each sub-class of the PIDs mimicked the series of *pax*-gene clusters, which generated a consistent set events involved in the biosynthesis of the PIDs.

Scheme 1.3. Proposed Biosynthesis Incorporating the Identified Gene Clusters.

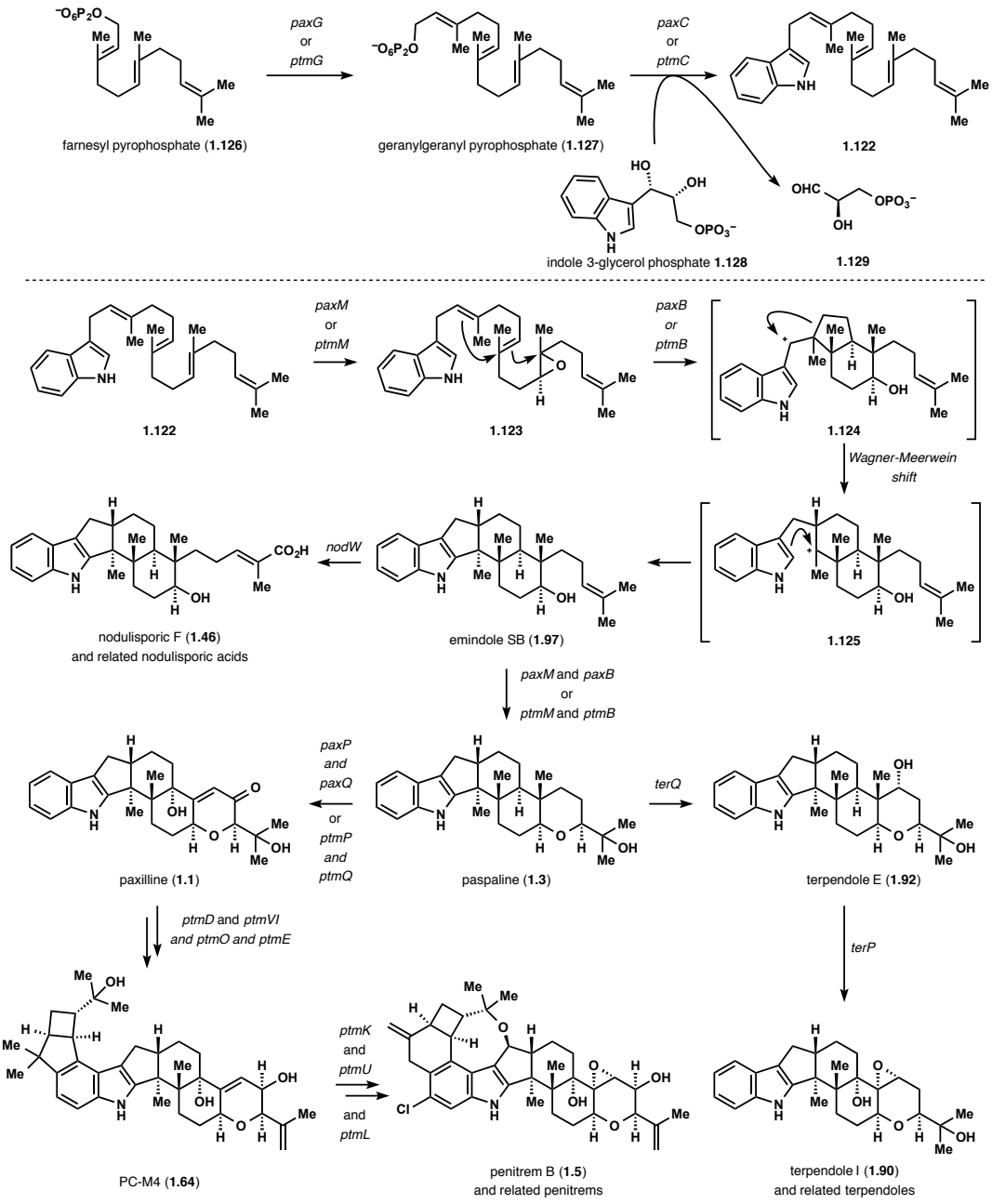

As research in this area shifted from identification of the gene clusters to determining the precise role of each gene cluster an initial study on P450 monooxygenases *paxP* and *paxQ* revealed their involvement in the conversion of paspaline (**1.3**) and paxilline (**1.1**) (Scheme 1.2).[23] These efforts laid the foundation for the identification of the role of each cluster in the

biosynthesis of various PIDs. As such, the biosynthetic machinery for the terpendoles,[22] paxilline,[24] the penitrems,[25] and nodulisporic acid F (**1.46**)[26] has successfully been reconstituted.

The conclusions of the initial labeling studies related to the biosynthesis of the PIDs are corroborated by the reconstitution studies, which allows for a plausible biosynthesis to be proposed (Scheme 1.3). The biosynthesis begins with the conversion of farnesyl pyrophosphate (**1.126**) to geranylgeranyl pyrophosphate (**1.127**) in the presence of a geranylgeranyl diphosphate synthase. Subsequent alkylation of indole 3-glycerol pyrophosphate (**1.128**), enabled by a prenyltransferase, assembles 3-geranylgeranyl indole (**1.122**), which possesses all of the carbon atoms contained in the pentacyclic core. Chemoselective epoxidation of **1.122,** mediated by a FAD dependent monooxygenase, delivers epoxide **1.123** that undergoes a polyene cyclization in the presence of a cyclase. This sequence of events terminates with the formation of emindole SB (**1.97**), which is the first isolated congener of the family possessing the conserved pentacyclic core. The PIDs diverge from emindole SB (**1.97**), with the assistance of various monooxygenases, to yield the nodulisporic acids and paspaline (**1.3**). Further divergence from paspaline (**1.3**) provides access to paxilline-like congeners (i.e. the penitrems) or the terpendoles.

1.1.3 Bioactivities of the Paxilline Indole Diterpenes

In addition to the array of structural architectures displayed by the PIDs a diverse set of bioactivities is also observed that render the PIDs relevant to human health. The first isolated congeners of the family were investigated as tremorgenic toxins. As such, they were implicated as the primary component produced by various strains of fungi that infected grass,[9c,14a,27] food,[11a,8c,1] and soil[12a] and were known to induce tremors in livestock. Tremorgenic activity was attributed to the inhibition of large conductance calcium-activated potassium (BK) channels.[28] In a recent study, mice lacking BK ion channels, *Kcnma1*, were unaffected by known tremorgenic

PIDs paxilline (**1.1**) and lolitrem B (**1.22**).[29] This activity is arguably the most widespread throughout the family and is observed in many of the identified subclasses of the PIDs.

As more congeners of the family were isolated a diverse set of beneficial activities was realized and ranged from inhibition of motor protein Eg5[14o,30] and acyl-CoA: cholesterol tranferase[13a] to antiviral[14l] and microbial[14j] properties. In addition, the PIDs were identified as insecticidal agents[31] that granted a chemical defense system to the fungi that produced them. Specifically, the nodulisporic acids were identified as selective activators of a hybrid receptor containing both glutamate and *gamma*-aminobutryic acid (GABA) gated ion channels[32] This selectivity is remarkable since pharmacological studies have indicated that invertebrate GABA receptors do not conform to that of mammalian GABA receptors.[33] As such, the nodulisporic acids were identified and investigated as insecticidal agents.[34] In a comparison with ivermectin,[35] a known activator of glutamate-gated chloride ion channels, the nodulisporic acids displayed binding to only one of the two distinct receptor populations that were known targets, which further broadened the selectivity of this sub-class of PIDs in the context of activation of ligand-gated ion channels.

Taken together, the balance of unique and diverse chemical structures and interesting set of bioactivities render the PIDs appealing and virtuous targets for synthetic organic chemists. As such, a number of groups in synthetic organic chemistry have displayed interest in the PIDs as indicated by the publication of creative approaches and successful synthetic campaigns.

1.2 Previous Total Syntheses and Studies Toward the Paxilline Indole Diterpenes

1.2.1 Amos B. Smith III's First-generation Synthesis of (–)-Paspaline

In 1985 the group led by Amos B. Smith III published a landmark enantioselective synthesis of (–)-paspaline (**1.3**).[36] This work represented the first synthetic effort toward any PID

and highlighted the challenges associated with the construction of the *trans*-hexahyrdoindane motif embedded in the pentacyclic core. The initial efforts toward (–)-paspaline (**1.3**) described by Smith and co-workers generated the foundation for a longitudinal synthetic program related to the PIDs that has resulted in the total synthesis of many congeners and continues today.

Scheme 1.4. Smith's First Generation Synthesis of (–)-Paspaline.

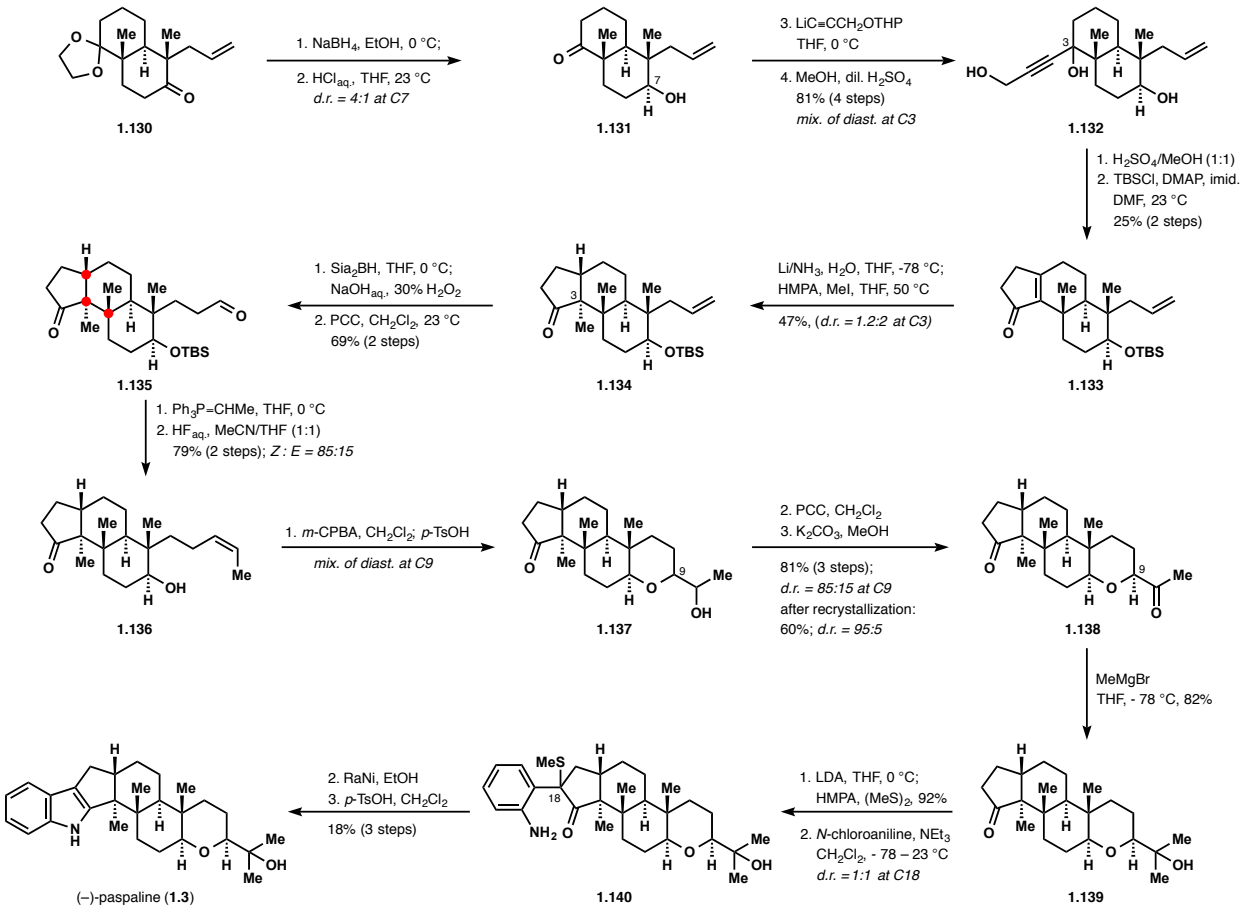

Smith's strategy involved a late-stage formation of the indole and a conjugate reduction-alkylation reaction sequence to install the *trans*-fused 5-6-ring system contained in the terpenoid core (Scheme 1.4). Following this approach, the synthesis commenced from (+)-Wieland-Miescher ketone,[37] which was converted to ketone **1.130** in three steps using a protocol developed by Smith and co-workers.[38] In order to install the cyclopentenone required for the proposed vicinal difunctionalization reaction sequence an annulation strategy[39] was employed

that delivered enone **1.133** in four steps from keto alcohol **1.131**. The proposed conjugate reduction-alkylation sequence on enone **1.133** proceeded with low diastereoselectivity and 47% of a mixture of diastereomeric tricycles was obtained. The undesired diastereomer, bearing a *cis*-fused 5-6-ring juncture, was the slightly favored product. While unfortunate, this result highlighted the inherent challenge associated with the installation of the stereotriad (highlighted in red in Scheme 1.4 on tricycle **1.135**) contained within the terpenoid core.

Conversion of tricycle **1.135** to tetracycle **1.139** was achieved using a series of functional group manipulations, which set the stage for indole assembly. Initial studies on model systems containing sterically hindered ketones investigated the Fischer indole synthesis,[40] however no indole formation was observed. Smith and co-workers proposed that the lack of desired reactivity indicated that sterically encumbered ketones were not susceptible to nucleophilic addition. This outcome guided the pursuit of alternative strategies that avoided initial attack at the carbonyl. As such, a Gassman indole synthesis[41] was pursued, which converted tetracyclic ketone **1.139** to (–)-paspaline (**1.3**) over four-steps and completed the first synthesis of a PID. While this work represented a significant achievement, the challenge of assembling the terpenoid core in a stereocontrolled manner remained. In the efforts that followed, Smith and others have developed unique and creative solutions aimed at the construction of the terpenoid core.

1.2.2 Amos B. Smith III's Second-Generation Formal Synthesis of (–)-Paspaline

In a second-generation approach toward (–)-paspaline (**1.3**) Smith and co-workers altered their approach and elected to install the axially oriented methyl group at C3 using a conjugate alkylation strategy (Scheme 1.5).[42] Following this approach, Smith accessed cyclohexenone **1.141** in four steps from (+)-Wieland-Miescher ketone. Initial studies revealed that copper mediated conjugate methylation of **1.141** delivered mixtures of 1,2- and 1,4-adducts, favoring the

former. After considerable experimentation,[43] application of a conjugate methylation procedure developed by Luche and co-workers[44] cleanly afforded enoxysilane **1.141** as a single diastereomer. The assembly of the key stereotriad permitted the pursuit of a ring contraction to cyclopentanone **1.144**, which was achieved following ozonolysis of the enoxysilane, aldol addition, and oxidative decarboxylation.

Scheme 1.5. Smith's Second Generation Formal Synthesis of (–)-Paspaline.

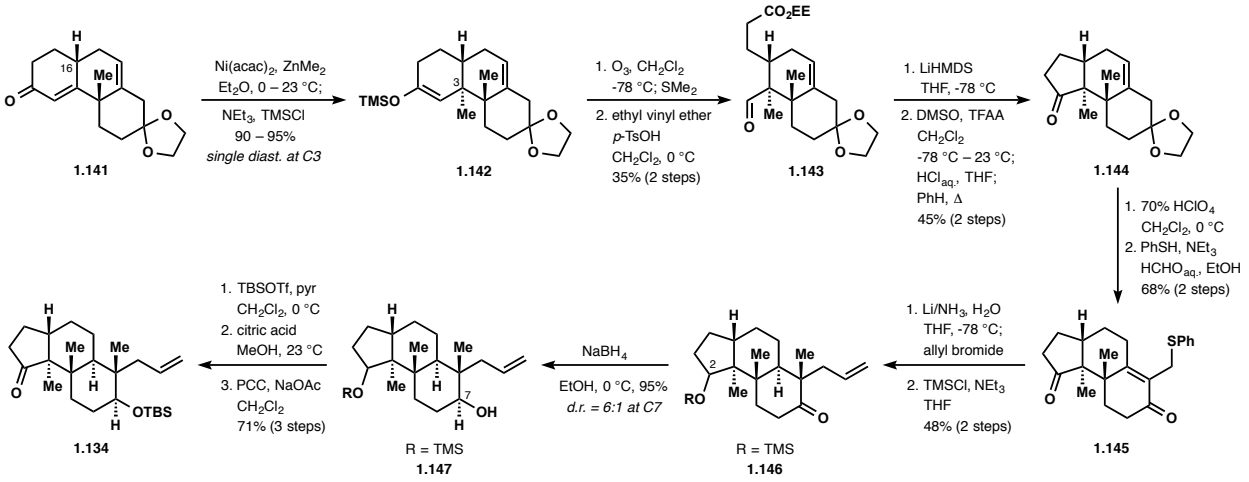

In order to complete the formal synthesis, the final stereocenter contained in the core and the allyl side chain had to be installed, which was achieved via reductive allylation[38] of phenyl sulfide[45] **1.145**. A final series of functional group manipulations converted **1.146** to tricycle **1.134**, which completed a formal synthesis of (–)-paspaline (**1.3**). While the second-generation approach developed by Smith and co-worker addressed the stereocontrolled assembly of the terpenoid core, the gains in stereocontrol came at the expense of step efficiency (17 steps to **1.134** vs. 11 for the first-generation approach). Nonetheless, Smith's research program achieved a monumental feat and developed a truly stereocontrolled formal synthesis of paspaline (**1.3**).

1.2.3 Amos B. Smith III's Total Syntheses of (–)-Paspalicine and (–)-Paspalinine

Scheme 1.6. Smith's Synthesis of (–)-Paspalicine and (–)-Paspalinine.

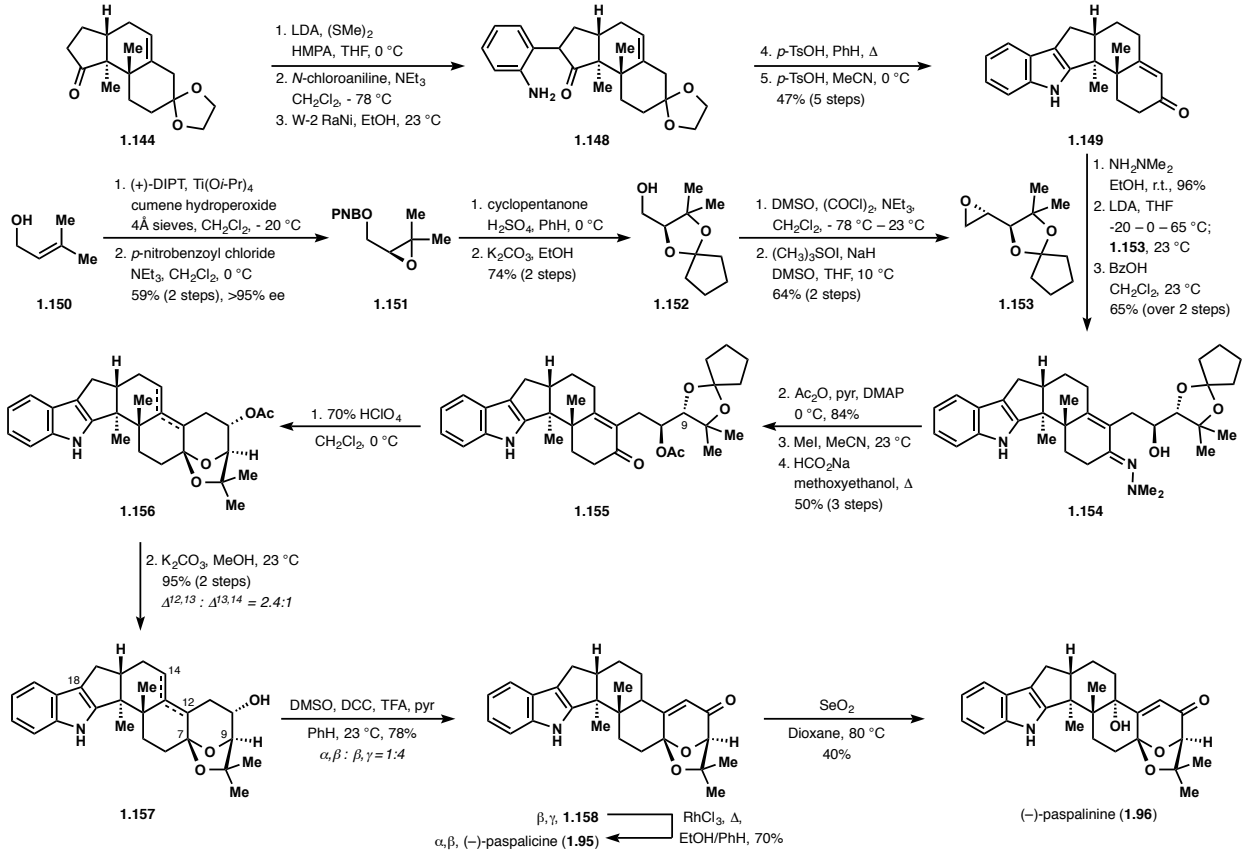

In order to display the generality of their approach, Smith and co-workers reported total syntheses of (–)-paspalicine (**1.95**) and (–)-paspalinine (**1.96**) using a common intermediate and a slightly revised strategy.[46] Their updated approach featured an early-stage installation of the indole, a convergent alkylation of a highly oxidized side-chain via Stork metalloenamine coupling,[47] and a late-stage oxidative conversion of (**1.95**) to (**1.96**) (Scheme 1.6).

Following this approach, Smith's synthesis commenced from **1.144**,[48] which was converted to indole **1.149** via Gassman indole synthesis (*vide supra*). After condensation of *N,N*-dimethylhydazine onto the cyclohexenone, Stork metalloenamine alkylation was pursued. As such, treatment with strong base and enantioenriched epoxide **1.153** delivered *N,N*-dimethylhydrazone **1.154** after treatment with benzoic acid to affect alkene isomerization into conjugation with the hydrazone. In order to chemoselectively form the

dioxabicyclo[3.2.1]octane, the free hydroxyl group was protected and the hydrazone moiety was hydrolyzed.[49] Acid-mediated removal of the ketal protecting group induced concomitant bridged bicycle formation and delivered a mixture homoallyilic and bis-homoallylic alcohols **1.157** after subsequent removal of the acetate-protecting group. Moffatt oxidation[50] and isomerization of the β,γ-alkene isomer into conjugation using a variant of Grieco's rhodium-catalyzed reaction[51] delivered (–)-paspalicine (**1.95**), which was subsequently converted to (–)-paspalinine (**1.96**) via selenium dioxide-mediated allylic oxidation.[52] During reaction development for the conversion of (**1.95**) to (**1.96**) Smith and co-workers discovered that the indole nucleus was prone to decomposition in the presence of various oxidants, which identified one of the key instability factors associated with the PIDs that has served as a guide in subsequent synthetic efforts. In addition, the completion of (–)-paspalinine (**1.95**) and (–)-paspalicine (**1.96**) from common intermediate **1.144** validated the general approach that Smith and co-workers had developed toward the PIDs.

1.2.4 J. Edwin Saxton's Approach Toward (–)-Paspalicine

J. Edwin Saxton and co-workers published a series of papers that took an interesting and unique approach to (–)-pasplicine (**1.95**).[53] While the efforts described did not lead to the completion of a synthesis, the strategy employed to assemble the crucial *trans* 5-6-ring juncture and the vicinal quaternary stereocenters bearing axial methyl groups made a lasting impact on target oriented syntheses related to the PIDs.

Saxton's strategy hinged on two key sequences: an oxidative ring expansion of an α-hydroxy furan via an Achmatowicz reaction followed by bicyclic ketal formation and a directed cyclopropanation-reductive cyclopropane opening sequence. Following this approach, Saxton set

Scheme 1.7. Saxton's Approach to the Bridged Terpenoid Core.

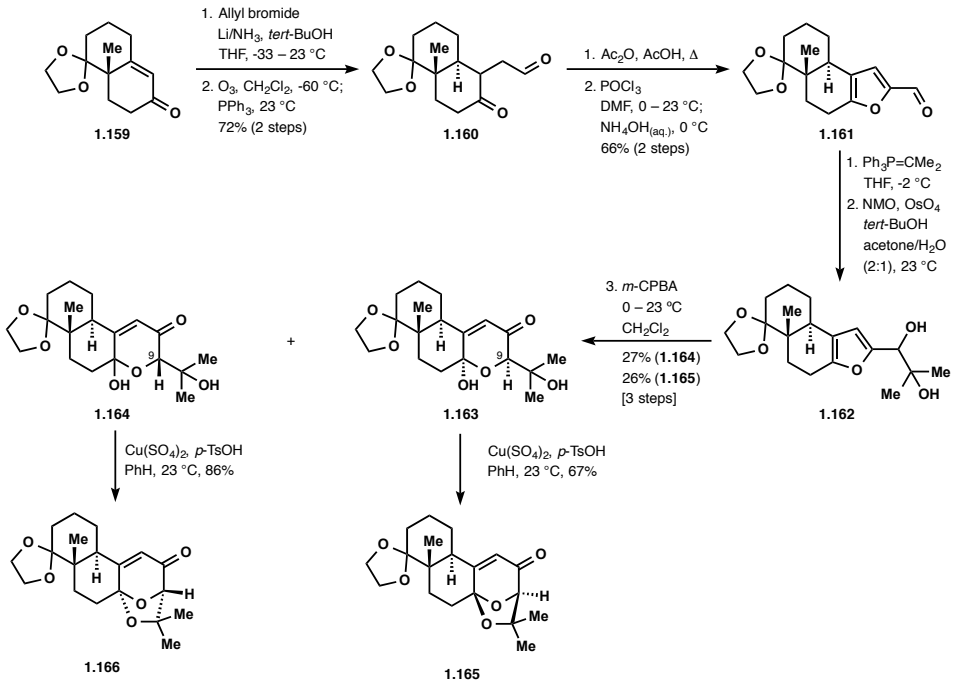

out to validate each sequence independently and accessed furan **1.162** in six steps from ketal **1.159** in pursuit of the oxidative ring expansion (Scheme 1.7). Subjection of **1.162** to *m*-CPBA induced oxidative rearrangement that resulted in a mixture of diastereomeric diols **1.163** and **1.164**. Initial studies revealed that **1.163** and **1.164** converged to bridged bicycle **1.166** when exposed to copper(II) sulfate, indicating a thermodynamic preference for the bridged bicycle with an unnaturally oriented isopropoxy bridge. Indeed, a theoretical energy minimization study by Smith and co-workers revealed that the unnatural bridged bicycle was lower in energy for both paspalicine (**1.95**) and paspalinine (**1.96**), which validated Saxton's empirical observations (Figure 1.3).[46b] Nonetheless, careful treatment with anhydrous copper(II) sulfate and catalytic acid could deliver each bridged bicycle, **1.165** and **1.166**, without epimerization.

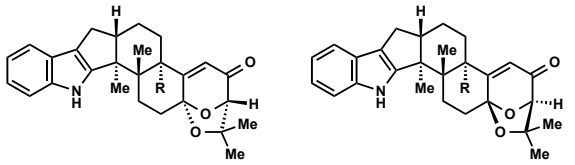

Figure 1.3. Smith's Energy Minimization Study.

Saxton's second strategy toward the terpenoid core of (–)-paspalicine (**1.95**) focused on a directed cyclopropanation-reductive cyclopropane opening to access the vicinal quaternary stereocenters bearing axial methyl groups (Scheme 1.8). Following this approach cyclopropanol **1.173** was accessed in four steps from ketal **1.169**.[54] Directed Simmons-Smith cyclopropanation[55] diasteroselectively delivered cyclopropane **1.174** after subsequent Swern oxidation.[56] Reductive cleavage of the cyclopropane moiety[57] afforded cyclopentanone **1.175** as a single diastereomer with the desired stereochemistry for the resultant methyl group. Unfortunately, the intermediate enolate generated from the reductive opening of the cyclopropane could not be trapped to form an appropriate functional handle for a Wender indole synthesis.[58]

Scheme 1.8. Saxton's Approach to the Vicinal Quaternary Stereocenters.

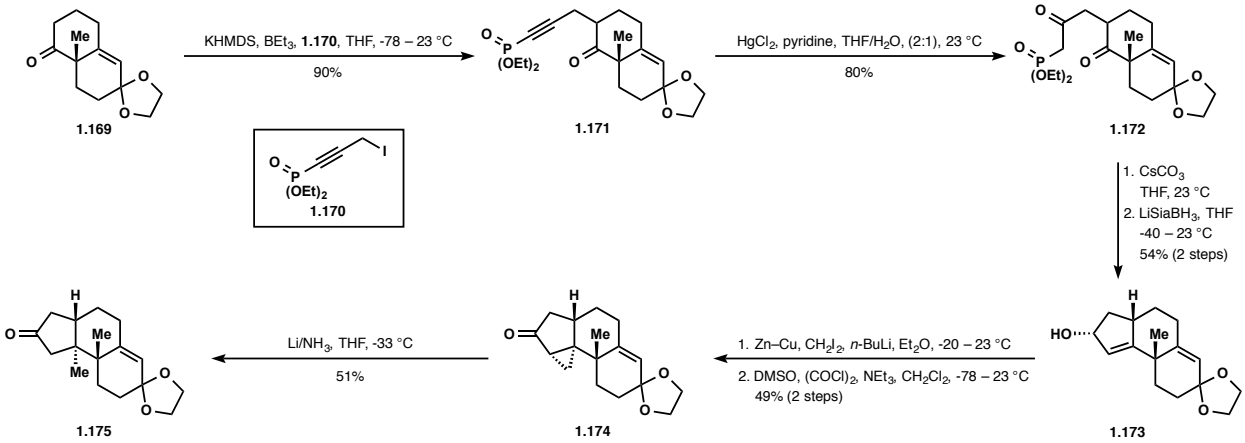

While Saxton's approach toward (–)-paspalicine (**1.95**) was unsuccessful in regards to completing a total synthesis, his construction of the vicinal quaternary stereocenters embedded in the terpenoid core proved to be a stereoselective, reliable, and efficient tactic. Specifically, the

exploitation of a directing-group to override some of the inherent challenges associated with the assembly of the terpenoid core proved to be a general strategy that could be applied in subsequent synthetic approaches to the PIDs.

1.2.5 Amos B. Smith III's Synthesis of (–)-Penitrem D

Scheme 1.9. Smith's Strategy Toward (–)-Penitrem D.

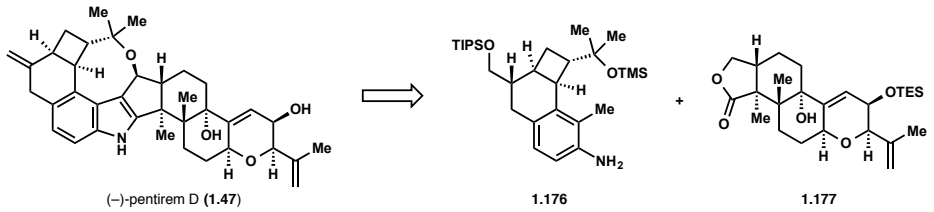

The penitrems are arguably the most structurally complex sub-class of the PIDs. As such, a successful synthetic campaign toward any congener would represent a significant achievement in target-oriented synthesis. Smith and co-workers reported a total synthesis of (–)-penitrem D (**1.47**) in 2000 that was the culmination of over a decade of synthetic work.[59] A convergent strategy was at the core of Smith's approach, which hinged on a modified Madelung indole synthesis[60] to unite two complex subtargets and form the indole nucleus (Scheme 1.9).

Scheme 1.10. Smith's Construction of the *trans-anti*-Stereotriad.

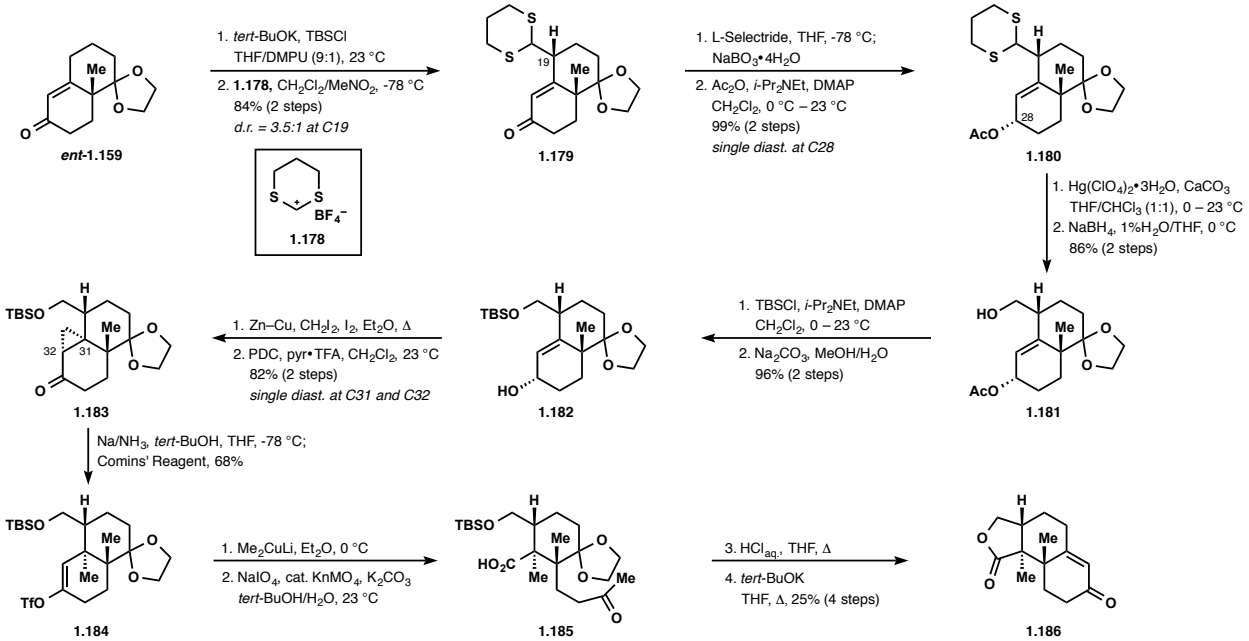

In accord with Smith's previous syntheses, construction of the stereotriad embedded in the terpenoid core proved to be a challenge. As a result, multiple approaches to the eastern fragment were pursued, but many were plagued with inefficiencies.[59c,d] Similar to Saxton's approach (*vide supra*), a strategy centered on reductive cleavage of a cyclopropane was ultimately utilized in the synthesis of eastern subtarget **1.177**.[59f]

Following this approach, allylic alcohol **1.182** was accessed from ketal *ent*-**1.159** in eight steps with moderate stereocontrol (Scheme 1.10). Subsequent cyclopropanation delivered cyclopropane **1.183** in high yield as a single diastereomer after oxidation with pyridinium dichromate.[61] Dissolving metal reduction and *in situ* trapping of the resulting sodium enolate as

Scheme 1.11. Smith's Final Assembly of the Eastern Subtarget.

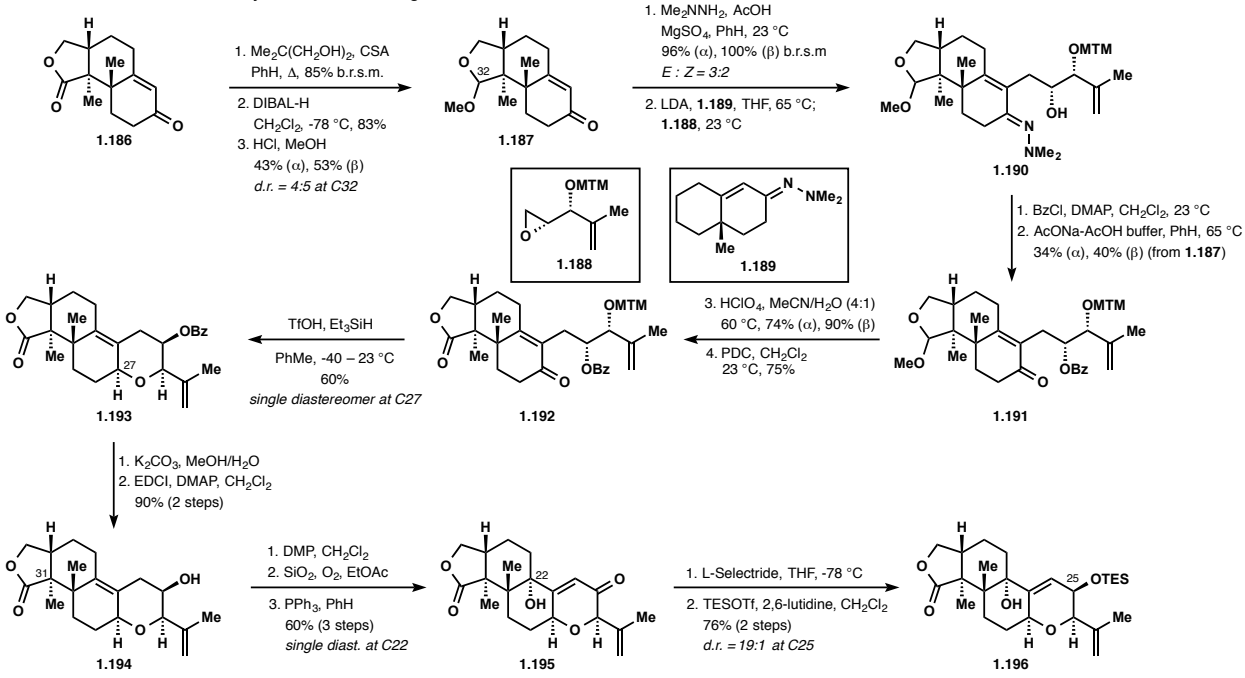

the vinyl triflate with Comins' reagent[62] afforded triflate **1.184**, which concluded the construction of the crucial stereotriad. A four-step sequence converted **1.184** to lactone **1.186**, which was identified as a general subtarget for the PIDs.[59f]

Drawing from their experience, Smith turned to the construction of the dihydropyran ring contained in penitrem D (**1.47**) (Scheme1.11). As such, **1.186** was converted to **1.190** over five steps[63] using an Stork metalloenamine alkylation strategy to unite tricycle **1.187** and epoxide **1.188**.[59c,64] The presence of auxiliary hydrazone **1.189** was essential to obtaining high yields. While the exact role of **1.189** was unknown, Smith and co-workers speculated that it facilitated equilibration of anions, which enabled a more efficient protocol. A series of functional group manipulations converted **1.190** to tricycle **1.192** and set the stage for the construction of the final ring contained in the eastern hemisphere subtarget.

Scheme 1.12. Formation of the *cis*-pyran.

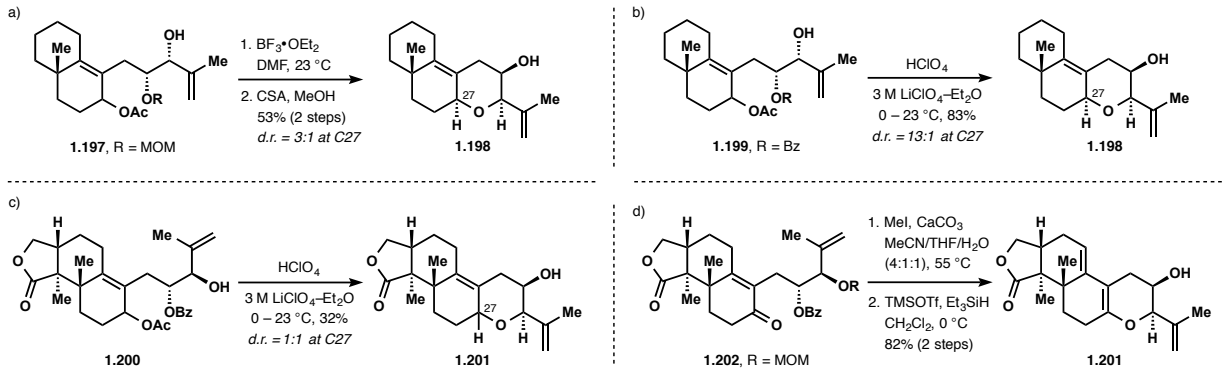

Formation of the *cis*-pyran proved to be a challenge. While an effort to acquire the desired *cis*-pyran was successful on a model system, application of the developed reaction conditions delivered an unselective process (Scheme 1.12a–c). Due to the lack of selectivity and low efficiency, the pursuit of pyran formation via ionizing conditions was abandoned in favor of a protocol developed by Nicolaou and co-workers.[65] Initial attempts using a two-step protocol delivered an undesired elimination product (Scheme 1.12d), but optimization of this approach ultimately delivered *cis*-pyran **1.193** as a single diastereomer (Scheme 1.11, **1.192** to **1.193**).

Scheme 1.13. Model Study Related to the Installation of the Hydroxyl Group at C22.

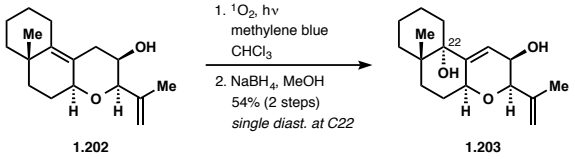

The final obstacle blocking the completion of the eastern hemisphere subtarget was incorporation of the hydroxyl group at C22. Results on a model system indicated that an ene reaction with singlet oxygen could provide access to the desired alcohol as a single diastereomer after reduction of the intermediate peroxide (Scheme 1.13).[66] However, this mode of reactivity did not translate to alkene **1.194** and no reaction was observed. Smith attributed the negative result to the presence of the axial methyl group at C31 as 1,3-diaxial interactions are know to inhibit photosensitized oxygenations.[67]

Undeterred and inspired by their successful oxidative conversion of (–)-paspalicine (**1.95**) to (–)-pasplinine (**1.96**) Smith pivoted and pursued an analogous oxidation of an enone. Following this approach, oxidation of the alcohol with Dess-Martin periodinane[68] and subsequent autooxidation[69] delivered alcohol **1.195** as a single diastereomer after reduction of the intermediate peroxide. Installation of the hydroxy group permitted the completion of eastern

Scheme 1.14. Preparation of the Western Hemisphere Subtarget.

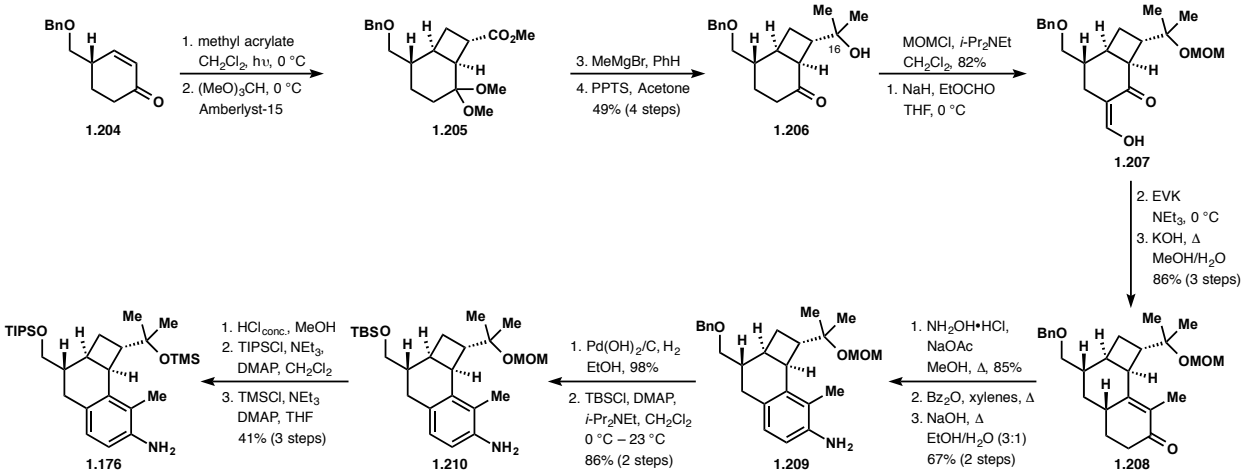

hemisphere subtarget **1.196** after chemo- and diastereoselective reduction of the ketone and protection of the newly formed alcohol.

Synthetic efforts focused on western hemisphere subtarget **1.176** began with a photochemical [2+2] cycloaddition between enone **1.204**[70] and methyl acrylate to construct the *cis*-cyclobutane found in the penitrems (Scheme 1.14). Following the cycloaddition, a series of functional group conversions delivered enol **1.207** in six steps from enone **1.204**. A Woodward–Wilds modification of the Robinson annulation[71] produced enone **1.208** and set the stage for a Semmler–Wolff aniline aromatization.[72] Following this approach, condensation of **1.208** with hydroxyl amine, *O*-benzylation, and treatment with aqueous base induced the formation of aniline **1.209**. A final sequence of protecting group manipulations led to the production of western hemisphere subtarget **1.176**.

Scheme 1.15. Endgame Approach to (–)-Penitrem D.

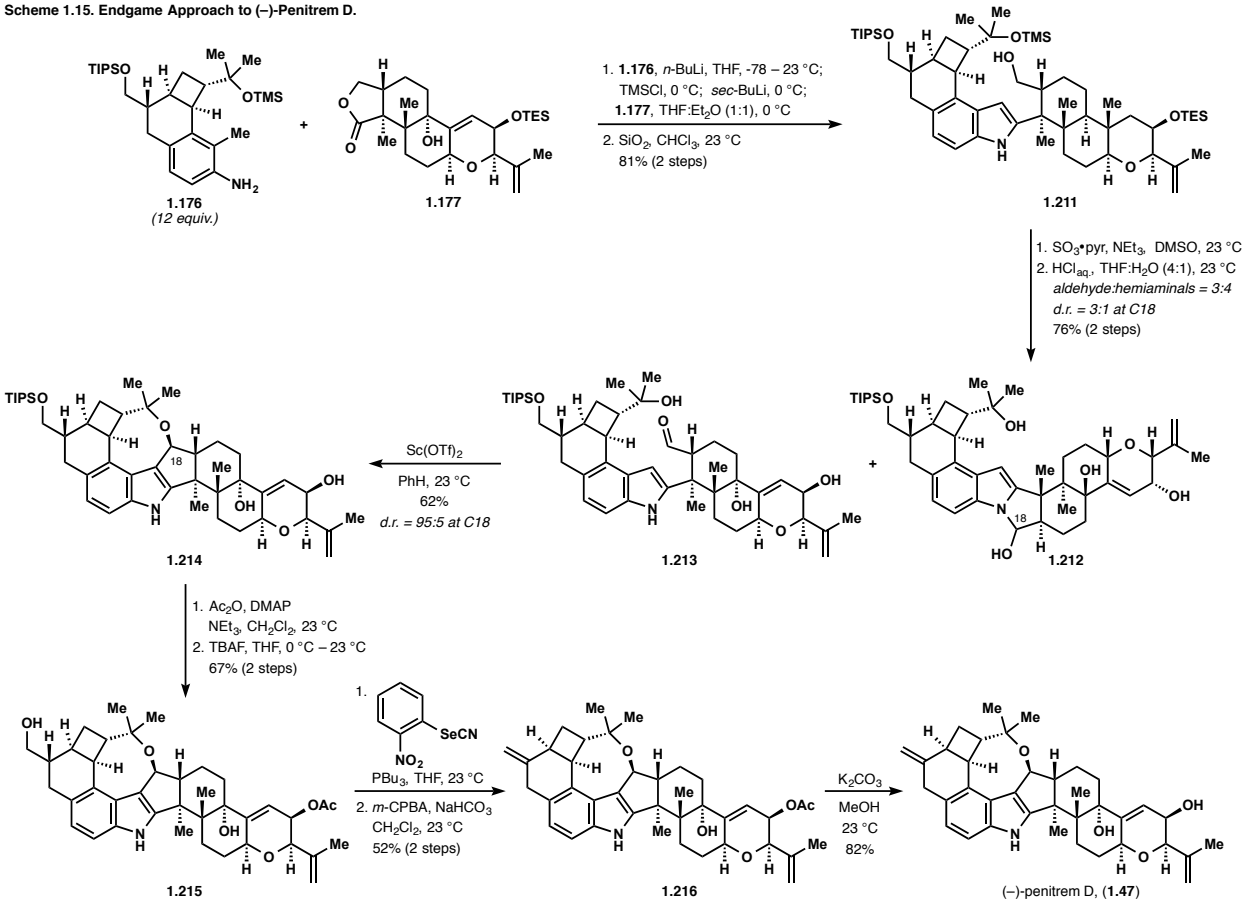

The stereocontrolled assembly of each hemisphere facilitated a final construction of (–)-penitrem D (**1.47**). As such, the crucial modified Madelung indole synthesis was investigated and gratifyingly delivered indole **1.211** after addition of the dianion of *N*-silyl analog of **1.176** into lactone **1.177** and silica gel mediated aza-Peterson olefination/tautomerization. Next, Parikh–Doering oxidation[73] and removal of the *O*-TES and *O*-TMS protecting groups produced a complex mixture containing aldehyde **1.213** and hemiaminal **1.212**.[74] A proposed oxocane formation cascade was investigated in the presence of a Brønsted acid, however a low yield for desired product **1.214** was observed along with considerable dehydration of the hemiaminal (product not shown). Fortunately, Lewis acidic conditions utilizing $Sc(OTf)_3$ delivered desired oxocane **1.214** with high diastereoselectivity. With the final ring formed, completion of (–)-penitrem D (**1.47**) was achieved following a series of protecting group manipulations and Grieco–Nishizawa selenation/elimination.[75]

The highlight of Smith's landmark synthesis of (–)-penitrem D (**1.47**) was the convergent modified Madelung indole assembly that united two complex fragments. While the efficiency of the transformation (12 equivalents of **1.176** was required) was not ideal, its accomplishment indicated that a convergent strategy focused on the synthesis of the indole nucleus was viable.

1.2.6 Amos B. Smith III's Total Synthesis of (–)-21-Isopentenylpaxilline

In 2003 Smith and co-worker disclosed a synthesis of (–)-isopentenylpaxilline (**1.112**) using a synthetic strategy similar to (–)-penitrem D (**1.47**; *vide supra*).[76] As such, the synthesis began with enone **1.186** and epoxide **1.218**,[77] which were united via Stork metalloenamine coupling.[47] A series of functional group manipulations provided access to enone **1.221**, which was converted to pyran **1.222** following reductive cyclization and epoxidation. A final protecting

group exchange of the *O*-TES protecting group for a benzoyl group delivered lactone **1.223** and completed the assembly of the terpenoid core.

Scheme 1.16. Preparation of Lactone 1.223.

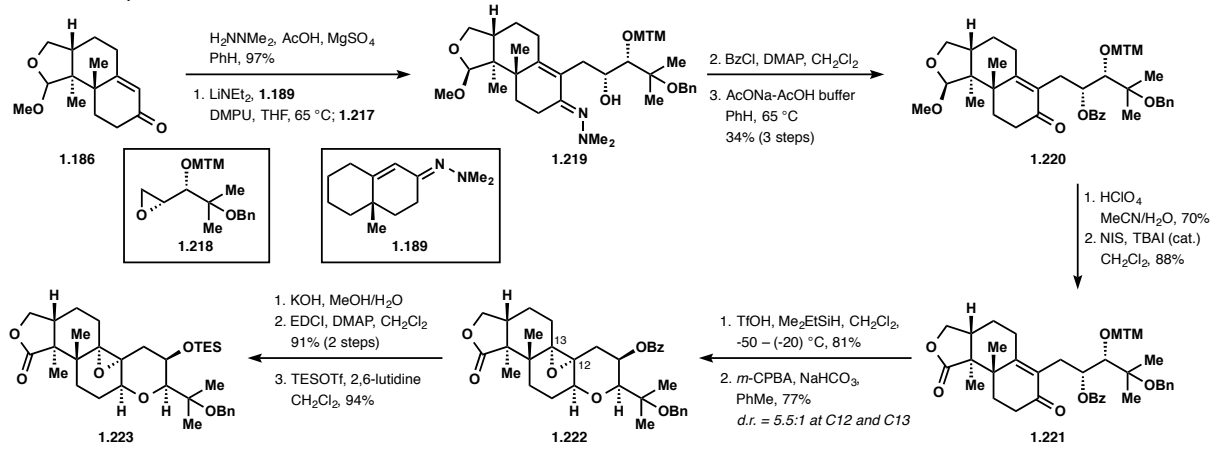

Application of the modified Madelung indole synthesis coupled lactone **1.223** and aniline **1.224**, delivered desired indole **1.225** (Scheme 1.17). The revealed alcohol was converted to a mesylate that was efficiently displaced via intramolecular attack by the indole.[78] Removal of the protecting groups and oxidation with Ph_3BiCO_3[79] completed the assembly of (–)-21-isopentenylpaxilline (**1.112**).

Scheme 1.17. Endgame Approach to (–)-21-Isopentenylpaxilline.

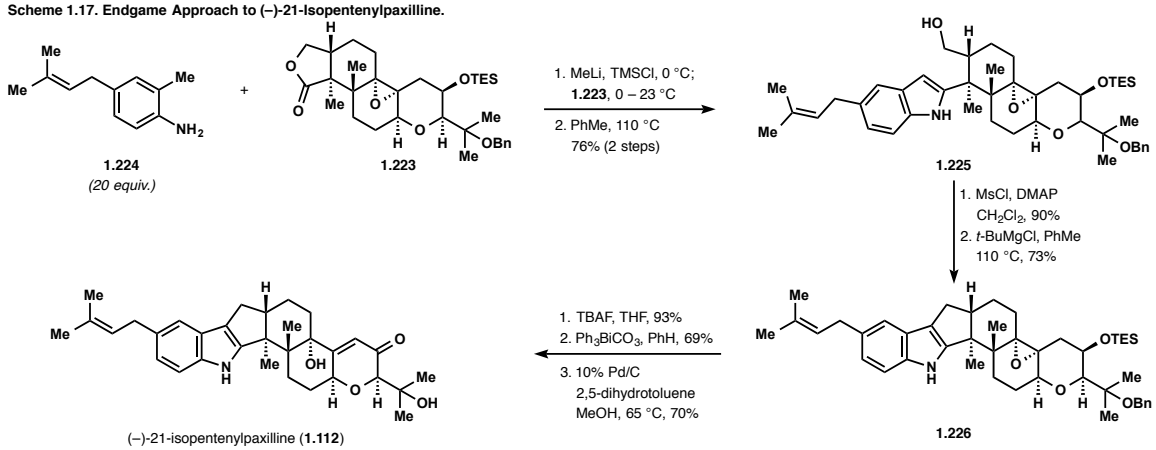

1.2.7 Philip Magnus' Approach to the Western Hemisphere of the Nodulisporic Acids

Scheme 1.18. Magnus' Approach to the Nodulisporic Acids.

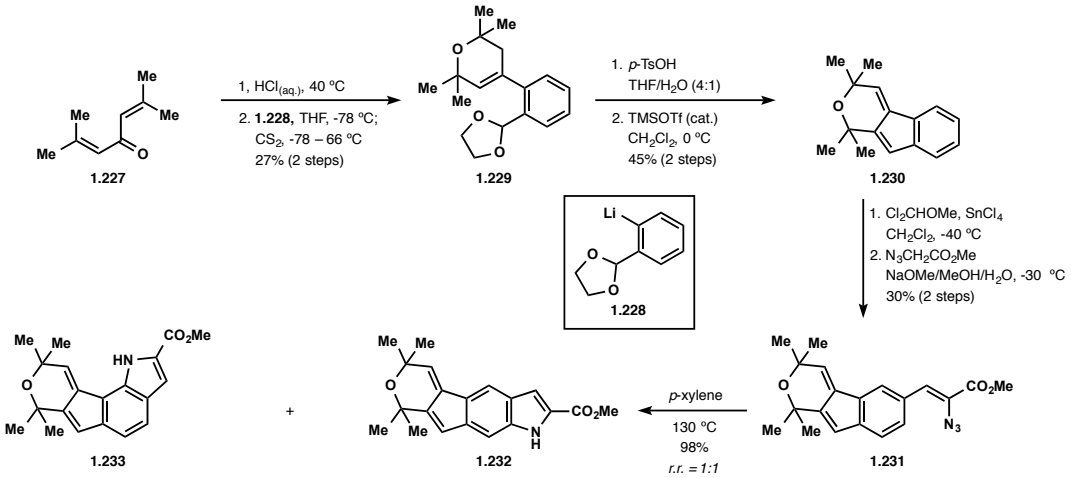

In 1999 Philip Magnus and co-worker published the first synthetic approach to the nodulisporic acid subclass of the PIDs (Scheme 1.18).[80] A key type II ene reaction[81] was proposed to forge the indane fragment characteristic to the nodulisporic acids. Following this approach, phorone **1.227** was converted to arene **1.229** via hydration/cyclization[82] and 1,2-aryllithium addition/Chugaev elimination[83] sequences. Hydrolysis of the ketal and treatment with Lewis acid induced the desired ene reaction and resulted in the formation of diene **1.230**. During reaction development Magnus and co-workers observed that the desired benzylic alcohol readily eliminated and formed diene **1.230**. While the benzylic alcohol represents the native functionality the diene was pursued due to its efficient formation and the belief that the benzylic alcohol could be reinstalled at a later point.

The preparation of the 6-5-6 tricyclic framework contained in the nodulisporic acids allowed the focus to shift to the synthesis of an indole via a Hemetsberger indole synthesis.[84] Following this approach, the arene ring was formylated with dichloro methyl ether[85] and the resulting aldehyde was exposed to α-azido methyl acetate. Heating induced indole formation, however a 1:1 mixture of separable regioisomers **1.232** and **1.233** was obtained in good yield. The synthesis of **1.232** completed the model study related to the nodulisporic acids.

Scheme 1.19. Reinstallation of the Benzylic Alcohol.

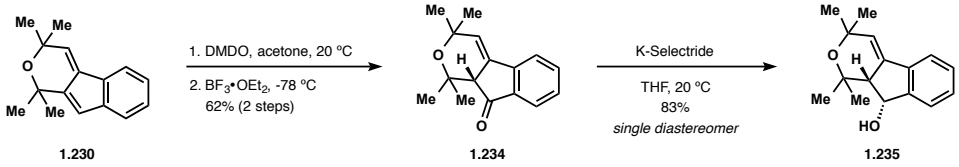

In addition to the assembly of indole **1.232** Magnus also reinstalled the benzylic alcohol found in the more highly oxidized nodulisporic acids (Scheme 1.19). As such, epoxidation of diene **1.230** with dimethyldioxirane and subsequent Meinwald rearrangement delivered indanone **1.234**. Reduction with K-Selectride diastereoselectively reinstalled the benzylic alcohol, albeit with the undesired stereochemistry. While Magnus did not further pursue the nodulisporic acids the enduring message from his studies related to the stability of the benzylic alcohol, which was found to be very sensitive to acidic conditions. This property of a key functionality was recognized as a consideration that must be kept in mind when pursuing the nodulisporic acids.

1.2.8 Michael A. Kerr's Approach to the Western Hemisphere of the Lolicines and Lolitrems

Scheme 1.20. Kerr's Approach Toward the Western Hemisphere of the Lolicines and Lolitrems.

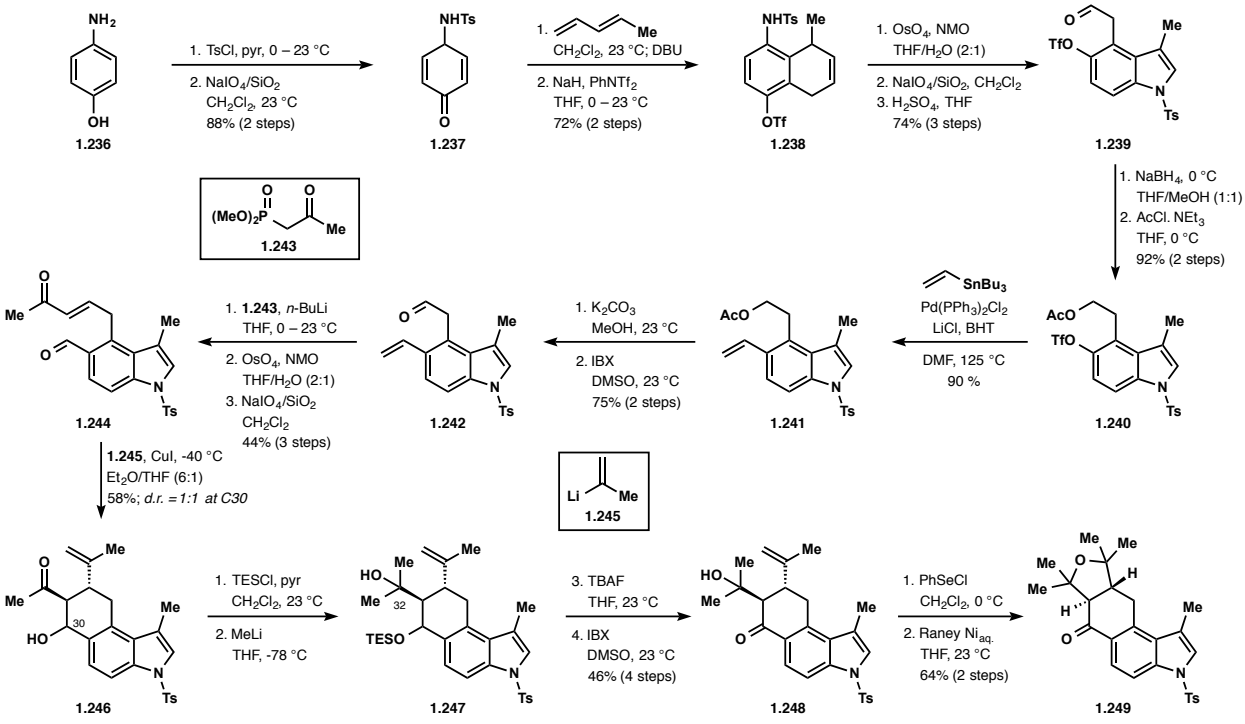

In 2006, Kerr and co-workers reported an approach to the western hemisphere of the lolicines and lolitrems.[86] Their strategy involved an early-stage Plieninger indole synthesis to construct a highly functionalized indole and a vicinal difunctionalization of an enone involving a 1,4-addition/aldol to form the dihydropyran fagment (Scheme 1.20). Following this approach, assembly of indole **1.249** began with the formation of dihydronaphthalene **1.238** via Diel–Alder between quinoid imine **1.237** and (*E*)-penta-1,3-diene. Subsequent Plieninger indole synthesis[87,88] delivered indole **1.239**, which was converted to aryl triflate **1.240** following reduction with $NaBH_4$ and acylation of resultant alcohol. Stille coupling[89] and reintroduction of the aldehyde afforded styrene **1.242**.

Horner–Wadsworth Emmons olefination and a two-step oxidative cleavage of the styrene led to the formation of enone **1.244**, which possessed the desired enone and aldehyde functionalities for the proposed vicinal difunctionalization. As such, **1.244** was treated with organolithium **1.245** in the presence of copper(I) iodide, which delivered benzyl alcohol **1.246** as an inconsequential mixture of diastereomers at C30 following the proposed 1,4-addition/aldol cascade. Installation of a tertiary alcohol at C32 and subsequent conversion of the benzylic alcohol delivered ketone **1.248**, which was positioned to form the 2,2,5,5-tetramethyltetrahydrofuran fragment contained in the lolicines and lolitrems. As such, alkoxy-selenation[90] of the alkene and reduction of the resulting selenide delivered western hemisphere target **1.249** and completed Kerr's efforts.

1.2.9 Shigefumi Kuwahara's Total Synthesis of (–)-Paspalinine

Scheme 1.21. Kuwahara's Synthesis of (–)-Paspalinine.

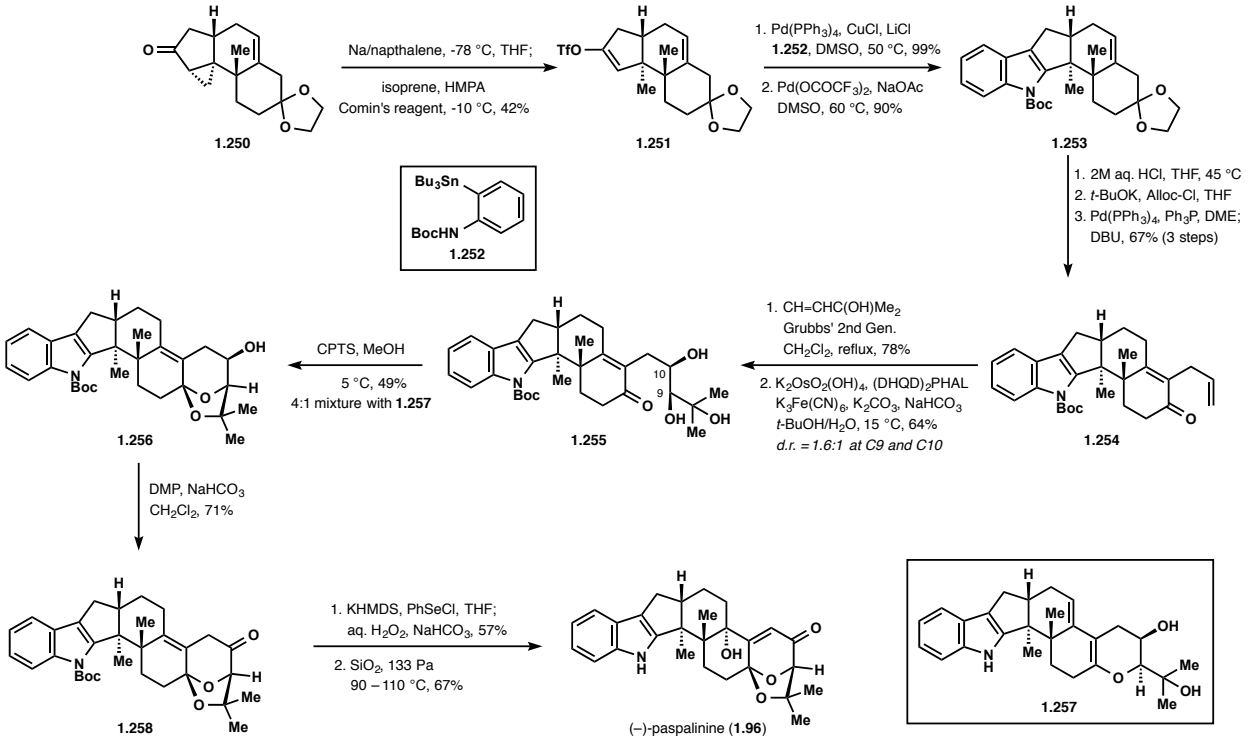

In 2012 Shigefumi Kuwahara and co-workers reported the synthesis of (–)-paspalinine (**1.96**) utilizing a strategy reminiscent of the one reported by Saxton almost 20 years prior (*vide supra*).[53c] As such, Kuwahara used reductive opening of cyclopropane **1.250**[91] to complete the assembly of the challenging vicinal quaternary stereocenters bearing axial methyl groups embedded in the terpenoid core (Scheme 1.21).[92] However, in contrast to Saxton's report, the intermediate enolate generated during the dissolving metal reduction was successfully trapped as vinyl triflate **1.251**. The ability to directly access the vinyl triflate facilitated indole assembly via a two-step process involving a Stille coupling with stannane **1.22**[93] and a Pd(II)-mediated oxidative cyclization,[94] which produced indole **1.253** with high efficiency.

After the successful installation of the indole moiety, elaboration of the right side to the dioxabicyclo[3.2.1]bicycle was pursued. As such, hydrolysis of the ketal and Tsuji allylation[95] delivered enone **1.254**. Cross metathesis in the presence of Grubbs' second generation catalyst[96]

converted the terminal alkene to an intermediate internal (*E*)-alkene that was subject to Sharpless asymmertric dihydroxylation,[97] which afforded triol **1.255** with relatively poor diastereocontrol. Exposure to Brønsted acid induced ketal formation and oxidation with Dess-Martin periodinane[68] delivered ketone **1.258**. During ketal formation, a minor elimination side product, diene **1.257**, was observed.

Installation of the final hydroxyl group was achieved via α-selenation, oxidation to the selenoxide, and [2,3]-sigmatropic rearrangement.[98] Finally, removal of the Boc protecting group completed the total synthesis and delivered (–)-paspalinine (**1.96**). This work represented the first successful total synthesis of a PID by a research group other than Amos B. Smith III. In addition, the strategy originally put forth by Saxton and co-workers was validated as nearly identical intermediates were used to assemble the challenging stereotriad contained in the terpenoid core of the PIDs.

1.2.10 Athanassios Giannis' Synthesis of 16-*epi*-Terpendole E.

In 2010 Giannis and co-workers reported unique strategy toward terpendole E (Scheme 1.22). Unlike all previous approaches that relied on a *de novo* synthesis of the indole, Giannis proposed an aldol condensation between terpenoid core **1.268** with protected indole-3-carboxaldehyde **1.269** and formation of the five-membered ring via a Nazarov cyclization.[99] Following this approach, the construction of the terpenoid core commenced from ketone **1.130**. Stereoselective reduction of the carbonyl[100] and hydroboration-oxidation delivered lactone **1.260**. Oxidation to enone **1.261** was a challenge; the evaluation of common dehydrogenation reactions[101] did not yield desired enone **1.261**. However, treatment of ketone **1.260** with strong base and *N*-*tert*-butylbenzenesulfinimidoyl chloride[102] delivered enone **1.261**.

Subsequent treatment with H_2O_2 and base induced epoxide formation of the enone

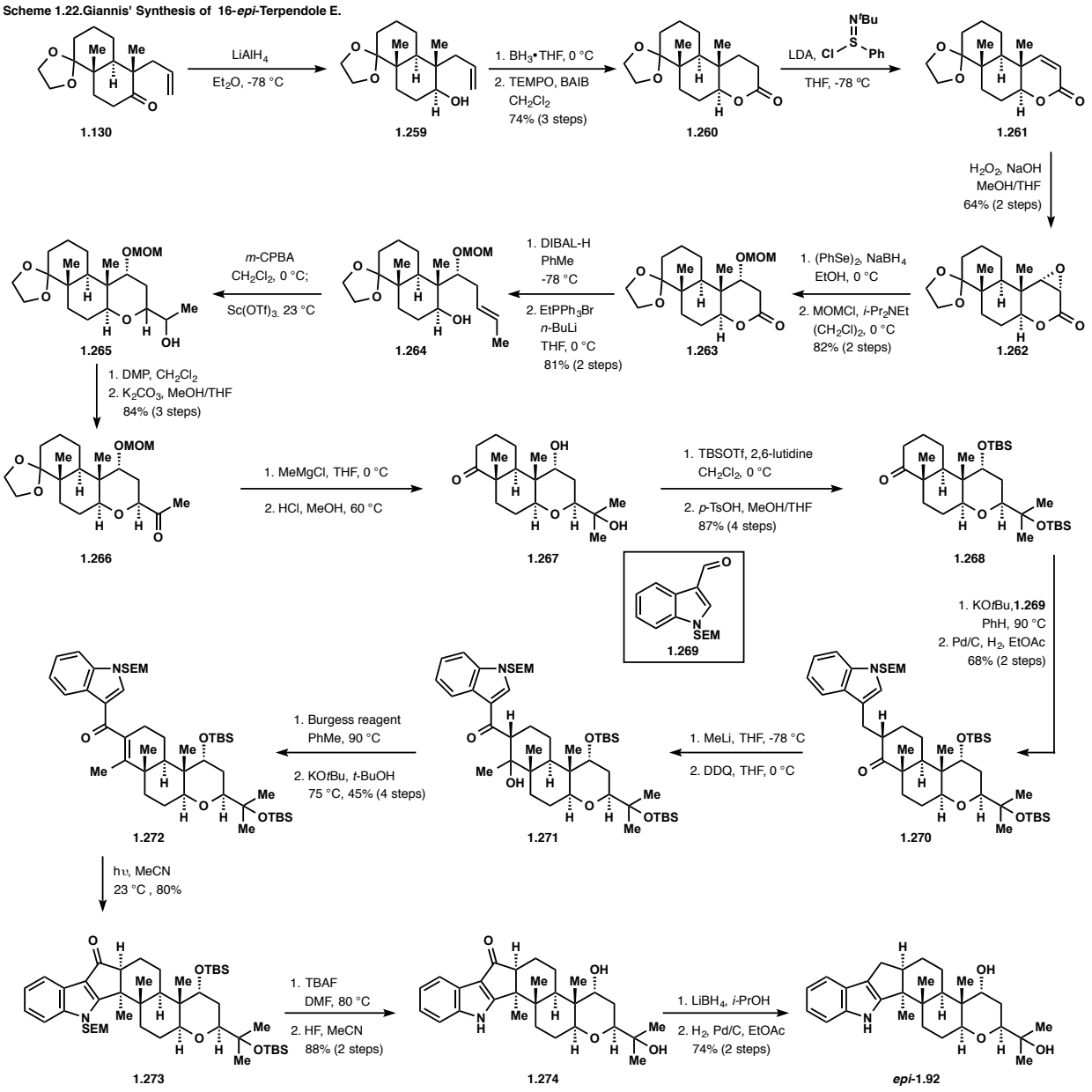

moiety. Regioselective organoselenium-mediated reduction[103] of the newly formed epoxide and protection of the resulting alcohol delivered lactone **1.263** as a single diastereomer. Reduction of the lactone and Wittig olefination of the corresponding lactol afforded alkene **1.264** as a mixture of isomers. Epoxidation and Lewis acid catalyzed intramolecular cyclization formed an inconsequential mixture of alcohols that could be converted to desired pyran **1.266** after Dess–Martin periodinane oxidation and base-mediated epimerization. Addition of methylmagnesium

bromide into the ketone, removal of the MOM-protecting group, and silylation of the resulting diol produced ketone **1.268** in excellent overall yield from pyran **1.266**.

The construction of ketone **1.268** allowed Giannis and co-workers to turn their attention to their proposed installation of the indole via aldol condensation. As such, treatment of ketone **1.268** with base in the presence of indole-3-carboxaldehyde **1.269** delivered indole **1.270** after hydrogenation of the resulting double bond. Addition of methyllithium into the ketone followed by benzylic oxidation with DDQ[104] afforded an inconsequential mixture of diastereomeric tertiary alcohols that were treated with Burgess reagent[105] to induce dehydration and delivered enone **1.272** after alkene isomerization.

Attempts at the proposed Nazarov cyclization under traditional Lewis or Brønsted acid conditions did not give the desired product. However, irradiation at 350 nm produced hexacycle **1.273**, which possessed the undesired stereochemistry at C16. Unfortunately, after removal of the silyl-protecting groups, attempts to epimerize the stereochemistry at C16 were unsuccessful. Nonetheless, reduction of the benzylic ketone afforded 16-*epi*-terpendole E (*epi*-**1.92**).

1.2.11 Masato Oikawa's Approach to the Eastern Hemisphere of Terpendole E

In 2010 Oikawa and co-workers reported an approach to the eastern hemisphere of terpendole E (**1.92**) (Scheme 1.23).[106] The pursued strategy provided insight related to the addition of organometallic reagents to aldehyde **1.279** to access the alcohol at C11. Construction of aldehyde **1.279** commenced from alcohol **1.275**[107] by way of Sharpless asymmetric epoxidation[108] and protection of the alcohol delivered epoxide **1.276**. Reductive opening of the epoxide with titanocene(III) chloride[109] induced a radical polyene cyclization that terminated with the formation of exocyclic alkene **1.278** after protection of the alcohol[110] formed in the reductive ring-opening event. A series of functional group manipulations converted **1.278** to

aldehyde **1.279**, which was poised for further elaboration via organometallic addition into the aldehyde moiety.

Scheme 1.23. Oikawa's Approach to the Eastern Hemisphere of Terpendole E.

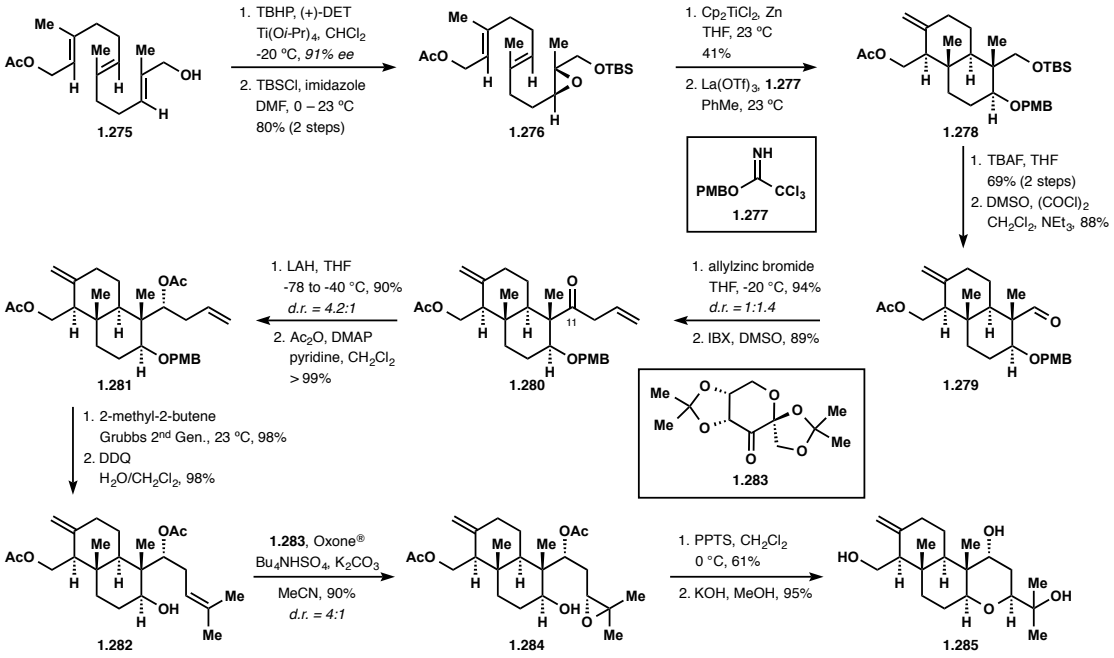

Upon treatment with allylzinc bromide a diastereomeric mixture of homoallylic alcohols with a slight preference for the undesired diastereomer (not shown) was observed. A brief survey of traditional allylmetal species on a model system using aldehyde **1.288** did not yield a more diastereoselective process (Table 1). In addition, attempts at the introduction of a dimethyl allyl organometallic delivered the undesired γ-addition product as the major regioisomer. Undeterred by these results, Oikawa continued forward and pursued an oxidation-reduction sequence to obtain the desired stereochemistry at C11.

Table 1.1. Addition of Allyl Metals to Aldehyde 1.288.

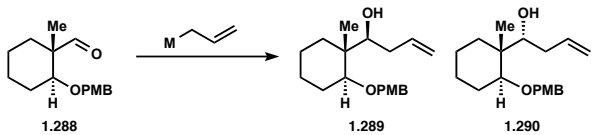

entry	*M*	**1.289** : **1.290**
1	MgBr	1:1.4
2	ZnBr	2.2:1
3	TMS	1:0

Treatment of the intermediate homoallylic alcohol (not shown) with *o*-iodoxybenzoic acid (IBX) in DMSO[111] delivered ketone **1.280**. Subsequent reduction with lithium aluminum hydride and acetylation of the resulting alcohol produced acetate **1.281** with synthetically useful diastereoselectivity.[112] Cross metathesis with 2-methyl-2-butene mediated by Grubbs' second-generation catalyst[97] and oxidative removal of the *p*-methoxybenzyl (PMB) group afforded trisubstituted alkene **1.282**. Construction of the pyran ring and completion of Oikawa's eastern hemisphere fragment **1.285** was achieved following diastereoselective Shi epoxidation,[113] Brønsted acid mediated pyran formation, and removal of the protecting groups. While the unselective addition of organometallic reagents into aldehyde **1.282** was unexpected, the identification of this challenge provides researchers with a consideration to be mindful of when planning a campaign toward relevant PIDs.

1.2.12 Shigefumi Kuwahara's Total Synthesis of (±)-Terpendole E

In 2015 Kuwahara and co-workers completed a synthesis of terpendole E (**1.92**) using a strategy that incorporated aspects from their synthesis of (–)-paspalinine (**1.96**) and Oikawa's approach to terpendole E (**1.47**) (Scheme 1.24).[114] As such, Kuwahara accessed terminal alkene **1.291**,[115] which was elaborated to silylated pyran **1.294** using a synthetic sequence similar to the one reported by Oikawa (*vide supra*).

At this stage of the synthetic sequence the focus turned to the construction of the vicinal quaternary stereocenters bearing axial methyl groups. Application of the strategy involving the reductive opening of a cyclopropane pioneered by Saxton and further developed in Kuwahara's synthesis of (–)-paspalinine (**1.96**) delivered indole **1.300** stereoselectively in six steps from enone **1.296**. Removal of the protecting groups completed the synthesis of terpendole E (**1.92**).

Scheme 1.24. Kuwahara's Synthesis of Terpendole E.

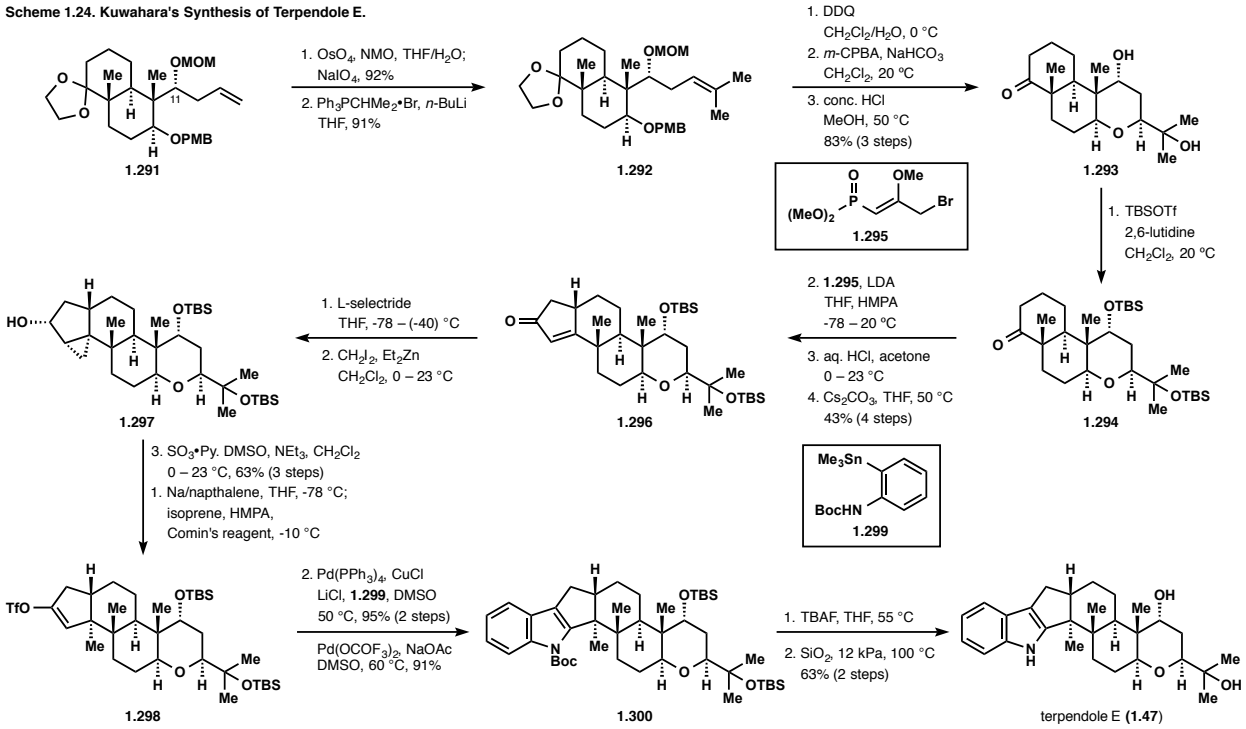

1.2.13 Jeffery S. Johnson's Total Synthesis of (–)-Paspaline

In 2015, Johnson and co-worker published the first successful synthesis of a PID that did not begin with the Wieland–Miescher ketone.[116] Johnson's synthesis began with a regioselective alkylation of *N,N*-dimethyl hydrazone **1.303** with iodide **1.304**,[117] which produced 1,3-dione **1.305** after hydrolysis of the hydrazone (Scheme 1.25). Inspired by a desymmetrizing biocatalytic reduction first investigated by Nakada[118] and Node,[119] Johnson exposed **1.305** to yeast from *Saccaromyces cerevisiae* type 2 (YSC-2) to deliver an intermediate β-hydroxy ketone (not shown) with excellent diastereo- and enantioselectivity.

The conversion of the product of desymmetrization to C13 tosyl hydrazone **1.306** was essential for the subsequent construction of the pyran ring. Initial attempts at the epoxidation of the trisubstituted alkene with a C13 ketone variant of **1.306** were not diastereoselective (*d.r.* = 2:1 at C9) and, of greater concern, opening of the epoxide was not regioselective and complicated by competing attack of the epoxide by the enol tautomer of the ketone. To enhance

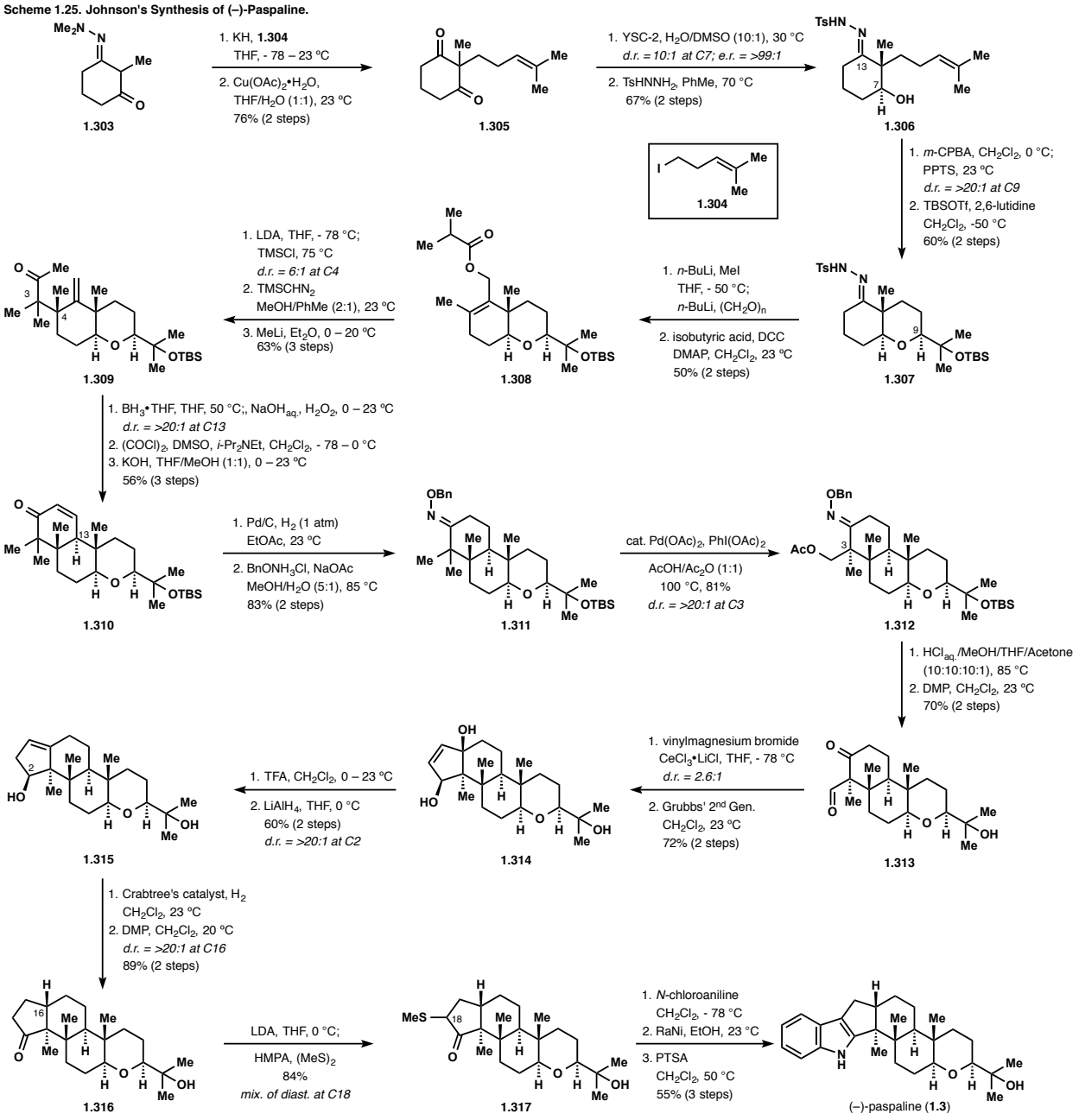

the regioselectivity, Johnson turned to hydrazone **1.306** and to their delight both hurdles observed with the ketone were rectified. As such, epoxidation of the trisubstituted alkene and subsequent *in situ* treatment with Brønsted acid afforded pyran **1.307** with excellent diastereoselectivity. Johnson hypothesized that the enhancement of the diastereoselectivity was a result of a conformational difference between the ketone and hydrazone. The dihedral angle

about the C7–C–OH and C12-CH_2CHCMe_2 (for clarity CH_2CHCMe_2 is denoted as R) appeared to be significantly larger for the hydrazone than the ketone (Figure 1.4). This difference could lead to the alcohol having a stronger directing effect for the epoxidation event and result in higher diastereoselectivity of the epoxidation.

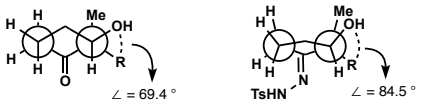

Figure 1.4. Calculated Dihedral Angles.

Johnson turned his attention to the installation of the axial methyl group at C4. Initial approaches pursued dissolving metal-mediated reductive alkylations of a cyclohexenone, but were not successful. Undeterred, Johnson turned to an Ireland–Claisen rearrangement[120] to forge the C3–C4 bond. Following this approach, α-methylation of the hydrazone followed by fragmentation of the hydrazone under Shapiro conditions[121] and trapping of the intermediate vinyllithium with paraformaldehyde delivered ester **1.308** after esterification of the newly formed alcohol with isobutyric acid. Treatment with strong base induced the desired rearrangement and installed the axial methyl group at C4 with good diastereocontrol; elaboration of the resulting acid to ketone **1.309** was achieved in two additional steps.

The construction of the final six-membered ring contained in the terpenoid core was pursued via an aldol condensation. As such, diastereoselective hydroboration and oxidation delivered an intermediate aldehyde that was converted to cyclohexenone **1.310**. Hydrogenation of the enone and condensation of *O*-benzyl hydroxylamine set the stage for desymmetrization of the gem-dimethyl groups via Pd(II)-catalyzed C–H activation.[122] Following this approach, exposure to catalytic $Pd(OAc)_2$ and stoichiometric bis(acetoxy)iodo benzene afforded acetate **1.312** with excellent diastereocontrol. A series of functional group manipulations delivered

dicarbonyl **1.313**, which enabled the assembly of allylic alcohol **1.314** after double addition of vinyl organocerium(III)[123] and ring-closing metathesis.

Completion of the terpenoid core hinged on the formation of the *trans*-ring junction contained in the hexahydroindane fragment. Elimination of the tertiary allylic alcohol produced a β,γ-enone (not shown) that underwent hydrogenation with the undesired facial selectivity.[124] To circumvent this issue, directed hydrogenation was pursued. As such, after elimination of the tertiary alcohol the resulting ketone was diastereoseletively reduced to afford alcohol **1.315**. Indeed, directed hydrogenation with Crabtree's catalyst produced the desired *trans*-ring junction. Oxidation of the alcohol to ketone **1.316** set the stage for a Gasman indole assembly (*vide supra*), which completed the synthesis of (–)-paspaline (**1.3**).

1.2.14 Amos B. Smith III's Total Synthesis of (+)-Nodulisporic Acid F

Scheme 1.26. Preparation of Common Subtarget for the Nodulisporic Acids.

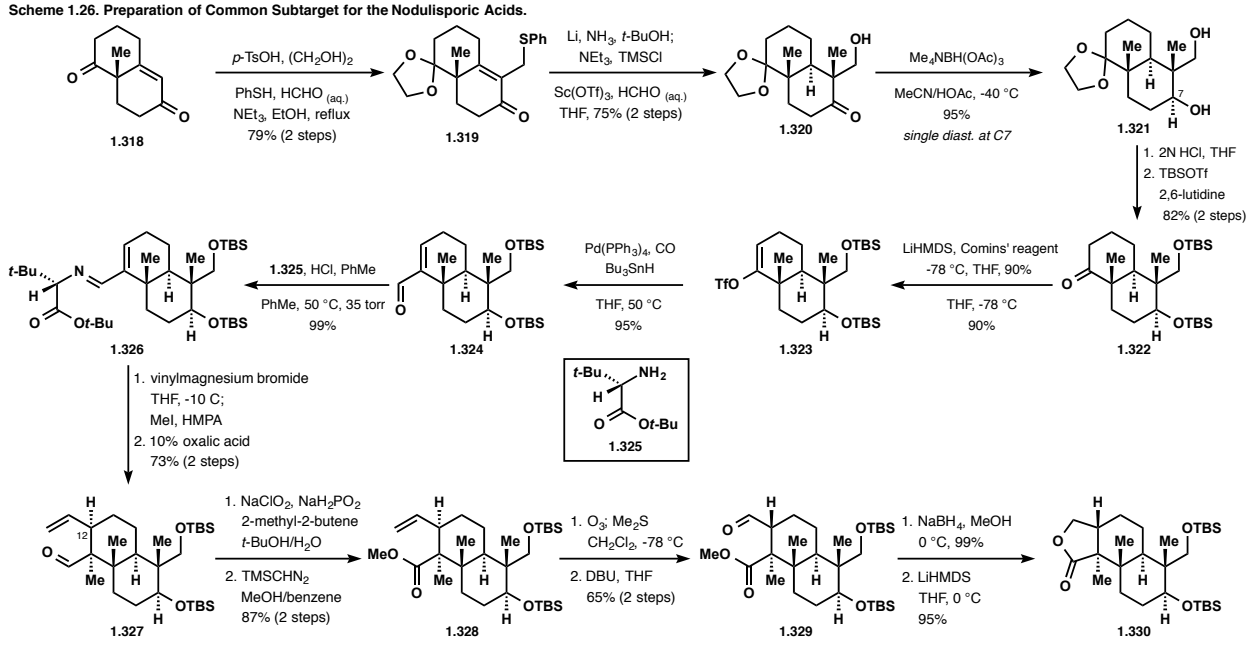

(–)-Nodulisporic acid A (**1.32**) was isolated in 1997[10a] and presented an attractive target for chemists because of its chemical structure and interesting bioactivity. To develop a platform to access more complex congeners of this subclass of the PIDs, Smith and co-workers pursued

the synthesis of the simplest congener, (+)-nodulisporic acid F (**1.46**).[125] As such, Smith identified lactone **1.330** as a common subtarget en route to the nodulisporic acids (Scheme 1.26). Unlike Smith's synthesis of penitrem D (*vide supra*) the strategy toward the *trans*-5-6 ring junction and *trans*-oriented methyl groups contained in the terpenoid core focused on a vicinal difunctionalization of an α,β-unsturated imine using a tactic developed by Koga and co-workers.[126]

Efforts toward this end began from (+)-Wieland Miescher ketone **1.318**. In a sequence of events reminiscent of Smith's previous efforts toward various other PIDs (*vide supra*), **1.318** was elaborated to cyclohexanone **1.322**. Vinyl triflate formation and palladium-catalyzed carbonylative formylation[127] delivered enal **1.323** that was desired for the proposed vicinal difunctionalization. Condensation of auxiliary **1.325**[128] with aldehyde **1.324** followed by addition of vinylmagnesium bromide and trapping of the intermediate enolate with iodomethane afforded aldehyde **1.327** after hydrolysis of the auxiliary.

Unfortunately, the undesired stereochemistry was obtained at C12. Nonetheless, Smith proposed that an epimerization event could rectify the outcome. Pinnick oxidation[129] of the aldehyde, methylation of the resulting carboxylic acid, ozonolysis of the alkene, and treatment with base delivered ester **1.329** with the correct stereochemistry at C12. Chemoselective reduction of the proposed aldehyde followed by treatment with strong base formed lactone **1.330** and completed the assembly of the common precursor en route to the nodulisporic acids.

Drawing from their experience constructing indole ring systems from lactones Smith and co-workers extended the modified Madelung indole synthesis that was successful in their campaigns toward penitrem D (**1.47**) and 21-isopentenylpaxilline (**1.112**; *vide supra*). Prior to formation of the indole, an efficient synthetic sequence was developed that converted protected

diol **1.330** to alkene **1.332** (Scheme 1.27). Formation of the indole proceeded smoothly using a similar protocol to the one developed Smith's synthesis of 21-isopentenyl paxilline **1.112**. Subsequent elaboration of the alkene was achieved using a hydroboration/Suzuki[130] reaction sequence to install the unsaturated acid-containing side-chain found in the nodulisporic acids. Saponification of the ester and removal of the silyl protecting group completed the synthesis and delivered (+)-nodulisporic acid F (**1.46**).

Scheme 1.27. Completion of Nodulisporic Acid F.

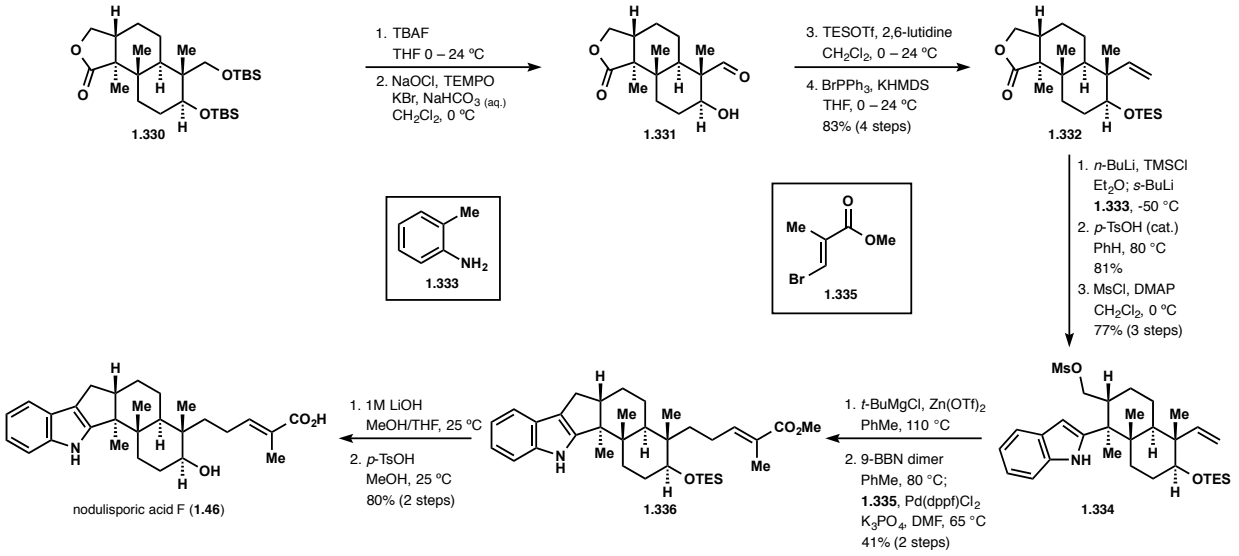

1.2.15 Amos B. Smith III's Synthesis of (–)-Nodulisporic Acid D

As Smith's synthetic campaign to the PIDs progressed, it became clear that the modified Madelung indole synthesis was a useful and viable way to construct the indole moiety contained in simple and complex congeners of the family.[131] However, when it came to complex nodulisporic acids the modified Madelung indole synthesis was inefficient (Scheme 1.28a).[132] While triple deprotonation of **1.337** and treatment with lactone **1.330** delivered ketone **1.338** subsequent elaboration to indole **1.339** required a lengthy and low-yielding synthetic sequence .[133] The driving force behind the poor conversion of **1.338** to **1.339** was the lability of the alcohol

at C24, which forced the development of a circuitous synthetic sequence. Tolerance of an alcohol functionality at C24 would be paramount to a successful convergent approach to nodulisporic

Scheme 1.28. Evolution of the Strategy Toward Formation of the Indole.

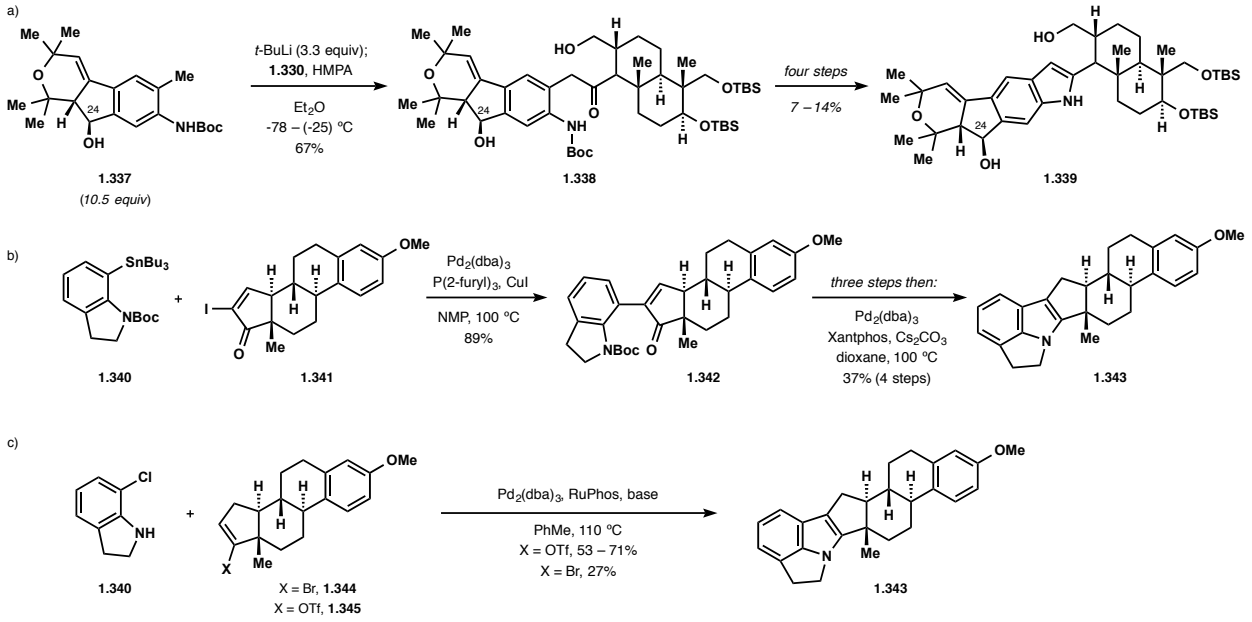

acid A (**1.32**), the most complex congener of the subclass, so Smith and co-workers changed their strategy related to indole assembly.

As such, initial studies were focused on a sequence involving a Stille cross-coupling[90,94b,134] and Buchwald–Hartwig amination[135] (Scheme 1.28b). While this strategy was successful, as evidenced by its ability to efficiently build strained indole **1.343**, Smith ultimately turned to an indole synthesis developed by Barluenga and co-workers[136] that converted a vinyl halide **1.344** or pseudohalide **1.341** directly to indole **1.343** (Scheme 1.28c). Notably, the relatively mild conditions for the one-pot indole formation should tolerate acid sensitive functional groups, which could permit access to scaffolds resembling nodulisporic acid A **1.32**.

As a platform to develop the indole synthesis in a complex setting Smith pursued the total synthesis of (–)-nodulisporic acid D **1.39**.[137] Following this approach the synthesis of the western hemisphere began with the reduction of carboxylic acid **1.346** and conversion of the resulting

benzylic alcohol to benzyl iodide **1.347** (Scheme 1.29).[138] Diastereoselective Enders alkylation[139] of known hydrazone **1.348**[132a] and subsequent removal of the auxiliary produced ketone **1.349** with the appropriate stereochemistry at C23. Regioselective vinyl triflate formation followed by reduction[140] of the nitro group delivered aniline **1.350**, which was converted to western hemisphere subtarget **1.351** via regioselective iodination[141] and Stille–Kelly[142] intramolecular coupling.

Scheme 1.29. Preparation of α-Chloro Aniline 1.351.

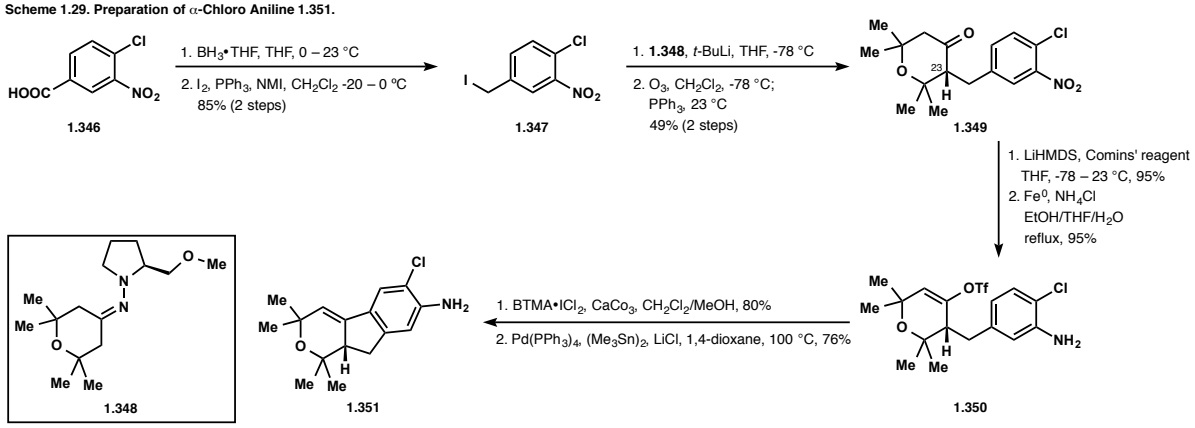

Efforts toward eastern hemisphere subtarget **1.356** began from aldehyde **1.324**, which was prepared en route to lactone **1.330** and (+)-nodulisporic acid F (**1.46**; *vide supra*) (Scheme 1.30). Direct installation of the vicinal quaternary stereocenters was achieved using a vicinal difunctionalization sequence. Following this approach, a copper-catalyzed conjugate addition of vinylmagnesium and *in situ* silylation of the resulting enolate delivered an intermediate TMS-enoxysilane (not shown). Subsequent treatment with methyllithium generated a lithium enolate that underwent *C*-methylation with iodomethane. During optimization efforts it was determined that alternative lower-order cuprate reagents (i.e. Gilman[143] or Normant[144]) were inferior for the diastereoselective installation of the vinyl group at C12 and the use of diglyme as a solvent was essential for regioselectivity and diastereoselectivity during the methylation event.

Scheme 1.30. Preparation of the Eastern Hemisphere Subtarget.

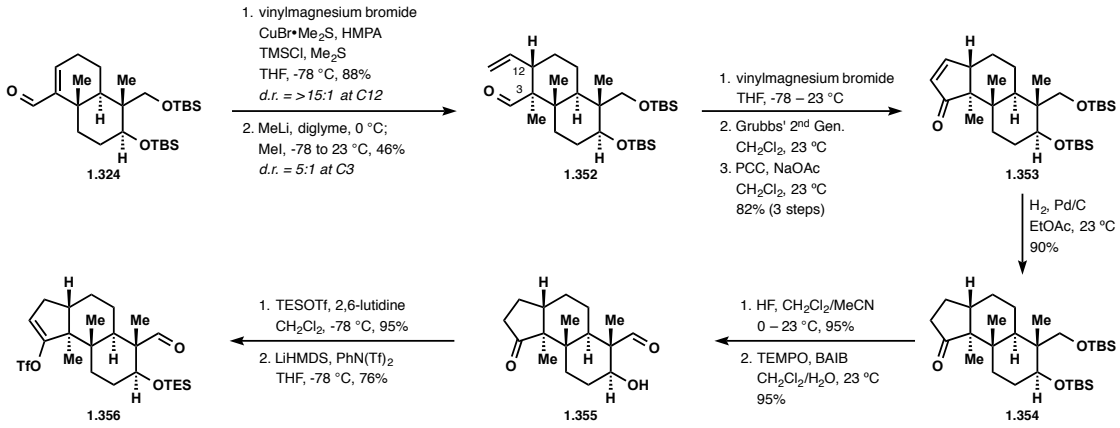

Execution of the vicinal difunctionalization installed the final stereocenters found in the terpenoid core. In order to complete the assembly of eastern hemisphere subtarget **1.358** construction of the final ring was pursued. Thus, elaboration of γ,δ-unsaturated aldehyde **1.352** to enone **1.353** was achieved following addition of vinylmagnesium bromide, ring-closing metathesis, and oxidation. A series of functional group manipulations completed the preparation of subtarget **1.356** in five steps from enone **1.353**.

Access to each coupling partner provided the opportunity to investigate the unifying indole synthesis (Scheme 1.31). Gratifyingly, the use of Buchwald's third generation RuPhos-based precatalyst, cesium carbonate, and mild heating in the presence of the two hemispheres, with only a slight excess of **1.351**, delivered the desired indole **1.357**. While the exact sequence of events was unclear, an intermediate imine (not shown) resulting from Buchwald–Hartwig amination and tautomerization was isolated, which led the authors to propose that the first bond-forming event resulted in C–N bond formation. The assembly of the indole nucleus left only the dienoic acid-containing side-chain to be installed. This was achieved after exchanging the protecting group on the secondary alcohol and Horner–Wadsworth–Emmons olefination[145] with phosphonate **1.359**. Saponification of the ester completed the synthesis (–)-nodulisporic acid D (**1.39**).

Scheme 1.31. Completion of Nodulisporic Acid D.

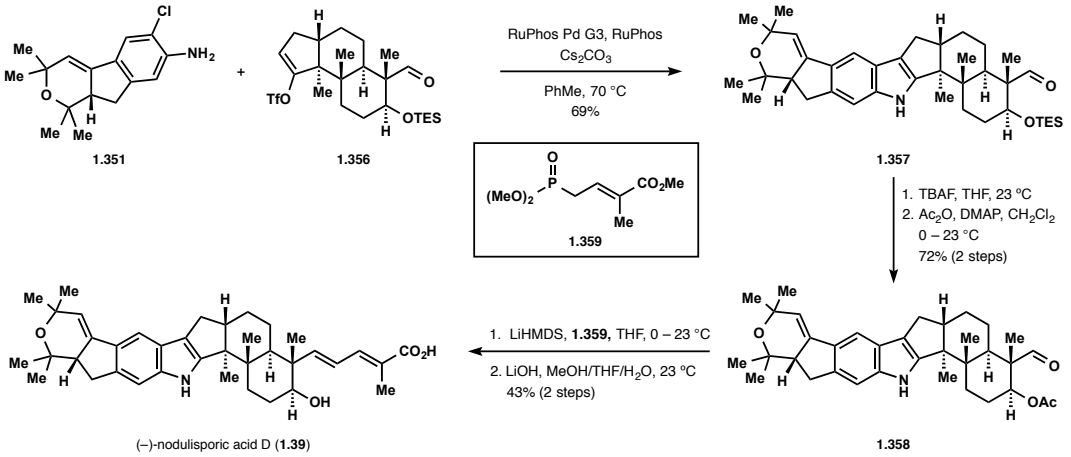

The application of the Barluenga indole synthesis in a complex setting was a major step forward for Smith's program focused on the PIDs. The ability to use almost equimolar amounts of each coupling partner demonstrated the superiority of the new strategy and the relatively mild conditions should lend themselves to the synthesis more complex and sensitive nodulisporic acids.

1.2.16 Hidetoshi Tokuyama's Approach to the Western Hemisphere of Penitrem E

In 2015, Tokuyama and co-workers published a brief, but interesting, assembly of the western hemisphere of penitrem E (**1.48**).[146] The strategy centered on a palladium-catalyzed Catellani reaction[147] and a Tf_2NH-catalyzed [2+2]-cycloaddition[148] to construct the unique ring-system appended to the indole nucleus (Scheme 1.32). Following this approach, alkyl iodide **1.362** was prepared in seven steps from *meso*-1,3-diol **1.359** via lipase-mediated desymmetrization and a series of straightforward functional group manipulations. The proposed Catellani reaction coupling alkyl iodide **1.362** with aryl iodide **1.364** proceeded smoothly and delivered tricycle **1.365**. Dihydroxylation and Lemieux–Johnson oxidative cleavage[149] of the resulting diol produced an intermediate ketone that was subsequently converted to enoxy silane **1.366**. When enoxy silane **1.366** was exposed to Tf_2NH and methacrolein a [2+2]-cycloaddition

ensued, which delivered cyclobutane **1.367** with poor diastereoselectivity for the desired isomer of the cyclobutane.[150] The ability to perform the [2+2]-cycloaddition with an enoxy silane granted access to the tertiary alcohol at C15, which is found in the most complex congeners of the penitrem subclass of PIDs.

Scheme 1.32. Tokuyama's Approach to the Western Hemisphere of Penitrem E.

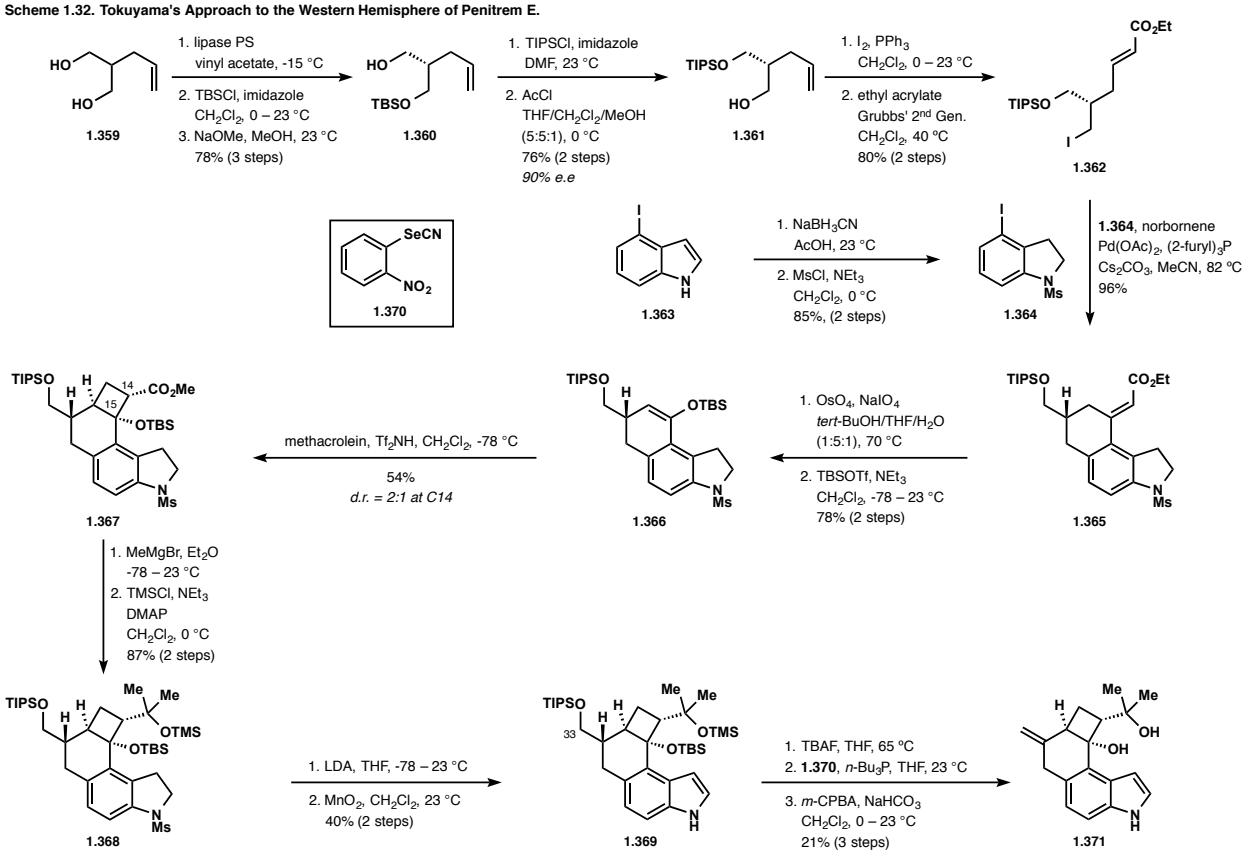

With the carbon framework assembled elaboration to protected triol **1.369** was achieved using simple functional group manipulations. Completion of the target western hemisphere surrogate **1.371** was accomplished following global deprotection and formation of the exocyclic alkene via Grieco–Nishizawa elimination.[75, 151] While the total synthesis of a natural product was not achieved, the approach was unique, creative, and provided access to a relevant polycyclic scaffold.

1.3 References and Notes

[1] (a) Wilson, B. J.; Wilson, C. H. *Science* **1964**, *144*, 177. (b) Gallagher, R. T.; Clardy, J.; Wilson, B. J. *Tetrahedron Lett.* **1980**, *21*, 239.
[2] von Fehr, T.; Acklin, W. *Helv. Chim Acta.* **1966**, *49*, 1907.
[3] Wilson, B. J.; Wilson, C. H.; Hayes, A. W. *Nature* **1968**, *220*, 78.
[4] Hou, C. T.; Ciegler, A.; Hesseltine, C. W. *Can. J. Microbiol.* **1971**, *17*, 599.
[5] Cole, R. J.; Kirksey, J. W.; Wells, J. M. *Can. J. Microbiol.* **1971**, *20*, 1159.
[6] Springer, J. P.; Clardy, J.; Wells, J. M.; Cole, R. J.; Kirksey, J. W *Tetrahedron Lett.* **1975**, *16*, 2531.
[7] It should be noted at this time that while paxilline was not the first isolated congener of the family, it was the first congener to succumb to unambiguous structural assignment. Thus, our lab uses paxilline as the namesake for the family.
[8] (a) Gallagher, R. T.; Latch, G. C. M.; Keogh, R. G. *Appl. Environ. Microbiol.* **1980**, *39*, 272. (b) Lauren, D. R.; Gallagher, R. T. *J. Chromatogr.* **1982**, *248*, 150. (c) de Jesus, A. E.; Steyn, P. S.; van Heerden, F. R.; Vleggaar, R. *J. Chem. Soc. Perkin Trans. 1* **1984**, 697. (d) Wilkins, A. L.; Miles, C. O.; Ede, R. M.; Gallahher, R. T.; Munday, S. C. *J. Agric. Food Chem.* **1992**, *40*, 1307. (e) Penn, J.; Swift, R.; Wigley, L. J.; Mantle, P. G.; Bilton, J. N.; Sheppard, R. N. *Phytochemistry* **1993**, *32*, 1431. (f) Kawahara, T.; Nagai, A.; Takagi, M.; Shin-ya, K. *J. Antibiot.* **2012**, *65*, 535.
[9] (a) Gallagher, R. T.; White, E. P.; Mortimer, P. H. *N. Z. Vet. J.* **1981**, *29*, 189. (b) Gallagher, R. T.; Campbell, A. G.; Hawkes, A. D.; Holland, P. T.; McGaveston, D. A.; Pansier, E. A.; Harvey, I. C. *N. Z. Vet. J.* **1982**, *30*, 183. (c) Gallagher, R. T.; Hawkes, A. D.; Steyn, P. S.; Vleggaar, R. *J. Chem. Soc., Chem. Commun.* **1984**, 614. (d) Miles, C. O.; Munday, S. C.; Wilkins, A. L.; Ede, R. M.; Towers, N. R. *J. Agric. Food Chem.* **1994**, *42*, 1488. (e) Munday-Finch, S. C.; Miles, C. O.; Wilkins, A. L.; Hawkes, A. D. *J. Agric. Food Chem.* **1995**, *43*, 1283. (f) Munday-Finch, S. C.; Wilkins, A. L.; Miles, C. O.; Ede, R. M.; Thomson, R. A. *J. Agric. Food Chem.* **1996**, *44*, 2782. (g) Munday-Finch, S. C.; Wilkins, A. L.; Miles, C. O.; Tomoda, H.; Ōmura, S. *J. Agric. Food Chem.* **1997**, *45*, 199. (h) Munday-Finch, S. C.; Wilkins, A. L.; Miles, C. O. *J. Agric. Food Chem.* **1998**, *46*, 590.
[10] (a) Ondeyka, J. G.; Helms, G. L.; Hensens, O. D.; Goetz, M. A.; Zink, D. L.; Tsipouras, A.; Shoop, W. L.; Slayton, L.; Dombrowski, A. W.; Polishook, J. D.; Ostlind, D. A.; Tsou, N. N.; Ball, R. G.; Singh, S. B. *J. Am. Chem. Soc.* **1997**, *119*, 8809. (b) Hensens, O. D.; Ondeyka, J. G.; Dombrowski, A. W.; Ostlind, D. A.; Zink, D. L. *Tetrahedron Lett.* **1999**, *40*, 5455. (c) Ondeyka, J. G.; Dahl-Roshak, A. M.; Tkacz, J. S.; Zink, D. L.; Zakson-Aiken, M.; Shoop, W. L.; Goetz, M. A.; Singh, S. B. *Bioorg. Med. Chem. Lett.* **2002**, *12*, 2941. (d) Ondeyka, J. G.; Byrne, K.; Vesey, D.; Zink, D. L.; Shoop, W. L.; Goetz, M. A.; Singh, S. B. *J. Nat. Prod.* **2003**, *66*, 121. (e) Singh, S. B.; Ondeyka, J. G.; Jayasuriya, H.; Zink, D. L.; Ha, S. N.; Dahl-Roshak, A.; Greene, J.; Kim, J. A.; Smith, M. M.; Shoop, W.; Tkacz, J. S. *J. Nat. Prod.* **2004**, *67*, 1496.
[11] (a) de Jesus, A. E.; Steyn, P. S.; van Heerden, F. R.; Vleggaar, R.; Wessels, P. L.; Hull, W. E. *J. Chem. Soc., Chem. Commun.* **1981**, 289. (b) de Jesus, A. E.; Steyn, P. S.; van Heerden, F. R.; Vleggaar, R.; Wessels, P. L. *J. Chem. Soc. Perkin Trans. I* **1983**, 1847. (c) de Jesus, A. E.; Steyn, P. S.; van Heerden, F. R.; Vleggaar, R.; Wessels, P. L. *J. Chem. Soc. Perkin Trans. 1* **1983**, 1857. (d) Penn, J.; Biddle, J. R.; Mantle, P. G.; Bilton, J. N.; Sheppard, R. N. *J. Chem. Soc. Perkin Trans 1* **1992**, 23. (e) Laakso, J. A.; Gloer, J. B.; Wicklow, D. T.; Dowd, P. F. *J. Org. Chem.* **1992**, *57*, 2066. (f) Laasko, J. A.; Gloer, J. B.; Wicklow, D. T.; Dowd, P. F. *J. Agric. Food Chem.* **1993**, *41*, 973. (g) Hayashi, H. H.; Asabu, Y.; Murao, S.; Nakayama, M.; Arai, M. *Chem. Express* **1993**, *8*, 233. (h) Naik, J. T.; Mantle, P. G.; Sheppard, R. N.; Waight, E. S. *J. Chem. Soc.*

Perkin Trans 1 **1995**, 1121. (j) González, M. C.; Lull, C.; Moya, P.; Ayala, I.; Primo, J.; Yúfera, E. P. *J. Agric. Food Chem.* **2003**, *51*, 2156. (k) Su, S.-S.; Song, A.-H.; Chen, G.; Wang, H.-F.; Li, Z.-Q.; Pei, Y.-H. *J. Asian Nat. Prod. Res.* **2014**, *16*, 285. (l) Zhang, P.; Li, X.-M.; Wang, B.-G. *Pytochemistry Lett.* **2015**, *12*, 182. (m) Gao, S.-S.; Li, X.-M.; Williams, K.; Proksch, P.; Ji, N.-Y.; Wang, B.-G. *J. Nat. Prod.* **2016**, *79*, 2066. For precursors to the penitrems see: (n) Yamaguchi, T.; Nozawa, K. Hosoe, T.; Nakajima, S.; Kawai, K.-I. *Phytochemistry* **1993**, *32*, 1177. (o) Rundberget, T.; Wilkins, A. L. *Phytochemistry* **2002**, *61*, 979. (p) Moldes-Anaya, A.; Rundberget, T.; Uhlig, S.; Rise, F.; Wilkins, A. L. *Toxicon* **2011**, *57*, 259.

[12] (a) Belofsky, G. N.; Gloer, J. B.; Wicklow, D. T.; Dowd, P. F. *Tetrahedron* **1995**, *51*, 3959. (b) Xu, M.; Gessner, G.; Groth, I.; Lange, C.; Christner, A.; Bruchn, T.; Deng, Z.; Li, X.; Heinemann, S. H.; Grabley, S.; Bringmann, G.; Sattler, I.; Lin, W. *Tetrahedron* **2007**, *63*, 435.

[13] (a) Huang, X.-H.; Tomoda, H.; Nishida, H.; Masuma, R.; Ōmura, S. *J. Antibiot.* **1995**, *48*, 1. (b) Huang, X.-H.; Nishida, H.; Tomoda, H.; Tabata, N.; Shiomi, K.; Yang, D.-J.; Takayanagi, H.; Ōmura, S. *J. Antibiot.* **1995**, *48*, 5. (c) Tomoda, H.; Tabata, N.; Yang, D.-J.; Takayanagi, H.; Ōmura, S. *J. Antibiot.* **1995**, *48*, 793. (d) Gatenby, W. A.; Munday-Finch, S. C.; Wilkins, A. L.; Miles, C. O. *J. Agric. Food Chem.* **1999**, *47*, 1092.

[14] (a) Cole, R. J.; Dorner, J. W; Lansden, J. A.; Cox, R. H.; Pape, C.; Cunfer, B.; Nicholson, S. S.; Bedell, D. M. *J. Agric. Food Chem.* **1977**, *25*, 1197. (b) Springer, J. P.; Clardy, J. *Tetrahedron Lett.* **1980**, *21*, 231. (c) Gallagher, R. T.; Finer, J.; Clardy, J.; Leutwiler, A.; Weibel, F.; Acklin, W.; Arigoni, D. *Tetrahedron Lett.* **1980**, *21*, 235. (d) Dorner, J. W.; Role, R. J.; Cox, R. H.; Cunfer, B. M. *J. Agric. Food Chem.* **1984**, *32*, 1069. (e) Nozwa, K.; Nakajima, S.; K. K-i. *J. Chem. Soc. Perkin Trans. 1* **1988**, 2607. (f) Hosoe, T.; Nozawa, K.; Udagawa, S.-i.; Nakajima, S.; Kawai, K.-i. *Chem. Pharm. Bull.* **1990**, *38*, 3473. (g) Munday-Finch, S. C.; Wilkins, A. L.; Miles, C. O. *Tetrahedron* **1996**, *41*, 327. (h) Li, C.; Gloer, J. B.; Wicklow, D. T.; Dowd, P. F. *Org. Lett.* **2002**, *4*, 3095. (i) Uchida, R.; Kim, Y.-P.; Namatame, I.; Tomoda, H.; Ōmura, S. *J. Antibiot.* **2006**, *59*, 93. (j) Ogata, M.; Ueda, J.-y.; Hoshi, M.; Hashimoto, J.; Nakashima, T.; Anazi, K.; Takagi, M.; Shin-ya, K. *J. Antibiot.* **2007**, *60*, 645. (k) Itabashi, T.; Hosoe, T.; Wakana, D.; Fukushima, K.; Takizawa, K.; Yaguchi, T.; Okada, K.; Takaki, G. M. d. C.; Kawai, K.-i. *J. Nat. Med.* **2009**, *63*, 96. (l) Fan, Y.; Wang, Y.; Liu, P.; Fu, P.; Zhu, T.; Wang, W.; Zhu, W. *J. Nat. Prod.* **2013**, *76*, 1328. (m) Matsui, C.; Ikeda, Y.; Iinuma, H.; Kushida, N.; Kunisada, T.; Simizu, S.; Umezawa, K. *J. Antiobiot.* **2014**, *67*, 787. (n) Zhang, Y.-H.; Huang, S.-D.; Pan, H.-Q.; Bian, X.-Q.; Wang, Z.-Y.; Han, A.-H.; Bai, J. *Magn. Reson. Chem.* **2014**, *52*, 306. (o) Tarui, Y.; Chinen, T.; Nagumo, Y.; Motoyama, T.; Hayashi, T.; Hirota, H.; Muroi, M.; Ishii, Y.; Kondo, H.; Osada, H.; Usui, T. *CHemBioChem* **2014**, *15*, 934.

[15] Acklin, W.; Weibel, F.; Arigoni, D. *Chimia* **1977**, *31*, 63.

[16] It should be noted that at the time of publication of the initial labeling studies emindole SB had yet to be isolated.

[17] (a) de Jesus, A. E.; Gorst-Allman, C. P.; Steyn, P. S.; van Heerden, F. R.; Vleggaar, R.; Wessels, P. L. *J. Chem. Soc. Perkin Trans. 1* **1983**, 1863. (b) Laws, I.; Mantle, P. G. *J. Gen. Microbiol.* **1989**, *135*, 2679. (c) Mantle, P. G.; Weedon, C. M. *Phytochemistry* **1994**, *36*, 1209. (d) Munday-Finch, S. C.; Wilkins, A. L.; Miles, C. O. *Phytochemistry* **1996**, *41*, 327. (e) Gatenby, W. A.; Munday-Finch, S. C.; Wilkins, A. L.; Miles, C. O. *J. Agric. Food Chem.* **1999**, *47*, 1092. (f) Bryne, K. M.; Smith, S. K.; Ondeyka, J. G. *J. Am. Chem. Soc.* **2002**, *124*, 7055.

[18] Young, C.; McMillan, L.; Telfer, E.; Scott, B. *Mol. Microbiol.* **2001**, *39*, 754.

[19] (a) Young, C. A.; Bryant, M. K.; Christensen, M. J.; Tapper, B. A.; Bryan, G. T.; Scott, B. *Mol. Gen. Genomics* **2005**, *274*, 13. (b) Young, C. A.; Felitti, S.; Shields, K.; Spangenberg, G.; Johnson, R. D.; Bryan, G. T.; Saikia, S.; Scott, B. *Fun. Gen. Biol.* **2006**, *43*, 679.
[20] Saikia, S.; Parker, E. J.; Koulman, A.; Scott, B. *FEBS Lett.* **2006**, *580*, 1625.
[21] Nicholson, M. J.; Koulman, A.; Monahan, B. J.; Pritchard, B. L.; Payne, G. A.; Scott, B. *Appl. Environ. Microbiol.* **2009**, *75*, 7469.
[22] Motoyama, T.; Hayashi, T.; Hirota, H.; Ueki, M.; Osada, H. *Chem. Biol.* **2012**, *19*, 1611.
[23] Saikia, S.; Parker, E. J.; Koulman, A.; Scott, B. *J. Biol. Chem.* **2007**, *282*, 16829.
[24] Tagami, K.; Liu, C.; Minami, A.; Noike, M.; Isaka, T.; Fueki, S.; Shichijo, Y.; Toshima, H.; Gomi, K.; Dairi, T.; Oikawa, H. *J. Am. Chem. Soc.* **2013**, *135*, 1260.
[25] Liu, C.; Tagami, K.; Minami, A.; Matsumoto, T.; Frisvad, J. C.; Suzuki, H.; Ishikawa, J.; Gomi, K.; Oikawa, H.
[26] Van de Bittner, K. C.; Nicholson, M. J.; Bustamante, L. Y.; Kessans, S. A.; Ram, A.; van Dolleweerd, C. J.; Scott, B.; Parker, E. J. *J. Am. Chem. Soc.* **2018**, *140*, 582.
[27] Uhlig, S.; Botha, C. J.; Vrålstad, Rolén, E.; Miles, C. O. *J. Agric. Food Chem.* **2009**, *57*, 11112.
[28] Knaus, H.-G.; McManus, O. B.; Lee, S. H.; Schmalhofer, W. A.; Garcia-Calvo, M.; Helms, L. M. H.; Sanchez, M.; Giangiacomo, K.; Reuben, J. P.; Smith, A. B. III; Kaczorowski, G. J.; Garcia, M. L. *Biochemistry* **1994**, *33*, 5819.
[29] Imlach, W. L.; Finch, S. C.; Dunlop, J.; Meredith, A. L.; Aldrich, R. W.; Dalziel, J. E. *J. Pharmacol. Exp. Ther.* **2008**, *327*, 657.
[30] Nakazawa, J.; Yajima, J.; Usui, T.; Ueki, M.; Takatsuki, A.; Imoto, M.; Toyoshima, Y. Y.; Osada, H. *Chem. Biol.* **2003**, *10*, 131.
[31] (a)Dowd, P. F.; Cole, R. J.; Vesonder, R. F. *J. Antibiot.* **1988**, *41*, 1868. (b) Prestidge, R. A.; Gallagher, R. T. *Ecol. Entomol.* **1988**, *13*, 429.
[32] Kane, N. S.; Hirschberg, B.; Qian, S.; Hunt, D.; Bande, T.; Brochu, R.; Ludmerer, S. W.; Zheng, Y.; Smith, M.; Arena, J. P.; Cohen, C. J.; Schmatz, D.; Warmke, J.; Cully, D. F. *Proc. Natl. Acad. Sci.* **2000**, *97*, 13949. Ludmerer, S. W.; Warren, V. A.; Williams, B. S.; Zheng, Y.; Hunt, D. C.; Ayer, M. B.; Wallace, M. A.; Chaudhary, A. G.; Egan, M. A.; Meinke, P. T.; Dean, D. C.; Garcia, M. L.; Cully, D. F.; Smith, M. M. *Biochemistry* **2002**, *41*, 6548.
[33] (a) Zhang, H.-G.; ffrench-Constant, R. H. Jackson, M. B. *J. Physiol.* **1994**, *479*, 65. (b) Zhang, H.-G.; Lee, H.-J. Rocheleau, T.; ffrench-Constant, R. H.; Jackson, M. B. *Mol. Pharmacol.* **1995**, *48*, 835. (c) Aydar, E.; Beadle, D. J. *J. Insect Physiol.* **1999**, *45*, 213.
[34] Meinke, P. T.; Smith, M. M.; Shoop, W. L. *Top. Curr. Med. Chem.* **2002**, *2*, 655.
[35] Ōmura, S. *Int. J. Antimicrob. Agents* **2008**, *31*, 91 and references therein.
[36] (a) Smith, A. B. III; Mewshaw, R. E. *J. Am. Chem. Soc.* **1985**, *107*, 1769. (b) Mewshaw, R. E.; Taylor, M. D.; Smith, A. B. III *J. Org. Chem.* **1989**, *54*, 3449.
[37] (a) Wieland, P.; Miescher, K. *Helv. Chim. Acta* **1950**, *33*, 2215. (b) Hiroi, K.; Yamada, S. *Chem. Pharm. Bull.* **1975**, *23*, 1103.
[38] Smith, A. B. III; Mewshaw, R. E. *J. Org. Chem.* **1984**, *49*, 3685.
[39] (a) Islam, A. M.; Raphael, R. A. *J. Chem. Soc.* **1953**, 2247. (b) MacAlpine, G. A.; Raphael, R. A.; Shaw, A.; Taylor, A. W.; Wild, H.-W. *J. Chem. Soc. Perkin Trans. 1* **1976**, 410.
[40] (a) Fischer, E.; Jourdan, F. *Ber.* **1883**, *16*, 2241. (b) Fischer, E.; Hess, O. *Ber.* **1884**, *17*, 559. for a review see: (c) Robinson, B. *Chem. Rev.* **1969**, *69*, 227 and references therein.
[41] Gassman, P. G.; van Bergen, T.; J.; Gilbert, D. P.; Cue, B. W., Jr. *J. Am. Chem. Soc.* **1974**, *96*, 5496.

[42] (a) Smith, A. B. III; Leenay, T. L. *Tetrahedron Lett.* **1988**, *29*, 2791. (b) Smith, A. B. III; Leenay, T. L. *J. Am. Chem. Soc.* **1989**, *111*, 5761.
[43] Nagata, W.; Yoshioka, M. *Tetrahedron Lett.* **1966**, *7*, 1913.
[44] (a) Luche, J.-L.; Petrier, C.; Lansard, J.-P.; Greene, A. E. *J. Org. Chem.* **1983**, *48*, 3837. (b) Greene, A. E.; Lansard, J.-P.; Luche, J.-L.; Petrier, C. *J. Org. Chem.* **1984**, *49*, 931.
[45] Kirk, D. N.; Petrow, V. *J. Chem. Soc.* **1962**, 1091.
[46] (a) Smith, A. B. III; Sunazuka, T.; Leenay, T. L.; Kingery-Wood, J. *J. Am. Chem. Soc.* **1990**, *112*, 8197. (b) Smith, A. B. III; Kingery-Wood, J.; Leenay, T. L.; Nolen, E. G.; Sunazuka, T. *J. Am. Chem. Soc.* **1992**, *114*, 1438.
[47] Stork, G.; Benaim, J. *J. Am. Chem. Soc.* **1971**, *93*, 5938.
[48] Prepared as in Smith's second-generation approach to (–)-paspaline **1.3**.
[49] Stork, G.; Ponaras, A. A. *J. Org. Chem.* **1976**, *41*, 2937.
[50] (a) Pfitzner, K. E.; Moffat, J. G. *J. Am. Chem. Soc.* **1965**, *87*, 5661. (b) Pfitzner, K. E.; Moffatt, J. G. *J. Am. Chem. Soc.* **1965**, *87*, 5670.
[51] (a) Grieco, P. A.; Nichizawa, M.; Marinovic, N.; Ehmann, W. J. *J. Am. Chem. Soc.* **1976**, *98*, 7102. (b) Clive, D. L.; Joussef, A. C. *J. Org. Chem.* **1990**, *55*, 1096.
[52] Furlenmeier, A.; Fürst, A.; Langemann, A.; Waldvogel, G.; Kerb, U.; Hocks, P.; Wiechert, R. *Helv. Chim. Acta.* **1966**, *49*, 1591.
[53] (a) Ali, A.; Saxton, J. E. *Tetrahedron Lett.* **1989**, *30*, 3197. (b) Ali, A.; Guile, S. D.; Saxton, J. E.; Thornton-Pett, M. *Tetrahedron* **1991**, *47*, 6407. (c) Guile, S. D.; Saxton, J. E.; Thornton-Pett, M. *J. Chem. Soc. Perkin Trans. 1* **1992**, 1763.
[54] Corey, E. J.; Virgil, S. C. *J. Am. Chem. Soc.* **1990**, *112*, 6429.
[55] (a) Simmons, H. E.; Smith, R. D. *J. Am. Chem. Soc.* **1958**, *80*, 5323. (b) Simmons, H. E.; Smith, R. D. *J. Am. Chem. Soc.* **1959**, *81*, 4256. (c) Dauben, W. G.; Berzein, G. H. *J. Am. Chem. Soc.* **1963**, *85*, 468.
[56] (a) Mancuso, A. J.; Huang, S.-L.; Swern, D. *J. Org. Chem.* **1978**, *43*, 2480. (b) Omura, K.; Swern, D. *Tetrahedron* **1978**, *34*, 1651 and references therein.
[57] (a) Dauben, W. G.; Deviny, E. J. *J. Org. Chem.* **1966**, *31*, 3794. (b) Stork, G.; Uyeo, S.; Wakamatsu, T.; Grieco, P.; Lebovitz, J. *J. Am. Chem. Soc.* **1971**, *93*, 4945.
[58] (a) Wender, P. A.; White, A. W. *Tetrahedron Lett.* **1981**, *22*, 1475. (b) Wender, P. A.; White, A. W. *Tetrahedron* **1983**, *39*, 3767.
[59] (a) Haseltine, J.; Visnick, M.; Smith, A. B., III *J. Org. Chem.* **1988**, *53*, 6160. (b) (b) Smith, A. B., III; Haseltine, J. N.; Visnick, M.; *Tetrahedron* **1989**, *45*, 2431. (c) Smith, A. B. III; Ohta, M.; Clark, W. M.; Leahy, J. W. *Tetrahedron Lett.* **1993**, *34*, 3033. (d) Smith, A. B., III; Nolen, E. G. Jr.; Shirai, R.; Blase, F. R.; Ohta, M.; Chida, N.; Hartz, R. A.; Fitch, D. M.; Clark, W. M.; Sprengeler, P A. *J. Org. Chem.* **1995**, *60*, 7837 (e) Smith, A. B. III; Kanoh, N.; Noriaki, M.; Rainier, J. D.; Blase, F. R.; Hartz, R. A. *Org. Lett.* **1999**, *1*, 1263 (f) Smith, A. B. III; Hartz, R. A.; Spoors, P. G.; Ranier, J. D. *Isr. J. Chem.* **1997**, *37*, 69. (g) Smith, A. B., III; Kanoh, N.; Ishiyama, H.; Hartz, R. A. *J. Am. Chem. Soc.* **2000**, *122*, 11254. (h) Smith, A. B., III; Kanoh, N.; Ishiyama, H.; Minakawa, N.; Rainier, J. D.; Hartz, R. A.; Cho, Y. S.; Cui, H.; Moser, W. H. *J. Am. Chem. Soc.* **2003**, *125*, 8228.
[60] (a) Madelung, W. *Ber.* **1912**, *45*, 1128. (b) Corriu, R. J. P.; Moreau, J. J. Some Uses of Silicon–Nitrogen Bonds in Organic Synthesis. In *Selectivity – a Goal for Synthetic Efficiency*, 1st, Bartmann, W.; Trost, B. M. Eds.; Verlag Chemie: Deerfield Beach, Fl., 1983; 14, pp 21–41. (c) Smith, A. B. III; Visnick, M. *Tetrahedron Lett.* **1985**, *26*, 3757. (d) Smith, A. B.; Visnick, M.; Haseltine, J. N.; Sprengeler, P. A. *Tetrahedron* **1986**, *42*, 2957.

[61] Corey, E. J.; Schmidt, G. *Tetrahedron Lett.* **1979**, *20*, 399.
[62] Comins, D. L.; Dehghani, A. *Tetrahedron Lett.* **1992**, *33*, 6299.
[63] The lactone moiety found on **1.186** precluded Enders' alkylation and was reduced and protected in order to achieve the desired mode of reactivity.
[64] Jackson, D. Y. *Synth. Commun.* **1988**, *18*, 337.
[65] Nicolaou, K. C.; Hwang, C.-K.; Nugiel, D. A. *J. Am. Chem. Soc.* **1989**, *111*, 4136.
[66] Schenck, G. O.; Eggert, H.; Denk, W. *Liebigs. Ann. Chem.* **1953**, *584*, 177.
[67] Nickon, A.; Schwartz, N.; DiGiorgio, J. B.; Widdowson, D. A. *J. Org. Chem.* **1965**, *30*, 1711.
[68] (a) Dess, D. B.; Martin, J. C. *J. Org. Chem.* **1983**, *48*, 4155. (b) Dess, D. B.; Martin, J. C. *J. Am. Chem. Soc.* **1991**, *113*, 7277.
[69] Nickon, A.; Mendelson, W. L. *J. Org. Chem.* **1965**, *30*, 2087.
[70] It is not explicitly clear how Smith and co-workers prepared enone **1.204**. While *ent*-**1.204** is prepared in 59f, there is no report of the preparation of **1.204**.
[71] (a) Shunk, R. B.; Wilds, A. L. *J. Am. Chem. Soc.* **1949**, *71*, 3946. (b) Woodward, R. B.; Sondheimer, F.; Taub, D.; Heusler, K.; McLamore, W. M. *J. Am. Chem. Soc.* **1952**, *74*, 4223.
[72] (a) Semmler, W. *Chem. Ber.* **1892**, *25*, 3352. (b) Wolff, L. *Annalen* **1902**, *322*, 351.
[73] Parikh, J. R.; Doering, W. E. *J. Am. Chem. Soc.* **1967**, *89*, 5505.
[74] Hemiaminal **2.212** was produced as an inconsequential mixture of diastereomers.
[75] Grieco, P. A.; Gilman, S.; Nishizawa, M. *J. Org. Chem.* **1976**, *41*, 1485.
[76] (a) Smith, A. B. III; Cui, H. *Org. Lett.* **2003**, *5*, 587. (b) Smith, A. B. III; Cui, H. *Helv. Chim. Acta.* **2003**, *86*, 3908.
[77] Prepared in eight steps from 1,2:5,6-di-*O*-isopropylidene-D-mannitol.
[78] While trivial at first glance, the use of *tert*-butylmagnesium chloride was essential to the formation of the desired product. Strategies centered on lithium-based organometallics initially formed the desired annulated indole, but oxidative cleavage of the C2–C18 bond was quantitatively observed and could not be avoided.
[79] Barton, D. H. R.; Kitchin, J. P.; Lester, D. J.; Motherwell, W. B.; Papoula, M. T. B. *Tetrahedron* **1981**, *37*, 73.
[80] Magnus, P.; Mansley, T. E. *Tetrahedron* **1999**, *6909*.
[81] (a) Oppolzer, W.; Snieckas, V. *Angew. Chem. Int. Ed.* **1978**, *17*, 476. (b) Andersen, N. H.; Hadley, S. W.; Kelly, J. D.; Bacon, E. R. *J. Org. Chem.* **1985**, *50*, 4144.
[82] Cabani, S.; Ceccanti, N. *J. Chem. Soc. (B)* **1977**, 77.
[83] (a) Chugaev, L. A. *Ber.* **1899**, *32*, 332. (b) Benkeser, R. A.; Hazdra, J. J. *J. Am. Chem. Soc.* **1959**, *81*, 228.
[84] (a) Hemetberger, H.; Knittel, D.; Weidmann, H. *Monatsh. Chem.* **1969**, *100*, 1599. (b) Moody, C. J. *J. Chem. Soc. Perkin Trans. 1* **1984**, 1333.
[85] (a) Rieche, A.; Gross, H.; Höft, E. *Chem. Ber.* **1960**, *93*, 88. (b) Rieche, A.; Gross, H.; Matthey, G. *Chem. Ber.* **1963**, *96*, 308.
[86] England, D. B.; Magolan, J.; Kerr, M. A. *Org. Lett.* **2006**, *8*, 2209.
[87] (a) Plieninger, H.; Suhr, K.; Werst, G.; Kiefer, B. *Chem. Ber.* **1956**, *89*, 270. (b) Plieninger, H.; Voekl, A. *Chem. Ber.* **1976**, *109*, 2121.
[88] (a) Banfield, S. C.; England, D. B.; Kerr, M. A. *Org. Lett.* **2001**, *3*, 3325. (b) Sqada, P. V.; Banfield, S. C.; Kerr, M. A. *Synlett* **2003**, 971. (c) England, D. B.; Kerr, M. A. *J. Org. Chem.* **2005**, *70*, 6519.
[89] Milstein, D.; Stille, J. K. *J. Am. Chem. Soc.* **1978**, *100*, 3636.
[90] Nicolaou, K. C.; Lysenko, Z. *Tetrahedron Lett.* **1977**, *18*, 1257.

[91] **1.250** was prepared in almost a nearly identical sequence as **1.174**; see reference 53c.
[92] Enomoto, M. Morita, A.; Kuwahara, S. *Angew. Chem. Int. Ed.* **2012**, *51*, 12833.
[93] (a) Salituro, F. G.; McDonald I. A. *J. Org. Chem.* **1988**, *53*, 6138. (b) Han, X.; Stoltz, B. M.; Corey, E. J. *J. Am. Chem. Soc.* **1999**, *121*, 7600.
[94] (a) Hegedus, L. S.; Allen, G. F.; Waterman, E. L. *J. Am. Chem. Soc.* **1976**, *98*, 2674. (b) Hegedus, L. S.; Allen, G. F.; Bozell, J. J.; Waterman, E. L. *J. Am. Chem. Soc.* **1978**, *100*, 5800.
[95] Tsuji, J.; Minami, I.; Shimizu, I. *Tetrahedron Lett.* **1983**, *24*, 1793.
[96] Scholl, M.; Ding, S.; Lee, C. W.; Grubbs, R. H. *Org. Lett.* **1999**, *1*, 953.
[97] Wang, Z.-M.; Sharpless, K. B. *Tetrahedron Lett.* **1993**, *34*, 8225.
[98] (a) Sharpless, K. B.; Lauer, R. F. *J. Am. Chem. Soc.* **1973**, *95*, 2697. (b) Reich, H. J. *J. Org. Chem.* **1975**, *40*, 2570. (c) Clive, D> L. J.; Chittattu, G.; Curtis, N. J.; Menchen, S. M. *J. Chem. Soc. Chem. Commun.* **1978**, 770.
[99] Santelli-Rouvier, C.; Santelli, M. *Synthesis* **1983**, 429 and references therein.
[100] Few diastereoselectivities were reported throughout the synthesis.
[101] (a) Larock, R. C.; Hightower, T. R.; Kraus, G. A.; Hahn, P.; Zheng, D. *Tetrahedron Lett.* **1995**, *36*, 2423. (b) Ito, Y.; Hirao, T.; Saegusa, T. *J. Org. Chem.* **1978**, *43*, 1011. (c) Nicolaou, K. C.; Gray, D. L. F.; Montagnon, T.; Harrison, S. T. *Angew. Chem. Int. Ed.* **2002**, *41*, 996.
[102] Matsuo, J.-i.; Aizawa, Y. *Tetrahedron Lett.* **2005**, *46*, 407.
[103] Miyashita, M.; Suzuki, T.; Hoshino, M.; Yoshikoshi, K. *Tetrahedron* **1997**, *53*, 12469.
[104] Oikawa, Y.; Yonemitsu, O. *J. Org. Chem.* **1977**, *42*, 1213.
[105] (a) Atkins, G. M. Jr.; Burgess, E. M. *J. Am. Chem. Soc.* **1968**, *90*, 4744. (b) Burgess, E. M.; Penton, H. R. Jr.; Taylor, E. A. *J. Org. Chem.* **1973**, *38*, 26.
[106] Oikawa, M.; Hashimoto, R.; Sasaki, M. *Eur. J. Org. Chem.* **2011**, 538.
[107] (a) Chehade, K. A. H.; Andres, D. A.; Morimoto, H.; Spielmann, H. P. *J. Org. Chem.* **2000**, *65*, 3027. (b) Suhara, Y.; Murakami, A.; Kamao, M.; Mimatsu, S.; Nakagawa, K.; Tsugawa, N.; Okano, T. *Bioorg. Med. Chem. Lett.* **2007**, *17*, 1622.
[108] Katsuki, T.; Sharpless, K. B. *J. Am. Chem. Soc.* **1980**, *102*, 5974.
[109] (a) Nugent, W. A.; RajanBabu, T. V. *J. Am. Chem. Soc.* **1988**, *110*, 8561. (b) RajanBabu, T. V.; Nugent, W. A. *J. Am. Chem. Soc.* **1994**, *116*, 986.
[110] Rai, A. N.; Basu, A. *Tetrahedron Lett.* **2003**, *44*, 2267.
[111] Frigerio, M.; Santagostino, M. *Tetrahedron Lett.* **1994**, *35*, 8019.
[112] Prior to acetylation, the diastereomeric alcohols were separated via flash chromatography.
[113] (a) Tu, Y.; Wang, Z.-X.; Shi, Y. *J. Am. Chem. Soc.* **1996**, *118*, 9806. (b) Wang, Z.-X.; Tu, Y.; Frohn, M.; Zhang, J.-R.; Shi, Y. *J. Am. Chem. Soc.* **1997**, *119*, 11224.
[114] (a) Teranishi, T.; Kuwahara, S. *Tetrahedron Lett.* **2014**, *55*, 1486. (b) Teranishi, T.; Murokawa, T.; Enomoto, M.; Kuwahara, S. *Biosci. Biotechnol. Biochem.* **2015**, *79*, 11.
[115] Prepared from an intermediate [previously reported by Snapper and co-workers (Murelli, R. P.; Cheung, A. K.; Snapper, M. L. *J. Org. Chem.* **2007**, *72*, 1545.)] using a sequence similar to Oikawa's report, see Ref. 114a.
[116] (a) Sharpe, R. J.; Johnson, J. S. *J. Org. Chem.* **2015**, *80*, 9740. (b) Sharpe, R. J.; Johnson, R. J. *J. Am. Chem. Soc.* **2015**, *137*, 4968.
[117] (a) Demir, A. S.; Enders, D. *Adv. Synth. Catal.* **1997**, *339*, 553. (b) Sharpe, R. J.; Portillo, M.; Vélez, R. A.; Johnson, J. S. *Synlett* **2015**, 2293.
[118] Watanabe, H.; Iwamoto, M.; Nakada, M. *J. Org. Chem.* **2005**, *70*, 4652.

[119] (a) Katoh, T.; Mizumoto, S.; Fudesaka, M.; Nakashima, Y.; Kajimoto, T.; Node, M. *Synlett* **2006**, 2176. (b) Katoh, T.; Mizumoto, S.; Fudesaka, M.; Takeo, M.; Kajimoto, T.; Node, M. *Tetrahedron: Asymmetry* **2006**, *17*, 1655.
[120] (a) Ireland, R. E.; Mueller, R. H. *J. Am. Chem. Soc.* **1972**, *94*, 5897. (b) Ireland, R. E.; Mueller, R. H.; Willard, A. K. *J. Am. Chem. Soc.* **1976**, *98*, 2868.
[121] (a) Shapiro, R. H.; Heath, M. J. *J. Am. Chem. Soc.* **1967**, *89*, 5734. (b) Kaufman, G.; Cook, F.; Shechter, H.; Bayless, J.; Friedman, L. *J. Am. Chem. Soc.* **1967**, *89*, 5736.
[122] For stoichiometric examples see: (a) Constable, A. G.; McDondald, W. S.; Sawkins, L. C.; Shaw, B. L. *J. Chem. Soc. Chem. Commun.* **1978**, 1061. (b) Constable, A. G.; McDondald, W. S.; Sawkins, L. C.; Shaw, B. L. *J. Chem. Soc. Dalton Trans.* **1980**, 1992. (c) Baldwin, J. E.; Jones, R. H.; Najera, C.; Yus, M. *Tetrahedron* **1985**, *41*, 699. (d) Carr, K.; Saxton, H. M.; Sutherland, J. K. *J. Chem. Soc. Perkin Trans. 1* **1988**, 1599. For an application in a synthetic arena see: Zhu, C.; Tang, P.; Yu, B. *J. Am. Chem. Soc.* **2008**, *130*, 5872. For catalytic variants see: (e) Desai, L. V.; Hull, K. L.; Sanford, M. S. *J. Am. Chem. Soc.* **2004**, *126*, 9542. (f) Neufeldt, S. R.; Sanford, M. S. *Org. Lett.* **2010**, *12*, 532. For an application in a synthetic arena see: (g) Siler, D. A.; Mighion, J. D.; Sorensen, E. J. *Angew. Chem. Int. Ed.* **2014**, *53*, 5332.
[123] Krasovskiy, A.; Kopp, F.; Knochel, P. *Angew. Chem. Int. Ed.* **2006**, *45*, 497.
[124] a) Sondheimer, F.; Burstein, S.; Mechoulam. *J. Am. Chem. Soc.* **1960**, *82*, 3209. (b) Abad, A.; Agullo, C.; Arno, M.; Domingo, L. R.; Zaragoza, R. J. *J. Org. Chem.* **1990**, *55*, 2369.
[125] (a) Smith, A. B. III; Cho, Y. S.; Ishiyama, H. *Org. Lett.* **2001**, *3*, 3971. (b) Smith, A. B. III; Kürti, L.; Davulcu, A. H.; Cho, Y. S. *Org. Proc. Res. Dev.* **2007**, *11*, 19. (c) Smith, A. B. III; Davulcu, A. H.; Cho, Y. S.; Ohmoto, K.; Kürti, L.; Ishiyama, H. *J. Org. Chem.* **2007**, *72*, 4596. (d) Smith, A. B. III; Davulcu, A. H.; Kürti, L. *Org. Lett.* **2006**, *8*, 1665.
[126] Kogen, H.; Tomioka, K.; Hashimoto, S.-I.; Koga, K. *Tetrahedron* **1981**, *37*, 3951.
[127] Cacchi, S.; Morera, E.; Ortar, G. *Tetrahedron Lett.* **1985**, *26*, 1109.
[128] Anderson, G. W.; Callahan, F. M. *J. Am. Chem. Soc.* **1960**, *82*, 3359.
[129] a) Lindgren, B. O.; Nilsson, T. *Acta. Chem. Scand.* **1973**, *27*, 888. (b) Kraus, G. A.; Taschner, M. J. *J. Org. Chem.* **1980**, *45*, 1175. (c) Kraus, G. A.; Roth, B. *J. Org. Chem.* **1980**, *45*, 4825. (d) Bal, B. S.; Childers, W. E. Jr.; Pinnick, H. W. *Tetrahedron* **1981**, *37*, 2091.
[130] (a) Miraura, N.; Ishiyama, T.; Ishikawa, M.; Suzuki, A. *Tetrahedron Lett.* **1986**, *27*, 6369. (b) Miyaura, N.; Ishiyama, T.; Sasaki, H.; Ishikawa, M.; Satoh, M.; Suzuki, A. *J. Am. Chem. Soc.* **1989**, *111*, 314.
[131] (a) Smith, A. B. III; Davulcu, A. H.; Kürti, L. *Org. Lett.* **2006**, *8*, 1669. (b) Smith, A. B. III; Davulcu, A. H.; Cho, Y. S.; Ohmoto, K.; Kürti, L.; Ishiyama, H. *J. Org. Chem.* **2007**, *72*, 4596.
[132] (a) Smith, A. B. III; Ishiyama, H.; Cho, Y. S.; Ohmoto, K. *Org. Lett.* **2001**, *3*, 3967. (b) Smith, A. B. III; Kürti, L.; Davulcu, A. H.; Cho, Y. S.; Ohmoto, K. *J. Org. Chem.* **2007**, *72*, 4611.
[133] Smith, A. B. III; Kürti, L.; Davulcu, A. H. *Org. Lett.* **2006**, *8*, 2167.
[134] (a) Liebeskind, L. S.; Fengl, R. W. *J. Org. Chem.* **1990**, *55*, 5359. (b) Farina, V.; Krishnan, B. *J. Am. Chem. Soc.* **1991**, *113*, 9585. (c) Farina, V.; Kapadia, S.; Krishnan, B.; Wang, C.; Liebeskind, L. S. *J. Org. Chem.* **1994**, *59*, 5905. (d) Lebsack, A. D.; Link, J. T.; Overman, L. E.; Stearns, B. A. *J. Am. Chem. Soc.* **2002**, *124*, 9008. (e) Overman, L. E.; Peterson, E. A. *Tetrahedron* **2003**, *59*, 6905.
[135] (a) Kosugi, M.; Kameyama, M.; Migita, T. *Chem. Lett.* **1983**, *12*, 927. (b) Guram, A. S.; Buchwald, S. L. *J. Am. Chem. Soc.* **1993**, *116*, 7901. (c) Paul, F.; Patt, J.; Hartwig, J. F. *J. Am. Chem. Soc.* **1994**, *116*, 5969. (d) Guram, A. S.; Rennels, R. A.; Buchwald, S. L. *Angew. Chem.*

Int. Ed. **1995**, *34*, 1348. (e) Louie, J.; Hartwig, J. F. *Tetrahedron Lett.* **1995**, *36*, 3609. (f) Wolfe, J. P.; Wagaw, S.; Buchwald, S. L. *J. Am. Chem. Soc.* **1996**, *118*, 7215.
[136] (a) Barluenga, J.; Fernández, A.; Aznar, F.; Valdés, C. *Chem. Eur. J.* **2005**, *11*, 2276. (b) Barluenga, J.; Valdés, C. *Chem. Commun.* **2005**, 4891.
[137] Zou, Y.; Melvin, J. E.; Gonzales, S. S.; Spafford, M. J.; Smith, A. B. III *J. Am. Chem. Soc.* **2015**, *137*, 7095.
[138] Garegg, P. J.; Samuelsson, B. *J. Chem. Soc. Chem. Commun.* **1977**, 978.
[139] (a) Enders, D.; Eichenauer, H. *Angew. Chem. Int. Ed.* **1976**, *15*, 549. (b) Enders, D.; Eichenauer, H. *Tetrahedron Lett.* **1977**, *18*, 191. (c) Enders, D.; Zamponi, A.; Raabe, G.; Runsink, J. *Synthesis* **1993**, 725. (d) Job, A.; Janeck, C. F.; Bettray, W.; Peters, R.; Enders, D. *Tetrahedron* **2002**, *58*, 2253.
[140] Ramadas, K.; Srinivasan, N. *Synth. Commun.* **1992**, *22*, 3189.
[141] Kajigaeshi, S.; Kakinami, T.; Yamasaki, H.; Fujisake, S.; Kondo, M.; Okamoto, T. *Chem. Lett.* **1987**, *16*, 2109.
[142] Ross, T. R.; Li, Q.; Bhusan, V. *Tetrahedron Lett.* **1990**, *31*, 161.
[143] Gilman, H.; Jones, R. G.; Woods, L. A. *J. Org. Chem.* **1952**, *17*, 1630.
[144] Normant, J. F.; Bourgain, M. *Tetrahedron Lett.* **1971**, *12*, 2583.
[145] (a) Horner, L.; Hoffmann, H.; Wippel, H. G. *Chem. Ber.* **1958**, *91*, 61. (b) Wadsworth, W. S. Jr.; Emmons, W. D. *J. Am. Chem. Soc.* **1961**, *83*, 1733.
[146] Yoshii, Y.; Otsu, T.; Hosokawa, N.; Takasu, K.; Okano, K.; Tokuyama, H. *Chem. Commun.* **2015**, *51*, 1070.
[147] Catellani, M.; Fagnola, M. C. *Angew. Chem. Int. Ed.* **1994**, *33*, 2421.
[148] Inanaga, K.; Takasu, K.; Ihara, M. *J. Am. Chem. Soc.* **2005**, *127*, 3668.
[149] Rappo, R.; Allen, D. S. Jr.; Lemieux, R. U.; Johnson, W. S. *J. Org. Chem.* **1956**, *21*, 478.
[150] A boat-like transition state was proposed to be the origin of the diastereoselectivity.
[151] Sharpless, K. B.; Young, M. W. *J. Org. Chem.* **1975**, *40*, 947.

Chapter 2: A Concise Approach to the Paxilline Indole Diterpenes

2.1 Retrosynthetic Analysis: Structure-goal and Transform-based Strategy

2.1.1 Introduction and General Synthetic Considerations

In 2014, our lab initiated synthetic studies related to the paxilline indole diterpenes (PIDs). We hoped to develop a general approach that would be concise in nature and amenable to the synthesis of a variety of simple and complex PIDs. While we devised a unique synthetic strategy we would be remiss to not acknowledge some of the general synthetic considerations that guided our approach.

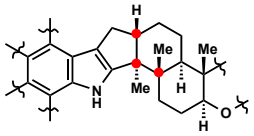

Figure 2.1. Common Pentacyclic Core.

There are two major considerations that should be taken into account when planning a synthesis of any PID. The first is related to the construction of the terpenoid core. The body of synthetic literature associated with the PIDs indicates that the selective installation of key functional groups contained within the terpenoid core is a significant challenge. Specifically, the assembly of a stereotriad containing the *trans*-fused hydrindane and the vicinal quaternary stereocenters bearing axial methyl groups (highlighted in red, Figure 2.1) is not straightforward. In regards to the formation of the key stereotriad, two general strategies have received considerable attention: vicinal difunctionalization of a polycyclic framework possessing an α,β-unsaturated carbonyl[1] and the use of a directing group to functionalize an alkene.[2] The former strategy, while seemingly attractive, does not deliver highly diastereoselective processes likely due to stereoelectronic considerations (Scheme 2.1a). The latter approach is effective in terms of diastereocontrol, but is rather circuitous, ultimately detracting from its appeal.

Scheme 2.1. Common Synthetic Strategies to the Key Stereotriad and Sensitive Nature of the Indole Nucleus.

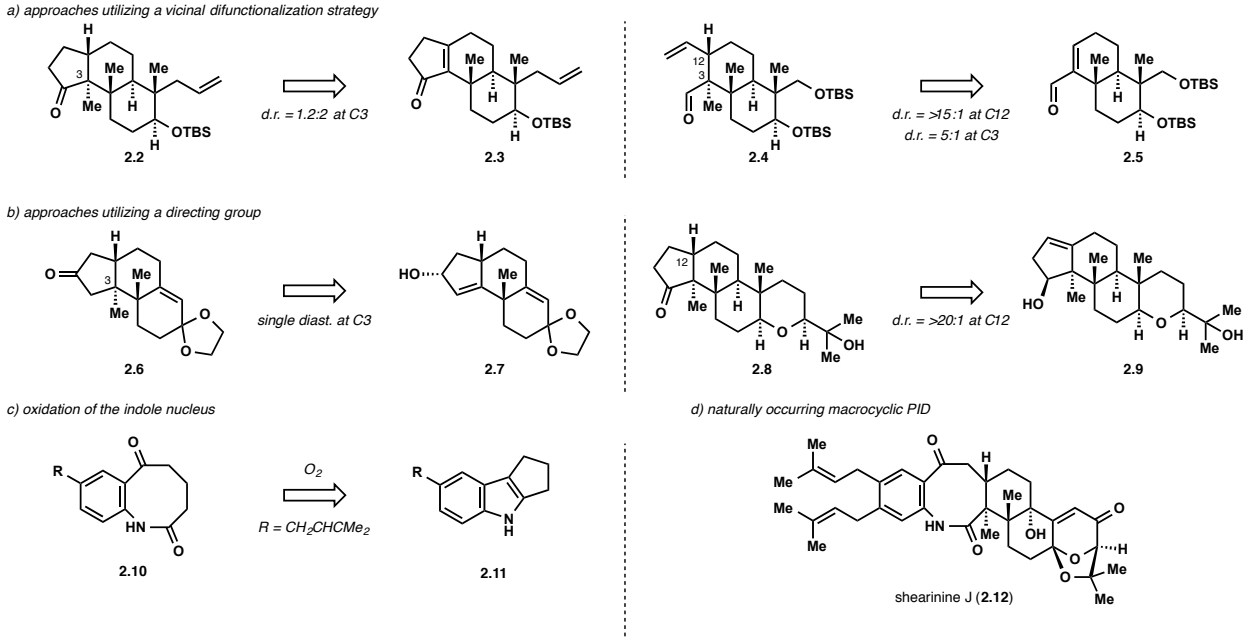

The second major consideration is the stability of the indole nucleus, which is prone to oxidation, potentially forming dicarbonyl analogs (Scheme 2.1c).[3] This property can be observed naturally as there are congeners of the family that contain a macrocyclic dicarbonyl which likely arises from prolonged exposure to atmospheric oxygen (Scheme 2.1d).[4] This property influences the types of reactions that can be proposed and pursued once the indole is installed. Taken together, the construction of the pentacyclic core is a synthetic challenge that requires careful synthetic planning. In addition, once the core is formed its somewhat sensitive nature limits the scope of reactions that are available for the further functionalization of advanced intermediates.

With these general considerations in mind, we devised a retrosynthesis that identified a tricarbocyclic subtarget and two key transforms for the assembly of the core of the PIDs. We believed that, if successful, the blend of structure-goal and transform-based strategies would render a concise and unique construction of the pentacyclic core, develop new chemistry, and offer the opportunity to prepare many congeners the family in a straightforward manner.[5]

2.1.2 Structure-goal: Tricarbocyclic Hexahydroindane 2.13

The PIDs possess a wide array of molecular complexities, but share a common pentacyclic core (Figure 2.1). As such, we identified tricarbocycle **2.13** as an intermediate that could serve as a molecular platform for the synthesis of the PIDs since it possessed each stereocenter found in the shared core and limited, but key, non-hydrocarbon functionalities (Scheme 2.2). We believed that the inclusion of each stereocenter found in the terpenoid core was essential, as it would allow for **2.13** to serve as a common precursor for many congeners of the family. In addition, we thought that key functionalities like a cyclopentanone and aldol motif would be amenable to subsequent synthetic modifications and provide useful handles for the assembly of **2.13**.[6]

Scheme 2.2. Identification of a Key Tricarbocyclic Subtarget.

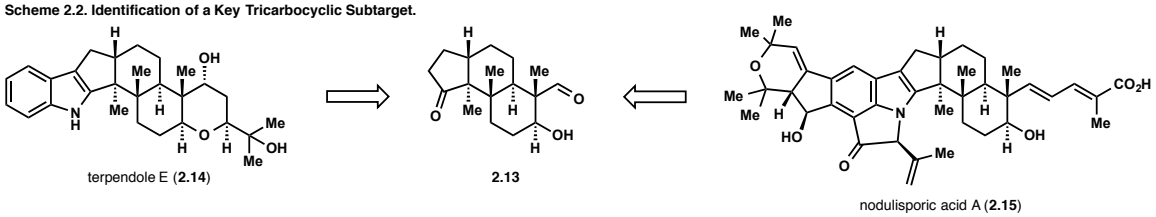

More specifically, the cyclopentanone moiety in **2.13** could serve as a handle for the construction of the indole nucleus with many transforms utilizing a ketone or ketone-derived precursor. In the context of complex congeners of the family [i.e. nodulisporic acid A (**2.15**)], the use of a precursor like **2.13** during indole formation would unite two fragments of similar complexity. The inherent reactivity of the aldol motif in **2.13** (electrophilic at the aldehyde and nucleophilic at the alcohol) could be leveraged as a bifunctional handle thus providing flexibility during subsequent elaboration to more complex terpenoid scaffolds [i.e. terpendole E (**2.14**)]. Taken together, we believe **2.13** has a set of functional groups that make it a versatile intermediate en route to various PIDs.

2.1.3 Radical-polar Crossover Polycyclization Cascade

In order to assemble tricarbocyclic subtarget **2.13** in a direct manner, we pursued a topological strategy involving a radical-polar crossover polycyclization transform by deconstructing an embedded cocyclic pair of bonds (C12–C7 and C4–C13, Scheme 2.3). More specifically, we envisioned that the application of aldol and conjugate addition transforms would indicate **2.17** as a hypothetical synthon for **2.13**. The successful execution of this approach was expected to deliver the all *trans*-decalin ring system and forge four of the six stereocenters in **2.13**.

Scheme 2.3. Radical-polar Crossover Polycyclization.

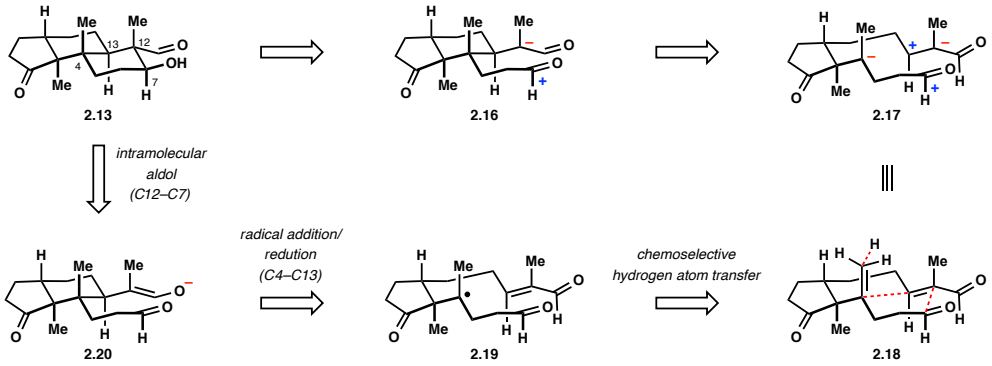

In a polar reaction manifold, generating a synthetic synthon possessing a reactivity profile similar to **2.17** would be challenging due to functional group compatibility. As such, we proposed accessing relevant intermediates via a radical-polar crossover reaction manifold from diene **2.18**. We believed that traversing a reaction coordinate in this way would deliver a chemoselective process.

Inspiration for this transformation came from recent work from the Baran lab wherein the authors developed a reductive alkene coupling between electron-rich and electron-deficient alkenes.[7] Their work suggested that tertiary radical **2.19** could be generated following a chemoselective hydrogen atom transfer (HAT) to the electron-rich alkene found on diene **2.18**. Subsequent radical conjugate addition would forge the C4–C13 bond. The resulting stabilized

tertiary radical (intermediate not shown) could undergo single-electron reduction and crossover from a neutral radical species to enolate **2.20**. Finally, intramolecular aldol addition with the pendent aldehyde would deliver the tricarbocyclic subtarget **2.13**. Aldol reactions were known in similar systems that utilize cobalt catalysis to reductively couple an electron-deficient alkene with an aldehyde,[8] which provided an intellectual foundation for the final step of the cascade. While the proposed polycyclization was likely to proceed through six-membered transition states, the desired stereochemical outcome would rely on a pseudo-axial orientation of each methyl group, which could present a challenge due to developing steric interactions (i.e. *syn*-pentane) in the transition state. In spite of this, we believed that the proposed transform would break apart a highly complex subtarget to a relatively simple precursor thus providing merit for its pursuit.

2.1.4 Intermolecular α-Alkenylation

Scheme 2.4. Retrosynthesis of the Polycyclization Precursor.

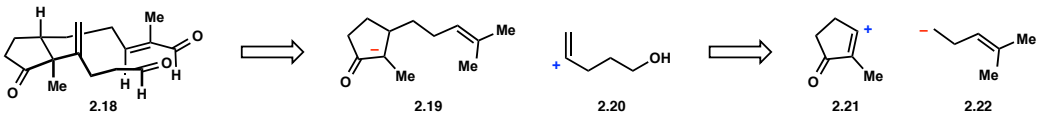

The polycyclization transform was proposed to initiate from a 1,1-disubstituted alkene that was linked to a cyclopentanone through a quaternary stereocenter. We envisioned that the most direct way to deconstruct the β,γ-unsaturation from the molecule would be via an α-alkenylation transform on an unsymmetric ketone using hypothetical synthons **2.19** and **2.20** (Scheme 2.4). Analysis of the literature did not reveal a direct precedent for the simultaneous installation of the quaternary stereocenter and 1,1-disubstituted alkene functionalities. However, we believed hypothetical retron **2.19** could be deconstructed via a conjugate addition transform. In addition, utilization of a formal vicinal difunctionalization strategy beginning with 2-methyl-cyclopenten-1-one (**2.21**) would diastereoselectively deliver relevant intermediates en route to

polycyclization precursor **2.18**. While there was a lack of a general method to directly access **2.18**, we viewed this as an opportunity to develop a new method that could find immediate utility in target-oriented synthesis.

2.2 Synthesis of Tricarbocyclic Hexahydroindane 2.13

2.2.1 Development of an Intermolecular α-Alkenylation

Our synthetic studies related to the PIDs began with the development of the proposed α-alkenylation. Since the formation of quaternary carbons is difficult due to the congested nature of the associated fully substituted atom, achieving the desired reactivity in a regioselective manner would be a challenge (phase 1, Scheme 2.5). In addition, if regioselectivity can be achieved a new issue of chemoselectivity arises since the desired product contains an enolizable position that can react with the alkene surrogate (phase 2, Scheme 2.5). Taken together, the developed method must be selective for the formation of quaternary stereocenters.

Scheme 2.5. Major Challenges Associated with the α-Alkenylation.

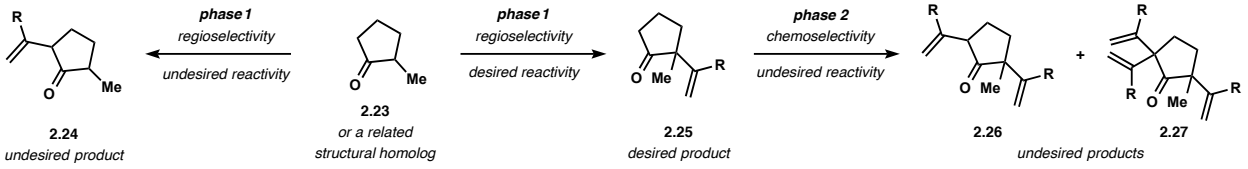

Prior to our studies there was little precedent for the regioselective intermolecular α-alkenylation of a ketone bearing two enolizable positions with limited examples of formation of quaternary stereocenters.[9] Initially, we pursued a palladium-catalyzed coupling between a metal enolate and a vinyl halide (Scheme 2.6). Unfortunately, we were unable to obtain the desired product and typically observed the formation of complex mixtures of products that resembled the formation of products similar to **2.26** and **2.27**.

Scheme 2.6. Palladium-catalyzed α-Alkenylation of Various Metal Enolates.

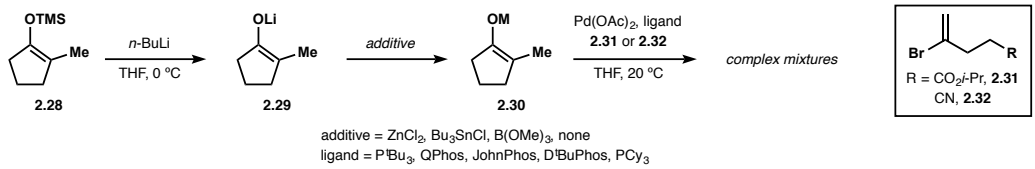

Concurrent to these efforts we pursued the activation of terminal alkynes using π-acids. We were inspired by work from Baba and co-workers who achieved α-alkenylation of silyl ketene acetals with phenyl acetylene using indium(III) bromide as a π-acid. This process delivered β,γ-unsaturated esters and achieved assembly of quaternary stereocenters.[10] Applying this approach, we treated enoxysilane **2.28** with terminal alkyne **2.35** and indium(III) bromide and obtained the desired β,γ-unsaturated ketone **2.37** in moderate yield (entry 1, Table 2.1). A major side-product of the reaction was hydrolysis of the enoxysilane, which we attributed to sensitive nature of the TMS protecting group. Indeed, the use of more hydrolytically stable enoxysilanes (–TBS and –TIPS) led to higher yields (entries 2 and 3, Table 1). A screen of known π-acids including InI_3, $InCl_3$, $ZnBr_2$, $AgSbF_6$, $[AuPPh_3]^+$, or $PdBr_2$ revealed that the observed reactivity was unique to $InBr_3$ as little-to-no desired product was observed in all cases. Substrate scope was briefly investigated using the optimized conditions and alkynes that contained relevant functional handles for our synthetic studies toward the PIDs. As such, substrates containing a halide, isopropyl ester, and alcohol functionalities successfully participated in the alkenylation (Table 2.2).

Table 2.1. Optimization of the α-Alkenylation Utilizing $InBr_3$.

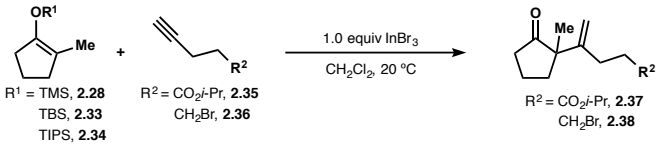

Entry	Enoxysilane	Alkyne	Product	Yield[a]
1	**2.28**	**2.35**	**2.37**	31%
2	**2.33**	**2.35**	**2.37**	45%
3	**2.34**	**2.36**	**2.38**	65%[b]

[a] Isolated yield. [b] Inseparable from $(i\text{-Pr})_3SiOH$.

Table 2.2. Examples of Regioselective Intermolecular Alkenylation.

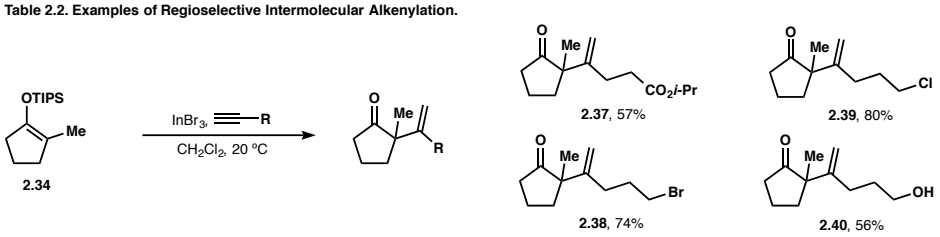

During reaction development, we discovered that isomeric enoxysilane **2.41** readily isomerized to **2.28** in the presence of indium(III) bromide (Scheme 2.7a). In addition, treatment of **2.41** with alkyne **2.36** and indium(III) bromide resulted in isomerization and alkenylation, which delivered **2.38** with high regioselectivity. At this stage, it is unclear how the isomerization occurs. Attempts at using proton scavengers (i.e. 2,6-di-*tert*-butyl pyridine) to rule out the involvement of Brønsted acids were inconclusive. This result appears to be idiosyncratic for enoxysilanes derived from 2-methylcyclopentanone (**2.23**) as six-membered and acyclic substrates, **2.40** and **2.43** respectively did not exhibit the apparent preference for building quaternary centers (Scheme 2.7b).

Scheme 2.7. Interesting Observations.

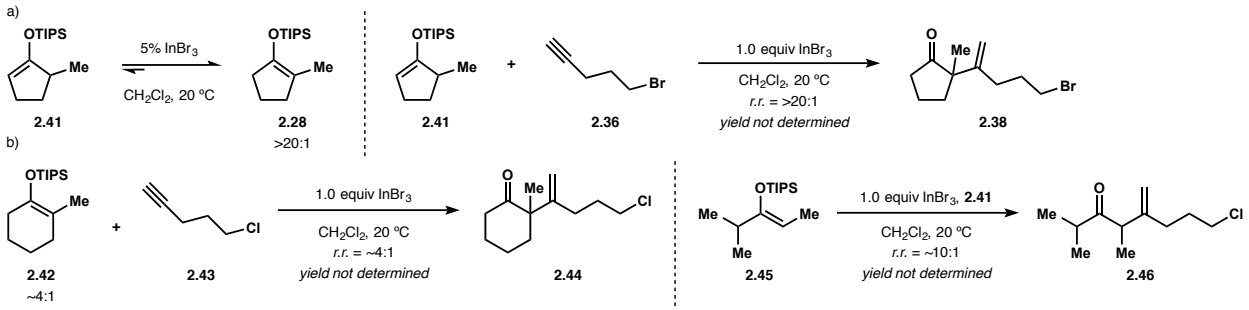

We proposed that the mechanism for the α-alkenylation involved a coordination event between alkyne **2.36** and indium(III) forming complex **2.45** (Scheme 2.8). This resulted in the liberation of an equivalent of a bromide ion, which served to activate enoxysilane **2.34**.[11] Once activated, nucleophilic attack by enoxysilane **2.46** onto alkyne-indium complex **2.45** resulted in the formation of desired vinylindium **2.48** and triisopropylsilyl bromide **2.47**. An acidic workup served to protonate **2.48** and delivered β,γ-unsaturated ketone **2.38**.[10]

Scheme 2.8. Proposed Mechanism of the α-Alkenylation.

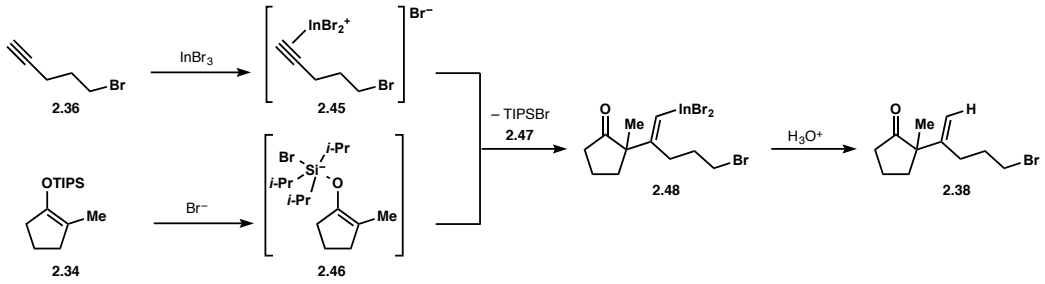

2.2.2 Synthesis of Polycyclization Precursor 2.18

Scheme 2.9. Preparation of the Polycyclization Precursor.

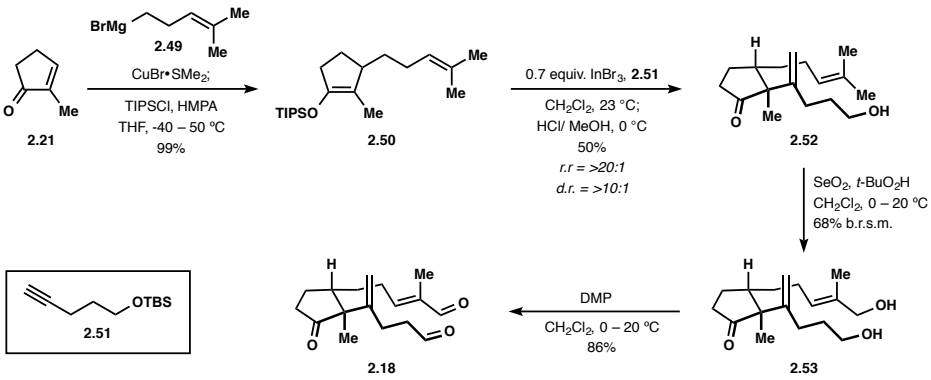

The development of the proposed α-alkenylation enabled our pursuit of polycyclization precursor **2.18**. Our synthesis began with a copper-catalyzed conjugate addition of Grignard **2.45** to 2-methyl-cyclopenten-1-one (**2.21**), which afforded enoxysilane **2.49** in a nearly quantitative yield (Scheme 2.9).[12] Subsequent treatment with *O*-TBS protected 4-pentyn-1-ol (**2.47**) and indium(III) bromide delivered the desired alkenylation product **2.52** in moderate yield. We found that treatment of the reaction mixture with a solution of 1% HCl in MeOH allowed for protonation of the intermediate vinylindium, deprotection the TBS group, and conversion of TIPSBr **2.47** to triisopropyl(methoxy)silane. The formation of triisopropyl(methoxy)silane helped avoid the formation of tiisopropylsilanol, which complicated the isolation of ketone **2.52**.

With alkenylation product **2.52** in hand we pursued the polycyclization precursor **2.18** via a series of oxidations. Following this approach, Sharpless allylic hydroxylation[13] delivered keto diol **2.53** in modest yield. Careful reaction monitoring of this process was required as prolonged

reaction times led to products resulting from overoxidation. Double oxidation of keto diol **2.53** using Dess–Martin periodinane[14] delivered tricarbonyl **2.18** and completed the synthesis of the polycyclization precursor.

2.2.3 Development of a Radical-polar Crossover Polycyclization Cascade

Scheme 2.10. Initial Results of the Polycyclization Cascade.

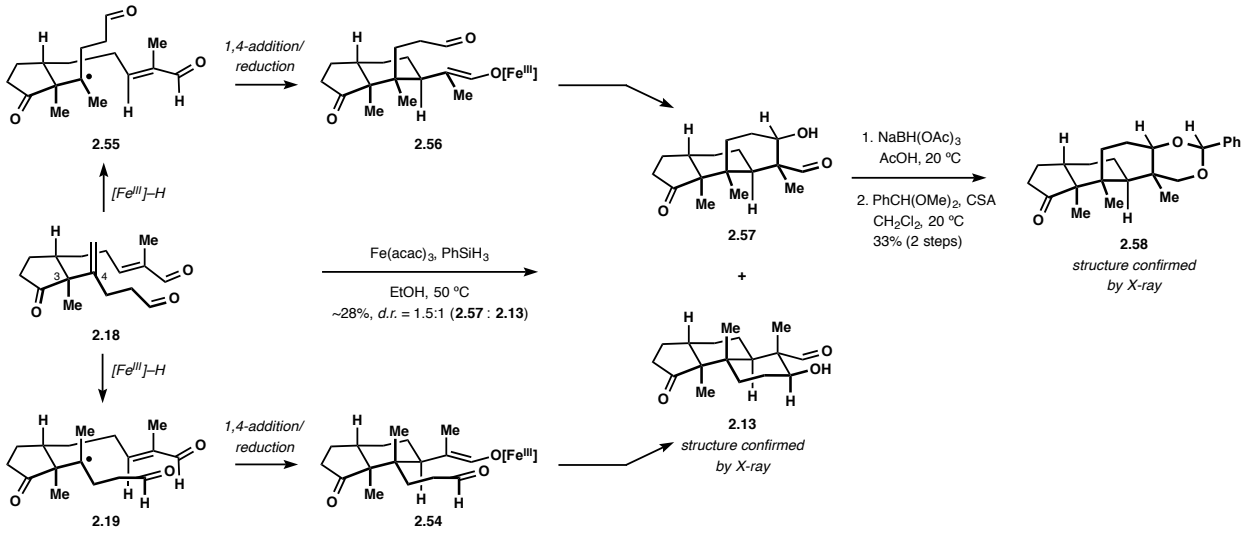

The preparation of **2.18** enabled the evaluation of the proposed polycyclization event. To our delight, exposure of **2.18** to conditions developed by Baran and co-workers[7] resulted in formation of products of the polycyclization cascade (Scheme 2.10). While desired tricycle **2.13** was isolated, it was accompanied by undesired tricycle **2.57** that resulted from a diastereomeric series of intermediates.[15] After chemoselective HAT, free rotation about the C3–C4 bond axis allowed access to intermediates **2.19** and **2.55**. Since there was a relatively small difference in size between the relevant substituents (i.e. methyl vs. *n*-alkyl) a similar activation barrier likely led to the observed outcome. Despite the notion that neutral radical intermediates are largely unaffected by exogenous reagents we attempted to optimize the polycyclization by screening various metal pre-catalysts, solvents, silanes, temperature regimes, or additives. However we were unable to find a set of conditions that improved the product ratio.[16, 17]

Scheme 2.11. Proposed Mechanism for the Radical-polar Crossover Polycyclization.

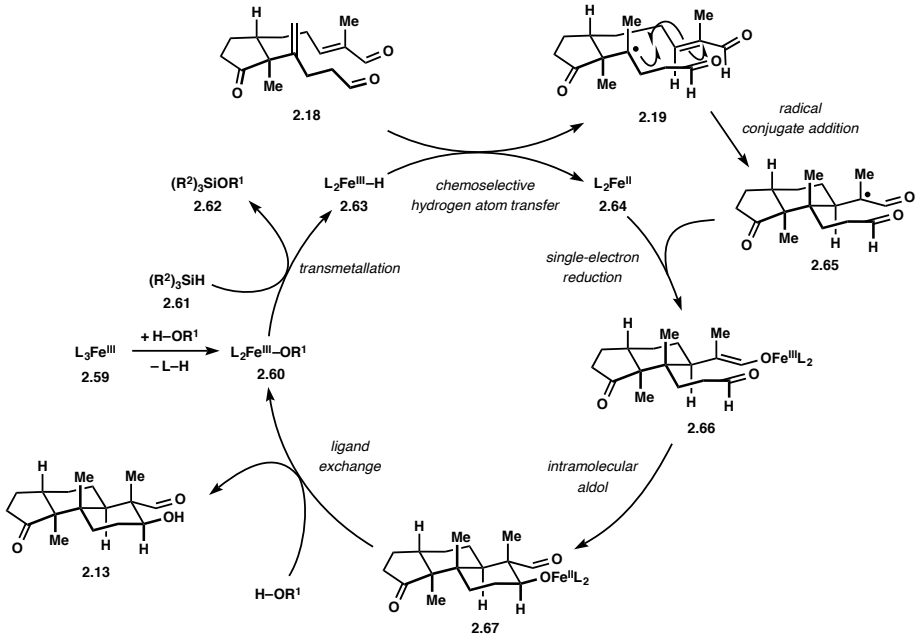

During our optimization efforts we made a series of observations that dramatically influenced our approach to the proposed polycyclization. We observed that an exogenous alcohol was essential to the success of the reaction as no reaction was observed in its absence. In addition, the use sub-stoichiometric or catalytic quantities of iron(III) acetylacetonate resulted in poor reaction conversion. These observations corroborated work from Holland, Baran, and co-workers[7c] that indicated that iron(III) alkoxide complexes were the catalytically active metal species in relevant reductive olefin coupling reactions. Taken together we proposed a mechanism for the polycyclization that is based on the one provided by Baran, Holland, and co-workers (Scheme 2.11).[7c,18]

The proposed cascade began with activation of the pre-catalyst **2.59** by the exogenous alcohol and produced iron(III) alkoxide **2.60**. Ensuing transmetallation with silane **2.61** provided access to the putative iron(III)-hydride **2.63** that participated in a chemoselective HAT event with the 1,1-disubstituted alkene. Subsequent radical conjugate addition by the resulting tertiary alkyl radical **2.19** resulted in formation of stabilized radical **2.65**. A single-electron reduction[19] of

2.65 and intramolecular aldol forged the second carbon-carbon bond of the cascade and completed the assembly of tricycle **2.13**.

Scheme 2.12. Mono(isopropoxy)phenylsilane as a Reductant

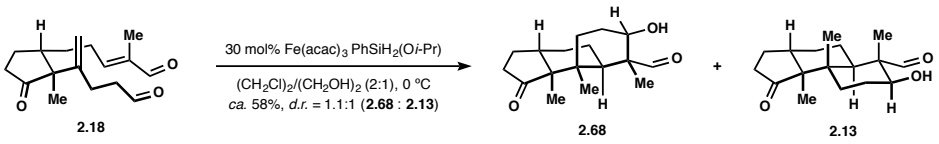

The second observation that we made during our optimization efforts was that the yield of the polycyclization was dramatically increased when mono(isopropoxy)phenylsilane was used as a reductant (Scheme 2.12).[20] The application of this reagent allowed the reaction to proceed at lower temperatures, which we believe limited undesired background reactivity involving the aldehydes contained on **2.18** (i.e. enolization of the C7 aldehyde and subsequent intermolecular aldol). Since diastereomers **2.13** and **2.68** were easily separable by chromatography, the increase in reaction yield provided access to synthetically useful quantities of **2.13**, which supported further studies toward the terpenoid core of various PIDs.

Scheme 2.13. Synthesis of the Terpenoid Core of JBIR-03.

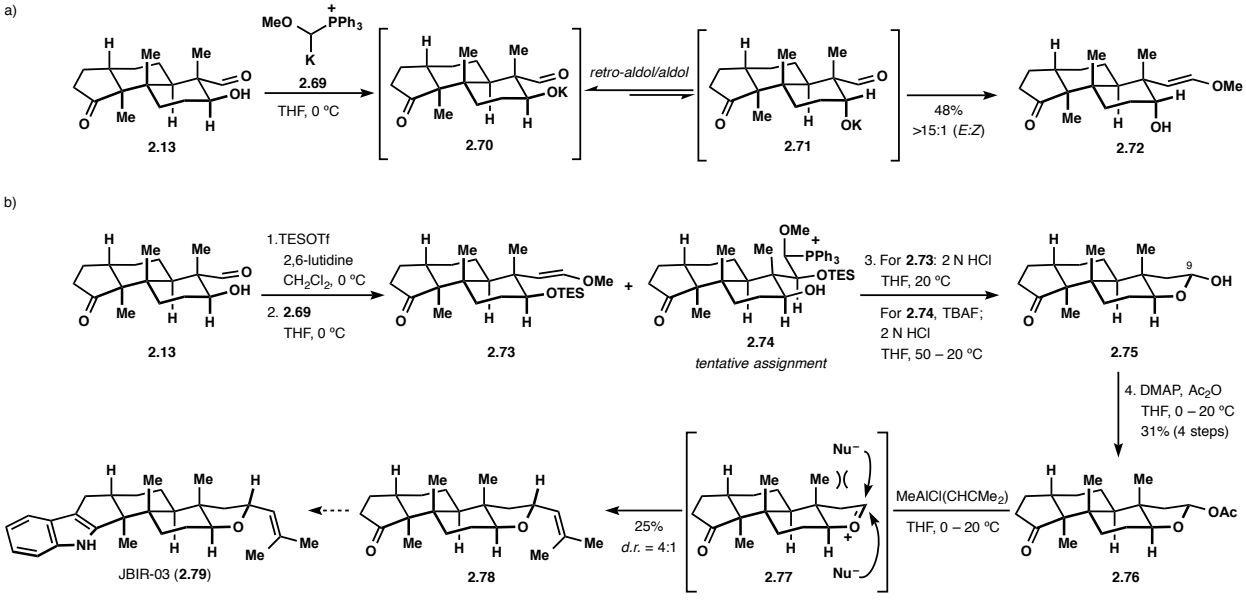

One such study led to the completion of the core of JBIR-03 (**2.79**; Scheme 2.13).[21] Our initial work in this area began with a one-carbon homologation of the aldehyde on **2.13** using methoxy(methylene)triphenylphosphorane.[22] To our surprise, epimeric olefination product **2.72** was obtained in moderate yield. We proposed that after deprotonation of the alcohol an equilibrium was established between **2.70** and **2.71** via a retro-aldol/aldol sequence and that the most reactive species resulted from the alkoxide being axially oriented (Scheme 2.13a).[23] We proposed that protection of the alcohol would eliminate the retro-aldol/aldol pathway and provide access to the desired olefination product. Indeed, protection of the alcohol on **2.13** as the TES-ether and subsequent treatment with methoxy(methylene)triphenylphosphorane delivered the desired olefination product **2.73** along with what was tentatively assigned as an interrupted-Wittig product **2.74** that resulted from silyl transfer after addition of the Wittig reagent (Scheme 2.13b). Gratifyingly, **2.73** and **2.74** converged to lactol **2.75**, which was found to exist as an inconsequential mixture of diastereomers at C9.

We envisioned that a nucleophilic addition into an oxacarbenium ion would be a straightforward way to install the 2-methyl-1-propenyl moiety found in the terpenoid core of JBIR-03 (**2.79**). Previous research indicated that an inside the envelop attack is favored for reactions involving nucleophilic addition into oxacarbeniums ions contained in mono- and bicyclic five-membered rings,[24] which, in our setting, would produce the undesired stereochemistry at C9. Notwithstanding, we posited that nucleophilic attack on an oxacarbenium ion like **2.77** would occur outside the envelop due to developing steric interactions in the transition state from the proximal axial methyl group. To test this hypothesis, we acylated the lactol and treated the resulting acetate with a heteroleptic vinyl organoaluminum complex,[25] which afforded the tetracyclic terpenoid core of JBIR-03 (**2.79**) with modest diastereoselectivity.

To our delight, NOESY experiments revealed that the *trans*-tetrahydrofuran was formed as major product.[26] The successful installation of the 2-methyl-1-propenyl moiety completed the synthesis of the tetracyclic core, which was achieved in 10 steps from commercially available material and validated our approach to the PIDs.

2.2.4 Revised Strategy Toward the Paxilline Indole Diterpenes

Scheme 2.14. Addition of Alcohol Nucleophiles into the C7 Aldehyde.

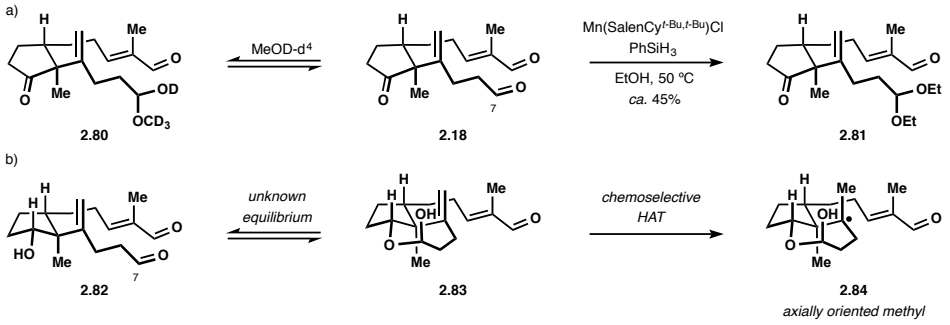

Despite the success of our studies related to the synthesis of the terpenoid core of JBIR-03 **2.79**, the poor diastereoselectivity of the polycyclization plagued the sequence and required further attention. Eventually, my co-worker, Eric J. Kuenstner, discovered a solution to the stereoselectivity problem. Thus, during our initial optimization efforts we repeatedly observed that the aldehyde at C7 was susceptible to the addition of alcohol nucleophiles forming hemiacetal **2.80** and acetal **2.81** (Scheme 2.14a). This inherent reactivity guided us to propose that cyclopentanol analog **2.82** could reversibly access 7-membered lactol **2.83** and conformationally restrict the 1,1-disubstituted alkene (Scheme 2.14b). We hoped that restricting the available conformations would orient the methyl group in the pseudo-axial position prior to the radical conjugate addition (i.e. **2.84**). If the molecule could be manipulated in this way, we hypothesized that a diastereoselective polycyclization favoring the *trans*-decalin would result.

To validate this hypothesis, Eric prepared alcohol **2.82** and observed that it existed as a ~1:2.5 mixture of **2.82**:**2.83** in deuterated chloroform (Scheme 2.15).[27] Importantly, when the

mixture of **2.82** and **2.83** was treated with the optimized reaction conditions for the polycyclization (*vide supra*) we observed selectivity for the desired tricycle.[28] Taken together, Eric discovered that the diastereochemical outcome of the polycyclization cascade was highly influenced by the tether and confirmed our hypothesis.

Scheme 2.15. Tether-controlled Polycyclization.

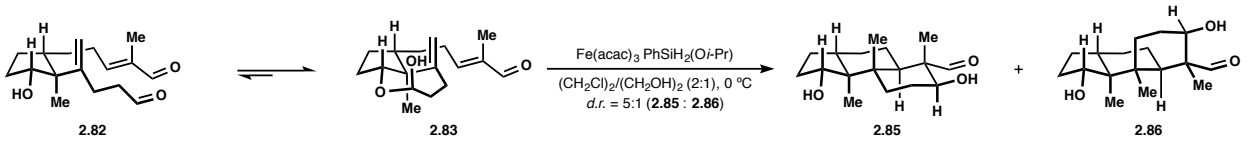

2.82 2.83 2.85 2.86

2.3 Tether-controlled Synthesis of Emindole SB

2.3.1 Synthesis of New Polycyclization Precursor 2.93

The insight that we gained from Eric's studies related to **2.82** had a dramatic impact on our approach to the PIDs. Alcohol **2.82** served as a substrate that provided access to a relevant tricarbocyclic framework in a stereoselective manner, however we believed that its utilization would require unnecessary functional group manipulations during its preparation that would ultimately detract from the overall efficiency of our synthetic approach.

Scheme 2.16. Tether Involving Hemiaminal Intermediates.

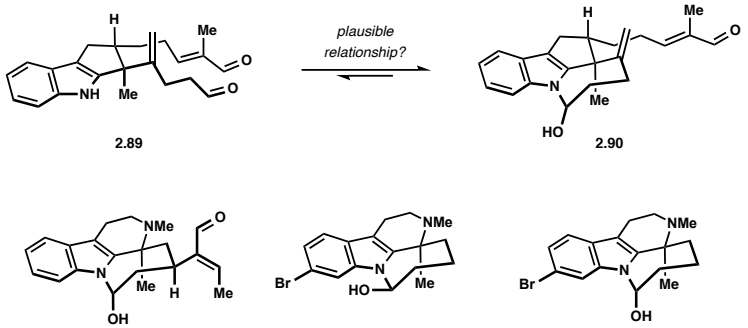

2.89 2.90

akagerine (**2.91**) aborescidine C (**2.92**) aborescidine D (**2.93**)

To address this concern, we proposed installing the indole nucleus early on in our synthetic sequence and accessing analogous hemiaminal intermediates en route to the various PIDs (Scheme 2.16). Structures bearing similar hemiaminal motifs can be found in select secondary metabolites (**2.91**–**2.93**), which provided a foundation for the pursuit of similar

intermediates.[29] To access a cyclization precursor like **2.89**, we believed that the cyclopentanone moiety in our early intermediates (i.e. **2.53**) would serve as a functional group handle for indole assembly without the need for lateral functional group manipulations.

Scheme 2.17. Synthesis of the Hemiaminal Polycyclization Precursor.

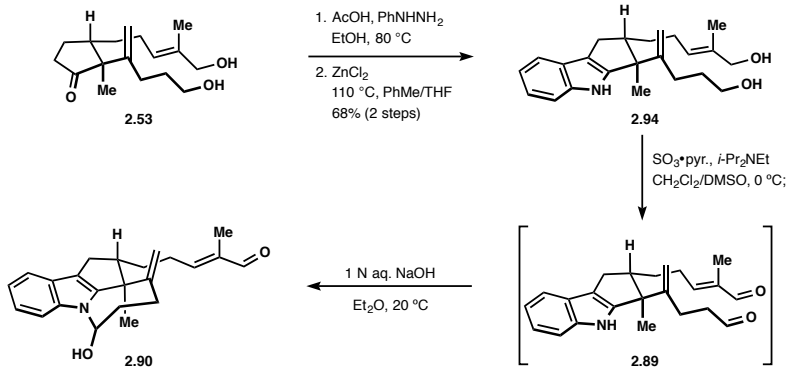

Following this approach, we pursued a Fischer indole synthesis[30] with ketone **2.53**. Our installation of the indole moiety was accomplished using a protocol developed by Wood and co-workers,[31] which produced indole diol **2.94** (Scheme 2.16). Oxidation of **2.94** proved to be a challenge due to the proclivity of the indole nucleus toward oxidation. As such, tactics that involved certain activated forms of dimethylsulfoxide (i.e. Moffatt, Corey–Kim, or Swern oxidation),[32] TEMPO,[33] or aerobic copper-catalysis[34] led to complex mixtures of products that were difficult to interpret. Fortunately, Parikh–Doering oxidation[35] produced the desired indole dialdehyde **2.89** without any undesired products resulting from degradation of the indole. During reaction development, we observed that careful control of the reaction temperature limited the formation of side products resulting from Pummerer rearrangement[36] and trapping of the putative thionium ion with **2.94**.

Scheme 2.18. Acid-mediated Decomposition of the Hemiaminal.

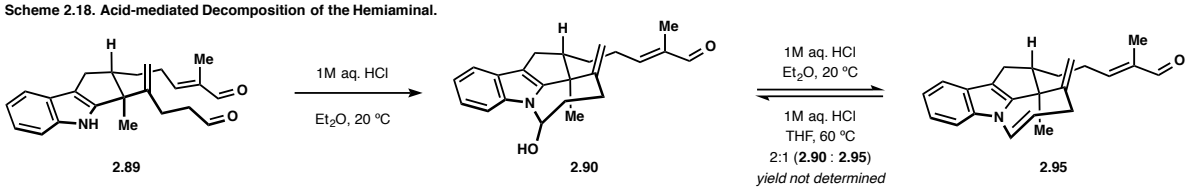

Dialdehyde **2.89** was a stable compound that could be isolated via chromatography and did not exhibit relevant hemiaminal signals when analyzed by ^{1}H NMR. Fortunately, we discovered that treatment with aqueous base during the reaction workup converted **2.89** to hemiaminal **2.90** without any discernable signs of decomposition. This result stood in stark contrast to our efforts related to the acid-mediated conversion of **2.89** to **2.90**, which produced **2.90** along with enamine **2.95** (Scheme 2.18). We discovered that dehydration of the series of intermediates containing the hemiaminal moiety readily occurred in the presence of dilute acid, however simple treatment with acid under heating reformed the hemiaminal moiety with modest efficiency.

2.3.2 Tether-controlled Cyclization

Scheme 2.19. Completion of the Common Pentacyclic Core.

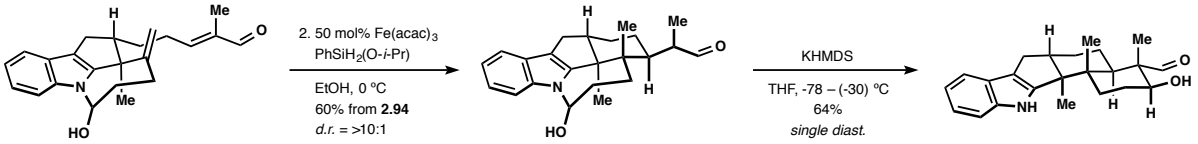

2.90 **2.96** **2.97**

When **2.90** was subject to cyclization conditions only the radical conjugate addition was observed as pentacycle **2.96** was obtained (Scheme 2.19).[37] Gratifyingly, the process was highly diastereoselective. In accord with our previous studies, the iron-catalyzed reductive olefin cyclization was sensitive toward atmospheric oxygen as undesired oxidation products were observed (Figure 2.2). We attributed this property of the reaction to the oxidation of an iron(III) enolate that resulted from the radical conjugate addition.[38]

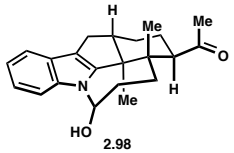

2.98

Figure 2.2. Representative Undesired Oxidation Product.

While we only affected one of the carbon–carbon forming steps from cyclization strategy, treatment with strong base induced cleavage of the hemiaminal and aldol addition. This sequence of events delivered the desired pentacyclic core as a single diastereomer. During our efforts to increase the efficiency of this process we discovered that potassium bases were unique in their ability to affect the desired transformation. No reaction conversion was observed in the presence of lithium bases, which suggested that cleavage of the hemiaminal did not occur (Scheme 2.20). We speculate that the lithium–oxygen bond was too strong and as a result deprotonation of the hemiaminal does not lead to ring opening and subsequent reactivity.

Scheme 2.20. Unique Reactivity Involving Lithium Bases.

2.99
O–K ~57 kcal/mol

2.100
O–Li ~81 kcal/mol

Additional work suggested that **2.97** was the kinetic product from the hemiaminal cleavage-aldol sequence as α,β-unsaturated aldehyde **2.107** was formed under thermodynamic conditions (Scheme 2.21).[39] Fortunately, careful addition of base and reaction monitoring delivered reliable quantities of desired pentacycle **2.97** that enabled further synthetic studies.

Scheme 2.21. Proposed Origin of Undesired Side Product 2.107.

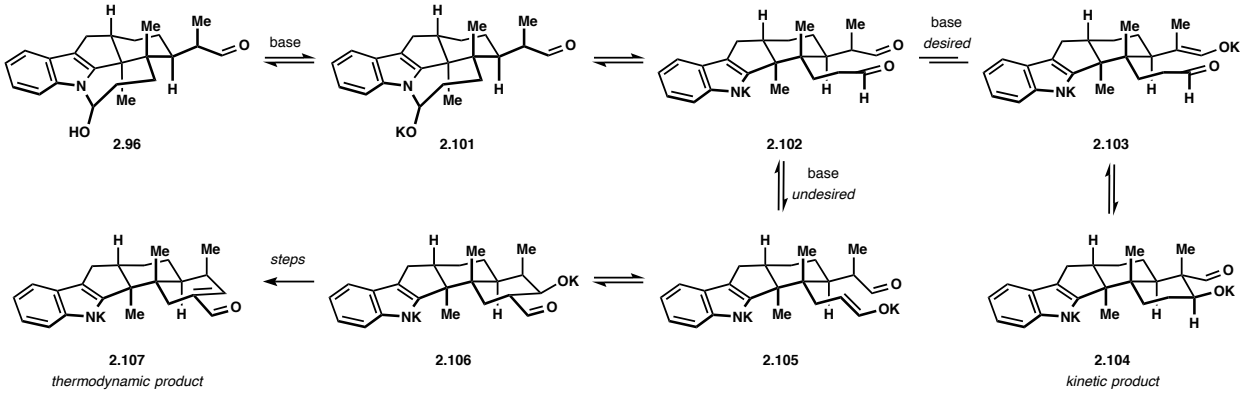

2.96 **2.101** **2.102** **2.103**

2.107
thermodynamic product

2.106 **2.105** **2.104**
kinetic product

The hemiaminal tether appeared to be crucial for the diastereoselective construction of **2.97**. Indeed, when indole dialdehyde **2.92** was used directly in the polycyclization we observed a new product that was believed to be diastereomer **2.108** along with desired pentacycle **2.97** (Scheme 2.22).[40] X-ray crystallographic analysis confirmed our tentative assignment by ^{1}H NMR and identified the new material as the undesired diastereomer **2.108** resulting from the alternative sterechemical course of the polycyclization cascade (*vide supra*, Scheme 2.10). In stark contrast to our studies with hemiaminal **2.93** the undesired *cis*-decalin was the major product of the reaction.

Scheme 2.22. Importance of the Tether.

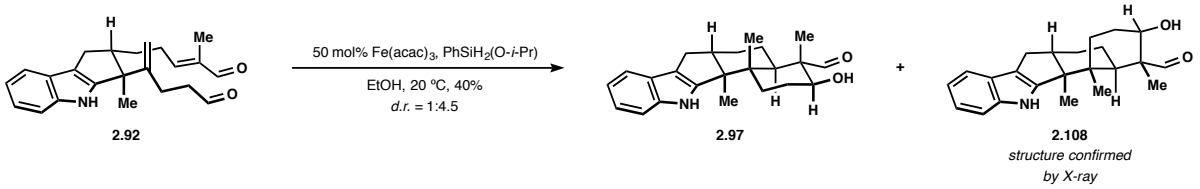

2.3.3 Completion of Emindole SB

The development of a stereocontrolled assembly of the pentacyclic core of the PIDs enabled us to pursue a proof-of-concept for our synthetic approach. We identified emindole SB,[41] the simpliest congener of the entire family and likely biosynthetic precursor to all other members,[42] as our initial target. We believed that we could access the dimethallyl side chain via homologation of the aldehyde moiety. Following this approach, we executed a Schlosser homologation[43] using (*Z*)-2-ethoxyvinyllithium, which delivered α,β-unsaturated aldehyde **2.109** after acidic workup (Scheme 2.23). A large excess of the organometallic reagent was necessary to suppress side reactions resulting from retro-aldol pathways. Chemoselective hydrogenation of the electron deficient alkene and Wittig olefination with isopropylidene triphenylphosphorane completed the synthesis and delivered emindole SB (**2.111**) in 11 steps from commercially available material.

Scheme 2.23. Synthesis of Emindole SB.

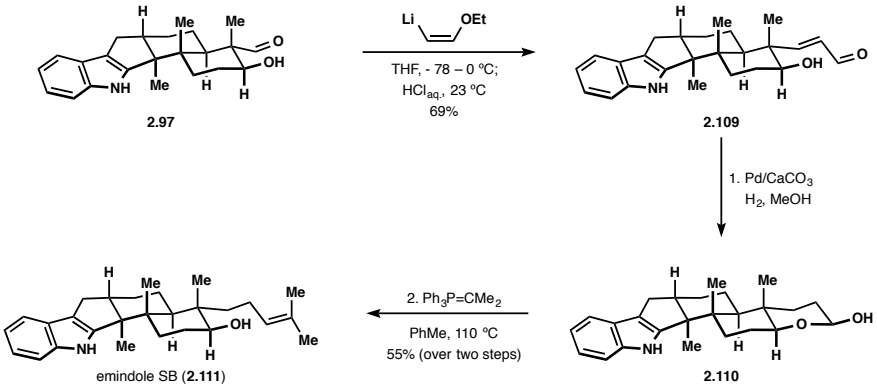

The successful assembly emindole SB (**2.111**) validated our synthetic approach to the PIDs. Importantly, the strategy that we pursued enabled the synthesis the common pentacyclic core **2.97** of various congeners of the family. We believe that the work described in this Chapter will serve as the foundation for further synthetic studies related to the PIDs.

2.4 Experimental Section

2.4.1 General Experimental Details

All reactions were carried out in flame- or oven-dried glassware under a positive pressure of dry nitrogen unless otherwise noted. Reaction solvents including diethylether (Et_2O, Fisher, HPLC Grade), tetrahydrofuran (THF, Fisher, HPLC Grade), methylene chloride (CH_2Cl_2, Fisher, HPLC Grade), benzene (PhH, Fisher, HPLC Grade), and toluene (PhMe, Fisher, HPLC Grade) were dried by percolation through a column packed with neutral alumina and a column packed with a supported copper catalyst for scavenging oxygen (Q5) under positive pressure of argon. Anhydrous, 1,2-dichloroethane (Fisher, ACS Grade), *N*,*N*-diisopropylamine (Oakwood Chemical, triethylamine (Oakwood Chemical), and *N*,*N*-diisopropylethylamine (Oakwood Chemical) were distilled from calcium hydride (~10% w/v) under a positive pressure of nitrogen. Anhydrous ethylene glycol [$(CH_2OH)_2$] was purchased from Sigma–Aldrich. Dimethyl sulfoxide (DMSO, EMD Chemicals) was dried over activated 3 Å molecular sieves (Acros Organics, 20%

w/w). Anhydrous hexamethphosphoramide (HMPA, Oakwood Chemical) was distilled from calcium hydride (10% w/v) under vacuum (*ca*. 0.1 torr). Solvents for extraction, thin layer chromatography (TLC) and flash column chromatography were purchased from Fisher (ACS Grade) and VWR (ACS Grade) and used without further purification. Chloroform-d and benzene-d_6 for ^{1}H and ^{13}C NMR analysis were purchased from Cambridge Isotope Laboratories and used without further purification. Commercially available reagents were used without further purification unless otherwise noted. All reactions were monitored by TLC using precoated siliga gel plates (EMD Chemicals, Siliga gel F_{254}). Flash column chromatography was performed over silica gel (Acros Organics, 60 Å, particle size 0.04 – 0.063 mm). ^{1}H NMR and ^{13}C NMR spectra were recorded on Bruker DRX-500 (BBO probe), Bruker DRX-500 (TCI cryoprobe), and Bruker AVANCE600 (TBI probe) spectrometers using residual solvent peaks as internal standards [$CHCl_3$: 7.26 ppm (^{1}H NMR), 77.16 ppm (^{13}C NMR); C_6H_6: 7.16 ppm (^{1}H NMR), 128.00 ppm (^{13}C NMR)]. High-resolution mass spectra (HRMS) were recorded on Waters LCT Premier TOF spectrometer with ESI and CI sources.

2.4.2 Experimental Procedures

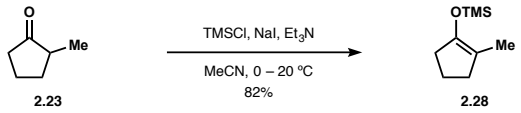

2.23 2.28

TMS-enoxysilane **2.28**:[44] Chlorotrimethylsilane (1.9 mL, 15.0 mmol) was added to a suspension of sodium iodide (2.4 g, 16.0 mmol) in acetonitrile (16 mL) at 0 ºC. After 20 minutes, 2-methyl cyclopentanone (1.1 mL, 10.0 mmol) and triethylamine (2.8 mL, 20.0 mmol) were added to the reaction mixture. The reaction mixture was vigorously stirred and allowed to warm to room temperature. After 1 hour the reaction was extracted with pentane (3x20 mL). The combined organic layers of pentane were washed with a solution of saturated aqueous $NaHCO_3$ (20 mL)

and brine (20 mL). The combined organic layers were dried over $MgSO_4$, filtered, and concentrated under reduced pressure to afford 1.4 g (82%) of **2.28** as a light yellow oil. This material was used without further purification. All the analytical data are identical with the literature.

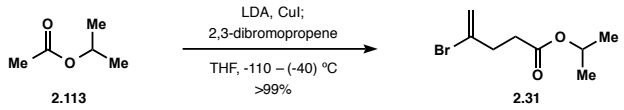

Isopropyl Ester **2.31**:[45] A solution of isopropyl acetate (2.0 mL, 10.0 mmol) and copper(I) iodide (7.6 g, 40.0 mmol) in THF (75 mL) was added to a solution of LDA [freshly prepared from *N*,*N*-diisopropylamine (2.8 mL, 20.0 mmol) and *n*-BuLi (8.2 mL, 2.44 M in hexanes, 20.0 mmol) in THF (25 mL) at -78 ºC] at ~(-105) ºC. The reaction was vigorously stirred and allowed to warm to ~(-40) ºC. Once at ~(-40) ºC (~1 hour) a solution of 2,3-dibromopropene (2.0 mL, 10.0 mmol) in THF (25 mL) was added in a slow and steady stream. The reaction mixture was stirred for 1 hour and quenched with a solution of saturated aqueous NH_4Cl (100 mL). The organic layer was washed with a solution of saturated aqueous NH_4Cl (75 mL per wash) until no blue tint could be observed in the organic layer (4 washes). The combined aqueous layers were extracted with diethyl ether (3x100 mL). The combined organic layers were washed with a solution of saturated aqueous NH_4Cl (100 mL) and brine (100 mL). The organic layer was dried over $MgSO_4$, filtered, and concentrated under reduced pressure. Purification by flash chromatography (gradient elution: 100% hexanes to 20% v/v ethyl acetate in hexanes) afforded 2.2 g (>99%) of isopropyl ester **2.31** as a clear, colorless oil. R_f = 0.19 (100% hexanes); ^{1}H NMR (500 MHz; $CDCl_3$): δ 5.63 (s, 1H), 5.43 (s, 1H), 5.02 (dt, *J* = 12.5, 6.3 Hz, 1H), 2.75 (t, *J* = 7.5 Hz, 2H), 2.54 (t, *J* = 7.5 Hz, 2H), 1.24 (d, *J* = 6.3 Hz, 6H); ^{13}C NMR (125 MHz; $CDCl_3$): δ 171.5, 132.3, 117.5, 77.0, 68.0, 36.7, 33.3, 21.8.

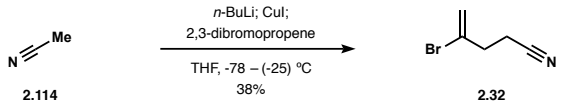

Nitrile **2.32**:[46] *n*-Butyllithium (14.0 mL, 2.44 M in hexanes, 34.1 mmol) was added to a solution of acetonitrile (1.8 mL, 34.1 mmol) in THF (50 mL) at -78 ºC. The reaction was vigorously stirred and allowed to slowly warm to ~(-40) ºC. Once at ~(-40) ºC (~1 hour) copper iodide (6.5 g, 34.1 mmol) was added. After an additional 15 minutes, 2,3-dibromopropene (1.2 mmol, 10.0 mmol) in THF (30 mL) was added in a slow and steady stream. The reaction was stirred for 1 hour and quenched with a solution of saturated aqueous NH_4Cl (50 mL). The layers were separated and the aqueous layer was extracted with diethyl ether (3x50 mL). The combined organic layers were dried over anhydrous sodium sulfate, filtered, and concentrated under reduced pressure. Purification by flash chromatography (gradient elution: 100% hexanes to 100% ethyl acetate) afforded 0.60 g (38%) of nitrile **2.32** as a clear, colorless oil. R_f = 0.5 (30% v/v ethyl acetate in hexanes); ^{1}H NMR (400 MHz; $CDCl_3$): δ 5.78 (t, *J* = 1.0 Hz, 1H), 5.58 (d, *J* = 2.1 Hz, 1H), 2.76 (t, *J* = 7.0 Hz, 2H), 2.65-2.62 (m, 2H); ^{13}C NMR (125 MHz; $CDCl_3$): δ 129.2, 120.1, 118.1, 77.4, 77.2, 76.9, 37.4, 16.9.

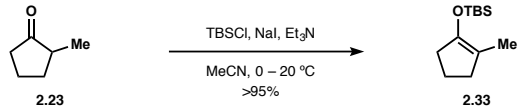

TBS-enoxysilane **2.33**:[47] *tert*-Butyl(chloro)dimethylsilane (2.6 g, 15.0 mmol) was added to a suspension of sodium iodide (2.4 g, 16.0 mmol) in acetonitrile (20 mL) at 0 ºC. After 20 minutes, 2-methyl cyclopentanone (1.1 mL, 10.0 mmol) and triethylamine (2.8 mL, 20.0 mmol) were added. The reaction was vigorously stirred and allowed to warm to room temperature. After 1 hour the reaction was extracted with pentane (3x20 mL). The combined layers of pentane were

washed with a solution of saturated aqueous $NaHCO_3$ (20 mL) and brine (20 mL). The combined organic layers were dried over $MgSO_4$, filtered, and concentrated under reduced pressure to afford 2.1 g (>95%) of **2.33** as a clear, colorless oil. This material was used without further purification. All the analytical data are identical with the literature.

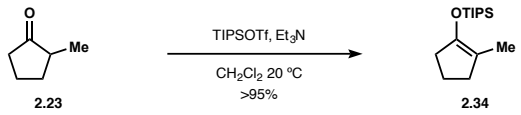

2.23 2.34

TIPS-enoxysilane **2.34**:[48] Triethylamine (5.0 mL, 36.0 mmol) was added to a solution of 2-methylcyclopentanone (2.1 mL, 20.0 mmol) in methylene chloride (60 mL) at room temperature. Triisopropylsilyl trifluoromethanesulfonate (5.4 mL, 20.0 mmol) was added in a dropwise manner over 10 minutes. After 30 minutes the reaction was quenched with a solution of saturated aqueous $NaHCO_3$ (15 mL) and diluted with hexanes (180 mL). The layers were separated and the combined organic layers were washed with brine (25 mL), dried over $MgSO_4$, filtered, and concentrated under reduced pressure to afford 5.1g (>99%) of **2.34** as a clear, colorless oil. This material was used without further purification. All the analytical data are identical with the literature.

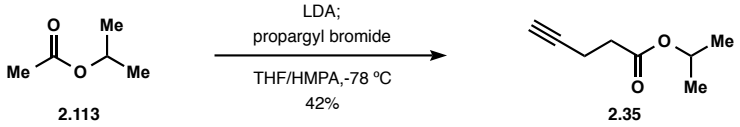

2.113 2.35

Isopropyl ester **2.35**:[49] Isopropyl acetate (1.2 mL, 10.0 mmol) was added to a solution of LDA [freshly prepared from *N*,*N*-diisopropylamine (1.7 mL, 12.0 mmol) and *n*-BuLi (4.9 mL, 2.44 M in hexanes, 12.0 mmol)] in THF (111 mL) at -78 ºC. After 1 hour HMPA (5.2 mL) and propargyl bromide (0.76 mL, 10 mmol) were added. The reaction was vigorously stirred and allowed to slowly warm to room temperature overnight. After 21 hours the reaction was quenched with a solution of saturated aqueous NH_4Cl (50 mL). The organic layer was washed with 1 N aqueous

solution of HCl (2x20 mL) and water (2x20 mL). The organic layer was dried over $MgSO_4$, filtered, and concentrated under reduced pressure. Purification by distillation under a nitrogen atmosphere afforded 0.59 g (52%) of **2.35** as a clear, colorless oil. ^{1}H NMR (500 MHz; $CDCl_3$): δ 5.04 (dt, *J* = 12.5, 6.3 Hz, 1H), 2.50 (s, 3H), 1.96 (d, *J* = 1.7 Hz, 1H), 1.24 (d, *J* = 6.3 Hz, 6H); ^{13}C NMR (126 MHz; $CDCl_3$): δ 171.3, 82.6, 68.9, 68.1, 33.7, 21.9, 14.5.

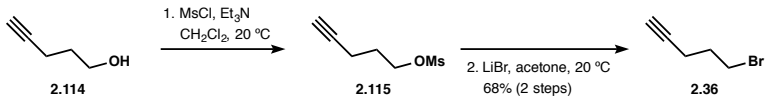

Alkyne **2.36**:[50] Methanesulfonyl chloride (1.25 mL, 16.1 mmol) was added to a solution of 4-pentyn-1-ol (1.0 mL, 10.8 mmol) and triethylamine (3.0 mL, 21.5 mmol) in methylene chloride (15 mL) at 0 ºC. The reaction was vigorously stirred and allowed to warm to room temperature. The reaction was monitored by ^{1}H NMR analysis of crude reaction aliquots in lieu of TLC due to stability issues of the mesylate. After 4 hours the reaction was quenched with a solution of saturated aqueous NH_4Cl (10 mL) and extracted with methylene chloride (3x10 mL). The combined organic layers were dried over anhydrous sodium sulfate, filtered, and concentrated under reduced pressure. Crude mesylate **2.115** was used immediately in the next step.

The crude mesylate was dissolved in acetone (15 mL) and anhydrous lithium bromide (1.87 g, 21.5 mmol) was added in a single portion. The reaction was vigorously stirred at room temperature for 40 hours. After consumption of the mesylate, the reaction was diluted with pentane (20 mL) and quenched with a solution of saturated aqueous $NaHCO_3$ (10 mL). The aqueous layer was extracted with pentane (20 mL) and the combined organic layers were dried over Anhydrous sodium sulfate, filtered, and concentrated under reduced pressure to afford 1.1 g (68%) of **2.36** as a clear, colorless oil. This material was used without further purification. All analytical data are identical to literature data.

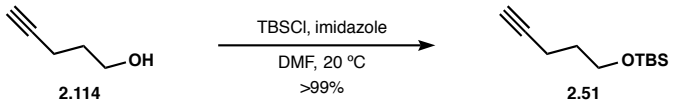

Alkyne **2.51**:[51] 4-pentyn-1-ol (18.6 mL, 200.0 mmol) was added to a solution of imidazole (34.0 g, 500.0 mmol) and *tert*-butyl(chloro)dimethylsilane (37.7 g, 250.0 mmol) in DMF (67 mL). The resulting solution was vigorously stirred at room temperature. After 1.5 hours the reaction was quenched with water (100 mL) and extracted with hexanes (4x100 mL). The combined organic layers were washed with brine (100 mL) dried over $MgSO_4$, filtered, and concentrated under reduced pressure. Purification by vacuum distillation (~50 ºC at 1.5 torr) afforded 35.0 g (88%) of **2.51** as a clear, colorless oil. All analytical data are identical to literature data.

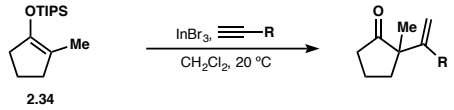

General α-alkenylation procedure:

A dram vial was charged with indium(III) bromide (1.0 equiv.) in a nitrogen atmosphere glovebox. The vial was sealed with a cap lined with a PTFE/silicone septa, removed from the glovebox, and quickly set under an inlet of dry nitrogen. The indium(III) bromide was suspended in methylene chloride (0.25 M) and enoxysilane (1.0 equiv.) and alkyne (3.0 equiv.) were sequentially added. The reaction was vigorously stirred at room temperature and monitored by TLC. Once the reaction was complete it was quenched with 1 N aqueous solution of HCl and diethyl ether. The combined organic layers were dried over Anhydrous sodium sulfate, filtered, and concentrated under reduced pressure.

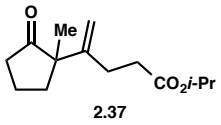

Comments: The reaction was performed on 0.5 mmol scale using TIPS-enoxysilane **2.34** and alkyne **2.35** and allowed to react for 15 hours. The product was purified using flash chromatography (7% v/v ethyl acetate in hexanes) and afforded 68.2 mg (57%) of **2.37** as a clear, colorless oil. ^{1}H NMR (600 MHz; $CDCl_3$): δ 5.00-4.95 (m, 1H), 4.88 (d, *J* = 0.5 Hz, 1H), 4.85 (d, *J* = 1.5 Hz, 1H), 2.45-2.42 (m, 2H), 2.32-2.23 (m, 5H), 1.87-1.82 (m, 2H), 1.69-1.64 (m, 1H), 1.20 (d, *J* = 6.2 Hz, 6H), 1.15 (d, *J* = 1.5 Hz, 3H).

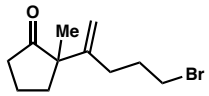

2.38

Comments: The reaction was performed on 0.1 mmol scale using TIPS-enoxysilane **2.34** and alkyne **2.36** and allowed to react for 2 hours. The yield (74%) was determined using dimethylsulfone as an internal standard. ^{1}H-NMR (600 MHz; $CDCl_3$): δ 4.95 (s, 1H), 4.93 (s, 1H), 3.43 (td, *J* = 6.6, 1.2 Hz, 2H), 2.33-2.24 (m, 3H), 2.16 (q, *J* = 7.4 Hz, 2H), 2.05-2.00 (m, 2H), 1.89 (q, *J* = 7.1 Hz, 2H), 1.71 (dt, *J* = 13.1, 7.2 Hz, 1H), 1.17 (s, 3H).

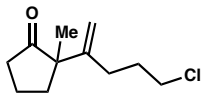

2.39

Comments: The reaction was performed on 1.0 mmol scale using TIPS-enoxysilane **2.34** and commercially avaialble 5-chloro-1-pentyne and allowed to react for 19.5 hours. The product was purified using flash chromatography (3% v/v ethyl acetate in hexanes) and afforded 238 mg (70%, slight *i*-Pr_3SiOH impurity present) of **2.39** as a clear, colorless oil. ^{1}H NMR (600 MHz; $CDCl_3$): δ 4.95 (s, 1H), 4.93 (s, 1H), 3.56 (t, *J* = 6.5 Hz, 2H), 2.27 (tdd, *J* = 12.5, 7.0, 5.5 Hz, 2H), 2.16 (dt, *J* = 11.4, 5.6 Hz, 3H), 1.97-1.85 (m, 4H), 1.70 (dt, *J* = 13.4, 6.9 Hz, 1H), 1.17 (s, 3H).

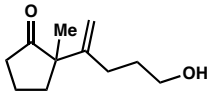

2.40

Comments: The reaction was performed on 0.5 mmol scale using TIPS-enoxysilane **2.34** and alkyne **2.51** (only 1.5 equiv.) and allowed to react for 2.5 hours. The reaction was quenched with 1% v/v aqueous HCl in MeOH. The product was purified using flash chromatography (30% v/v ethyl acetate in hexanes) and afforded 50.6 mg (56%) of **2.40** as a clear, colorless oil. ^{1}H NMR (600 MHz; $CDCl_3$): δ 4.95-4.93 (m, 2H), 3.67 (td, *J* = 6.3, 2.3 Hz, 2H), 2.30-2.25 (m, 3H), 2.15-2.02 (m, 2H), 1.90-1.85 (m, 2H), 1.77-1.67 (m, 3H), 1.48 (s, 1H), 1.17 (s, 3H).

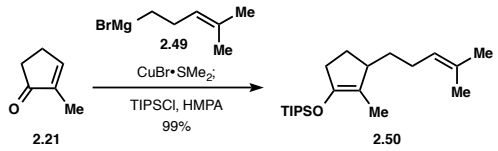

2.21 2.50

Preparation of **2.49**: Homoprenyl bromide (5.3 g, 33.3 mmol, ¼ of total) was added to a suspension of magnesium turnings (5.4 g, 221.7 mmol) in THF (22 mL). After observation of an initial exotherm, the remaining bromide (16.4 g, 99.7 mmol) and THF (44 mL) were added in roughly 10 portions to maintain a mild exotherm. After the addition was complete the reaction mixture was heated to 50 ºC for 1 hour, cooled to room temperature, and left to age overnight. Titration revealed a 0.75 M solution had been prepared.

Enoxysilane **2.50**: While hot, an oven-dried three-neck round bottom flask was equipped with an oven-dried addition funnel in the center position, an inlet of anhydrous nitrogen in one of the side positions, and a septum in the other side position. The assembled system was allowed to cool to room temperature under a stream of nitrogen by venting through the top of the addition funnel. Once cooled, the flask was charged with CuBr•SMe_2 (2.1 g, 10.0 mmol) and THF (22 mL). The flask was submerged in a cooling bath maintained at ~ (-35) ºC. While the suspension was cooling, the addition funnel was charged with the freshly prepared Grignard solution. The

Grignard solution was added in a dropwise manner over 15 – 20 minutes and a dark blue solution was formed. After the addition was complete the cooling bath was further cooled to ~(-45) ºC and 2-methyl-cyclopenten-1-one (7.4 mL, 75.0 mmol) was added in a dropwise manner via a syringe pump. After the addition was complete stirring was continued at ~(-45) ºC. After 15 minutes, the flask was removed from the cooling bath and allowed to slowly warm to room temperature. Once at room temperature, triisopropylchlorosilane (32.0 mL, 150.0 mmol) and HMPA (59.0 mL. 337.0 mmol) were added and the flask was warmed to 50 ºC. After 3 hours the solution was cooled to 0 ºC and quenched with a 3:1 mixture of saturated aqueous NH_4Cl:NH_4OH (70 mL). The organic layer was diluted with hexanes (200 mL) and washed with a 3:1 mixture of a saturated aqueous NH_4Cl:NH_4OH until no traces of a blue color was observed (3x80 mL). The combined aqueous layers were extracted with hexanes (2x200 mL). The combined organic layers were washed with brine (100 mL), dried over Anhydrous sodium sulfate, filtered, and concentrated under reduced pressure. Purification by flash chromatography over silica gel deactivated with 1% Et_3N in hexanes (elution 100% hexanes) afforded 25.2 g (>99%) of **2.50** as a clear, colorless oil. R_f = 0.6 (100% hexanes); ^{1}H NMR (500 MHz, C_6D_6): δ 5.27–5.24 (m, 1H), 2.49–2.45 (m, 1H), 2.36–2.24 (m, 2H), 2.15–2.08 (m, 1H), 2.06–1.92 (m, 2H), 1.73–1.67 (m, 7H), 1.59 (s, 3H), 1.44 (ddt, *J* = 12.5, 8.9, 6.2 Hz, 1H), 1.28–1.21 (m, 2H), 1.13 (t, *J* = 4.0 Hz, 21H); ^{13}C NMR (125 MHz; C_6D_6): δ 147.4, 130.9, 125.6, 115.4, 44.8, 35.0, 33.4, 27.0, 25.9, 25.9, 18.2, 17.7, 13.3, 10.7; HRMS (CI) calculated for $C_{21}H_{41}OSi$ $[M]^+$: 336.2849, found: 336.2853.

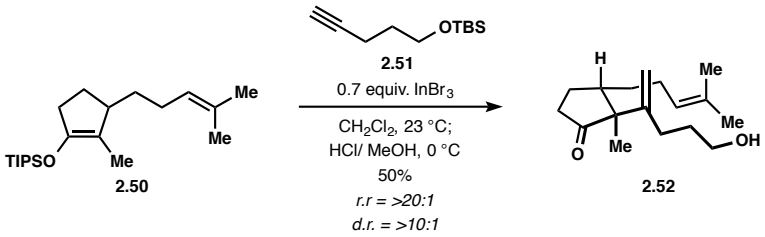

Alcohol **2.52**: A Schlenk flask was charged with $InBr_3$ (10.6 g, 30.0 mmol) in a nitrogen atmosphere glovebox. The flask was sealed with a plastic cap, removed from the glovebox, and connected to a double bank vacuum manifold. The plastic cap was replaced with a rubber septum under a positive atmosphere of nitrogen. The flask was charged with a solution of enoxysilane **2.50** (16.4 g, 48.8 mmol) and **2.51** (15.0 mL, 63.6 mmol) in CH_2Cl_2 (100 mL) via a cannula. The resulting mixture was vigorously stirred at room temperature. After 16 hours the flask was cooled to 0 ºC and quenched with 1% HCl in MeOH (100 mL, prepared using a concentrated aqueous solution of HCl). After 30 minutes the solution was transferred to a recovery flask and concentrated under reduced pressure. The residue was partitioned between methylene chloride (100 mL) and water (50 mL). The aqueous layer was extracted with methylene chloride (3x100 mL). The combined organics were washed with water (100 mL) and brine (100 mL), dried over anhydrous sodium sulfate, filtered, and concentrated under reduced pressure. Purification by flash chromatography (gradient elution: 100% hexanes to 30% v/v ethyl acetate in hexanes) afforded 6.4 g (50%) of **2.52** as a clear, colorless oil. R_f = 0.24 (30% v/v ethyl acetate in hexanes); ^{1}H NMR (500 MHz; $CDCl_3$): δ 5.09–5.06 (m, 2H), 5.03 (s, 1H), 3.70–3.60 (m, 2H), 2.48–2.42 (m, 1H), 2.28–1.85 (m, 8H), 1.78–1.71 (m, 2H), 1.68 (s, 3H), 1.60 (s, 3H), 1.56–1.51 (m, 1H), 1.43–1.37 (m, 1H), 1.27–1.20 (m, 1H), 1.00 (d, J = 1.3 Hz, 3H); ^{13}C NMR (125 MHz; $CDCl_3$): δ 222.6, 148.5, 132.1, 124.4, 112.4, 62.2, 59.1, 43.1, 38.0, 31.3, 29.7, 28.7, 26.1, 25.8, 25.4, 17.8, 14.9; HRMS (CI) calculated $C_{17}H_{28}O_2$ $[M]^+$: 264.2089, found, 264.2090.

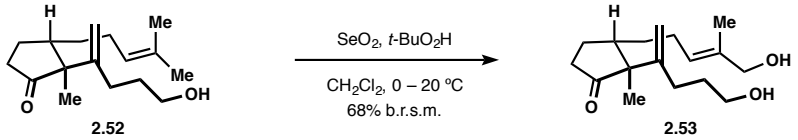

Diol **2.53**: A solution of tert-butyl hydroperoxide (11.4 mL of 5.82 M solution in decane, 66.3 mmol) was added to a mixture of alcohol **2.52** (6.3 g, 23.9 mmol) and selenium dioxide (1.47 g, 13.3 mmol) in methylene chloride (80 mL) at 0 °C. The resulting suspension was warmed up to room temperature and stirred 2.5 hours. The reaction was quenched with 10% w/v aqueous solution of Na_2CO_3 and extracted with diethyl ether. The aqueous layer was extracted with diethyl ether, and the combined organic layers were washed with brine, dried over anhydrous sodium sulfate, and concentrated under reduced pressure. Purification by flash chromatography (gradient elution: 20% v/v ethyl acetate in hexanes to 100% ethyl acetate) afforded 0.6 g (10%) of starting alcohol **2.52** and 4.1 g (68% yield based on recovered starting material) of diol **2.53** as a colorless oil. R_f = 0.13 (50% v/v ethyl acetate in hexanes); ^{1}H NMR (500 MHz; $CDCl_3$): δ 5.40-5.37 (m, 1H), 5.08 (s, 1H), 5.04 (s, 1H), 4.00 (s, 2H), 3.68-3.59 (m, 2H), 2.46 (dt, *J* = 16.8, 7.9 Hz, 1H), 2.32-1.98 (m, 7H), 1.94-1.88 (m, 1H), 1.75-1.71 (m, 2H), 1.65 (s, 3H), 1.57-1.42 (m, 2H), 1.37-1.31 (m, 1H), 1.27-1.23 (m, 1H), 1.00 (s, 3H); ^{13}C NMR (125 MHz; $CDCl_3$): δ 222.2, 148.6, 135.7, 125.0, 112.6, 68.6, 62.3, 59.0, 42.1, 38.0, 31.5, 29.3, 28.9, 25.4, 25.0, 14.8, 13.9; HRMS (CI) calculated for $C_{17}H_{28}O_3$ $[M+Na]^+$: 303.1936, found: 303.1932.

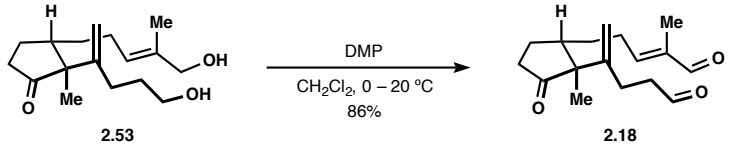

Dialdehyde **2.18**: Dess–Martin periodinane (1.6 g, 3.73 mmol) was added to a solution of diol **2.53** (418.1 mg, 1.49 mmol) in methylene chloride (8.0 mL) at 0 ºC. The reaction was vigorously stirred and allowed to warm to room temperature. After 1 hour the reaction was quenched with

water (5 mL) and a solution of saturated aqueous $NaHCO_3$ (9 mL) and diluted with ethyl acetate (20 mL). The biphasic mixture was filtered through a plug of celite and the plug was thoroughly rinsed with ethyl acetate (~100 mL). The combined organic layers were washed with brine (20 mL), dried over Anhydrous sodium sulfate, filtered, and concentrated under reduced pressure. Purification by flash chromatography gradient elution: 100% hexanes to 50% v/v ethyl acetate in hexanes) afforded 360 mg (86%) of **2.18** as a clear, colorless oil. R_f = 0.19 (30% v/v ethyl acetate in hexanes); ^{1}H NMR (500 MHz; $CDCl_3$): δ 9.77 (s, 1H), 9.41 (s, 1H), 6.48 (td, *J* = 7.2, 0.9 Hz, 1H), 5.05 (s, 1H), 5.01 (d, *J* = 1.3 Hz, 1H), 2.70-2.65 (m, 1H), 2.52-2.10 (m, 9H), 1.75 (s, 3H), 1.64-1.53 (m, 2H), 1.46-1.38 (m, 1H), 1.04 (s, 3H); ^{13}C NMR (125 MHz; $CDCl_3$): δ 220.7, 201.6, 195.2, 153.8, 147.7, 139.8, 112.8, 58.6, 43.5, 42.5, 37.8, 28.5, 27.1, 25.3, 24.6, 15.0, 9.4. HRMS (CI) calculated for $C_{17}H_{24}O_3$ $[M+Na]^+$: 299.1623, found: 299.1626.

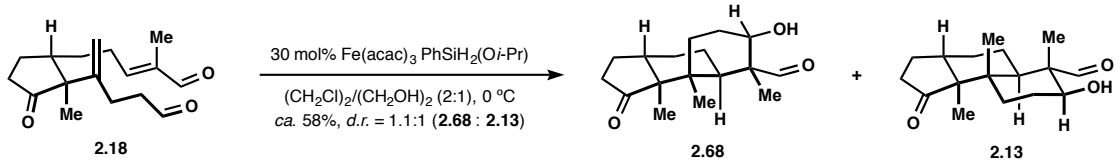

Tricycles **2.68** and **2.13**: A Schlenk flask was charged with iron(III) acetylacetonate (0.144 g, 0.41 mmol), dialdehyde **2.18** (0.340 g, 1.22 mmol), 1,2-dichloroethane (12 mL), and anhydrous ethylene glycol (6 mL). The mixture was degassed using a freeze-pump-thaw technique (3 cycles), cooled to 0 ˚C, and treated with (isopropoxy)phenylsilane[52] (0.600 g, 3.66 mmol). The reaction was stirred 1.5 h and quenched with 1 N aqueous solution of HCl (50 mL) and water (50 mL) Diethyl ether (100 mL) was added, and the mixture was stirred until the organic layer appeared colorless. The layers were separated, and the organic layer was dried over anhydrous sodium sulfate and concentrated under reduced pressure. Purification by flash chromatography (gradient elution: 100% hexanes to 50% v/v ethyl acetate in hexanes) afforded 0.199 g (ca. 58% yield) of a mixture of tricycles **2.68** and **2.13**. The mixture was separated by flash

chromatography (gradient elution: 100% hexanes to 20% v/v acetone in hexanes) to afford 0.081 g (24% yield) of pure tricycle **2.13** as a white solid and 0.074 g (22% yield) of pure hydroxyaldehyde **2.68** as a colorless amorphous solid. Crystals of **2.13**, suitable for X-ray crystallographic analysis, were obtained by slow evaporation from a solution of hexanes. For **2.13**: R_f = 0.16 (20% v/v acetone in hexanes); ^{1}H NMR (600 MHz, $CDCl_3$): ^{1}H NMR (600 MHz; $CDCl_3$): δ 9.39 (s, 1H), 3.74 (dt, *J* = 10.9, 5.2 Hz, 1H), 2.36–2.31 (m, 1H), 2.24–2.17 (m, 2H), 2.05–1.99 (m, 1H), 1.85-1.61 (m, 6H), 1.55–1.36 (m, 4H), 1.12 (td, *J* = 8.1, 3.0 Hz, 1H), 1.08 (s, 3H), 1.03 (s, 3H), 0.98 (s, 3H).; ^{13}C NMR (125 MHz, $CDCl_3$): δ 220.50 40.04 24.67 206.69 38.58 23.85 72.32 37.39 17.62 55.76 30.47 10.54 55.16 26.48 8.73 40.36 25.56. For **2.68**: R_f = 0.23 (20% v/v acetone in hexanes); ^{1}H NMR (500 MHz, $CDCl_3$): ^{1}H NMR (600 MHz; $CDCl_3$): δ 9.35 (s, 1H), 4.29 (t, *J* = 7.6 Hz, 1H), 2.36–2.30 (m, 1H), 2.11 (tdd, *J* = 12.0, 6.2, 3.1 Hz, 1H), 2.04–1.97 (m, 2H), 1.82–1.71 (m, 4H), 1.62–1.48 (m, 4H), 1.44 (d, *J* = 8.9 Hz, 3H), 1.43–1.38 (m, 3H), 1.26 (s, 3H), 1.00 (s, 3H).); ^{13}C NMR (125 MHz, $CDCl_3$): δ 219.87 39.55 25.16 205.17 39.20 23.29 67.27 36.96 22.70 54.04 27.60 17.23 53.59 25.89 11.67 45.04 25.60; HRMS calculated for $C_{17}H_{28}O_3N$ $[M+NH_4]^+$: 296.2226, found: 296.2231.

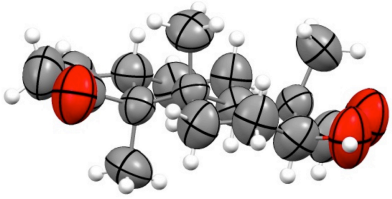

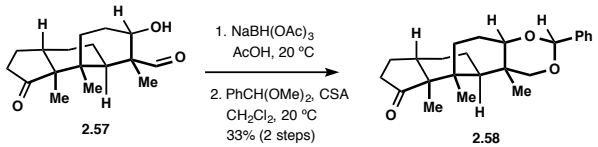

Ketal **2.58** was prepared by Eric J. Kuenstner as reported in the literature.[53]

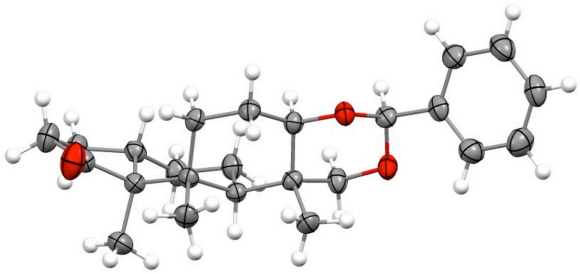

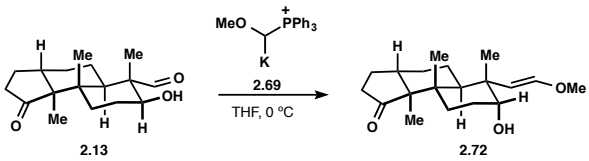

Axial alcohol **2.72**: A solution of phosphorane **2.69** [0.53 mL, 0.4 mmol, freshly prepared from (methoxymethyl)triphenylphosphonium bromide (514 mg, 1.5 mmol) and potassium *tert*-pentoxide (0.14 mL, 1.0 M in C_6H_{12}) in toluene (2.0 mL)] was added to tricycle **2.13** (20 mg, 0.07 mmol) in toluene (0.2 mL) at 0 ºC. The reaction was vigorously stirred at 0 ºC. After 3.5 hours the reaction was quenched with water, diluted with diethyl ether, dried over anhydrous sodium sulfate, filtered, and concentrated under reduced pressure. Purification by flash chromatography (gradient elution: 100% hexanes to 20% v/v ethyl acetate in hexanes) afforded ~7 mg (~33%) of **2.72** as a thin film. ^{1}H NMR (600 MHz; $CDCl_3$): δ 5.86 (d, J = 7.2 Hz, 1H), 4.01 (d, J = 7.2 Hz, 1H), 3.76 (t, J = 2.6 Hz, 1H), 3.58 (d, J = 3.0 Hz, 3H), 2.31 (dd, J = 19.2, 8.4 Hz, 1H), 2.22 (dddd, J = 12.2, 9.1, 6.0, 3.1 Hz, 1H), 2.13 (dd, J = 12.1, 2.7 Hz, 2H), 2.06–1.96 (m, 2H), 1.85 (tt, J = 14.0, 2.9 Hz, 1H), 1.78 (dtd, J = 15.1, 7.7, 4.5 Hz, 2H), 1.69 (ddq, J = 14.1, 7.0, 3.5 Hz, 2H), 1.56–1.49 (m, 2H), 1.42–1.34 (m, 2H), 1.07 (s, 3H), 1.03 (s, 3H), 1.00 (s, 3H); ^{13}C NMR (125 MHz; $CDCl_3$): δ 221.3, 146.4, 113.7, 72.6, 60.1, 44.5, 40.8, 39.7, 38.5, 37.6, 29.7, 26.4, 24.7, 23.85, 23.80, 23.65, 19.7, 17.8, 10.5.

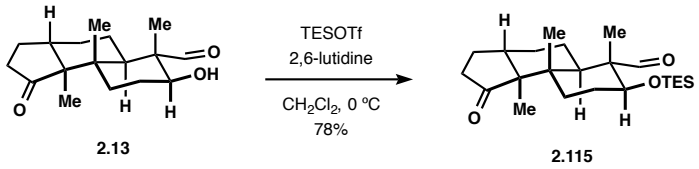

2.13 2.115

TES Ether **2.115**: Triethylsilyl trifluoromethanesulfonate (20 μL, 0.09 mmol) and 2,6-lutidine (16 μL, 0.14 mmol) were added to a solution of tricycle **2.13** (16.8 mg, 0.06 mmol) in methylene chloride (1.2 mL) at 0 ºC. The reaction was vigorously stirred at 0 ºC. After 1 hour the reaction was quenched with a solution of saturated aqueous $NaHCO_3$ (50 μL), diluted with methylene chloride, filtered through a plug of anhydrous sodium sulfate, and concentrated under reduced pressure. Purification by flash chromatography (gradient elution: 100% hexanes to 10% v/v ethyl acetate in hexanes) afforded 18.5 mg (78%) of TES ether **2.115** as a thin film. R_f = 0.21 (5% v/v ethyl acetate in hexanes); ^{1}H NMR (500 MHz; $CDCl_3$): δ 9.31 (s, 1H), 3.74 (dd, *J* = 11.3, 4.7 Hz, 1H), 2.32 (dd, *J* = 19.3, 7.8 Hz, 1H), 2.17 (ddt, *J* = 13.2, 6.8, 3.4 Hz, 2H), 2.00 (dt, *J* = 19.2, 9.5 Hz, 1H), 1.83–1.63 (m, 5H), 1.60–1.50 (m, 3H), 1.45–1.32 (m, 2H), 1.07 (s, 3H), 1.02 (s, 3H), 0.97 (s, 3H), 0.90 (t, *J* = 8.0 Hz, 9H), 0.52 (qd, *J* = 7.9, 3.9 Hz, 6H); ^{13}C NMR (125 MHz; $CDCl_3$): δ 220.6, 207.3, 73.8, 55.92, 55.83, 40.4, 39.7, 38.5, 37.4, 30.5, 27.1, 25.6, 24.6, 23.9, 17.7, 10.5, 9.3, 6.9, 5.2; LRMS (ESI) calculated for $C_{23}H_{40}O_3SiNa$ $[M+Na]^+$: 415.3, found: 415.2.

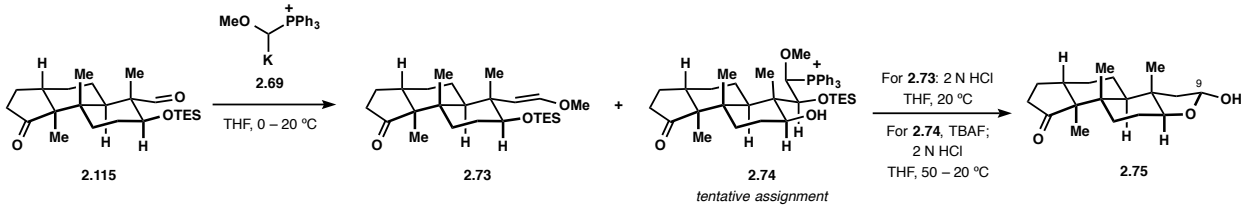

2.115 2.73 2.74 2.75

tentative assignment

Alkene **2.73** and phosphonium salt **2.74**: A Schlenk flask was charged with (methoxymethyl)triphenylphosphonium chloride (48.1 mg, 0.14 mmol) and toluene (1.0 mL). The flask was exposed to hi-vacuum, to azeotrope off any residual water, until a free-flowing

white powder remained. The flask was placed under an atmosphere of nitrogen and THF (0.6 mL) was added. The suspension was cooled to 0 ºC and potassium hexamethyldisilizide (0.28 mL, 0.5 M in toluene, 0.14 mmol) was added. The reaction was vigorously stirred at 0 ºC. After 20 minutes a solution of TES ether **2.115** (18.5 mg, 0.05 mmol) in THF (0.5 mL) was added via a cannula. The reaction was vigorously stirred and allowed to warm to room temperature. After 1 hour the reaction was quenched with 1 N aqueous solution of solution of HCl (0.5 mL) and diluted with diethyl ether (5 mL). The layers were separated and the organic layer was dried over anhydrous sodium sulfate, filtered, and concentrated under reduced pressure. Purification by flash chromatography (gradient elution: 100% hexanes to 5% ethyl acetate in hexanes; 5% methanol in methylene chloride) afforded **2.73** and **2.74**. Diagnostic ^{1}H NMR signals for **2.73**: ^{1}H NMR (600 MHz; $CDCl_3$): δ 6.04 (d, *J* = 12.8 Hz, 1H), 5.65 (t, *J* = 4.9 Hz, 2.8H), 4.39 (d, *J* = 12.7 Hz, 1H), 3.86 (d, *J* = 7.3 Hz, 2.6H), 3.69 (dd, *J* = 11.3, 4.3 Hz, 2.6H), 3.21 (dd, *J* = 11.3, 4.4 Hz, 1H). Diagnostic ^{1}H NMR signals for **2.74**: ^{1}H NMR (600 MHz; $CDCl_3$): δ 8.11 (dd, *J* = 11.6, 8.0 Hz, 13H), 8.01 (dd, *J* = 11.8, 7.9 Hz, 7H), 6.91 (d, *J* = 9.9 Hz, 1H), 6.41 (d, *J* = 7.4 Hz, 2H), 5.48-5.46 (m, 2H), 4.56-4.53 (m, 1H), 3.78 (t, *J* = 5.6 Hz, 2H), 3.61 (dd, *J* = 9.2, 8.1 Hz, 1H).

Lactol **2.75** from alkene **2.73**: A dram vial was charged with **2.73**, 2 N aqueous solution of HCl (0.2 mL) and THF (0.4 mL). The reaction was vigorously stirred at room temperature. After 1 hour the reaction was neutralized with a solution of saturated aqueous $NaHCO_3$ and extracted with methylene chloride. The organic layers were dried over anhydrous sodium sulfate, filtered and concentrated under reduced pressure. The crude material was combined with the crude material from the conversion of **2.74** to **2.75**. R_f = 0.18 (30% v/v ethyl acetate in hexanes); Diagnostic ^{1}H NMR signals **2.75**: ^{1}H NMR (500 MHz; $CDCl_3$): δ 5.57 (t, *J* = 5.0 Hz, 1H), 3.49 (dd, *J* = 11.9, 3.3 Hz, 1H).

Lactol **2.75** from alkene **2.73**: A dram vial was charged with **2.74**, THF (0.4 mL) and TBAF (5 drops, 1 M in THF). The vial was vigorously stirred and heated at 50 ºC. After 1.5 hours the vial was cooled to 20 ºC and a 2 N aqueous solution of HCl (0.4 mL) was added. After an additional 24 hours the reaction was neutralized with a solution of saturated aqueous $NaHCO_3$ and extracted with methylene chloride. The organic layers were dried over anhydrous sodium sulfate, filtered and concentrated under reduced pressure. The crude material was combined with the crude material from the conversion of **2.73** to **2.75**. R_f = 0.18 (30% v/v ethyl acetate in hexanes).

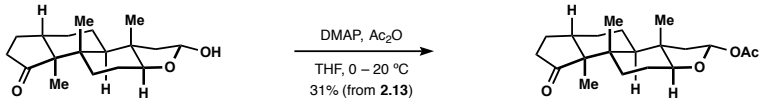

2.75 **2.76**

Acetate **2.76**: Acetic anhydride (18 µL, 0.19 mmol) was added to a solution of crude **2.73** and **2.74** (~0.047 mmol) and DMAP (11 mg, 0.09 mmol) in THF (0.5 mL) at 0 ºC. The reaction was vigorously stirred and allowed to warm to room temperature. After 50 minutes the reaction mixture was diluted with diethyl ether (3 mL) and quenched with a mixture of brine:water (2:1, 1.5 mL). The organic layer was dried over anhydrous sodium sulfate, filtered, and concentrated under reduced pressure. Purification by flash chromatography (gradiuent elution: 100% hexanes to 15% v/v ethyl acetate in hexanes) afforded 6.2 mg (31% from **2.13**) of acetate **2.76** as a thin film. R_f = 0.44 (30% v/v ethyl acetate in hexanes); ^{1}H NMR (600 MHz; $CDCl_3$) [minor presence of grease]: δ 6.27 (t, *J* = 5.5 Hz, 1H), 3.43 (dd, *J* = 12.3, 3.5 Hz, 1H), 2.33 (dd, *J* = 18.9, 8.1 Hz, 1H), 2.25 (dt, *J* = 13.7, 3.2 Hz, 1H), 2.18 (td, *J* = 6.1, 3.7 Hz, 3H), 2.07 (s, 3H), 2.04–1.97 (m, 2H), 1.91–1.88 (m, 1H), 1.85–1.80 (m, 1H), 1.75–1.68 (m, 3H), 1.63–1.58 (m, 3H), 1.54–1.49 (m, 3H), 1.44–1.39 (m, 3H), 0.99 (s, 3H), 0.95 (s, 3H), 0.84 (d, *J* = 1.1 Hz, 3H); ^{13}C NMR (150 MHz; $CDCl_3$): δ 220.9, 170.8, 98.5, 87.1, 56.4, 48.4, 46.6, 45.4, 40.39, 40.34, 37.5, 31.8, 25.8, 24.7, 24.1, 21.65, 21.53, 20.0, 16.0, 10.6.

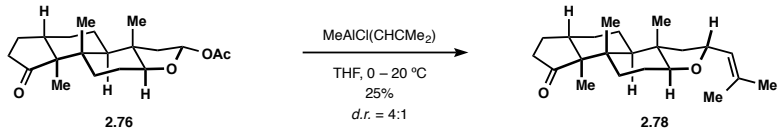

2.76 2.78

Preparation of $MeAlCl(CHCMe_2)$: A Schlenk flask was charged with $AlCl_3$ (66.7 mg, 0.5 mmol) in a nitrogen atmosphere glovebox. The flask was sealed with a plastic cap, removed from the glovebox, and connected to a double bank vacuum manifold. The plastic cap was replaced with a rubber septum under a positive atmosphere of nitrogen. The flask was cooled to 0 ºC and THF (1.6 mL) was added. The reaction mixture was allowed to age at 0 ºC until homogeneity was achieved (~15 minutes). Vigorous stirring was initiated and methylmagnesium bromide (0.18 mL, 2.77 M in diethyl ether, 0.5 mmol) was added and a heterogeneous mixture resulted. After 5 minutes the flask was allowed to warm to room temperature. After an additional 30 minutes 2-methyl-1-propenylmagnesium bromide (1.1 mL. 0.46 M in THF, 0.5 mmol) was added dropwise and homogeneity ensued. The solution was stirred for an additional 25 minutes prior to use.

Tetracycle **2.78**: $MeAlCl(CHCMe_2)$ (0.44 mL, 0.074, 0.17 M, freshly prepared) was added to a solution of acetate **2.76** (6.2 mg, 0.019 mmol) in THF (0.2 mL) at 0 ºC. The reaction was vigorously stirred and allowed to warm to room temperature. After 1 hour the reaction was quenched with a solution of saturated aqueous NH_4Cl (0.1 mL), diluted with diethyl ether (10 mL), and filtered through a plug of anhydrous sodium sulfate. Purification by flash chromatography (gradient elution: 100% hexanes to 15% v/v ethyl acetate in hexanes) afforded 1.6 mg (*ca*. 25%) of tetracycle **2.78** as a thin film. $R_f = 0.37$ (20% v/v ethyl acetate in hexanes); ^1H NMR (600 MHz; $CDCl_3$) [water impurity present]: δ 5.30 (d, $J = 8.9$ Hz, 1H), 4.78 (q, $J = 7.8$ Hz, 1H), 3.14 (dd, $J = 11.8, 3.4$ Hz, 1H), 2.32 (dd, $J = 19.2, 8.5$ Hz, 1H), 2.22-2.17 (m, 2H), 2.05-1.97 (m, 2H), 1.90 (dd, $J = 11.4, 6.8$ Hz, 1H), 1.85-1.79 (m, 2H), 1.72 (s, 4H), 1.68 (s, 3H),

1.64-1.50 (m, 15H), 1.46-1.40 (m, 4H), 1.19-1.16 (m, 1H), 1.00 (s, 3H), 0.93 (s, 3H), 0.86 (s, 3H); LRMS (ESI) calculated for $C_{22}H_{34}O_2Na$ $[M+Na]^+$: 353.2, found: 353.4.

NOESY Correlations

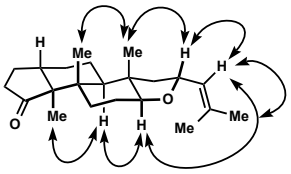

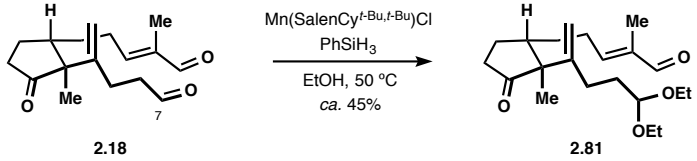

2.18 **2.81**

Ketal **2.81**: A solution of dialdehyde **2.18** (11.1 mg, 0.04 mmol) and Mn(SalenCy$^{t\text{-Bu},t\text{-Bu}}$)Cl in ethanol (0.8 mL) was sparged with nitrogen for 30 minutes. After degassing was complete phenylsilane (10 µL, 0.08 mmol) was charged into the solution. The reaction was heated to 50 ºC and vigorously stirred. After 45 minutes the reaction was cooled to room temperature and diluted with diethyl ether (15 mL). The solution was washed with 1 N aqueous solution of HCl (1 mL), dried over anhydrous sodium sulfate, filtered, and concentrated under reduced pressure. Purification by flash chromatography (gradient elution: 100% hexanes to 30% v/v ethyl acetate in hexanes) afforded ~5 mg (~36%) as a thin film. ^{1}H NMR (500 MHz; $CDCl_3$): δ 9.40 (s, 1H), 6.45 (td, *J* = 7.3, 1.1 Hz, 1H), 5.09 (s, 1H), 5.02 (s, 1H), 4.46 (t, *J* = 5.5 Hz, 1H), 3.67-3.58 (m, 2H), 3.51–3.44 (m, 2H), 2.50–2.16 (m, 6H), 1.95 (ttd, *J* = 15.7, 10.5, 5.1 Hz, 2H), 1.84–1.77 (m, 1H), 1.75–1.73 (m, 3H), 1.63–1.53 (m, 3H), 1.45–1.38 (m, 1H), 1.19 (t, *J* = 7.0 Hz, 6H), 1.03 (s, 3H); ^{13}C NMR (125 MHz; $CDCl_3$): δ 220.8, 195.2, 153.8, 148.8, 139.8, 112.4, 102.6, 61.6, 61.0, 43.4, 37.9, 32.7, 28.6, 27.6, 27.2, 25.4, 15.5, 15.1.

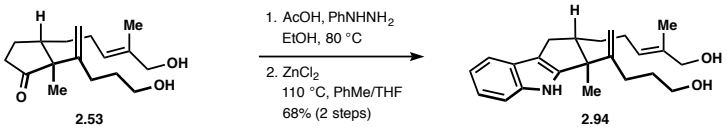

2.53 **2.94**

Indole diol **2.94**: Acetic acid (1.5 mL, 25.7 mmol) and phenylhydrazine (2.5 mL, 25.7 mmol) were added to a solution of keto-diol **2.53** (4.8 g, 17.1 mmol) in ethanol (17 mL). The reaction mixture was heated to 80 ºC and vigorously stirred. After 2 hours the mixture was allowed to cool to room temperature and concentrated under reduced pressure. Excess phenylhydrazine was removed by flash chromatography (10% acetone in methylene chloride) to afford 5.8 g (92%) of the crude hydrazone (not shown). An oven-dried three-neck flask was equipped with a distillation head in the middle position, rubber septa in the two side positions, and a nitrogen inlet on the distillation head. The assembled system was allowed to cool to room temperature under a stream of nitrogen. Once cooled, a solution of the crude hydrazone (5.8 g) in toluene (200 mL) and a solution of anhydrous $ZnCl_2$ (30 mL,, 15.0 mmol, 0.5 M in THF) were added. The reaction solution was vigorously stirred and heated to 110 ºC. Additional portions of anhydrous $ZnCl_2$ (15 mL, 7.5 mmol, 0.5 M in THF) were added after 9 hours, 29 hours, and 40 hours. After 45 hours the reaction was judged complete (monitored by ^{1}H NMR analysis of aliquots) and was cooled to room temperature. The solution was transferred via cannula to a vigorously stirred solution of saturated aqueous $NaHCO_3$ (350 mL). A solid residue resulted and was triturated with methylene chloride (3x400 mL). The combined organic solutions were washed with water (300 mL) and brine (300 mL), dried over anhydrous sodium sulfate, filtered, and concentrated under reduced pressure. Purification by flash chromatography (gradient elution: 30 v/v ethyl acetate to 40% v/v ethyl acetate in hexanes) afforded 2.7 g (68% from **2.53**) of indole diol **2.94** as a yellow foam. R_f = 0.25 (50% v/v ethyl acetate in hexanes); ^{1}H NMR (500 MHz; $CDCl_3$): δ 7.91 (s, 1H), 7.47–7.45 (m, 1H), 7.29–7.27 (m, 1H), 7.11–7.07 (m, 2H), 5.43 (td, *J* = 7.2, 1.2 Hz, 1H), 5.13 (s, 1H), 5.05 (s, 1H), 3.99 (s, 2H), 3.57 (tt, *J* = 8.6, 4.3 Hz, 2H), 3.08 (dd, *J* = 13.7, 7.6 Hz, 1H), 2.83 (ddd, *J* = 8.2, 6.6, 3.6 Hz, 1H), 2.43 (dd, *J* = 13.7, 9.0 Hz,

1H), 2.23–1.94 (m, 6H), 1.76–1.71 (m, 2H), 1.69 (s, 3H), 1.63–1.50 (m, 2H), 1.21 (s, 3H); ^{13}C NMR (125 MHz; $CDCl_3$): δ 152.6, 149.5, 140.3, 135.5, 125.4, 124.9, 120.7, 119.6, 118.7, 117.0, 111.7, 110.5, 68.7, 62.6, 51.4, 50.9, 32.1, 29.72, 29.61, 28.5, 25.8, 19.2, 13.9; HRMS (ESI) calculated for $C_{23}H_{31}NO_2Na$ $[M+Na]^+$: 376.2253, found: 376.2242.

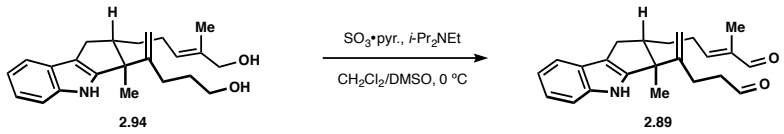

Indole dialdehyde **2.89**: *i*-Pr_2NEt (0.18 mL, 1.0 mmol) followed by a solution of SO_3•pyr (127.7 mg, 0.8 mmol) in DMSO (1.7 mL) were added to a solution of indole diol **2.94** (35 mg, 0.1 mmol) in methylene chloride (0.6 mL) at 0 ºC. The reaction was vigorously stirred at 0 ºC. After 20 minutes the reaction was quenched with water (5 mL) and extracted with diethyl ether (3x10 mL). The combined organic layers were washed with brine (5 mL), dried over anhydrous $MgSO_4$, filtered, and concentrated under reduced pressure. ^{1}H NMR (600 MHz; C_6H_6): δ 9.39 (s, 1H), 9.16 (s, 1H), 7.65 (d, *J* = 7.6 Hz, 1H), 7.27–7.19 (m, 5H), 5.94 (t, *J* = 7.3 Hz, 1H), 4.96 (s, 1H), 4.67 (s, 1H), 2.87 (dd, *J* = 13.6, 7.5 Hz, 1H), 2.59–2.54 (m, 1H), 2.23 (dd, *J* = 13.7, 9.0 Hz, 1H), 2.07–1.89 (m, 8H), 1.70 (s, 3H), 1.38–1.33 (m, 2H), 1.30–1.22 (m, 1H), 1.05 (s, 3H).

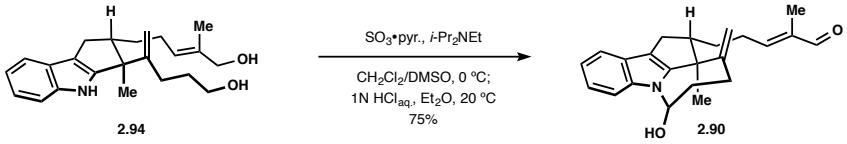

Hemiaminal **2.90**: *i*-Pr_2NEt (2.1 mL, 12.0 mmol) followed by a solution of SO_3•pyr (1.4 g, 9.0 mmol) in DMSO (4.2 mL) were added to a solution of indole diol **2.94** (530 mg, 1.5 mmol) in methylene chloride (10.8 mL) at 0 ºC. The reaction was vigorously stirred at 0 ºC. After 30 minutes the reaction was allowed to warm to room temperature. After an additional hour the reaction was quenched with a 1 N aqueous solution of NaOH (5 mL). The resulting solution was vigorously stirred at room temperature. After 2 hours the mixture was extracted with methylene

chloride (3x60 mL). The combined organic layers were washed with brine (20 mL), dried over anhydrous sodium sulfate, filtered and concentrated under reduced pressure. The crude oil was dissolved in DMSO (15 mL) and treated with a 1 N aqueous solution of HCl (2.5 mL). The reaction mixture was vigorously stirred overnight. The solution was diluted with water (50 mL) and extrached with diethyl ether (3x75 mL). To combined organic layers were washed with brine (20 mL), dried over anhydrous magnesium sulfate, filtered, and concentrated under reduced pressure. Purification by flash chromatography (gradient elution: 100% hexanes to 20% v/v ethyl acetate in hexanes afforded 0.39 g (75%) of hemiaminal **2.90**. R_f = 0.35 (20% v/v ethyl acetate in hexanes); ^{1}H NMR (600 MHz; C_6H_6): δ 9.34 (s, 1H), 7.63 (d, *J* = 7.7 Hz, 1H), 7.29–7.27 (m, 1H), 7.22 (td, *J* = 7.7, 1.2 Hz, 1H), 7.01 (d, *J* = 8.2 Hz, 1H), 5.95 (td, *J* = 7.4, 1.0 Hz, 1H), 5.58 (dt, *J* = 4.4, 2.2 Hz, 1H), 4.80 (s, 1H), 4.71 (s, 1H), 3.28–3.23 (m, 1H), 2.91–2.87 (m, 2H), 2.30–2.26 (m, 1H), 2.16–2.11 (m, 1H), 2.09–2.04 (m, 2H), 1.97 (dt, *J* = 16.1, 7.8 Hz, 1H), 1.73 (t, *J* = 2.3 Hz, 1H), 1.70 (d, *J* = 0.6 Hz, 3H), 1.63–1.57 (m, 1H), 1.50–1.43 (m, 2H), 1.35 (s, 3H); ^{13}C NMR (151 MHz; C6D6): δ 194.0, 153.7, 152.8, 140.2, 139.9, 125.2, 121.0, 120.4, 119.3, 115.2, 110.4, 109.7, 108.6, 75.0, 52.0, 50.6, 36.0, 29.6, 29.3, 28.9, 27.7, 20.6, 9.3; HRMS (ESI) calculated for $C_{23}H_{27}NO_2Na$ $[M+Na]^+$: 372.1939, found: 372.1936.

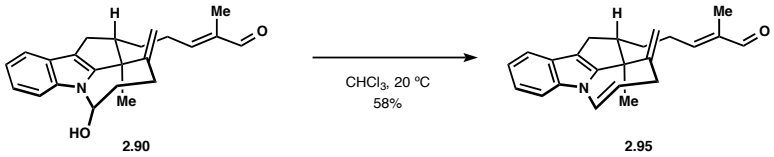

Enamine **2.95**: Hemiaminal **2.90** (170 mg, 0.49 mmol) was dissolved in chloroform and allowed to age overnight. Chloroform was removed under reduced pressure. Purification by flash chromatography afforded 98.4 mg (58%) of enamine **2.95**. ^{1}H NMR (600 MHz; $CDCl_3$): δ 9.45 (s, 1H), 7.44–7.42 (m, 1H), 7.34 (d, *J* = 8.0 Hz, 1H), 7.17–7.11 (m, 2H), 6.95 (dt, *J* = 9.0, 1.6 Hz, 1H), 6.60–6.58 (m, 1H), 5.19 (dt, *J* = 9.0, 5.6 Hz, 1H), 4.95 (s, 1H), 4.88 (s, 1H), 3.21–3.02 (m,

4H), 2.63–2.54 (m, 2H), 2.48 (dq, J = 15.6, 7.8 Hz, 1H), 1.91 (dddd, J = 13.1, 9.8, 6.8, 3.2 Hz, 1H), 1.86-1.80 (m, 4H), 1.24 (s, 3H).

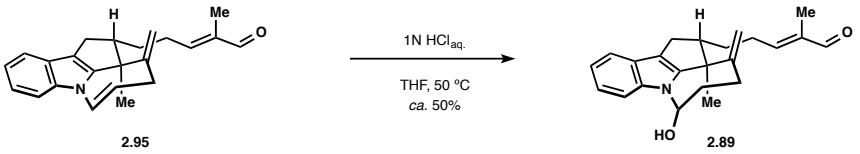

Hemiaminal **2.89**: An open flask was charged with enamine **2.95** (98.4 mg), THF (4 mL), and a 1 N aqueous solution of HCl (4 mL). The mixture was heated to 40 ºC and vigorously stirred. After 15 hours the reaction was cooled to room temperature and neutralized. The organic layer was dried over anhydrous sodium sulfate, filtered, and concentrated under reduced pressure. Purification by flash chromatography afforded 52 mg (*ca.* 50%) of hemiaminal **2.89**.

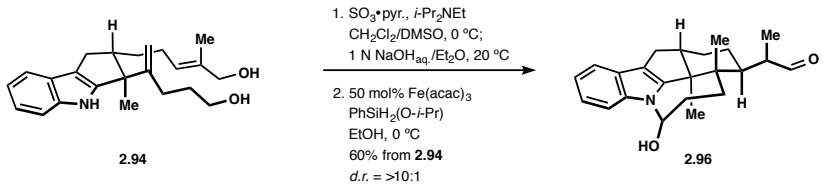

Pentacycle **2.96**: *i*-Pr$_2$NEt (1.0 mL, 5.7 mmol) followed by a solution of SO$_3$•pyr (0.72 g, 4.5 mmol) in DMSO (8.1 mL) were added to a solution of indole diol **2.94** (200. mg, 0.57 mmol) in methylene chloride (3.3 mL) at 0 ºC. The reaction was vigorously stirred at 0 ºC. After 30 minutes the reaction was quenched with water (11 mL) and extracted diethyl ether (3x10 mL). The combined organic layers were treated with a 1 N aqueous solution of NaOH (10 mL) and the biphasic mixture was vigorously stirred at room temperature. After 1 hour the organic layer washed with brine (10 mL), dried over anhydrous magnesium sulfate, filtered, and concentrated under reduced pressure. The crude hemiaminal **2.93** was used without further purification. Iron(III) acetylacetonate (0.102 g, 0.29 mmol) was added to a solution of the crude hemiaminal **2.93** in ethanol (11 mL). The resulting mixture was thoroughly degassed using a frezze-pump-thaw technique (three cycles). The solution was cooled to 0 ºC and was treated with

(isopropoxy)phenylsilane[50] (0.284 g, 1.71 mmol). The reaction mixture was vigorously stirred at 0 ºC. After 1 hour the reaction was quenched with a degassed (sparged with argon) solution of saturated aqueous $NaHCO_3$ (11 mL). The aqueous layer was diluted with water (11 mL) and brine (11 mL). The combine aqueous layer was extracted with diethyl ether (3x35 mL). The combined organic layers were washed with brine (35 mL), dried over anhydrous magnesium sulfate, filtered, and concentrated under reduced pressure. Purification by flash chromatography (elution with 10% v/v ethyl aceate in hexanes) afforded 0.12 g of pentacycle **2.96** (60% from **2.94**) as a tan solid. R_f = 0.23 (20% v/v ethyl acetate in hexanes); ^{1}H NMR (500 MHz; C_6H_6): δ 9.48 (d, *J* = 2.8 Hz, 1H), 7.58 (d, *J* = 7.8 Hz, 1H), 7.24 (t, *J* = 7.4 Hz, 1H), 7.20–7.18 (m, 1H), 7.06 (d, *J* = 8.1 Hz, 1H), 5.62 (s, 1H), 2.67 (dd, *J* = 12.8, 6.3 Hz, 1H), 2.47 (dd, *J* = 6.2, 3.7 Hz, 1H), 2.37 (dd, *J* = 12.8, 10.3 Hz, 1H), 2.21 (dt, *J* = 7.0, 2.5 Hz, 1H), 2.08 (t, *J* = 12.7 Hz, 1H), 1.87–1.83 (m, 2H), 1.78–1.68 (m, 2H), 1.53–1.41 (m, 2H), 1.31–1.21 (m, 3H), 1.10 (d, *J* = 8.0 Hz, 3H), 0.89 (dd, *J* = 6.9, 4.7 Hz, 3H), 0.73 (s, 3H); ^{13}C NMR (125 MHz; $CDCl_3$): δ 204.7, 152.7, 140.1, 128.4, 127.1, 120.4, 119.4, 116.3, 109.9, 75.8, 50.0, 47.4, 45.73, 45.68, 40.9, 30.1, 29.6, 28.5, 25.1, 24.7, 18.8, 15.4, 14.6; HRMS (ESI) $C_{23}H_{29}NO_2Na$ $[M+Na]^+$: 374.2096, found: 374.2092.

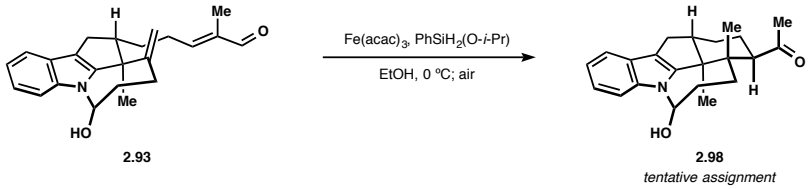

2.93 2.98
tentative assignment

Methyl ketone **2.98**: A dram vial was charged with hemiaminal **2.93** (5 mg, 0.014 mmol), iron(III) acetylacetonate (5 mg, 0.014 mmol), and EtOH (0.3 mL). The vial was cooled to 0 ºC and (isopropoxy)phenylsilane[50] (7 µL, 0.043) was added. The reaction was vigorously stirred at 0 ºC. After 30 minutes the reaction was quench by bubbling air through the solution and solvent

was removed under reduced pressure. Purification was performed by flash chromatography. Diagnostic ^{1}H NMR signals: ^{1}H NMR (600 MHz; $CDCl_3$): δ 7.43–7.41 (m, 1H), 7.34 (d, *J* = 8.1 Hz, 1H), 7.14–7.08 (m, 2H), 6.17 (t, *J* = 2.8 Hz, 1H), 3.06–3.03 (m, 1H), 2.80–2.74 (m, 2H), 2.52–2.48 (m, 1H), 2.42–2.37 (m, 1H), 2.30–2.24 (m, 3H), 2.21 (s, 3H), 1.99–1.91 (m, 1H), 1.81–1.76 (m, 4H), 1.22 (s, 3H), 1.06 (s, 3H).

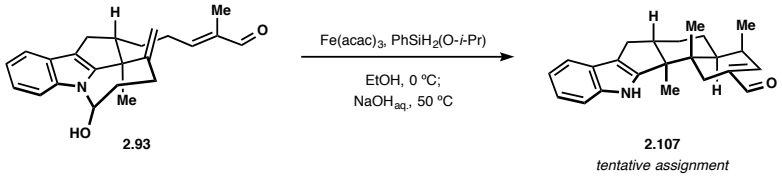

2.93 2.107
tentative assignment

Aldehyde **2.107**: Iron(III) acetylacetonate (5 mg, 0.019 mmol) was added to a solution of hemiaminal **2.93** (5 mg, 0.019 mmol) in ethanol (0. mL). The resulting mixture was thoroughly degassed using a frezze-pump-thaw technique (three cycles). The solution was cooled to 0 ºC and was treated with (isopropoxy)phenylsilane[50] (7 μL, 0.043 mmol). The reaction mixture was vigorously stirred at 0 ºC. After 1 h the reaction was quenched with a 1 N aqueous solution of NaOH (0.2 mL) and heated to 50 ºC. After 40 minutes the reaction was cooled to room temperature and neutralized with a 1 N aqueous solution of HCl (0.2 mL). The mixture was extracted with diethyl ether (3x7 mL). The combined organic layers were washed with a 1 N aqueous solution of HCl (1 mL), dried over anhydrous sodium sulfate, filtered and concentrated under reduced pressure. Purification by flash chromatography (gradient elution: 100% hexanes to 7% v/v ethyl acetate in hexanes) afforded 1.5 mg (*ca.* 30%) of aldehyde **2.107** as a thin film. ^{1}H NMR (600 MHz; $CDCl_3$): δ 9.52 (s, 1H), 7.98 (s, 1H), 7.44 (d, *J* = 7.4 Hz, 1H), 7.34 (d, *J* = 7.5 Hz, 1H), 7.12–7.06 (m, 2H), 6.64 (t, *J* = 2.0 Hz, 1H), 2.82 (dddd, *J* = 13.3, 10.1, 6.6, 3.3 Hz, 1H), 2.72 (dd, *J* = 13.3, 6.5 Hz, 1H), 2.53 (d, *J* = 16.7 Hz, 1H), 2.39 (dd, *J* = 13.3, 10.6 Hz, 1H), 2.31 (d, *J* = 16.4 Hz, 1H), 1.98 (ddd, *J* = 11.4, 5.4, 3.4 Hz, 1H), 1.77 (dtd, *J* = 10.4, 5.1, 2.5 Hz,

1H), 1.69 (qd, *J* = 12.9, 4.2 Hz, 1H), 1.27–1.22 (m, 4H), 1.20 (t, *J* = 6.3 Hz, 3H), 1.01 (s, 3H), 0.91 (s, 3H).

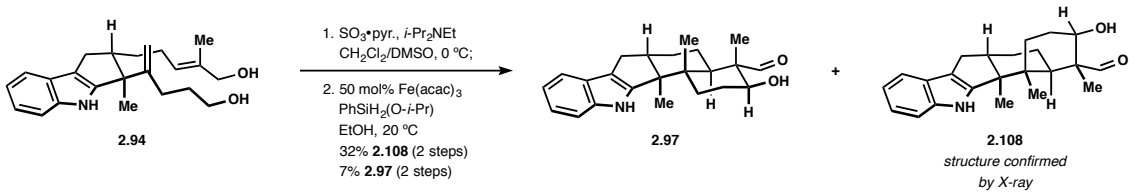

Undesired Pentacycle **2.108**: *i*-Pr_2NEt (0.18 mL, 1.0 mmol) followed by a solution of SO_3•pyr (127.7 mg, 0.8 mmol) in DMSO (1.7 mL) were added to a solution of indole diol **2.94** (35 mg, 0.1 mmol) in methylene chloride (0.6 mL) at 0 ºC. The reaction was vigorously stirred at 0 ºC. After 20 minutes the reaction was quenched with water (5 mL) and extracted with diethyl ether (3x10 mL). The combined organic layers were washed with brine (5 mL), dried over anhydrous $MgSO_4$, filtered, and concentrated under reduced pressure. The crude dialdehyde **2.92** was used without further purification. Iron(III) acetylacetonate (17.7 mg, 0.05 mmol) was added to a solution of the crude hemiaminal **2.93** in ethanol (2 mL). The resulting mixture was thoroughly degassed using a frezze-pump-thaw technique (three cycles). The solution was cooled to 0 ºC and was treated with (isopropoxy)phenylsilane[50] (50 μL, 0.3 mmol). The reaction mixture was vigorously stirred at 0 ºC. After 30 minutes the reaction was quenched with a degassed (sparged with argon) solution of saturated aqueous $NaHCO_3$ (1 mL). The aqueous layer was extracted with diethyl ether (3x10 mL). The combined organic layers were washed with a solution of 1 N aqueous HCl (4 mL), a solution of saturated aqueous $NaHCO_3$ (5 mL), and brine (3 mL). The organic layer was dried over anhydrous magnesium sulfate, filtered, and concentrated under reduced pressure. Purification by flash chromatography (gradient elution: 100% hexanes to 30% v/v ethyl aceate in hexanes) afforded 11.3 mg (32%) of the undesired pentacycle **2.108** and 2.5 mg (7%) of the desired pentacycle **2.97** as thin films. Crystals of **2.108**, suitable for X-ray

crystallographic analysis, were obtained by slow evaporation from a solution of hexanes. ^{1}H NMR (500 MHz; $CDCl_3$): δ 9.41 (s, 1H), 7.82 (s, 1H), 7.43 (d, *J* = 7.2 Hz, 1H), 7.30 (d, *J* = 7.5 Hz, 1H), 7.09 (quintet, *J* = 6.8 Hz, 2H), 4.32 (t, *J* = 8.4 Hz, 1H), 2.77–2.67 (m, 2H), 2.47 (br s, 1H), 2.35 (dd, *J* = 12.9, 10.1 Hz, 1H), 2.15 (t, *J* = 9.2 Hz, 1H), 2.05 (dd, *J* = 22.5, 9.3 Hz, 1H), 1.81 (q, *J* = 4.8 Hz, 2H), 1.65 (dd, *J* = 12.7, 5.3 Hz, 3H), 1.51–1.47 (m, 5H), 1.38-1.34 (m, 1H), 1.31 (s, 3H), 1.04 (s, 3H). ^{13}C NMR (125 MHz; $CDCl_3$): δ 205.3, 149.6, 140.0, 124.9, 120.9, 119.9, 118.57, 118.51, 111.6, 67.4, 54.2, 51.8, 47.6, 44.7, 39.5, 28.5, 28.3, 27.2, 26.9, 26.0, 24.4, 17.3, 15.6.

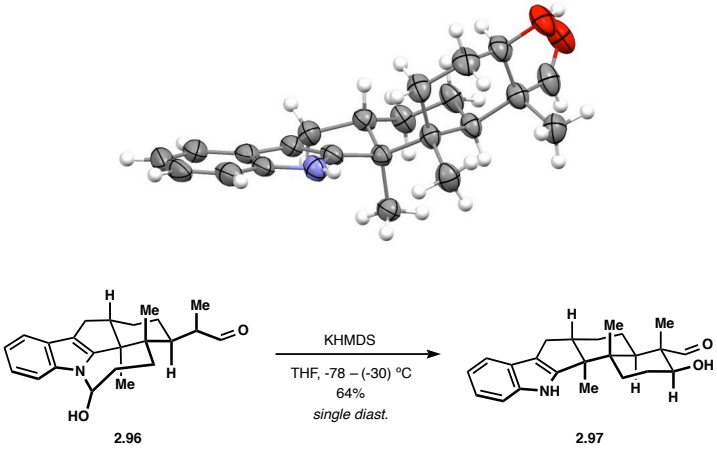

2.96 2.97

Pentacyclic core **2.97**: A solution of pentacycle **2.96** (50. mg, 0.14 mmol) in THF (2.9 mL) was degassed using a freeze-pump-thaw technique (three cycles). The solution was cooled to -78 ºC and treated dropwise with a solution of KHMDS (0.313 mL, 0.16 mmol, 0.5 M in toluene). The reaction was vigorously stirred at -78 ºC. After 30 minutes the reaction was warmed to ~(-30) ºC and rapidly quenched with a 1 N aqueous solution of HCl (2.85 mL). The mixture allowed to warm to room temperature and concentrated under reduced pressure. The residue was partitioned between water (15 mL) and diethyl ether (15 mL). The aqueous layer was extracted with diethyl ether (3x30 mL). The combined organic layers were washed with brine, dried over anhydrous magnesium sulfate, filtered, and concentrated under reduced pressure. Purification by flash

chromatography (elution with 30% v/v ethyl acetate in hexanes) afforded 32 mg (64%) of the pentacycle core **2.97** as a white powder. R_f = 0.23 (40% v/v ethyl acetate in hexanes); ^{1}H NMR (500 MHz; $CDCl_3$): δ 9.44 (s, 1H), 7.76 (s, 1H), 7.44 (dd, *J* = 6.3, 2.4 Hz, 1H), 7.31 (dd, *J* = 6.4, 2.3 Hz, 1H), 7.12–7.07 (m, 2H), 3.83 (dd, *J* = 10.9, 4.1 Hz, 1H), 2.77 (dddd, *J* = 13.0, 9.9, 6.5, 3.2 Hz, 1H), 2.70 (dd, *J* = 13.2, 6.4 Hz, 1H), 2.36 (dd, *J* = 13.2, 10.6 Hz, 1H), 2.07 (dd, *J* = 12.7, 3.3 Hz, 1H), 2.00 (td, *J* = 12.9, 3.7 Hz, 1H), 1.94–1.82 (m, 2H), 1.78–1.74 (m, 1H), 1.69–1.52 (m, 4H), 1.21 (dd, *J* = 13.1, 2.8 Hz, 1H), 1.14 (s, 3H), 1.12 (s, 3H), 1.07 (s, 3H); ^{13} C NMR (125 MHz; $CDCl_3$): δ 206.9, 150.1, 140.1, 125.1, 120.8, 119.8, 118.63, 118.46, 111.6, 72.1, 55.3, 52.8, 48.8, 39.8, 38.7, 33.2, 27.5, 26.7, 25.4, 25.0, 18.8, 14.7, 8.5; HRMS (ESI) calculated for $C_{23}H_{30}NO_2$ $[M+H]^+$: 352.227, found: 352.2290.

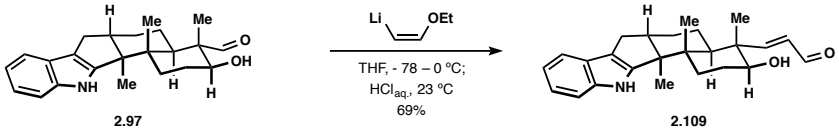

Aldehyde **2.109**: *tert*-Butyllithium (2.1 mL, 3.0 mmol, 1.45 M in pentane) was added to a solution of (*Z*)-2-bromo-ethoxyethene (0.16 mL, 15 mmol) in THF (3.0 mL) at -78 ºC. The reaction was vigorously stirred at -78 ºC. After 45 minutes a solution of hydroxyaldehyde **2.97** (53 mg, 0.15 mmol) in THF (5.5 mL) was added in a slow and steady stream. The resulting solution was vigorously stirred at -78 ºC. After 30 minutes the reaction was allowed to warm to 0 ºC. After an additional 30 minutes the reaction was quenched with a 2 N aqueous solution of HCl (5 mL) and warmed to room temperature. After 1 hour the mixture was neutralized with a solution of saturated aqueous $NaHCO_3$. The aqueous layer was extracted with diethyl ether (3x15 mL). The combined organic layers were washed with brine (15 mL), dried over anhydrous magnesium sulfate, filtered, and concentrated under reduced pressure. Purification by flash chromatography (gradient elution: 100% hexanes to 60% v/v ethyl acetate in hexanes) afforded

39 mg (69%) of aldehyde **2.109** as a yellow solid. R_f = 0.13 (40% v/v ethyl acetate in hexanes); ^{1}H-NMR (500 MHz; $CDCl_3$): δ 9.62 (d, *J* = 7.6 Hz, 1H), 7.71 (s, 1H), 7.44-7.42 (m, 1H), 7.30 (dd, *J* = 6.4, 2.1 Hz, 1H), 7.11-7.06 (m, 2H), 6.66 (d, *J* = 15.9 Hz, 1H), 6.18 (dd, *J* = 15.9, 7.6 Hz, 1H), 3.55 (dd, *J* = 10.7, 4.2 Hz, 1H), 2.76 (dddd, *J* = 13.1, 9.9, 6.5, 3.2 Hz, 1H), 2.69 (dd, *J* = 13.2, 6.4 Hz, 1H), 2.34 (dd, *J* = 13.2, 10.6 Hz, 1H), 2.02 (td, *J* = 12.7, 3.9 Hz, 1H), 1.93-1.86 (m, 2H), 1.82-1.74 (m, 2H), 1.70-1.59 (m, 2H), 1.53-1.38 (m, 3H), 1.17 (s, 3H), 1.11 (s, 3H), 1.05 (s, 3H); ^{13}C NMR (125 MHz; $CDCl_3$): δ 193.9, 168.1, 150.2, 140.1, 133.1, 125.2, 120.8, 119.8, 118.6, 118.6 111.6, 76.3, 53.2, 48.9, 47.8, 44.3, 39.1, 33.3, 27.5, 26.5, 25.2, 25.0, 19.3, 14.7, 11.1; HRMS (ESI) calculated for $C_{25}H_{32}NO_2$ $[M+H]^+$: calculated 378.2433, found: 378.2443.

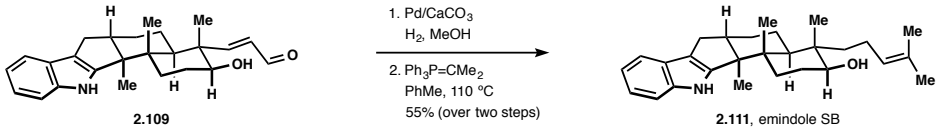

Emindole SB **2.111**: $Pd/CaCO_3$ (5% w/w, 20.4 mg, 0.0096 mmol) was added to a solution of aldehyde **2.109** (36.3 mg, 0.096 mmol) in MeOH (12 mL) and water (0.5 mL). The flask was sealed with a septum and the solution was sparged with nitrogen (~5 minutes). Once degassed, the solution was sparged with hydrogen (~5 min). The hydrogen atmosphere was maintained and the reaction was vigorously stirred at room temperature. After 2 hours the reaction was deactivated by sparging the solution with nitrogen (~10 minutes). The degasses suspension was filtered through Celite and the filter cake was washed with ethyl acetate. The combined organic solutions were concentrated under reduced pressure. The resulting residue was partitioned between ethyl acetate (45 mL) and brine (15 mL). The organic layer was dried over anhydrous magnesium sulfate and concentrated under reduced pressure. The resulting crude mixture of lactols was used in the following step without further purification. KHMDS (0.96 mL, 0.48 mmol, 0.5 M in toluene) was added to a suspension of isopropyltriphenylphosphonium iodide

(0.218 g, 0.5 mmol) in toluene (1.0 mL) at 0 ºC. The reaction was vigorously stirred at 0 ºC and a deep-red solution developed. After 20 minutes a solution of the crude mixture of lactols in toluene (2.0 mL) was added and the reaction was heated to 100 ºC. After 1 hour the reaction was allowed to cool to room temperature and quenched with a solution of saturated aqueous NH_4Cl. The layers were separated and the aqueous layer was diluted with water (10 mL) and extracted with diethyl ether (3x20 mL). The combined organic layers were washed with water (10 mL) and brine (10 mL), dried over anhydrous magnesium sulfate, filtered, and concentrated under reduced pressure.Purification by flash chromatography(gradient elution: 100% hexanes to 30% v/v ethyl acetate in hexanes) afforded 21.4 mg (55%) of emindole SB **2.111** as a white powder. R_f = 0.15 (20% ethyl acetate in hexanes); ^{1}H NMR (500 MHz; $CDCl_3$): δ 7.72 (s, 1H), 7.44–7.42 (m, 1H), 7.30 (dd, *J* = 5.8, 3.1 Hz, 1H), 7.10–7.06 (m, 2H), 5.15–5.12 (m, 1H), 3.59 (t, *J* = 7.9 Hz, 1H), 2.76 (dddd, *J* = 13.0, 9.9, 6.5, 3.2 Hz, 1H), 2.68 (dd, *J* = 13.2, 6.4 Hz, 1H), 2.34 (dd, *J* = 13.2, 10.6 Hz, 1H), 1.98–1.74 (m, 7H), 1.71 (s, 3H), 1.66–1.63 (m, 4H), 1.61–1.51 (m, 3H), 1.43 (dd, *J* = 13.0, 4.3 Hz, 1H), 1.33 (ddd, *J* = 14.6, 12.1, 5.3 Hz, 2H), 1.11 (s, 3H), 1.03 (s, 3H), 0.83 (s, 3H); ^{13}C NMR (125 MHz; $CDCl_3$): δ 150.9, 139.9, 131.4, 125.1, 124.6, 120.4, 119.6, 118.40, 118.28, 111.4, 77.0, 73.3, 53.1, 48.8, 41.2, 39.8, 39.3, 37.5, 33.5, 27.5, 25.8, 25.1, 22.7, 21.4, 19.2, 17.7, 16.5, 14.7; HRMS (ESI) calculated for $C_{28}H_{40}NO_2$ $[M+H]^+$: 406.3110, found: 406.3116.

2.5 References and Notes

[1] (a) Smith, A. B. III; Mewshaw, R. *J. Am. Chem. Soc.* **1985**, *107*, 1769. (b) Smith, A. B. III; Leenay, T. L. *Tetrahedron Lett.* **1988**, *29*, 2787. (c) Smith, A. B. III; Leenay, T. L. *Tetrahedron Lett.* **1988**, *29*, 2791. (d) Mewshaw, R. E.; Taylor, M. D.; Smith, A. B. III *J. Org. Chem.* **1989**, *54*, 3449. (e) Smith, A. B. III; Cho, Y. S.; Ishiyama, H. *Org. Lett.* **2001**, *3*, 3971. (e) Smith, A. B. III; Kürti, L.; Davulcu, A. H.; Cho, Y. S. *Org. Proc. Res. Dev.* **2007**, *11*, 19. (f) Zou, Y.; Melvin, J. E.; Gonzales, S. S.; Spafford, M. J.; Smith, A. B. III *J. Am. Chem. Soc.* **2015**, *137*, 7095.
[2] (a) Guile, S. D.; Saxton, E.; Thornton-Pett, M. *J. Chem. Soc. Perkin Trans. 1* **1992**, 1763. (b) Smith, A. B. III; Hartz, R. A.; Spoors, G.; Rainer, J. D. *Isr. J. Chem.* **1997**, *37*, 69. (c) Enomoto,

M.; Morita, A.; Kuwahara, S. *Angew. Chem. Int. Ed.* **2012**, *51*, 12833. (d) Teranishi, T.; Murokawa, T.; Enomoto, M.; Kuwahara, S. *Biosci. Biotechnol. Biochem.* **2015**, *79*, 11. (e) Sharpe, R. J.; Johnson, J. S. *J. Am. Chem. Soc.* **2015**, *137*, 4968. (f) Sharpe, R. J.; Johnson, J. S. *J. Org. Chem.* **2015**, *80*, 9740.

[3] (a) Smith, A. B. III; Kingery-Wood, J.; Leenay, T. L.; Nolen, E. G.; Sunazuka, T. *J. Am. Chem. Soc.* **1992**, *114*, 1438. (b) Smith, A. B. III; Cui, H. *Org. Lett.* **2003**, *5*, 587.

[4] (a) Belofsky, G. N.; Gloer, J. B.; Wicklow, D. T.; Dowd, P. F. *Tetrahedron* **1995**, *51*, 3959. (b) Rundberget, T.; Wilkins, A. L. *Phytochemistry* **2002**, *61*, 979. (c) Xu, M.; Gessner, G.; Groth, I.; Lange, C.; Christner, A.; Bruchn, T.; Deng, Z.; Li, X.; Heinemann, S. H.; Grabley, S.; Bringmann, G.; Sattler, I.; Lin, W. *Tetrahedron* **2007**, *63*, 435. (d) Gao, S.-S.; Li, X.-M.; Williams, K.; Proksch, P.; Ji, N.-Y.; Wang, B.-G. *J. Nat. Prod.* **2016**, *79*, 2066.

[5] Corey, E. J.; Cheng, X. M. In *The Logic of Chemical Synthesis*; John Wiley & Sons; New York, NY, 1995.

[6] During the development of our synthetic studies related to the assembly of **2.13** Smith and co-workers also identified the same intermediate as a common subtarget in their latest synthetic iteration related to the PIDs. See ref. 1f.

[7] (a) Lo, J. C.; Yabe, Y.; Baran, P. S. *J. Am. Chem. Soc.* **2014**, *136*, 1304. (b) Lo, J. C.; Gui, J.; Yabe, Y.; Pan, C.-M.; Baran, P. S. *Nature* **2014**, *516*, 343. (c) Lo, J. C.; Kim, D.; Pan, C.-M.; Edwards, J. T.; Yabe, Y.; Gui, J.; Qin, T.; Gutiérrez, S.; Giacoboni, J.; Smith, M. W.; Holland, P. L.; Baran, P. S. *J. Am. Chem. Soc.* **2017**, *139*, 2484.

[8] (a) Isayama, S.; Mukaiyama, T. *Chem. Lett.* **1989**, 2005. (b) Baik, T.-G.; Luis, A. L.; Wang, L.-C.; Krische, M. J. *J Am. Chem. Soc.* **2001**, *123*, 5112. (c) Wang, L.-C.; Jang, H.-Y.; Roh, Y.; Lynch, V.; Schultz, A. J.; Wang, X.; Krische, M. J. *J. Am. Chem. Soc.* **2002**, *124*, 9448.

[9] (a) Kosugi, M.; Hagiwara, I.; Migita, T. *Chem. Lett.* (b) Yamaguchi, M.; Tsukagoshi, T.; Arisawa, M. *J. Am. Chem. Soc.* **1999**, *121*, 4074. (c) Ooi, T.; Goto, R.; Maruoka, K. *J. Am. Chem. Soc.* **2003**, *125*, 10494. (d) Su, W.; Raders, S.; Verkade, J. G.; Liao, X.; Hartwig, J. F. *Angew. Chem. Int. Ed.* **2006**, *45*, 5852. (e) Datta, G. K.; Larhed, M. *Org. Biomol. Chem.* **2008**, *6*, 674. (f) Grigalunas, M.; Anker, T.; Morrby, P.-O.; Wiest, O.; Helquist, P. *J. Am. Chem. Soc.* **2015**, *137*, 7019.

[10] Nichimoto, Y.; Moritoh, R.; Yasuda, M; Baba, A. *Angew. Chem. Int. Ed.* **2009**, *48*, 4577.

[11] Sakurai, H. *Synlett* **1989**, 1.

[12] (a) Karasch, M. S.; Tawney, P. O. *J. Am. Chem. Soc.* **1941**, *63*, 2308. (b) Posner, G. H. In *Organic Reactions*; Dauben, W. G., Fried, J., McKusick, B. C., Kende, A. S., Meinwald, J., Marshall, J. A., Trost, B. M., Eds.; Robert E. Krieger: Malabar, FL, 1972, 17, p 1–113 and references therein.

[13] Umbreit, M. A.; Sharpless, K. B. *J. Am. Chem. Soc.* **1977**, *99*, 5526.

[14] (a) Dess, D. B.; Martin, J. C. *J. Org. Chem.* **1983**, *48*, 4155. (b) Dess, D. B.; Martin, J. C. *J. Am. Chem. Soc.* **1991**, *113*, 7277.

[15] We unambiguously confirmed the structures of each diastereomeric tricycle after growing crystals suitable for X-ray diffraction of **2.13** and ketal derivative **2.58**.

[16] During reaction development, we discovered that the reaction was sensitive of atmospheric oxygen. As such, reactions were thoroughly degassed to avoid trapping of intermediate radical species. See: Mailliard, B.; Ingold, K. U.; Scaiano, J. C. *J. Am. Chem. Soc.* **1983**, *105*, 5095.

[17] For an extensive list of conditions that were investigated, see Appendix A for further details.

[18] For clarity only the series of intermediates that lead to the formation of the desired tricycle is shown.

[19] For relevant redox potentials see: (a) Anderson, C. W.; Lung, K. R.; Nile, T. A. *Inorg. Chim. Acta* **1984**, *85*, 33. (b) Fu, Y.; Liu, L.; Yu, H.-Z.; Wang, Y.-M.; Guo, Q.-X. *J. Am. Chem. Soc.* **2005**, *127*, 7227. For conversion of redox potentials see: Pavlishchuk, V. V.; Addison, A. W. *Inorg. Chim. Acta* **2000**, *298*, 97.
[20] The superior nature of $PhSiH_2(O\textit{i}\text{-Pr})$ was privately disclosed via personal communication with Ryan A. Shenvi. We are indebted to Ryan for informing us about $PhSiH_2(O\textit{i}\text{-Pr})$ ahead of publication: Obradors, C. L.; Martinez, R.; Shenvi, R. A. *J. Am. Chem. Soc.* **2016**, *138*, 4962.
[21] Ogata, M.; Ueda, J.-y.; Hoshi, M.; Hashimoto, J.; Nakashima, T.; Anzai, K.; Takagi, M.; Shin-ya, K. *J. Antibiot.* **2007**, *60*, 645.
[22] Levine, S. G. *J. Am. Chem. Soc.* **1958**, *80*, 6150.
[23] Seeman, J. I. *Chem. Rev.* **1983**, *83*, 83 and references therein.
[24] (a) Larsen, C. H.; Ridgeway, B. H.; Shaw, J. T.; Woerpel, K. A. *J. Am. Chem. Soc.* **1999**, *121*, 12208. (b) Smith, D. M.; Tran, M. B.; Woerpel, K. A. *J. Am. Chem. Soc.* **2003**, *125*, 14149.
[25] Luo, S.–H.; Hugelshofer, C. L.; Hua, J.; Jing, S.-X.; Li, C.-H.; Liu, Y.; Li, X.-N.; Zhao, X.; Magauer, T.; Li, S.-H. *Org. Lett.* **2014**, *16*, 6416.
[26] See Section 2.4.2 and Appendix C for relevant spectra and correlations.
[27] Eric J. Kuenstner prepared and performed all of the experiments involving **2.82**.
[28] Each diastereomer (**2.85** and **286**) was confirmed by direct comparison, after reduction, with triols **2.87** and **2.88**. Authentic triols **2.87** and **2.88** were generated from **2.13** and **2.57**, respectively.

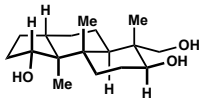

2.87

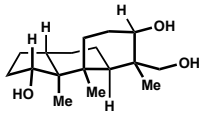

2.88

[29] (a) Angenot, L.; Dideberg, O.; Dupont, L. *Tetrahedron Lett.* **1975**, *16*, 1357. (b) Chbani, M.; Païs, M.; Delauneux, J.-M.; Debitus, C. *J. Nat. Prod.* **1993**, *56*, 99. (c) Schubot, F. D.; Hossain, M. B.; van der Helm, D.; Païs, M.; Debitus, C. *J. Chem. Crystallogr.* **1998**, *28*, 23.
[30] a) Fischer, E.; Jourdan, F. *Ber.* **1883**, *16*, 2241. (b) Fischer, E.; Hess, O. *Ber.* **1884**, *17*, 559. for a review see: (c) Robinson, B. *Chem. Rev.* **1969**, *69*, 227 and references therein.
[31] Vaswani, R. G.; Day, J. J.; Wood, J. L. *Org. Lett.* **2009**, *11*, 4532.
[32] (a) Pfitzner, K. E.; Moffatt, J. G. *J. Am. Chem. Soc.* **1963**, *85*, 3027. (b) Corey, E. J.; Kim, C. U. *J. Am. Chem. Soc.* **1971**, *94*, 7586. (c) Omura, K.; Sharma, A. K.; Swern, D. *J. Org. Chem.* **1976**, *41*, 957. (d) Mancuso, A. J.; Huang, S.-L.; Swern, D. *J. Org. Chem.* **1978**, *43*, 2480.
[33] De Mico, A.; Margarita, R.; Parlanti, L.; Vescovi, A.; Piancatelli, G. *J. Org. Chem.* **1997**, *62*, 6974.
[34] Gamez, P.; Arends, I. W. C. E.; Reedijk, J.; Sheldon, R. A. *Chem. Commun.* **2003**, 2414.
[35] Parikh, J. R.; Doering, W. von E. *J. Am. Chem. Soc.* **1967**, *89*, 5505.
[36] Padwa, A.; Gunn, D. E. Jr.; Osterhout, M. H. *Synthesis* **1997**, 1353 and references therein.
[37] We found it best to use **2.93** as crude material from the Parikh–Doering oxidation due to loss of mass balance during the isolation of **2.93**. We speculate that the loss of material arises from the sensitive nature of the hemiaminal moiety.
[38] Chuang, G. J.; Lee, W. W. E.; Rotter, T. *J. Am. Chem. Soc.* **2011**, *133*, 1760.
[39] The scheme depicted in Scheme 2.19 is likely a simplified version of a much more complex system.
[40] The absence of the hemiaminal motif permitted the propagation of the entire polycyclization cascade.

[41] (a) Nozawa, K.; Nakajima, S.; Kawai, K.-i.; Udagawa, S.-i. *J. Chem. Soc. Perkin Trans. 1* **1988**, 2607. (b) Fan, Y.; Wang, Y.; Liu, P.; Fu, P.; Zhu, T.; Wang, W.; Zhu, W. *J. Nat. Prod.* **2013**, *76*, 1328.
[42] (a) Motoyama, T.; Hayashi, T.; Hirota, H.; Ueki, M.; Osada, H. *Chem. Biol.* **2012**, *19*, 1611. (b) Tagami, K.; Liu, C.; Minami, A.; Noike, M.; Isaka, T.; Fueki, S.; Shichijo, Y.; Toshima, H.; Gomi, K.; Dairi, T.; Oikawa, H. *J. Am. Chem. Soc.* **2013**, *135*, 1260. (c) Liu, C.; Tagami, K.; Minami, Matsumoto, T.; Frisvad, J. C.; Suzuki, H.; Ishikawa, J.; Oikawa, H. *Angew. Chem. Int. Ed.* **2015**, *54*, 5748. (d) Van de Bittner, K. C.; Nicholson, M. J.; Bustamante, L. Y.; Kessans, S. A.; Ram, A.; van Dolleweerd, C. J.; Scott, B.; Parker, E. J. *J. Am. Chem. Soc.* **2018**, *140*, 582.
[43] Lau, K. S. Y.; Schlosser, M. *J. Org. Chem.* **1976**, *43*, 1595.
[44] Duhamel, P.; Hennequin, L.; Poirier, J. M.; Tavel, G.; Vottero, C. *Tetrahedron* **1986**, *42*, 4777.
[45] Kuwajima, I.; Doi, Y. *Tetrahedron Lett.* **1972**, *13*, 1163.
[46] Kuwajima, I.; Corey, E. J. *Tetrahedron Lett.* **1972**, *13*, 487.
[47] Sarabèr, F. C. E.; Baranovsky, A.; Jansen, B. J. M.; Posthumus, M. A.; de Groot, A. *Tetrahedron* **2006**, *62*, 1726.
[48] Yu, J.-Q.; Wu, H.-C.; Corey, E. J. *Org. Lett.* **2005**, *7*, 1415.
[49] Beauchard, A.; Phillips, V. A.; Lloyd, M. D.; Threadgill, M. D. *Tetrahedron* **2009**, *65*, 8176.
[50] Rivero, M. R.; Alonso, I.; Carretero, J. C. *Chem. Eur. J.* **2004**, *10*, 5443.
[51] Guo, H.; O-Doherty, G. A. *Org. Lett.* **2005**, *7*, 3921.
[52] Gunji, Y.; Yamashita, Y.; Ikeno, T.; Yamada, T. *Chem. Lett.* **2006**, *35*, 714.
[53] George, D. T.; Kuenstner, E. J.; Pronin, S. V. *J. Am. Chem. Soc.* **2015**, *137*, 15410.

Chapter 3: Synthetic Studies Toward (–)-11-ketopaspaline

3.1 Research-guided Strategy

3.1.1 Previous Synthetic Studies Toward 11-ketopaspaline[1]

In 2015, our lab completed the total synthesis of emindole SB,[2,3] which served as a proof-of-concept for our synthetic strategy related to the paxilline indole diterpenes (PIDs). We envisioned that the research foundation provided by our work would enable the synthesis of various members of the family. While our approach was successful, we identified areas of improvement that we hoped to address as our strategy evolved toward the PIDs.

Scheme 3.1. Tether-controlled Assembly of the Pentacyclic Core.

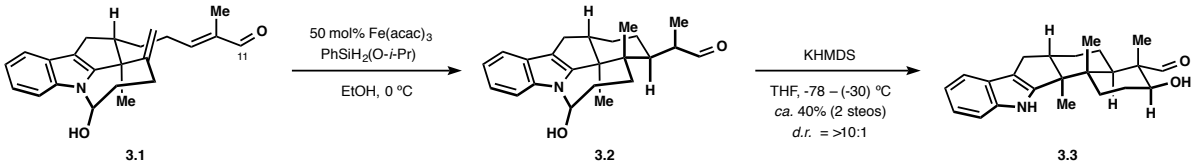

3.1 **3.2** **3.3**

A defining feature of our approach was a concise and stereocontrolled assembly of the pentacyclic core enabled by a tether-controlled radical conjugate addition/aldol addition reaction sequence (Scheme 3.1).[4] This series of events facilitated the synthesis of a crucial intermediate **3.3** that possessed key functional handles we aimed to leverage during subsequent chemical modifications en route to numerous congeners of the family. However, we observed that a variety of electrophiles and nucleophiles exhibited poor reactivity toward the aldol motif found in **3.3** and only highly reactive organometallic reagents were effective at elaborating **3.3** to the desired intermediates.

To overcome the poor reactivity observed for the aldol motif, we proposed incorporating the desired substituents on our tetracyclic precursor prior to the radical conjugate addition event (i.e. **3.1** to **3.2**). Following this approach, Eric J. Kuenstner pursued the radical conjugate addition/aldol addition sequence using diketone **3.4** (Scheme 3.2a). While the first phase of our

sequence proceeded as expected, the desired pentacycle was not observed and complex mixtures of products resulted when **3.5** was treated with various bases. We proposed that the acidic proton associated with the 1,3-diketone moiety complicated regioselective enolate generation. As a result, the proton at C12 was less acidic than the enolizable protons at C6, which would allow an undesired enolate to preferentially form. To determine whether a substrate bearing a ketone at C11 could be converted to a product possessing the desired connectivity pattern, Eric turned to methyl ketone **3.6** (Scheme 3.2b). In line with our previous results, the hydrogen atom transfer (HAT) initiated radical conjugate addition delivered the desired pentacyclic hemiaminal **3.7**. However, when **3.7** was treated with various bases we observed the formation of products (i.e. **3.8**) that resulted from regioselective deprotonation at C6 rather than C12.

Scheme 3.2. Approaches Utilizing Ketone Cyclization Precursors.

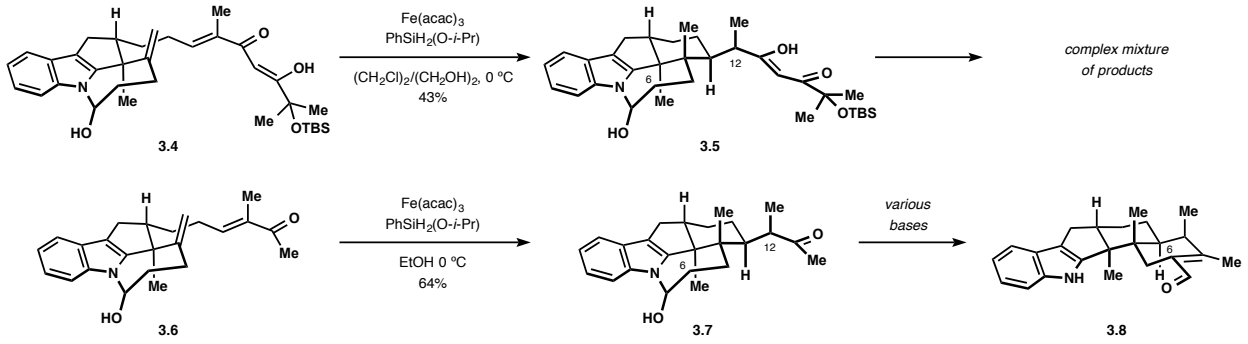

At this stage we recognized that it would be a challenge to achieve regioselective enolate generation as substrates bearing a ketone would have at least three activated positions adjacent to a carbonyl (Scheme 3.3a). To overcome this challenge, we considered revisiting our initial approach to the PIDs. In our initial studies we discovered that dialdehyde **3.10** was converted to a mixture of tricycles **3.11** and **3.12** in good yield, but with poor diastereoselectivity via a radical-polar crossover polycyclization (Scheme 3.3b). At the time, we were unable to develop a solution to the poor stereoselectivity that we observed, however Devon J. Schatz recently discovered *O*-TMS cyanohydrin **3.13** delivered the desired tricycle with a high level of

diastereocontrol (Scheme 3.3c).[5] In the polycyclization cascade, the putative enolate for the aldol addition was regioselectively generated via single-electron reduction of a stabilized tertiary radical and reacted with the pendent aldehyde (*vide infra*). Taken together, we posited that we could take advantage of the reaction mechanism of the polycyclization cascade to access relevant tricarbocyclic products bearing a ketone at C11 (Scheme 3.3d). More specifically, after chemoselective HAT to the electron-rich alkene and radical conjugate addition, the stabilized tertiary radical could be reduced to regioselectively form iron(III)-enolate **3.17** that can rapidly react with the pendent aldehyde via an intramolecular aldol addition. We regarded the fundamental reactivity embedded within the mechanism of the polycyclization as a way to tolerate multiple enolizable positions. Indeed, when Eric attempted the polycyclization cascade on ketone **3.14** he isolated the tricyclic framework **3.12**.[6]

Scheme 3.3. Challenge Associated with the Heminal Substrate and Potential Solution.

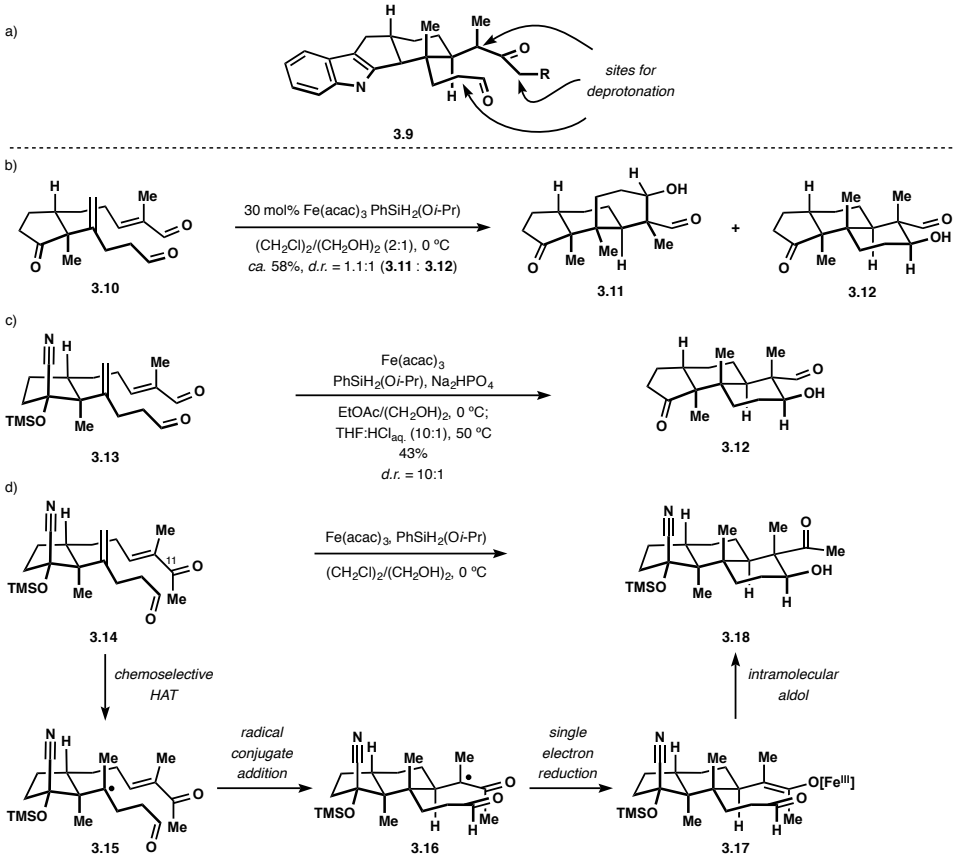

3.1.2 Revised Strategy Toward 11-ketopaspaline[7]

The success of the polycyclization of ketone **3.14** led us to pursue more complex polycyclization precursors. Our initial studies investigated the polycyclization using 1,3-diketone **3.19** as a precursor (Scheme 3.4). However, a lengthy and inefficient synthetic sequence plagued the preparation of **3.19** and attempts at the polycyclization with **3.19** produced an intractable mixture of products that was difficult to interpret.[8] We proposed that the observed difference in reactivity between the methyl ketone **3.14** and 1,3-diketone **3.19** was a result in a slight modulation in the reduction potential of the intermediate stabilized tertiary alkyl radical (i.e. **3.16**),[9] which could have made reduction of the stabilized radical an unfavorable process.

Scheme 3.4. Undesired Reactivity Associated with 3.19

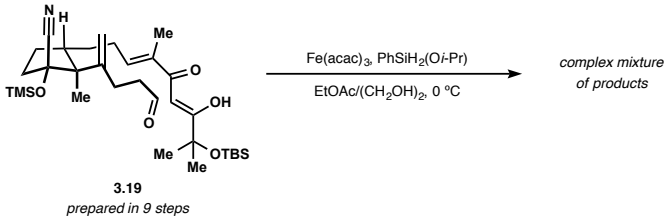

3.19
prepared in 9 steps

Undeterred by this result, we pursued the polycyclization cascade using ketone substrates lacking the 1,3-diketone moiety. We reasoned that the isolation of **3.18** (Scheme 3.3d) as the product of the polycyclization indicated that proton transfer or enolate isomerization did not occur. As such, we proposed that a substrate possessing oxygenated functional groups at the β'-position (C9) would be tolerated in the polycyclization cascade. Following this approach we identified β-keto epoxide **3.22** as a polycyclization precursor (Scheme 3.5). We proposed that the epoxide could be directly utilized in the cascade to deliver a tetracyclic core **3.21** en route to 11-ketopaspaline (**3.20**). As such, we initiated studies related to the development of a stereocontrolled assembly of the core of 11-ketopaspaline (**3.20**) using **3.22** as a polycyclization precursor.

Scheme 3.5. Retrosynthesis of 11-ketopaspaline.

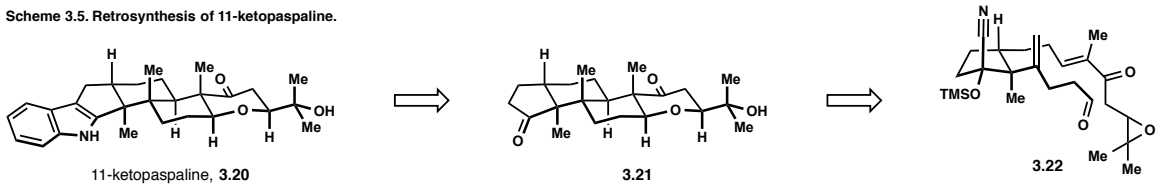

3.2 Polycyclization Cascade Utilizing β-keto epoxide 3.22

3.2.1 Synthesis of β-keto epoxide 3.22

Our initial synthetic strategy toward β-keto epoxide **3.22** involved a Horner–Wadsworth–Emmons (HWE) olefination[10] as a way to introduce the enone moiety. Our efforts toward this end began with a vicinal difunctionalization sequence of 2-methyl-cyclopenten-1-one (**2.24**) using a synthetic sequence similar to one applied in our synthesis of emindole SB (Scheme 3.6). Following this approach, a copper-catalyzed conjugate addition of the Grignard reagent derived from *O*-TIPS-3-bromo-1-propanol to enone **2.24** and subsequent α-alkenylation of the resulting enoxysilane delivered β,γ-unsaturated ketone **3.27**. Unlike our previous studies related to the α-alkenylation of unsymmetric ketones,[2] we observed a considerable amount of regioisomeric β,γ-unsaturated ketone **3.28** that was inseparable from **3.27**. Nonetheless, cyanosilylation[11] of the cyclopentanone and oxidation with Dess–Martin periodinane[12] completed the synthesis of the aldehyde partner **3.29** for the HWE olefination.

Scheme 3.6. Synthesis of the Aldehyde for the HWE Olefination

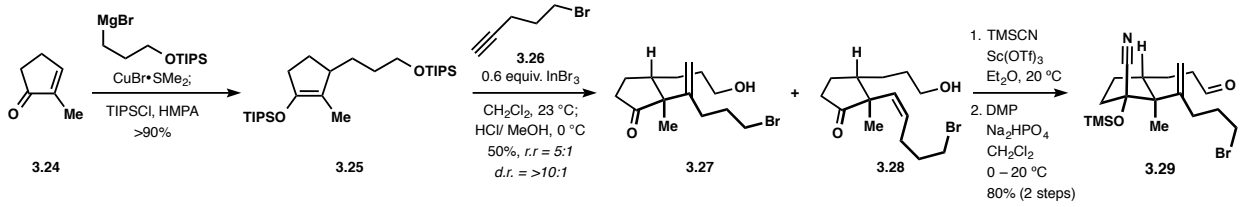

While the preparation of **3.29** was relatively straightforward, the synthesis of a suitable phosphonate ester for the HWE olefination was a challenge (Scheme 3.7). Initially, we hoped to access a relevant phosphonate ester containing a β-keto epoxide motif from esters **3.34** and **3.39**[13] or acyl chloride **3.35**[14] via phospha-Claisen condensation.[15] However, when **3.34**, **3.39**, or

3.35 were treated with **3.41** only elimination products were observed due to the sensitivity of the epoxide moiety.[16] Undeterred, we turned to silylated bromohydrin **3.40** which we believed could serve as a surrogate for the epoxide motif. To our delight, we were able to convert silylated bromohydrin **3.40** to phosphonate **3.42** via a phospha-Claisen condensation with **3.41**.[17]

Scheme 3.7. Preparation of the Phosphonate Ester.

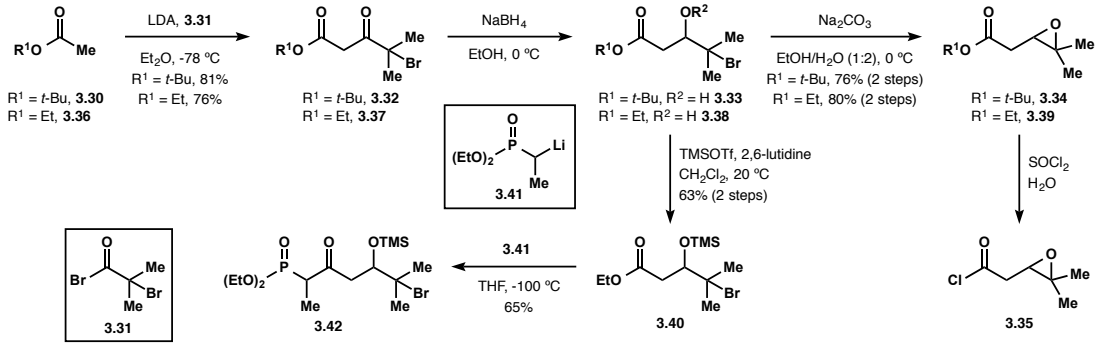

The convergent union of **3.29** and **3.42** via HWE olefination delivered synthetically useful quantities of **3.43** (Scheme 3.8). Unfortunately, Ganem oxidation[18] using trimethylamine-*N*-oxide (TMANO) of the primary alkyl bromide to the corresponding aldehyde proceeded with low overall efficiency. In addition, attempts to remove the TMS-protecting group led decomposition and elimination of the putative epoxide moiety. While this synthetic sequence provided a concise approach to an advanced intermediate (six steps) the relatively low reaction yields and sensitivity of the array of functional groups provided an impetus for the development of an alternative approach to β-keto epoxide **3.22**.

Scheme 3.8. HWE Olefination and Conversion to the Polycyclization Precursor.

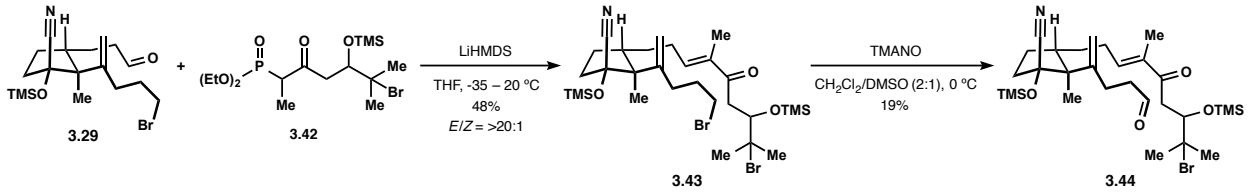

As such, our revised studies related to β-keto epoxide **3.22** began with the conversion of known intermediate **3.45**[2] to *O*-TMS cyanohydrin **3.44** via cyanosilylation of the cyclopentanone

and chemoselective Sharpless allylic hydroxylation of the trisubstituted alkene (Scheme 3.6).[19] In order to install various side chains at C11 we pursued a chemoselective allylic alcohol oxidation. Following this approach, oxidation of the allylic alcohol **3.46** with manganese(IV) oxide[20] and regioselective α-prenylation[21] of the resulting aldehyde delivered triene **3.47** as an inconsequential mixture of alcohols at C11. Double oxidation of the primary and allylic alcohols with Dess–Martin periodinane delivered dicarbonyl **3.50** that was poised for a chemoselective epoxidation.[22] Initial attempts at the epoxidation delivered products resulting from over-oxidation of the aldehyde. However, exposure to *m*-CPBA at sub-ambient temperatures and treatment of the reaction mixture with 2-methyl-2-butene afforded the desired polycyclization precursor **3.22** as a mixture of diastereomeric epoxides.[23] The completion of our synthesis of **3.22** permitted further studies related to the proposed polycyclization cascade.

Scheme 3.9. Synthesis of β-keto Epoxide 3.22.

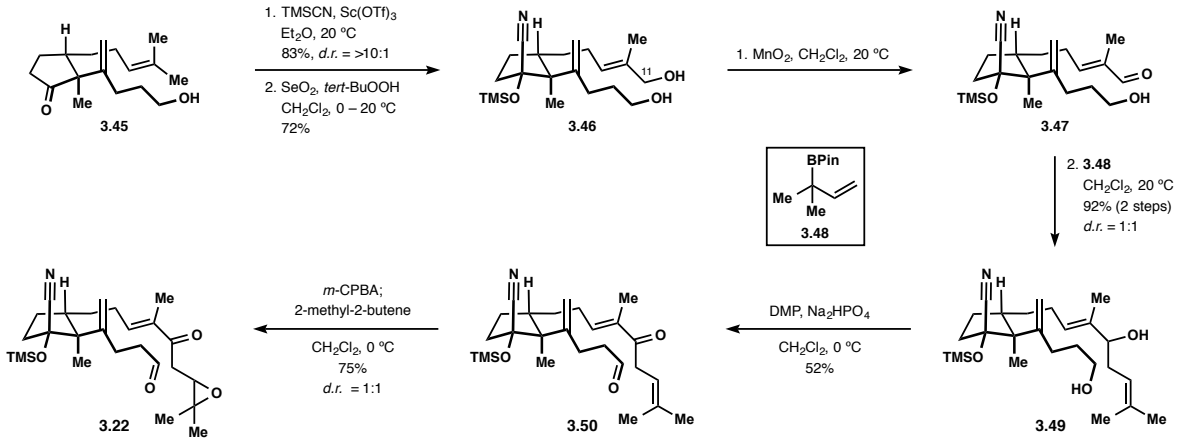

3.2.2 Unexpected Outcomes of the Polycyclization and Revised Strategy.

Our initial attempts at the polycyclization using **3.22** produced the desired terpenoid framework that resulted from the proposed radical-polar crossover polycyclization (Scheme 3.10a). However, the product was obtained in low yield and efficiency. To our surprise we

discovered that the stereocenter at C7 possessed an axially oriented alcohol as indicated by the appearance of the C7–H resonance in the ^{1}H NMR.[24]

Scheme 3.10. Unexpected Stereochemical Outcome from the Polycyclization Cascade.

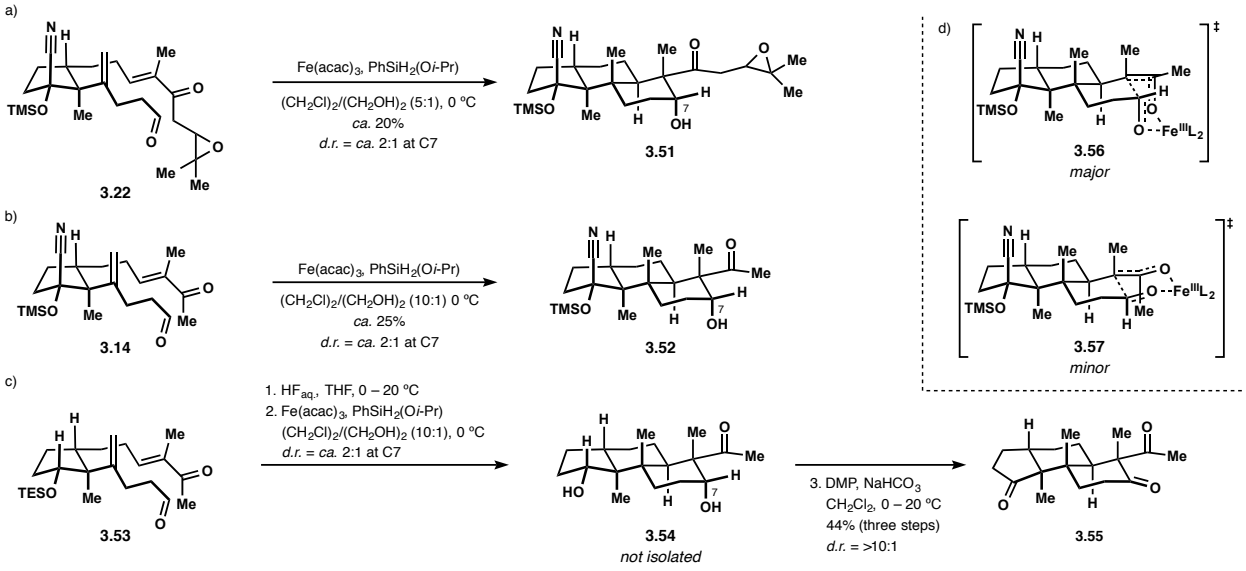

We investigated whether the formation of the axial alcohol was the result of the complex side chain on the ketone and revisited methyl ketone **3.14**. To our surprise tricycle **3.52** with an axially oriented alcohol was obtained (Scheme 3.10b).[25] In addition, secondary alcohol **3.53** also converted to tricycle **3.54** with the axial hydroxyl group (Scheme 3.10c). Two diastereomeric transition structures (for example, **3.56** and **3.57**) likely lead to the formation of the undesired (major) and desired (minor) diastereomers (Scheme 3.10d). We believe that formation of the undesired *Z*-enolate **3.56** is slightly favored due to minimization of allylic strain and leads to the preferential formation of the axially oriented alcohol.

The stereocenter at C7 in **3.51** could be epimerized upon treatment with base, however the epoxide was also cleaved during this process and delivered a corresponding α,β-unsaturated-γ-hydroxy ketone (not shown). The undesired diastereoselectivity observed during the aldol addition and inability to chemoselectively epimerize the stereocenter at C7 represented a major problem for our approach to 11-ketopaspaline (**3.20**).

We observed in our studies involving various polycyclization precursors (**3.22**, **3.14**, and **3.53**; Scheme 3.10a–c) that **3.53** gave a higher overall yield for the terpenoid framework. We speculated that the difference in efficiency resulted from the steric bulk of the *O*-TMS protected cyanohydrin, which decreased the chemoselectivity of the initial HAT event. As the chemoselectivity decreased, competitive HAT to the electron-deficient alkene occurred, which could lead to products arising from intermolecular reductive aldol addition.[26] This notion was corroborated by unrelated studies on a bimolecular version of the polycyclization cascade as a product resulting from an intermolecular reductive aldol reaction pathway between methacrolein (**3.58**) and aldehyde **3.59**[27] was favored over the desired cyclization pathway (Scheme 3.11).[28]

Scheme 3.11. Unselective HAT.

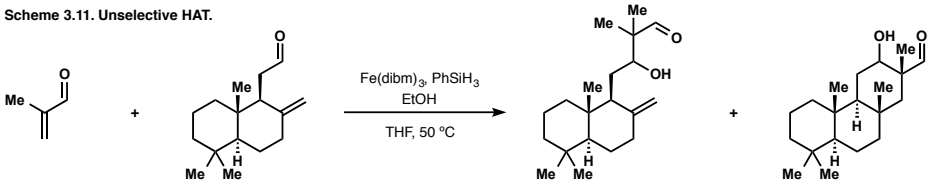

3.58 *1.2 equiv.* + **3.59** *1.0 equiv.* → **3.60** *ca.* 47% *d.r.* = 3:1 + **3.61** *ca.* 25%

Taken together, we elected to pursue future polycyclization cascades involving an α,β-unsaturated ketone on substrates similar to **3.53**. We believed that we could reinstall the cyclopentanone motif and oblate the stereochemistry at C7 via an oxidation event (i.e. **3.54** to **3.55**; Scheme 3.10c). We thought this could be strategic as the ketone at C7 could serve as a synthetic handle to access the tetracyclic core **3.21** of 11-ketopaspaline (**3.20**) via reduction of a ketal intermediate (i.e. **3.66**; Scheme 3.12).[29] As such, we identified tetracycle **3.64** as a new subtarget.

Scheme 3.12. Revised Approach to 11-ketopaspaline.

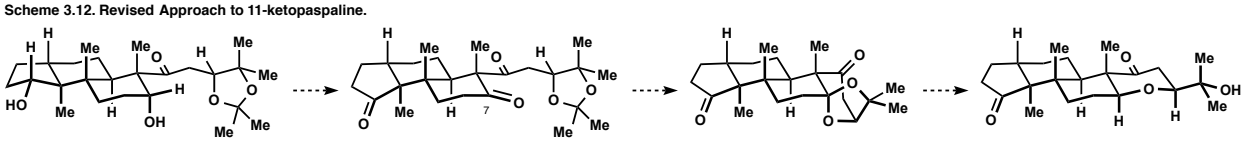

3.64 *product of the polycyclization* → **3.65** → **3.66** → **3.21** *tetracyclic core of 11-ketopaspaline*

3.3 Polycyclization Cascade Utilizing Protected Triol 3.67.

3.3.1 Retrosynthesis of Protected Diol 3.64.

Scheme 3.13. Retrosynthesis of 3.64.

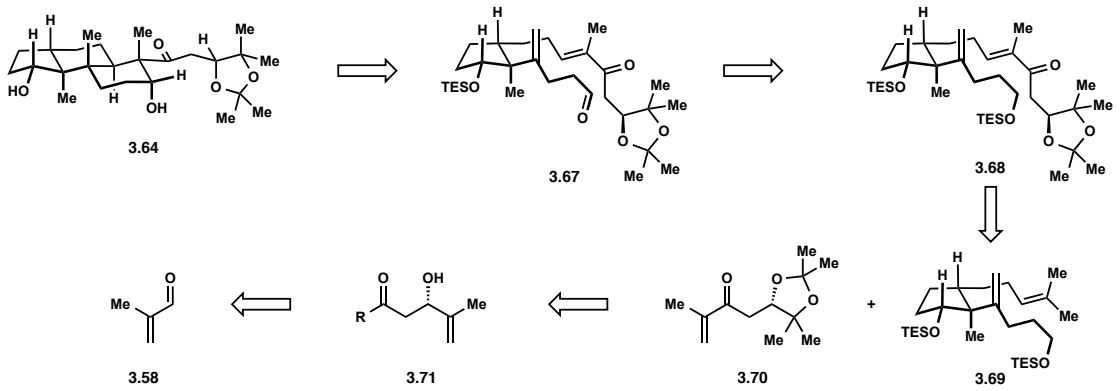

Our retrosynthesis of **3.64** involved the polycyclization, chemoselective oxidation[30] and cross metathesis[31] transforms, which identified diene **3.69** and enone **3.70** as key synthons. We believed that **3.69** could be accessed from intermediates previously described (i.e. **3.45**) and **3.70** could be accessed from hypothetical synthon **3.71** via a radical-polar crossover ketal formation. Finally, an enantioselective aldol transform would provide access to **3.71** from methacrolein (**3.58**).

Scheme 3.14. Proposed Radical-polar Crossover Ketal Formation.

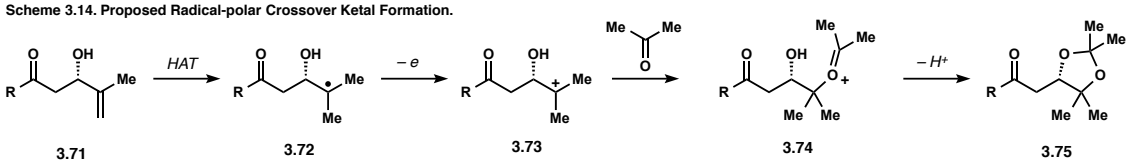

We elected to pursue this route because of its concise nature and the opportunity to develop new chemistry. Specifically, the conversion of hypothetical synthon **3.71** to enone **3.70** would involve the formal protonation of the 1,1-disubstituted alkene in the presence of an aldol motif. Due to the sensitive nature of an allylic alcohol, we believed that we could achieve the formal protonation of the alkene via a radical-polar crossover reaction manifold (Scheme 3.14). We were inspired by work from Shigehisa and co-workers wherein hydroalkoxylation of simple

alkenes was achieved via a proposed radical-polar crossover mechanism.[32] Furthermore, work by Eric E. Touney related to the development of a 1,2-pinacol rearrangement of allylic alcohols indicated that ketal products could be obtained in the presence of acetone.[33] Taken together, we believed we could immediately apply Eric's discovery in the preparation of enone **3.70**.

Scheme 3.15. Proof-of-concept for the Cross-metathesis.

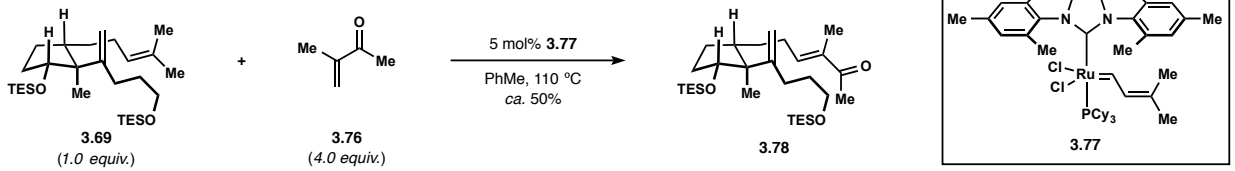

Despite widespread application in the context of total synthesis there are limited examples utilizing cross-metathesis involving two complex alkene partners,[34] with examples involving two polysubstituted alkenes particularly scarce.[35] Outside of the context of target-oriented synthesis the preparation of trisubstituted alkenes via cross-metathesis is typically limited to the reaction between terminal alkenes, or their surrogates, and simple 1,1-disubstituted alkenes.[36] Furthermore, cross-metathesis reactions do not readily initiate with tri-substituted alkenes.[37] For our proposed cross-metathesis this meant that the ruthenium catalyst would likely have to initiate with enone **3.70** and form a metathesis-active ketone-carbene. However, metal alkylidenes derived from α,β-unsaturated carbonyl compounds are known to be unstable in solution,[38] which represented an additional challenge for the proposed cross-metathesis. In spite of these potential problems we attempted the cross-metathesis between **3.69** and 3-methyl-3-buten-2-one (**3.76**) and obtained *ca*. 50% yield of enone **3.78** (Scheme 3.15). This result indicated that the strategy involving the proposed cross-metathesis was viable and provided an impetus for further studies.

3.3.2 Enantioselective Synthesis of Enone 3.70

We acknowledged from the outset that the proposed aldol between an acetate equivalent or methyl ketone and methacrolein (**3.58**) would be a challenge. There are methods that utilize auxiliaries to achieve highly diastereoselective acetate aldol additions,[39] but the synthesis of each auxiliary is prohibitively lengthy. For this reason, we decided to pursue aldol additions relying on simple chiral auxiliaries or catalysts. Following this approach, we investigated an array of stereoselective aldol reactions to access products resembling **3.71** (Scheme 3.16). However, our attempts at a Reformatsky reaction[40] were unsuccessful at delivering an efficient and stereoselective process (Scheme 3.16a and b). In addition, while we could obtain modest enantioselectivity via a Mukaiyama aldol reaction[41] the enantioselectivity and yield dramatically decreased as we increased the scale of the reaction (Scheme 3.16c).

Scheme 3.16. Studies Toward the Stereoselective Synthesis of the Allylic Alcohol Motif.

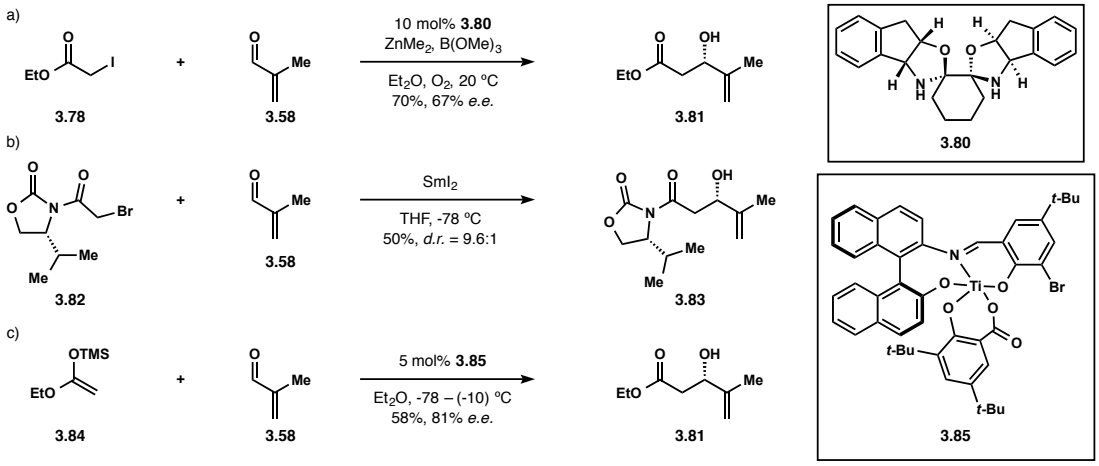

Ultimately, we elected to go with the Evans aldol[42] between commercially available (S)-3-acetyl-4-benyzl-2-oxazolidinone (**3.86**) and methacrolein (**3.58**) due to the availability of reagents and the ability to scale the reaction despite poor diastereoselectivity (Scheme 3.17). We believed that the major diastereomer of the aldol addition resulted from a Zimmerman–Traxler transition structure where the dipole was minimized[43] and the directing group of the auxiliary was exo to the pericyclic transition state (**3.88**).[44] Alternatively, the minor diastereomer resulted

from a structure with opposite facial selectivity and only the directing group of the auxiliary exo to the pericyclic transition state (**3.89**). While the diastereoselectivity was low for the reaction, aldol adduct **3.87** was isolated as a highly enriched diastereomer (*d.r.* >95:5) via simple flash chromatography.

Scheme 3.17. Stereoselective Synthesis of the Allylic Alcohol Motif.

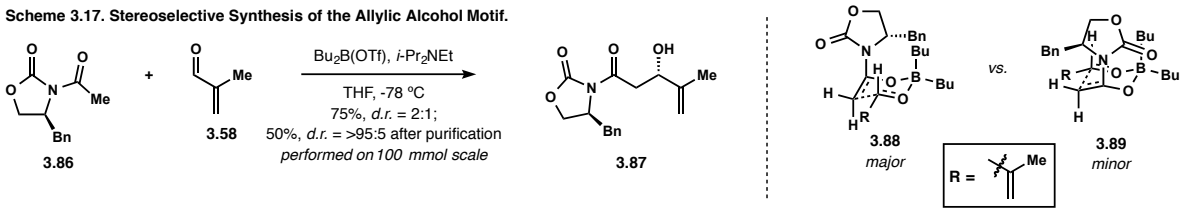

Access to allylic alcohol **3.87** permitted synthetic studies related to the direct formation of the ketal moiety. Previous related research by Shigehisa[30] and our lab indicated that a combination of a cobalt(II)salen catalyst, *N*-fluoro-2,4,6-trimethylpyridinium salt, and silane could affect the proposed mode of reactivity. Based on the previous proposals, the cascade began with an oxidation of the cobalt(II)salen catalyst **3.88** in the presence of a *N*-fluoro-2,4,6-trimethylpyridinium salt **3.89** (Scheme 3.18).

Scheme 3.18. Proposed Mechanism for the Radical-polar Crossover Ketal Formation.

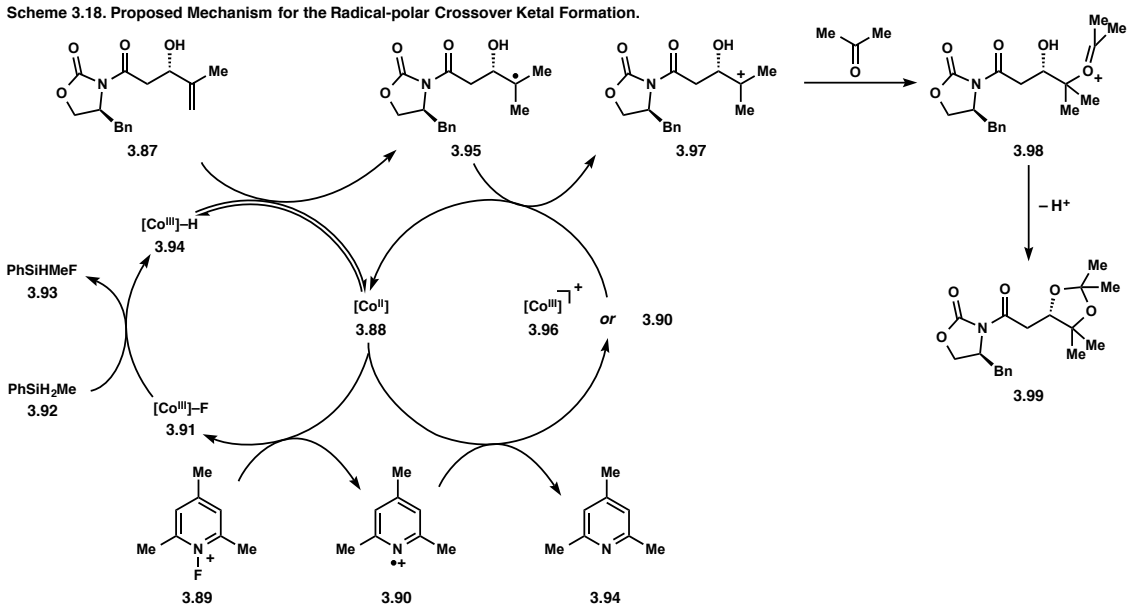

The resulting cobalt(III)–fluoride complex **3.91** underwent transmetallation with a silane (i.e. **3.92**) and delivered a putative cobalt(III)–hydride **3.94**. Ensuing regioselective HAT between metal hydride **3.94** and the substrate **3.87** regenerated the catalyst **3.88** and produced tertiary radical **3.95**. Subsequent single-electron oxidation of **3.95** by either the pyridinium radical cation **3.90** or cationic cobalt(III) **3.96** resulted in formation of tertiary carbocation **3.97**. A nucleophilic attack by acetone at carbocation **3.97** generated oxocarbenium **3.98**, which was positioned to form ketal **3.99** after attack by the secondary alcohol and deprotonation.

Scheme 3.19. Radical-polar Crossover Ketal Formation.

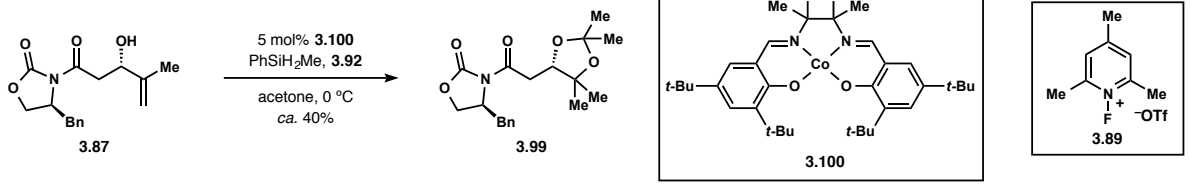

With this mechanism in mind, we set out to investigate ketal formation. We were able to isolate the desired ketal **3.88**, however only in modest yield indicating that further development is likely required (Scheme 3.19). We observed in our initial studies that an excess (3.0 equivalents) of silane and oxidant were necessary to achieve full conversion. Full conversion of silane **3.92** to **3.93** by GCMS was observed so we speculate that either the metal hydride **3.94** or unstable cationic intermediates **3.97** or **3.98** eliminated under the reaction conditions, which led to wasting of the oxidant and silane. Gas evolution, a sign of hydrogen formation, was also observed in the early-stages of the reaction, which could indicate the decomposition of **3.94**. The reaction was highly dependent on the nature of the oxidant, as *N*-fluorobenzenesulphonimide and Selectfluor® were ineffective at facilitating the reaction. Of greater concern was the appearance of the crude reaction mixtures by ^{1}H NMR, which displayed signals associated with the desired product and only minor quantities of side products.

In spite of the unoptimized ketal formation, we were able to continue with our efforts toward 11-ketopaspaline (**3.20**). As such, we converted **3.99** to the desired enone **3.70** in two steps through the intermediacy of Weinreb amide **3.101**,[45] which completed the synthesis of one of the partners for the proposed cross-metathesis (Scheme 3.20).

Scheme 3.20. Completion of the Enone.

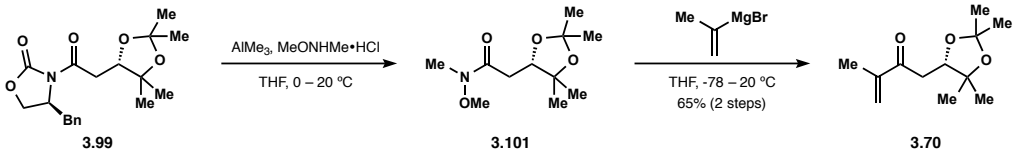

3.3.3 Enantioselective Synthesis of Ketal 3.66

Concurrent to the synthetic efforts related to **3.70** we prepared enantioenriched trisubstituted alkene **3.69** using a synthetic sequence that resembled our first approach to the PIDs.[2] Following this approach, we performed an enantioselective copper-catalyzed conjugate addition of Grignard reagent **3.103** to 2-methyl-cyclopenten-1-one (**3.102**) using a procedure developed by Devon J. Schatz[46,47] and obtained the desired enoxy silane **3.105** in good yield and enantioenrichment (Scheme 3.21).[48,49] Application of the α-alkenylation methodology that our lab developed[2] delivered β,γ-unsaturated ketone **3.107**. We were able to complete the synthesis of trisubstituted alkene **3.69** following diastereoselective reduction and protection of the resulting diol.

Scheme 3.21. Preparation of the Trisubstituted Alkene.

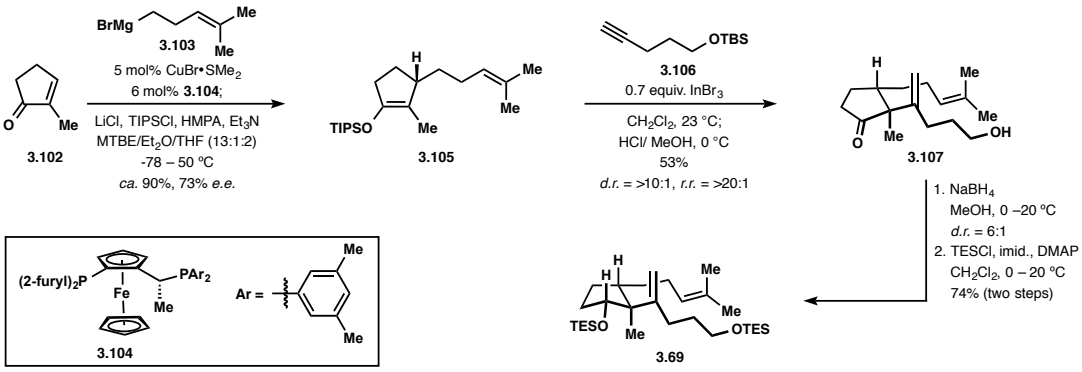

The preparation of **3.69** and **3.70** enabled our pursuit of the cross metathesis. Unlike our model study involving 3-methyl-3-buten-2-one (**3.76**) and racemic **3.69** (*vide supra*; Scheme 3.15), the metathesis between **3.69** and **3.70** did not proceed with the same level of efficiency and a stoichiometric quantity of the ruthenium complex **3.77** was required (Scheme 3.22). While the exact reaction mechanism remains unknown we believe that **3.77** reacts with **3.70** to form an α,β-unsaturated carbonyl metal alkylidene that undergoes cross-metathesis with **3.69** as relevant metal alkylidenes have displayed reactivity toward trisubstituted alkenes.[38] A slight excess of enone **3.70** was utilized as we observed conversion of **3.70** to trisubstituted enone **3.108**. The formation of **3.108** indicated that ruthenium complex **3.77** was decomposing as the reaction progressed since propene is a product of decomposition for similar Grubbs catalysts.[50] We attempted to increase the efficiency of the process and utilize a catalytic loading of ruthenium complexes by employing other known metathesis alkylidene complexes,[51] however low yield and poor catalyst turnover was observed.

Scheme 3.22. Validation of the Cross-metathesis.

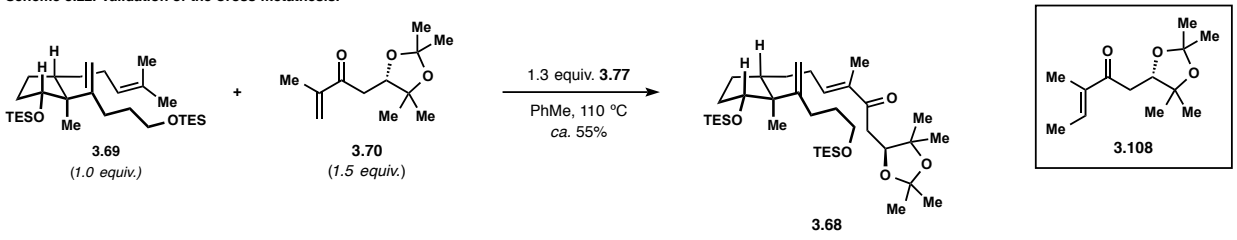

Undeterred by the low efficiency of the cross-metathesis, we continued our studies toward 11-ketopaspaline (**3.20**). As such, the chemoselective oxidation of the primary TES-protected alcohol was achieved using a Swern oxidation to afford aldehyde **3.67** in modest yield (Scheme 3.23).[36,52] During the development of the reaction we discovered that extended reaction times led to oxidation of the secondary TES-protected alcohol. As a result, we favored terminating the reaction at a low level of conversion to obtain the desired product **3.67** and recovered starting material **3.68**. Deprotection of the secondary alcohol was achieved following

treatment with aqueous hydrofluoric acid, which delivered alcohol **3.109**. In corroboration with our previous results,[2] alcohol **3.109** was observed to exist in equilibrium with lactol **3.110** in $CDCl_3$ as a ~2:1 mixture (**3.110** : **3.109**).

Scheme 3.23. Sythesis of the Tricarbocyclic Core.

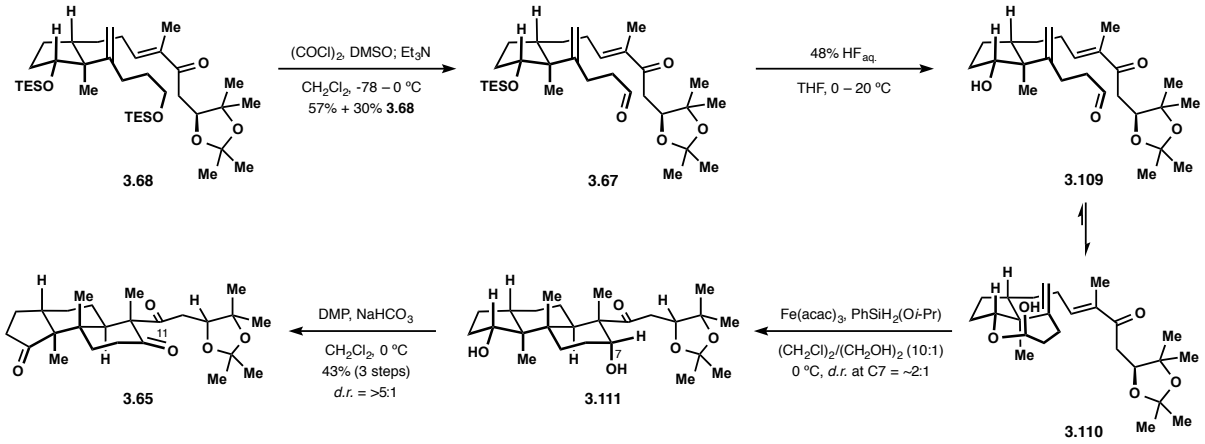

Direct subjection of **3.109** to polycyclization conditions delivered a mixture of epimeric alcohols at C7 with a preference for the axial alcohol **3.111**. In order to restore the cyclopentanone motif for indole assembly and oblate the stereochemistry at C7, double oxidation with Dess–Martin periodinane[11] was pursued using the crude material from the polycyclization cascade. Following the sequence of deprotection, polycyclization, and double oxidation we were able to obtain a modest yield of tricarbonyl **3.65**.[53] While the polycyclization was unselective for the desired stereochemistry at C7, the overall sequence involving the double oxidation offered a stereoselective construction of the tricyclic core **3.66**.

3.3.4 Completion of 7-epi-11-ketopaspaline and dehydro-11-ketopaspaline

Scheme 3.24. Preparation of Vinyl Triflate 3.112.

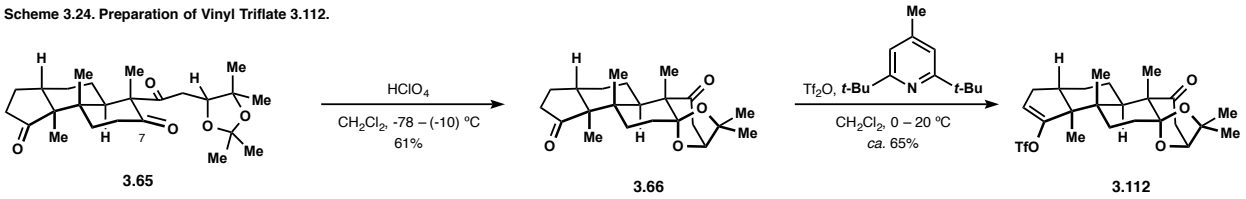

Our endgame strategy toward 11-ketopaspaline (**3.20**) involved reduction of the ketal moiety and indole assembly from the cyclopentanone. In order to install the desired ketal functionality we treated tricarbonyl **3.65** with perchloric acid to induce removal of the acetonide moiety and intramolecular ketal formation at C7 (Scheme 3.24). While the sensitive nature of the β-hydroxy ketone motif resulted in the formation of side products from elimination pathways, careful reaction monitoring facilitated the assembly of pentacycle **3.66**. With the ketal formed we were confident that the caged dioxabicycle would hinder enolization at the proximal ketone in the presence of bulky bases. Indeed, treatment with trifluoromethansulfonic anhydride and 2,6-di-*tert*-butyl-4-methyl pyridine chemoselectively introduced the vinyl triflate functional group onto the 5-membered ring and delivered **3.112**.

Scheme 3.25. Synthesis of 7-*epi*-11-ketopaspaline.

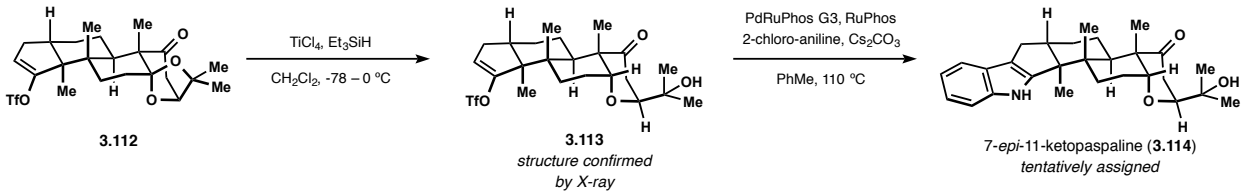

3.112

3.113
structure confirmed by X-ray

7-*epi*-11-ketopaspaline (**3.114**)
tentatively assigned

The preparation of **3.112** allowed our attention to focus on the introduction of the final stereocenter contained in the terpenoid core of 11-ketopaspaline (**3.20**). As such, we hoped to induce invertive displacement of the ketal moiety with a hydride donor in the presence of Lewis acid to reveal the tetracyclic core. However, upon treatment with $TiCl_4$ and Et_3SiH we observed clean conversion to tetracycle **3.113** with the incorrect stereochemistry at C7 (Scheme 3.25). Analysis of the correlations from a NOESY experiment supported our initial assignment of **3.113** and X-ray crystallographic analysis of a suitable crystal confirmed our assignment. Given the outcome of the reduction we believe that oxacarbenium ion formation readily occurred, which rendered the desired *re*-face inaccessible due to its position on the concave face of the molecule. As a result, exclusive hydride delivery from the convex face into the *si*-face of the oxacarbenium

ion occurred. While this stereochemical outcome was undesired, we investigated the indole assembly via a Barluenga indole synthesis[3c,54] and tentatively accessed 7-*epi*-11-ketopaspaline (**3.114**).[55]

Scheme 3.26. Synthesis of dehydro-11-ketopaspaline.

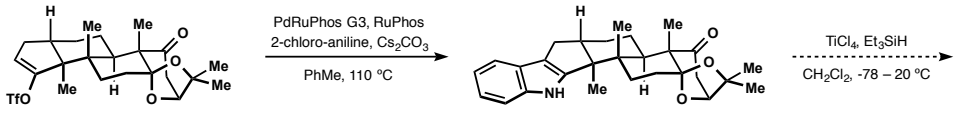

3.112

dehydro-11-ketopaspaline (**3.115**)
tentatively assigned

As a potential solution, we tentatively converted **3.112** to dehydro-11-ketopaspaline (**3.115**)[55] in hope that the indole moiety would induce subtle electronic or structural changes that could influence the stereochemical outcome of the reduction event (Scheme 3.26). Unfortunately, attempts at the reduction of **3.115** resulted in no reaction and recovery of the starting material. At the preliminary stage of our efforts in this area, it is unclear as to why the indole nucleus deactivates the ketal toward reduction.

3.3.5. Conclusions and Outlook

While the synthesis of 11-ketopaspaline (**3.20**) remains unfinished the efforts described in this Chapter have achieved the synthesis of an advanced intermediate **3.66** that possesses many of the structural elements found in the terpenoid core. The full propagation of the polycyclization cascade solved a key challenge related to regioselective enolate generation that plagued our initial synthetic studies related to the expansion of our program related to the PIDs. Given the preliminary nature of our results on the late-stage reduction of the ketal moiety it remains unclear if the current approach ultimately leads to a fundamentally flawed synthetic sequence. Efforts related to solving the reduction are ongoing and are pursuing alternative combinations of Lewis acids and reducing agents in addition to directed strategies.[56] It is our hope that a solution to the diastereoselective reduction will be developed and reported in the near future.[57]

3.4 Experimental Section

3.4.1. General Experimental Details

All reactions were carried out in flame- or oven-dried glassware under a positive pressure of dry nitrogen unless otherwise noted. Reaction solvents including diethylether (Et_2O, Fisher, HPLC Grade), tetrahydrofuran (THF, Fisher, HPLC Grade), methylene chloride (CH_2Cl_2, Fisher, HPLC Grade), benzene (PhH, Fisher, HPLC Grade), and toluene (PhMe, Fisher, HPLC Grade) were dried by percolation through a column packed with neutral alumina and a column packed with a supported copper catalyst for scavenging oxygen (Q5) under positive pressure of argon. Anhydrous, 1,2-dichloroethane (Fisher, ACS Grade), *N*,*N*-diisopropylamine (Oakwood Chemical, triethylamine (Oakwood Chemical), and *N*,*N*-diisopropylethylamine (Oakwood Chemical) were distilled from calcium hydride (~10% w/v) under a positive pressure of nitrogen. Anhydrous ethylene glycol [$(CH_2OH)_2$] was purchased from Sigma–Aldrich. Dimethyl sulfoxide (DMSO, EMD Chemicals) was dried over activated 3 Å molecular sieves (Acros Organics, 20% w/w). Anhydrous hexamethphosphoramide (HMPA, Oakwood Chemical) was distilled from calcium hydride (10% w/v) under vacuum (*ca*. 0.1 torr). Solvents for extraction, thin layer chromatography (TLC) and flash column chromatography were purchased from Fisher (ACS Grade) and VWR (ACS Grade) and used without further purification. Chloroform-d and benzene-d_6 for ^1H and ^{13}C NMR analysis were purchased from Cambridge Isotope Laboratories and used without further purification. Commercially available reagents were used without further purification unless otherwise noted. All reactions were monitored by TLC using precoated siliga gel plates (EMD Chemicals, Siliga gel F_{254}). Flash column chromatography was performed over silica gel (Acros Organics, 60 Å, particle size 0.04 – 0.063 mm). ^1H NMR and ^{13}C NMR spectra were recorded on Bruker DRX-500 (BBO probe), Bruker DRX-500 (TCI cryoprobe), and Bruker

AVANCE600 (TBI probe) spectrometers using residual solvent peaks as internal standards [$CHCl_3$: 7.26 ppm (^{1}H NMR), 77.00 ppm (^{13}C NMR); C_6H_6: 7.16 ppm (^{1}H NMR), 128.00 ppm (^{13}C NMR)]. High-resolution mass spectra (HRMS) were recorded on Waters LCT Premier TOF spectrometer with ESI and CI sources. Enantiomeric excess (*e.e.*) was determined using an Agilent Technologies 7820A Gas Chromatography System equipped with a 30m x 0.250 mm HP-Chiral-20B column. Optical rotations were measured with a Jasco P-1010 polarimeter.

3.4.2. Experimental Procedures

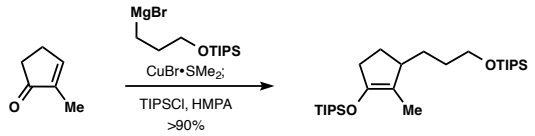

3.24 3.25

Grignard preparation: A Schlenk flask was charged with magnesium turnings (1.63 g, 67.0 mmol, freshly activated by mechanical grinding with a mortar and pestel) in a nitrogen atmosphere glovebox. The flask was sealed with a plastic cap, removed from the glovebox, and connected to a double bank vacuum manifold. The plastic cap was replaced with a rubber septum under a positive atmosphere of nitrogen. THF (61 mL) and 5 drops of a solution of iodine (1.0 M in MTBE) were added to form a yellow tinted suspension. *O*-triisopropylsilyl-3-bromo-propan-1-ol[58] (16.5 g, 55.9 mmol) was added in a single portion and the mixture was agitated in a sonicator until the yellow tint disappeared. The resulting colorless mixture was vigorously stirred in a water bath to control the exotherm. After 2 hours titration revealed a 0.49 M solution had been prepared.

Enoxysilane **3.25**: While hot, an oven-dried three-neck round bottom flask was equipped with an oven-dried addition funnel in the center position, an inlet of anhydrous nitrogen in one of the side positions, and a septum in the other side position. The assembled system was allowed to cool to room temperature under a stream of nitrogen by venting through the top of the addition

funnel. Once cooled, the flask was charged with CuBr•SMe_2 (0.6 g, 2.9 mmol) and THF (5 mL). The flask was submerged in a cooling bath maintained at ~(-35) ºC. While the suspension was cooling, the addition funnel was charged with the freshly prepared Grignard solution. The Grignard solution was added in a dropwise manner over 30 minutes. After the addition was complete the cooling bath was further cooled to ~(-45) ºC and 2-methyl-cyclopenten-1-one (2.8 mL, 28.5 mmol) was added in a dropwise manner via a syringe pump. After the addition was complete stirring was continued at ~(-45) ºC. After 45 minutes, triisopropylchlorosilane (11.6 mL, 57.0 mmol) was added and the flask was removed from the cooling bath and allowed to slowly warm to room temperature. Once at room temperature HMPA (22.3 mL. 128.3 mmol) were added and the flask was warmed to 50 ºC. After 3 hours the solution was cooled to 0 ºC and quenched with a 3:1 mixture of saturated aqueous NH_4Cl:NH_4OH (30 mL). The organic layer was diluted with hexanes (50 mL) and washed with a 3:1 mixture of a saturated aqueous NH_4Cl:NH_4OH until no traces of a blue color was observed (2x60 mL). The combined aqueous layers were extracted with hexanes (2x100 mL). The combined organic layers were washed with brine (45 mL), dried over anhydrous sodium sulfate, filtered, and concentrated under reduced pressure. Purification by flash chromatography over silica gel deactivated with 1% Et_3N in hexanes (elution 100% hexanes) afforded 14.4 g (>99%) of **3.25** as a clear, colorless oil that was contaminated with Wurtz coupling and protonation of the Grignard. ^{1}H NMR (500 MHz; C_6H_6): δ 3.69–3.66 (m, 2H), 2.47 (td, *J* = 2.1, 0.9 Hz, 1H), 2.33–2.27 (m, 2H), 1.96 (dtd, *J* = 12.9, 8.6, 4.6 Hz, 1H), 1.77–1.63 (m, 5H), 1.58–1.49 (m, 2H), 1.48–1.41 (m, 1H), 1.32–1.24 (m, 1H), 1.16–1.06 (m, 47H).

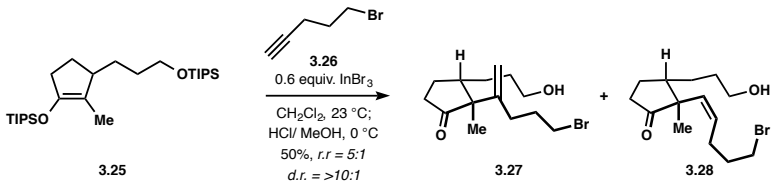

Alcohol **3.27**: A Schlenk flask was charged with $InBr_3$ (0.52 g, 1.5 mmol) in a nitrogen atmosphere glovebox. The flask was sealed with a plastic cap, removed from the glovebox, and connected to a double bank vacuum manifold. The plastic cap was replaced with a rubber septum under a positive atmosphere of nitrogen. The flask was charged with a solution of enoxysilane **3.25** (1.47 g, 2.5 mmol) and **3.26** (0.48 mL, 3.25 mmol) in CH_2Cl_2 (3.5 mL) via a cannula. The resulting mixture was vigorously stirred at room temperature. After 16 hours the flask was cooled to 0 ºC and quenched with 1% HCl in MeOH (3.5 mL, prepared using a concentrated aqueous solution of HCl). After 4.5 hours the solution was transferred to a recovery flask and concentrated under reduced pressure. The residue was partitioned between diethyl ether (10 mL) and water (3 mL). The aqueous layer was extracted with diethyl ether (3x10 mL). The combined organics were washed with water (3 mL) and brine (3 mL), dried over anhydrous magnesium sulfate, filtered, and concentrated under reduced pressure. Purification by flash chromatography (gradient elution: 100% hexanes to 35% ethyl acetate in hexanes) afforded 379.4 mg (50%) of a 5:1 mixture of **3.27**:**3.28** as a clear, colorless oil. ^{1}H-NMR (500 MHz; $CDCl_3$): δ 5.05 (d, J = 8.9 Hz, 1H), 3.68–3.66 (m, 2H), 3.47–3.37 (m, 2H), 2.49–2.43 (m, 1H), 2.30–1.97 (m, 6H), 1.73–1.65 (m, 1H), 1.60–1.43 (m, 5H), 1.31–1.24 (m, 1H), 1.02 (s, 3H).

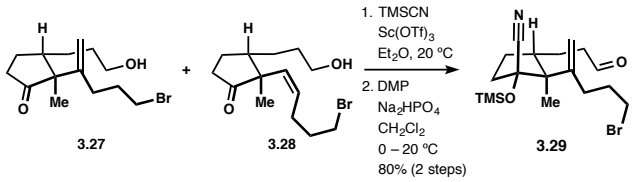

O-TMS cyanohydrin **3.29**: A Schlenk flask was charged with $Sc(OTf)_3$ (64.0 mg, 0.13 mmol). The flask was gently heated with a heat gun under reduced pressure to remove trace quantities of moisture. TMSCN (0.78 mL, 6.25 mmol) followed by a solution of alcohol **3.27** (379.4 mg, 1.25 mmol) in diethyl ether (2.8 mL) were added. The reaction was vigorously stirred at room temperature. After 30 minutes the reaction was quenched with a solution of saturated aqueous $NaHCO_3$ (3.5 mL). The aqueous layer was extracted with diethyl ether (3x15 mL). The combined organic layers were washed with water (5 mL) and brine (5 mL), dried over anhydrous magnesium sulfate, filtered, and concentrated under reduced pressure. The crude alcohol was used without further purification. ^{1}H NMR (500 MHz; $CDCl_3$): δ 5.06 (t, *J* = 1.4 Hz, 1H), 5.00 (s, 1H), 3.68–3.62 (m, 3H), 3.50–3.41 (m, 3H), 2.41–2.25 (m, 5H), 2.11–2.01 (m, 3H), 1.96–1.89 (m, 2H), 1.65–1.41 (m, 13H), 0.99 (s, 3H), 0.23 (s, 9H).

Dess–Martin periodinane (715.6 mg, 1.68 mmol) and Na_2HPO_4 (497.1 mg, 3.37 mmol) were added to a solution of the crude alcohol (452.7 mg, 1.12 mmol) in methylene chloride (2.5 mL) at 0 ºC. The reaction was vigorously stirred and allowed to warm to room temperature. After 2 hours the reaction was quenched with a solution of saturated aqueous $NaHCO_3$:$Na_2S_2O_3$:water (1:1:1, 5 mL total). The biphasic mixture was vigorously stirred at room temperature. After 5 minutes the aqueous layer was extracted with methylene chloride (3x10 mL). The combined organic layers were washed with water (5 mL) and brine (5 mL), dried over anhydrous magnesium sulfate, filtered, and concentrated under reduced pressure. Purification by flash chromatography (gradient elution: 100% hexanes to 15% ethyl acetate in hexanes) afforded 361. mg (80% from **3.27**/**3.28**) as a clear, colorless oil. ^{1}H NMR (500 MHz; $CDCl_3$): δ 9.79 (s, 1H), 5.08 (s, 1H), 5.02 (s, 1H), 3.50–3.42 (m, 2H), 2.53–2.25 (m, 7H), 2.11–1.86 (m, 6H), 1.44–1.38 (m, 2H), 1.01 (s, 3H), 0.24 (s, 9H).

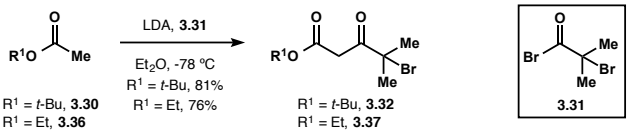

General Procedure:[11] Acetate **3.30** or **3.36** (1.0 equiv., freshly distilled from powdered 3 Å molecular sieves) was added to a solution of LDA [freshly prepared from *N*,*N*-diisopropylamine (1.05 equiv.) and *n*-BuLi (1.03 equiv., 2.45 –2.50 M in hexanes) in diethyl ether (0.3M) at 0 ºC] in a dropwise manner at –78 ºC. The reaction was vigorously stirred at -78 ºC. After 45 minutes acyl bromide **3.31** (1.2 equiv.) was added in a dropwise manner. After an additional 90 minutes the reaction was quenched with a solution of saturated aqueous NH_4Cl and extracted with diethyl ether. The combined organics were dried over anhydrous sodium sulfate, filtered, and concentrated under reduced pressure. Purification by flash chromatography afforded purified products.

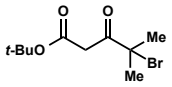

3.32

Comments: The reaction was performed on 3.0 mmol scale. A gradient elution (100% hexanes to 5% ethyl acetate in hexanes) was used during purification, which afforded 639.8 mg (81%) of **3.32** as a clear, colorless oil. ^{1}H NMR (500 MHz; $CDCl_3$): δ 3.78 (s, 2H), 1.89 (s, 6H), 1.47 (s, 9H).

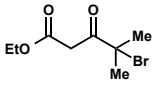

3.37

Comments: The reaction was performed on 15.0 mmol scale. A gradient elution (100% hexanes to 10% ethyl acetate in hexanes) was used during purification, which afforded 2.72 g (76%) of **3.37** as a clear, colorless oil. ^{1}H NMR (500 MHz; $CDCl_3$): 4.21 (q, J = 7.1 Hz, 2H), 3.87 (s, 2H), 1.89 (s, 6H), 1.28 (t, J = 7.1 Hz, 3H).

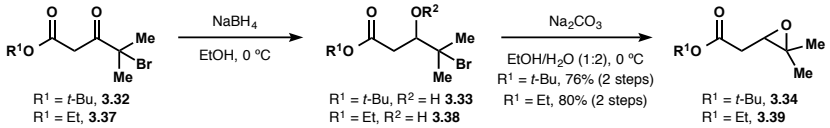

General Procedure: Sodium borohydride (0.5 equiv.) was added to a solution of β-keto ester (1.0 equiv.) in EtOH (0.1 M) at 0 ºC. The reaction was vigorously stirred at 0 ºC. After 30 minutes the reaction was quenched with water and warmed to room temperature. The aqueous layer was extracted with methylene chloride and the combined organic layers were washed with brine, dried over anhydrous sodium sulfate, filtered, and concentrated under reduced pressure. The crude β-hydroxy ester was used without further purification.

Solid Na_2CO_3 (1.0 equiv) was added to a solution of the crude β-hydroxy ester (1.0 equiv) in aqueous EtOH (0.1 M, 1:2; EtOH:H_2O). The reaction was vigorously stirred at room temperature. After 10 minutes the reaction was partitioned with pentane and the aqueous layer was quickly extracted with additional pentane. The combined organic layers were dried over anhydrous sodium sulfate, filtered, and concentrated under reduced pressure.

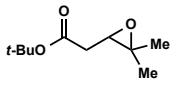

3.34

Comments: The reaction was performed on 1.78 mmol scale and the crude material was used without further purification. ^{1}H NMR (500 MHz; $CDCl_3$): δ 3.07 (t, J = 6.3 Hz, 1H), 2.57 (dd, J = 16.5, 6.3 Hz, 1H), 2.43 (dd, J = 16.5, 6.3 Hz, 1H), 1.47 (s, 9H), 1.35 (s, 3H), 1.28 (s, 3H).

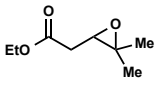

3.39

Comments: The reaction was performed on 2.19 mmol scale and the crude material was used without further purification. ^{1}H NMR (500 MHz; $CDCl_3$): δ 4.19 (qd, J = 7.1, 1.7 Hz, 2H), 3.12

(t, J = 6.3 Hz, 1H), 2.63 (dd, J = 16.6, 6.4 Hz, 1H), 2.53 (dd, J = 16.6, 6.1 Hz, 1H), 1.35 (s, 3H), 1.29 (t, J = 3.6 Hz, 6H).

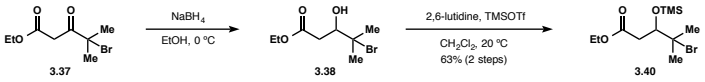

O-TMS Ether **3.40**: Sodium borohydride (199.4 mg, 5.2 mmol) was added to a solution of β-keto ester (2.5 g, 10.5 mmol) in EtOH (105 mL) at 0 ºC. The reaction was vigorously stirred at 0 ºC. After 20 minutes the reaction was quenched with a solution of 0.2 M aqueous HCl (50 mL) and warmed to room temperature. The aqueous layer was extracted with methylene chloride (3x150 mL). The combined organic layers were dried over anhydrous sodium sulfate, filtered, and concentrated under reduced pressure. The crude β-hydroxy ester was used without further purification.

2,6-lutidine (3.0 mL, 26.0 mmol) was added to a solution of crude β-hydroxy ester **3.38** (~10.5 mmol) in methylene chloride (80 mL) at room temperature. TMSOTf (2.4 mL, 13.0 mmol) was added in a slow steady stream. The reaction was vigorously stirred at room temperature. After 2 hours the reaction was quenched with a solution of brine. The aqueous layer was extracted with diethyl ether (3x75 mL). The combined organic layers were washed with brine (60 mL), dried over anhydrous sodium sulfate, filtered, and concentrated under reduced pressure. Purification by flash chromatography (elution with 2% v/v ethyl acetate in hexanes) afforded 2.04 g (63%) of ester **3.40** as a clear, colorless oil. ^{1}H NMR (500 MHz; $CDCl_3$): δ 4.25 (dd, J = 8.9, 2.4 Hz, 1H), 4.16 (q, J = 7.2 Hz, 2H), 2.93 (dd, J = 15.9, 2.4 Hz, 1H), 2.49 (dd, J = 15.9, 9.0 Hz, 1H), 1.73 (s, 3H), 1.68 (s, 3H), 1.28 (t, J = 7.2 Hz, 3H), 0.13 (s, 9H).

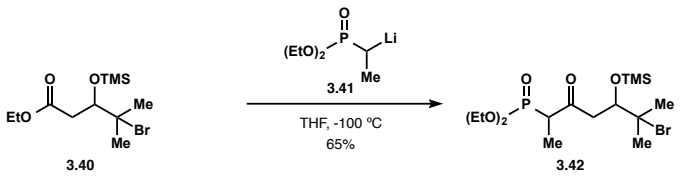

β-keto phosphonate **3.42**: *n*-BuLi (5.25 mL, 13.4 mmol, 2.55 M in hexanes) was added to a solution of diethyl ethylphosphonate (2.17 mL, 13.4 mmol) in THF (30 mL) at -78 ºC. The reaction was vigorously stirred at -78 ºC. After 20 minutes the flask was further cooled to -100 ºC and a solution of ester **3.40** (2.04 g, 6.6 mmol) in THF (5 mL) was added dropwise over 10 minutes. The reaction was vigorously stirred at -100 ºC. After 30 minutes the reaction was quenched with a solution of 0.2 M aqueous HCl (50 mL) and allowed to warm to room temperature. The aqueous layer was extracted with ethyl acetate (3x50 mL). The combined organic layers were washed with solutions of saturated aqueous $NaHCO_3$ (25 mL) and brine (25 mL), dried over anhydrous sodium sulfate, filtered, and concentrated. Purification by flash chromatography (gradient elution 30% v/v ethyl acetate in hexanes to 50% v/v ethyl acetate in hexanes) afforded 1.85 g (65%) of β-keto phosphonate **3.42** as a light yellow oil. Isolated as a mixture of tautomers. ^{1}H NMR (500 MHz; $CDCl_3$): δ 4.28–4.26 (m, 2H), 4.18–4.10 (m, 9H), 3.37 (dd, *J* = 18.3, 2.1 Hz, 1H), 3.21 (s, 3H), 3.04 (dd, *J* = 18.4, 7.1 Hz, 1H), 2.83 (dd, *J* = 18.2, 8.3 Hz, 1H), 2.04 (s, 1H), 1.71 (d, *J* = 1.9 Hz, 5H), 1.69 (s, 3H), 1.68 (s, 2H), 1.35-1.32 (m, 14H), 0.13 (s, 7H), 0.11 (s, 9H).

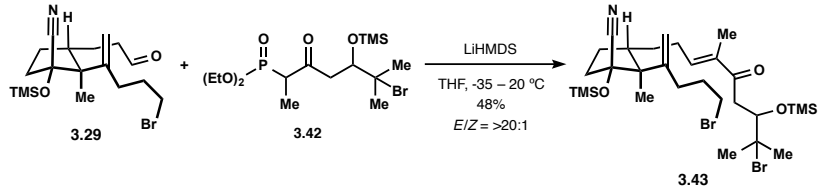

Enone **3.43**: A solution of β-keto phosphonate **3.42** (194.5 mg, 0.45 mmol) in THF (0.7 mL) was added to a solution of LiHMDS [freshly prepared from HMDS (94 μL, 0.45 mmol) and *n*-BuLi (175 μL, 0.45 mmol, 2.55 M in hexanes) in THF (0.9 mL) at -35 ºC] in THF at -35 ºC. The reaction was vigorously stirred and allowed to warm to room temperature. After 40 minutes the reaction was cooled to -35 ºC and a solution of aldehyde **3.29** (160.2 mg, 0.4 mmol) in THF (0.6

mL) was added in a dropwise manner. The reaction was vigorously stirred and allowed to slowly warm to room temperature. After 3.5 hours the reaction was quenched with a solution of saturated aqueous NH_4Cl (2.0 mL). The aqueous layer was extracted with ethyl acetate (4x7 mL). The combined organic layers were dried over anhydrous magnesium sulfate, filtered, and concentrated under reduced pressure. Purification by flash chromatography (gradient elution: 100% hexanes to 3% v/v ethyl acetate in hexanes) afforded 143.6 mg (48%) of enone **3.43** as a light yellow oil. ^{1}H NMR (500 MHz; $CDCl_3$): δ 6.62 (t, *J* = 6.9 Hz, 1H), 5.05 (s, 1H), 4.97 (s, 1H), 4.28 (td, *J* = 5.7, 3.4 Hz, 1H), 3.47–3.39 (m, 2H), 3.06–2.95 (m, 2H), 2.41–2.24 (m, 5H), 2.18 (ddd, *J* = 14.0, 7.1, 3.2 Hz, 1H), 2.11–2.01 (m, 3H), 1.96–1.90 (m, 1H), 1.77 (s, 3H), 1.69 (d, *J* = 1.2 Hz, 6H), 1.52–1.41 (m, 1H), 1.28–1.23 (m, 1H), 0.98 (s, 3H), 0.22 (s, 9H), 0.06 (s, 9H).

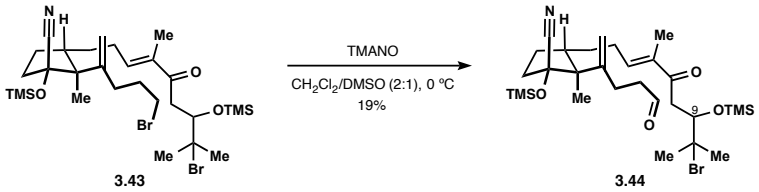

Aldehyde **3.44**: A solutions of trimethylamine-*N*-oxide (22.5 mg, 0.3 mmol) in DMSO (0.4 mL) followed by triethylamine (80 μL, 0.008 mmol, 0.1 M in methylene chloride) were added to a solution of bromide **3.43** (80.3 mg, 0.12 mmol) in methylene chloride (0.8 mL) at 0 ºC. The reaction was vigorously stirred at 0 ºC. After 1 hour the reaction was warmed to room temperature and an additional 15 mg (0.15 mmol) of trimethylamine-*N*-oxide was added. After an additional hour the reaction was heated to 30 ºC. After 20 hours the reaction was cooled to room temperature and quenched with water (1 mL). The aqueous layer was extracted with diethyl ether (4x7 mL). The combined organic layers were washed with water (3 mL) and brine (3 mL), dried over anhydrous magnesium sulfate, filtered, and concentrated under reduced

pressure. Purification by flash chromatography (gradient elution: 100% hexanes to 7.5% v/v ethyl acetate in hexanes) afforded 14.0 mg (19%) mixture of diastereomeric aldehydes at C9 **3.44** as a thin film. ^{1}H NMR (500 MHz; $CDCl_3$): δ 9.80 (s, 1H), 6.63 (t, *J* = 6.9 Hz, 1H), 5.00 (d, *J* = 4.6 Hz, 2H), 4.30 (dt, *J* = 7.1, 3.6 Hz, 1H), 3.07-2.97 (m, 2H), 2.62 (dq, *J* = 30.5, 7.9 Hz, 3H), 2.48-2.25 (m, 6H), 2.22-2.07 (m, 3H), 1.95 (td, *J* = 13.0, 6.6 Hz, 1H), 1.79 (s, 3H), 1.71 (s, 6H), 1.54-1.46 (m, 2H), 1.31-1.22 (m, 3H), 1.02 (s, 3H), 0.23 (s, 9H), 0.07 (s, 9H). ^{13}C NMR (125 MHz; $CDCl_3$): δ 202.0, 199.3, 148.4, 142.39, 142.36, 138.05, 138.02, 121.7, 111.4, 82.6, 76.34, 76.31, 70.1, 56.2, 42.8, 42.1, 40.90, 40.86, 36.7, 31.45, 31.39, 30.36, 30.32, 29.52, 29.40, 27.7, 25.39, 25.36, 23.7, 12.7, 11.5, 1.1, 0.43, 0.40.

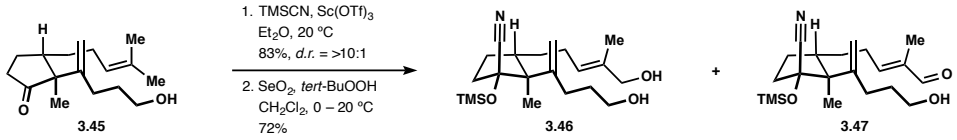

Diol **3.46**: A Schlenk flask was charged with $Sc(OTf)_3$ (1.33 g, 2.7 mmol). The flask was gently heated with a heat gun under reduced pressure to remove trace quantities of moisture. TMSCN (17.2 mL, 137.2 mmol, freshly distilled) followed by a solution of ketone **3.45**[2] (7.26 g, 27.4 mmol) in diethyl ether (60 mL mL) were added to the flask. The resulting solution was vigorously stirred at room temperature. After 2 hours the reaction was quenched with a solution of saturated aqueous $NaHCO_3$ (60 mL) and biphasic mixture was vigorously stirred for an additional 30 minutes. The aqueous layer was extracted with diethyl ether (3x100 mL). The combined organic layers were washed with water (50 mL) and brine (50 mL), dried over anhydrous magnesium sulfate, filtered, and concentrated under reduced pressure. Purification by flash chromatography (gradient elution: 100% hexanes to 20% v/v ethyl acetate in hexanes) afforded 8.26 g (83%) of an intermediate cyanohydrin. ^{1}H NMR (500 MHz; $CDCl_3$): δ 5.13–5.09 (m, 1H), 5.07 (s, 1H), 4.99 (s, 1H), 3.72–3.65 (m, 2H), 2.40–2.24 (m, 3H), 2.22–2.15 (m, 1H),

2.11–1.99 (m, 2H), 1.95–1.88 (m, 2H), 1.78 (dqd, J = 8.7, 6.7, 1.9 Hz, 2H), 1.69 (s, 3H), 1.61 (s, 3H), 1.58–1.56 (m, 1H), 1.45 (tdd, J = 12.9, 9.4, 3.7 Hz, 1H), 1.27–1.24 (m, 1H), 1.16–1.09 (m, 1H), 0.97 (s, 3H), 0.22 (s, 9H).

A solution of tert-butyl hydroperoxide (11.9 mL, 68.1 mmol, 5.82 M solution in decane) was added to a mixture of the above cyanohydrin (8.26 g, 22.7 mmol) and selenium dioxide (1.26 g, 11.4 mmol) in methylene chloride (68 mL) at 0 °C. The resulting suspension was vigorously stirred and allowed to warm to room temperature. After 2.5 hours the reaction was quenched with a solution of saturated aqueous $NaHCO_3$ (80 mL). The aqueous layer was extracted with diethyl ether (3x100mL). The combined organic layers were washed with water (75 mL) and brine (75 mL), dried over anhydrous sodium sulfate, and concentrated under reduced pressure. Purification by flash chromatography (gradient elution: 100% hexanes to 90% v/v ethyl acetate in hexanes) afforded 1.04 g (13%) of aldehyde **3.47**, 4.84 g (59%) of diol **3.46**, and ~2 g (*ca.* 25%) of starting alcohol **2.45** as clear, colorless oils. For **3.46**: ^{1}H NMR (500 MHz; $CDCl_3$): δ 5.44–5.40 (m, 1H), 5.07 (t, J = 1.5 Hz, 1H), 5.00 (s, 1H), 4.00 (s, 2H), 3.72–3.66 (m, 2H), 2.40–2.17 (m, 4H), 2.09 (dtdd, J = 12.8, 4.8, 4.6, 4.5 Hz, 2H), 2.02–1.89 (m, 2H), 1.81–1.74 (m, 2H), 1.67 (s, 3H), 1.61–1.52 (m, 4H), 1.50–1.35 (m, 3H), 1.22–1.14 (m, 1H), 0.97 (s, 3H), 0.22 (s, 9H). For **3.47**: ^{1}H NMR (500 MHz; $CDCl_3$): δ 9.39 (s, 1H), 6.48 (td, J = 7.4, 1.3 Hz, 1H), 5.10 (t, J = 1.4 Hz, 1H), 4.97 (s, 1H), 3.73–3.65 (m, 2H), 2.40 (dtd, J = 13.4, 9.0, 4.0 Hz, 2H), 2.33–2.26 (m, 2H), 2.20 (dt, J = 16.1, 8.0 Hz, 1H), 2.10 (dtd, J = 13.2, 9.6, 6.1 Hz, 1H), 1.95 (td, J = 12.9, 6.3 Hz, 1H), 1.81–1.70 (m, 6H), 1.53–1.45 (m, 1H), 1.33–1.25 (m, 2H), 1.00 (s, 3H), 0.23 (s, 9H).

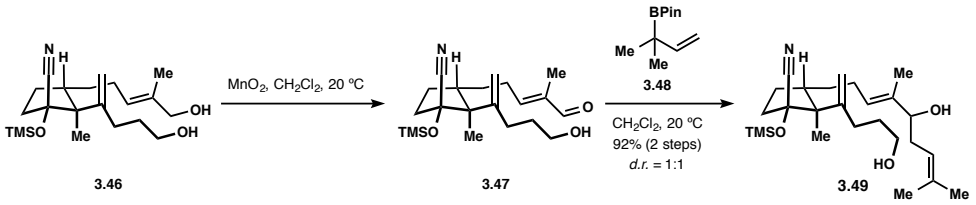

Diol **3.49**: MnO_2 (5.22 g, 60.0 mmol) was added to a solution of diol **3.46** (1.0 g, 2.9 mmol) in methylene chloride (30.0 mL). The heterogeneous mixture was vigorously stirred at room temperature. After 23 hours the mixture was filtered through a plug of Celite. The filter cake was thoroughly rinsed with methylene chloride and the combined organic material was concentrated under reduced pressure. Crude aldehyde **3.47** was used without further purification. ^{1}H NMR (500 MHz; $CDCl_3$): δ 9.39 (s, 1H), 6.48 (td, *J* = 7.4, 1.3 Hz, 1H), 5.10 (t, *J* = 1.4 Hz, 1H), 4.97 (s, 1H), 3.73–3.65 (m, 2H), 2.40 (dtd, *J* = 13.4, 9.0, 4.0 Hz, 2H), 2.33–2.26 (m, 2H), 2.20 (dt, *J* = 16.1, 8.0 Hz, 1H), 2.10 (dtd, *J* = 13.2, 9.6, 6.1 Hz, 1H), 1.95 (td, *J* = 12.9, 6.3 Hz, 1H), 1.81–1.70 (m, 6H), 1.53–1.45 (m, 1H), 1.33–1.25 (m, 2H), 1.00 (s, 3H), 0.23 (s, 9H).

Pinacol borane **3.48**[59] (1.13 g, 5.8 mmol) was added to a solution of aldehyde **3.49** in methylene chloride (10 mL). The solution was vigorously stirred at room temperature. After 24 hours the reaction was quenched with a solution of saturated aqueous $NaHCO_3$. The aqueous layer was extracted with methylene chloride (3x15 mL). The combined organic layers were washed with brine (7 mL), dried over anhydrous sodium sulfate, filtered, and concentrated under reduced pressure. Purification by flash chromatography afforded 1.19 g (92% from **3.46**) of diol **3.49** as a clear, colorless oil. ^{1}H NMR (500 MHz; $CDCl_3$): δ 5.43–5.40 (m, 1H), 5.12–5.09 (m, 1H), 5.07 (d, *J* = 1.5 Hz, 1H), 5.00 (s, 1H), 3.99–3.97 (m, 1H), 3.69 (t, *J* = 2.5 Hz, 2H), 2.40–2.18 (m, 6H), 2.08 (dtd, *J* = 12.7, 9.1, 5.8 Hz, 2H), 2.00–1.89 (m, 3H), 1.77 (tddd, *J* = 8.9, 6.7, 4.5, 2.2 Hz, 2H), 1.72 (s, 3H), 1.64–1.56 (m, 8H), 1.45 (dq, *J* = 12.6, 4.1 Hz, 1H), 1.24 (s, 3H), 0.97 (s, 3H), 0.21 (d, *J* = 1.8 Hz, 9H).

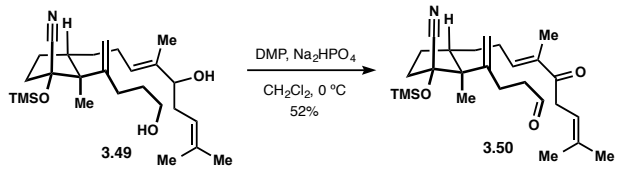

Dicarbonyl **3.50**: Dess–Martin periodinane (2.8 g, 6.6 mmol) and Na_2HPO_4 (1.89 g, 13.3 mmol) were added to a solution of diol **3.49** (1.19 g, 2.7 mmol) in methylene chloride (13.5 mL) at 0 ºC. The reaction was vigorously stirred at 0 ºC. After 3.5 hours the reaction was quenched with a solution of 10% aqueous Na_2CO_3 (4 mL). The aqueous layer was extracted with methylene chloride (3x15 mL). The combined organic layers were washed with brine (5 mL), dried over anhydrous magnesium sulfate, filtered and concentrated under reduced pressure. Purification by flash chromatography (gradient elution: 100% hexanes to 10% v/v ethyl acetate in hexanes) afforded 0.61 g (52%) of dicarbonyl **3.50** as a clear, colorless oil. ^{1}H NMR (600 MHz; $CDCl_3$): δ 9.81 (t, *J* = 1.4 Hz, 1H), 6.60 (td, *J* = 7.2, 1.3 Hz, 1H), 5.31–5.29 (m, 1H), 5.00 (d, *J* = 5.0 Hz, 2H), 3.36 (d, *J* = 6.9 Hz, 2H), 2.68–2.58 (m, 3H), 2.47–2.34 (m, 3H), 2.32–2.26 (m, 1H), 2.21–2.08 (m, 2H), 1.95 (td, *J* = 13.0, 6.5 Hz, 1H), 1.78 (d, *J* = 0.9 Hz, 3H), 1.74 (d, *J* = 1.2 Hz, 3H), 1.64 (s, 3H), 1.50 (tdd, *J* = 12.9, 9.4, 3.6 Hz, 1H), 1.30–1.23 (m, 1H), 1.02 (s, 3H), 0.23 (s, 9H).

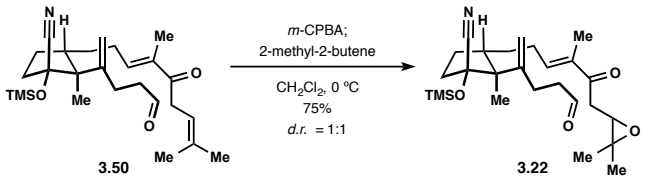

Epoxide **3.22**: *m*-CPBA (368.1 mg, 1.6 mmol, 75%) was added to a solution of dicarbonyl **3.50** (0.61 g, 1.4 mmol) in methylene chloride (28 mL) at 0 ºC. The reaction was vigorously stirred and the temperature was maintained at 0 ºC. After 1.25 hours the reaction was quench by the addition of 2-methyl-2-butene (0.89 mL, 8.4 mmol). After an additional 20 minutes the reaction was allowed to warm to room temperature and a solution of saturated aqueous $NaHCO_3$ (5 mL) was added. The aqueous layer was extracted with methylene chloride (20 mL). The combined

organic layers were washed with brine (10 mL), dried over anhydrous sodium sulfate, filtered, and concentrated under reduced pressure. Purification by flash chromatography (gradient elution: 100% hexanes to 30% v/v ethyl acetate in hexanes) afforded 0.48 g (75%) a diastereomeric mixture of epoxides **3.22** as a clear, colorless oil. ^{1}H NMR (500 MHz; C_6H_6): δ 9.41 (q, *J* = 1.2 Hz, 1H), 6.38–6.34 (m, 1H), 4.99–4.98 (m, 1H), 4.86 (q, *J* = 1.5 Hz, 1H), 3.15 (q, *J* = 6.1 Hz, 1H), 2.88 (dd, *J* = 16.5, 6.1 Hz, 1H), 2.55 (ddd, *J* = 16.5, 5.6, 4.2 Hz, 2H), 2.37–2.25 (m, 2H), 2.19–2.08 (m, 3H), 1.82 (d, *J* = 0.8 Hz, 3H), 1.80–1.68 (m, 2H), 1.60–1.54 (m, 1H), 1.51–1.45 (m, 1H), 1.18 (d, *J* = 4.0 Hz, 3H), 1.09 (s, 3H), 1.02–0.85 (m, 3H), 0.77 (s, 3H), 0.20 (s, 9H).

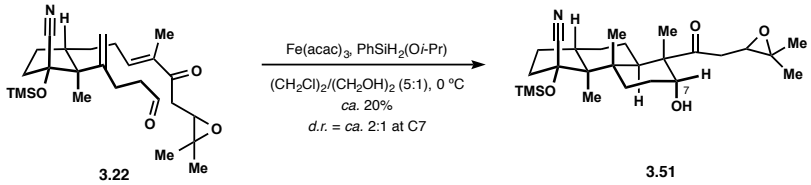

3.22 3.51

Axial alcohol **3.51**: A Schlenk flask was charged with iron(III) acetylacetonate (37.2 mg, 0.11 mmol), a solution of epoxide **3.22** (80.6 mg, 0.18 mmol) in 1,2-dichloroethane (3.6 mL), and ethylene glycol (0.7 mL). The mixture was degassed using a freeze-pump-thaw technique (3 cycles), cooled to 0 ºC, and treated with (isopropoxy)phenylsilane[60] (45 mg, 0.27 mmol). The biphasic reaction mixture was vigorously stirred at 0 ºC. After 2 hours the reaction was quenched with a degassed 1 N aqueous solution of HCl (3.8 mL). The aqueous layer was extracted with diethyl ether (4x7 mL). The combined organic layers were washed with solutions of 1 N aqueous HCl (3.8 mL) and saturated aqueous $NaHCO_3$ (3.8 mL), dried over anhydrous sodium sulfate, filtered, and concentrated under reduced pressure. Analysis of the crude ^{1}H NMR spectrum indicated that the d.r. at C7 was *ca.* 2:1. Purification by flash chromatography afforded 18.6 mg (22%) of axial alcohol **3.51** as a thin yellow film. Diagnostic ^{1}H NMR signals for **3.51**: ^{1}H NMR (600 MHz; C_6H_6): δ 3.53 (br s, 1H), 3.37 (br s, 1H); diagnostic ^{1}H NMR signals for 7-*epi*-**3.51**:

^{1}H NMR (500 MHz; C_6H_6): δ 3.67–3.63 (m, 2H), 3.57 (dd, *J* = 11.8, 4.1 Hz, 1H). The broad singlet at 3.53 ppm is assigned to the C7-proton. In our experience, the axial orientation of the C7 proton results in well-defined signal due to proton spin-coupling constants related to axial-axial/axial-equatorial types of coupling. However, we anticipate that an undefined, and broad, signal could result from axial-equatorial/equatorial-equatorial types of coupling.

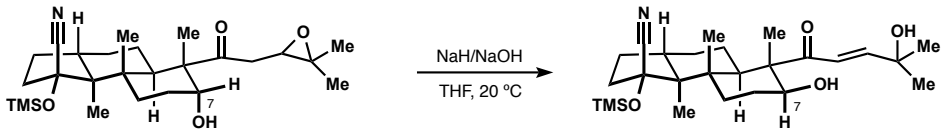

3.51 **dehydro-7-*epi*-3.51**

Enone **dehydro-7-*epi*-3.51**: Solid NaH (1.0 mg, 0.016 mmol, 60%, likely contains NaOH) was added to a solution of axial alcohol **3.51** (7.5 mg, 0.016 mmol) in THF (0.3) at room temperature. The mixture was vigorously stirred at room temperature. After 30 minutes the reaction was quenched with a solution of saturated aqueous NH_4Cl (0.4 mL) and diluted with diethyl ether (15 mL). The organic layer was dried over anhydrous sodium sulfate, filtered, and concentrated under reduced pressure. Purification by flash chromatography (gradient elution 100% hexanes to 60% ethyl acetate in hexanes) afforded 4 mg of enone **dehydro-7-*epi*-3.51** as a thin film. Diagnostic ^{1}H NMR signals for **dehydro-7-*epi*-3.51**: ^{1}H NMR (600 MHz; C_6H_6): δ 7.04–7.01 (d, *J* =18.9 Hz, 2H), 4.01 (dd, *J* = 11.6, 4.4 Hz, 1H).

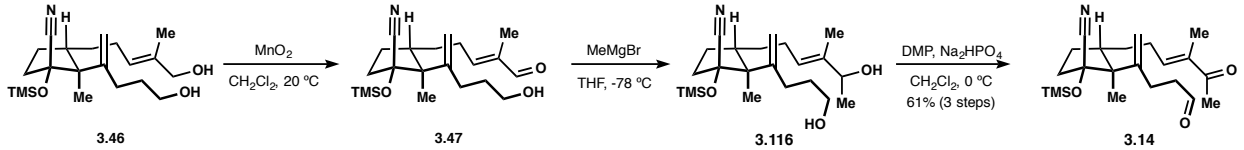

3.46 **3.47** **3.116** **3.14**

Dicarbonyl **3.14**: MnO_2 (1.74 g, 20.0 mmol) was added to a solution of diol **3.46** (379.1 mg, 1.0 mmol) in methylene chloride (10.0 mL). The heterogeneous mixture was vigorously stirred at room temperature. After 23 hours the mixture was filtered through a plug of Celite. The filter

cake was thoroughly rinsed with methylene chloride and the combined organic material was concentrated under reduced pressure. Crude aldehyde **3.47** was used without further purification.

A solution of crude aldehyde **3.47** in THF (4.0 mL) was added in a dropwise manner to a solution of methylmagnesium bromide (0.79 mL, 2.2 mmol, 2.8 M in diethyl ether) in THF (2.0 mL) at -78 ºC. A precipitate immediately formed and the reaction was allowed to warm to 0 ºC. After 10 minutes the reaction was quenched with a solution of saturated aqueous NH_4Cl (3 mL). The aqueous layer was extracted with methylene chloride (3x7 mL). The combined organic layers were washed with brine (4 mL), dried over anhydrous sodium sulfate, filtered, and concentrated under reduced pressure. Crude diol **3.116** was used without further purification.

Dess–Martin periodinane (1.06 g, 2.5 mmol) and Na_2HPO_4 (0.71 g, 5.0 mmol) were added to a solution of crude diol **3.116** in methylene chloride (5.0 mL) at 0 ºC. The reaction was vigorously stirred at 0 ºC. After 1.5 hours the reaction was quenched with a solution of 10% aqueous Na_2CO_3 (2 mL). The aqueous layer was extracted with methylene chloride (3x10 mL). The combined organic layers were washed with brine (4 mL), dried over anhydrous sodium sulfate, filtered, and concentrated under reduced pressure. Purification by flash chromatpgraphy (gradient elution: 100% hexanes to 30% v/v ethyl acetate in hexanes) afforded 238.7 mg (61% over 3 steps) of dicarbonyl **3.14** as a clear, colorless oil. ^{1}H NMR (500 MHz; $CDCl_3$): δ 9.80 (t, *J* = 1.4 Hz, 1H), 6.59 (td, *J* = 7.2, 1.2 Hz, 1H), 5.01 (s, 1H), 4.99 (s, 1H), 2.68–2.57 (m, 3H), 2.48–2.25 (m, 8H), 2.22–2.07 (m, 2H), 1.95 (td, *J* = 12.9, 6.4 Hz, 1H), 1.77 (s, 3H), 1.72–1.66 (m, 1H), 1.50 (tdd, *J* = 12.9, 9.2, 3.7 Hz, 1H), 1.26 (dtd, *J* = 13.4, 10.5, 5.2 Hz, 1H), 1.02 (s, 3H), 0.23 (s, 9H); ^{13}C NMR (150 MHz; $CDCl_3$): δ 202.1, 199.8, 148.6, 142.7, 138.2, 121.8, 111.5, 82.7, 56.3, 42.9, 40.9, 36.8, 30.4, 27.7, 25.60, 25.46, 23.8, 12.8, 11.3, 1.3.

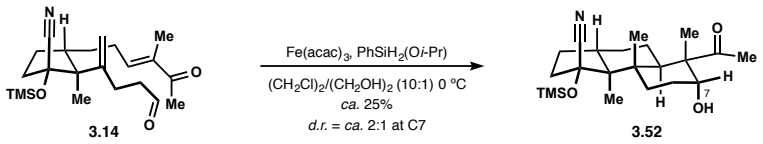

Tricycle **3.52**: A Schlenk flask was charged with iron(III) acetylacetonate (13.2 mg, 0.075 mmol), a solution of dicarbonyl **3.14** (9.7 mg, 0.025 mmol) in 1,2-dichloroethane (0.5 mL), and ethylene glycol (0.1 mL). The mixture was degassed using a freeze-pump-thaw technique (3 cycles), cooled to 0 ºC, and treated with (isopropoxy)phenylsilane (13 μL, 0.075 mmol). The biphasic reaction mixture was vigorously stirred at 20 ºC. After 1 hour the reaction was quenched with a degassed 1 N aqueous solution of HCl (1.0 mL). The organic layer was diluted with ethyl acetate (25 mL) and separated from the aqueous layer. The organic layer were washed with solutions of water (3 mL) and brine (3 mL), dried over anhydrous sodium sulfate, filtered, and concentrated under reduced pressure. Analysis of the crude ^{1}H NMR spectrum indicated that the d.r. at C7 was *ca.* 2:1. Purification by flash chromatography afforded 2.2 mg (*ca.* 22%) of axial alcohol **3.52** as a thin yellow film. ^{1}H NMR (600 MHz; $CDCl_3$): δ 3.91 (s, 1H), 2.67 (dd, *J* = 12.0, 2.8 Hz, 1H), 2.39–2.34 (m, 2H), 2.23 (s, 3H), 2.06–2.00 (m, 3H), 1.92–1.83 (m, 2H), 1.74-1.65 (m, 3H), 1.55 (s, 3H), 1.49–1.42 (m, 4H), 1.32 (s, 3H), 1.15 (s, 3H), 0.28 (s, 9H).

NOESY Correlations

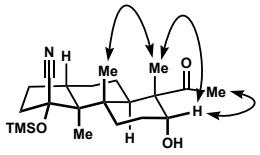

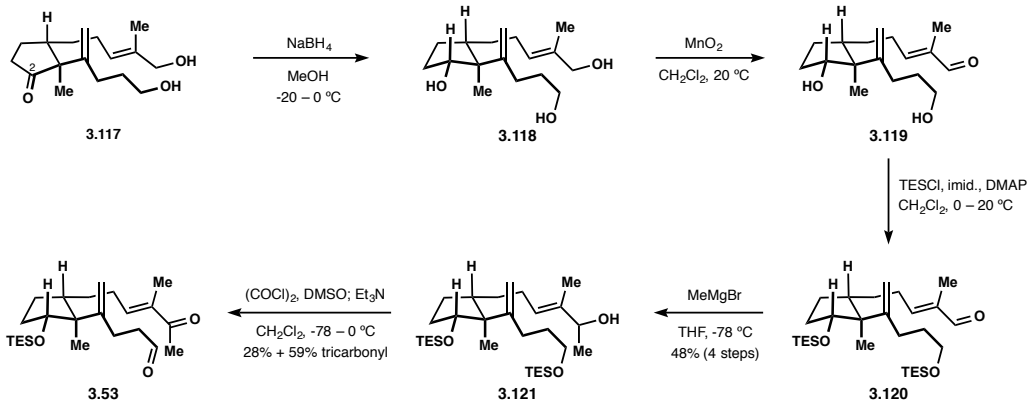

Triol **3.120**: Three equal portions of sodium borohydride (0.35 g total, 9.2 mmol) were added to a solution of ketone **3.117**[2a] (3.45 g, 12.3 mmol) in methanol (43 mL) at ~(-20) ºC. The reaction was vigorously stirred and slowly allowed to warm to room temperature. Additional charges of sodium borohydride (48 mmol total) were added in portions over 2 hours. After 16 hours the reaction was cooled to 0 ºC and quenched with a solution of aqueous 1 N HCl (15 mL). The volatiles were concentrated under reduced pressure and the remaining aqueous layer was partitioned with ethyl acetate (75 mL). The resulting biphasic mixture was filtered through a pad of Celite. The filter cake was thoroughly rinsed with ethyl acetate (3x75 mL). The combined organic layers were washed with brine (20 mL), dried over anhydrous sodium sulfate, filtered, and concentrated under reduced pressure. Analysis of the crude ^{1}H NMR spectrum indicated that the d.r. at C2 was *ca.* 10:1. The crude triol **3.118** was used without further purification.

Aldehyde **3.119**: MnO_2 (16.5 g, 190.0 mmol) was added to a solution of triol **3.118** in methylene chloride (100 mL). The heterogeneous mixture was vigorously stirred at room temperature. After 23 hours the mixture was filtered through a plug of Celite. The filter cake was thoroughly rinsed with methylene chloride and the combined organic material was concentrated under reduced pressure. Crude aldehyde **3.119** was used without further purification.

Bis(silyl)ether **3.120**: Triethylchlorosilane (0.6 mL, 3.6 mmol), imidazole (262.1 mg, 3.85 mmol), and 4-(dimethylamino)pyridine (11.0 mg, 0.09 mmol) were added to a solution of aldehyde (10% of total) in methylene chloride (7.7 mL) at 0 ºC. The reaction was vigorously stirred and allowed to warm to room temperature. After 1 hour the reaction was quenched with a solution of saturated aqueous $NaHCO_3$ (10 mL). The aqueous layer was extracted with methylene chloride (3x10 mL). The combined organic layers were dried over anhydrous magnesium sulfate, filtered, and concentrated under reduced pressure. The residue was dissolved in pentane and filtered through a small plug of silica. Solvent was removed under reduced pressure to afford a clear, colorless oil that was used without further purification. R_f = 0.44 (5% v/v ethyl acetate in hexanes).

Allylic alcohol **3.121**: Methylmagnesium bromide (0.42 mL, 1.16 mmol, 2.77 M in diethyl ether) was added to a solution of **3.120** in THF (7.7 mL) at -78 ºC. The reaction was vigorously stirred and allowed to warm to 0 ºC. After 10 minutes the reaction was quenched with a solution of saturated aqueous NH_4Cl (3 mL). The aqueous layer was extracted with diethyl ether (3x10 mL). The combined organic layers were washed with brine (4 mL), dried over anhydrous magnesium sulfate, filtered, and concentrated under reduced pressure. Purification by flash chromatography afforded 302.4 mg (48% over 4 steps) of diastereomeric allylic alcohols **3.120** as a clear, colorless oil. R_f = 0.27 (5% v/v ethyl acetate in hexanes); ^{1}H-NMR (500 MHz; $CDCl_3$): δ 5.36 (q, *J* = 7.0 Hz, 1H), 4.90 (s, 2H), 4.17 (dd, *J* = 6.0, 2.9 Hz, 1H), 3.97 (t, *J* = 8.5 Hz, 1H), 3.64 (qd, *J* = 5.0, 2.0 Hz, 2H), 2.04–1.96 (m, 3H), 1.94–1.78 (m, 4H), 1.71–1.63 (m, 3H), 1.60 (s, 3H), 1.50 (ddt, *J* = 12.6, 8.4, 4.2 Hz, 1H), 1.34 (dt, *J* = 11.3, 5.4 Hz, 2H), 1.23 (d, *J* = 6.4 Hz, 3H), 1.16–1.08 (m, 1H), 0.97 (t, *J* = 8.0 Hz, 9H), 0.90 (t, *J* = 7.9 Hz, 9H), 0.87 (s, 3H), 0.61 (q, *J* = 7.9 Hz, 6H), 0.50 (q, *J* = 7.8 Hz, 6H); ^{13}C NMR (125 MHz; $CDCl_3$): δ 152.8, 138.79, 138.74,

125.3, 125.1, 110.52, 110.46, 78.4, 73.49, 73.37, 63.4, 53.1, 41.62, 41.58, 32.7, 31.39, 31.38, 30.51, 30.48, 27.65, 27.60, 26.49, 26.43, 26.03, 25.99, 21.8, 11.66, 11.65, 6.99, 6.94, 5.1, 4.6.

Dicarbonyl **3.53**: Oxalyl chloride (0.11 mL, 1.27 mmol) was added to a solution of DMSO (0.18 mL, 2.53 mmol) in methylene chloride (3.2 mL) at -78 ºC. The reaction was vigorously stirred at -78 ºC. After 20 minutes a solution of allylic alcohol **3.121** (302.4 mg, 0.58 mmol) in methylene chloride (8.6 mL) was added dropwise over 10 minutes with a syringe pump. The reaction was vigorously stirred at -78 ºC. After 1 hour triethylamine (0.71 mL, 5.07 mmol) was added in a dropwise manner and the reaction was allowed to warm to 0 ºC. After an additional 10 minutes the reaction was quenched with water (5 mL). The aqueous layer was extracted with methylene chloride (3x20 mL). The combined organic layers were washed with brine (10 mL), dried over anhydrous magnesium sulfate, filtered, and concentrated under reduced pressure. Purification by flash chromatography afforded 66.9 mg (28%) of dicarbonyl **3.53** and 99.0 mg (59%) of the corresponding tricarbonyl as clear, colorless oils. ^{1}H NMR (600 MHz; $CDCl_3$): δ 9.78 (t, *J* = 1.5 Hz, 1H), 6.57–6.55 (m, 1H), 4.93 (s, 1H), 4.80 (t, *J* = 1.5 Hz, 1H), 3.95 (t, *J* = 8.6 Hz, 1H), 2.63–2.54 (m, 2H), 2.40–2.31 (m, 2H), 2.26 (s, 3H), 2.23–2.18 (m, 1H), 2.10 (ddq, *J* = 14.1, 6.8, 6.3 Hz, 1H), 1.95–1.87 (m, 2H), 1.85–1.79 (m, 1H), 1.72 (d, *J* = 0.9 Hz, 3H), 1.51 (tdd, *J* = 12.9, 8.5, 4.6 Hz, 1H), 1.42 (dddd, *J* = 13.2, 9.9, 6.9, 3.1 Hz, 1H), 1.37–1.31 (m, 1H), 1.25–1.19 (m, 1H), 0.88 (dd, *J* = 10.6, 5.3 Hz, 12H), 0.48 (qd, *J* = 8.0, 3.1 Hz, 6H); ^{13}C NMR (150 MHz; CDCl3): δ 202.2, 199.9, 151.4, 143.8, 137.8, 110.5, 78.7, 53.0, 42.9, 42.0, 31.0, 29.6, 27.7, 26.3, 25.5, 23.4, 11.6, 11.2, 6.9, 5.1.

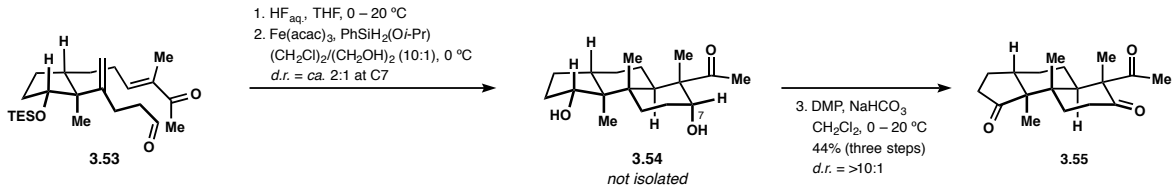

Desilylated **3.53**: Aqueous hydrofluoric acid (12 μL, 0.32 mmol, 48%) was added to a solution of dicarbonyl **3.53** (66.9 mg, 0.16 mmol) in THF (3.0 mL) at 0 ºC. The reaction mixture was vigorously stirred at 0 ºC. After 30 minutes an additional 12 μL (0.32 mmol) of HF was added and the reaction was allowed to warm to room temperature. After an additional 1.5 hours the reaction was neutralized with a solution of saturated aqueous $NaHCO_3$ (1 mL). The aqueous layer was diluted with water (1 mL) and extracted with diethyl ether (3x7 mL). The combined organic layers were washed with water (2 mL) and brine (2 mL), dried over anhydrous sodium sulfate, filtered, and concentrated under reduced pressure. The crude desilylated **3.53** was used without further purification. $R_f = 0.24$ (30% v/v ethyl acetate in hexanes).

Tricycle **3.54**: A Schlenk flask was charged with iron(III) acetylacetonate (56.5 mg, 0.16 mmol), a solution of desilylated **3.53** in 1,2-dichloroethane (7.3 mL), and ethylene glycol (0.7 mL). The mixture was degassed using a freeze-pump-thaw technique (3 cycles), cooled to 0 ºC, and treated with (isopropoxy)phenylsilane (55 μL, 0.32 mmol). The biphasic reaction mixture was vigorously stirred at 0 ºC. After 30 minutes the reaction was quenched with a solution of degassed 1 N aqueous HCl (4.0 mL). The organic layer was diluted with diethyl ether (15 mL) and vigorously stirred until the organic layer was clear and colorless. The aqueous layer was extracted with diethyl ether (3x15 mL). The organic layer were washed with solutions of water (4 mL) and brine (4 mL), dried over anhydrous sodium sulfate, filtered, and concentrated under reduced pressure. Analysis of the crude ^1H NMR spectrum revealed that a 2:1 mixture of diastereomers at C7. The crude tricycle **3.54** was used without further purification. $R_f = 0.22$ (70% v/v ethyl acetate in hexanes).

Tricarbonyl **3.55**: Dess–Martin periodinane (203.6 mg, 0.48 mmol) and $NaHCO_3$ (80.6 mg, 0.96 mmol) were added to a solution of the crude tricycle **3.54** in methylene chloride (1.0 mL) at 0 ºC.

The reaction mixture was vigorously stirred and allowed to warm to room temperature. After 2 hours the reaction was cooled to 0 ºC and quenched with a 1:1 mixture of saturated aqueous $NaHCO_3$:$Na_2S_2O_3$ (0.8 mL). The heterogeneous material was filtered off and the aqueous layer was extracted with diethyl ether (3x7 mL). The combined organic layers were washed with a solution of saturated aqueous $NaHCO_3$ (3 mL), water (3 mL), and brine (3 mL). The organic layer was dried over anhydrous sodium sulfate, filtered, and concentrated under reduced pressure. Analysis of the crude ^{1}H NMR spectrum revealed that a >10:1 mixture of diastereomeric *trans*:*cis* tricycles. Purification by flash chromatography (gradient elution: 100% hexanes to 15% ethyl acetate in hexanes) afforded 20.5 mg (44% over 3 steps) of tricarbonyl **3.55** as a white film. R_f = 0.5 (40% v/v ethyl acetate in hexanes); ^{1}H-NMR (600 MHz; $CDCl_3$): δ 2.61 (tdd, *J* = 12.8, 5.2, 4.1 Hz, 2H), 2.48-2.34 (m, 3H), 2.21 (dddt, *J* = 15.3, 12.2, 6.1, 3.0 Hz, 1H), 2.10 (s, 3H), 2.09-2.00 (m, 2H), 1.86 (dddd, *J* = 12.5, 9.1, 6.1, 1.0 Hz, 1H), 1.71 (dt, *J* = 8.8, 3.0 Hz, 1H), 1.58 (tdd, *J* = 12.5, 9.6, 8.7 Hz, 1H), 1.45-1.39 (m, 2H), 1.28 (s, 3H), 1.15 (s, 3H), 1.10 (dt, *J* = 9.5, 3.0 Hz, 1H), 1.01 (s, 3H); ^{13}C NMR (150 MHz; $CDCl_3$): δ 220.0, 212.4, 206.9, 66.4, 55.4, 41.7, 40.4, 38.3, 37.3, 35.3, 30.8, 27.4, 25.3, 24.7, 23.7, 16.7, 16.3, 10.7.

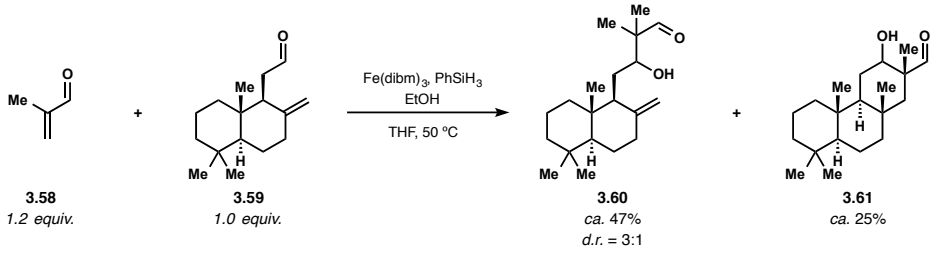

3.58 *1.2 equiv.* **3.59** *1.0 equiv.* **3.60** *ca.* 47% *d.r.* = 3:1 **3.61** *ca.* 25%

Bimolecular coupling: A dram vial was charged with $Fe(dibm)_3$ (7.8 mg, 0.015 mmol), aldehyde **3.59**[24] (11.7 mg, 0.05 mmol), methacrolein **3.58** (5 µL, 0.06 mmol), ethanol (9 µL, 0.15 mmol), phenylsilane (6.8 µL, 0.055 mmol), and THF (0.25 mL). The resulting solution was degassed by sparging with argon (~10 minutes). After degassing the reaction mixture was vigorously stirred

and heated to 50 ºC. After 3 hours the reaction was quenched with a solution of 1 N aqueous HCl (0.4 mL). The aqueous layer was extracted with diethyl ether. The combined organic layers were washed with brine, dried over sodium sulfate, filtered, and concentrated under reduced pressure. Purification by flash chromatography (gradient elution: 100% hexanes to 15% v/v ethyl acetate in hexanes) afforded 7.2 mg (*ca.* 48%) of bicycle **3.60** (*d.r.* = 2:1) and 4.9 mg (*ca*. 25%) of tricycle **3.61** as thin films. Diagnostic ^{1}H NMR signals for **3.60**: ^{1}H NMR (500 MHz; $CDCl_3$): δ 9.56 (s, 1H), 9.52 (s, 2H), 4.90 (d, *J* = 1.2 Hz, 1H), 4.83 (d, *J* = 1.4 Hz, 2H), 4.74 (s, 1H), 4.39 (d, *J* = 1.0 Hz, 2H), 3.78 (ddd, *J* = 10.2, 5.5, 1.5 Hz, 2H), 3.69 (dt, *J* = 9.0, 4.0 Hz, 1H), 1.11 (s, 6H), 1.11 (s, 3H), 1.09 (s, 6H), 1.07 (s, 3H), 0.88 (s, 3H), 0.88 (s, 6H), 0.81 (s, 6H), 0.80 (s, 3H 0.68 (s, 6H), 0.67 (s, 3H). Diagnostic^{1}H NMR signals for **3.61**: ^{1}H NMR (500 MHz; $CDCl_3$): δ 9.45 (s, 1H), 3.95 (d, *J* = 11.5 Hz, 1H), 1.28 (s, 3H), 1.12 (s, 3H), 0.91 (s, 3H), 0.89 (s, 3H), 0.88 (s, 3H).

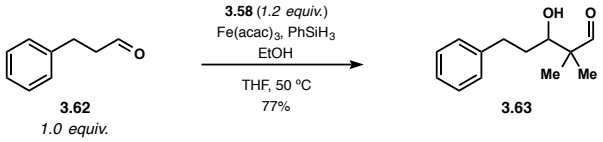

β-hydroxy aldehyde **3.63**: A Schlenk flask was charged with iron(III) acetylacetonate (10.6 mg, 0.03 mmol), THF (1.0 mL), aldehyde **3.62** (13 μ, 0.1 mmol), methacrolein **3.58** (10 μL, 0.12 mmol), phenylsilane (14 μL, 0.11 mmol), and ethanol (12 μL, and ethylene glycol (0.1 mL). The mixture was degassed using a freeze-pump-thaw technique (3 cycles). The reaction mixture was vigorously stirred and heated to 50 ºC. After 1.5 hours the reaction was quenched with a solution of degassed 1 N HCl (1.0 mL). The organic layer was diluted with diethyl ether and separated from the aqueous layer. The organic layer were washed with solutions of 1 N aqueous HCl and brine, dried over anhydrous magnesium sulfate, filtered, and concentrated under reduced pressure. Purification by flash chromatography (gradient elution: 100% hexanes to 30% v/v ethyl

acetate in hexanes) afforded 15.8 mg (77%) of β-hydroxy aldehyde **3.63** as a clear, colorless oil. ^{1}H-NMR (499 MHz; $CDCl_3$): δ 9.49 (s, 1H), 7.30 (t, *J* = 7.4 Hz, 2H), 7.22–7.19 (m, 3H), 3.75 (dd, *J* = 10.4, 1.8 Hz, 1H), 2.94 (td, *J* = 9.2, 4.8 Hz, 1H), 2.66 (ddd, *J* = 13.7, 9.2, 7.2 Hz, 1H), 2.25 (br s, 1H), 1.78–1.65 (m, 2H), 1.09 (s, 3H), 1.03 (s, 3H).

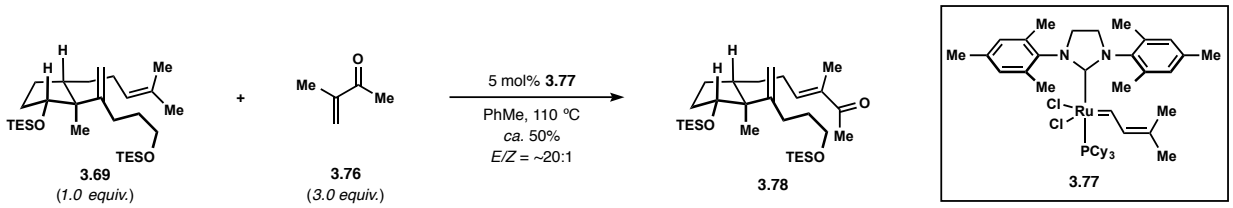

Enone **3.78**: A dram vial was charged with trisubstituted alkene **3.69** (20.1 mg, 0.041 mmol), toluene (0.3 mL), 3-methyl-3-buten-2-one (12.5 μL, 0.123 mmol), and ruthenium alkylidene **3.77** (1.7 mg, 0.002 mmol). The reaction mixture was vigorously stirred and heated to 110 °C. After 30 minutes the reaction mixture was cooled to room temperature and concentrated under reduced pressure. Purification by flash chromatography (gradient elution 100% hexanes to 2% v/v ethyl acetate in hexanes) afforded 11.4 mg (*ca.* 50%) of enone **3.78** as a thin film with *E/Z* = ~20:1. ^{1}H NMR (500 MHz; $CDCl_3$): δ 6.59–6.56 (m, 1H), 4.91 (s, 2H), 3.98 (t, *J* = 8.5 Hz, 1H), 3.64 (t, *J* = 6.5 Hz, 2H), 2.28 (s, 3H), 2.26–2.18 (m, 1H), 2.13–2.07 (m, 1H), 2.06–1.98 (m, 2H), 1.97–1.77 (m, 4H), 1.74 (s, 3H), 1.71–1.66 (m, 3H), 1.56–1.29 (m, 2H), 1.23–1.18 (m, 1H), 0.96 (t, *J* = 7.9 Hz, 9H), 0.91 (t, *J* = 7.8 Hz, 12H), 0.59 (t, *J* = 8.0 Hz, 6H), 0.53–0.48 (m, 6H).

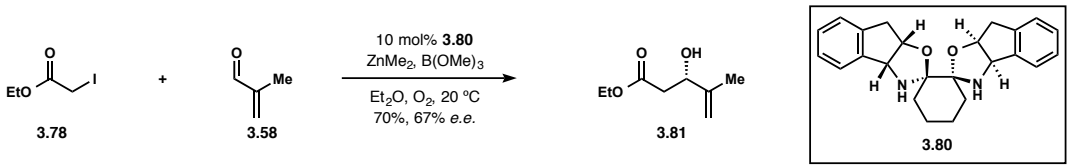

β-hydroxy ester **3.81**: A two-neck flask was outfitted with a drying tube in the vertical position and a septum in the side position. An inlet of nitrogen from a balloon was connected to the drying tube. Ligand **3.80** (18.7 mg, 0.05 mmol) and diethyl ether (10 mL) were added to the

flask. The mixture was vigorously stirred for 5 minutes. Ethyl iodoacetate (0.12 mL, 1.0 mmol) was added to the solution. After 5 minutes $B(OMe)_3$ (57 μL, 0.5 mmol) was added to the solution and an inlet of oxygen from a balloon was attached to the drying tube. The headspace was briefly flushed (~20 seconds). After 5 minutes $ZnMe_2$ (1.65 mL, 2.0 mmol, 1.2 M in toluene) was added over 20 minutes via a syringe pump. Immediately after the initiation of the addition of $ZnMe_2$, a solution of methacrolein (41 μL, 0.5 mmol) in diethyl ether (2.0 mL) was quickly added to the flask. After an additional 10 minutes a second portion of $ZnMe_2$ (1.65 mL, 2.0 mmol, 1.2 M in toluene) was added over 20 minutes via a syringe pump. After an additional 1 hour the reaction mixture was cooled to 0 ºC and quenched with a solution of 1 N aqueous HCl (5 mL). The aqueous layer was extracted with methylene chloride (3x15 mL). The combined organic layers were washed with water (7 mL) and brine (7 mL), dried over anhydrous sodium sulfate, filtered, and concentrated under reduced pressure. Purification by flash chromatography (gradient elution: 100% hexanes to 30% v/v ethyl acetate in hexanes) afforded 55.4 mg (70%) of β-hydroxy ester **3.81** as a clear, colorless oil. ^{1}H NMR (500 MHz; $CDCl_3$): δ 5.04 (d, J = 0.7 Hz, 1H), 4.88 (td, J = 1.5, 0.6 Hz, 1H), 4.47 (dd, J = 7.8, 3.7 Hz, 1H), 4.18 (q, J = 7.1 Hz, 2H), 2.91 (d, J = 3.5 Hz, 1H), 2.61-2.52 (m, 2H), 1.76 (s, 3H), 1.28 (t, J = 7.1 Hz, 3H); the *e.e* was determined to be 67%.

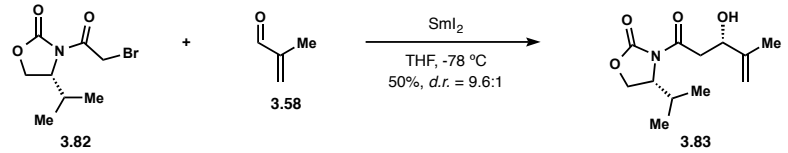

α-bromo acyl oxazolidinone **3.82**: *n*-BuLi (2.02 mL, 5.05 mmol, 2.5 M in hexanes) was added to a solution of (R)-4-isopropyl-2-oxazolidinone (645.8 mg, 5.0 mmol) in THF (25 mL) at -78 ºC. The reaction mixture was vigorously stirred at -78 ºC. After 45 minutes a solution of α-bromo acetyl bromide (0.48 mL, 5.5 mmol) in THF (8 mL) was added in a dropwise manner over 5 minutes. After an additional 1 hour the reaction was quenched with a mixture of saturated

aqueous NH_4Cl:$NaHCO_3$ (1:2, 7.5 mL total). The aqueous layer was extracted with diethyl ether (3x25 mL). The combined organic layers were dried over anhydrous sodium sulfate, filtered, and concentrated under reduced pressure. Purification by flash chromatography (gradient elution: 100% hexanes to 30%v/v ethyl acetate in hexanes) afforded 825.6 mg (66%) of α-bromo acyl oxazolidinone **3.82** as an off-white solid. ^{1}H-NMR (500 MHz; $CDCl_3$): δ 4.60 (d, *J* = 12.2 Hz, 1H), 4.46 (dt, *J* = 8.4, 3.5 Hz, 1H), 4.43 (d, *J* = 12.2 Hz, 1H), 4.34 (t, *J* = 8.8 Hz, 1H), 4.27 (dd, *J* = 9.2, 3.1 Hz, 1H), 2.42 (dtd, *J* = 14.0, 7.0, 3.9 Hz, 1H), 0.94 (d, *J* = 7.0 Hz, 3H), 0.91 (d, *J* = 6.9 Hz, 3H).

Allylic alcohol **3.83**: A Schlenk flask was charged with a solution of SmI_2 (54 mL, 5.37 mmol, 0.1M in THF) in a nitrogen atmosphere glovebox. The flask was sealed with a plastic cap, removed from the glovebox, and attached to a double bank vacuum manifold. The solution was vigorously stirred and cooled to -78 ºC. A solution of α-bromo acyl oxazolidinone **3.82** (671.3 mg, 2.68 mmol) and methacrolein (0.22 mL, 2.68 mmol) in THF (2.0 mL) was added in a dropwise manner over 5 minutes. After 30 minutes the reaction was quenched with a solution of 0.1 N aqueous HCl (65 mL). The aqueous layer was extracted with diethyl ether (3x60 mL). The combined organic layers were washed with solutions of saturated aqueous $Na_2S_2O_3$ (45 mL) and brine (45 mL), dried over anhydrous sodium sulfate, filtered, and concentrated under reduced pressure. Purification by flash chromatography (gradient elution: 100% hexanes to 90% ethyl acetate in hexanes) afforded 324.1 mg (50%) of allylic alcohol **3.83** and 33.7 mg (5%) of the minor diastereomer. ^{1}H-NMR (500 MHz; $CDCl_3$): δ 5.07 (s, 1H), 4.91 (s, 1H), 4.59-4.56 (m, 1H), 4.46 (dt, *J* = 8.2, 3.5 Hz, 1H), 4.29 (t, *J* = 8.7 Hz, 1H), 4.23 (dd, *J* = 9.2, 3.0 Hz, 1H), 3.26 (dd, *J* = 16.9, 2.9 Hz, 1H), 3.14 (dd, *J* = 16.9, 9.4 Hz, 1H), 2.82 (d, *J* = 4.3 Hz, 1H), 2.39 (dtt, *J* = 10.4, 6.9, 3.5 Hz, 1H), 1.80 (s, 3H), 0.94 (d, *J* = 7.0 Hz, 3H), 0.90 (d, *J* = 6.9 Hz, 4H).

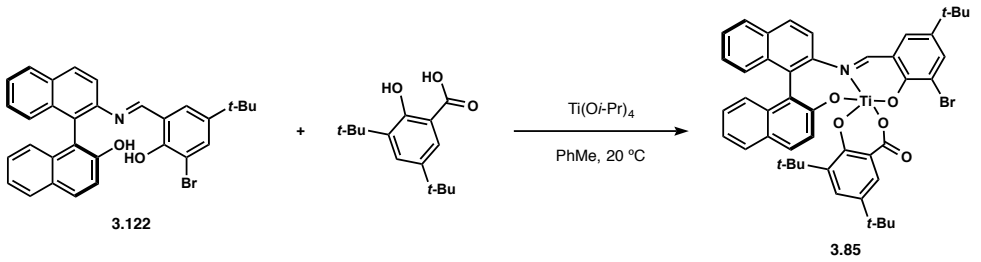

Catalyst **3.85**: Ti(O*i*-Pr)$_4$ (7.1 μL, 0.025 mmol) was added to a solution of imine **3.122** (28.8 mg, 0.055 mmol) in toluene (1.5 mL). The reaction mixture was vigorously stirred at room temperature. After 30 minutes a solution of 3,5-di-*tert*-butyl-salicyclic acid (8.1 mg, 0.03 mmol, azeotroped from toluene) in toluene (0.5 mL) was added in a dropwise manner. After an additional 45 minutes solvent was removed under reduced pressure without exposure to air. Catalyst **3.85** was used without further purification.

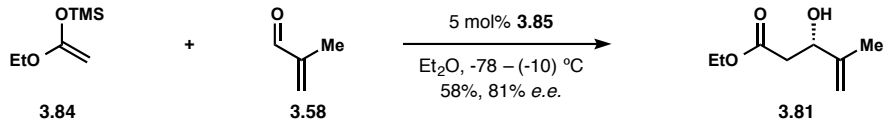

β-hydroxy ester **3.81**: The catalyst residue was dissolved in diethyl ether (1.0 mL) and the resulting solution was cooled to -78 ºC. Silyl ketene acetal **3.84** (120.2 mg, 0.75 mmol) and methacrolein (41.2 μL, 0.5 mmol) were sequentially added and the reaction mixture was allowed to slowly warm to ~(-15) – (-10) ºC. After 4.5 hours the reaction mixture was cooled to -78 ºC and quenched TFA (0.3 mL) was added. The solution was vigorously stirred and allowed to warm to room temperature overnight. After an additional 13 hours the reaction mixture was cooled to 0 ºC, diluted with diethyl ether (5 mL), and neutralized with a solution of saturated aqueous $NaHCO_3$ (1.5 mL). The aqueous layer was extracted with diethyl ether (3x7 mL). The combined organic layers were washed with water (2 mL) and brine (2 mL), dried over anhydrous sodium sulfate, filtered and concentrated under reduced pressure. Purification by flash chromatography (gradient elution: 100% hexanes to 15% v/v ethyl acetate in hexanes) afforded

46.1 mg (58%) of β-hydroxy ester **3.81** as a light yellow oil. ^{1}H NMR (500 MHz; $CDCl_3$): δ 5.01 (s, 1H), 4.86 (s, 1H), 4.46 (dd, *J* = 8.1, 4.4 Hz, 1H), 4.18-4.14 (m, 2H), 3.80 (s, 1H), 2.59-2.50 (m, 2H), 1.74 (s, 3H), 1.25 (t, *J* = 7.1 Hz, 3H); ^{13}C NMR (125 MHz; $CDCl_3$): δ 172.7, 145.5, 111.6, 71.7, 61.0, 40.1, 18.3, 14.2. The *e.e.* was determined to be 81%.

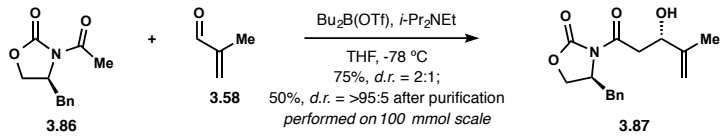

3.86 + 3.58 → 3.87

Allylic alcohol **3.87**: A solution of $Bu_2B(OTf)$ (23.4 mL, 23.4 mmol, 1 M in methylene chloride) followed by *i*-Pr_2NEt (4.46 mL, 25.6 mmol) were added to a solution of acyl oxazolidinone **3.86**[61] (4.68 g, 21.3 mmol) in THF (71 mL) at 0 ºC. The reaction mixture was vigorously stirred and the temperature was maintained at 0 ºC. After 30 minutes the reaction mixture was cooled to -78 ºC and methacrolein **3.58** (1.94 mL, 23.4 mmol) was added in a single portion. After an additional 40 minutes the reaction mixture was allowed to warm to room temperature. After an additional 1 hour the reaction was quenched with a solution of 0.2 M aqueous pH 7 phosphate buffer (45 mL). The aqueous layer was extracted with diethyl ether (3x75 mL). The combined organic layers were washed with water (30 mL) and brine (30 mL), dried over anhydrous sodium sulfate, filtered, and concentrated under reduced pressure. Analysis of the crude ^{1}H NMR spectra revealed that the diastereoselectivity of the transformation was 2:1. Purification by flash chromatography (gradient elution: 100% hexanes to 30% v/v diethyl ether in hexanes) afforded 3.07 g (50%) of allylic alcohol **3.87** as a clear, colorless oil that solidified upon standing at room temperature. R_f = 0.26 (30% v/v ethyl acetate in hexanes); ^{1}H NMR (500 MHz; $CDCl_3$): δ 7.34 (t, *J* = 7.3 Hz, 2H), 7.29 (d, *J* = 7.2 Hz, 1H), 7.23–7.21 (m, 2H), 5.08 (s, 1H), 4.92 (s, 1H), 4.71 (ddt, *J* = 9.5, 7.2, 3.5 Hz, 1H), 4.58 (dt, *J* = 8.9, 4.2 Hz, 1H), 4.25–4.18 (m, 2H), 3.29 (dq, *J* = 18.3, 7.1 Hz, 2H), 3.16 (dd, *J* = 17.0, 3.0 Hz, 1H), 3.00 (d, *J* = 4.6 Hz,

1H), 2.81 (dd, J = 13.5, 9.4 Hz, 1H), 1.81 (s, 3H); ^{13}C NMR (125 MHz; $CDCl_3$): δ 172.6, 153.6, 145.7, 135.2, 129.6, 129.2, 127.6, 111.7, 71.6, 66.5, 55.3, 41.4, 38.0, 18.5.

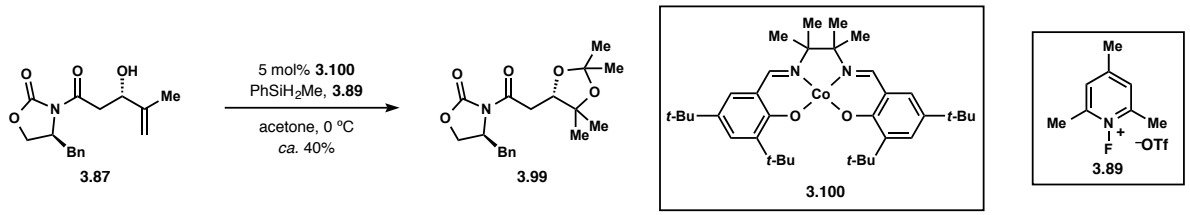

Ketal **3.99**: A Schlenk flask was charged with cobalt salen **3.100** (30.3 mg, 0.05 mmol), oxidant **3.89** (867.7 mg, 3.0 mmol), acetone (10.0 mL), and allylic alcohol **3.87** (289.3 mg, 1.0 mmol). The heterogeneous mixture was degassed using a freeze-pump-thaw technique (3 cycles), cooled to 0 ºC, and treated methy(phenyl)silane (0.3 mL, 2.2 mmol). The reaction mixture was vigorously stirred at and allowed to warm to room temperature. After 14 hours solvent was removed under reduced pressure. The residue was dissolved in diethyl ether (20 mL). The resulting solution was washed with a solution of saturated aqueous $NaHCO_3$ (5 mL). The aqueous layer was extracted with diethyl ether (2x10 mL). The combined organic layers were washed with brine (5 mL), dried over anhydrous sodium sulfate, filtered, and concentrated under reduced pressure. Purification by flash chromatography (gradient elution: 100% hexanes to 15% v/v ethyl acetate in hexanes) afforded 149.1 mg (43%) of ketal **3.99** and 2,4,6-collidine as a minor contaminant. ^{1}H NMR (500 MHz; $CDCl_3$): δ 7.35–7.32 (m, 2H), 7.29 (dt, J = 7.4, 1.8 Hz, 1H), 7.24–7.22 (m, 2H), 4.71 (ddt, J = 9.6, 7.5, 3.3 Hz, 1H), 4.30 (dd, J = 9.3, 3.1 Hz, 1H), 4.24–4.17 (m, 2H), 3.33 (ddd, J = 22.1, 15.3, 6.5 Hz, 2H), 3.03 (dd, J = 16.8, 3.1 Hz, 1H), 2.79 (dd, J = 13.4, 9.6 Hz, 1H), 1.46 (s, 3H), 1.41 (s, 3H), 1.32 (s, 3H), 1.18 (s, 3H).

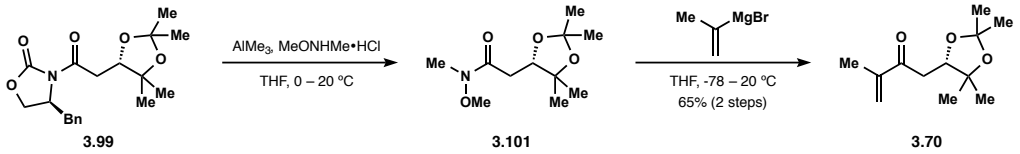

Weinreb amide **3.101**: Trimethylaluminum (0.35 mL, 3.6 mmol) was added to a suspension of *N*,*O*-dimethyl hydroxyl amine (351 mg, 3.6 mmol) in THF (3.6 mL) at 0 ºC. The reaction was vigorously stirred at 0 ºC and gas evolution was observed. After 30 minutes a solution of ketal **3.99** (250 mg, 0.72 mmol) in THF (3.6 mL) via a cannula. After 4 hours the reaction was quenched with a solution of 1 M aqueous HCl (7.2 mL). The aqueous layer was extracted with diethyl ether (3x20 mL). The combined organic layers were washed with water (7 mL) and brine (7 mL), dried over anhydrous magnesium sulfate, filtered, and concentrated under reduced pressure. The crude Weinreb amide **3.101** was used without further purification. ^{1}H NMR (400 MHz; $CDCl_3$): δ 4.29 (dd, *J* = 8.6, 4.2 Hz, 1H), 3.73 (s, 3H), 3.21 (s, 3H), 2.86 (dd, *J* = 15.6, 8.6 Hz, 1H), 2.41 (dd, *J* = 15.7, 4.1 Hz, 1H), 1.42 (s, 3H), 1.37 (s, 3H), 1.31 (s, 3H), 1.15 (s, 3H).

Enone **3.70**: Isopropenylmagnesium bromide (4.3 mL, 2.16 mmol, 0.5 M in THF) was added to a solution of Weinreb amide **3.101** in THF (0.7 mL) at -78 ºC. The reaction was vigorously stirred and allowed to warm to room temperature. After 30 minutes the reaction was quenched with a solution of 1 N aqueous HCl (3 mL). The aqueous layer were extracted with methylene chloride (3x15 mL). The combined organic layers were washed with brine (5 mL), dried over anhydrous magnesium sulfate, filtered, and concentrated under reduced pressure. Purification by flash chromatography (gradient elution: 100% hexanes to 15% v/v diethyl ether in hexanes) afforded 99.4 mg (65% over 2 steps) of enone **3.70** as a clear, colorless oil. ^{1}H NMR (500 MHz; $CDCl_3$): δ 6.00 (s, 1H), 5.83 (d, *J* = 1.4 Hz, 1H), 4.29 (dd, *J* = 8.1, 4.2 Hz, 1H), 3.09 (dd, *J* = 16.5, 8.1 Hz, 1H), 2.65 (dd, *J* = 16.5, 4.2 Hz, 1H), 1.89 (s, 3H), 1.40 (s, 3H), 1.36 (s, 3H), 1.28 (s, 4H), 1.12 (s, 3H).

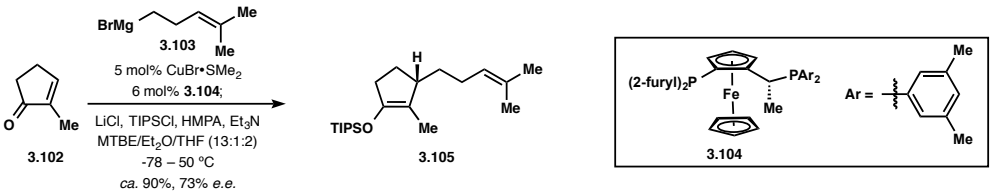

Grignardd **3.103**: An oven-dried three-neck flask was equipped with an inlet of nitrogen in one of the side positions and rubber septa in the remaining positions. The apparatus was cooled under a positive pressure of nitrogen. Once cool, the flask was charged with magnesium turnings (0.97 g, ~40 mmol) and diethyl ether (2.5 mL). Homoprenyl bromide (2.6 mL, 20.0 mmol) and diethyl ether (7.5 mL) were added in roughly 10 equal portions over the course of 30 minutes to avoid a vigorous exotherm. After the addition, titration revealed that a 1.15 M solution had been prepared.

Enoxysilane **3.105**: A Schlenk flask was charged with ligand **3.104** (371.1 mg, 0.6 mmol) in a nitrogen atmosphere glovebox. The flask was sealed with a plastic cap, removed from the glovebox, and connected to a double bank vacuum manifold. The plastic cap was replaced with a rubber septum under a positive atmosphere of nitrogen. The flask was charged with CuBr•SMe_2 (102.8 mg, 0.5 mmol) and methyl *tert*-butyl ether (133 mL, freshly distilled from sodium benzophenone ketyl). The resulting suspension was sonicated until a homogenous solution was observed (30–45 minutes). The solution was cooled to -78 ºC and vigorously stirred. 2-methyl-cyclopenten-1-one (0.98 mL, 10.0 mmol) was added in a single portion. After addition of the enone Grignard **3.104** (13 mL) was added dropwise over 30 minutes. The reaction mixture was vigorously stirred and the temperature was maintained at -78 ºC. After 20 hours a solution of LiCl (423.9 mg, 10.0 mmol, anhydrous) in THF (20 mL), TIPSCl (6.4 mL, 30.0 mmol), HMPA, 13.9 mL, 80.0 mmol), and triethylamine (4.9 mL, 35.0 mmol) were added to the reaction mixture. Stirring was maintained and the flask was slowly warmed to 50 ºC. After 3 hours the

flask was cooled to 0 ºC and quenched with a with a 3:1 mixture of saturated aqueous NH_4Cl:NH_4OH (55 mL). The organic layer was diluted with hexanes (100 mL) and washed with a 3:1 mixture of a saturated aqueous NH_4Cl:NH_4OH until no traces of a blue color was observed (3x55 mL). The combined aqueous layers were extracted with hexanes (2x75 mL). The combined organic layers were washed with brine (55 mL), dried over anhydrous sodium sulfate, filtered, and concentrated under reduced pressure. Purification by flash chromatography over silica gel deactivated with 1% Et_3N in hexanes (gradient elution: 100% hexanes to 10% ethyl acetate in hexanes) afforded 3.36 g (>90%) of enoxysilane **3.105** as a clear, colorless oil. The product was isolated with <10% Wurtz coupling of homoprenyl bromide. R_f = 0.6 (100% hexanes); ^{1}H-NMR (500 MHz; C_6H_6): δ 5.27–5.24 (m, 1H), 2.49–2.45 (m, 1H), 2.36–2.24 (m, 2H), 2.15–2.08 (m, 1H), 2.06–1.92 (m, 2H), 1.73–1.67 (m, 7H), 1.59 (s, 3H), 1.44 (ddt, *J* = 12.5, 8.9, 6.2 Hz, 1H), 1.28–1.21 (m, 2H), 1.13 (t, *J* = 4.0 Hz, 21H); ^{13}C NMR (125 MHz; C_6D_6): δ 147.4, 130.9, 125.6, 115.4, 44.8, 35.0, 33.4, 27.0, 25.9, 25.9, 18.2, 17.7, 13.3, 10.7; HRMS (CI) calculated for $C_{21}H_{41}OSi$ $[M]^+$: 336.2849, found: 336.2853; $[\alpha]_D^{20}$ -1.34 (*c* = 1.0, $CHCl_3$). A small sample was hydrolyzed form determination of the enantioenrichment: 73% *e.e.*

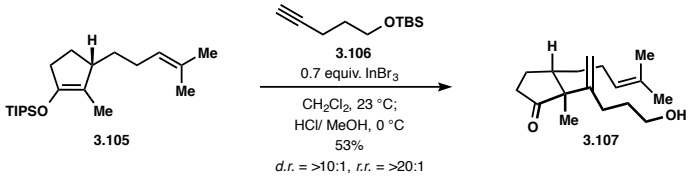

Ketone **3.107**: A Schlenk flask was charged with $InBr_3$ (1.95 g, 5.5 mmol) in a nitrogen atmosphere glovebox. The flask was sealed with a plastic cap, removed from the glovebox, and connected to a double bank vacuum manifold. The plastic cap was replaced with a rubber septum under a positive atmosphere of nitrogen. The flask was charged with a solution of enoxysilane **3.105** (3.03 g, 9.0 mmol) and **1.106** (2.33 g, 11.7 mmol) in CH_2Cl_2 (13.0 mL) via a cannula. The resulting mixture was vigorously stirred at room temperature. After 21 hours the flask was

cooled to 0 ºC and quenched with 1% HCl in MeOH (5 mL, prepared using a concentrated aqueous solution of HCl). After 1 hour the solution was neutralized with a solution of saturated aqueous $NaHCO_3$ (7 mL). The aqueous layer was extracted with ethyl acetate (3x20 mL). The combined organic layers were washed with water (7 mL) and brine (7 mL), dried over anhydrous sodium sulfate, filtered, and concentrated under reduced pressure. Purification by flash chromatography (gradient elution: 100% hexanes to 30% v/v ethyl acetate in hexanes) afforded 1.26 g (53%) of **3.107** as a clear, colorless oil. R_f = 0.24 (30% v/v ethyl acetate in hexanes); ^{1}H NMR (500 MHz; $CDCl_3$): δ 5.09–5.06 (m, 2H), 5.03 (s, 1H), 3.70–3.60 (m, 2H), 2.48–2.42 (m, 1H), 2.28–1.85 (m, 8H), 1.78–1.71 (m, 2H), 1.68 (s, 3H), 1.60 (s, 3H), 1.56–1.51 (m, 1H), 1.43–1.37 (m, 1H), 1.27–1.20 (m, 1H), 1.00 (d, *J* = 1.3 Hz, 3H); ^{13}C NMR (125 MHz; $CDCl_3$): δ 222.6, 148.5, 132.1, 124.4, 112.4, 62.2, 59.1, 43.1, 38.0, 31.3, 29.7, 28.7, 26.1, 25.8, 25.4, 17.8, 14.9; HRMS (CI) calculated $C_{17}H_{28}O_2$ $[M]^+$: 264.2089, found, 264.2090; $[\alpha]_D^{20}$ -13.14 (*c* = 1.0, $CHCl_3$).

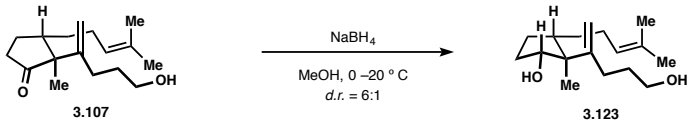

Diol **3.123**: Sodium borohydride (115.4 mg, 3.05 mmol) was added to a solution of ketone **3.107** (403.3 mg, 1.53 mmol) at ~(-20) ºC. The reaction mixture was vigorously stirred and slowly allowed to warm to room temperature. After 18 hours the reaction was cooled to 0 ºC and quenched with a solution of saturated aqueous NH_4Cl (1 mL) and water (1 mL). The aqueous layer was extracted with ethyl acetate (4x10 mL). The combined organic layers were washed with water (4 mL) and brine (4 mL), dried over anhydrous sodium sulfate, filtered, and concentrated under reduced pressure. Purification by flash chromatography (gradient elution: 30% ethyl acetate in hexanes to 50% ethyl acetate in hexanes) afforded 300.0 mg (74%) of diol

3.123 as a waxy white solid. Analysis of the crude ^{1}H NMR spectrum indicated that the d.r. at C2 was *ca.* 6:1 R_f = 0.22 (50% v/v hexanes in ethyl acetate); ^{1}H NMR (600 MHz; $CDCl_3$): δ 5.08–5.05 (m, 1H), 4.99 (d, *J* = 5.4 Hz, 2H), 4.03 (t, *J* = 9.0 Hz, 1H), 3.70 (tq, *J* = 11.5, 5.7 Hz, 2H), 2.11 (t, *J* = 7.7 Hz, 1H), 2.04 (ddd, *J* = 17.8, 8.9, 4.4 Hz, 1H), 1.97–1.93 (m, 1H), 1.92–1.75 (m, 6H), 1.67 (s, 3H), 1.58 (s, 3H), 1.52 (ddt, *J* = 17.5, 8.4, 4.3 Hz, 2H), 1.37–1.25 (m, 2H), 1.14-1.08 (m, 1H), 0.89 (s, 3H); ^{13}C NMR (150 MHz; CDCl3): δ 152.7, 131.7, 124.8, 111.3, 77.6, 62.8, 52.8, 42.1, 32.1, 30.8, 29.6, 26.9, 26.5, 26.2, 25.8, 17.8, 11.3; HRMS (ESI) calculated $C_{17}H_{30}O_2Na$ $[M+Na]^+$: 289.2144, found, 289.2141; $[\alpha]_D^{20}$ 14.59 (*c* = 1.0, $CHCl_3$).

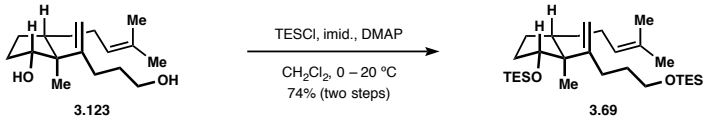

Trisubstituted alkene **3.69**: Imidazole (371.7 mg, 5.46 mmol) and DMAP (14.8 mg, 0.12 mmol) were added to a solution of diol **3.123** (290.0 mg, 1.09 mmol) in methylene chloride (11 mL) at 0 ºC. After 1 minute chlorotriethylsilane (0.64 mL, 3.82 mmol) was added. The reaction mixture was vigorously stirred and allowed to warm to room temperature. After 2 hours the reaction was diluted with methylene chloride (10 mL) and quenched with a solution of saturated aqueous $NaHCO_3$ (3 mL). The aqueous layer was extracted with methylene chloride (3x10 mL). The combined organic layers were washed with water (3 mL) and brine (3 mL), dried over anhydrous magnesium sulfate, filtered, and concentrated under reduced pressure. Purification by flash chromatography (gradient elution: 100% hexanes to 2% v/v ethyl acetate in hexanes) afforded 544.7 mg (>95%) of trisubstituted alkene **3.69** as a clear, colorless oil. R_f = 0.19 (2% v/v ethyl acetate in hexanes); ^{1}H NMR (600 MHz; $CDCl_3$): δ 5.08–5.06 (m, 1H), 4.89 (s, 2H), 3.96 (t, *J* = 8.5 Hz, 1H), 3.66–3.61 (m, 2H), 2.03–1.77 (m, 7H), 1.70–1.67 (m, 5H), 1.58 (s, 3H), 1.49 (ddd, *J* = 12.7, 8.3, 4.5 Hz, 1H), 1.35–1.25 (m, 2H), 1.10–1.05 (m, 1H), 0.97 (t, *J* = 7.9 Hz, 9H), 0.90

(t, *J* = 7.9 Hz, 9H), 0.86 (s, 3H), 0.63–0.59 (q, *J* = 7.8 Hz, 6H), 0.52–0.48 (m, 6H); ^{13}C NMR (150 MHz; $CDCl_3$): δ 152.8, 131.4, 125.1, 110.1, 78.5, 63.3, 53.1, 41.8, 32.5, 31.4, 30.8, 27.5, 26.7, 26.4, 25.8, 17.8, 11.7, 7.01, 6.96, 5.1, 4.6; HRMS (ESI) calculated $C_{29}H_{58}O_2Si_2Na$ $[M+Na]^+$: 517.3873, found, 517.3856; $[\alpha]_D^{20}$ 9.06 (*c* = 1.0, $CHCl_3$).

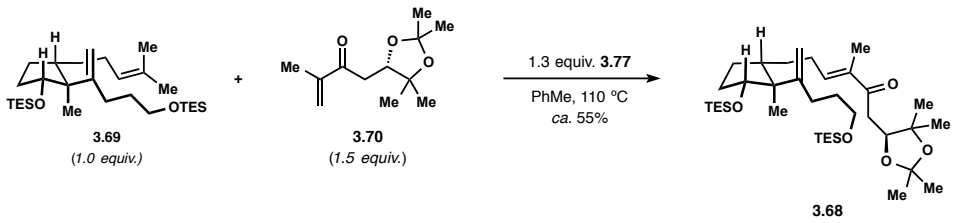

Enone **3.68**: A Schlenk flask was charged with trisubstituted alkene **3.69** (320 mg, 0.65 mmol), toluene (6.5 mL), enone **3.70** (200 mg, 0.97 mmol), and ruthenium alkylidene **3.77** (537 mg, 0.65 mmol). The reaction mixture was vigorously stirred and heated to 110 ºC. After 1 hour an additional charge of **3.77** (150 mg, 0.18 mmol) was added. After an additional 1.75 hours the reaction mixture was cooled to room temperature and concentrated under reduced pressure. Purification by flash chromatography (gradient elution 100% hexanes to 3% v/v ethyl acetate in hexanes) afforded 265.4 mg [63%, contaminated with an unknown compound(s)] of enone **3.78** as a thin film with *E/Z* = ~20:1. Diagnostic ^{1}H NMR signals: ^{1}H NMR (500 MHz; $CDCl_3$): δ 6.64-6.61 (m, 1H), 4.90 (s, 2H), 4.28 (dd, *J* = 8.1, 4.2 Hz, 1H), 3.97 (t, *J* = 8.5 Hz, 1H), 3.64 (t, *J* = 6.5 Hz, 2H), 1.76 (s, 3H), 1.40 (s, 3H), 1.35 (s, 3H), 1.28 (s, 3H), 1.12 (s, 3H), 0.96 (t, *J* = 8.0 Hz, 9H), 0.92-0.89 (m, 12H), 0.60 (q, *J* = 8.0 Hz, 6H), 0.50 (qd, *J* = 8.0, 1.4 Hz, 6H).

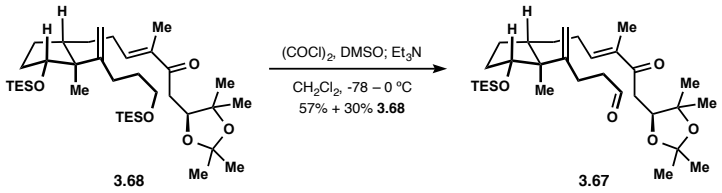

Dicarbonyl **3.67**: Oxalyl chloride (0.10 mL, 1.23 mmol) was added to a solution of DMSO (0.17 mL, 2.46 mmol) in methylene chloride (8.6 mL) at -78 ºC. The reaction was vigorously stirred at

-78 ºC. After 30 minutes a solution of enone **3.68** (265.4 mg, 0.41 mmol) in methylene chloride (4.3 mL) was added with assistance from a cannula. The reaction was vigorously stirred at -78 ºC. After 1 hour triethylamine (0.83 mL, 5.92 mmol) was added in a dropwise manner and the reaction was allowed to warm to 20 ºC. After an additional 30 minutes the reaction was quenched with water (5 mL). The aqueous layer was extracted with methylene chloride (3x15 mL). The combined organic layers were washed with a solution of saturated aqueous $NaHCO_3$ (5 mL), water (5 mL), and brine (10 mL). The combined organic layers were dried over anhydrous sodium sulfate, filtered, and concentrated under reduced pressure. Purification by flash chromatography (gradient elution: 100% hexanes to 10% v/v ethyl acetate in hexanes) afforded 124.3 mg (57%) of dicarbonyl **3.67** and 79.3 mg (30%) of starting enone **3.68** as clear, colorless oils. R_f = 0.47 (20% v/v ethyl acetate in hexanes); ^{1}H NMR (500 MHz; $CDCl_3$): δ 9.77 (t, *J* = 1.5 Hz, 1H), 6.60 (t, *J* = 7.2 Hz, 1H), 4.92 (s, 1H), 4.79 (s, 1H), 4.26 (dd, *J* = 8.1, 4.1 Hz, 1H), 3.94 (t, *J* = 8.5 Hz, 1H), 3.03 (dd, *J* = 16.4, 8.1 Hz, 1H), 2.60–2.54 (m, 3H), 2.35 (dq, *J* = 15.8, 8.0 Hz, 2H), 2.26–2.18 (m, 1H), 2.10 (dq, *J* = 15.7, 7.8 Hz, 1H), 1.94–1.78 (m, 3H), 1.74 (s, 3H), 1.51–1.39 (m, 4H), 1.37 (s, 4H), 1.32 (s, 3H), 1.25 (s, 3H), 1.09 (s, 3H), 0.87 (dd, *J* = 10.5, 5.7 Hz, 12H), 0.47 (qd, *J* = 8.0, 2.2 Hz, 6H); ^{13}C NMR (125 MHz; $CDCl_3$): δ 202.0, 198.6, 151.4, 143.6, 137.6, 110.4, 106.9, 80.1, 79.1, 78.8, 53.0, 42.8, 42.1, 37.3, 31.0, 29.5, 28.5, 27.8, 26.9, 26.25, 26.07, 23.4, 11.55, 11.38, 6.9, 5.0; $[\alpha]_D^{20}$ 13.84 (*c* = 1.0, $CHCl_3$).

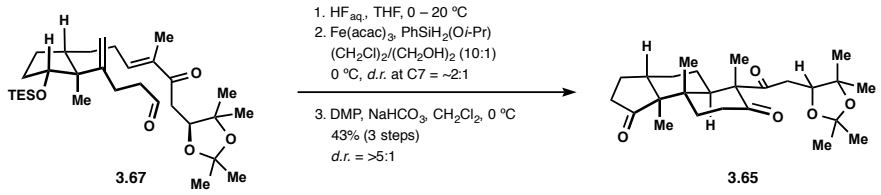

Tricarbonyl **3.65**: Aqueous hydrofluoric acid (19 μL, 0.52 mmol, 48%) was added to a solution of dicarbonyl **3.67** (147.7 mg, 0.0.28 mmol) in THF (5.2 mL) at 0 ºC. The reaction mixture was

vigorously stirred at 0 ºC. After 15 minutes the reaction mixture was allowed to warm to room temperature. After an additional 15 minutes 50 μL (1.25 mmol) of HF was added. After an additional 2 hours the reaction was neutralized with a solution of saturated aqueous $NaHCO_3$ (3 mL). The aqueous layer was extracted with diethyl ether (3x7 mL). The combined organic layers were washed with water (2 mL) and brine (2 mL), dried over anhydrous sodium sulfate, filtered, and concentrated under reduced pressure. The crude desilylated material existed as a *ca.* 2:1 mixture of **3.110** : **3.109** by analysis of the crude ^{1}H NMR. This material was used without further purification. R_f = 0.30 (30% v/v ethyl acetate in hexanes).

A Schlenk flask was charged with iron(III) acetylacetonate (98.9 mg, 0.28 mmol), a solution of the crude material from the previous step in 1,2-dichloroethane (14 mL), and ethylene glycol (1.4 mL). The mixture was degassed using a freeze-pump-thaw technique (3 cycles), cooled to 0 ºC, and treated with (isopropoxy)phenylsilane (100 μL, 0.52 mmol). The biphasic reaction mixture was vigorously stirred at 0 ºC. After 1 hour the reaction was quenched with a solution of degassed water (2.0 mL). The aqueous layer was extracted with diethyl ether (3x15 mL). The organic layer were washed with a solution of 1 N aqueous HCl (3x3 mL), water (5 mL), and brine (3 mL). The combined organic layers were dried over anhydrous sodium sulfate, filtered, and concentrated under reduced pressure. Analysis of the crude ^{1}H NMR spectrum revealed that a 2:1 mixture of diastereomers at C7. The crude tricycle **3.111** was used without further purification.

Dess–Martin periodinane (475.0 mg, 0.1.12 mmol) and $NaHCO_3$ (188.2 mg, 2.24 mmol) were added to a solution of the crude tricycle **3.111** in methylene chloride (2.8 mL) at 0 ºC. The reaction mixture was vigorously stirred and allowed to warm to room temperature. After 1.5 hours the reaction was cooled to 0 ºC and quenched with a 1:1 mixture of saturated aqueous

$NaHCO_3$:$Na_2S_2O_3$ (2 mL). The heterogeneous material was filtered off and the aqueous layer was extracted with methylene chloride (3x7 mL). The combined organic layers were washed with a solution of saturated aqueous $NaHCO_3$ (3 mL), water (3 mL), and brine (3 mL). The organic layer was dried over anhydrous sodium sulfate, filtered, and concentrated under reduced pressure. Analysis of the crude ^{1}H NMR spectrum revealed that a >5:1 mixture of diastereomeric *trans*:*cis* tricycles. Purification by flash chromatography (gradient elution: 100% hexanes to 15% ethyl acetate in hexanes) afforded 50.1 mg (43% over 3 steps) of tricarbonyl **3.65** as a white film. R_f = 0.46 (30% v/v ethyl acetate in hexanes); ^{1}H NMR (500 MHz; $CDCl_3$): δ 4.15 (dd, *J* = 9.9, 2.0 Hz, 1H), 2.70–2.63 (m, 2H), 2.57 (ddd, *J* = 13.7, 6.2, 2.3 Hz, 1H), 2.51–2.41 (m, 2H), 2.36 (dd, *J* = 19.4, 8.4 Hz, 1H), 2.24 (dd, *J* = 15.1, 2.0 Hz, 2H), 2.08–2.04 (m, 1H), 1.95 (td, *J* = 14.0, 4.7 Hz, 1H), 1.85 (ddd, *J* = 12.4, 8.8, 6.2 Hz, 1H), 1.65 (dq, *J* = 8.9, 3.2 Hz, 1H), 1.60–1.51 (m, 1H), 1.41–1.35 (m, 6H), 1.26 (m, 6H), 1.20 (m, 6H), 1.05 (s, 3H), 1.03 (s, 3H); ^{13}C NMR (125 MHz; $CDCl_3$): δ 220.1, 213.2, 206.0, 106.9, 80.5, 80.0, 66.3, 55.7, 41.0, 40.5, 38.9, 38.1, 37.3, 35.4, 30.4, 28.6, 26.9, 25.4, 24.9, 24.1, 23.7, 23.4, 16.3, 15.7, 10.4; HRMS (ESI) calculated $C_{25}H_{38}O_5Na$ [M+Na]$^+$: 441.2617, found, 441.2598; $[\alpha]_D^{20}$ -30.85 (*c* = 1.0, $CHCl_3$).

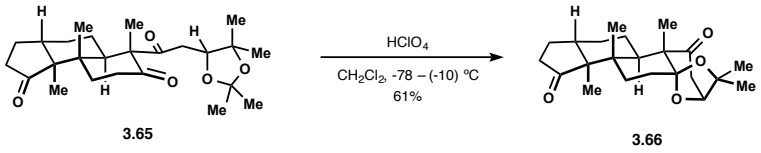

3.65 3.66

Ketal **3.66**: Aqueous perchloric acid (20 μL, 0.24 mmol, 48%) was added to a solution of tricarbonyl **3.65** (50.1 mg, 0.12 mmol) in methylene chloride (1.0 mL) at -78 ºC. The reaction mixture was vigorously stirred and allowed to slowly warm to ~(-10) ºC. The temperature was maintained between -20 – (-10) ºC for 6 hours. The reaction was quenched with a solution of saturated aqueous $NaHCO_3$ (1.0 mL). The aqueous layer was extracted with methylene chloride (3x7 mL). The combined organic layers were washed with brine (3 mL), dried over anhydrous

sodium sulfate, filtered, and concentrated under reduced pressure. Purification by flash chromatography (gradient elution: 100% hexanes to 20% v/v ethyl acetate in hexanes) afforded 26.6 mg (61%) of ketal **3.66** as a white film. R_f = 0.27 (20% v/v ethyl acetate in hexanes); ^{1}H NMR (500 MHz; $CDCl_3$): δ 4.23 (d, *J* = 5.6 Hz, 1H), 2.75 (dd, *J* = 16.7, 5.7 Hz, 1H), 2.44 (d, *J* = 16.7 Hz, 1H), 2.32 (dd, *J* = 19.3, 8.5 Hz, 1H), 2.20–2.07 (m, 5H), 2.00 (t, *J* = 9.6 Hz, 1H), 1.79 (ddd, *J* = 12.4, 8.9, 6.1 Hz, 1H), 1.67–1.58 (m, 2H), 1.50 (tt, *J* = 12.2, 9.2 Hz, 1H), 1.37–1.26 (m, 6H), 1.17 (s, 3H), 1.07 (s, 3H), 1.01 (s, 3H), 0.98 (s, 3H); ^{13}C NMR (125 MHz; $CDCl_3$): δ 220.6, 211.5, 110.8, 82.0, 79.5, 59.6, 56.3, 41.8, 40.7, 40.3, 39.3, 37.6, 29.2, 28.80, 28.66, 25.6, 23.8, 23.13, 23.03, 18.5, 14.0, 10.6; HRMS (ESI) calculated $C_{22}H_{32}O_4Na$ $[M+Na]^+$: 383.2198, found, 383.2207; $[\alpha]_D^{20}$ 30.31 (*c* = 1.0, $CHCl_3$).

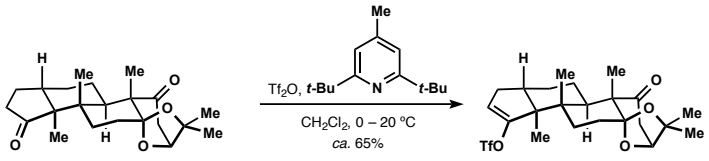

3.66 **3.112**

Vinyl triflate **3.112**: Trifluoromethanesulfonic anhydride (38 μL, 0.22 mmol, freshly prepared from TfOH and P_2O_5) was added to a solution of ketal **3.66** (26.6 mg, 0.074 mmol) and 2,6-di-*tert*-butyl-4-methyl pyridine (53 μL, 0.22 mmol) in methylene chloride (3.7 mL) at 0 ºC. The reaction mixture was vigorously stirred and allowed to warm to room temperature. After 5 hours an addition charge of trifluoromethanesulfonic anhydride (17 μL, 0.1 mmol) and 2,6-di-*tert*-butyl-4-methyl pyridine (24 μL, 0.1 mmol). After an additional 6 hours the reaction mixture was cooled to 0 ºC and quenched with a solution of saturated aqueous $NaHCO_3$ (0.8 mL). The biphasic mixture was diluted with methylene chloride (5 mL) and water (1 mL). The aqueous layer was extracted with methylene chloride (3x7 mL). The combined organic layers were dried over anhydrous sodium sulfate. Purification by flash chromatography (gradient elution: 100%

hexanes to 7.5% v/v ethyl acetate in hexanes) afforded 40. mg (*ca.* 65% based on impurity) of vinyl triflate **3.112** as a white film along with $(TfOCH_2CH_2)_2$[62] as an impurity. R_f = 0.47 (20% v/v ethyl acetate in hexanes); ^{1}H NMR (500 MHz; $CDCl_3$): δ 5.56 (dd, *J* = 3.1, 1.8 Hz, 1H), 4.58 (q, *J* = 4.8 Hz, 5H), 4.22 (d, *J* = 5.4 Hz, 1H), 2.73 (dd, *J* = 16.6, 5.7 Hz, 1H), 2.45 (d, *J* = 16.6 Hz, 1H), 2.29–1.95 (m, 12H), 1.65 (ddd, *J* = 20.8, 9.3, 2.6 Hz, 2H), 1.58 (dq, *J* = 8.8, 3.0 Hz, 1H), 1.33–1.29 (m, 4H), 1.18 (s, 3H), 1.15 (t, *J* = 2.9 Hz, 1H), 1.13 (s, 3H), 1.11 (s, 3H), 1.09 (s, 3H) [10 extra protons from impurity]; ^{13}C NMR (150 MHz; $CDCl_3$): δ 211.5, 157.8, *118.7 (q, J = 319.5 Hz)*, 118.6 (q, *J* = 320.2 Hz) 114.6, 110.7, 82.2, 79.5, *75.9*, 59.8, 55.0, 42.7, 41.9, 40.4, 39.2, 30.3, 29.9, 28.88, 28.76, *25.5*, 24.4, 23.9, 23.0, 19.1, 13.8, 12.2 [italicized signals are from the impurity].

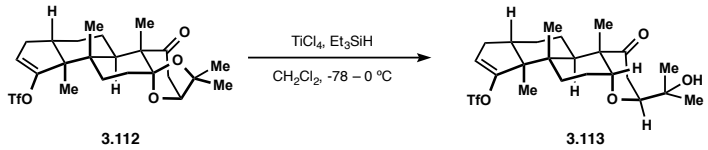

3.112 **3.113**

Tertiary alcohol **3.113**: A solution of $TiCl_4$ (20 μL, 0.022 mmol, 0.1 M in methylene chloride) was added to a solution of ketal **3.112** (<5 mg, <0.011 mmol) and triethylsilane (5 μL, 0.033 mmol) in methylene chloride (0.6 mL) at -78 ºC. The reaction was vigorously stirred and the temperature was maintained at -78 ºC. After 1 hour the reaction was warmed to 0 ºC. After an additional 1 hour the reaction was warmed to room temperature. After an additional hour the reaction was quenched with a solution of saturated aqueous $NaHCO_3$ (50 μL) and diluted with methylene chloride. The resulting solution was filtered through a plug of anhydrous sodium sulfate and concentrated under reduced pressure. Purification by flash chromatography (gradient elution: 100% hexanes to 50% ethyl acetate in hexanes) afforded (~1.6 mg) of tertiary alcohol **3.113** as a thin film. Crystals of **3.113**, suitable for X-ray crystallographic analysis, were obtained by slow evaporation from a solution of hexanes. R_f = 0.4 (30% v/v ethyl acetate in

hexanes); ^{1}H NMR (600 MHz; $CDCl_3$): δ 5.61 (dd, *J* = 3.2, 1.8 Hz, 1H), 4.24 (t, *J* = 3.2 Hz, 1H), 3.99 (dd, *J* = 7.3, 3.6 Hz, 1H), 2.76 (dd, *J* = 15.3, 7.3 Hz, 1H), 2.59 (dd, *J* = 15.3, 3.7 Hz, 1H), 2.39 (dd, *J* = 12.7, 3.5 Hz, 1H), 2.35–2.29 (m, 1H), 2.24–2.20 (m, 1H), 2.15 (td, *J* = 13.2, 4.3 Hz, 1H), 2.05 (ddd, *J* = 14.8, 11.0, 1.8 Hz, 1H), 1.94 (tdd, *J* = 13.9, 4.1, 2.7 Hz, 1H), 1.80 (dq, *J* = 14.6, 3.8 Hz, 1H), 1.52 (br s, 1H), 1.50-1.38 (m, 5H), 1.36 (s, 3H), 1.25 (s, 3H), 1.19 (s, 3H), 1.17 (s, 3H), 1.08 (s, 3H); ^{13}C NMR (150 MHz; CDCl3): δ 212.9, 157.9, 114.4, 79.2, 75.2, 75.0, 54.9, 52.9, 42.8, 39.6, 37.6, 36.7, 30.3, 29.9, 27.9, 26.2, 24.8, 24.0, 23.9, 18.7, 14.9, 12.4 [^{13}C signal for CF_3 not detectable].

NOESY Correlations

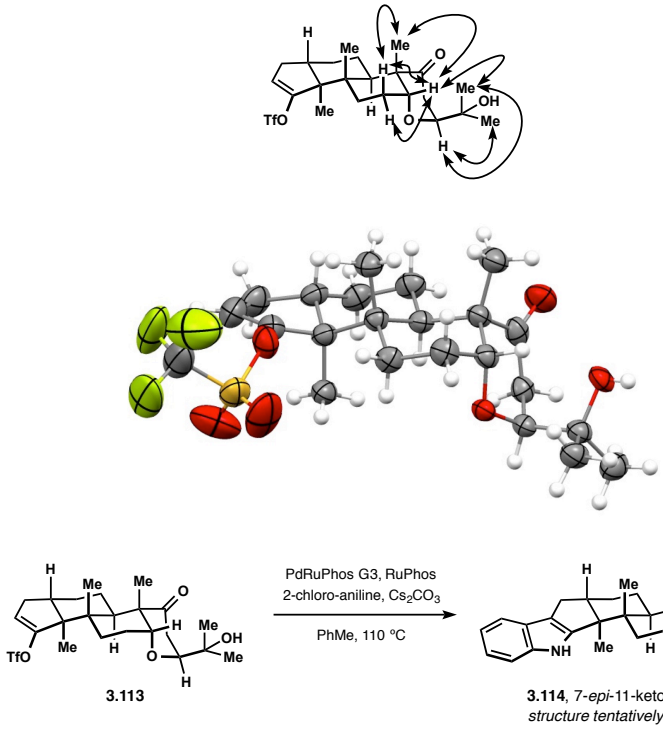

7-*epi*-11-ketopaspaline **3.114**: A dram vial was charged with a solution of vinyl triflate **3.113** (~1.6 mg) in toluene. The volatiles were removed under reduced pressure and the vial was brought into a nitrogen atmosphere glovebox. The vial was charged with RuPhos Pd G3 (0.6 mg, 0.0007 mmol), RuPhos (1.0 mg, 0.0021 mmol), Cs_2CO_3 (2.3 mg, 0.007 mmol), toluene (0.2 mL),

and a solution of 2-chloroaniline (42 μL, 0.0042 mmol, 0.1 M in toluene). The vial was sealed with a PTFE lined cap and heated to 110 ºC. After 16 hours the reaction mixture was cooled to room temperature and removed from the glovebox. Volatiles were removed under reduced pressure. Purification by preparative TLC afforded material that was tentatively identified as 7-*epi*-11-ketopaspaline **3.114**. Diagnostic ^{1}H NMR signals: ^{1}H NMR (500 MHz; $CDCl_3$): δ 7.78 (br s, 1H), 7.49–7.48 (m, 1H), 7.37–7.34 (m, 2H), 7.14 (ddd, *J* = 6.9, 4.1, 2.2 Hz, 2H), 4.32 (t, *J* = 3.0 Hz, 1H), 4.04 (dd, *J* = 7.4, 3.7 Hz, 1H).

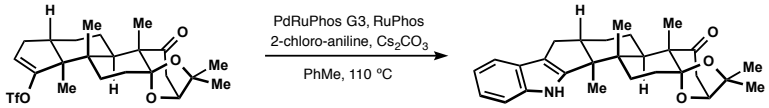

3.112 **3.115**, dehydro-11-ketopaspaline *structure tentatively assigned*

Dehydro-11-ketopaspaline **3.115**: A dram vial was charged with a solution of vinyl triflate **3.113** (3 mg, 0.006) in toluene. The volatiles were removed under reduced pressure and the vial was brought into a nitrogen atmosphere glovebox. The vial was charged with RuPhos Pd G3 (2.5 mg, 0.003 mmol), RuPhos (4.2 mg, 0.009 mmol), Cs_2CO_3 (5.9 mg, 0.018 mmol), toluene (0.2 mL), and a solution of 2-chloroaniline (120 μL, 0.012 mmol, 0.1 M in toluene). The vial was sealed with a PTFE lined cap and heated to 110 ºC. After 16 hours the reaction mixture was cooled to room temperature and removed from the glovebox. Volatiles were removed under reduced pressure. Purification by flash chromatography (gradient elution: 100% pentane to 20% v/v ethyl acetate in pentane) afforded 1.5 mg (*ca.* 58%) of dehydro-11-ketopaspaline **3.115** as a thin film. Diagnostic ^{1}H NMR signals: ^{1}H NMR (500 MHz; $CDCl_3$): δ 7.72 (s, 1H), 7.42 (dd, *J* = 6.3, 2.5 Hz, 1H), 7.31 (dd, *J* = 6.5, 2.3 Hz, 1H), 7.09–7.05 (m, 2H), 4.28 (d, *J* = 5.4 Hz, 1 H).

3.5 References and Notes

[1] It should be noted that Eric J. Kuenstner (EJK) and Devon J. Schatz (DJS) performed the majority of the research discussed in section 3.1.1.

[2] (a) George, D. T.; Kuenstner, E. J.; Pronin, S. V. *J. Am. Chem. Soc.* **2015**, *137*, 15410.
[3] George, D. T.; Kuenstner, E. J.; Pronin, S. *Synlett*, **2017**, *28*, 12.
[4] (a) Lo, J. C.; Yabe, Y.; Baran, P. S. *J. Am. Chem. Soc.* **2014**, *136*, 1304. (b) Lo, J. C.; Gui, J.; Yabe, Y.; Pan, C.-M.; Baran, P. S. *Nature* **2014**, *516*, 343. (c) Lo, J. C.; Kim, D.; Pan, C.-M.; Edwards, J. T.; Yabe, Y.; Gui, J.; Qin, T.; Gutiérrez, S.; Giacoboni, J.; Smith, M. W.; Holland, P. L.; Baran, P. S. *J. Am. Chem. Soc.* **2017**, *139*, 2484.
[5] The origin of the diastereoselectivity is currently being investigated.
[6] The initial structural assignment of **3.18** was incorrect. See Section 3.2.2 for further details.
[7] David T. George (DTG) performed all experiments discussed for the remainder of Chapter 3 unless otherwise noted.
[8] Speculative analysis of isolated mixtures indicated that products related to radical conjugate addition and the desired polycyclization might have formed, but in extremely low efficiency. Isolated materials never resembled a single component by NMR, which made the evaluation of this reaction extremely difficult.
[9] Fu, Y.; Lui, L.; Yu, H.-Z.; Wand, Y.-M.; Guo, Q.-X. *J. Am. Chem. Soc.* **2005**, *127*, 7227.
[10] Wadsworth, W. S. Jr.; Emmons, W. D. *J. Am. Chem. Soc.* **1961**, *83*, 1733.
[11] (a) Evan, D. A.; Truesdale, L. K.; Carroll, G. L. *J. Chem. Soc. Chem. Commun.* **1973**, 55. (b) Evans, D. A.; Carroll, G. L.; Truesdale, L. K. *J. Org. Chem.* **1974**, *39*, 914.
[12] (a) Dess, D. B.; Martin, J. C. *J. Org. Chem.* **1983**, *48*, 4155. (b) Dess, D. B.; Martin, J. C. *J. Am. Chem. Soc.* **1991**, *113*, 7277.
[13] Foley, C. N.; Leighton, J. L. *Org. Lett.* **2015**, *17*, 5858.
[14] Greenberg, J. A.; Sammakia, T. *J. Org. Chem.* **2017**, *82*, 3245.
[15] Corey, E. J.; Kwiatkowski, G. T. *J. Am. Chem. Soc.* **1966**, *88*, 4643.
[16] Solvent, temperature, and order of addition did not have an effect on the outcome.
[17] Boger, D. L.; Curran, T. T. *J. Org. Chem.* **1002**, *57*, 2235.
[18] Godfrey, A. G.; Ganem, B. *Tetrahedron Lett.* **1990**, *31*, 4825,
[19] Umbreit, M. A.; Sharpless, K. B. *J. Am. Chem. Soc.* **1977**, *99*, 5526.
[20] Fatiadi, A. J. *Synthesis* **1976**, 65.
[21] Hoffmann, R. W.; Wolff, J. J. *Chem. Ber.* **1991**, *124*, 563.
[22] Swern, D. *Chem. Rev.* **1949**, *45*, 1 and references therein.
[23] Due to the exploratory nature of this work we were not concerned with developing a diastereoselective epoxidation. We were confident we could evaluate the ensuing polycyclization on the mixture of diastereomers without any issues.
[24] See Section 3.4 for further details.
[25] The unselective aldol addition was not acknowledged in Section 3.1.1 because it was not known until the results discussed in Section 3.2.2.
[26] (a) Isayama, S.; Mukaiyama, T. *Chem. Lett.* **1989**, 2005. (b) Baik, T.-G.; Luis, A. L.; Wang, L.-C.; Krische, M. J. *J. Am. Chem. Soc.* **2001**, *123*, 5112. (c) Wang, L.-C.; Jang, H.;-Y.; Roh, Y.; Lynch, V.; Schultz, A. J.; Wand, X.; Krische, M. J. *J. Am. Chem. Soc.* **2002**, *124*, 9448.
[27] Kumar, C. N. S. S. P.; Chein, R.-J. *Org. Lett.* **2014**, *16*, 2990.
[28] In fact, reductive aldol involving methacrolein **3.58** appeared to be an efficient process as reaction with hydrocinnamaldehdye **3.62** produced aldol product **3.63** in high yield.

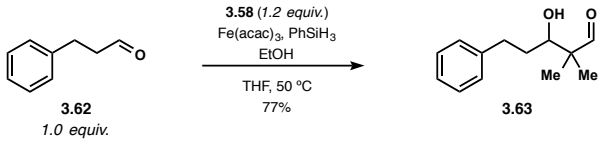

[29] (a) Smith, A. B. III; Kanoh, N.; Ishiyama, H.; Hartz, R. A. *J. Am. Chem. Soc.* **2000**, *122*, 11254. (b) Smith, A. B. III; Kanoh, N.; Ishiyama, H.; Minakawa, N.; Rainier, J. D.; Hartz, R. A.; Cho, Y. S.; Cui, H.; Moser, W. H. *J. Am. Chem. Soc.* **2003**, *125*, 8228.
[30] (a) Afonso, C. M.; Barros, M. T.; Maycock, C. D. *J. Chem. Soc. Perkin Trans. 1* **1987**, 1221. (b) Chen, J.; Forsyth, C. J. *Proc. Natl. Acad. Sci.* **2004**, *101*, 12067.
[31] Chatterjee, A. K.; Choi, T.-L.; Sanders, D. P.; Grubbs, R. H. *J. Am. Chem. Soc.* **2003**, *125*, 11360 and references therein.
[32] (a) Shigehisa, H.; Aoki, T.; Yamaguchi, S.; Shimizu, N.; Hiroya, K. *J. Am. Chem. Soc.* **2013**, *135*, 10306. (b) Shigehisa, H.; Hayashi, M.; Ohkawa, H.; Suzuki, T.; Okayashi, H.; Mukai, M.; Yamazaki, A.; Kawai, R.; Kikuchi, H.; Satoh, Y.; Fukuyama, A.; Hiroya, K. *J. Am. Chem. Soc.* **2016**, *138*, 10597.
[33] Touney, E. E.; Pronin, S. V. *Unpublished results*.
[34] (a) Nicolaou, K. C.; Bulger, P. G.; Sarlah, D. *Angew. Chem. Int. Ed.* **2005**, *44*, 4490. (b) Vanderwal, C. D.; Atwood, B. R. *Aldrichimica Acta* **2017**, *50*, 17.
[35] Burnley, J.; Wang, Z. J.; Jackson, W. R.; Robinson, A. J. *J. Org. Chem.* **2017**, *82*, 8497.
[36] For seminal work in this area see: Chatterjee, A. K.; Grubbs, R. H. *Org. Lett* **1999**, *1*, 1751.
[37] For seminal work in this area see: Chatterjee, A. K.; Sanders, D. P.; Grubbs, R. H. *Org. Lett.* **2002**, *4*, 1939.
[38] Ulman, M.; Belderrain, T. R.; Grubbs, R. H.*Tetrahedron Lett.* **2000**, *41*, 4689.
[39] (a) Guz, N. R.; Phillips, A. J. *Org. Lett.* **2002**, *4*, 2253. (b) Zhang, Y.; Phillips, A. J.; Sammakia, T. *Org. Lett.* **2004**, *6*, 23. (c) Zhang, Y.; Sammakia, T. *Org. Lett.* **2004**, *6*, 3139. (d) Crimmins, M. T.; Shamszad, M. *Org. Lett.* **2007**, *9*, 149.
[40] (a) Fukuzawa, S.-i.; Matsuzawa, H.; Yoshimitsu, S.-i. *J. Org. Chem.* **2000**, *65*, 1702. (b) Wolf, C.; Moskowitz, M. *J. Org. Chem.* **2011**, *76*, 6372.
[41] Carreira, E. M.; Singer, R. A.; Lee, W. *J. Am. Chem. Soc.* **1994**, *116*, 8837.
[42] Evans, D. A.; Bartoli, J.; Shih, T. L. *J. Am. Chem. Soc.* **1981**, *103*, 2127.
[43] Noe, E. A.; Raban, M. *J. Am. Chem. Soc.* **1975**, *97*, 5811.
[44] Evans, D. A.; Takacs, J. M.; McGee, L. R.; Ennis, M. D.; Mathre, D. J.; Bartoli, J. *Pure Appl. Chem.* **1981**, *53*, 1109.
[45] (a) Basha, A.; Lipton, M.; Weinreb, S. M. *Tetrahedron Lett.* **1977**, *18*, 4171. (b) Levin, J. I.; Turos, E.; Weinreb, S. M. *Synth. Commun.* **1982**, *12*, 989. (c) Evans, D. A.; Bender, S. L.; Morris, J. *J. Am. Chem. Soc.* **1988**, 1*110*, 2506. (d) Nahm, S.; Weinreb, S. M. *Tetrahedron Lett.* **1981**, *22*, 3815.
[46] Calvo, B. C.; Madduri, A. V. R.; Harutyunyan, S. R.; Minnaard, A. J. *Adv. Synth. Catal.* **2014**, *356*, 2061.
[47] The optimization of this protocol was performed by Devon J. Schatz.
[48] While 72% *e.e.* appears quite modest there is a gap in chemical space performing highly enantioselective conjugate additions of 2-substituted cyclopenten-1-ones. As such, our level of stereoenrichment will be one of the highest reported to date.
[49] **3.105** was contaminated with a minor (~5–10%) of Wurtz coupling of the homoprenyl unit.
[50] (a) van Rensburg, W. J.; Steynberg, P. J.; Meyer, W. H.; Kirk, M. M.; Forman, G. S. *J. Am. Chem. Soc.* **2004**, *126*, 14332. (b) Romero, P. E.; Piers, W. E. *J. Am. Chem. Soc.* **2005**, *127*, 5032. (c) Romero, P. E.; Piers, W. E. *J. Am. Chem. Soc.* **2007**, *129*, 1698. (d) Hong, S. H.; Wenzel, A. G.; Salguero, T. T.; Day, M. W.; Grubbs, R. H. *J. Am. Chem. Soc.* **2007**, *129*, 7961.

[51] (a) Scholl, M.; Ding, S.; Lee, C. W.; Grubbs, R. H. *Org. Lett.* **199**, *1*, 953. (b) Garber, S. B.; Kingsbury, J. S.; Gray, B. L.; Hoveyda, A. H. *J. Am. Chem. Soc.* **2000**, *122*, 8168. (c) Stewart, I. C.; Douglas, C. J.; Grubbs, R. H. *Org. Lett.* **2008**, *10*, 441.
[52] Mancuso, A. J.; Swern, D. *Synthesis* **1981**, 165 and references therein.
[53] During isolation of **3.65** we were able to resolve **3.65** and increase its level of enantioenrichment. We were able to achieve resolution due to the level of enantioenrichment of enone **3.70**, which set the stereochemistry at C9
[54] (a) Barluenga, J.; Fernández, M. A.; Aznar, F.; Valdés *Chem. Eur. J.* **2005**, *11*, 2276. (b) Barluenga, J.; Valdés, C. *Chem. Commun.* **2005**, 4891.
[55] Structural assignment is tentative due only to a lack of full characterization data.
[56] Saksena, A. K.; Mangiaracina, P. *Tetrahedron Lett.* **1983**, *24*, 273.
[57] At this point we realized that my (D.T.G.) time in the Pronin group had come to an end and my synthetic efforts toward 11-ketopaspaline **3.20** would remain incomplete. It is my greatest regret that I was unable to complete the synthesis; I tirelessly gave this project everything that I had to offer from an intellectual and technical standpoint. It is my hope that my efforts guide a successful strategy to 11-ketopaspaline **3.20** and any related congeners of the PIDs.
[58] Pal, K.; Koner, A. L. *Chem. Eur. J.* **2017**, *23*, 8610.
[59] Clary, J. W.; Rettenmaier, T. J.; Sneilling, R.; Bryks, W.; Banwell, J.; Wipke, W. T.; Singaram, B. *J. Org. Chem.* **2011**, *76*, 9602.
[60] Gunji, Y.; Yamashita, Y.; Ikeno, T.; Yamada, T. *Chem. Lett.* **2006**, *35*, 714.
[61] May, A. E.; Willoughby, P. H.; Hoye, T. R. *J. Org. Chem.* **2008**, *73*, 3292.
[62] Medina-Molner, A.; Rohner, M.; Pandiaranjan, D.; Springler, B. *Dalton Trans.* **2015**, *44*, 3664.

Chapter 4: New Chemical Methods Linking Radical and Cationic Intermediates

4.1 Cationic Intermediates from Carbon-centered Radicals

4.1.1 Hydrofunctionalization of Alkenes via a Radical-polar Crossover Reaction Mechanism

Simple, unactivated alkenes are readily available feedstock organic compounds and methods focused on their modification are invaluable resources for chemists. Although a wide variety of transformations are available that functionalize simple alkenes, Brønsted acid-catalyzed hydrofunctionalization of alkenes involving direct protonation is arguably the most straightforward as the resulting carbocation intermediate can be simply intercepted with a nucleophile (Scheme 4.1a). In nature, this sequence of elementary steps likely occurs in a variety of biosynthetic pathways where enzymatic pockets help lower the transition state energies associated with protonation events and exert absolute stereocontrol over the transformations.[1] The lowering the transition state energy barrier is a crucial feature as it facilitates carbocation generation at a biologically relevant pH, which is remarkable given the relatively low basicity of simple alkenes.[2] In an artificial setting, however, the low basicity is often overcome with the use of a strong Brønsted acid, which severely limits functional group tolerance.

Scheme 4.1. General Mechanism for Brønsted Acid Mediated Alkene Hydrofunctionalization.

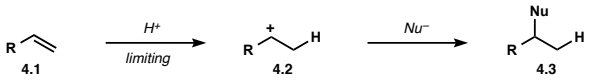

In order to broaden the reaction scope of the hydrofunctionalization of simple alkenes via carbocationic intermediates alternative reaction manifolds were recently developed that combined two elementary steps: transition metal-catalyzed hydrogen atom transfer (HAT) to simple alkenes and single-electron oxidation of carbon-centered radicals (Scheme 4.2). The

former elementary step, metal-catalyzed HAT, is a mode of reactivity that has seen a renaissance in the last decade.[3] The reaction conditions associated with metal-catalyzed HAT are typically mild, which delivers chemoselective reactions that tolerate variety of functional groups (i.e. heteroatom, carbonyl, halide, free and protected alcohols). Delivery of the hydrogen atom affords carbon-centered radicals from alkenes with Markovnikov selectivity, which mirrors the regioselectivity of direct protonation with Brønsted acids. Taken together, metal-catalyzed HAT represents a mild and regioselective method to generate carbon-centered radicals from simple alkenes.

Scheme 4.2. General Mechanism for Radical-polar Crossover Alkene Hydrofunctionalization.

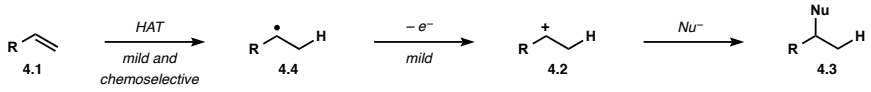

The latter elementary step, oxidation of carbon-centered radicals, is a kinetically and thermodynamically facile way to access high-energy carbocationic intermediates. This is due to the inherent kinetics of electron transfer, which can occur much faster than nuclear vibrations,[4] and the relatively low oxidation potential associated with secondary and tertiary carbon-centered radicals.[5] Since transition metal salts[6] and complexes[7] are capable single-electron oxidants toward carbon-centered radicals a method linking HAT and oxidation would offer mild and chemoselective access to carbocationic intermediates.

4.1.2. Intermolecular Hydroalkoxylation of Simple Alkenes

In 2013 Sigehisa, Hiroya, and co-workers published a report on the hydroalkoxylation of alkenes via a proposed radical-polar crossover reaction mechanism (Scheme 4.3a).[8] The optimized reaction converted terminal alkene **4.5** to ethyl ether **4.14** with high efficiency under mild reaction conditions. The authors speculated that oxidation of the cobalt catalyst **4.6** and subsequent transmetallation with phenylsilane[9] could provide access to the crucial cobalt(III)–

hydride **4.10**. Since cobalt(salen)–hydrides are well-known agents of HAT,[10] ensuing regioselective HAT from cobalt(III) hydride **4.10** to alkene **4.5** produced secondary radical **4.12**. Subsequent oxidation to form carbocation **4.13** and solvolysis produced ethyl ether **4.14**. The authors provided support for their proposed mechanism with experiments involving a radical clock and deuterium labeled reagents (Scheme 4.3b and c). As such, when vinyl cyclopropane **4.15** was subject to the optimized reaction conditions homo allylic ether **4.16** was obtained, which suggested that radical intermediates likely are involved in the process (Scheme 4.3b). In addition, deuterium labeling studies revealed that the reductant was the source of the hydrogen atom in the product (Scheme 4.3c).

Scheme 4.3. Radical-polar Crossover Alkene Hydrofunctionalization.

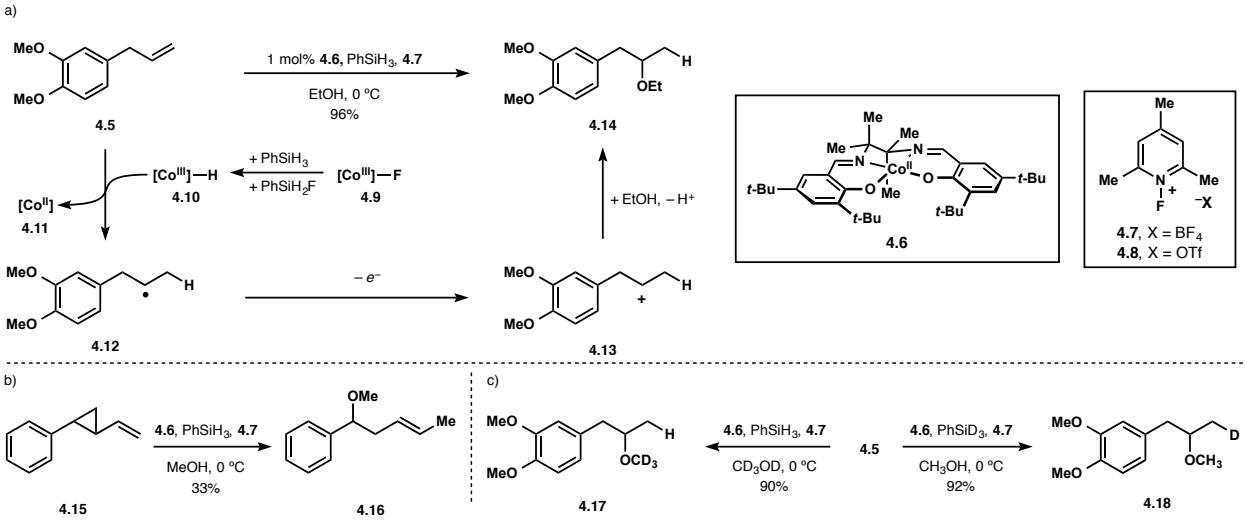

The reaction was applied to the hydroalkoxylation to a variety of terminal alkenes and isolated examples 1,1-disubstituted and trisubstituted alkenes to form methyl and *tert*-butyl ethers (Scheme 4.4a). The yields for *tert*-butyl ether formation were generally lower likely as a result of the poor nucleophilicity of *tert*-butanol, but synthetically useful yields were still obtained. In an isolated example, stoichiometric quantities of alkene **4.5** and alcohol **4.39** were coupled in an intermolecular fashion, which highlighted the potential of this method (Scheme

4.4b). In a subsequent report, the same authors extended this methodology to include the hydroalkoxylation of simple alkenes using fluorinated alcohols.[11] Importantly, this set of work represented the first examples uniting transition metal-catalyzed HAT and single-electron oxidation of carbon-centered radicals.

Scheme 4.4. Representative Reaction Scope for Hydroalkoxylation.

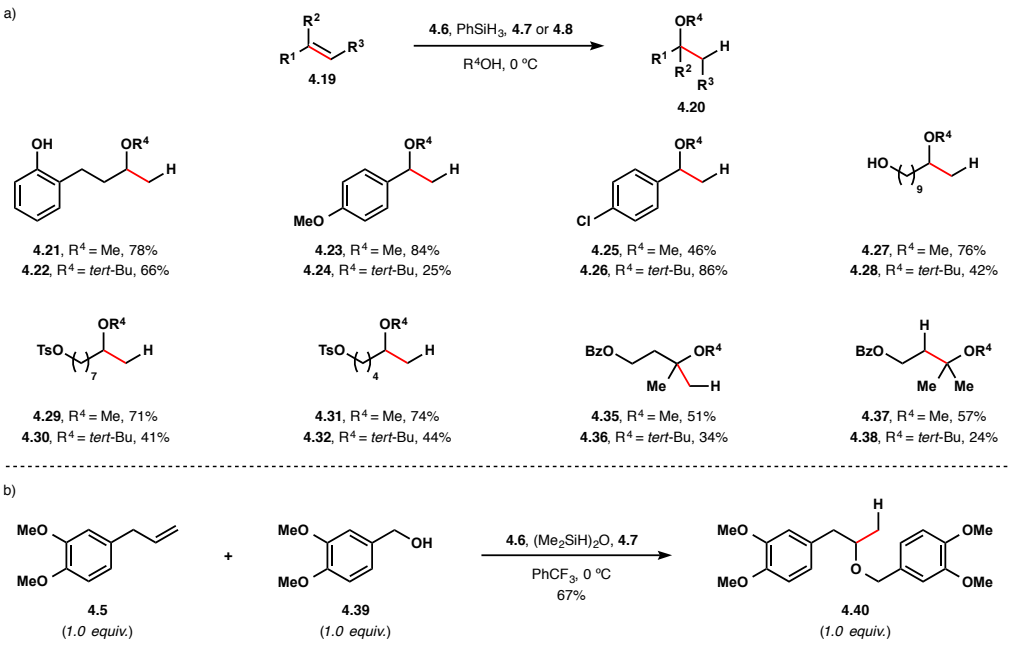

4.1.3. Intramolecular Hydroamination of Simple Alkenes

In 2014, Shigehisa and co-workers expanded the radical-polar crossover reaction manifold to include the hydroamination of simple alkenes.[12] Unlike their previous work (*vide supra*) the scope of this work was limited to intramolecular carbon–nitrogen bond formation (Scheme 4.5a). Protection of the nitrogen atom was critical to reaction progress as substrates bearing free amines were unreactive. Within this context, small rings were efficiently prepared (**4.43**–**4.47**). While a protecting group was required, its nature did not have a strong influence on the outcome of the reaction as amides bearing an unprotected phenol (**4.48**), benzaldehyde (**4.49**), acyl pyrrole (**4.50**), and epoxide (**4.51**) moieties were tolerated. An interesting study revealed that a tethered hydroxyl group could compete with the protected nitrogen during the

trapping of the putative carbocation (Scheme 4.5b). As such, the free-alcohol variant of **4.52** formed tetrahydrofuran **4.54** without the formation pyrrolidine **4.53**. However, pyrrolidine **4.53** could be formed as more acid-tolerant protecting groups were substituted on the hydroxyl group. In fact, complete selectivity for pyrrolidine formation was achieved when the acetate variant of **4.52** was exposed to the optimized reaction conditions. While Shigehisa and co-workers did not report any examples of intermolecular carbon–nitrogen bond formation, the disclosed method provided access to amine hetereocycles via a radical-polar crossover reaction mechanism under mild reaction conditions.

Scheme 4.5. Representative Reaction Scope for Hydroamination

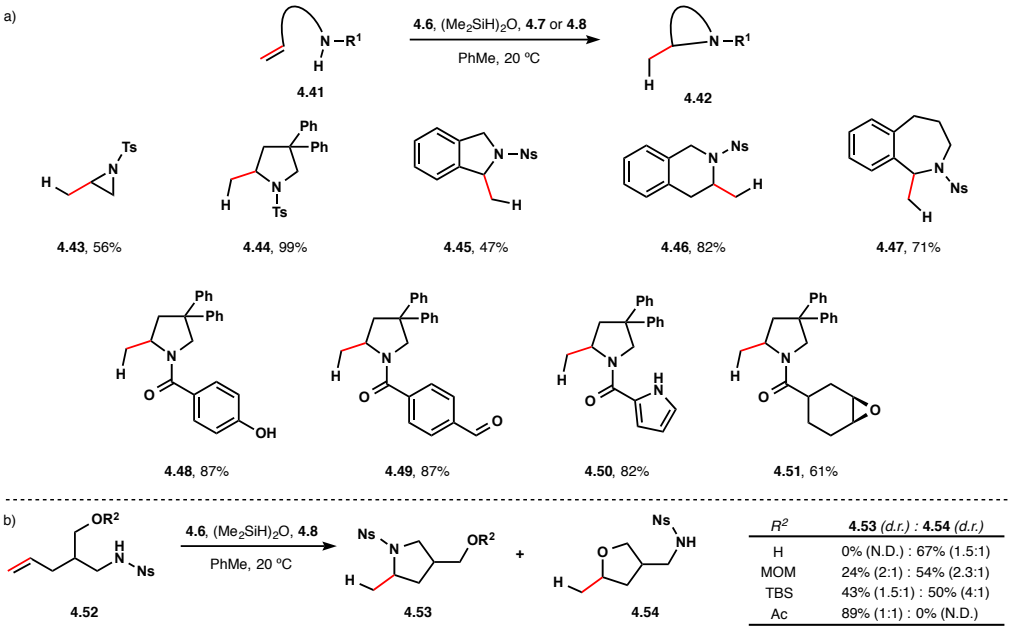

R^2	**4.53** *(d.r.)* : **4.54** *(d.r.)*
H	0% (N.D.) : 67% (1.5:1)
MOM	24% (2:1) : 54% (2.3:1)
TBS	43% (1.5:1) : 50% (4:1)
Ac	89% (1:1) : 0% (N.D.)

4.1.4 Synthesis of Oxygen Heterocycles from Simple Alkenes

In 2016 Shigehisa and co-workers published a report on the synthesis of oxygen heterocycles from simple alkenes via a radical-polar crossover mechanism.[13] This work offered an intramolecular variant to their original work on intermolecular hydroalkoxylation (*vide supra*). As such, 5- and 6-membered cyclic ethers and lactones assembled functionalized ring systems (Scheme 4.6). Cyclization performed with almost equal efficiency for etherification and

lactonization, which highlighted the utility of the carbocation generated from the radical-polar crossover mechanism. Furthermore, protected alcohols and carboxylic acids also were competent precursors to ethers and lactones, which corroborated previous studies.[11]

Scheme 4.6. Representative Reaction Scope for 5- and 6-membered Ether and Lactone Formation.

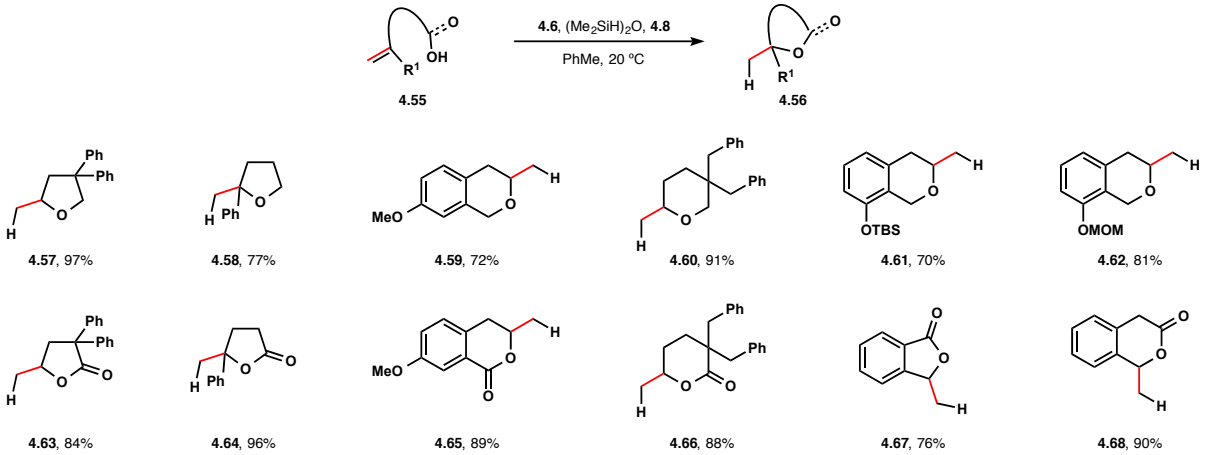

While small rings were efficiently formed, a low yield was reported for 7-membered ring formation (Scheme 4.7). However, a survey of similar cobalt(salen) complexes identified cobalt catalyst **4.70** as an efficient facilitator of medium-sized ring formation. As such, 7-, 8-, and 9-membered ethers and lactones were prepared using catalyst **4.70**. While medium-sized rings were formed, there was a considerable decrease in yield relative to small-sized ring formation. However, the decrease in yield was attributed to competing alkene isomerization, which is a known side-reaction for cobalt(salen) HAT reactions.[14]

Scheme 4.7. Representative Reaction Scope for Medium-sized Ring Formation

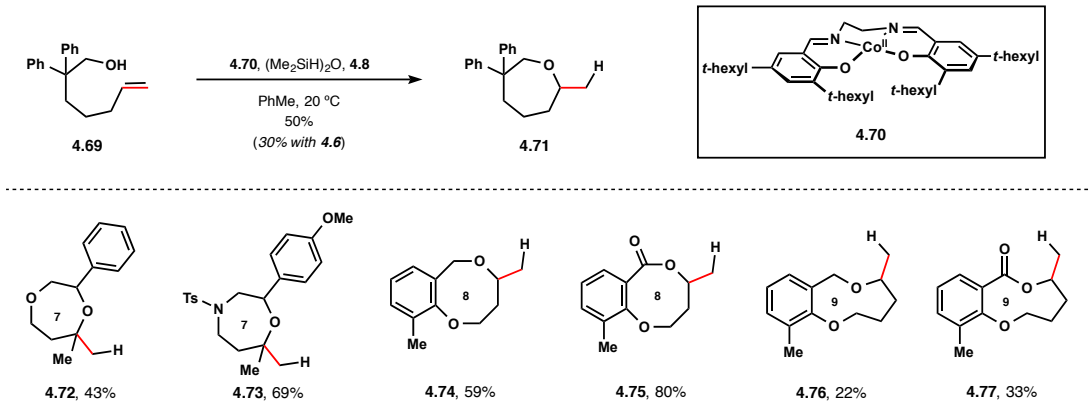

In addition to the expansion of the reaction scope for hydroalkoxylation of simple alkenes, Shigehisa and co-workers also provided further insight into the mechanism of the reaction. One observation indicated that the collidine (**4.85**) by-product was not an innocent spectator (Scheme 4.8a). As such, the cleaved protecting groups were transferred to collidine (**4.85**) as evidenced by the efficient formation of pyridinium salts **4.79**, **4.81**, and **4.83**. Analogous pyridinium salts were also observed during lactone formation from γ,δ-unsaturated esters. The presence of these pyridinium salts guided a mechanistic proposal involving a hypothetical interaction between oxonium **4.84** and **4.85** that would result in liberation of cyclized product **4.57** and salt **4.79**, **4.81**, or **4.83**.

Scheme 4.8. Interesting Observations.

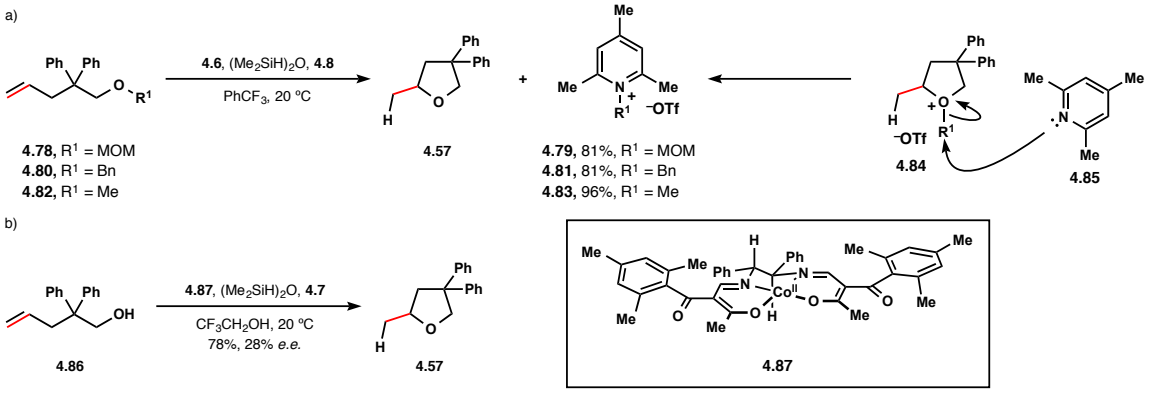

Shigehisa and co-workers also observed that alcohol **4.86** converted to tetrahydrofuran **4.57** with a modest level of enantioenrichment when β-oxoaldiminato cobalt complex **4.87**[15] was used as the catalyst (Scheme 4.8b). The originally proposed mechanism (Scheme 4.3a) did not involve the cobalt catalyst during stereodefining step, but the observation of enantioenriched material calls that proposal into question. Shigehisa and co-workers posited that simultaneous oxidation by a cationic cobalt complex and trapping of the carbocation could explain the observed enrichment. Nonetheless, it remains unclear how enantioenrichment was achieved, as other pathways could be operative.[16]

4.2 Development of a Mild and Chemoselective Ritter Reaction

4.2.1 Method Development

Our lab has interest in accessing polar intermediates from carbon-centered radicals via single-electron reduction or oxidation. We believe that traversing a reaction coordinate in this manner will result in mild and chemoselective reactions that will function in highly complex synthetic settings.[17] With this in mind, we identified simple alkenes as precursors to carbocationic intermediates that could be utilized in target oriented synthesis.[18] More specifically, we were inspired by work from Shigehisa and co-workers (*vide supra*) and hypothesized that we could execute a cationic polyene cyclization[19] via a radical-polar crossover reaction manifold (Scheme 4.9a). We hoped to leverage the apparent chemoselectivity exhibited by cobalt(salen) catalysts[20] to regioselectively generate tertiary radical **4.89** from polyene **4.88**. Subsequent oxidation of the resulting carbon-centered would generate a highly reactive intermediate that could facilitate the formation of bicycle **4.91** via a cationic polyene cyclization cascade. While this specific sequence of elementary steps represented a long-term goal we initially pursued the intramolecular *tert*-alkylation of enoxysilane **4.92** to build a foundation for our research program in this area (Scheme 4.9b).

Scheme 4.9. Research Goals.

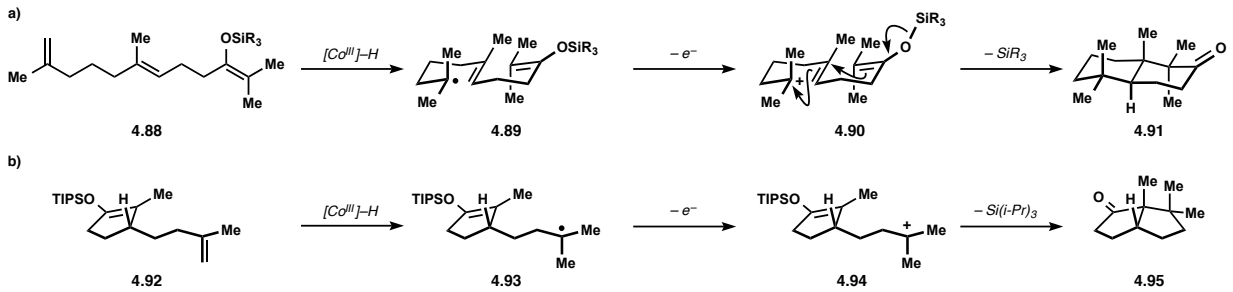

Our efforts in this area were moderately successful, as we were able to isolate the desired bicycle **4.95** with low overall efficiency (Scheme 4.10). The use of a Lewis basic solvent (i.e. acetonitrile) was crucial to product formation, as only side-reactions (i.e. alkene isomerization,[14]

hydrogenation,[20] hydrofluorination[21]) were operative in nonpolar mediums. However, we also isolated *tert*-alkyl acetamide **4.97** as a minor product that we believed formed from nitrilium ion **4.96** and adventitious moisture.

Scheme 4.10. Evidence of Alkylation and Amidation.

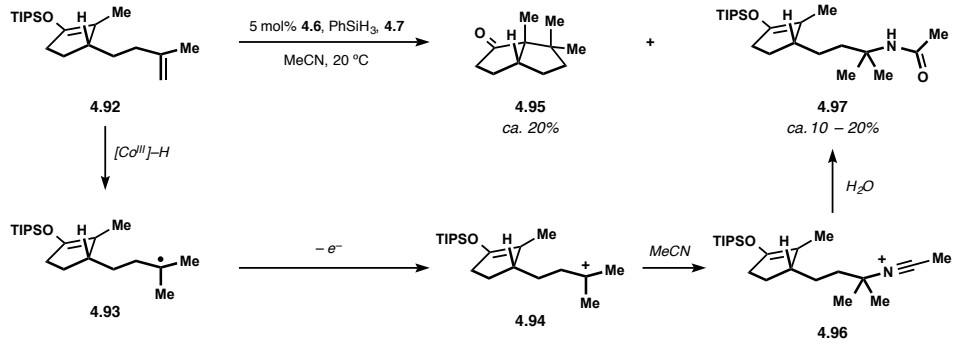

While the formation of **4.97** was unexpected,[22] we realized that further development of a hydroamidation reaction in the presence of an acid-sensitive functional group (i.e. enoxysilane) could lead to a mild complement of the Ritter reaction.[23] As such, we shifted our focus and pursued the hydroamidation of the 1,1-disubstituted alkene on dihydrocarvone (**4.98**; Table 4.1). Our initial attempts at forming *tert*-alkyl acetamide **4.99** were moderately successful (Entry 1, Table 4.1). However, analysis of the crude reaction mixtures by ^{1}H NMR indicated that alkene isomerization occurred and a considerable amount of starting material remained. We hypothesized that elimination of the intermediate nitrilium ion was the cause of the apparent lack of desired reactivity.

Table 4.1. Optimization of the Radical-polar Crosover Ritter Reaction.

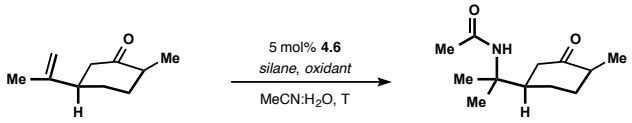

entry	*silane*	*oxidant*	*H_2O (equiv.)*	*T (°C)*	*yield*
1	$PhSiH_3$	**4.7**	trace	0	38%
2	$PhSiH_3$	**4.7**	5.0	0	51%
3	$PhSiHMe_2$	**4.8**	5.0	-30 – (-40)	77%

In order to promote the conversion of the nitrilium ion to the desired *tert*-alkyl acetamide we introduced a superstoichiometric quantity of water into the reaction mixture (Entry 2, Table

4.1). While we saw a considerable increase in yield for the desired product, we also observed vigorous gas evolution upon addition of the silane to the reaction mixture. We proposed that the evolved gas was hydrogen and resulted from compatibility issues between phenylsilane and water. Gratifyingly, the application of dimethyl(phenyl)silane as the reductant limited gas evolution and resulted in a higher yield for the desired product **4.99** (Entry 3, Table 4.1).

Scheme 4.11. Preliminary Substrate Scope for the Radical-polar Crossover Ritter Reaction.

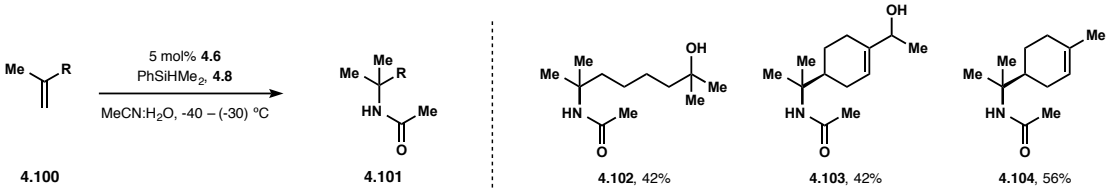

Substrate scope was briefly investigated using the optimized conditions and substrates bearing sensitive functional groups (Scheme 4.11). As such, tertiary alcohol (**4.101**), secondary allylic alcohol (**4.102**), and trisubstituted alkene (**4.103**) functional groups were tolerated and the desired *tert*-alkyl acetamides were obtained in synthetically useful yields. While the method remains largely undeveloped, we believe that the preliminary results in this area display that carbocationic intermediates can be generated under mild reaction conditions. Hopefully, further reaction development will be pursued and disclosed in the future.

4.3 Hydrofunctionalization of Simple Monosubstituted Alkenes via Organocobalt Intermediates

4.3.1 Method Development

In accord with our interest related to generating charged intermediates from neutral radical precursors we pursued basic research focused on the generation of cationic secondary organocobalt(IV) complexes from simple monosubstituted alkenes. We were inspired by preceding research that indicated that cobalt(II) complexes are scavengers of alkyl radicals (**4.111** to **4.112**, Scheme 4.12)[24] and that secondary organocobalt(III) intermediates result from

HAT events.[16e–f] In addition, oxidation of secondary organocobalt(III) complexes deliver cationic alkylcobalt(IV) complexes (**4.112** to **4.113**) that react as electrophiles in the presence of halogen nucleophiles via heterolytic displacement of the carbon–cobalt bond with inversion of stereochemistry (**4.113** to **4.115**).[16a–d]

Scheme 4.12. Hydrofunctionalization via Alkylcobalt Intermediates.

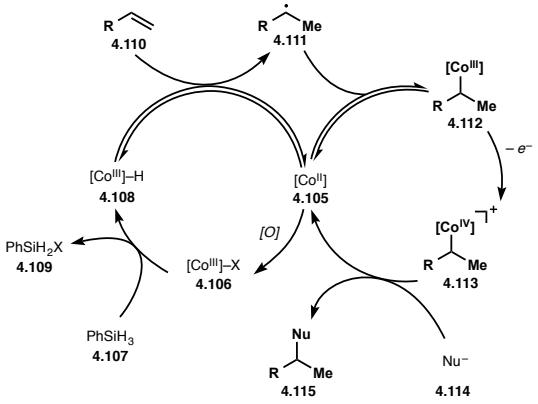

With this in mind, we proposed a catalytic reaction that linked each of these elementary steps (Scheme 4.12). Unlike traditional hydrofunctionalization of simple alkenes initiated by a HAT,[3b] the proposed method would involve the stereospecific displacement of a carbon–cobalt bond in the stereodefining step (**4.113** to **4.115**). We posited that this key departure would offer the opportunity to form enantioenriched products from simple alkenes.

While we were excited by the prospects of the proposed method the carbon–cobalt bond in secondary organocobalt(III) complexes is quite weak (~20 kcal/mol), which represented a potential challenge.[25] Undeterred by this concern, we set out to develop a catalytic reaction as described in Scheme 4.11. We believed that the development of a reaction operating in the proposed manifold would offer a fundamentally new way to access enantioenriched products from simple terminal alkenes.

Table 4.2. Optimization of Hydronitration of Terminal Alkene.

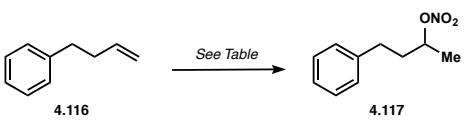

4.116 4.117

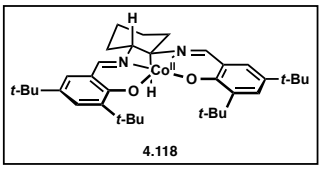

4.118

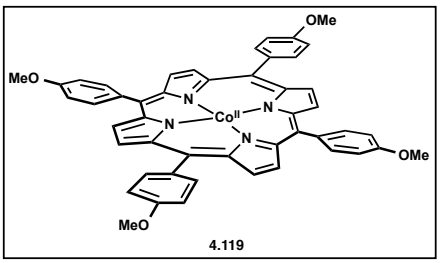

4.119

entry	*solvent*	*silane* (*equiv.*)	*catalyst (mol%)*	*oxidant* (*equiv.*)	*additive* (*equiv.*)	*T* (°C)	*yield*
1	CH_2Cl_2	$PhSiH_3$ (4.0)	**4.118** (2.5%)	CAN (4.4)	$Bu_4N(ONO_2)$ (1.0)	20	52%
2	CH_2Cl_2	$PhSiH_2(Oi\text{-}Pr)$ (4.0)	**4.118** (2.5%)	CAN (4.4)	$Bu_4N(ONO_2)$ (1.0)	-20	42%
3	EtOAc	$PhSiH_2(Oi\text{-}Pr)$ (2.0)	**4.118** (5.0%)	CAN (4.4)	$Bu_4N(ONO_2)$ (1.0)	-20	61%
4	EtOAc	$PhSiH_2(Oi\text{-}Pr)$ (2.0)	**4.118** (5.0%)	CAN (4.4)	$Bu_4N(ONO_2)$ (0.33)	-20	72%
5	EtOAc	$PhSiH_2(Oi\text{-}Pr)$ (2.0)	**4.119** (5.0%)	CAN (4.4)	$Bu_4N(ONO_2)$ (1.0)	-20	46%

As a platform initiate our program in this area we developed a hydronitration reaction using 4-phenyl-1-butene (**4.116**) as a model substrate (Table 4.2). We elected to use a combination of ceric(IV) ammonium nitrate (CAN) as the oxidant and phase-transfer reagent tetrabutylammonium nitrate (TBAN) to limit the amount oxidant in solution, which we believed would decrease background reactivity involving direct oxidation of a carbon-centered radical. In the early phases of reaction development we obtained a moderate yield for the desired nitrate ester **4.117** along with an appreciable amount (*ca.* 30%) of 4-phenylbutan-2-one (**4.124**; Entry 1, Table 4.2). The presence of **4.124** was concerning as it likely meant radical intermediates were present during the course of the reaction. Reducing the reaction temperature eliminated the formation of 4.124, however a slightly lower yield of **4.117** was also observed (Entry 2, Table 4.2). A survey of solvents revealed that polar solvents had a positive influence on the yield. As such, when the reaction was run in ethyl acetate a significant increase in yield was observed (Entry 3, Table 4.2). Final optimization of the loading of phase-transfer reagent indicated that a sub-stoichiometric amount of TBAN gave a slightly higher yield (Entry 4, Table 4.2). We also surveyed a variety of cobalt(II) catalysts, however only porphyrin **4.119** produced nitrate ester **4.114** with a similar level of efficiency (Entry 5, Table 4.2).[26]

Scheme 4.13. Mechanistic Probe: Potential Radical Resulting from HAT.

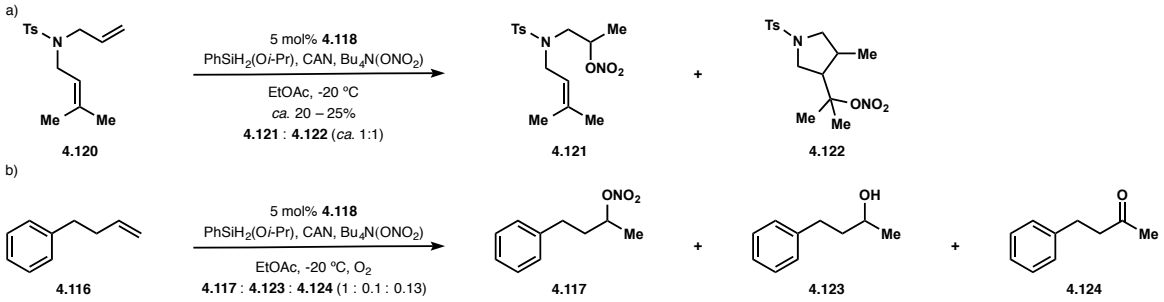

At this stage we were satisfied with the level of efficiency for hydronitration and turned our attention to probing the mechanism of the reaction. We first investigated the lifetime of radical intermediates that could form after HAT (i.e. **4.111**). Following this approach we attempted to affect hydronitration on 1,6-diene **4.120** (Scheme 4.13a). To our delight, we observed about equimolar production of the desired nitrate ester **4.121** and pyrrolidine **4.122**. This indicated that the lifetime of the putative radical intermediate was relatively short since the rate of radical cyclization is on the order of 10^5–10^7.[27] In addition, we observed only a minor amount of Mukaiyama hydration products when the reaction was run under an atmosphere of oxygen (Scheme 4.13b). Taken together these results suggested that the lifetime of the radical formed after HAT was short.

Scheme 4.14. Mechanistic Probe: Formation of Organocobalt(III) via HAT.

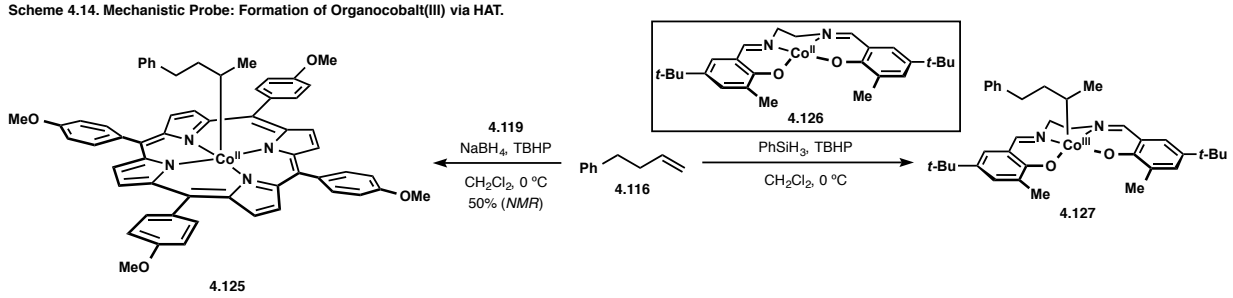

Our studies on the lifetime of the putative radical do not indicate whether the radical rapidly recombines with the cobalt(II) complex or if direct oxidation to a discreet carbocation occurs. In order to determine if secondary organocobalt(III) complexes were viable intermediates, we attempted to observe alkyl cobalt complexes directly from the HAT event.

Inspired by Setsune and co-workers we set out to generate secondary organocobalt(III) complexes from 4-phenyl-1-butene (**4.116**) (Scheme 4.14).[16f] We first validated Setsune's procedure to determine if **4.116** was a viable precursor to secondary organocobalt(III) complexes. Gratifyingly, we observed formation of organocobalt **4.125** in good yield. Emboldened by this result, we attempted formal hydrometallation between cobalt(II) complex **4.126** and **4.116** and observed formation of what we believed to be the desired secondary organocobalt(III) complex **4.127**. We were able to confirm the identity of **4.127** by independent synthesis from 2-bromo-4-phenyl butane (**4.130**; Scheme 4.15).[28,29] Unlike the synthesis of organocobalt(III) **4.125**, the formation of **4.127** via HAT was not efficient and products arising from Mukaiyama hydration (**4.123** and **4.124**) were observed in the crude ^{1}H NMR spectrum. This indicated that homolysis of the relatively weak carbon–cobalt bond likely occurred.[25]

Scheme 4.15. Independent Synthesis of Secondary Organocobalt(III) 4.129.

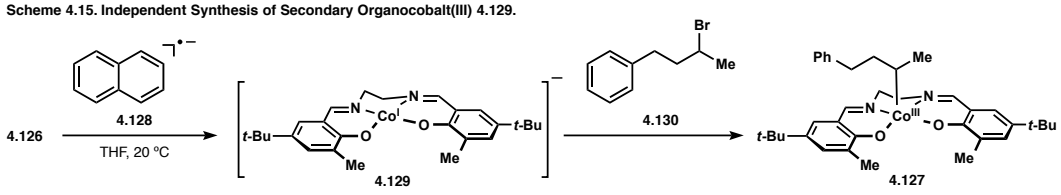

However, the generation of secondary organocobalt(III) complexes from alkene **4.116** via HAT allowed us to probe the oxidation event using a relevant ligand scaffold. Since cobalt(II) porphyrin **4.119** was a competent catalyst for hydronitration (Entry 5, Table 4.2) and secondary organocobalt(III) **4.125** was efficiently formed we decided to pursue oxidative displacement using **4.125**. Following this approach we treated **4.125** with CAN and TBAN and observed conversion to the desired nitrate ester **4.117** (Scheme 4.16a). In order to determine if the reaction proceeded with inversion of stereochemistry, we executed a similar oxidative displacement on enantioenriched secondary organocobalt(III) **4.132** and obtained nitrate ester **4.117** with modest retention of enantioenrichment (Scheme 4.16b).

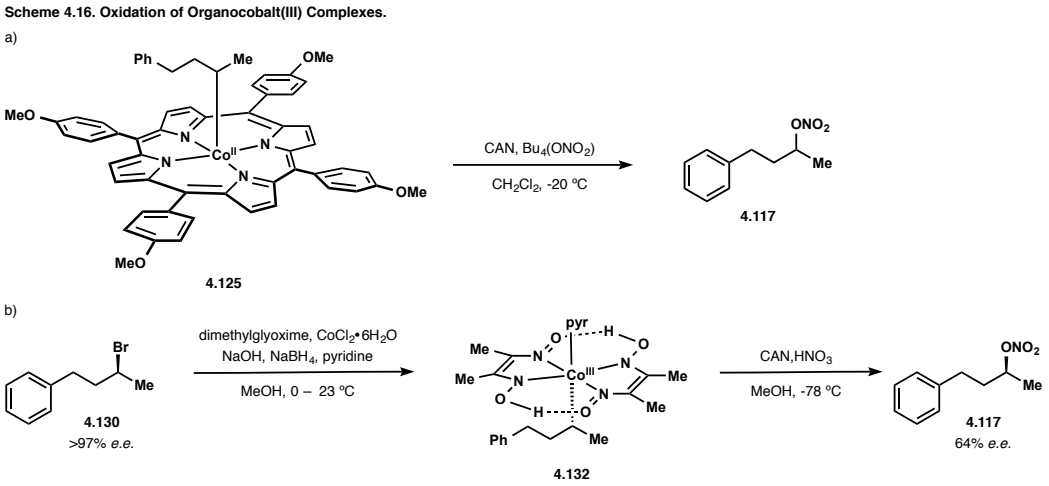

4.3.2 Conclusions and Outlook

The preliminary nature of the results described in Section 4.3.1 require further attention in order to draw any conclusions related to the mechanism of the hydronitration of terminal alkenes. For example, oxidative displacement of secondary organocobalt(III) complex **4.127** would be more relevant to the developed reaction than the results from Scheme 4.15. Finally, the reaction must be pursued using chiral ligand scaffolds to determine if enantioenriched products can be obtained.[30]

4.4 Experimental Section

4.4.1 General Experimental Details

All reactions were carried out in flame- or oven-dried glassware under a positive pressure of dry nitrogen unless otherwise noted. Reaction solvents including diethylether (Et_2O, Fisher, HPLC Grade), tetrahydrofuran (THF, Fisher, HPLC Grade), methylene chloride (CH_2Cl_2, Fisher, HPLC Grade), benzene (PhH, Fisher, HPLC Grade), and toluene (PhMe, Fisher, HPLC Grade) were dried by percolation through a column packed with neutral alumina and a column packed with a supported copper catalyst for scavenging oxygen (Q5) under positive pressure of argon. Anhydrous, 1,2-dichloroethane (Fisher, ACS Grade), *N*,*N*-diisopropylamine (Oakwood

Chemical, triethylamine (Oakwood Chemical), and *N*,*N*-diisopropylethylamine (Oakwood Chemical) were distilled from calcium hydride (~10% w/v) under a positive pressure of nitrogen. Anhydrous ethylene glycol [$(CH_2OH)_2$] was purchased from Sigma–Aldrich. Dimethyl sulfoxide (DMSO, EMD Chemicals) was dried over activated 3 Å molecular sieves (Acros Organics, 20% w/w). Anhydrous hexamethphosphoramide (HMPA, Oakwood Chemical) was distilled from calcium hydride (10% w/v) under vacuum (*ca*. 0.1 torr). Solvents for extraction, thin layer chromatography (TLC) and flash column chromatography were purchased from Fisher (ACS Grade) and VWR (ACS Grade) and used without further purification. Chloroform-d and benzene-d_6 for ^{1}H and ^{13}C NMR analysis were purchased from Cambridge Isotope Laboratories and used without further purification. Commercially available reagents were used without further purification unless otherwise noted. All reactions were monitored by TLC using precoated siliga gel plates (EMD Chemicals, Siliga gel F_{254}). Flash column chromatography was performed over silica gel (Acros Organics, 60 Å, particle size 0.04 – 0.063 mm). ^{1}H NMR and ^{13}C NMR spectra were recorded on Bruker DRX-500 (BBO probe), Bruker DRX-500 (TCI cryoprobe), and Bruker AVANCE600 (TBI probe) spectrometers using residual solvent peaks as internal standards [$CHCl_3$: 7.26 ppm (^{1}H NMR), 77.16 ppm (^{13}C NMR); C_6H_6: 7.16 ppm (^{1}H NMR), 128.00 ppm (^{13}C NMR)]. High-resolution mass spectra (HRMS) were recorded on Waters LCT Premier TOF spectrometer with ESI and CI sources. IR spectra were recorded on a FT-IR spectrometer and are reported in terms of frequency of absorption (cm^{-1}). Enantioenrichment was determined using an Agilent Technologies 1100 Series High-performance Liquid Chromatography system equipped with a Daicel Chemical Industries, Ltd. Chiralcel OD-H (0.46 cm ϕ x 25 cm) column using *n*-hexane and 2-propanol (HPLC grade) as eluting solvents.

4.4.2 Experimental Procedures

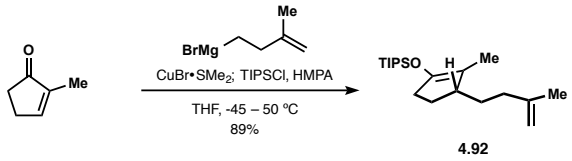

Grignard Preparation: 4-bromo-2-methylbut-1-ene[31] (1.0 g, 7.0 mmol) was added in a single portion to a suspension of magnesium turnings (255. mg, 10.5 mmol) in THF (1.0 mL). Additional THF (4.4 mL) was added over 30 minutes to control the exotherm. The Grignard solution titrated to 0.53 M.

Enoxysilane **4.92**: The freshly prepared Grignard solution (6.5 mL) was added to a suspension of $CuBr•SMe_2$ (71.9 mg, 0.35 mmol) in THF (0.5 mL) at -35 ºC in a dropwise manner over 10 minutes. The resulting solution was vigorously stirred and the temperature was maintained at -35 ºC. After 30 minutes the temperature was cooled to -45 ºC and 2-methyl-cyclopenten-1-one (0.3 mL, 3.0 mmol) was added in a dropwise manner over 10 minutes. After 30 minutes TIPSCl (1.1 mL, 6.0 mmol) was added in a single portion and the reaction mixture was allowed to warm to room temperature. HMPA (2.4 mL, 13.8 mmol) was added and the reaction mixture was further warmed to 50 ºC. After 4 hours the reaction mixture was allowed to cool to room temperature. The reaction was quenched with a 3:1 mixture of saturated aqueous NH_4Cl:NH_4OH (5 mL). The organic layer was diluted with hexanes (10 mL) and washed with a 3:1 mixture of a saturated aqueous NH_4Cl:NH_4OH until no traces of a blue color was observed in the aqueous layer (2x5 mL). The organic layer was washed with brine, dried over anhydrous magnesium sulfate, filtered, and concentrated under reduced pressure. Purification by flash chromatography over silica gel deactivated with 1% Et_3N in hexanes (elution 100% hexanes) afforded 858.2 mg (89%) of enoxysilane **4.92** as a clear, colorless oil. ^1H NMR (600 MHz; C_6H_6): δ 4.84 (s, 1H), 4.82 (s, 1H), 2.41 (dd, J = 3.4, 1.1 Hz, 1H), 2.28 (tddddd, J = 15.8, 11.3, 9.1, 6.8, 4.6, 2.3 Hz, 2H), 2.05

(ddd, J = 14.6, 10.6, 4.3 Hz, 1H), 1.97–1.91 (m, 2H), 1.81–1.75 (m, 1H), 1.68 (s, 3H), 1.66 (d, J = 0.9 Hz, 3H), 1.38 (ddt, J = 12.5, 9.1, 6.2 Hz, 1H), 1.31–1.25 (m, 1H), 1.11 (s, 21H).

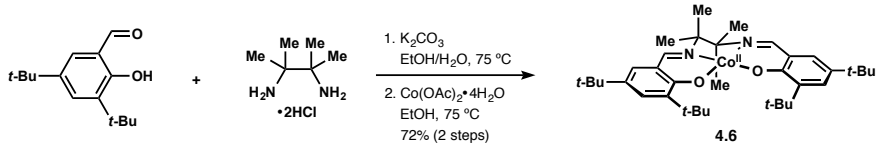

Cobalt(II) complex **4.6**: A 10 mL round bottom flask was charged with 3,5-di-*tert*-butyl salicyaldehyde (234.3 mg, 1.0 mmol), 2,3-dimethyl-2,3-diaminobutane bis(hydrogenchloride) (94.6 mg, 0.5 mmol), ethanol (1.2 mL), and a solution of K_2CO_3 (138.2 mg, 1.0 mmol) in water (0.7 mmol). The resulting solution was heated to 75 ºC for 4 hours. A precipitate formed and was collected by filtration. The collected residue was washed with cold (0 ºC) ethanol (~2 mL). The crude bis-imine was used without further purification. The crude bis-imine was suspended in ethanol (2 mL) and treated with cobalt(II) acetate tetrahydrate (125 mg, 0.5 mmol). The resulting solution was heated to 75 ºC for 2 hours. The mixture was cooled to 0 ºC and **4.6** was collected via filtration to afford 219. mg (72%) of cobalt(II) complex **4.6** as a red solid. LRMS (ESI) $C_{36}H_{54}N_2O_2Co$ $[M]^+$ calculated 605.3518, found 605.6.

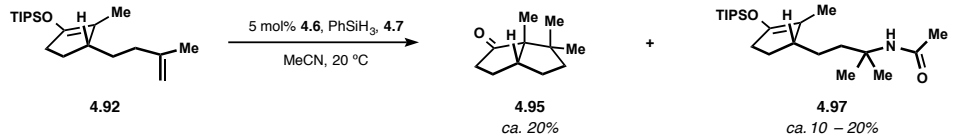

Bicycle **4.95** and *tert*-alkyl amide **4.97**: A Schlenk flask was charged with cobalt(II) complex **4.6** (1.0 mg, 0.0015 mmol) and *N*-fluoro-2,4,6-trimethylpyridinium tetrafluoroborate (15.0 mg, 0.066 mmol). The flask was cooled to -40 ºC and a degassed solution of enoxysilane (9.7 mg, 0.03 mmol) and phenysilane (7.4 μL, 0.06 mmol) in acetonitrile (0.5 mL) was added down the side of the flask. After 2 hours the volatiles were removed under reduced pressure. Purification by flash chromatography (gradient elution: 100% hexanes to 30% v/v ethyl acetate in hexanes) afforded 1.4 mg (*ca.* 20%) of **4.95** and 1.6 (*ca*. 15%) of **4.97** as thin films. Diagnostic ^{1}H NMR

signals for **4.95**: ^{1}H-NMR (500 MHz; $CDCl_3$): δ 1.05 (s, 3H), 1.00 (s, 3H), 0.95 (s, 3H), 0.91 (s, 3H); diagnostic ^{1}H NMR signals for **4.97**: ^{1}H-NMR (500 MHz; $CDCl_3$): δ 5.18 (s, 1H), 1.97 (s, 3H), 1.59 (s, 3H), 1.36 (s, 6H), 1.14 (d, J = 6.1 Hz, 21H); LRMS (CI) $C_{22}H_{43}NO_2Si$ $[M]^+$ calculated 381.3083, found 381.6; $C_{22}H_{44}NO_2Si$ $[M+H]^+$ calculated 382.3141, found 382.6.

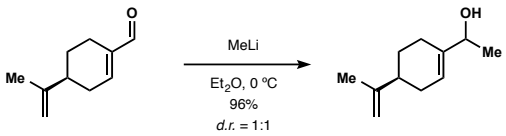

Allylic alcohol: A solution of methyllithium (2.4 mL, 3.9 mmol, 1.6 M in hexanes) was added in a dropwise manner over 10 minutes to a solution of (S)-perilladehyde (590 µL, 3.5 mmol, 92%) in diethyl ether (5.25 mL) at 0 ºC. The resulting mixture was vigorously stirred and the temperature was maintained at 0 ºC. After 2 hours the reaction was quenched with water (7 mL). The organic layer was diluted with diethyl ether (10 mL), washed with brine (5 mL), dried over anhydrous sodium sulfate, filtered, and concentrated under reduced pressure. Purification by flash chromatography (elution: 20% v/v diethyl ether in pentane) afforded 557.4 mg (96%) of a 1:1 mixture of diastereomeric allylic alcohols as a clear, colorless oil. ^{1}H-NMR (500 MHz; $CDCl_3$): δ 5.69 (dd, J = 2.7, 1.9 Hz, 1H), 4.72 (s, 1H), 4.71 (d, J = 2.2 Hz, 1H), 4.23–4.18 (m, 1H), 2.22–2.02 (m, 4H), 1.98–1.90 (m, 1H), 1.89–1.83 (m, 1H), 1.74 (s, 3H), 1.50–1.42 (m, 1H), 1.41–1.37 (m, 1H), 1.26 (apparent dd, J = 6.4, 1.9 Hz, 3H).

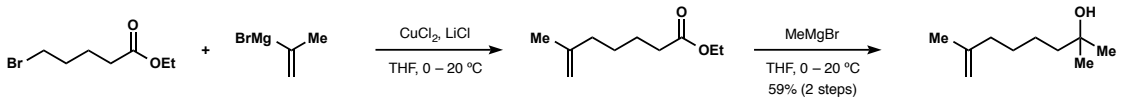

Ester:[32] A round bottom flask was charged with copper(II) chloride (0.1 g, 0.75 mmol) and lithium chloride (63.6 mg, 1.5 mmol). The mixture of solids was gently heated un vacuum to remove trace quantities of water. THF (7.5 mL) was added and formation of a homogeneous orange solution was observed. The mixture was vigorously stirred and cooled to 0 ºC. A solution

of 5-bromo-ethyl valerate (0.8 mL, 5.0 mmol) in THF (18 mL) was charged into the flask. After 30 minutes isopropenyl magnesium bromide (10 mL, 5.5 mmol, 0.56 M in diethyl ether) was added in a dropwise manner over 10 minutes. The reaction mixture was allowed to slowly warm to room temperature. After 14 hours the reaction was quenched with a solution of saturated aqueous NH_4Cl (25 mL). The resulting biphasic mixture was vigorously stirred for 30 minutes. The aqueous layer was extracted with diethyl ether (3x30 mL). The combined organic layers were washed with a solution of saturated aqueous NH_4Cl (25 mL), water (25 mL), and brine (25 mL). The organic layer was dried over anhydrous magnesium sulfate, filtered, and concentrated under reduced pressure. The crude ester was used without further purification.

Tertiary alcohol: A solution of methylmagnesium bromide (3.1 mL, 9.0 mmol, 2.86 M in diethyl ether) was added in a dropwise manner over 30 minutes to a solution of the crude ester in THF (8.2 mL) at 0 ºC. The reaction mixture was vigorously stirred and allowed to slowly warm to room temperature. After 1.5 hours the reaction was quenched with a solution of saturated aqueous NH_4Cl (7 mL). The aqueous layer was diluted with water (7 mL) and extracted with diethyl ether (3x15 mL). The combined organic layers were washed with brine (10 mL), dried over anhydrous magnesium sulfate, filtered, and concentrated under reduced pressure. Purification by flash chromatography (gradient elution: 100% hexanes to 10% ethyl acetate in hexanes) afforded 344.3 mg (59% over 2 steps) of tertiary alcohol as a clear, colorless oil. ^1H NMR (500 MHz; $CDCl_3$): δ 4.69 (t, J = 0.7 Hz, 1H), 4.67 (dd, J = 2.1, 0.9 Hz, 1H), 2.03 (t, J = 7.4 Hz, 2H), 1.71 (s, 3H), 1.50–1.42 (m, 4H), 1.38–1.32 (m, 2H), 1.21 (s, 6H), 1.20 (br s, 1 H).

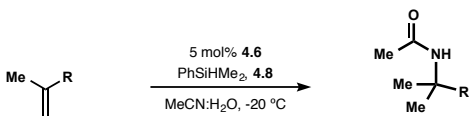

4.100 4.101

General Procedure: An appropriately sized vessel was charged with cobalt(II) complex **4.6** (0.05 equiv.) and acetonitrile (1/5 of total volume, 0.06 M overall), water (5.0 equiv.), substrate (1.0 equiv.), and dimethyl(phenyl)silane (4 equiv.). The resulting solution was vigorously stirred and cooled to ~(-30) ºC. A solution of *N*-fluoro-2,4,6-trimethylpyridinium trifluoromethanesulfonate (1.1 equiv.) in acetonitrile (4/5 of total volume, 0.06 M overall) was added in a slow steady stream. The temperature was maintained bewteen -40 – (-30) ºC. The reaction was monitored by TLC and upon completion the volatiles were removed under reduced pressure. Purification by flash chromatography afforded *tert*-alkyl acetamide products.

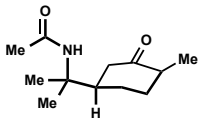

4.99
mixture of isomers

Comments for **4.99**: The reaction was performed on 0.15 mmol scale. 24.3 mg (77%). ^{1}H NMR (600 MHz; $CDCl_3$): δ 5.32 (br s, 1H), 2.53–2.48 (m, 1H), 2.39 (d, *J* = 13.0 Hz, 1H), 2.27 (dt, *J* = 12.7, 6.3 Hz, 1H), 2.08 (td, *J* = 8.9, 4.0 Hz, 2H), 1.90 (s, 4H), 1.44 (qd, *J* = 12.7, 3.1 Hz, 1H), 1.34–1.31 (m, 4H), 1.26 (s, 3H), 0.99 (d, *J* = 6.5 Hz, 3H); ^{13}C NMR (125 MHz; $CDCl_3$): δ 212.6, 169.6, 56.0, 45.8, 44.9, 43.3, 34.3, 26.7, 24.57, 24.54, 24.1, 14.4.

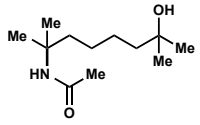

4.102

Comments: The reaction was performed on 0.15 mmol scale. 12.8 mg (42%). ^{1}H NMR (600 MHz; $CDCl_3$): δ 5.20 (br s, 1H), 1.90 (s, 3H), 1.69 (dd, *J* = 10.2, 6.6 Hz, 2H), 1.46 (dd, *J* = 10.9, 5.5 Hz, 2H), 1.34 (dt, *J* = 16.8, 6.8 Hz, 2H), 1.28 (s, 6H), 1.24 (dd, *J* = 10.0, 5.9 Hz, 2H), 1.19 (s, 6H); ^{13}C NMR (125 MHz; $CDCl_3$): δ 169.5, 71.1, 53.8, 44.0, 40.2, 29.4, 27.1, 24.78, 24.76, 24.65.

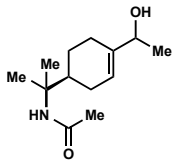

4.103

Comments: The reaction was performed on 0.15 mmol scale. 14.1 mg (42%), 1:1 mixture of diastereomeric allylic alcohols. ^{1}H NMR (600 MHz; $CDCl_3$): δ 5.65 (td, J = 5.7, 2.8 Hz, 1H), 5.23 (br s, 1H), 4.17 (apparent dq, J = 27.2, 6.4 Hz, 1H), 2.26–2.19 (m, 1H), 2.07–2.01 (m, 3H), 1.92 (s, 3H), 1.85–1.77 (m, 2H), 1.50 (br s, 1H), 1.30 (s, 3H), 1.27 (s, 3H), 1.23 (apparent t, J = 6.1 Hz, 3H).

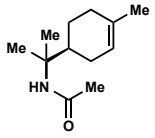

4.104

Comments: The reaction was performed on 0.15 mmol scale. 16.3 mg (56%). ^{1}H NMR (500 MHz; $CDCl_3$): δ 5.35 (br s, 1H), 5.24 (s, 1H), 2.14–2.09 (m, 1H), 2.03–1.95 (m, 3H), 1.91 (s, 3H), 1.75 (tdd, J = 8.7, 3.9, 2.6 Hz, 2H), 1.62 (s, 3H), 1.29 (s, 3H), 1.27 (s, 3H); ^{13}C NMR (125 MHz; $CDCl_3$): δ 169.4, 134.1, 120.5, 56.4, 41.1, 31.2, 26.7, 24.7, 24.29, 24.23, 24.0, 23.4.

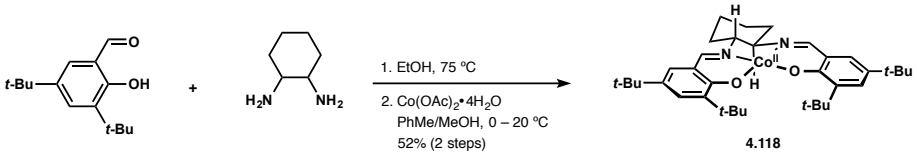

4.118

Cobalt(II) complex **4.118**: A round bottom flask was charged with 3,5-di-*tert*-butyl salicyaldehyde (2.3 g, 10.0 mmol), (±)-*trans*-1,2-diaminocyclohexane (0.6 mL, 5.0 mmol), and ethanol (30 mL). The resulting solution was heated to 75 ºC for 4 hours. A precipitate formed and was collected by filtration. The remaining residue washed with cold (0 ºC) ethanol (~5 mL). The crude bis-imine was used without further purification The intermediate crude bis-imine was dissolved in degassed toluene (40 mL) and treated with a degassed solution of cobalt(II) acetate

tetrahydrate (1.01 g, 4.07 mmol) in methanol (120 mL). The resulting mixture was vigorously stirred for 40 minutes, cooled to 0 ºC, and filtered to afford 2.3 g (52% over two steps) of **4.118** as an orange solid. LRMS (ESI) $C_{36}H_{52}N_2O_2Co$ $[M]^+$ calculated 603.3361, found 603.6.

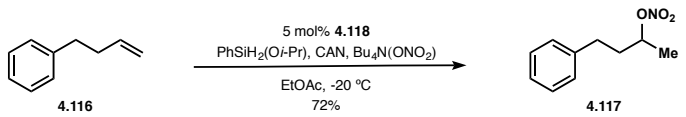

Nitrate ester **4.117**: A round bottom flask was charged with cobalt(II) complex **4.118** (10.9 mg, 0.015 mmol), CAN (723.7 mg, 1.32 mmol), $Bu_4N(ONO_2)$ (30.4 mg, 0.1 mmol), anhydrous ethyl acetate (6 mL), and alkene **4.116** (45 μL, 0.3 mmol). The resulting heterogeneous solution was degassed by sparging with argon gas while submerged in a sonicated bath of water (15 minutes). The reaction mixture was cooled to ~(-20) ºC and vigorously stirred. $PhSiH_2(O\textit{i}\text{-Pr})$ (100 mg, 0.6 mmol) was added in a dropwise manner. After 8.5 hours the reaction was quenched with water (4 mL). The aqueous layer was extracted with methylene chloride (3x10 mL). The combined organics were washed with water (5 mL) and brine (5 mL), dried over anhydrous sodium sulfate, filtered, and concentrated under reduced pressure. Purification by flash chromatography afforded 41.5 mg (72%) of nitrate ester **4.117** as a clear, colorless oil. ^{1}H NMR (500 MHz; $CDCl_3$): δ 7.30 (t, J = 7.5 Hz, 2H), 7.23–7.20 (m, 1H), 7.17 (d, J = 7.1 Hz, 2H), 5.07 (ttd, J = 6.4, 6.3, 6.1 Hz, 1H), 2.79–2.66 (m, 2H), 2.08-2.01 (m, 1H), 1.90 (dddd, J = 14.4, 9.5, 6.7, 5.1 Hz, 1H), 1.39 (d, J = 6.2 Hz, 3H); ^{13}C NMR (125 MHz; $CDCl_3$): δ 140.6, 128.8, 128.4, 126.4, 80.6, 35.8, 31.5, 18.7.

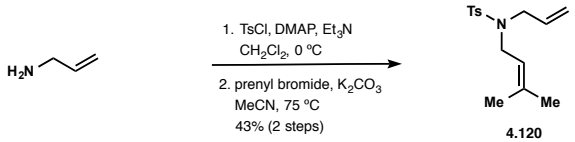

Radical clock **4.120**: *p*-Toluenesulfonyl chloride (2.1 g, 11.0 mmol) was added to a solution of allyl amine (0.75 mL, 10.0 mmol), 4-(dimethylamino)-pyridine (61.1 mg, 0.5 mmol), and

triethylamine (4.2 mL, 30.0 mmol) in methylene chloride (50 mL) at 0 ºC. The reaction mixture was vigorously stirred and the temperature was maintained at 0 ºC. After 45 minutes the reaction was quenched with a solution of saturated aqueous NH_4Cl (50 mL). The aqueous layer was extracted with ethyl acetate (3x50 mL). The combined organic layers were washed with brine (50 mL), dried over anhydrous magnesium sulfate, filtered, and concentrated under reduced pressure. The crude protected allyl amine was used without further purification. ^{1}H-NMR (500 MHz; $CDCl_3$): δ 7.76–7.75 (m, 2H), 7.32 (d, *J* = 8.0 Hz, 2H), 5.73 (ddt, *J* = 17.1, 10.3, 5.9 Hz, 1H), 5.19–5.15 (m, 1H), 5.11 (dq, *J* = 10.2, 1.3 Hz, 1H), 4.35–4.32 (m, 1H), 3.59 (tt, *J* = 6.0, 1.4 Hz, 2H), 2.44 (s, 3H).

Prenyl bromide (1.3 mL, 11.0 mmol) was added to a solution of the crue protected allyl amine and K_2CO_3 (1.5 g, 10.5 mmol) in acetonitrile (25 mL). The reaction mixture was vigorously stirred and heated to 75 ºC. After 19 hours the reaction mixture was cooled to room temperature and filtered through a plug of Celite. The filter cake was thoroughly rinsed with ethyl acetate. The volatile organic material was removed under reduced pressure. Purification by flash chromatography (gradient elution: 100% hexanes to 10% v/v ethyl acetate in hexanes) afforded 1.2 g (43% over 2 steps) of radical clock **4.120** as a clear, colorless oil. ^{1}H NMR (500 MHz; $CDCl_3$): δ 7.69 (dd, *J* = 8.4, 1.9 Hz, 2H), 7.29 (d, *J* = 8.0 Hz, 2H), 5.64 (ddt, *J* = 16.8, 10.5, 6.3 Hz, 1H), 5.15–5.13 (m, 1H), 5.11 (t, *J* = 1.3 Hz, 1H), 4.97 (dddt, *J* = 7.1, 5.7, 2.8, 1.4 Hz, 1H), 3.77 (apparent t, *J* = 6.3 Hz, 4H), 2.42 (s, 3H), 1.65 (d, *J* = 0.8 Hz, 3H), 1.58 (s, 3H); ^{13}C NMR (125 MHz; $CDCl_3$): δ 143.1, 137.8, 137.0, 133.4, 129.7, 127.3, 119.0, 118.5, 49.4, 44.6, 25.9, 21.7, 18.0.

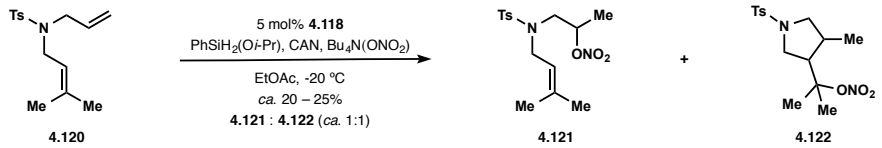

Radical Clock Experiment: A 2-dram vial was charged with cobalt(II) complex **4.118** (3.0 mg, 0.005 mmol), CAN (241.2 mg, 0.44 mmol), $Bu_4N(ONO_2)$ (30.4 mg, 0.1 mmol), anhydrous ethyl acetate (2 mL), and diene **4.120** (27.9 mg, 0.1 mmol). The resulting heterogeneous solution was degassed by sparging with argon gas while submerged in a sonicated bath of water (15 minutes). The reaction mixture was cooled to ~(-20) ºC and vigorously stirred. $PhSiH_2(O\textit{i}\text{-Pr})$ (33 mg, 0.2 mmol) was added in a dropwise manner. After 2 hours the reaction was quenched with water (2 mL). The aqueous layer was extracted with methylene chloride (3x10 mL). The combined organics were washed with water (2 mL) and brine (2 mL), dried over anhydrous sodium sulfate, filtered, and concentrated under reduced pressure. Analysis of the crude ^{1}H NMR revealed that the ratio of **4.121** : **4.122** was *ca.* 1:1.Purification by flash chromatography (gradient elution: 100% hexanes to 15% v/v ethyl acetate in hexanes) afforded two fractions of material: 4.3 mg (~10%) of a mixture of **4.122** (major) and **4.121** (minor); 4.7 mg (~10%) of a mixture of **4.121** (major) and **4.122** (minor). Diagnostic ^{1}H signals for **4.121**: ^{1}H NMR (500 MHz; $CDCl_3$): δ 5.34–5.28 (m, 1H), 4.91 (td, *J* = 7.2, 1.3 Hz, 1H), 3.82 (qd, *J* = 13.6, 7.2 Hz, 2H), 3.29 (dd, *J* = 15.0, 5.1 Hz, 1H), 3.23-3.18 (m, 2H), 1.66 (s, 3H), 1.62 (s, 3H), 1.37 (dd, *J* = 6.4, 1.3 Hz, 3H). Diagnostic ^{1}H signals for **4.122**: ^{1}H-NMR (500 MHz; $CDCl_3$): δ 4.00 (dd, *J* = 13.5, 1.2 Hz, 1H), 3.56 (d, *J* = 13.5 Hz, 1H), 3.28 (d, *J* = 9.1 Hz, 1H), 3.07 (dd, *J* = 9.1, 6.4 Hz, 1H), 2.85 (quintet, *J* = 6.7 Hz, 1H), 1.66 (s, 3H), 1.58 (s, 3H), 1.10 (d, *J* = 7.0 Hz, 3H).

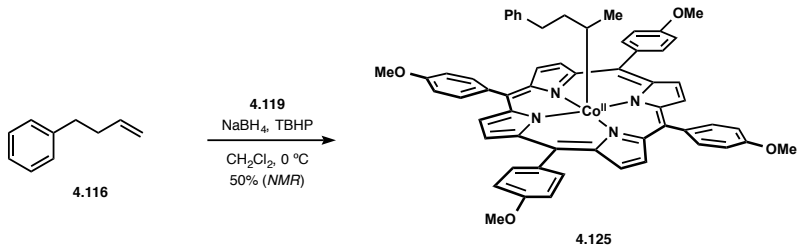

Secondary organocobalt(III) **4.125**: [*NOTE 1: The reaction, workup, and all handling of material was performed in the absence of light*] A round bottom flask was charged with cobalt(II)

tetramethoxyphenylporphryin (7.1 mg, 0.009 mmol), benzene (6 mL), methanol (0.2 mL), 4-phenyl-1-butene **4.116** (45 μL, 0.3 mmol), sodium borohydride (11.3 mg, 0.3 mmol), and *tert*-butyl hydrogen peroxide (66 μL, 0.46 mmol, 5.5 M in *n*-decane). After 1 hour the volatiles were removed under reduced pressure. The yield was determined using mesitylene as an internal standard. Diagnostic ^{1}H NMR signals: ^{1}H NMR (500 MHz; $CDCl_3$): δ -3.32–(-3.39) (m, 1H), -3.54–(-3.62) (m, 1H), -4.99 (d, J = 6.6 Hz, 3H).

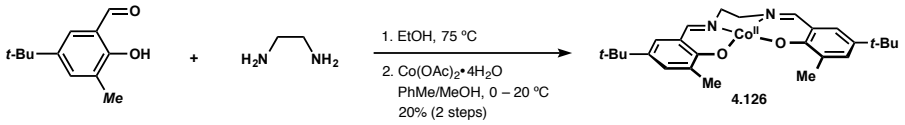

4.126

Cobalt(II) complex **4.126**: A round bottom flask was charged with 3-methyl-5-*tert*-butyl salicyaldehyde[33] (0.95 g, 5.0 mmol), ethylene diamine (0.17 mL, 2.5 mmol), and ethanol (7 mL). The resulting solution was heated to 75 ºC for 1 hours. The resulting precipitate was collected by filtration and washed with cold (0 ºC) ethanol (~5 mL). The resulting crude diimine was dissolved in degassed toluene (18 mL) and treated with a degassed solution of cobalt(II) acetate tetrahydrate (0.46 g, 1.9 mmol) in methanol (56 mL). The resulting mixture was vigorously stirred for 40 minutes, cooled to 0 ºC, and filtered to afford 0.47 g (20% over two steps) of **4.126** as an orange solid. LRMS (ESI) $C_{26}H_{34}N_2O_2Co$ $[M]^+$ calculated 465.1952, found 465.4.

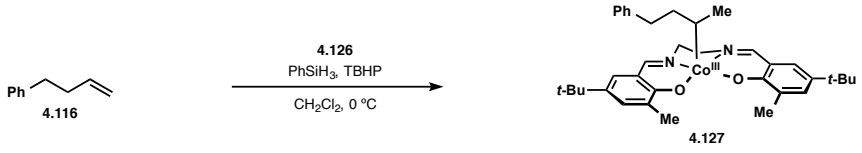

4.127

Secondary organocobalt(III) **4.127**: [*NOTE: The reaction, workup, and all handling of material was performed in the absence of light*] *tert*-butyl hydrogen peroxide (11 μL, 0.06 mmol, 5.5 M in *n*-decane) was added to a solution of cobalt(II) complex **4.126** (4.7 mg, 0.01 mmol), 4-phenyl-1-butene (7.5 μL, 0.05 mmol), and phenylsilane (7.5 μL, 0.06 mmol) in methylene chloride (1.5 mL) at 0 ºC. The reaction mixture mixture was vigorously stirred and the temperature was

maintained at 0 ºC. After 30 minutes all of the volatile material was removed under reduced pressure. Diagnostic ^{1}H NMR signals: ^{1}H-NMR (500 MHz; $CDCl_3$): δ 3.99 (m, 1H), 3.85 (br s, 2H), 3.68 (br s, 2H), -0.37 (d, J = 6.4 Hz, 3H).

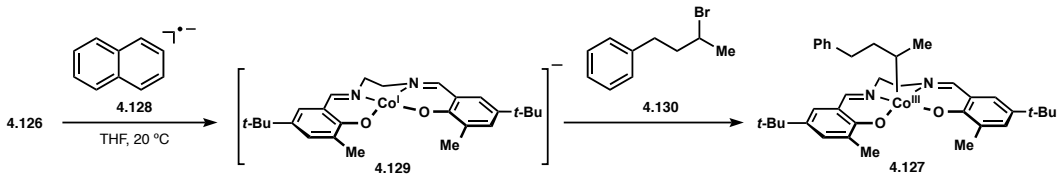

Secondary organocobalt(III) **4.127**: [*NOTE 1: The reaction, workup, and all handling of material was performed in the absence of light*] [*NOTE 2: THF was obtained from a reservoir that was distilled from sodium benzophenone ketyl radical]* Sodium naphthalenide [90 μL, 0.03 mmol, 0.34 M in THF (freshly prepared from a slight excess of Na^0 metal and naphthalene in THF)] was added to a solution of cobalt(II) complex **4.126** (11.6 mg, 0.025 mmol) in THF (1.0 mL). The reaction mixture was vigorously stirred and a persistent dark green solution formed. After 5 minutes 2-bromo-4-phenyl butane[34] (26 mg, 0.125 mmol, degassed by freeze-pump-thaw technique) was added in a dropwise manner. The color immediately changes to red/orange and the volatiles are removed after 30 minutes. Diagnostic ^{1}H NMR signals: ^{1}H-NMR (500 MHz; $CDCl_3$): δ 3.83 (br s, 2H), 3.64 (br s, 2H), -0.40 (d, J = 6.4 Hz, 3H).

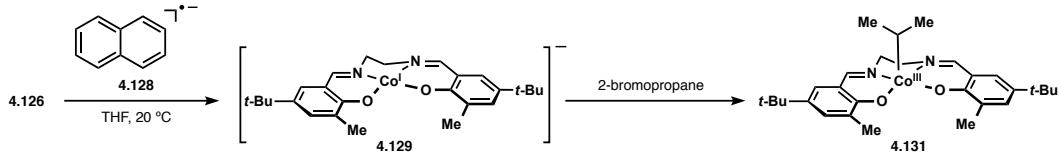

Secondary organocobalt(III) **4.131**: [*NOTE 1: The reaction, workup, and all handling of material was performed in the absence of light*] [*NOTE 2: THF was obtained from a reservoir that was distilled from sodium benzophenone ketyl radical]* Sodium naphthalenide [0.17, 0.058 mmol, 0.34 M in THF (freshly prepared from a slight excess of Na^0 metal and naphthalene in THF)] was added to a solution of cobalt(II) complex **4.126** (23.3 mg, 0.05 mmol) in THF (1.5 mL). The

reaction mixture was vigorously stirred and a persistent dark green solution formed. After 5 minutes 2-bromopropane (50 μL, 0.5 mmol, degassed by freeze-pump-thaw technique) was added in a dropwise manner. The color immediately changes to red/orange and the volatiles are removed after 5 minutes. ^{1}H NMR (500 MHz; $CDCl_3$): δ 7.85 (br s, 2H), 7.22 (br s, 2H), 6.82 (br s, 2H), 4.17 (m, J = 5.6 Hz, 1H), 3.83 (br s, 2H), 3.67 (br s, 2H), 2.43 (s, 6H), 1.24 (s, 18H), -0.29 (d, J = 5.9 Hz, 6H); LRMS (ESI) $C_{29}H_{41}N_2O_2Co$ $[M]^+$ calculated 508.2500, found 508.1.

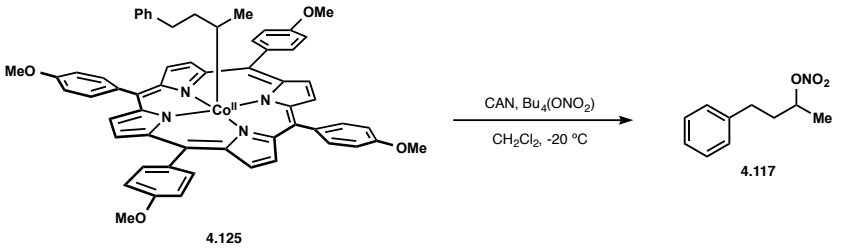

4.125 4.117

Nitrate ester **4.117**: [*NOTE: The reaction, workup, and all handling of material was performed in the absence of light*] A round bottom flask was charged with cobalt(II) tetramethoxyphenylporphryin (7.9 mg, 0.01 mmol), benzene (2 mL), methanol (070 μL), 4-phenyl-1-butene **4.116** (15 μL, 0.1 mmol), sodium borohydride (3.8 mg, 0.1 mmol), and *tert*-butyl hydrogen peroxide (22 μL, 0.12 mmol, 5.5 M in *n*-decane). After 1 hour the volatiles were removed under reduced pressure. Diagnostic ^{1}H NMR signals: ^{1}H NMR (500 MHz; $CDCl_3$): δ -3.48–(-3.51) (m, 1H), -3.69–(-3.73) (m, 1H), -5.11 (d, J = 6.3 Hz, 3H).

The crude residue was dissolved in methylene chloride (1.5 mL), sparged with argon (~10 minutes), and cooled to ~(-20) ºC. CAN (6.0 mg, 0.011 mmol) and $Bu_4N(ONO_2)$ (1.0 mg, 0.003 mmol) were charged into the flask. After 2 hours the reaction was quenched with water and extracted with methylene chloride. The combined organic layers were washed with brine, dried over anhydrous magnesium sulfate filtered, and concentrated. Analysis of the crude ^{1}H NMR confirmed the formation of **4.117**. Diagnostic ^{1}H NMR signal: ^{1}H NMR (600 MHz; $CDCl_3$): δ 1.39 (d, J = 6.2 Hz, 3H).

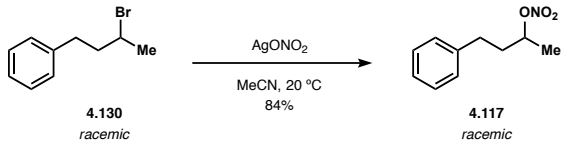

4.130
racemic

4.117
racemic

Nitrate **4.117**:[35] [*NOTE: Reaction was run in the dark*] A Schlenk flask as charged with silver(I) nitrate (51.0 mg, 0.3 mmol), acetonitrile (0.5 mL), and 2-bromo-4-phenyl butane (34 μL, 0.2 mmol). The reaction was vigorously stirred at room temperature. After 21 hours the reaction was diluted with diethyl ether and filtered through a plug of Celite. The volatile organic material was removed under reduced pressure. Purification through a plug of silica gel delivered 32.6 mg (84%) of nitrate **4.117** as a clear, colorless oil. All analytical data are in agreement with our previous studies. (*R*)- and (*S*)-**4.117** were resolved by HPLC using an OD-H Chiracel column (0.1% 2-propanol in *n*-hexane, 1 mL/min).

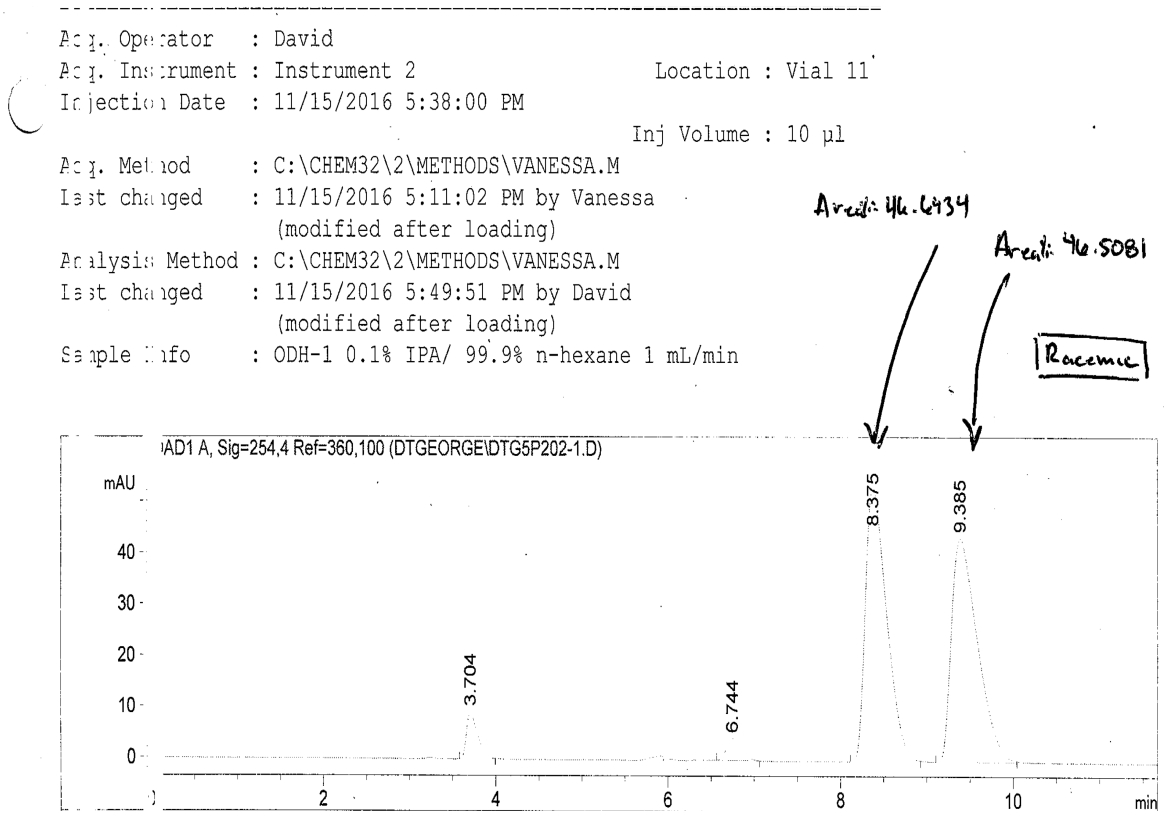

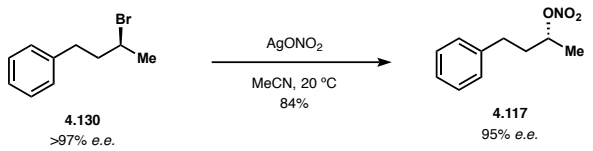

4.130
>97% *e.e.*

4.117
95% *e.e.*

R)-nitrate **4.117**:[35] [*NOTE: Reaction was run in the dark*] A Schlenk flask as charged with silver(I) nitrate (39.7 mg, 0.23 mmol), acetonitrile (0.4 mL), and (*S*)-2-bromo-4-phenyl butane[34] (33.2 mg, 0.16 mmol). The reaction was vigorously stirred at room temperature. After 21 hours the reaction was diluted with diethyl ether and filtered through a plug of Celite. The volatile organic material was removed under reduced pressure. Purification through a plug of silica gel delivered 25.8 mg (83%) of nitrate **4.117** as a clear, colorless oil. All analytical data are in agreement with our previous studies. (*R*)- and (*S*)-**4.117** were resolved by HPLC using an OD-H Chiracel column (0.1% 2-propanol in *n*-hexane, 1 mL/min). The *e.e.* was determined to be 95%.

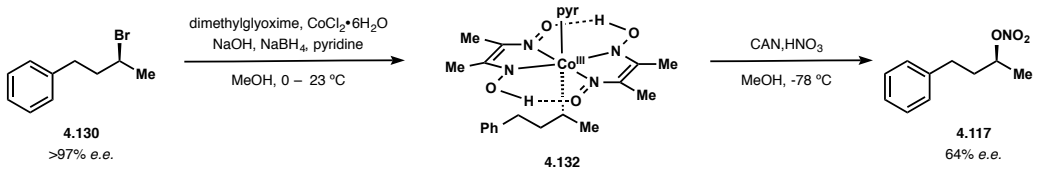

(*S*)-nitrate **4.117**: [*NOTE: The reaction, workup, and all handling of material was performed in the absence of light*] A Schlenk flask was charged with degassed methanol (3.5 mL) and $CoCl_2$•$6H_2O$ (119.0 mg, 0.5 mmol). The resulting mixture was vigorously stirred until homogeneity was observed (~10 minutes). Dimethylglyoxime (116.1 mg, 1.0 mmol) added. After 10 minutes pyridine (40 μL, 0.5 mmol) and an aqueous solution of NaOH (1.0 mL, 1.0 mmol, 1.07 M) were added. After an additional 15 minutes the mixture was cooled to 0 ºC and an aqueous solution of NaOH (0.4 mL, 0.5 mmol, 1.07 M) and sodium borohydride (37.8 mg, 1.0 mmol) was added. A dark solution immediately forms, which is indicative of anionic $Co^{I}(dmg)_2$. After an additional 5 minutes (*S*)-2-bromo-4-phenyl butane[34] (86 μL, 0.5 mmol) was added dropwise. The reaction mixture was vigorously stirred and allowed to warm to room temperature. After 4 hours the reaction was quenched with water (4.5 mL). The aqueous layer was extracted with methylene chloride (3x7 mL). The combined organic layers were dried over anhydrous sodium sulfate, filtered, and concentrated under reduced pressure. Secondary organocobalt(III) **4.132** was recrystallized from MeOH. ^{1}H NMR for **4.132**: ^{1}H-NMR (500 MHz; $CDCl_3$): δ 8.63 (s, 1H), 8.62 (s, 1H), 7.74–7.71 (m, 1H), 7.28 (dd, *J* = 13.8, 6.3 Hz, 2H), 7.18–7.16 (m, 2H), 2.75 (ddd, *J* = 13.5, 8.0, 4.7 Hz, 1H), 2.58–2.52 (m, 1H), 2.13 (s, 6H), 2.10 (s, 6H), 2.03-1.97 (m, 1H), 1.75–1.71 (m, 1H), 1.29–1.22 (m, 1H), 0.55 (d, *J* = 6.8 Hz, 3H).

CAN (27.4 mg, 0.05 mmol) was added to a degassed solution of secondary organocobalt(III) **4.132** (20 mg, 0.05 mmol) and nitric acid (40 μL, 0.04 mmol, 1 M aqueous solution) in methanol (0.4 mL) at -78 ºC. The reaction mixture was vigorously stirred and slowly allowed to warm to

room temperature. After 4 hours the reaction was quenched with a solution of aqueous 1 N HCl. The aqueous layer was extracted with diethyl ether (3x7 mL). The combined organic layers were washed with a solution of 1 N HCl (1 mL) and brine (1 mL), dried over anhydrous magnesium sulfate, filtered, and concentrated under reduced pressure. Purification by flash chromatography afforded nitrate **4.117** as a thin film. (*R*)- and (*S*)-**4.117** were resolved by HPLC using an OD-H Chiracel column (0.1% 2-propanol in *n*-hexane, 1 mL/min). The *e.e.* was determined to be 64%.

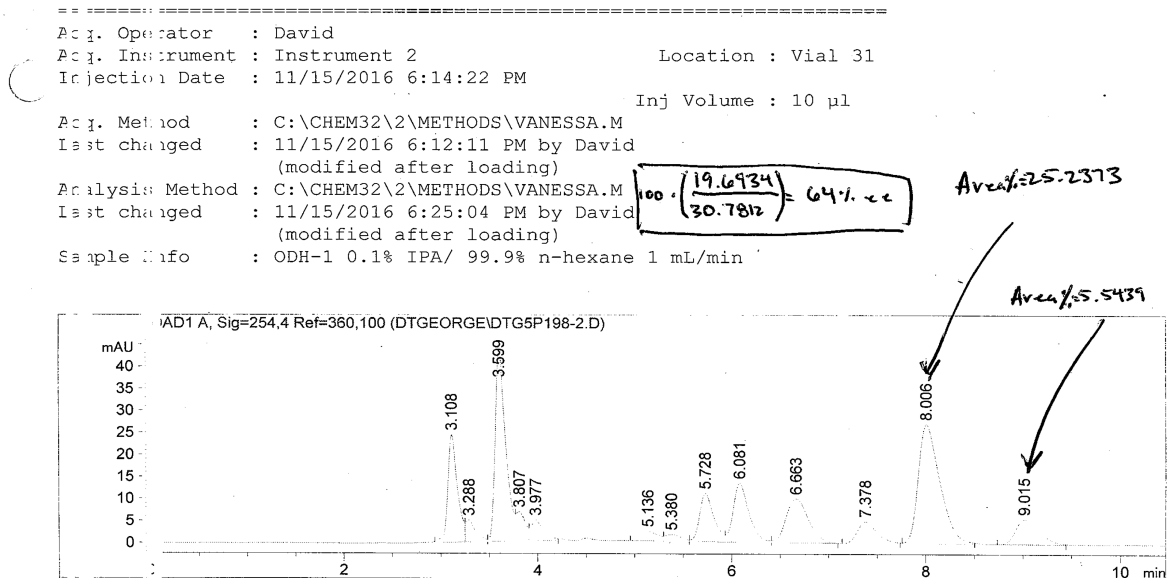

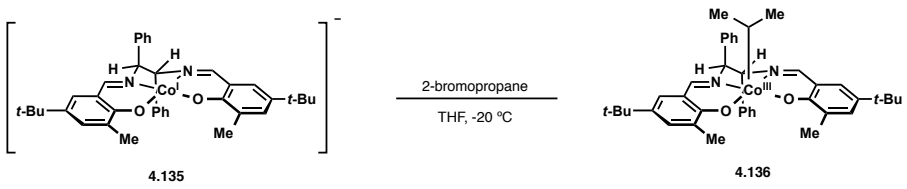

Secondary organocobalt(III) **4.136**: [*NOTE 1: The reaction, workup, and all handling of material was performed in the absence of light*] [*NOTE 2: THF was obtained from a reservoir that was distilled from sodium benzophenone ketyl radical]* Sodium naphthalenide [35 µL 0.015 mmol, 0.34 M in THF (freshly prepared from a slight excess of Na^0 metal and naphthalene in THF)] was added to a solution of cobalt(II) complex (6.2 mg, 0.01 mmol) in THF (0.4 mL). The reaction mixture was vigorously stirred and a persistent dark green solution formed. After 5

minutes 2-bromopropane (5 μL, 0.03 mmol, degassed by freeze-pump-thaw technique) was added in a dropwise manner. The color immediately changes to red/orange and the volatiles are removed after 5 minutes. Diagnostic ^{1}H NMR signals: ^{1}H NMR (500 MHz; DMSO-d_6): δ 5.29–5.26 (m, 1H), 4.93 (d, J = 10.4 Hz, 1H), 4.10–4.04 (m, 1H), 0.12 (dd, J = 13.2, 6.3 Hz, 6H). LRMS (ESI) $C_{41}H_{49}N_2O_2Co$ $[M]^+$ calculated 660.3126, found 660.2.

4.5 References and Notes

[1] (a) Turbek, C. S.; Smith, D. A.; Schardl, C. L. *FEMS Microbiol. Lett.* **1992**, *94*, 187. (b) Hoshino, T.; Sato, T. *Chem. Commun.* **2002**, 291 and references therein. (c) Bevers, L. E.; Pinkse, M. W. H.; Herhaert, P. D. E. M.; Hagen, W. R. *J. Bacteriol.* **2009**, *191*, 5010.
[2] Reed, C. A. *Chem. Commun.* **2005**, 1669
[3] (a) Inoki, S.; Kato, K.; Takai, T.; Ishiyama, S.; Yamada, T.; Mukaiyama, T. *Chem. Lett.* **1989**, 515. (b) Crossley, S. W. M.; Obradors, C.; Martinez, R. M.; Shenvi, R. A. *Chem. Rev.* **2016**, *116*, 8912 and references therein.
[4] Anslyn E. V.; Dougherty, D. A. In *Modern Physical Organic Chemistry*; University Science Books: United States of America, 2006, pp. 403–406.
[5] Fu, Y.; Liu, L.; Yu, H.-Z.; Wang, Y.-M.; Guo, Q.-X. *J. Am. Chem. Soc.* **2005**, *127*, 7227.
[6] (a) Kochi, J. K. *J. Am. Chem. Soc.* **1963**, *85*, 1958. (b) Kochi, J. K.; Subramanian, R. V. *J. Am. Chem. Soc.* **1965**, *87*, 4855. (c) Kochi, J. K.; Bemis, A. *J. Am. Chem. Soc.* **1968**, *90*, 4038. (d) Kochi, J. K.; Bemis, A.; Jenkins, C. L. *J. Am. Chem. Soc.* **1968**, *90*, 4616. (e) Lande, S. S.; Kochi, J. K. *J. Am. Chem. Soc.* **1968**, *90*, 5196. (f) Wong, C. L.; Kochi, J. K. *J. Am. Chem. Soc.* **1979**, *101*, 5593. (g) Rollick, K. L.; Kochi, J. K.; *J. Am. Chem. Soc.* **1982**, *104*, 1319. (h) Grodkowski, J.; Neta, P.; Schlesener, C. J.; Kochi, J. K. *J. Phys. Chen.* **1985**, *89*, 4374.
[7] Kapturkiewicz, A.; Behr, B. *Inorg. Chim. Acta* **1983**, *69*, 247.
[8] Shigehisa, H.; Aoki, T.; Yamaguchi, S.; Shimizu, N.; Hiroya, K. *J. Am. Chem. Soc.* **2013**, *135*, 10306.
[9] Ding, K.; Dugan, T. R.; Brennessel, W. W.; Bill, E.; Holland, P. L. *Organometallics* **2009**, *28*, 6650.
[10] (a) Gaspar, B.; Carreira, E. M. *Angew. Chem. Int. Ed.* **2007**, *46*, 4519. (b) Gaspar, B.; Carreira, E. M. *Angew. Chem. Int. Ed.* **2008**, *47*, 5758. (c) Gaspar, B.; Carreira, E. M. *J. Am. Chem. Soc.* **2009**, *131*, 13214. (d) Firijavallabhan, V.; Alvarez, C.; Njoroge, F. G. *J. Org. Chem.* **2011**, *76*, 6442.
[11] Shigehisa, H.; Kikuchi, H.; Hiroya, K. *Chem. Pharm. Bull.* **2016**, *64*, 371.
[12] Shigehisa, H.; Koseki, N.; Shimizu, N.; Fujisawa, M.; Niitsu, M.; Hiroya, K. *J. Am. Chem. Soc.* **2014**, *136*, 13534.
[13] Shigehisa, H.; Hayashi, M.; Ohkawa, H.; Suzuki, T.; Okayasu, H.; Mukai, M.; Yamazaki, A.; Kawai, R.; Kikuchi, H.; Satoh, Y.; Fukuyama, A.; Hiroya, K. *J. Am. Chem. Soc.* **2016**, *138*, 10597.
[14] Crossley, S. W. M.; Barabé, F.; Shenvi, R. A. *J. Am. Chem. Soc.* **2014**, *136*, 16788.
[15] Nagata, T.; Yorozu, K.; Yamada, T.; Mukaiyama, T. *Angew. Chem. Int. Ed.* **1995**, *34*, 2145.

[16] (A) Anderson, S. N.; Ballard, D. H.; Chrzastowski, J. Z.; Dodd, D.; Johnson, M. D. *J. Chem. Soc. Chem. Commun.* **1972**, 687. (b) Levitin, I.; Sigan, A. L.; Vol'pin, M. E. *J. Chem. Soc. Chem. Commun.* **1975**, 469. (c) Magnuson, R. H.; Halpern, J.; Levitin, I. Y.; Vol'pin, M. E. *J. Chem. Soc. Chem. Commun.* **1978**, 44. (c) Halpern, J.; Chan, M. S.; Roche, T. S.; Tom, G. M. *Acta Chem. Scand.* **1979**, *33A*, 141. (d) Vol'pin, M. E.; Levitin, I. Y.; Sigan, A. L.; Halpern, J.; Tom, G. M. *Inorg. Chim. Acta* **1980**, *41*, 271. (e) Okamoto, T.; Oka, S. *J. Org. Chem.* **1984**, *49*, 1589. (f) Setsune, J.-i.; Ishimaru, Y.; Moriyama, T.; Kitao, T. *J. Chem. Soc. Chem. Commun.* **1991**, 555. (g) Gridnev, A. A.; Ittel, S. D.; Wayland, B. B.; Fryd, M. *Organometallics* **1996**, *15*, 5116.

[17] George, D. T.; Kuenstner, E. J.; Pronin, S. V. *J. Am. Chem. Soc.* **2015**, *137*, 15410.

[18] Yoder, R. A.; Johnston, J. N. *Chem. Rev.* **2005**, *105*, 4730 and references therein.

[19] (a) Abe, I.; Rohmer, M.; Prestwich, G. D. *Chem. Rev.* **1993**, *93*, 2189 and references therein. (b) Wendt, K. U.; Schulz, G. E.; Corey, E. J.; Liu, D. R. *Angew. Chem. Int. Ed.* **2000**, *39*, 2812 and references therein.

[20] Iwasaki, K.; Wan, K. K.; Oppedisano, A.; Crossley, S. W. M.; Shenvi, R. A. *J. Am. Chem. Soc.* **2014**, *136*, 1300.

[21] Shigehisa, H.; Nishi, E.; Fujisawa, Hiroya, K. *Org. Lett.* **2013**, *15*, 5158.

[22] The reaction was performed in a flame dried vessel under anhydrous nitrogen using anhydrous solvent.

[23] (a) Ritter, J. J.; Manieri, P. P. *J. Am. Chem. Soc.* **1948**, *70*, 4045. (b) Ritter, J. J.; Kalish, J. *J. Am. Chem. Soc.* **1948**, *70*, 4048.

[24] Samsel, E. G.; Kochi, J. K. *J. Am. Chem. Soc.* **1986**, *108*, 4790.

[25] Simões, J. A. M.; Beauchamp, J. L. *Chem. Rev.* **1990**, *90*, 629 and references therein.

[26] For a list of all complexes investigated, see Appendix B.

[27] (a) Newcomb, M. *Tetrahedron* **1993**, *49*, 1151 and references therein. (b) Newcomb, M.; Filipkowski, M. A.; Johnson, C. C. *Tetrahedron Lett.* **1995**, *36*, 3643. (c) Newcomb, M.; Choi, S. Y.; Horner, J. H. *J. Org. Chem.* **1999**, *64*, 1225.

[28] Schrauzer, G. N.; Deutsch, E. *J. Am. Chem. Soc.* **1969**, *91*, 3341.

[29] The identification of **4.124** is tentative due to the lack of characterization data. However, isopropyl variant **4.129** of **4.124** was prepared in relatively high purity, which provided valuable ^{1}H NMR information.

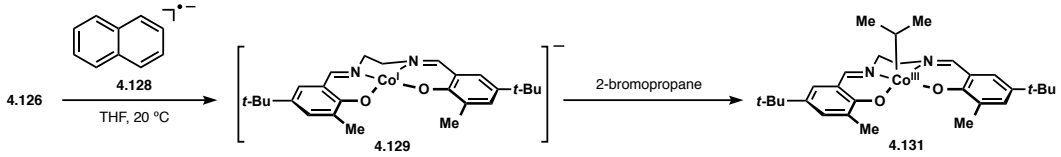

[30] The extent of our work with chiral ligand scaffolds revealed that secondary organocobalt(III) complexes were observable species, but further studies are required (Scheme 4.16).

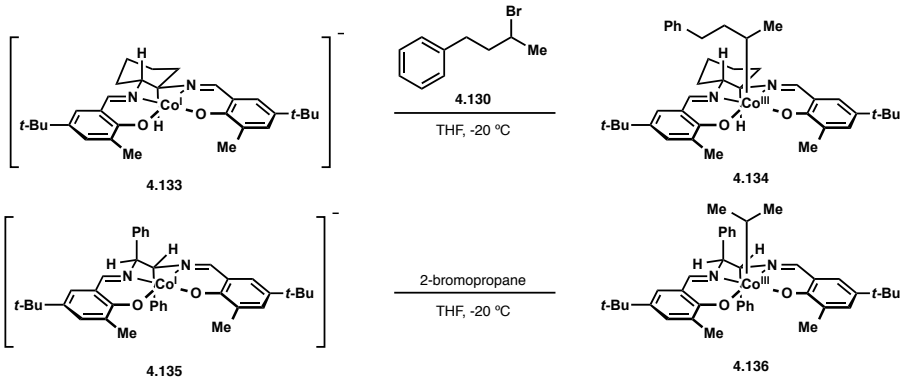

[31] Leach, A. G.; Wang, R.; Wohlhieter, G. E.; Khan, S. I.; Jung, M. E.; Houk, K. N. *J. Am. Chem. Soc.* **2003**, *125*, 4271.
[32] Poth, D.; Wollenberg, K. C.; Vences, M.; Schulz, S. *Angew. Chem. Int. Ed.* **2012**, *51*, 2187.
[33] (a) Damm, W.; Giese, B.; Hartung, J.; Hasskerl, T.; Houk, K. N.; Hüter, O.; Zipse, H. *J. Am. Chem. Soc.* **1992**, *114*, 4067. (b) Rudzevich, V.; Schollmeyer, D.; Braekers, D.; Desreux, J. F.; Diss, R.; Wipff, G.; Böhmer, V. *J. Org. Chem.* **2005**, *70*, 6027.
[34] Denmark, S. E.; Cresswell, A. J. *J. Org. Chem.* **2013**, *78*, 12593.
[35] Kornblum, N.; Hardies, D. E. *J. Am. Chem. Soc.* **1966**, *88*, 1707.

Appendix A: Optimization Efforts for the Conversion of 2.18 to 2.13

entry	*pre-catalyst*	*silane*	*solvent*	*temperature* (°C)	*d.r. (**2.13** : **2.68**)*	*additional comments*
1	$Fe(acac)_3$	$PhSiH_3$	EtOH	50	1:1.5	–
2	$Co(acac)_2$	$PhSiH_3$	EtOH	50	–	formed **2.81**
3	$Co(Cy^{t\text{-}Bu,t\text{-}Bu}Salen)Cl$	$PhSiH_3$	EtOH	50	1:1.5	**–**
4	$Mn(Cy^{t\text{-}Bu,t\text{-}Bu}Salen)Cl$	$PhSiH_3$	EtOH	50	–	formed **2.81**
5	$Mn(Cy^{t\text{-}Bu,t\text{-}Bu}Salen)Cl$	$PhSiH_3$	PhH	50	–	N/R
6	$Co(Cy^{t\text{-}Bu,t\text{-}Bu}Salen)Cl$	$PhSiH_3$	PhH	50	–	hydrogenation of α,β-unsaturation
7	$Co(Cy^{t\text{-}Bu,t\text{-}Bu}Salen)Cl$	$PhSiH_3$	*tert*-BuOH	30	1:1	–
8	$Co(Cy^{t\text{-}Bu,t\text{-}Bu}Salen)Cl$	$PhSiH_3$	CF_3CH_2OH	50	1:1	–
9	$Co(Cy^{t\text{-}Bu,t\text{-}Bu}Salen)Cl$	$PhSiH_3$	EtOH	20	1:1.5	–
10	$Fe(acac)_3$	$PhSiH_3$	CF_3CH_2OH	50	–	N/R
11	$Fe(acac)_3$	$PhSiH_3$	Acetone	50	1:1	Reaction proceeds after addition of 10% v/v ethanol
12	$Fe(acac)_3$	$PhSiH_3$	DMF	50	1:1	Reaction proceeds after addition of 10% v/v ethanol
13	$Fe(acac)_3$	$PhSiH_3$	*tert*-BuOH	50	1:1	–
14	$Fe(acac)_3$	$PhSiH_3$	EtOAc/EtOH (10:1)	50	1:1	–
15	$Fe(acac)_3$	$PhSiH_3$	PhH/EtOH (10:1)	50	1:1	–
16	$Fe(acac)_3$	$PhSiH_3$	$PhCF_3$/EtOH (10:1)	50	1:1	–
17	$Fe(acac)_3$	$PhSiH_3$	CH_2Cl_2/EtOH (10:1)	50	1:1	–
18	$Fe(acac)_3$	$PhSiH_3$	MeCN/EtOH (10:1)	50	1:1	–
19	$Fe(acac)_3$	$PhSiH_3$	*i*-PrOH	50	1:1	–
20	$Fe(acac)_3$	$PhSiH_3$	Acetone/EtOH (10:1)	50	1:1	–
21	$Fe_2(ox)_3 \bullet 6H_2O$	$PhSiH_3$	EtOH	50	1.8:1	–
22	$FeCl_3$	$PhSiH_3$	EtOH	50	–	N/R
23	$Fe_2(ox)_3 \bullet 6H_2O$	$PhSiH_3$	DMF/H_2O (1:1)	50	1:1	–
24	$Fe_2(ox)_3 \bullet 6H_2O$	$PhSiH_3$	Acetone/H_2O (1:1)	50	3:1	–
25	$Fe_2(ox)_3 \bullet 6H_2O$	$PhSiH_3$	MeCN/H_2O (1:1)	50	3:1	–
26	$Fe_2(ox)_3 \bullet 6H_2O$	$PhSiH_3$	Acetone/H_2O (10:1)	30	1:1	–
27	$Fe_2(ox)_3 \bullet 6H_2O$	$PhSiH_3$	Acetone/H_2O (10:1)	30	1:1	–
28	$Fe(acac)_3$	Ph_2SiH_2	Acetone/EtOH (10:1)	30	–	N/R
29	$Fe(acac)_3$	$Si(OEt)_3H$	Acetone/EtOH (10:1)	30	–	N/R
30	$Fe(acac)_3$	$MeSi(OEt)_2H$	Acetone/EtOH (10:1)	30	–	N/R
31	$Fe(acac)_3$	$PhSiH_3$	EtOH	20	–	CsF added; aldehyde reduction observed
32	$Fe(acac)_3$	**A**	EtOH	20	–	Aldehyde reduciton observed
33	$Fe(dibm)_3$	$PhSiH_3$	EtOH	50	1:1	–
34	$Fe(acac)_3$	**B**	EtOH	20	–	Aldehyde reduciton observed
35	$Fe(acac)_3$	**B**	DMF	20	–	Aldehyde reduciton observed
36	$Fe(acac)_3$	**B**	CH_2Cl_2	20	–	Aldehyde reduciton observed
37	$Fe(acac)_3$	**B**	PhH	20	–	Aldehyde reduciton observed
38	$Fe(acac)_3$	$PhSiH_2(O\textit{i}\text{-Pr})$	$(CH_2Cl)_2$/$(CH_2OH)_2$	0	1:1	–

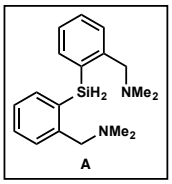

A

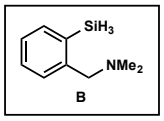

B

Appendix B: Qualitative Assessment of Various Cobalt(II) Catalysts

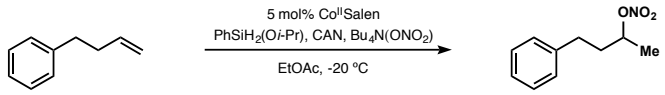

Forms desired product?

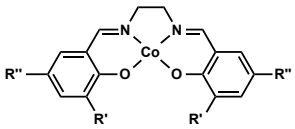

R'	R''	product?
Me	*tert*-Bu	yes

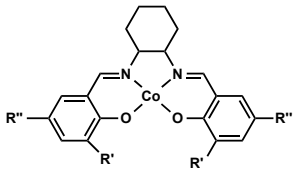

R'	R''	product?
tert-Bu	*tert*-Bu	yes
H	H	no
H	*tert*-Bu	no
H	OMe	no
Me	*tert*-Bu	yes

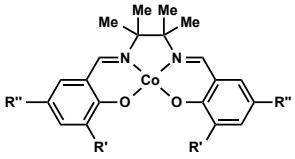

R'	R''	product?
tert-Bu	*tert*-Bu	yes

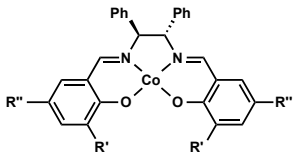

R'	R''	product?
Me	*tert*-Bu	yes

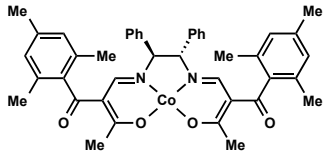

no

Appendix C: Chapter 2 NMR Spectra

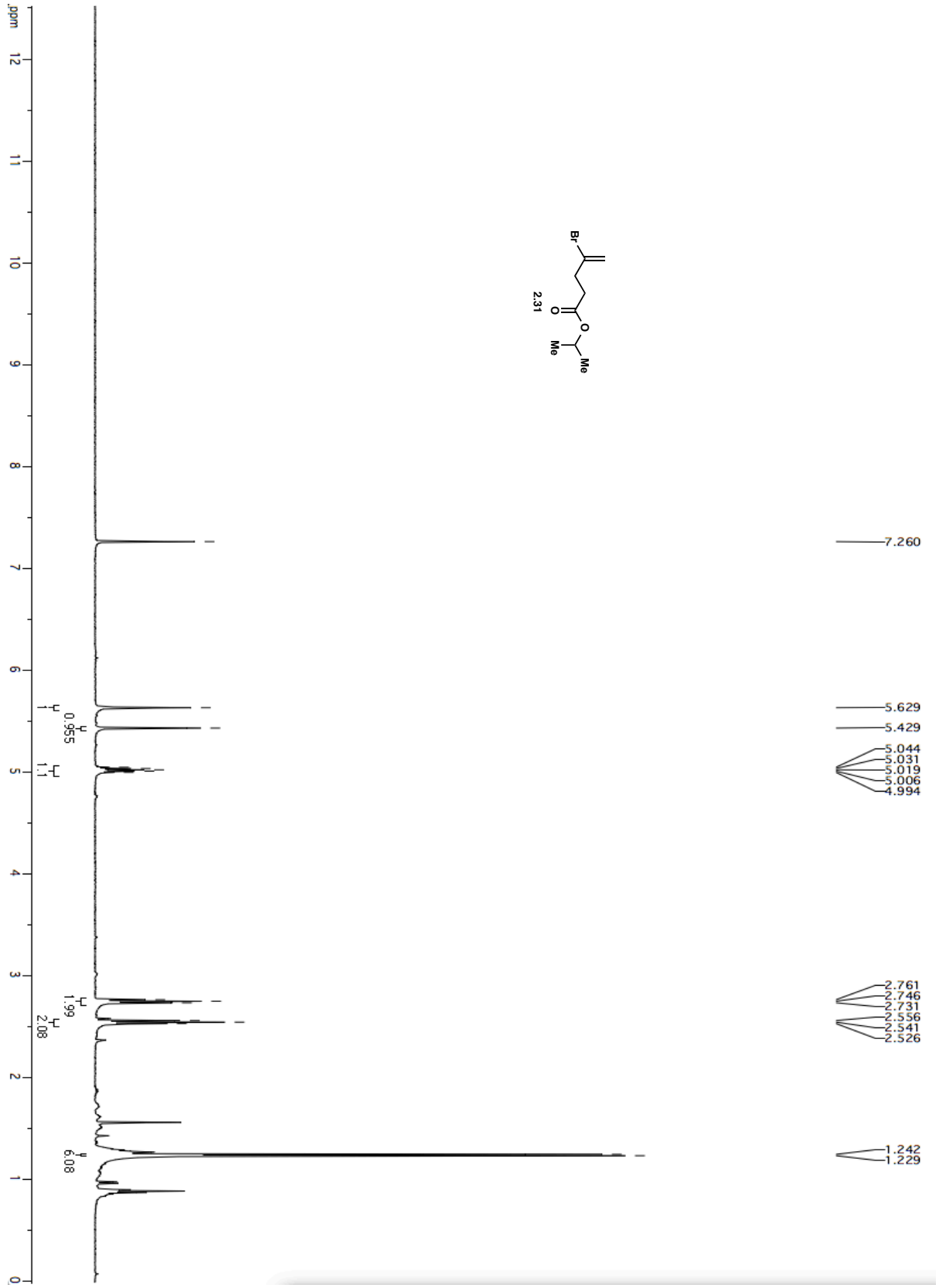
ppm
12
11
10
9
8
7
6
5
4
3
2
1
0
Br
O
O
Me
Me
2.31
7.260
5.629
5.429
5.044
5.031
5.019
5.006
4.994
2.761
2.746
2.731
2.556
2.541
2.526
1.242
1.229
1
0.955
1.1
1.99
2.08
6.08

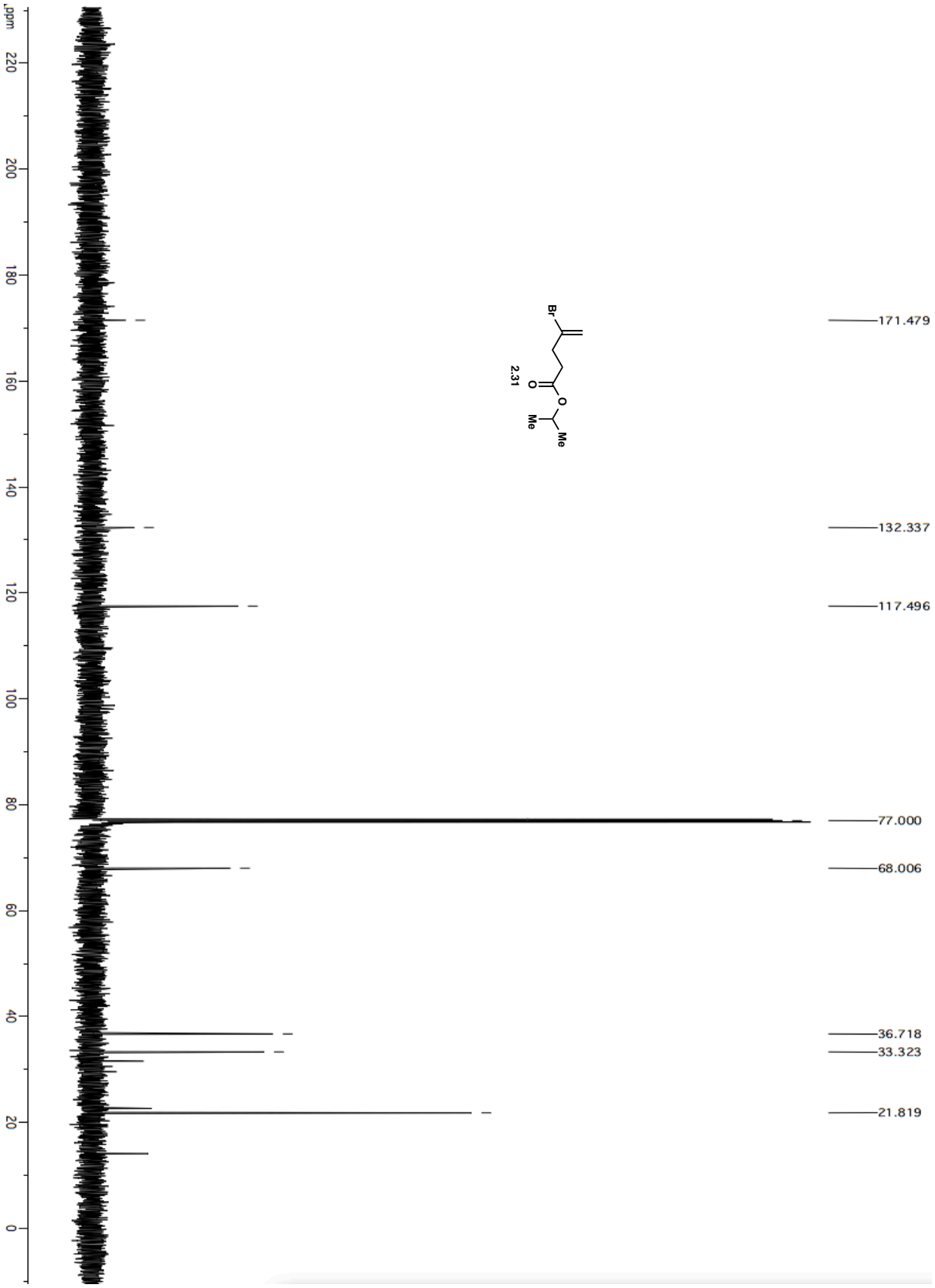
ppm
220
200
180
160
140
120
100
80
60
40
20
0
Br
2.31
O
O
Me
Me
171.479
132.337
117.496
77.000
68.006
36.718
33.323
21.819

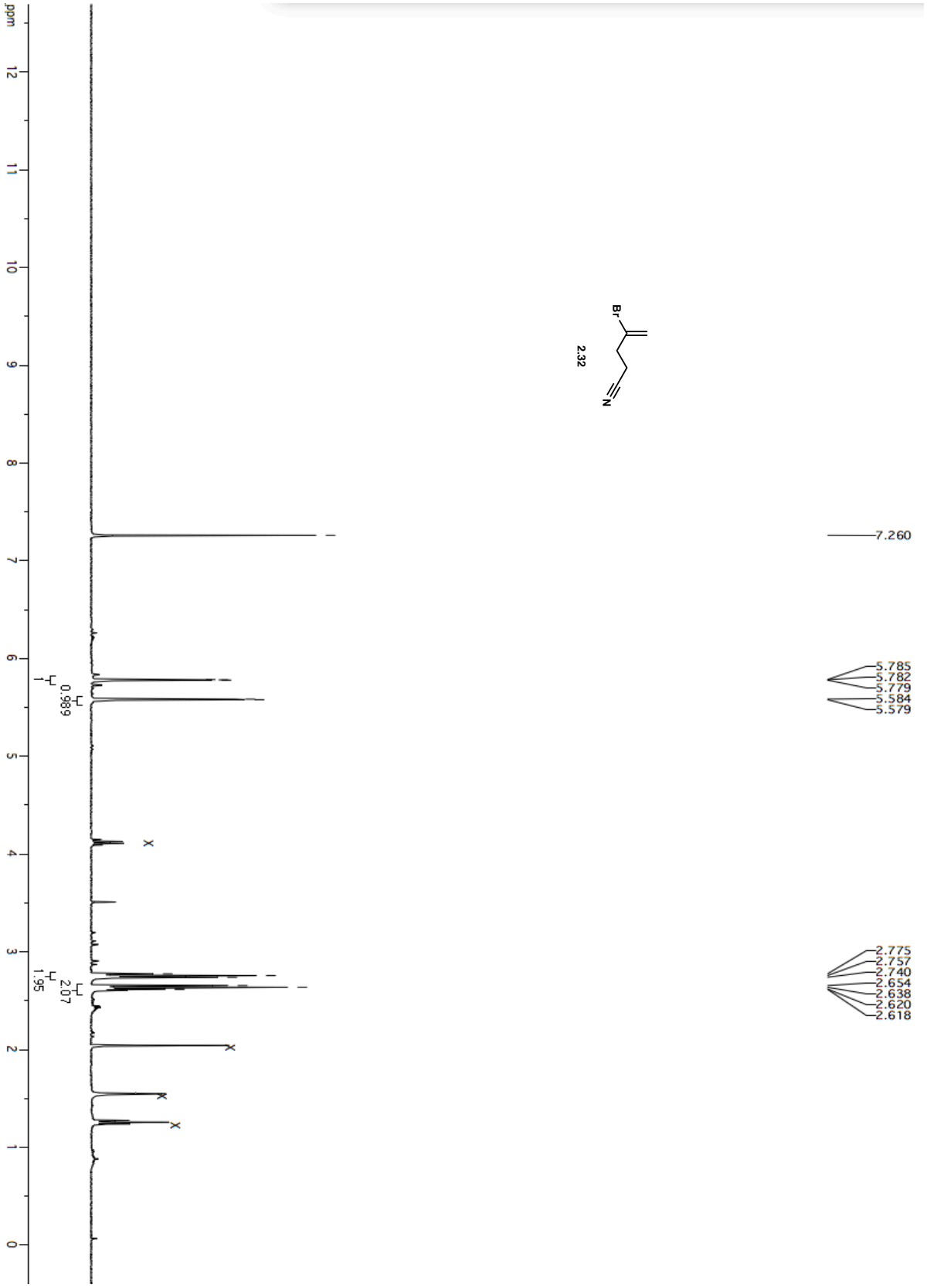
ppm
12
11
10
9
8
7
6
5
4
3
2
1
0
1.00
0.989
2.07
1.95
2.32
Br
N
7.260
5.785
5.782
5.779
5.584
5.579
2.775
2.757
2.740
2.654
2.638
2.620
2.618

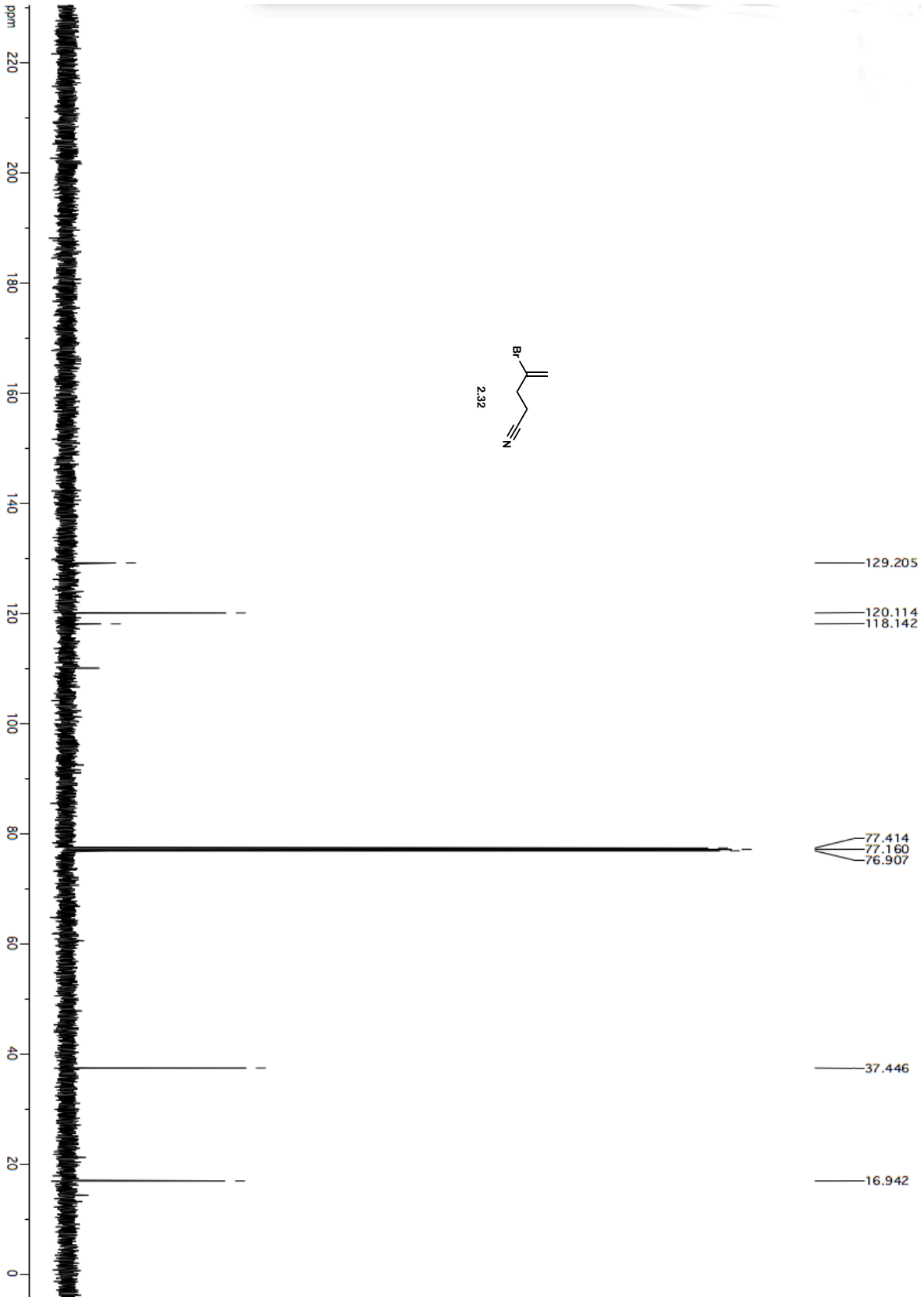
ppm
220
200
180
160
140
120
100
80
60
40
20
0
Br
N
2.32
129.205
120.114
118.142
77.414
77.160
76.907
37.446
16.942

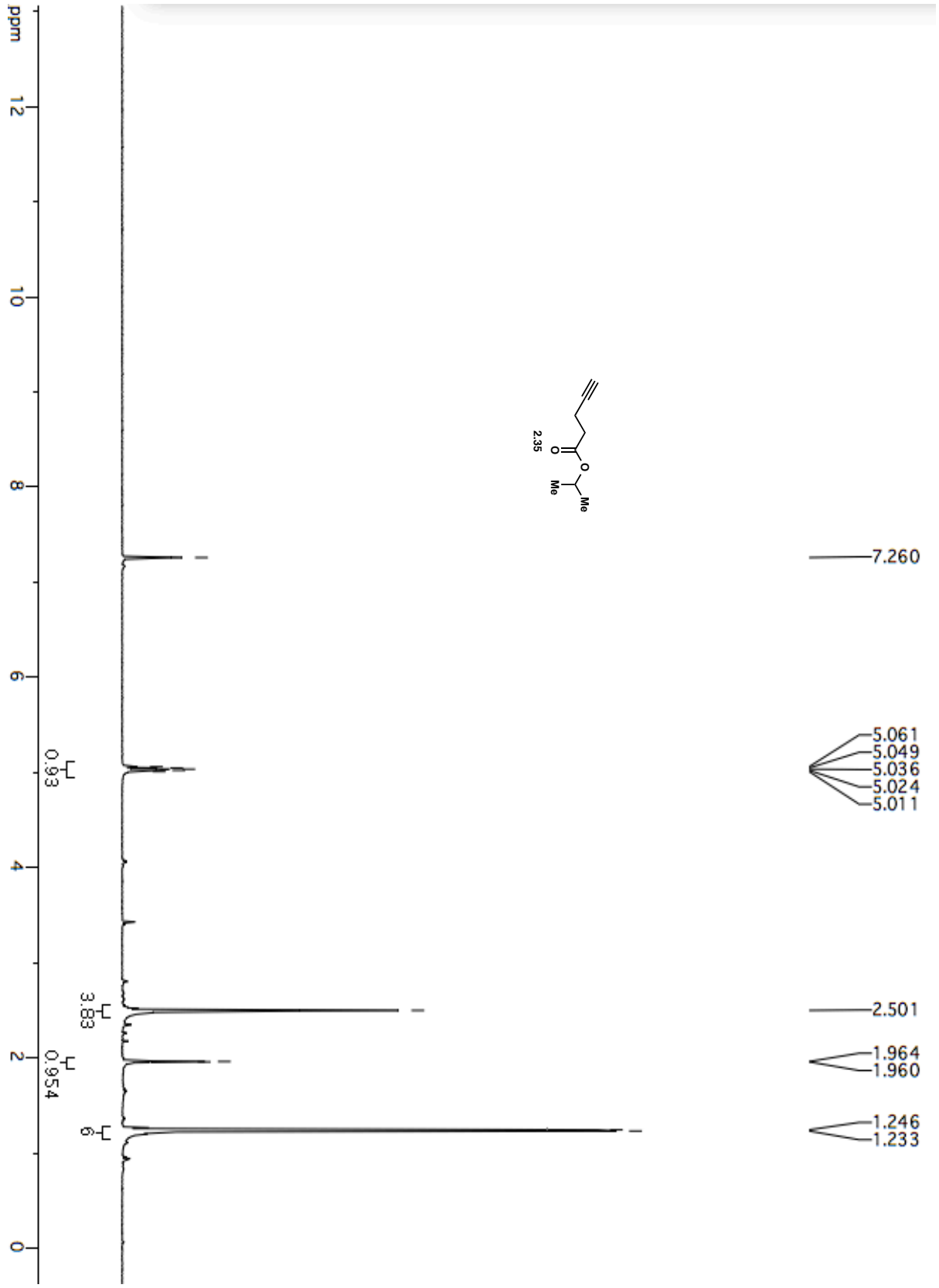
ppm
12
10
8
6
4
2
0
0.93
3.83
0.954
6
2.35
O
O
Me
Me
7.260
5.061
5.049
5.036
5.024
5.011
2.501
1.964
1.960
1.246
1.233

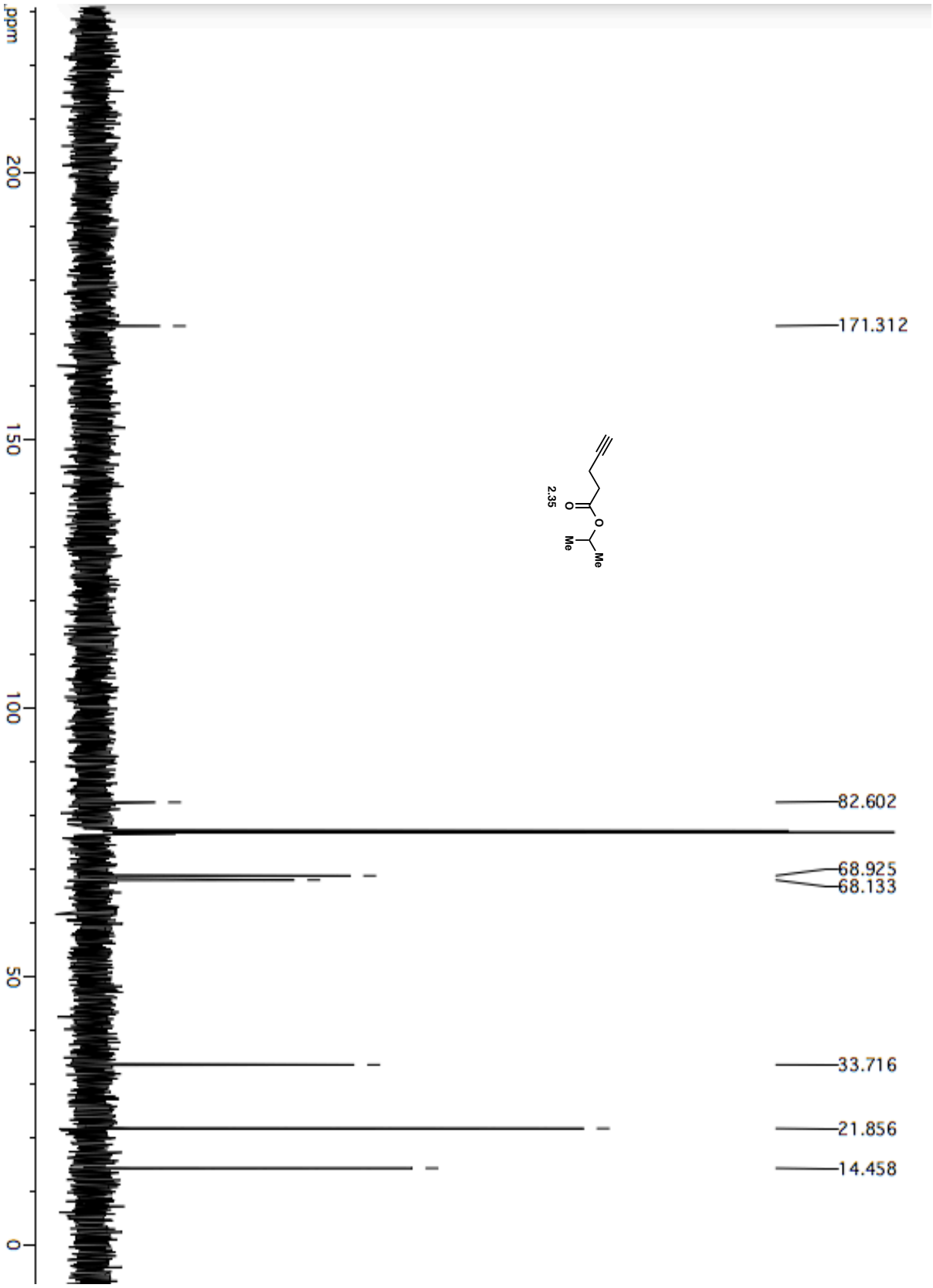
ppm
200
150
100
50
0
171.312
82.602
68.925
68.133
33.716
21.856
14.458
2.35
O
O
Me
Me

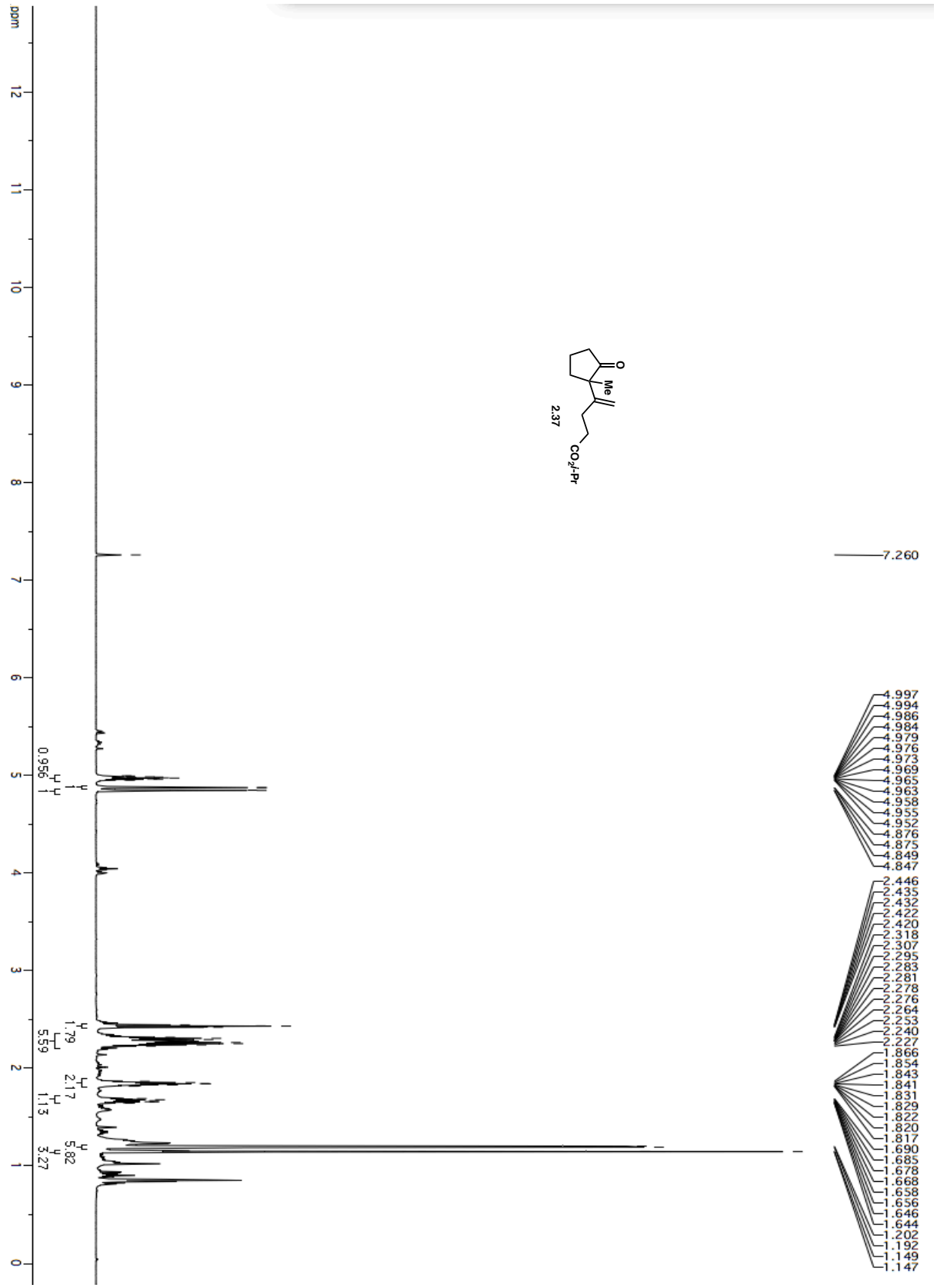
ppm
12
11
10
9
8
7
6
5
4
3
2
1
0
O
Me
2.37
CO2i-Pr
7.260
4.997
4.994
4.986
4.984
4.979
4.976
4.973
4.969
4.965
4.963
4.958
4.955
4.952
4.876
4.875
4.849
4.847
2.446
2.435
2.432
2.422
2.420
2.318
2.307
2.295
2.283
2.281
2.278
2.276
2.264
2.253
2.240
2.227
1.866
1.854
1.843
1.841
1.831
1.829
1.822
1.820
1.817
1.690
1.685
1.678
1.668
1.658
1.656
1.646
1.644
1.202
1.192
1.149
1.147
0.956
1
1.79
5.59
2.17
1.13
5.82
3.27

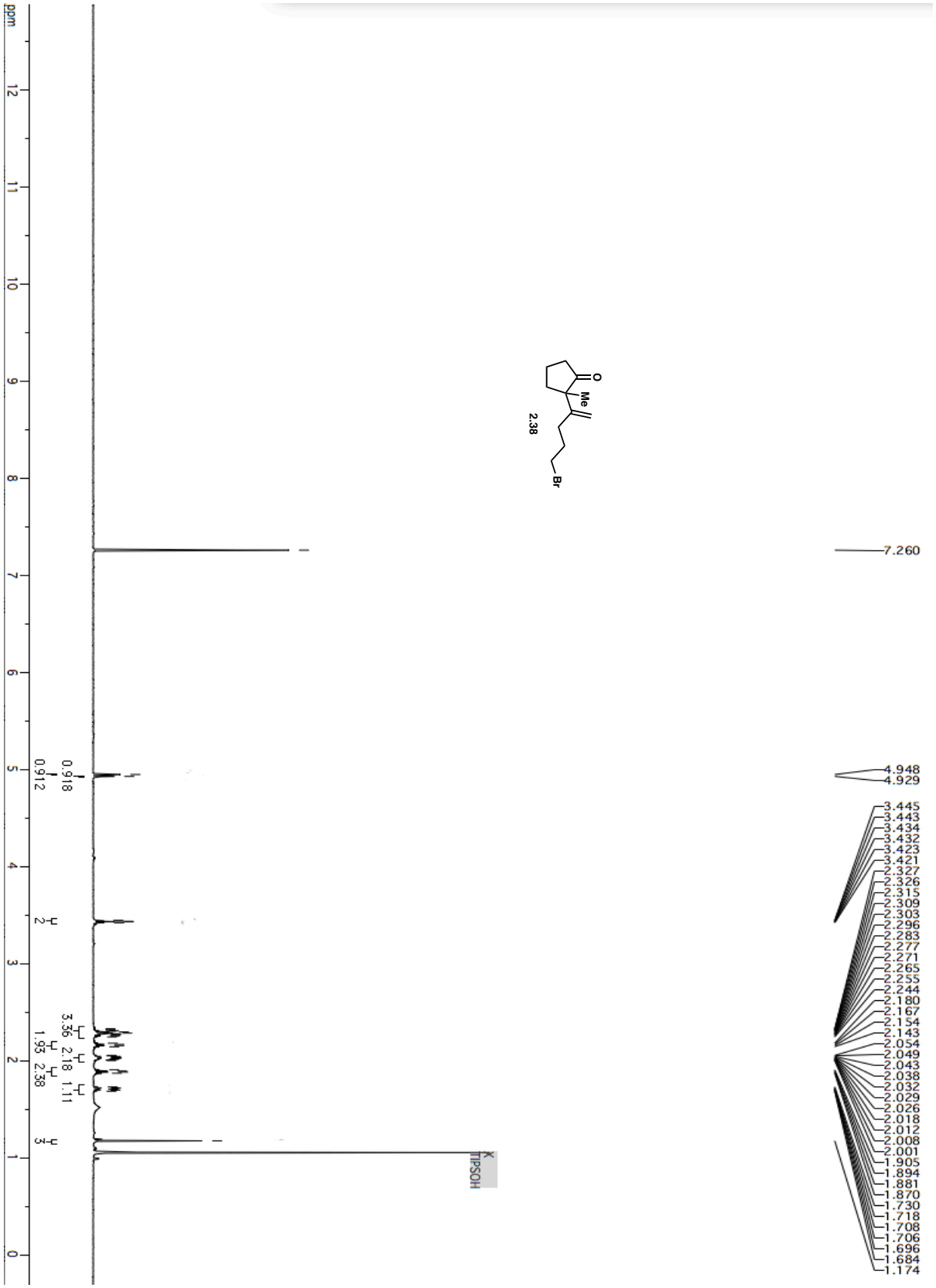
O
Me
2.38
Br
7.260
4.948
4.929
3.445
3.443
3.434
3.432
3.423
3.421
2.327
2.326
2.315
2.309
2.303
2.296
2.283
2.277
2.271
2.265
2.255
2.244
2.180
2.167
2.154
2.143
2.054
2.049
2.043
2.038
2.032
2.029
2.026
2.018
2.012
2.008
2.001
1.905
1.894
1.881
1.870
1.730
1.718
1.708
1.706
1.696
1.684
1.174
TIPSOH
0.918
0.912
3.36
2.18
1.93
2.38
1.11
ppm

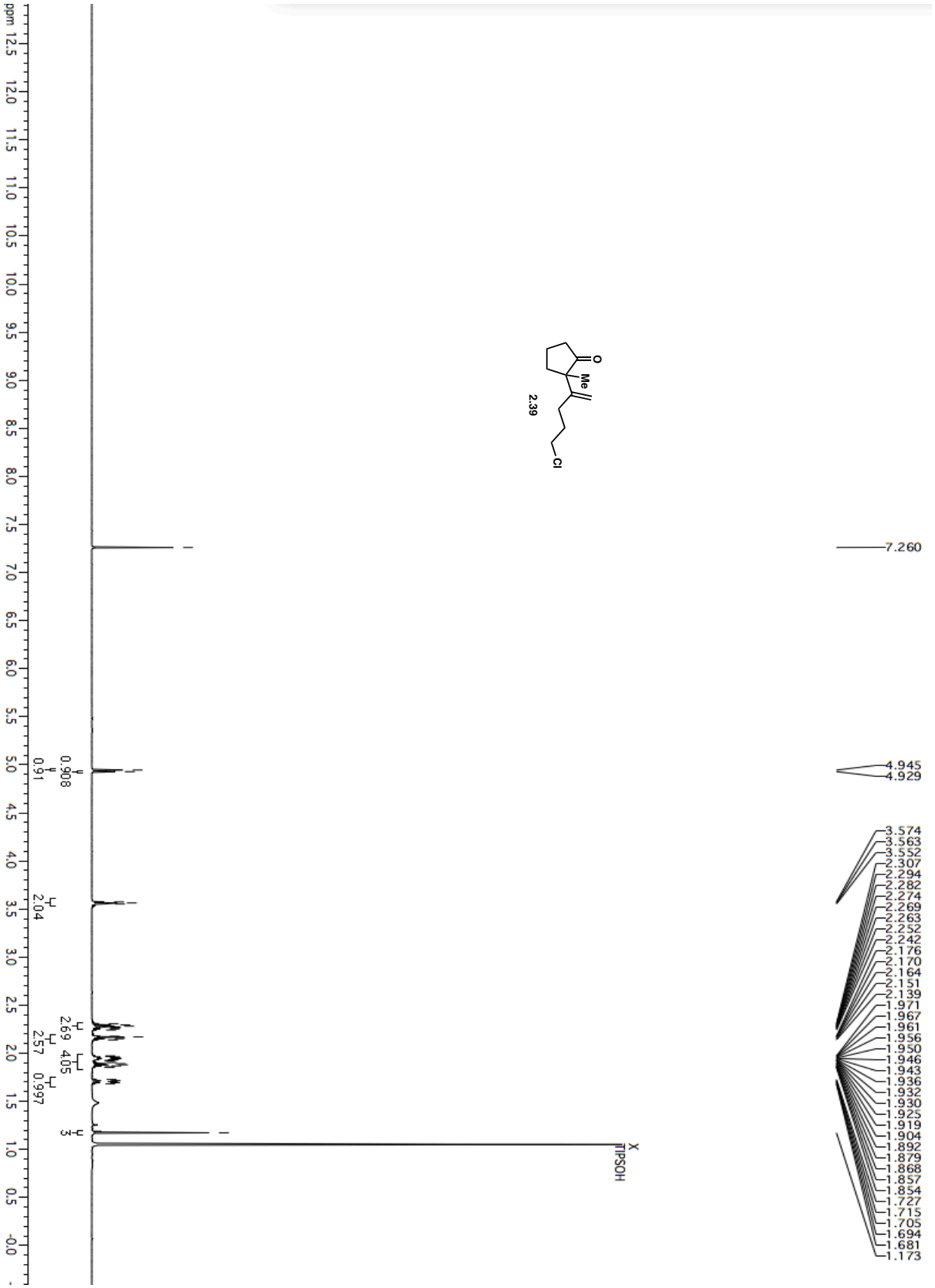
ppm 12.5 12.0 11.5 11.0 10.5 10.0 9.5 9.0 8.5 8.0 7.5 7.0 6.5 6.0 5.5 5.0 4.5 4.0 3.5 3.0 2.5 2.0 1.5 1.0 0.5 -0.0
0.91
0.908
2.04
2.69
4.05
2.57
0.997
3
X
TIPSOH
O
Me
2.39
Cl
7.260
4.945
4.929
3.574
3.563
3.552
2.307
2.294
2.282
2.274
2.269
2.263
2.252
2.242
2.176
2.170
2.164
2.151
2.139
1.971
1.967
1.961
1.956
1.950
1.946
1.943
1.936
1.932
1.930
1.925
1.919
1.904
1.892
1.879
1.868
1.857
1.854
1.727
1.715
1.705
1.694
1.681
1.173

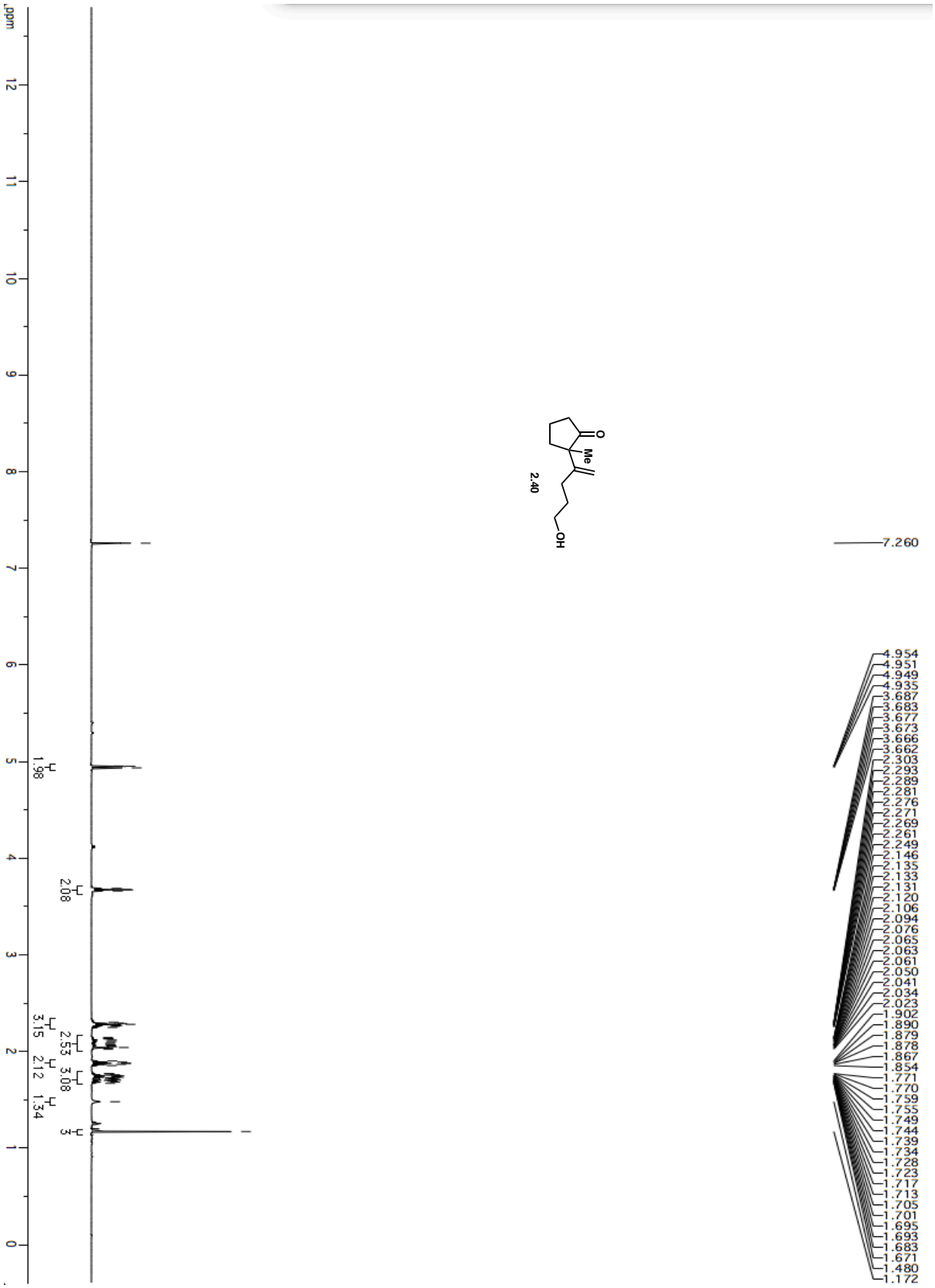
ppm
12
11
10
9
8
7
6
5
4
3
2
1
0
1.98
2.08
3.15
2.53
3.08
2.12
1.34
3
O
Me
2.40
OH
7.260
4.954
4.951
4.949
4.935
3.687
3.683
3.677
3.673
3.666
3.662
2.303
2.293
2.289
2.281
2.276
2.271
2.269
2.261
2.249
2.146
2.135
2.133
2.131
2.120
2.106
2.094
2.076
2.065
2.063
2.061
2.050
2.041
2.034
2.023
1.902
1.890
1.879
1.878
1.867
1.854
1.771
1.770
1.759
1.755
1.749
1.744
1.739
1.734
1.728
1.723
1.717
1.713
1.705
1.701
1.695
1.693
1.683
1.671
1.480
1.172

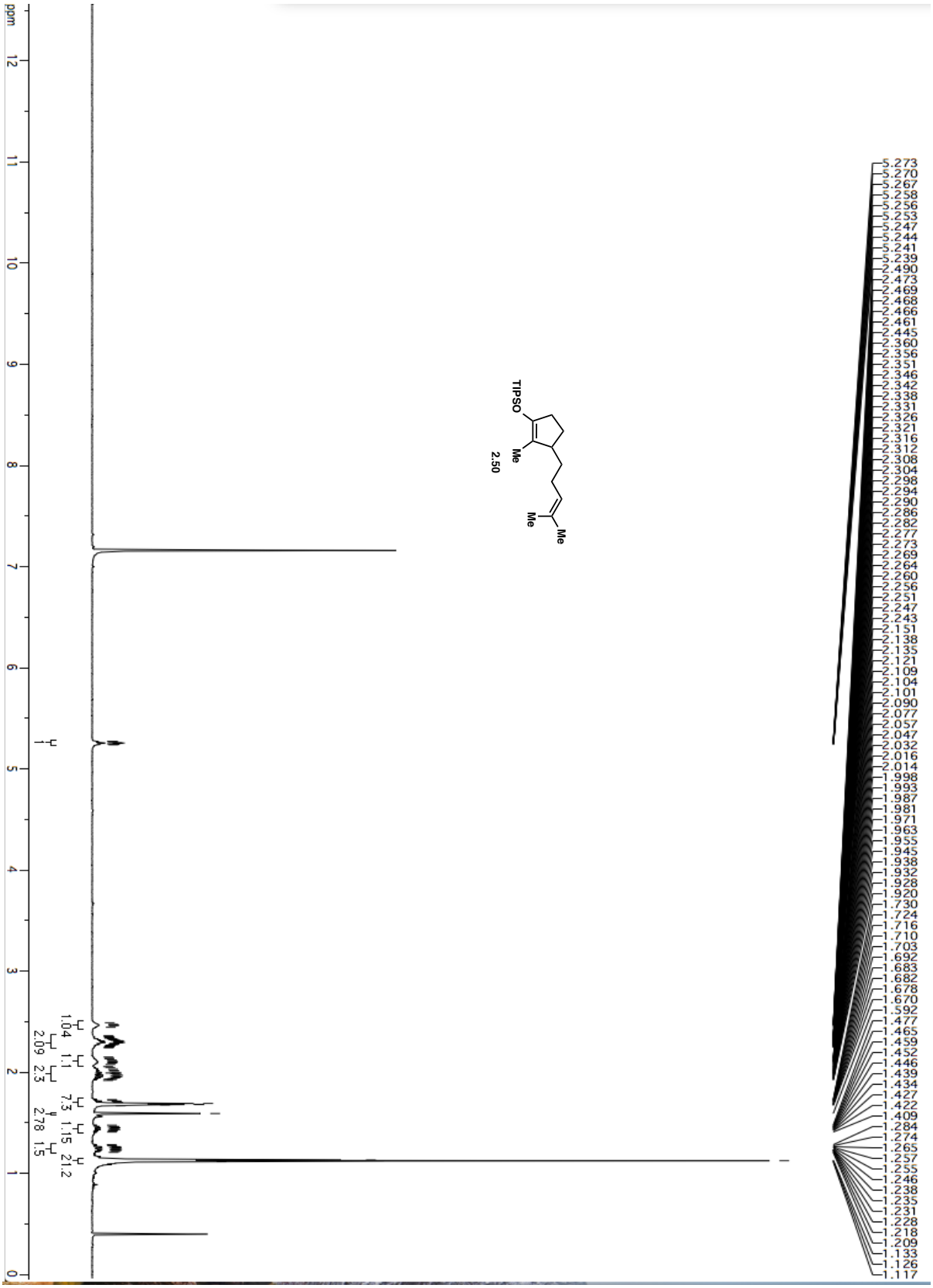
TIPSO
Me
2.50
Me
Me
ppm
1
1.04
1.1
7.3
1.15
21.2
2.09
2.3
2.78
1.5

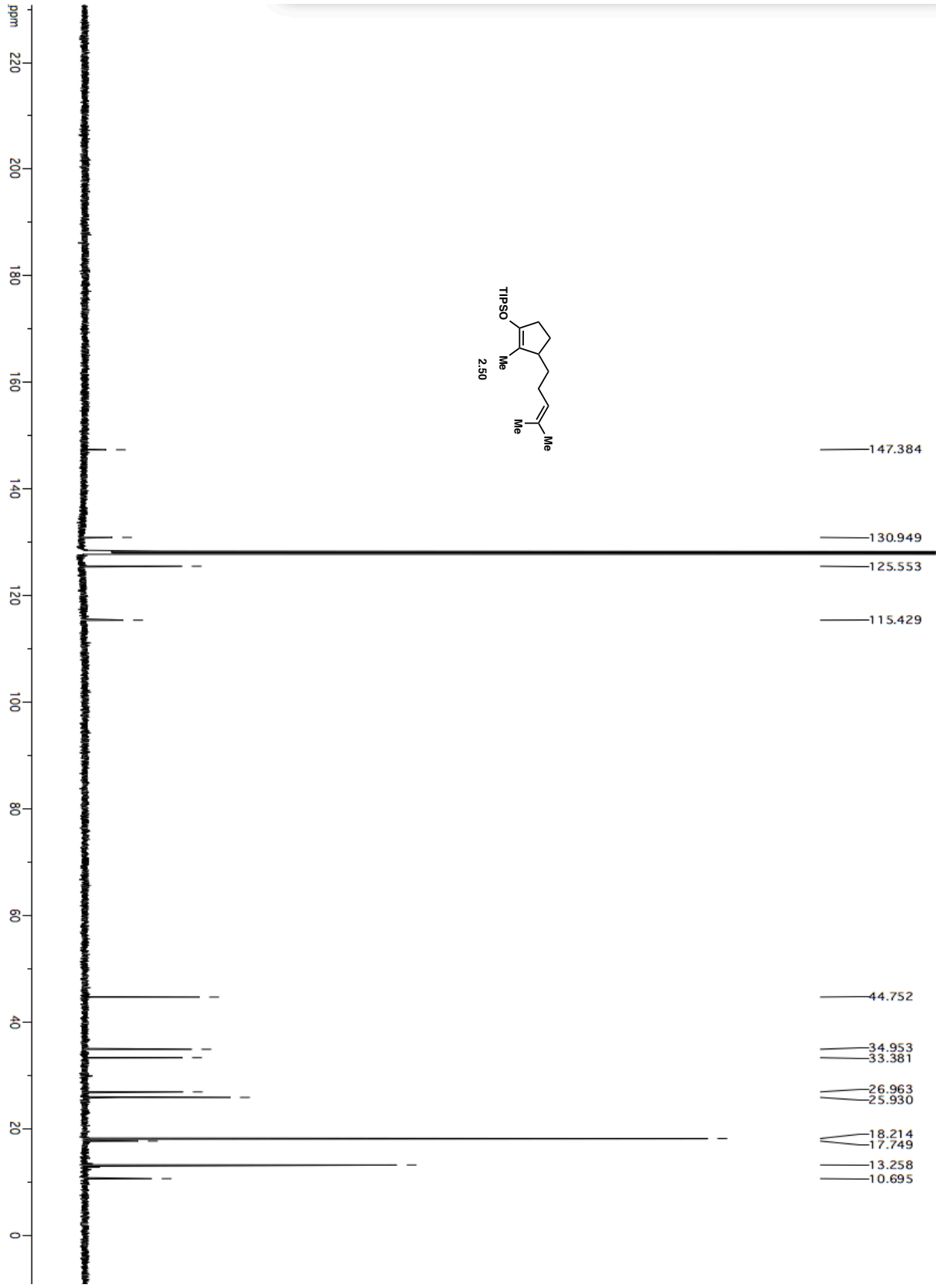
ppm
220
200
180
160
140
120
100
80
60
40
20
0
TIPSO
Me
2.50
Me
Me
147.384
130.949
125.553
115.429
44.752
34.953
33.381
26.963
25.930
18.214
17.749
13.258
10.695

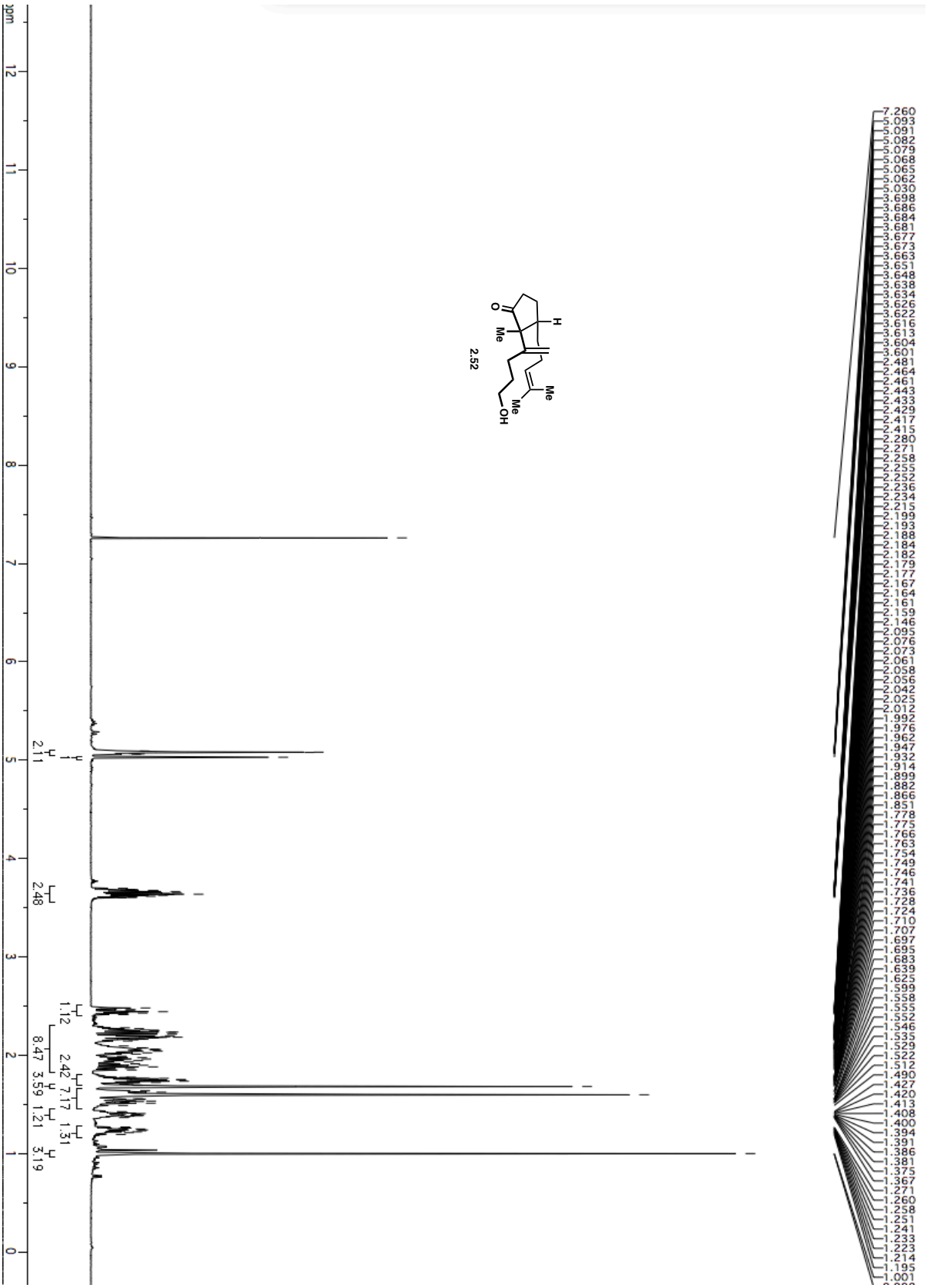
ppm
12
11
10
9
8
7
6
5
4
3
2
1
0
2.11
2.48
1.12
2.42
7.17
1.31
8.47
3.59
1.21
3.19
O
Me
H
Me
Me
OH
2.52
7.260
5.093
5.091
5.082
5.079
5.068
5.065
5.062
5.030
3.698
3.686
3.684
3.681
3.677
3.673
3.663
3.651
3.648
3.638
3.634
3.626
3.622
3.616
3.613
3.604
3.601
2.481
2.464
2.461
2.443
2.433
2.429
2.417
2.415
2.280
2.271
2.258
2.255
2.252
2.236
2.234
2.215
2.199
2.193
2.188
2.184
2.182
2.179
2.177
2.167
2.164
2.161
2.159
2.146
2.095
2.076
2.073
2.061
2.058
2.056
2.042
2.025
2.012
1.992
1.976
1.962
1.947
1.932
1.914
1.899
1.882
1.866
1.851
1.778
1.775
1.766
1.763
1.754
1.749
1.746
1.741
1.736
1.728
1.724
1.710
1.707
1.697
1.695
1.683
1.639
1.625
1.599
1.558
1.555
1.552
1.546
1.535
1.529
1.522
1.512
1.490
1.427
1.420
1.413
1.408
1.400
1.394
1.391
1.386
1.381
1.375
1.367
1.271
1.260
1.258
1.251
1.241
1.233
1.223
1.214
1.195
1.001

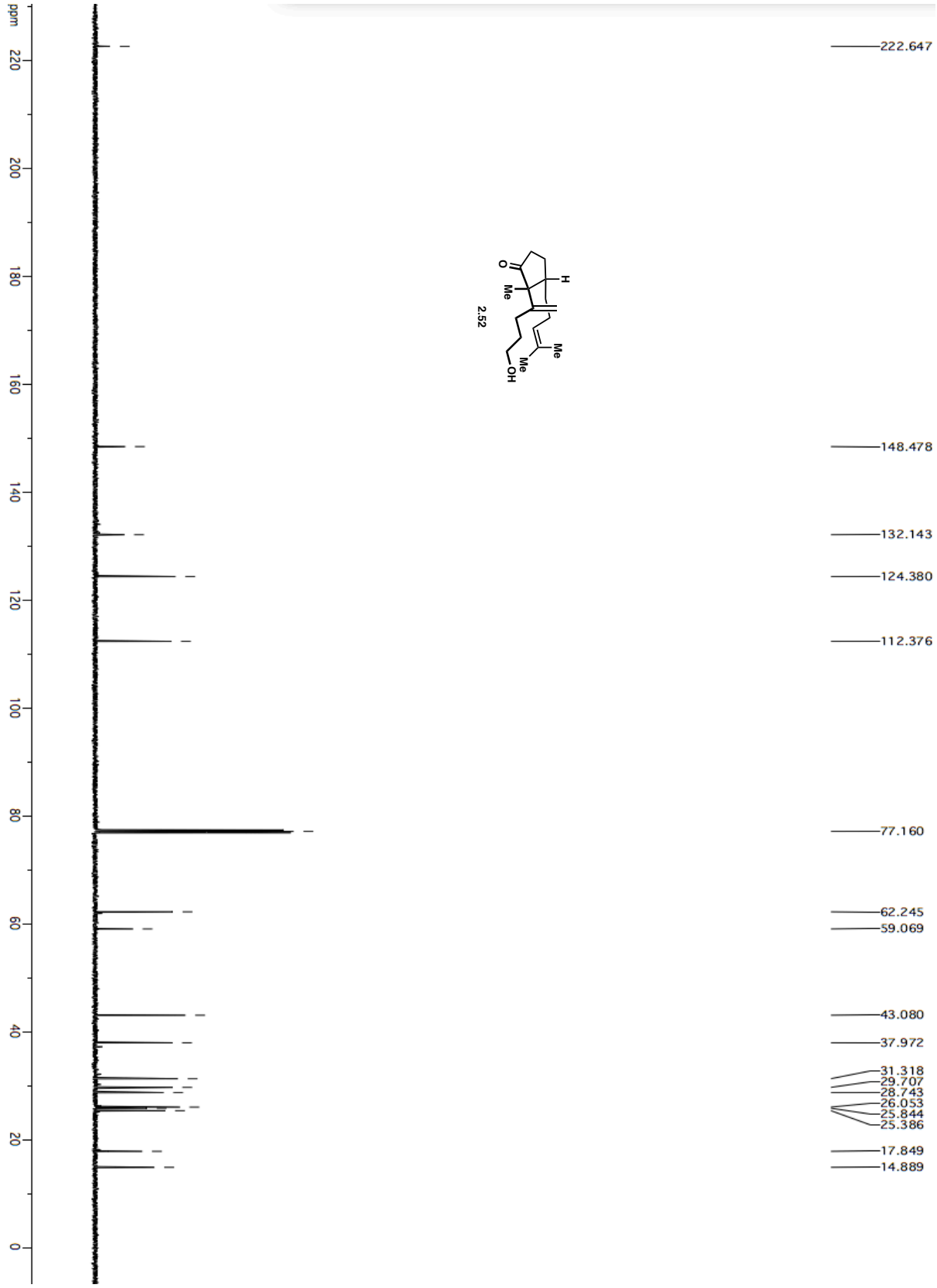
ppm
220
200
180
160
140
120
100
80
60
40
20
0
222.647
148.478
132.143
124.380
112.376
77.160
62.245
59.069
43.080
37.972
31.318
29.707
28.743
26.053
25.844
25.386
17.849
14.889
2.52
O
Me
H
Me
Me
OH

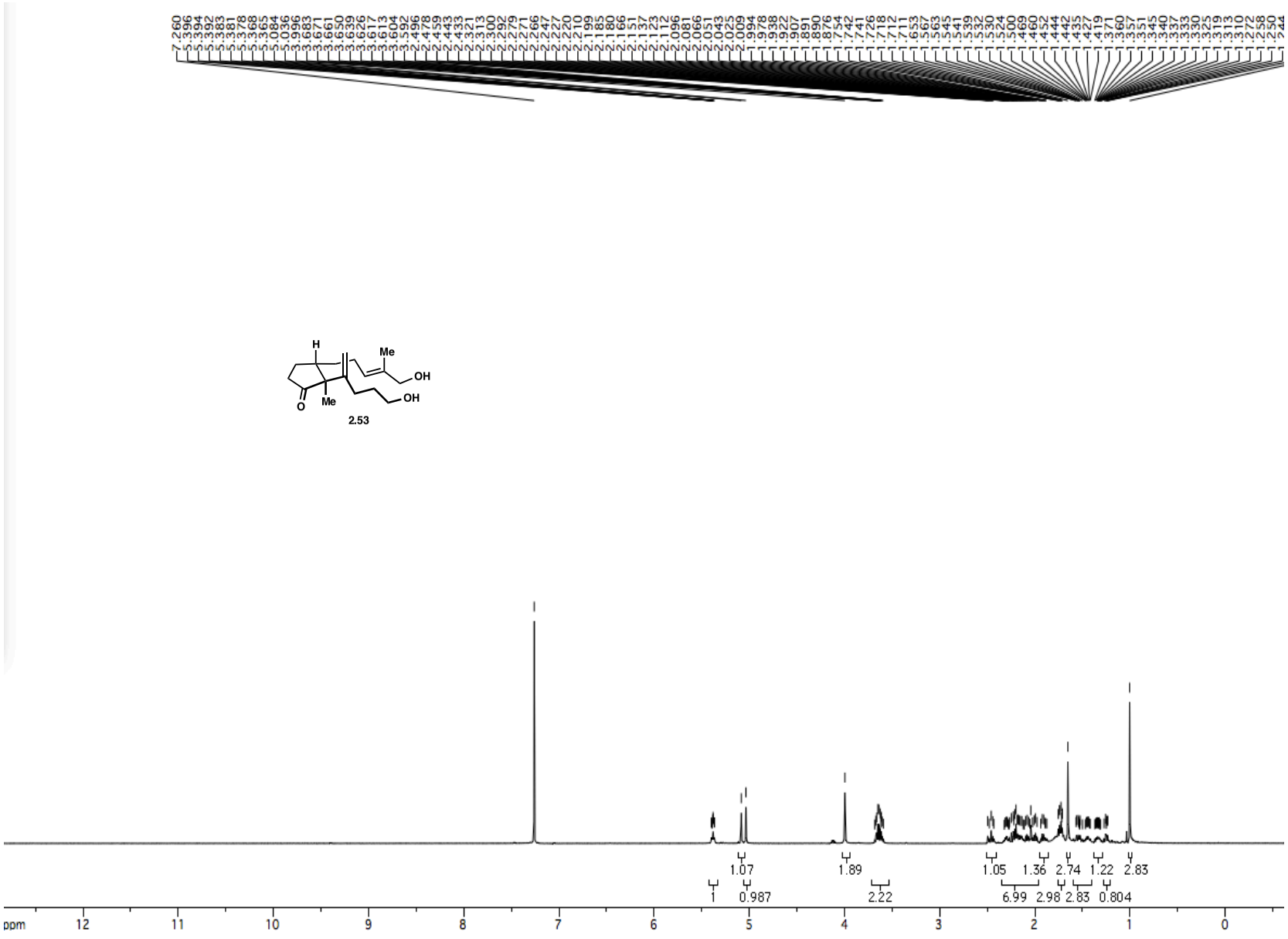
7.260
5.396
5.394
5.392
5.383
5.381
5.378
5.368
5.365
5.084
5.036
3.996
3.683
3.671
3.661
3.650
3.639
3.626
3.617
3.613
3.604
3.592
2.496
2.478
2.459
2.443
2.433
2.321
2.313
2.300
2.292
2.279
2.271
2.266
2.247
2.227
2.220
2.210
2.199
2.185
2.180
2.166
2.151
2.137
2.123
2.112
2.096
2.081
2.066
2.051
2.043
2.025
2.009
1.994
1.978
1.938
1.922
1.907
1.891
1.890
1.876
1.754
1.742
1.741
1.726
1.718
1.712
1.711
1.653
1.567
1.563
1.545
1.541
1.539
1.532
1.530
1.524
1.500
1.469
1.460
1.452
1.444
1.442
1.435
1.427
1.419
1.371
1.360
1.357
1.351
1.345
1.340
1.337
1.333
1.330
1.325
1.319
1.313
1.310
1.272
1.258
1.250
1.244
H
Me
OH
O
Me
OH
2.53
1.07
1.89
1.05
1.36
2.74
1.22
2.83
1
0.987
2.22
6.99
2.98
2.83
0.804
ppm
12
11
10
9
8
7
6
5
4
3
2
1
0

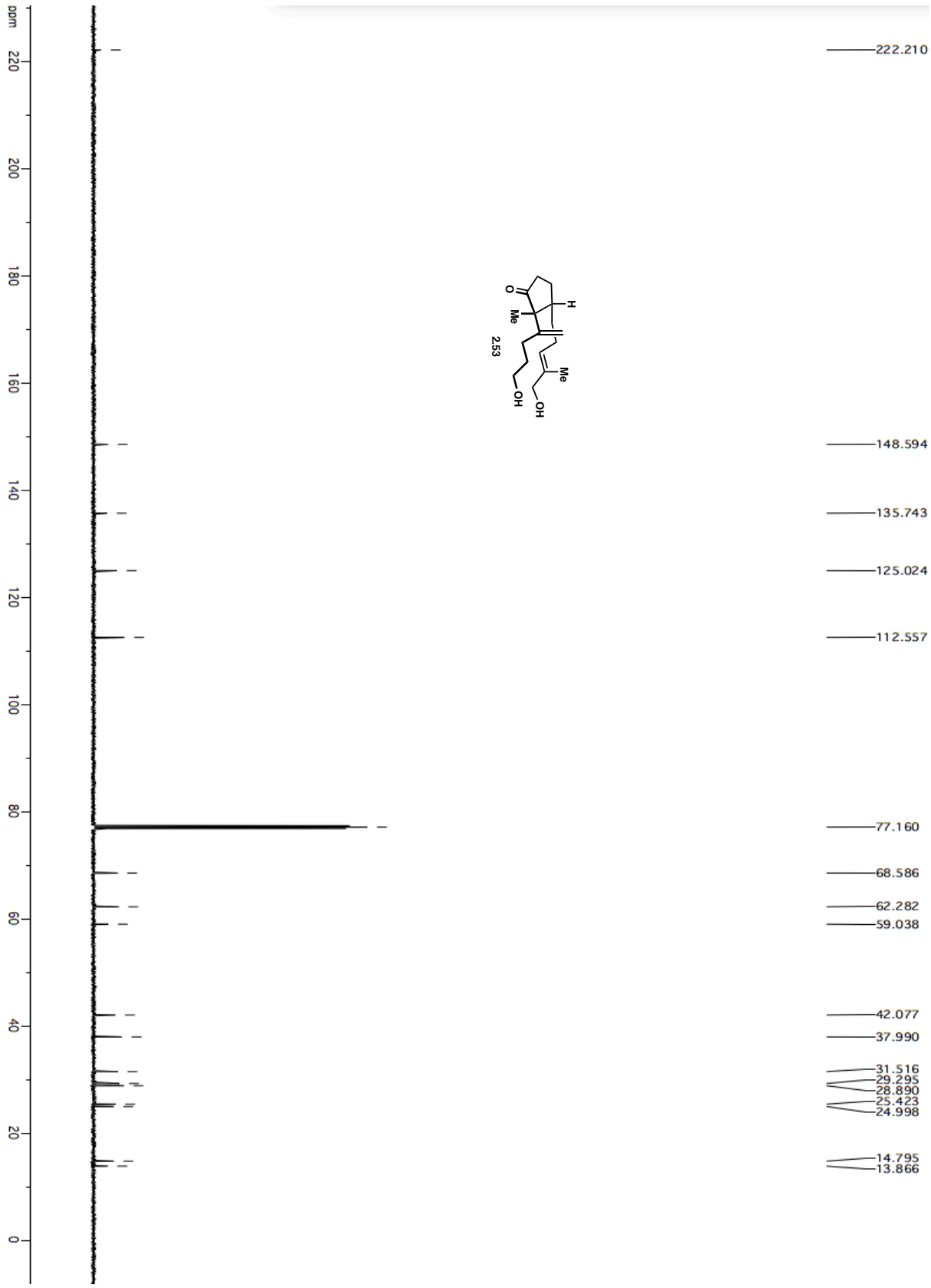
ppm
220
200
180
160
140
120
100
80
60
40
20
0
222.210
148.594
135.743
125.024
112.557
77.160
68.586
62.282
59.038
42.077
37.990
31.516
29.295
28.890
25.423
24.998
14.795
13.866
O
Me
H
2.53
Me
OH
OH

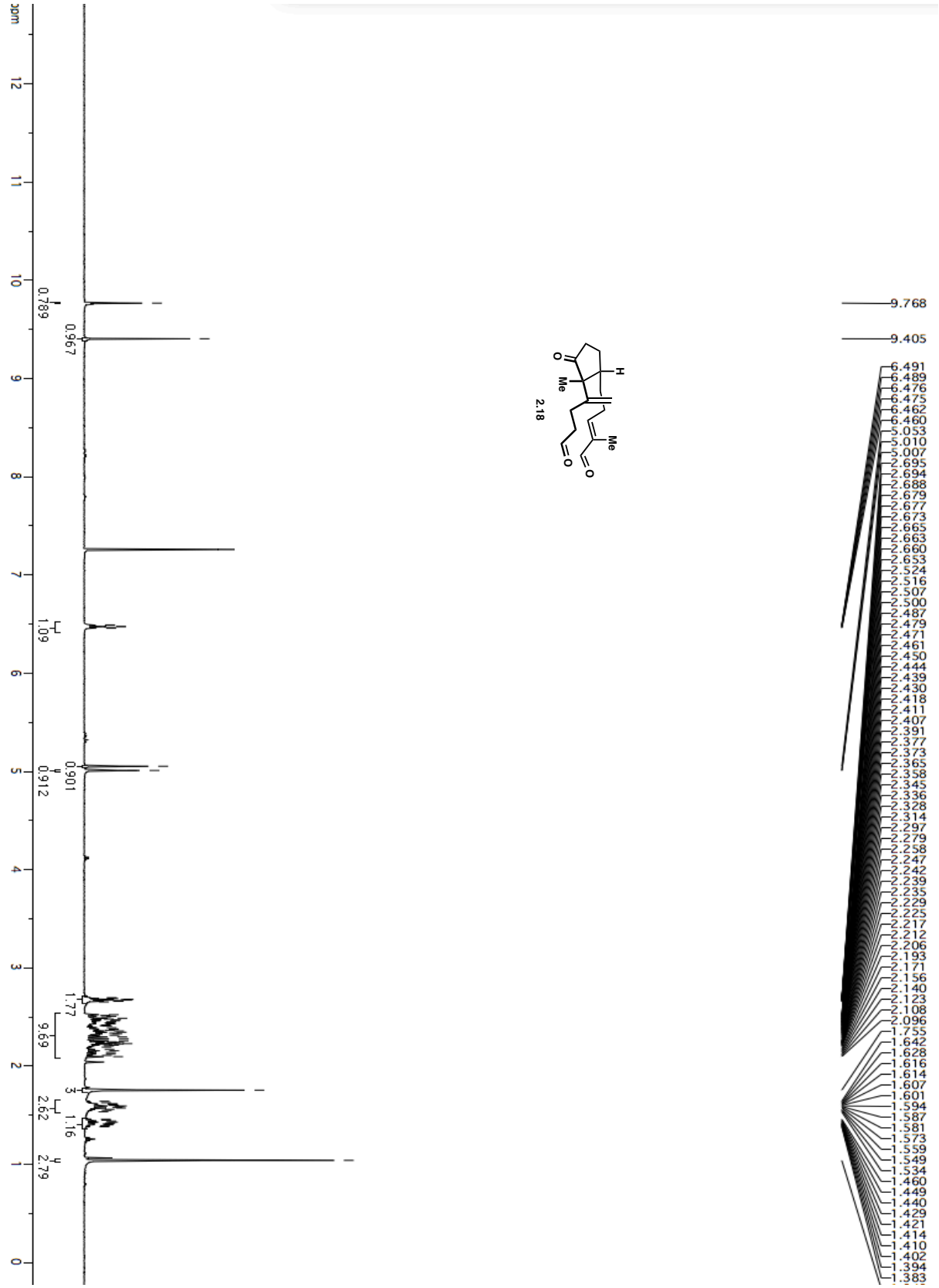
ppm
12
11
10
9
8
7
6
5
4
3
2
1
0
0.789
0.967
1.09
0.901
0.912
1.77
9.69
3
2.62
1.16
2.79
Me
Me
H
O
O
O
2.18
9.768
9.405
6.491
6.489
6.476
6.475
6.462
6.460
5.053
5.010
5.007
2.695
2.694
2.688
2.679
2.677
2.673
2.665
2.663
2.660
2.653
2.524
2.516
2.507
2.500
2.487
2.479
2.471
2.461
2.450
2.444
2.439
2.430
2.418
2.411
2.407
2.391
2.377
2.373
2.365
2.358
2.345
2.336
2.328
2.314
2.297
2.279
2.258
2.247
2.242
2.239
2.235
2.229
2.225
2.217
2.212
2.206
2.193
2.171
2.156
2.140
2.123
2.108
2.096
1.755
1.642
1.628
1.616
1.614
1.607
1.601
1.594
1.587
1.581
1.573
1.559
1.549
1.534
1.460
1.449
1.440
1.429
1.421
1.414
1.410
1.402
1.394
1.383

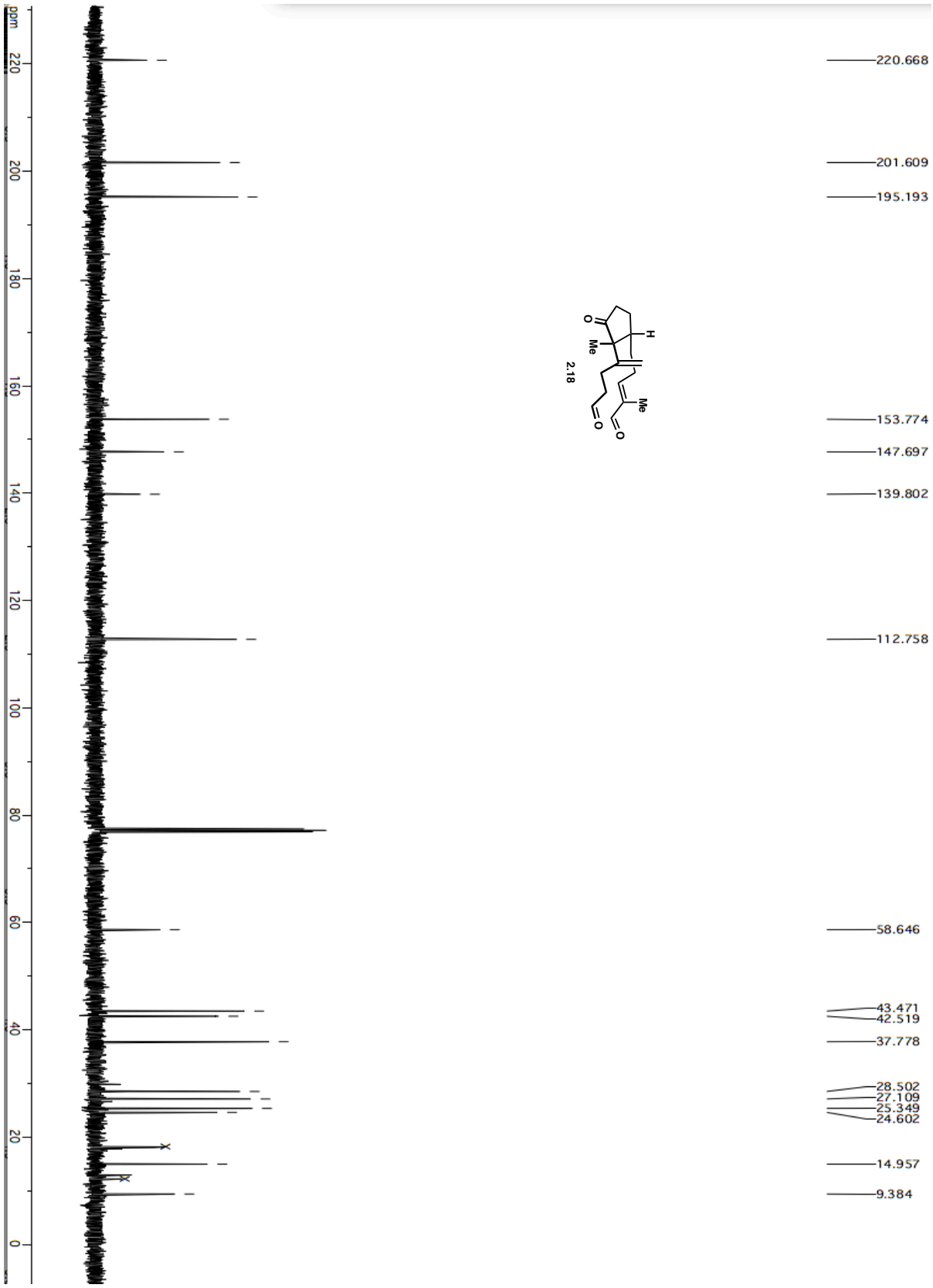
ppm
220
200
180
160
140
120
100
80
60
40
20
0
220.668
201.609
195.193
153.774
147.697
139.802
112.758
58.646
43.471
42.519
37.778
28.502
27.109
25.349
24.602
14.957
9.384
2.18
O
Me
H
Me
O
O

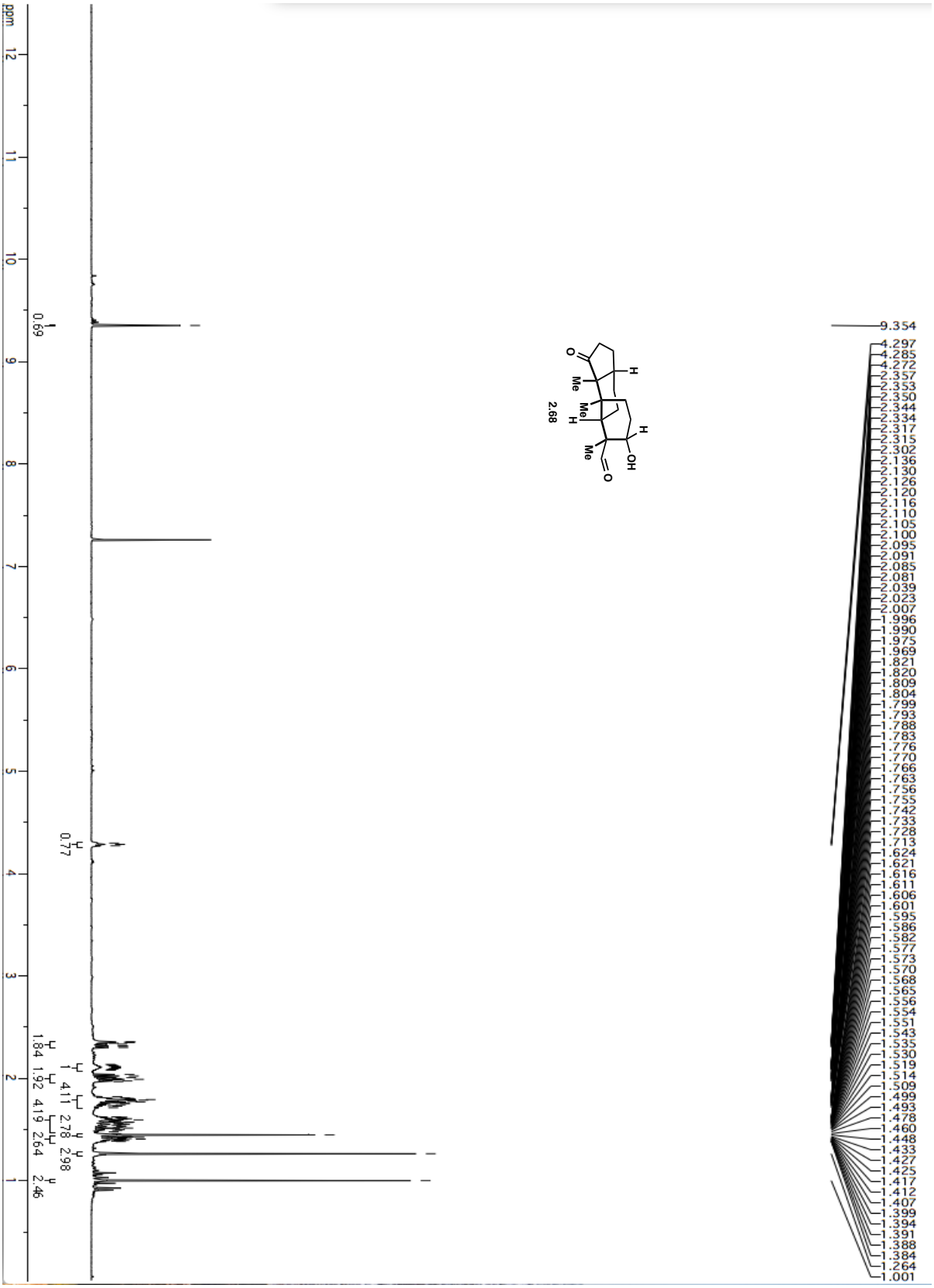
ppm
12
11
10
9
8
7
6
5
4
3
2
1
0.69
0.77
1.84
1.92
4.19
2.64
4.11
2.78
2.98
2.46
2.68
O
H
Me
Me
Me
H
H
OH
Me
O
9.354
4.297
4.285
4.272
2.357
2.353
2.350
2.344
2.334
2.317
2.315
2.302
2.136
2.130
2.126
2.120
2.116
2.110
2.105
2.100
2.095
2.091
2.085
2.081
2.039
2.023
2.007
1.996
1.990
1.975
1.969
1.821
1.820
1.809
1.804
1.799
1.793
1.788
1.783
1.776
1.770
1.766
1.763
1.756
1.755
1.742
1.733
1.728
1.713
1.624
1.621
1.616
1.611
1.606
1.601
1.595
1.586
1.582
1.577
1.573
1.570
1.568
1.565
1.556
1.554
1.551
1.543
1.535
1.530
1.519
1.514
1.509
1.499
1.493
1.478
1.460
1.448
1.433
1.427
1.425
1.417
1.412
1.407
1.399
1.394
1.391
1.388
1.384
1.264
1.001

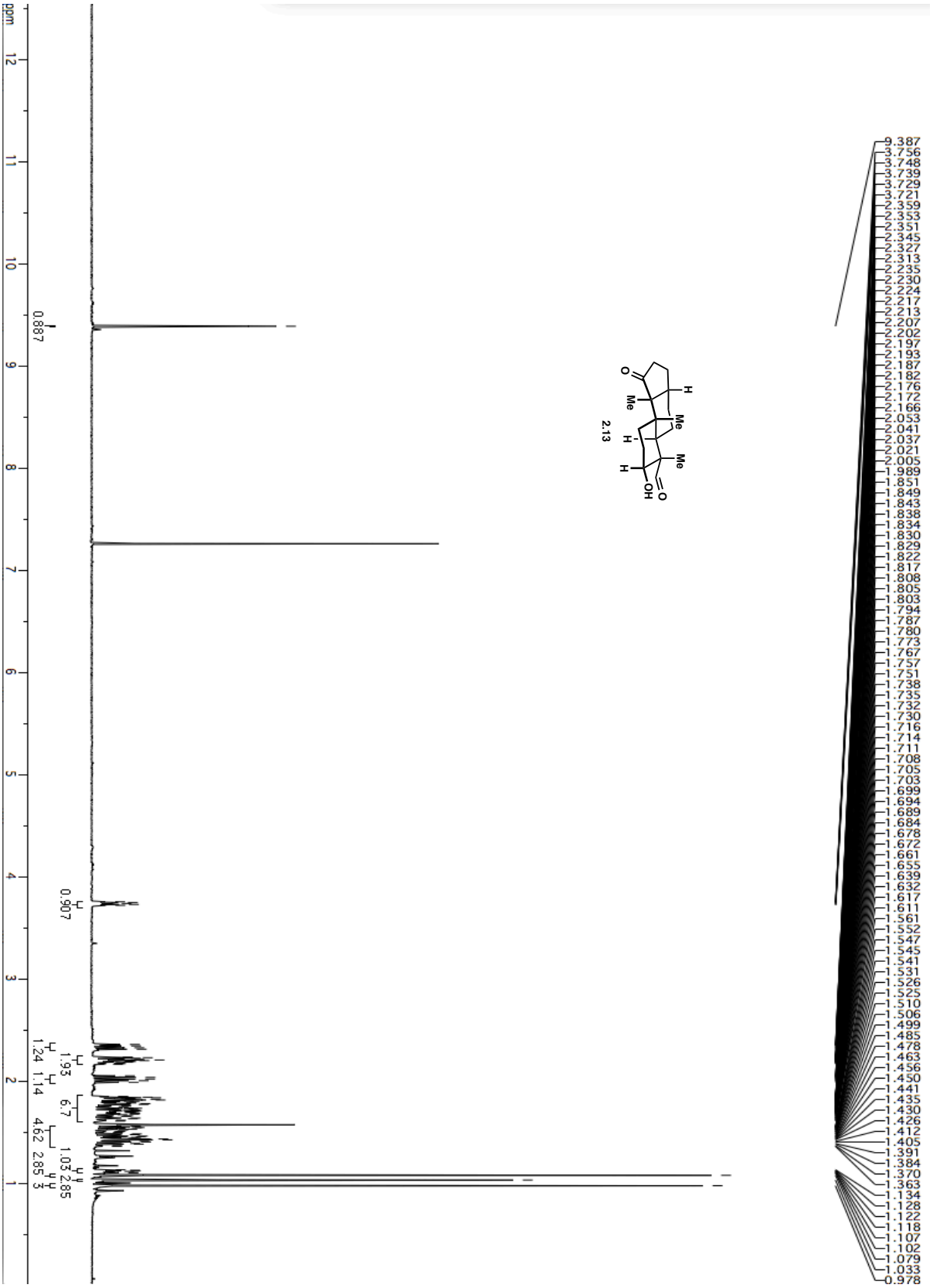
ppm
12
11
10
9
8
7
6
5
4
3
2
1
0.887
0.907
1.93
6.7
1.24
1.14
4.62
1.03
2.85
3
2.85
2.13
O
Me
H
Me
Me
H
H
OH
O
9.387
3.756
3.748
3.739
3.729
3.721
2.359
2.353
2.351
2.345
2.327
2.313
2.235
2.230
2.224
2.217
2.213
2.207
2.202
2.197
2.193
2.187
2.182
2.176
2.172
2.166
2.053
2.041
2.037
2.021
2.005
1.989
1.851
1.849
1.843
1.838
1.834
1.830
1.829
1.822
1.817
1.808
1.805
1.803
1.794
1.787
1.780
1.773
1.767
1.757
1.751
1.738
1.735
1.732
1.730
1.716
1.714
1.711
1.708
1.705
1.703
1.699
1.694
1.689
1.684
1.678
1.672
1.661
1.655
1.639
1.632
1.617
1.611
1.561
1.552
1.547
1.545
1.541
1.531
1.526
1.525
1.510
1.506
1.499
1.485
1.478
1.463
1.456
1.450
1.441
1.435
1.430
1.426
1.412
1.405
1.391
1.384
1.370
1.363
1.134
1.128
1.122
1.118
1.107
1.102
1.079
1.033
0.978

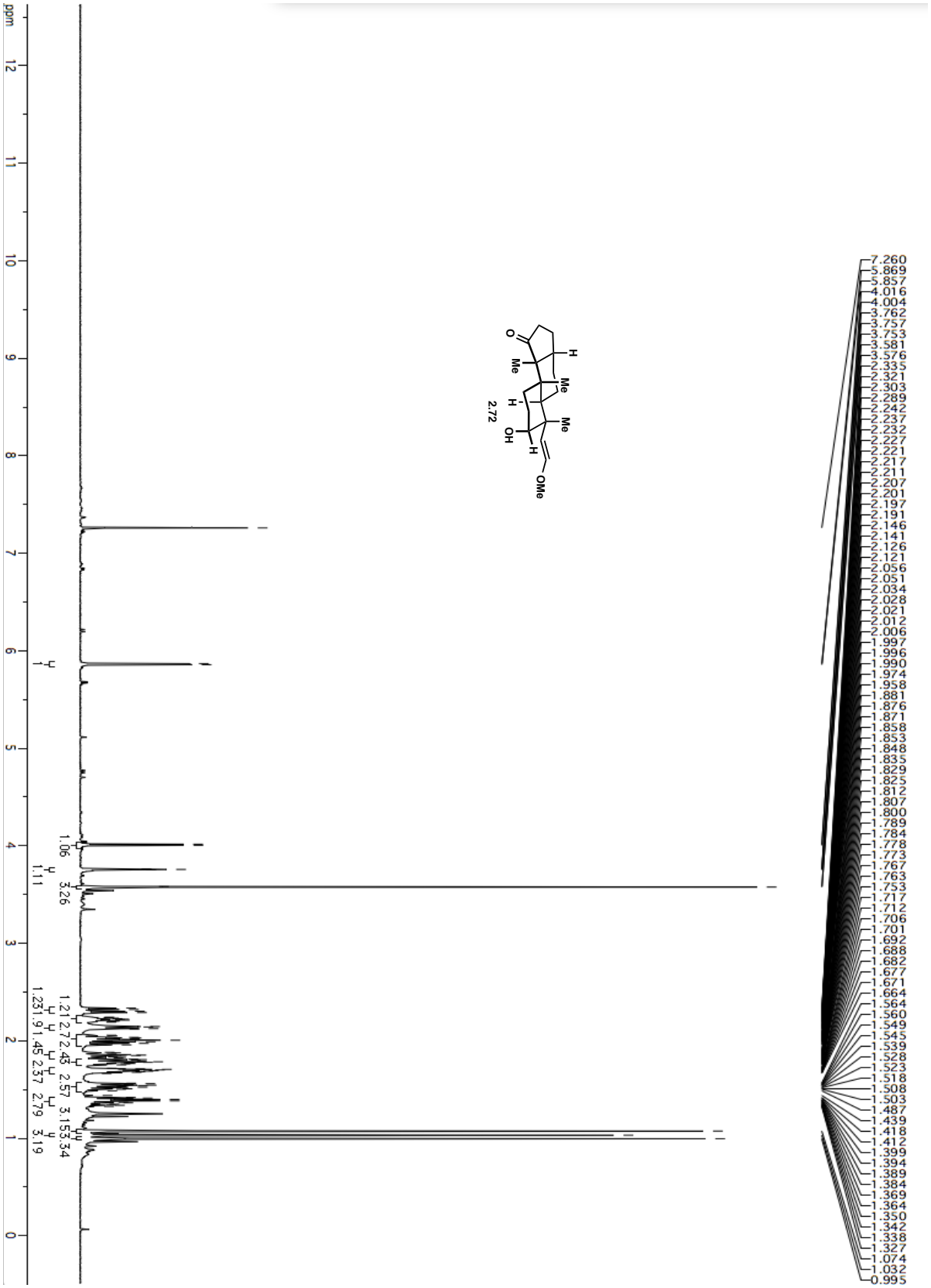
ppm
12
11
10
9
8
7
6
5
4
3
2
1
0
1
1.06
3.26
1.11
1.21
2.72
2.43
2.57
3.15
3.34
1.23
1.91
1.45
2.37
2.79
3.19
2.72
O
Me
H
Me
Me
H
OH
H
OMe
7.260
5.869
5.857
4.016
4.004
3.762
3.757
3.753
3.581
3.576
2.335
2.321
2.303
2.289
2.242
2.237
2.232
2.227
2.221
2.217
2.211
2.207
2.201
2.197
2.191
2.146
2.141
2.126
2.121
2.056
2.051
2.034
2.028
2.021
2.012
2.006
1.997
1.996
1.990
1.974
1.958
1.881
1.876
1.871
1.858
1.853
1.848
1.835
1.829
1.825
1.812
1.807
1.800
1.789
1.784
1.778
1.773
1.767
1.763
1.753
1.717
1.712
1.706
1.701
1.692
1.688
1.682
1.677
1.671
1.664
1.564
1.560
1.549
1.545
1.539
1.528
1.523
1.518
1.508
1.503
1.487
1.439
1.418
1.412
1.399
1.394
1.389
1.384
1.369
1.364
1.350
1.342
1.338
1.327
1.074
1.032
0.995

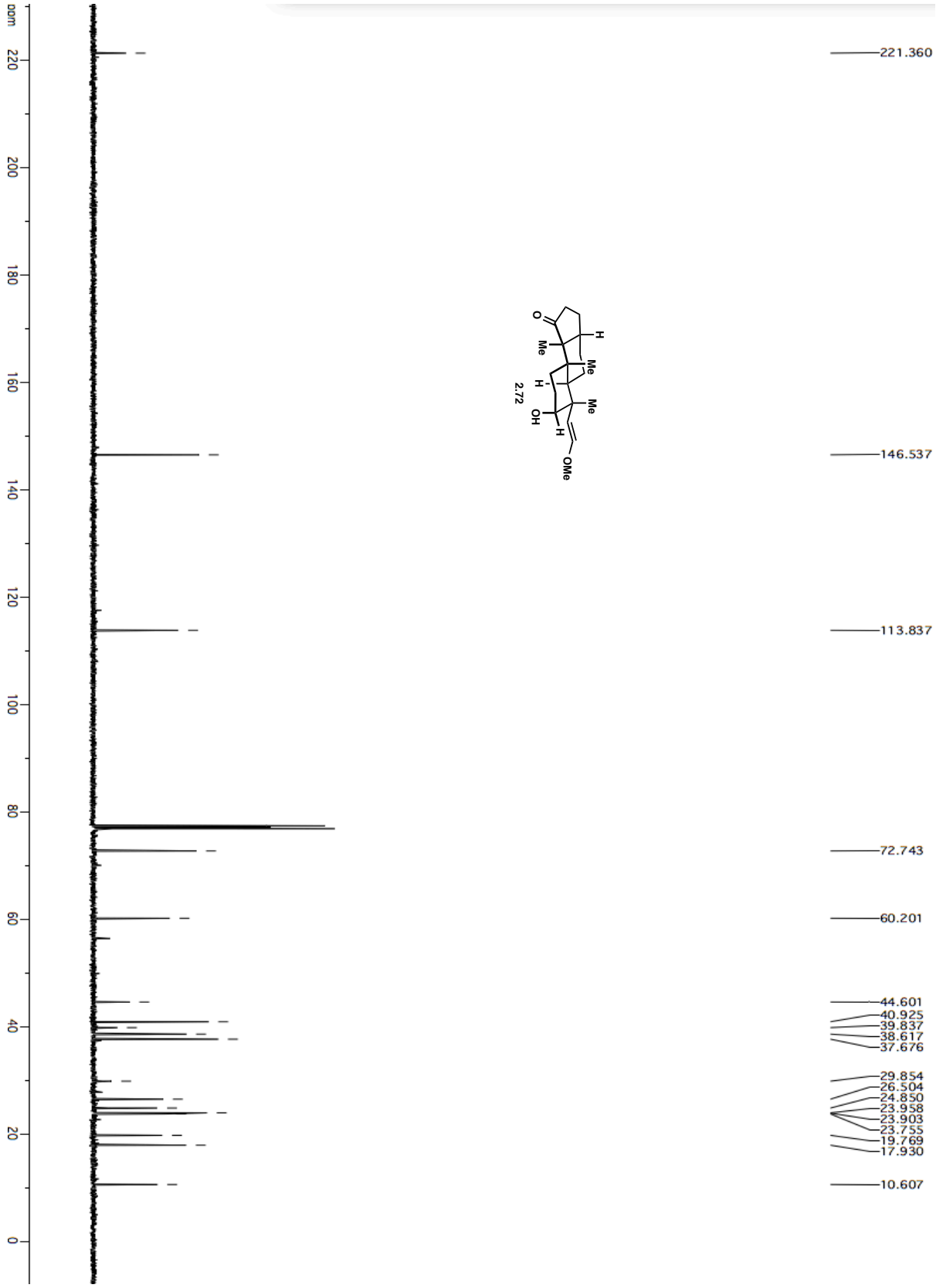
ppm
220
200
180
160
140
120
100
80
60
40
20
0
O
Me
H
Me
H
Me
OH
H
OMe
2.72
221.360
146.537
113.837
72.743
60.201
44.601
40.925
39.837
38.617
37.676
29.854
26.504
24.850
23.958
23.903
23.755
19.769
17.930
10.607

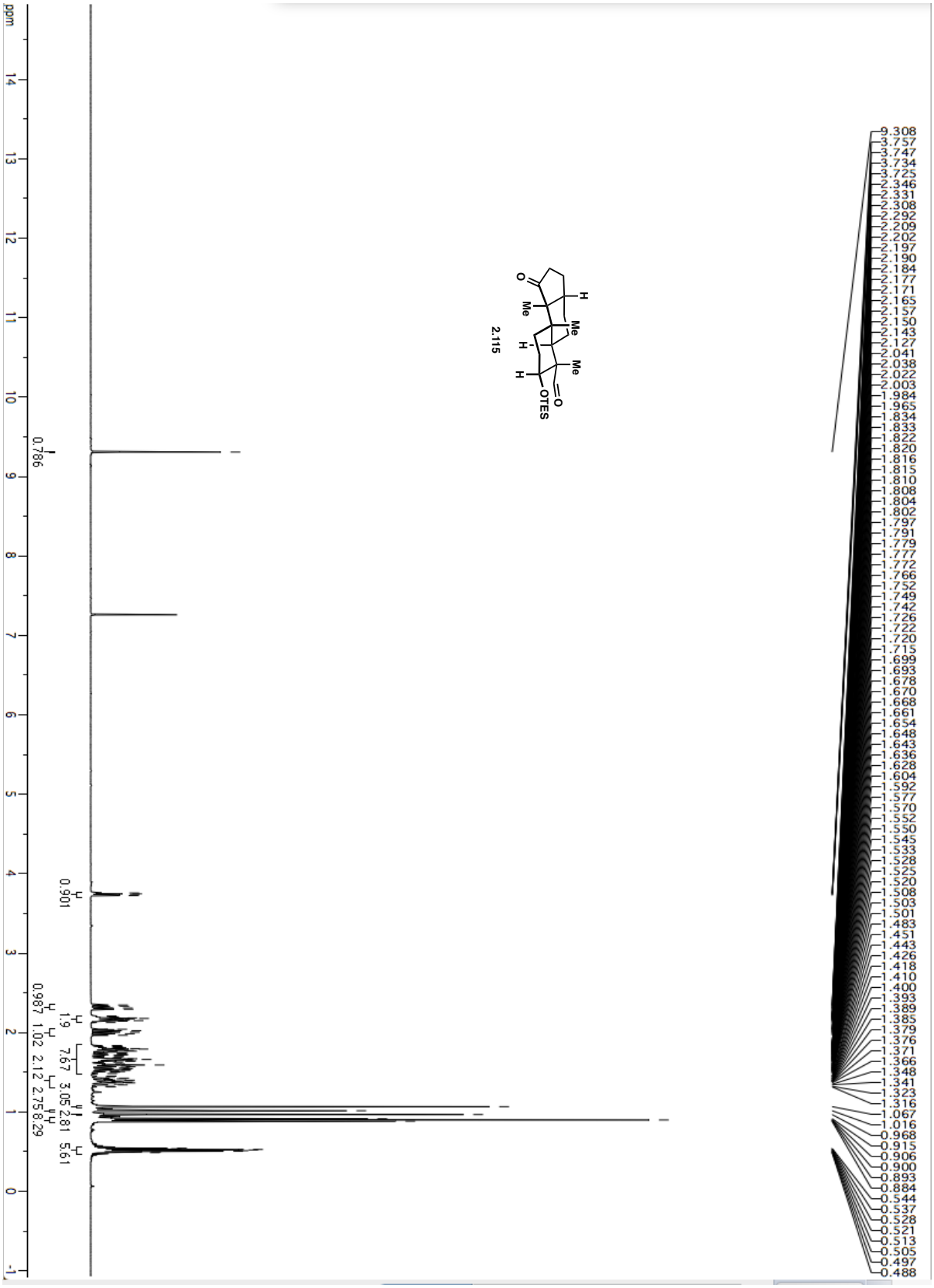
ppm
14
13
12
11
10
9
8
7
6
5
4
3
2
1
0
-1
0.786
0.901
0.987
1.9
7.67
1.02
3.05
2.12
2.81
2.75
8.29
5.61
2.115
O
Me
H
Me
Me
H
H
O
OTES
9.308
3.757
3.747
3.734
3.725
2.346
2.331
2.308
2.292
2.209
2.202
2.197
2.190
2.184
2.177
2.171
2.165
2.157
2.150
2.143
2.127
2.041
2.038
2.022
2.003
1.984
1.965
1.834
1.833
1.822
1.820
1.816
1.815
1.810
1.808
1.804
1.802
1.797
1.791
1.779
1.777
1.772
1.766
1.752
1.749
1.742
1.726
1.722
1.720
1.715
1.699
1.693
1.678
1.670
1.668
1.661
1.654
1.648
1.643
1.636
1.628
1.604
1.592
1.577
1.570
1.552
1.550
1.545
1.533
1.528
1.525
1.520
1.508
1.503
1.501
1.483
1.451
1.443
1.426
1.418
1.410
1.400
1.393
1.389
1.385
1.379
1.376
1.371
1.366
1.348
1.341
1.323
1.316
1.067
1.016
0.968
0.915
0.906
0.900
0.893
0.884
0.544
0.537
0.528
0.521
0.513
0.505
0.497
0.488

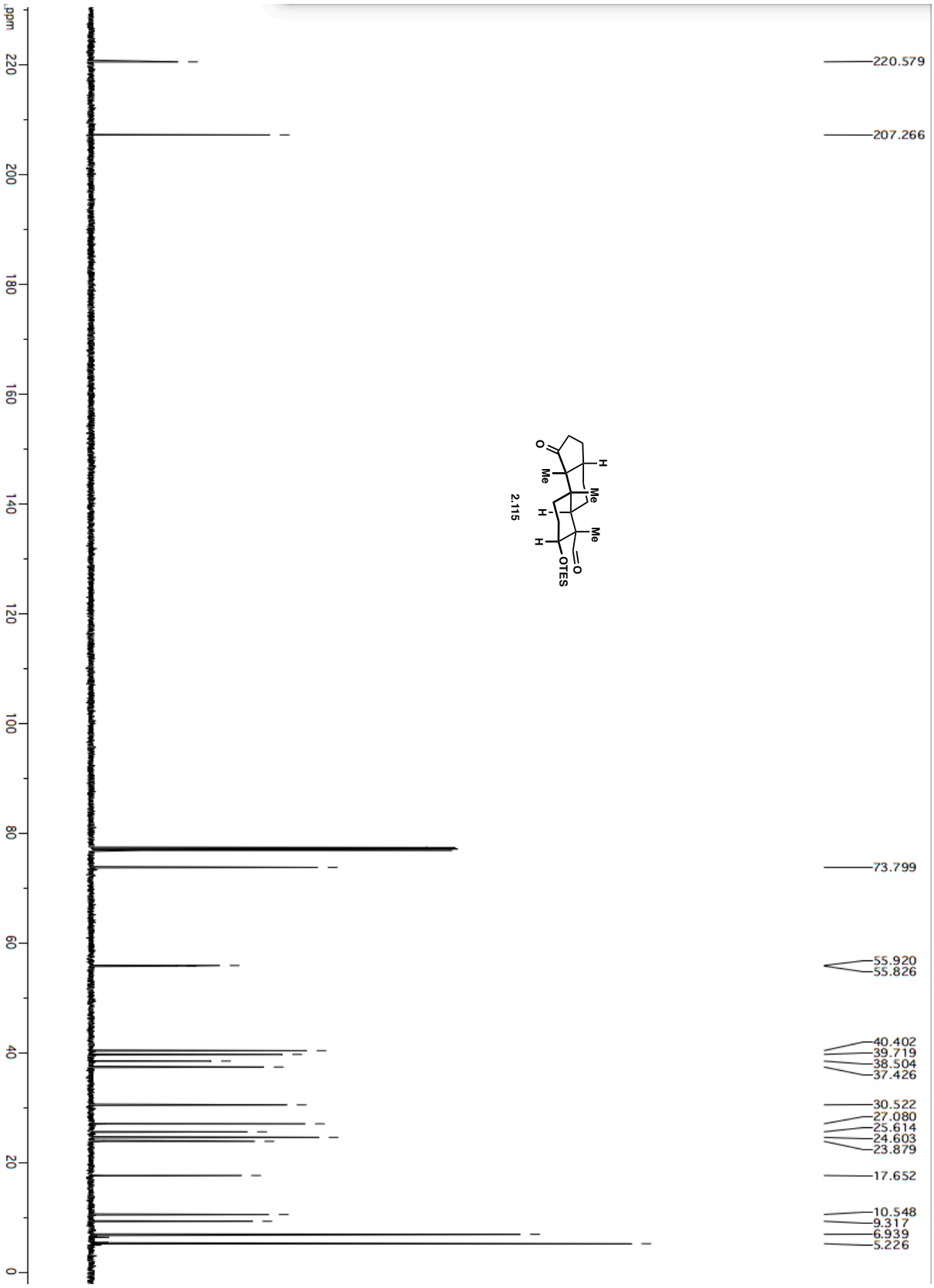
ppm
220
200
180
160
140
120
100
80
60
40
20
0
220.579
207.266
73.799
55.920
55.826
40.402
39.719
38.504
37.426
30.522
27.080
25.614
24.603
23.879
17.652
10.548
9.317
6.939
5.226
2.115
O
Me
H
Me
H
Me
H
O
OTES

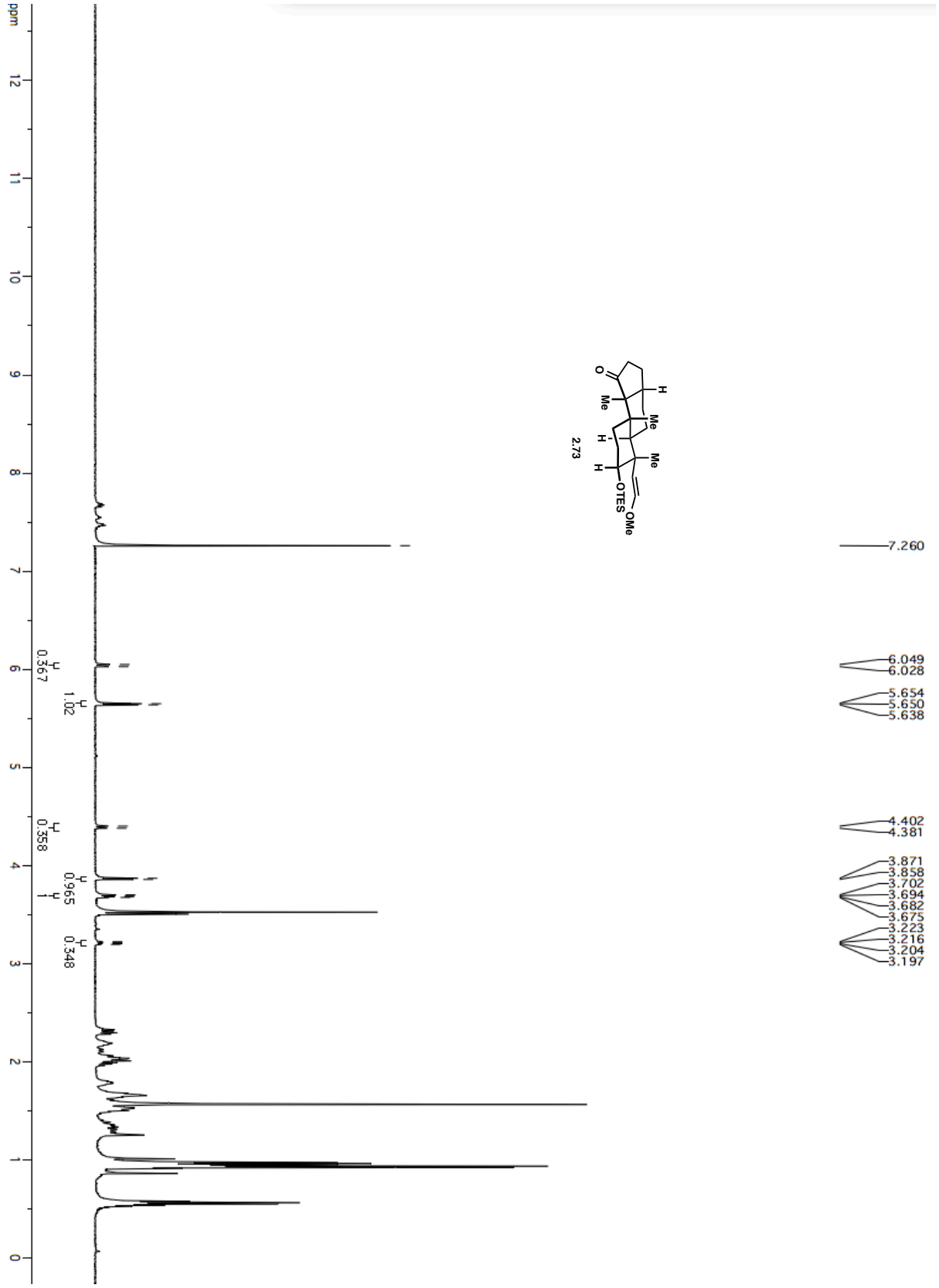
ppm
12
11
10
9
8
7
6
5
4
3
2
1
0
0.367
1.02
0.358
0.965
1
0.348
2.73
7.260
6.049
6.028
5.654
5.650
5.638
4.402
4.381
3.871
3.858
3.702
3.694
3.682
3.675
3.223
3.216
3.204
3.197

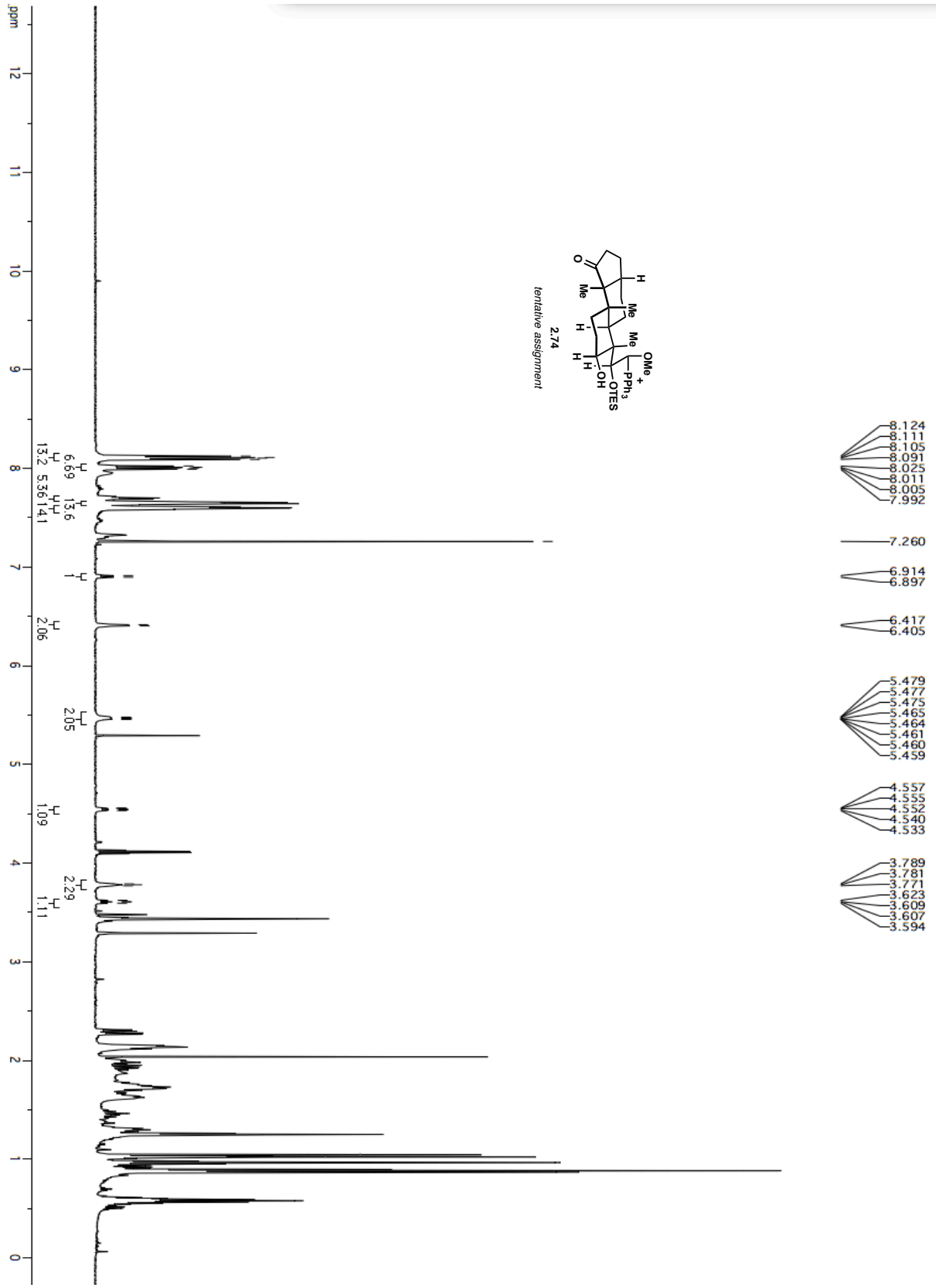
ppm
12
11
10
9
8
7
6
5
4
3
2
1
0
13.2
6.69
13.6
5.36
14.1
1
2.06
2.05
1.09
2.29
1.11
2.74
tentative assignment
8.124
8.111
8.105
8.091
8.025
8.011
8.005
7.992
7.260
6.914
6.897
6.417
6.405
5.479
5.477
5.475
5.465
5.464
5.461
5.460
5.459
4.557
4.555
4.552
4.540
4.533
3.789
3.781
3.771
3.623
3.609
3.607
3.594

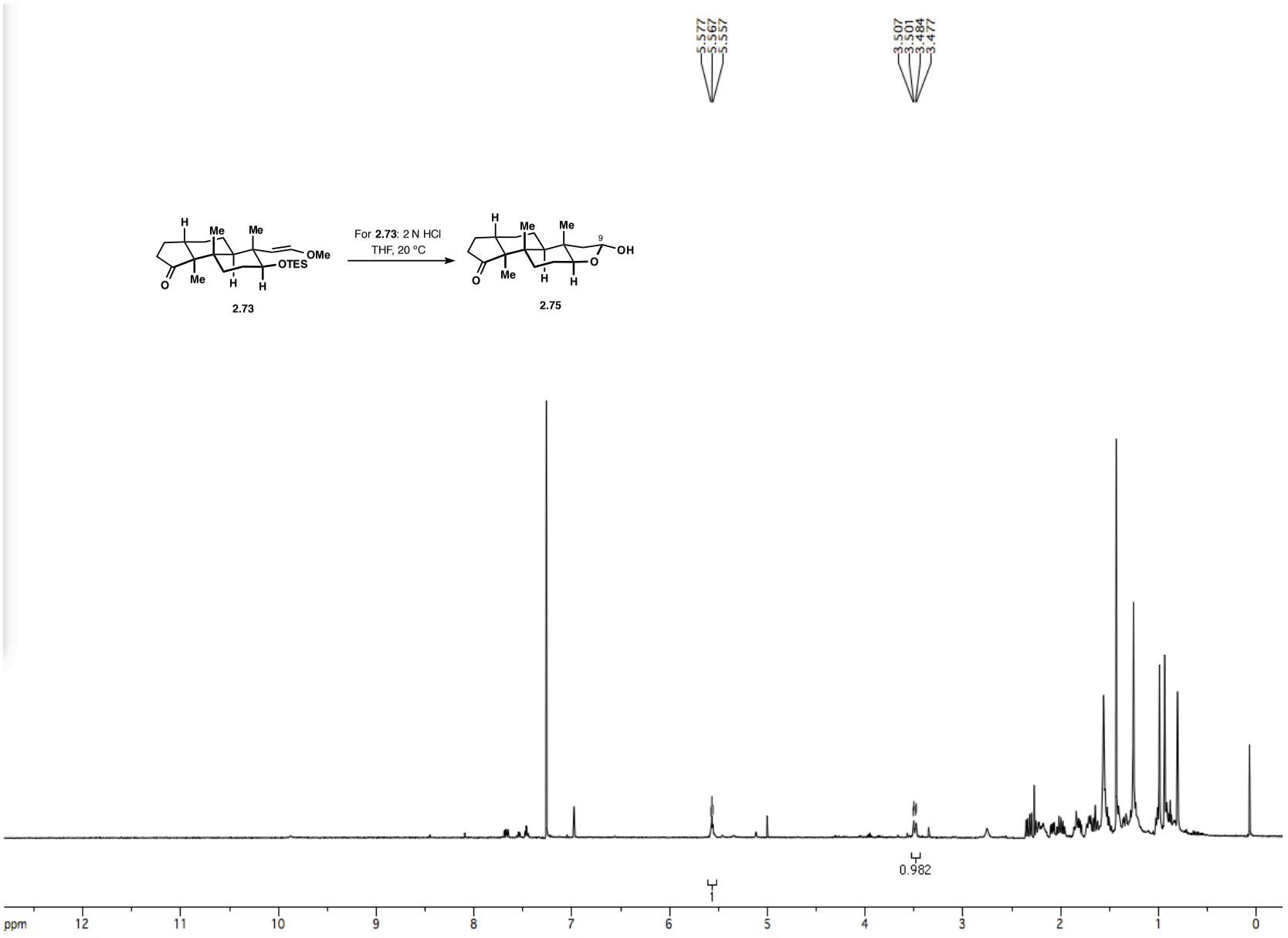
5.577
5.567
5.557
3.507
3.501
3.484
3.477
For 2.73: 2 N HCl
THF, 20 °C
OMe
OTES
OH
Me
H
O
2.73
2.75
0.982
ppm
12
11
10
9
8
7
6
5
4
3
2
1
0

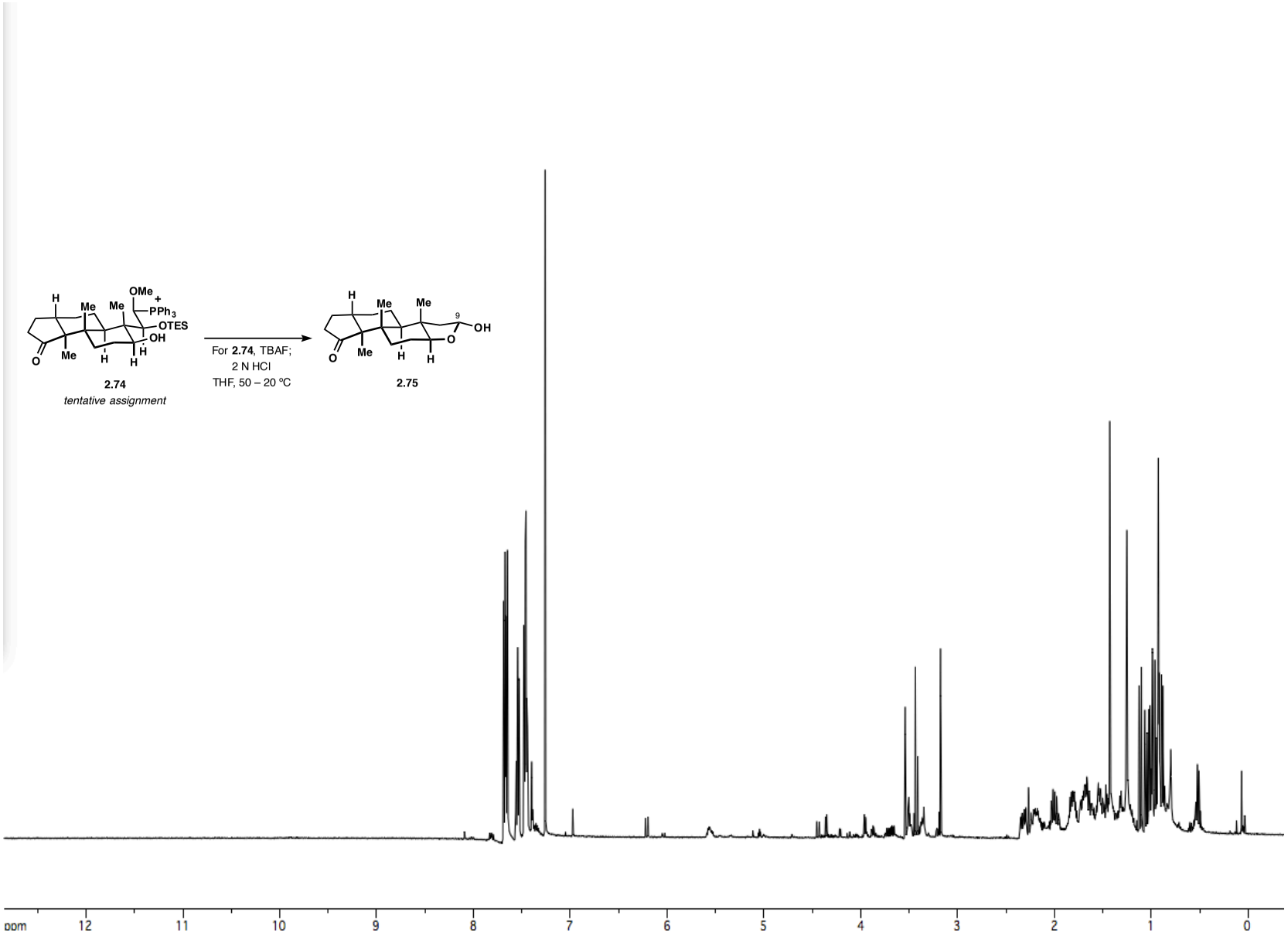
H
Me
Me
OMe
PPh3
OTES
OH
Me
O
H
H
2.74
tentative assignment
For 2.74, TBAF;
2 N HCl
THF, 50 – 20 °C
H
Me
Me
9
OH
O
Me
H
H
2.75
ppm
12
11
10
9
8
7
6
5
4
3
2
1
0

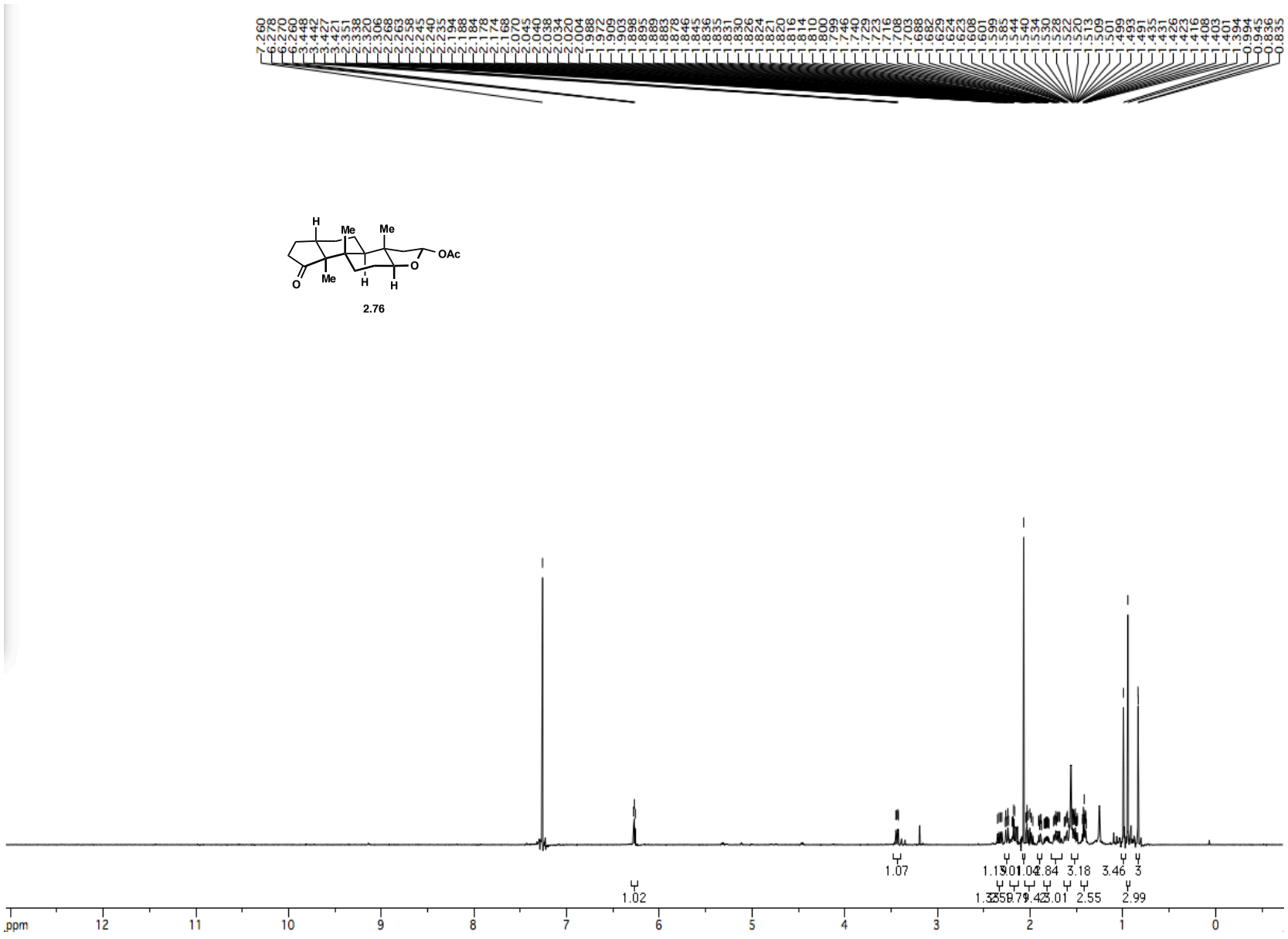
7.260
6.278
6.270
6.260
3.448
3.442
3.427
3.421
2.351
2.338
2.320
2.306
2.268
2.263
2.258
2.245
2.240
2.235
2.194
2.188
2.178
2.174
2.168
2.070
2.045
2.040
2.038
2.034
2.020
2.004
1.988
1.972
1.909
1.903
1.898
1.895
1.889
1.883
1.878
1.846
1.845
1.836
1.835
1.831
1.830
1.826
1.824
1.821
1.820
1.816
1.814
1.810
1.800
1.799
1.746
1.740
1.729
1.723
1.716
1.708
1.703
1.688
1.682
1.629
1.624
1.623
1.608
1.601
1.599
1.595
1.544
1.540
1.534
1.530
1.528
1.522
1.520
1.513
1.509
1.501
1.499
1.493
1.491
1.435
1.431
1.426
1.423
1.416
1.408
1.403
1.401
1.394
0.994
0.945
0.836
0.835
H
Me
Me
OAc
O
Me
H
H
O
2.76
1.07
1.02
1.13
3.01
1.04
2.84
3.18
3.46
3
2.55
2.99
ppm
12
11
10
9
8
7
6
5
4
3
2
1
0

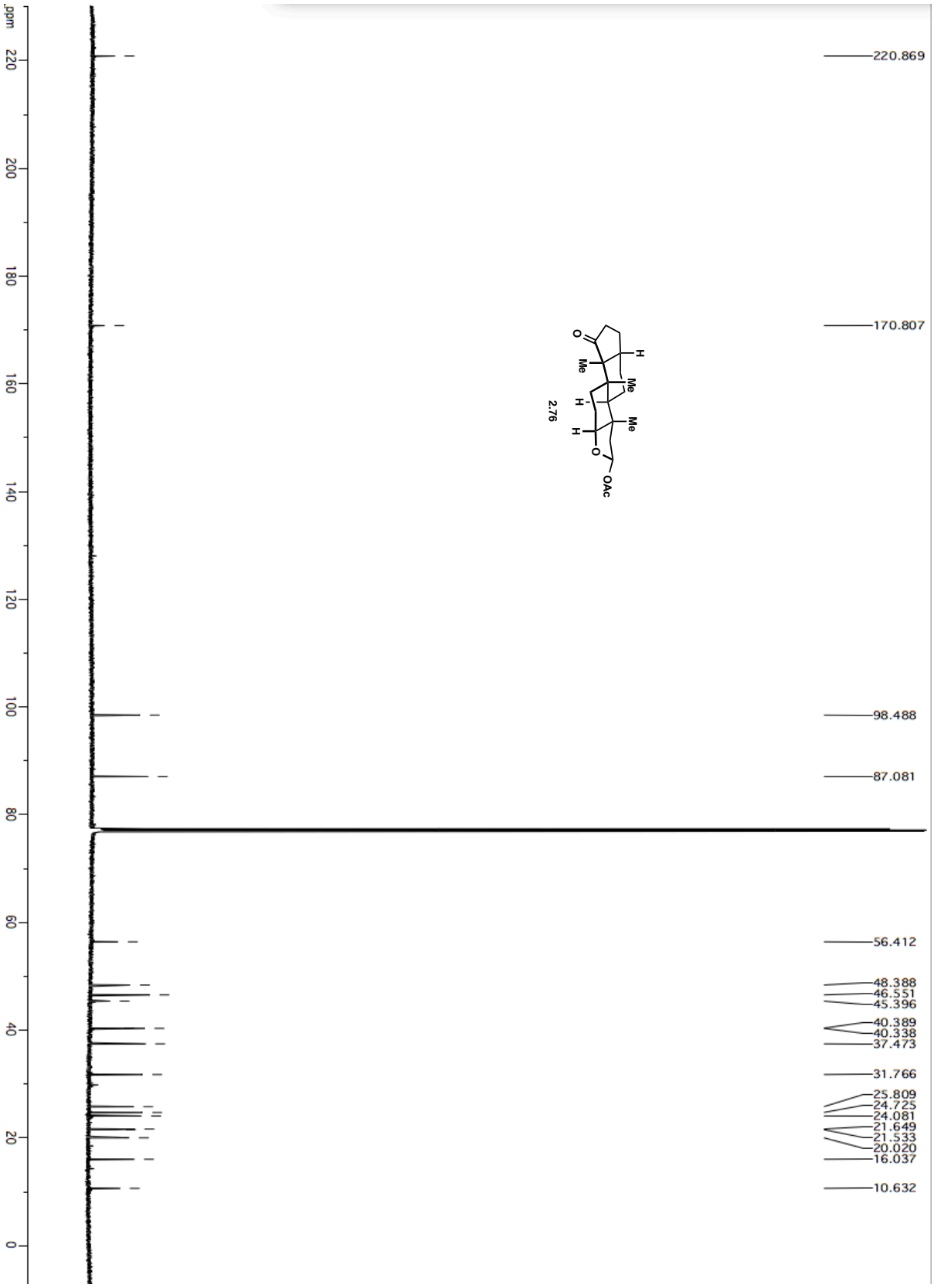
ppm
220
200
180
160
140
120
100
80
60
40
20
0
220.869
170.807
98.488
87.081
56.412
48.388
46.551
45.396
40.389
40.338
37.473
31.766
25.809
24.725
24.081
21.649
21.533
20.020
16.037
10.632
2.76
O
Me
H
Me
H
Me
H
O
OAc

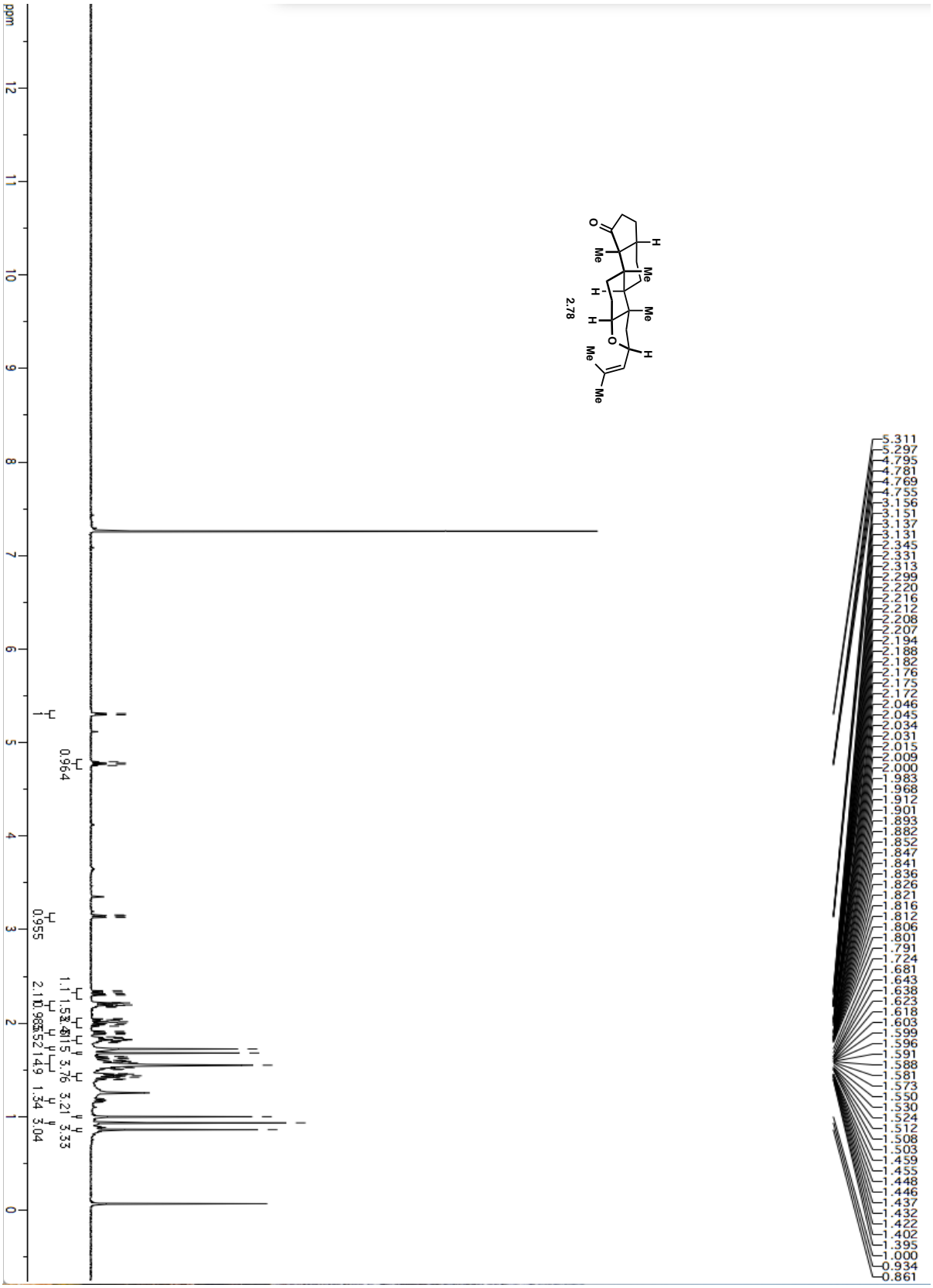
ppm
12
11
10
9
8
7
6
5
4
3
2
1
0
0.964
0.955
2.78
5.311
5.297
4.795
4.781
4.769
4.755
3.156
3.151
3.137
3.131
2.345
2.331
2.313
2.299
2.220
2.216
2.212
2.208
2.207
2.194
2.188
2.182
2.176
2.175
2.172
2.046
2.045
2.034
2.031
2.015
2.009
2.000
1.983
1.968
1.912
1.901
1.893
1.882
1.852
1.847
1.841
1.836
1.826
1.821
1.816
1.812
1.806
1.801
1.791
1.724
1.681
1.643
1.638
1.623
1.618
1.603
1.599
1.596
1.591
1.588
1.581
1.573
1.550
1.530
1.524
1.512
1.508
1.503
1.459
1.455
1.448
1.446
1.437
1.432
1.422
1.402
1.395
1.000
0.934
0.861

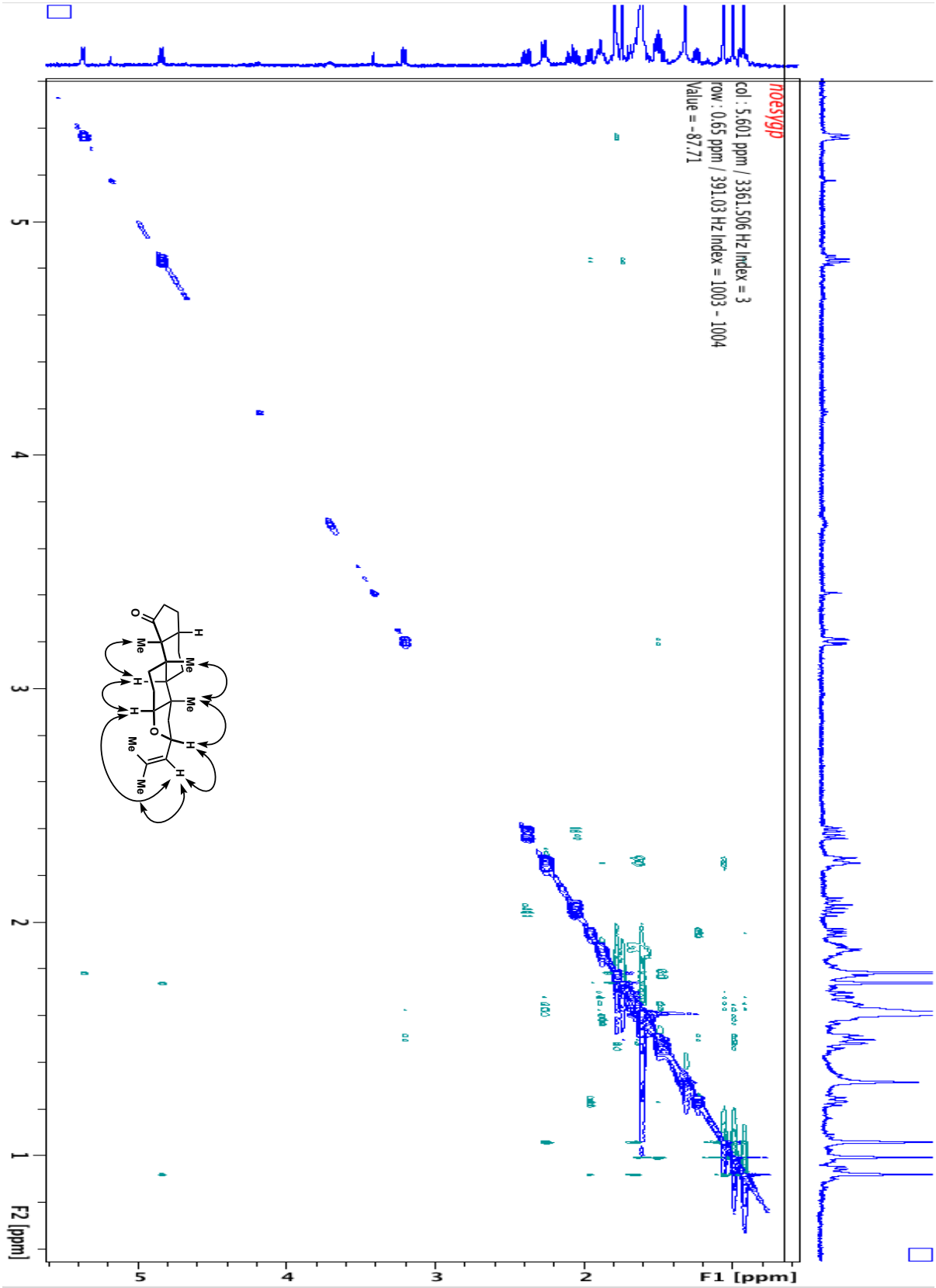
noesygp
col : 5.601 ppm / 3361.506 Hz Index = 3
row : 0.65 ppm / 391.03 Hz Index = 1003 - 1004
Value = -87.71
F1 [ppm]
F2 [ppm]
5
4
3
2
1
O
H
Me
Me
Me
H
H
H
O
H
Me
Me
H
Me

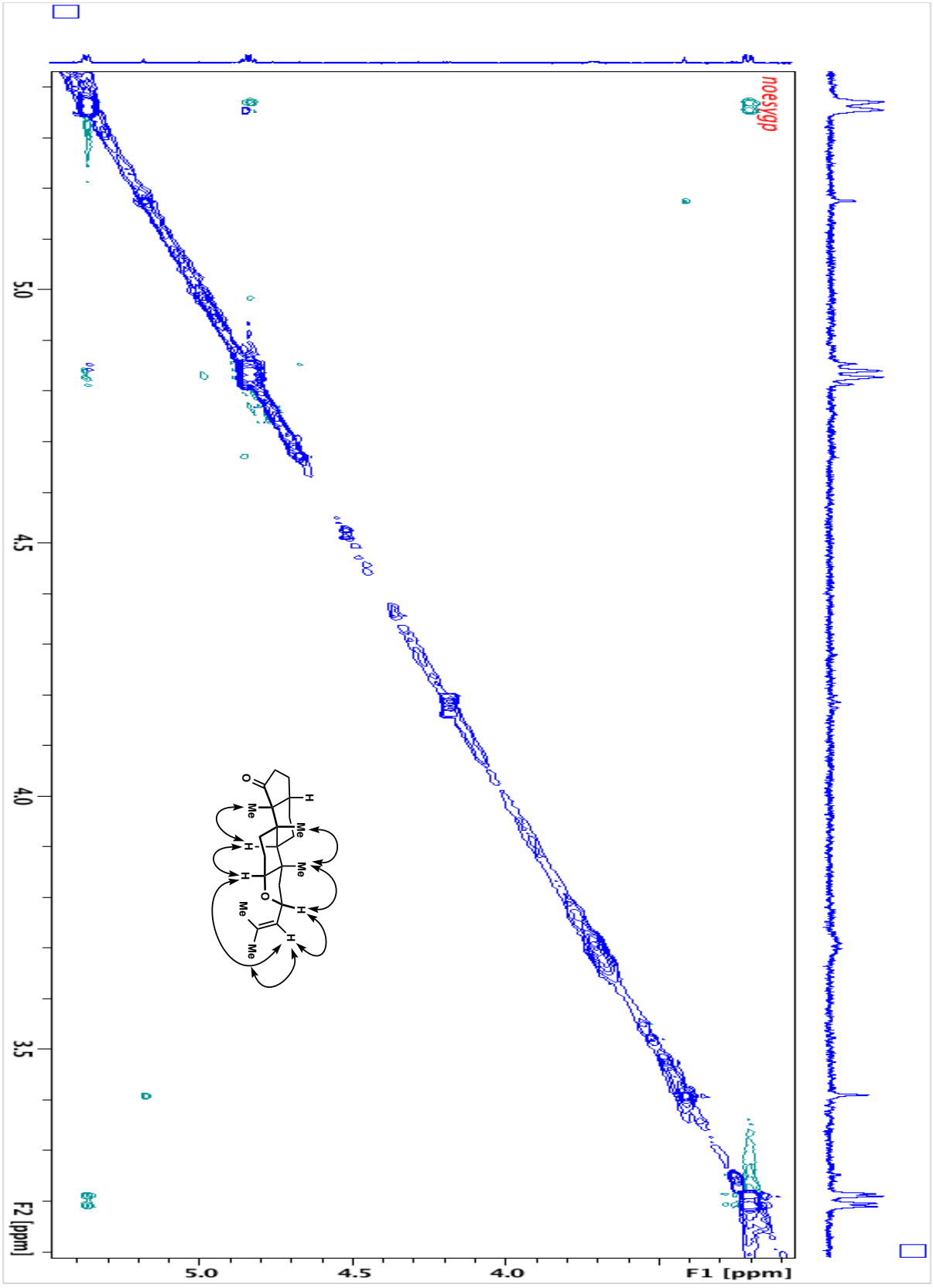
noesygp
F2 [ppm]
F1 [ppm]
5.0
4.5
4.0
3.5
O
H
Me
Me
Me
H
H
O
H
Me
Me
H

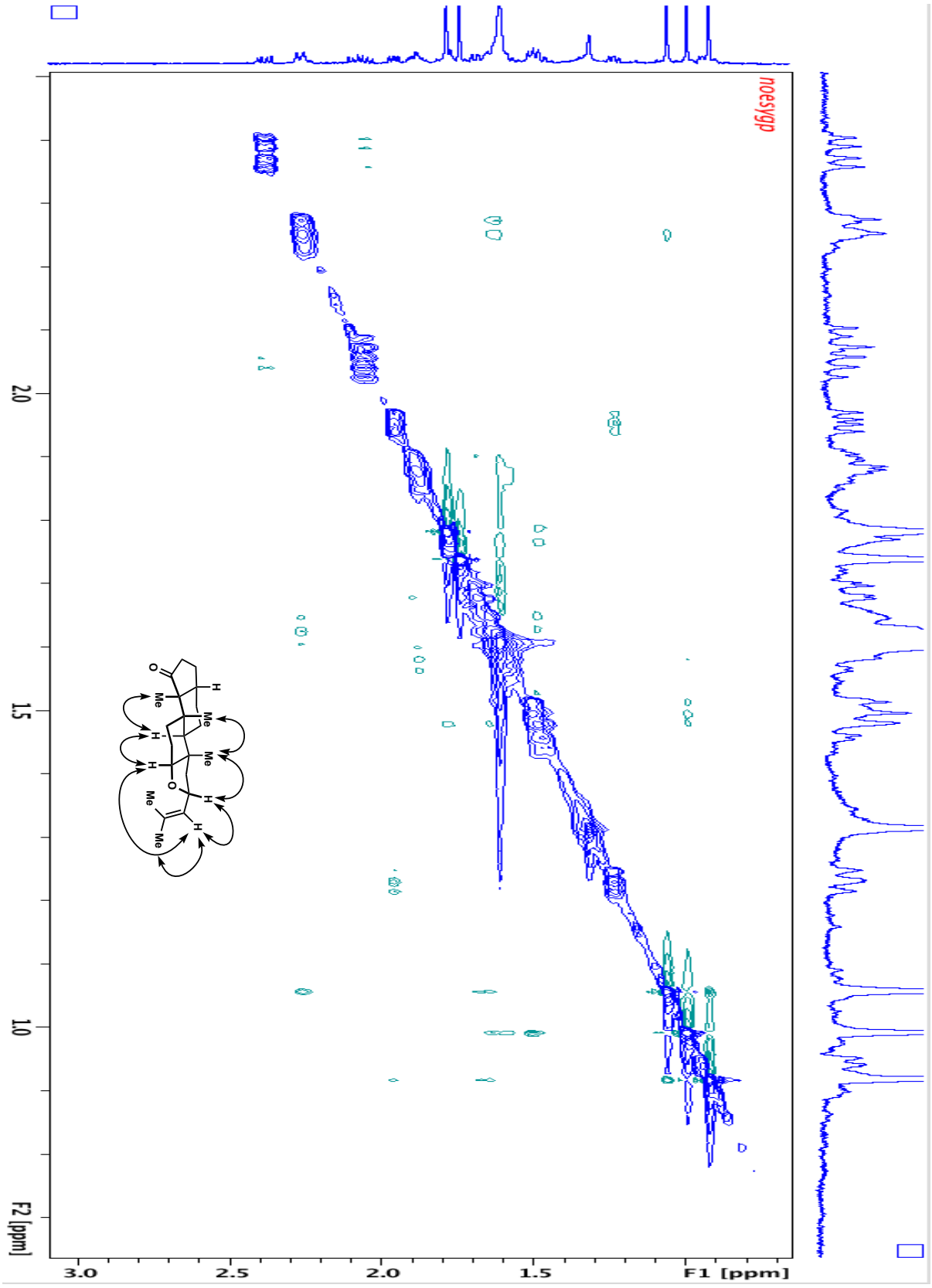
noesygp
F2 [ppm]
F1 [ppm]
3.0
2.5
2.0
1.5
1.0
Me
Me
Me
Me
Me
H
H
H
H
O
O

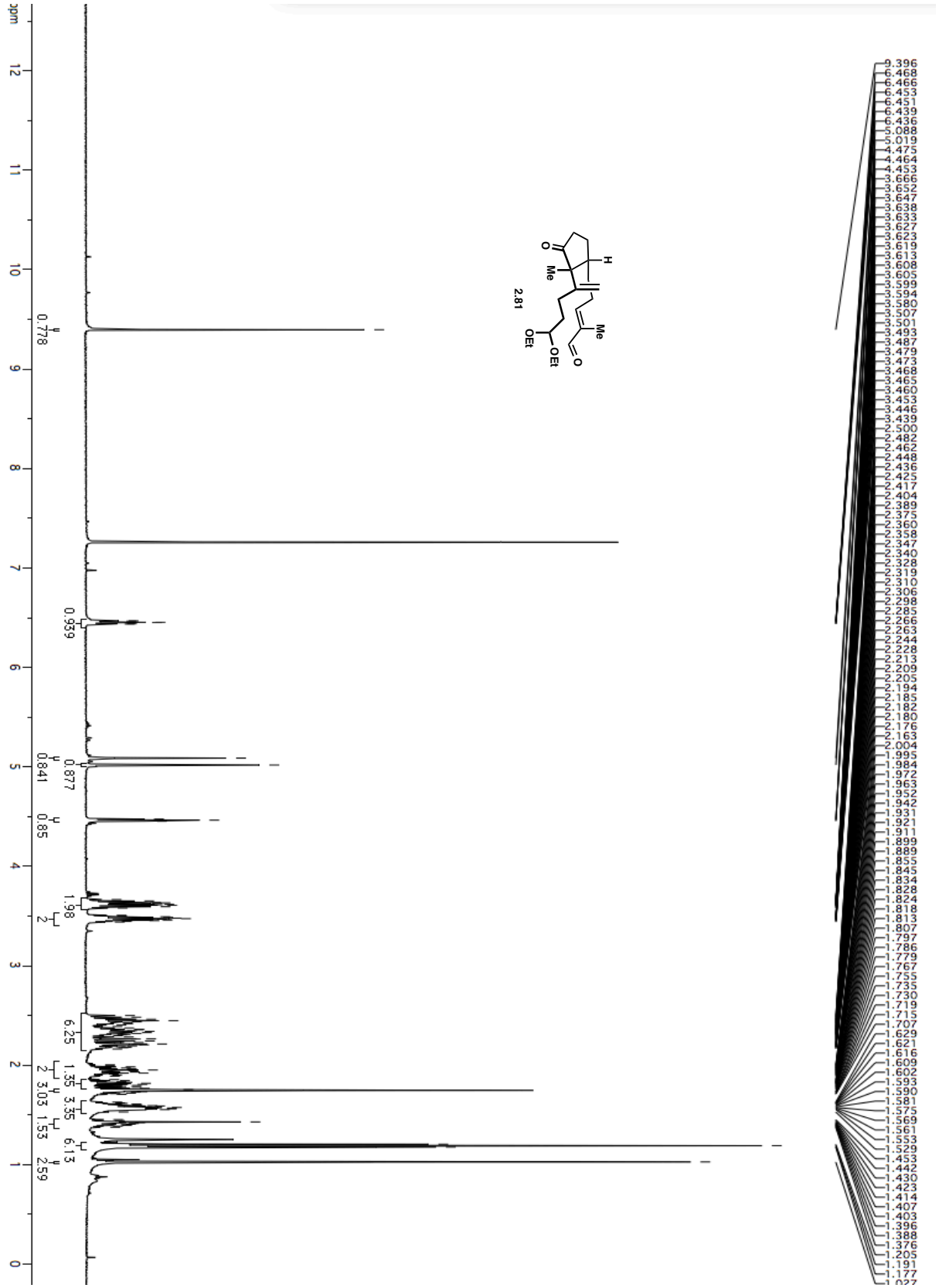
ppm
0.778
0.939
0.841
0.877
0.85
1.98
6.25
1.35
3.03
3.35
1.53
6.13
2.59
2.81
Me
O
H
Me
OEt
OEt
O

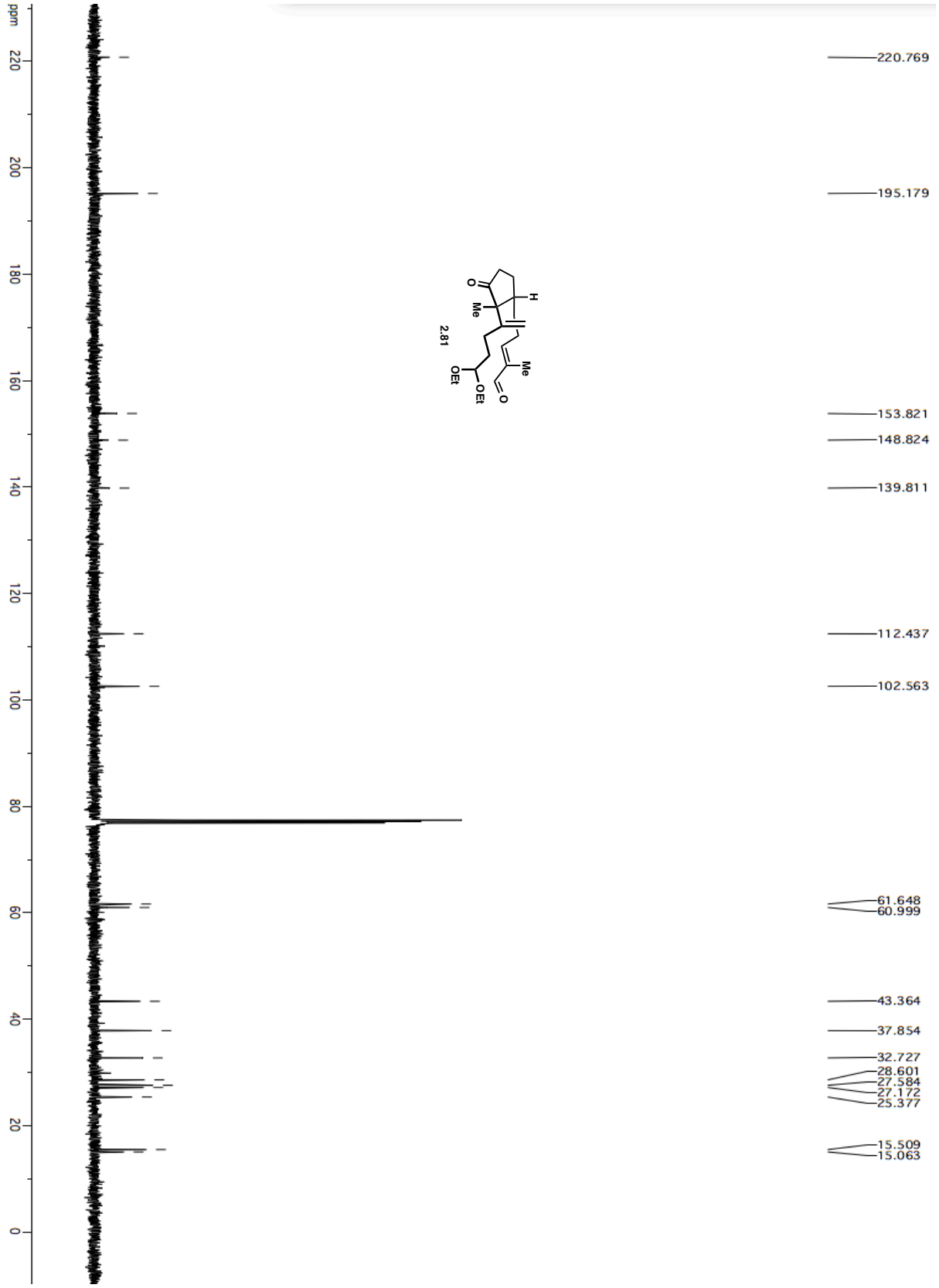
ppm
220
200
180
160
140
120
100
80
60
40
20
0
220.769
195.179
153.821
148.824
139.811
112.437
102.563
61.648
60.999
43.364
37.854
32.727
28.601
27.584
27.172
25.377
15.509
15.063
O
Me
H
2.81
OEt
Me
O

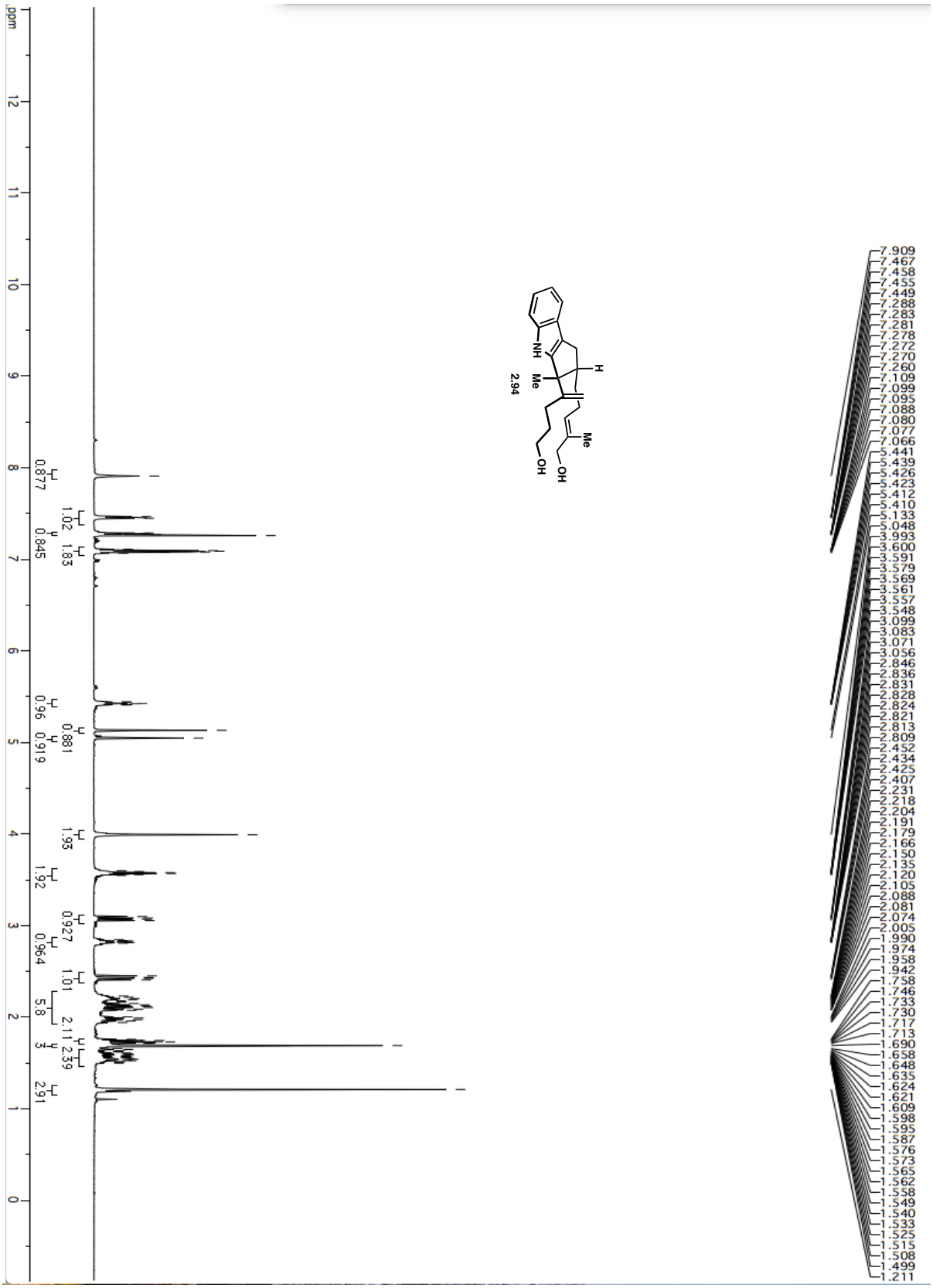
NH
Me
2.94
H
Me
OH
OH
7.909
7.467
7.458
7.455
7.449
7.288
7.283
7.281
7.278
7.272
7.270
7.260
7.109
7.099
7.095
7.088
7.080
7.077
7.066
5.441
5.439
5.426
5.423
5.412
5.410
5.133
5.048
3.993
3.600
3.591
3.579
3.569
3.561
3.557
3.548
3.099
3.083
3.071
3.056
2.846
2.836
2.831
2.828
2.824
2.821
2.813
2.809
2.452
2.434
2.425
2.407
2.231
2.218
2.204
2.191
2.179
2.166
2.150
2.135
2.120
2.105
2.088
2.081
2.074
2.005
1.990
1.974
1.958
1.942
1.758
1.746
1.733
1.730
1.717
1.713
1.690
1.658
1.648
1.635
1.624
1.621
1.609
1.598
1.595
1.587
1.576
1.573
1.565
1.562
1.558
1.549
1.540
1.533
1.525
1.515
1.508
1.499
1.211
ppm
0.877
1.02
1.83
0.845
0.96
0.881
0.919
1.93
1.92
0.927
0.964
1.01
5.8
2.11
2.39
3
2.91

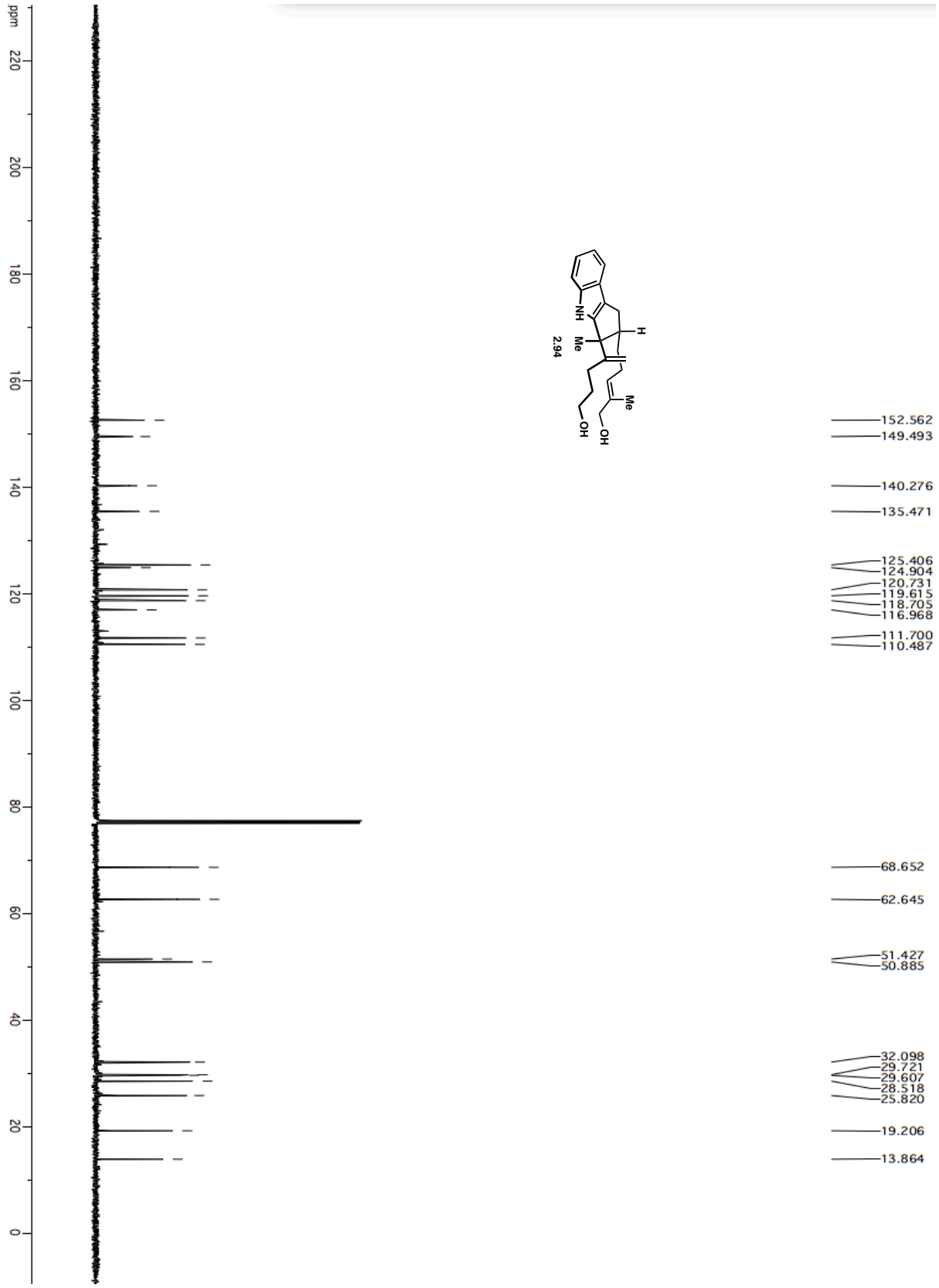
ppm
220
200
180
160
140
120
100
80
60
40
20
0
NH
Me
2.94
H
Me
OH
OH
152.562
149.493
140.276
135.471
125.406
124.904
120.731
119.615
118.705
116.968
111.700
110.487
68.652
62.645
51.427
50.885
32.098
29.721
29.607
28.518
25.820
19.206
13.864

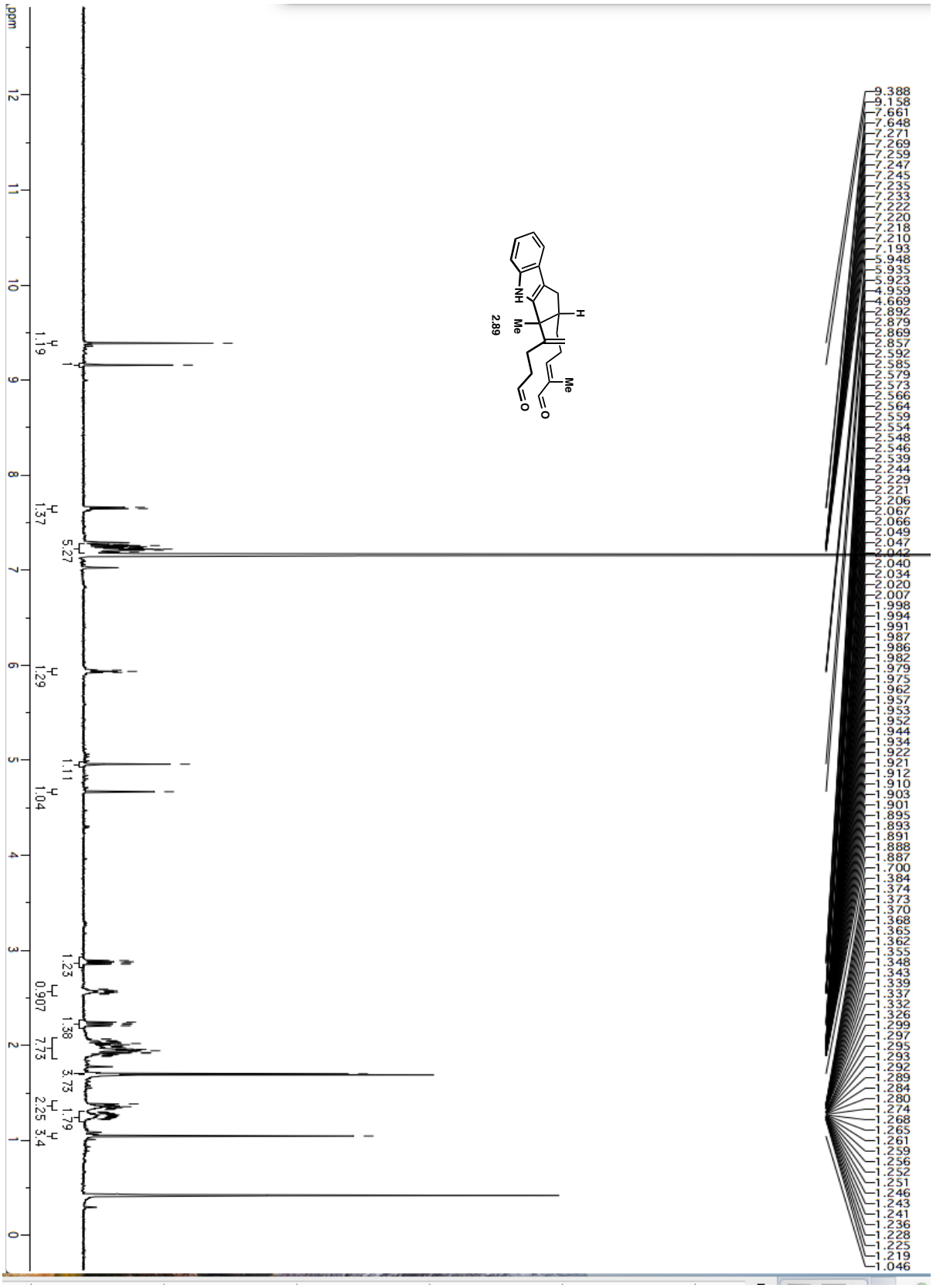
ppm
12
11
10
9
8
7
6
5
4
3
2
1
0
1.19
1
1.37
5.27
1.29
1.11
1.04
1.23
0.907
1.38
7.73
3.73
1.79
2.25
3.4
NH
Me
2.89
H
Me
O
O
9.388
9.158
7.661
7.648
7.271
7.269
7.259
7.247
7.245
7.235
7.233
7.222
7.220
7.218
7.210
7.193
5.948
5.935
5.923
4.959
4.669
2.892
2.879
2.869
2.857
2.592
2.585
2.579
2.573
2.566
2.564
2.559
2.554
2.548
2.546
2.539
2.244
2.229
2.221
2.206
2.067
2.066
2.049
2.047
2.042
2.040
2.034
2.020
2.007
1.998
1.994
1.991
1.987
1.986
1.982
1.979
1.975
1.962
1.957
1.953
1.952
1.944
1.934
1.922
1.921
1.912
1.910
1.903
1.901
1.895
1.893
1.891
1.888
1.887
1.700
1.384
1.374
1.373
1.370
1.368
1.365
1.362
1.355
1.348
1.343
1.339
1.337
1.332
1.326
1.299
1.297
1.295
1.293
1.292
1.289
1.284
1.280
1.274
1.268
1.265
1.261
1.259
1.256
1.252
1.251
1.246
1.243
1.241
1.236
1.228
1.225
1.219
1.046

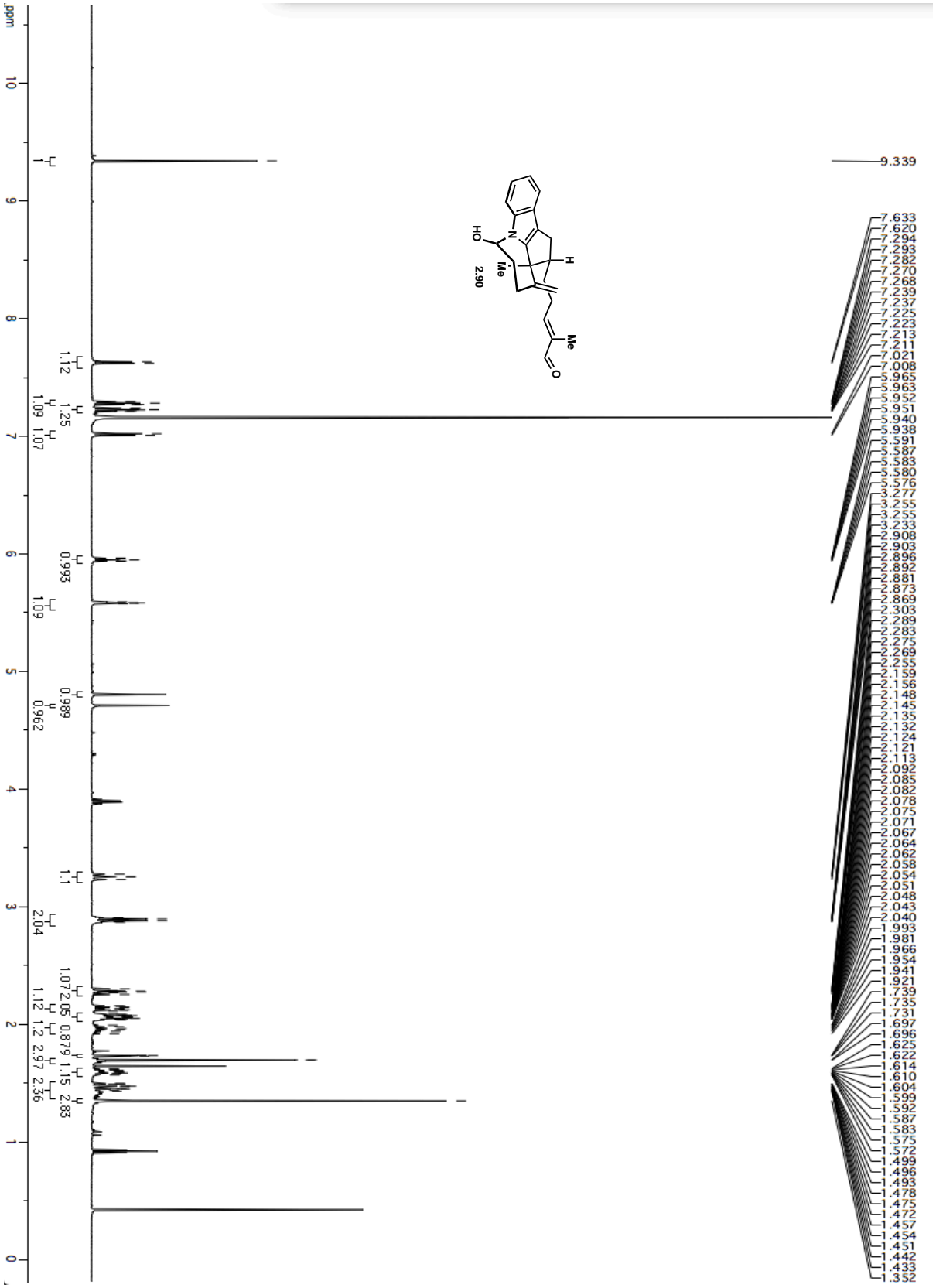
ppm
9.339
7.633
7.620
7.294
7.293
7.282
7.270
7.268
7.239
7.237
7.225
7.223
7.213
7.211
7.021
7.008
5.965
5.963
5.952
5.951
5.940
5.938
5.591
5.587
5.583
5.580
5.576
3.277
3.255
3.255
3.233
2.908
2.903
2.896
2.892
2.881
2.873
2.869
2.303
2.289
2.283
2.275
2.269
2.255
2.159
2.156
2.148
2.145
2.135
2.132
2.124
2.121
2.113
2.092
2.085
2.082
2.078
2.075
2.071
2.067
2.064
2.062
2.058
2.054
2.051
2.048
2.043
2.040
1.993
1.981
1.966
1.954
1.941
1.921
1.739
1.735
1.731
1.697
1.696
1.625
1.622
1.614
1.610
1.604
1.599
1.592
1.587
1.583
1.575
1.572
1.499
1.496
1.493
1.478
1.475
1.472
1.457
1.454
1.451
1.442
1.433
1.352
1.12
1.25
1.09
1.07
0.993
1.09
0.989
0.962
1.1
2.04
1.07
2.05
0.879
1.15
2.83
1.12
1.2
2.97
2.36
HO
N
Me
2.90
H
Me
O

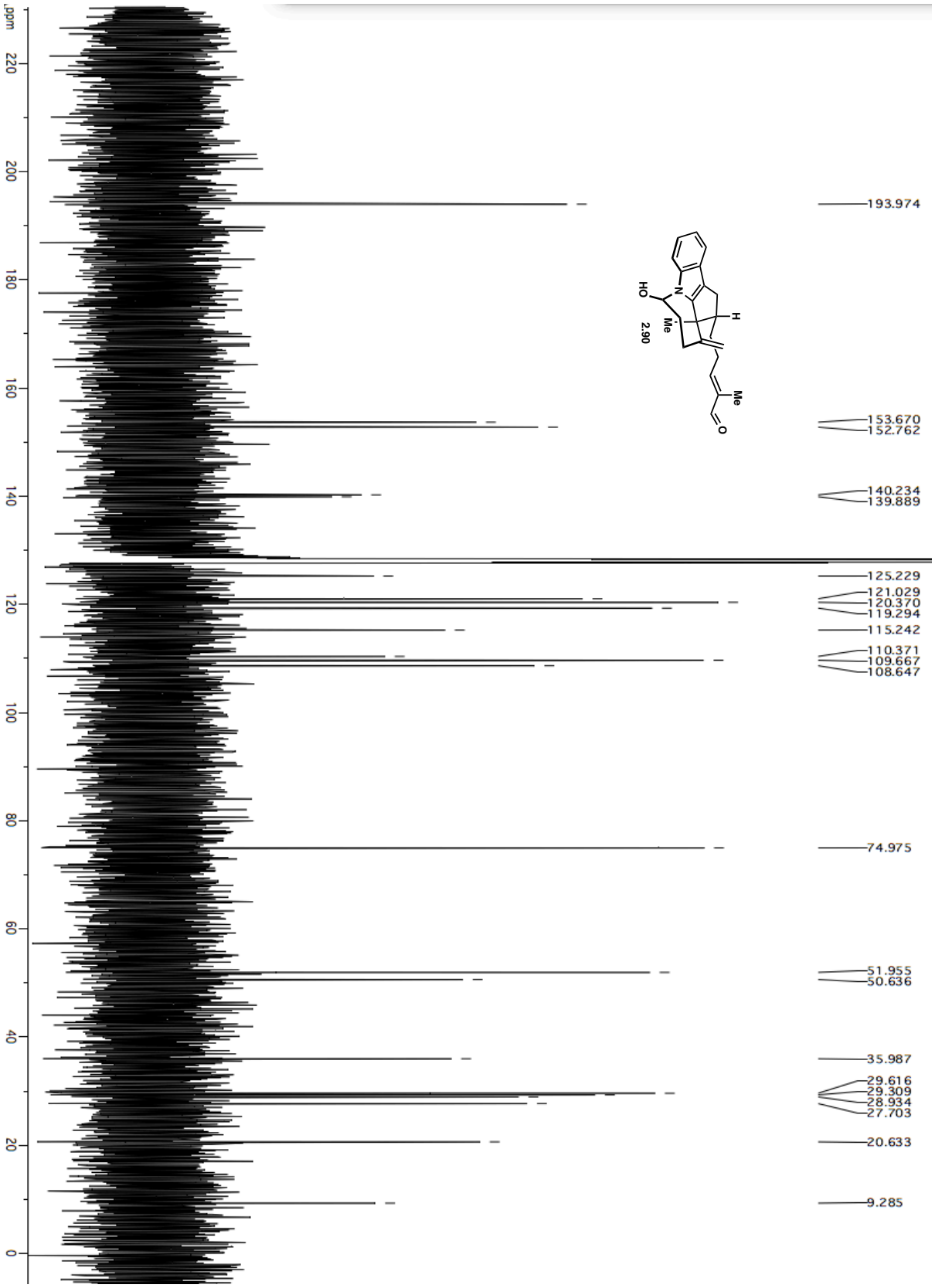
ppm
220
200
180
160
140
120
100
80
60
40
20
0
193.974
153.670
152.762
140.234
139.889
125.229
121.029
120.370
119.294
115.242
110.371
109.667
108.647
74.975
51.955
50.636
35.987
29.616
29.309
28.934
27.703
20.633
9.285
HO
N
Me
2.90
H
Me
O

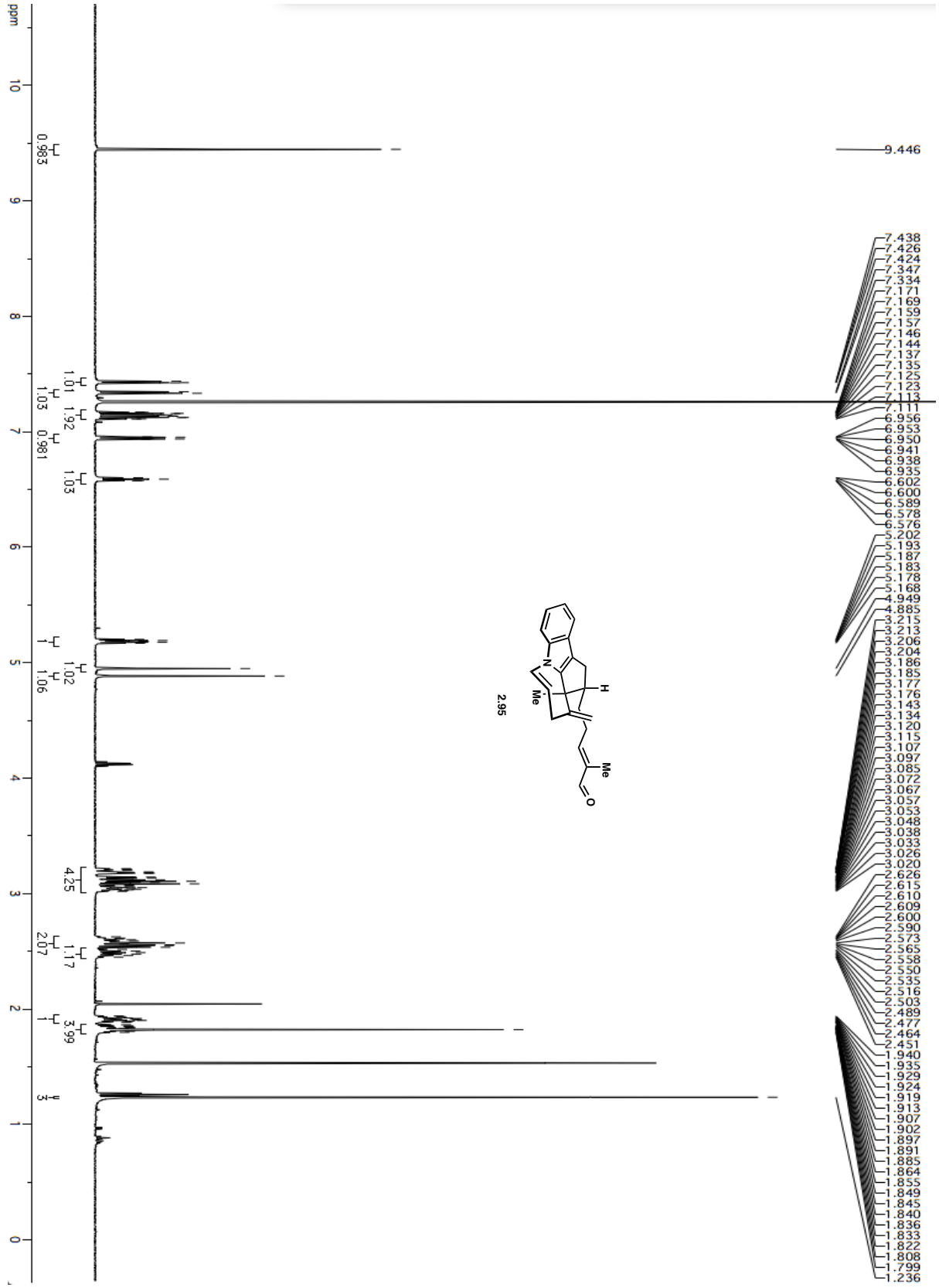
9.446
7.438
7.426
7.424
7.347
7.334
7.171
7.169
7.159
7.157
7.146
7.144
7.137
7.135
7.125
7.123
7.113
7.111
6.956
6.953
6.950
6.941
6.938
6.935
6.602
6.600
6.589
6.578
6.576
5.202
5.193
5.187
5.183
5.178
5.168
4.949
4.885
3.215
3.213
3.206
3.204
3.186
3.185
3.177
3.176
3.143
3.134
3.120
3.115
3.107
3.097
3.085
3.072
3.067
3.057
3.053
3.048
3.038
3.033
3.026
3.020
2.626
2.615
2.610
2.609
2.600
2.590
2.573
2.565
2.558
2.550
2.535
2.516
2.503
2.489
2.477
2.464
2.451
1.940
1.935
1.929
1.924
1.919
1.913
1.907
1.902
1.897
1.891
1.885
1.864
1.855
1.849
1.845
1.840
1.836
1.833
1.822
1.808
1.799
1.236
0.983
1.01
1.03
1.92
0.981
1.03
1.02
1.06
4.25
2.07
1.17
3.99
3
2.95
N
Me
H
Me
O
ppm

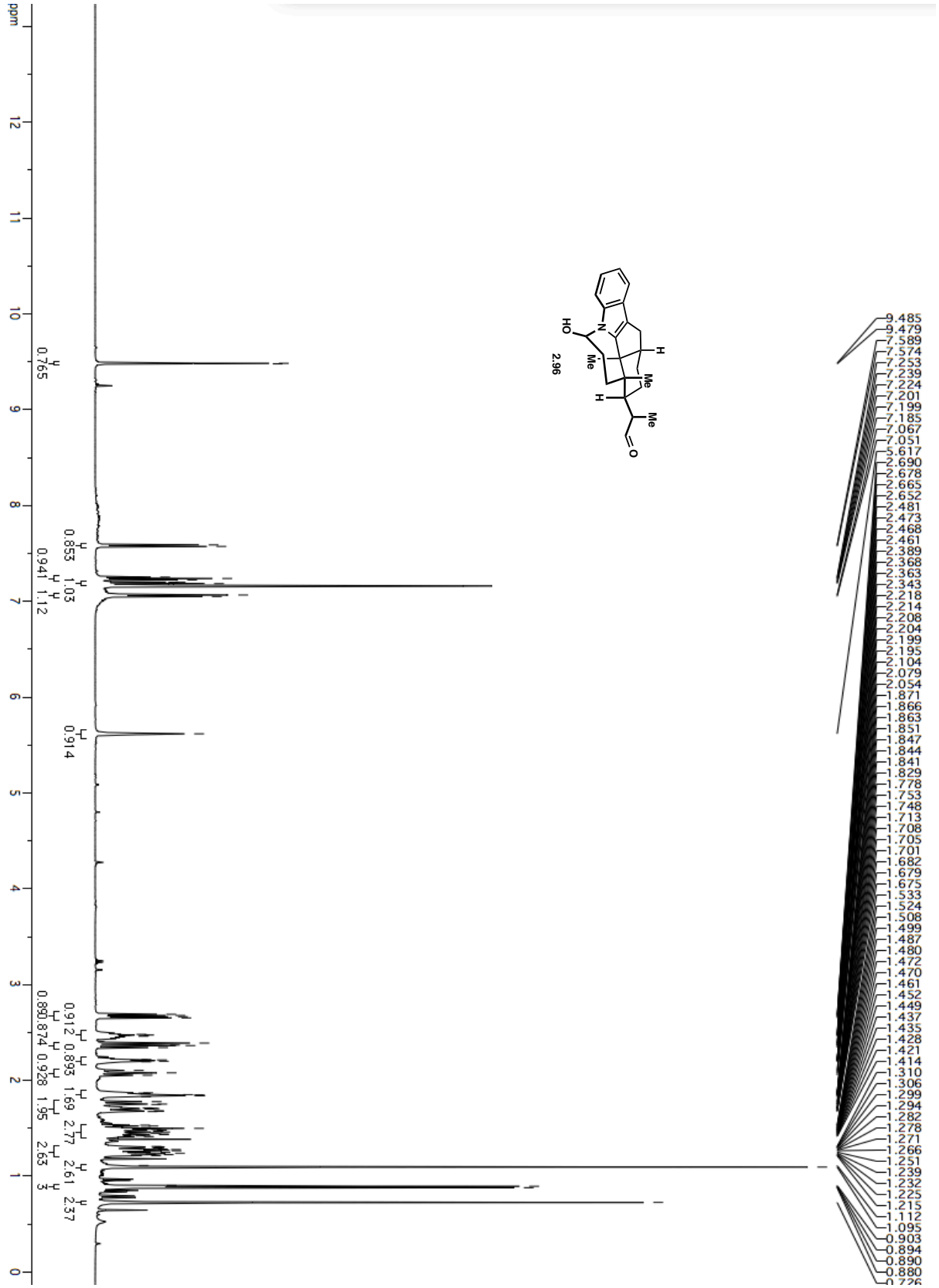
ppm
0.765
0.853
1.03
0.941
1.12
0.914
0.912
0.893
1.69
0.890
0.874
0.928
1.95
2.77
2.61
2.63
3
2.37
2.96
HO
N
Me
H
Me
H
Me
O
9.485
9.479
7.589
7.574
7.253
7.239
7.224
7.201
7.199
7.185
7.067
7.051
5.617
2.690
2.678
2.665
2.652
2.481
2.473
2.468
2.461
2.389
2.368
2.363
2.343
2.218
2.214
2.208
2.204
2.199
2.195
2.104
2.079
2.054
1.871
1.866
1.863
1.851
1.847
1.844
1.841
1.829
1.778
1.753
1.748
1.713
1.708
1.705
1.701
1.682
1.679
1.675
1.533
1.524
1.508
1.499
1.487
1.480
1.472
1.470
1.461
1.452
1.449
1.437
1.435
1.428
1.421
1.414
1.310
1.306
1.299
1.294
1.282
1.278
1.271
1.266
1.251
1.239
1.232
1.225
1.215
1.112
1.095
0.903
0.894
0.890
0.880

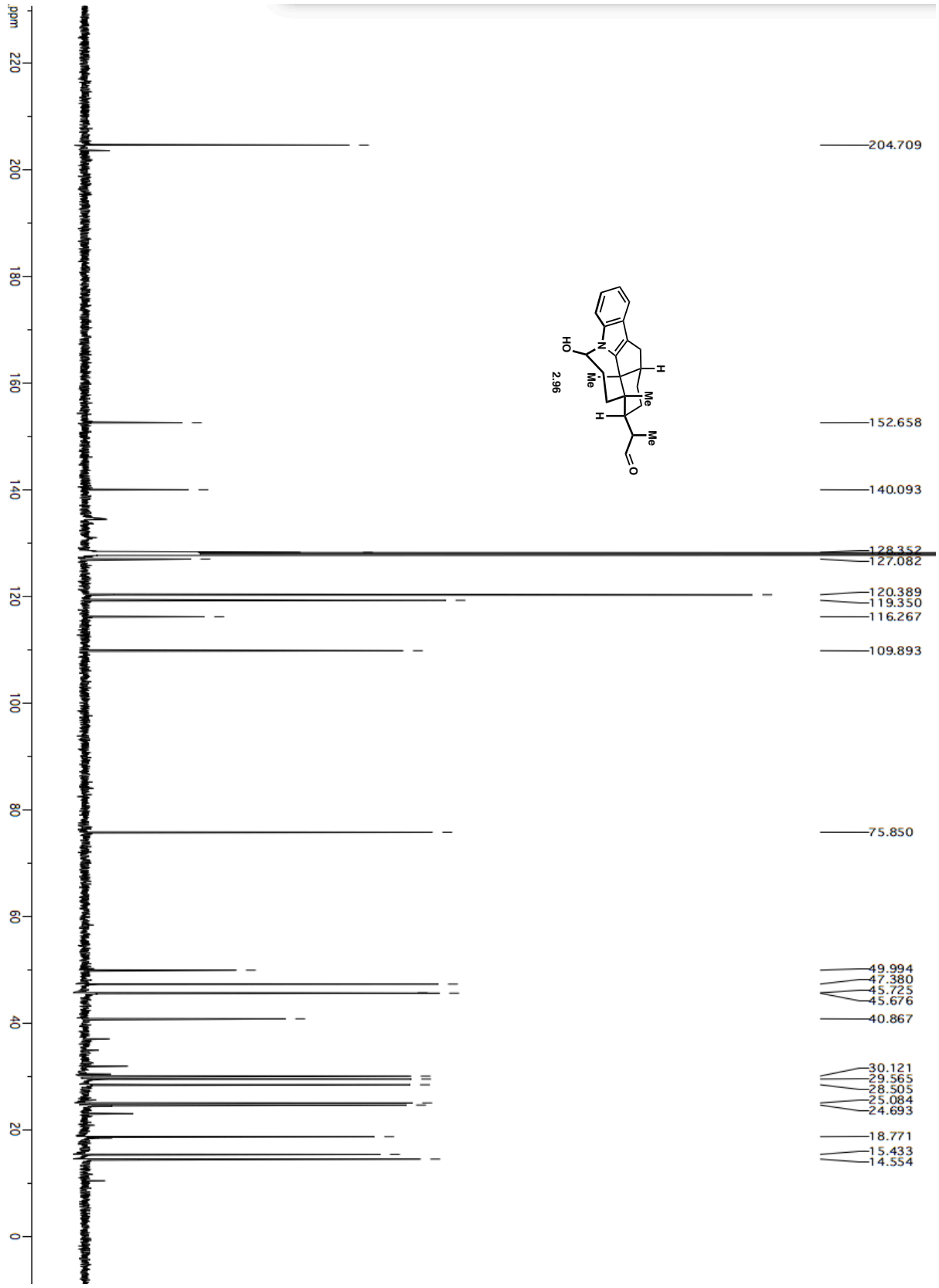
ppm
220
200
180
160
140
120
100
80
60
40
20
0
204.709
152.658
140.093
128.352
127.082
120.389
119.350
116.267
109.893
75.850
49.994
47.380
45.725
45.676
40.867
30.121
29.565
28.505
25.084
24.693
18.771
15.433
14.554
HO
N
Me
2.96
H
Me
H
Me
O

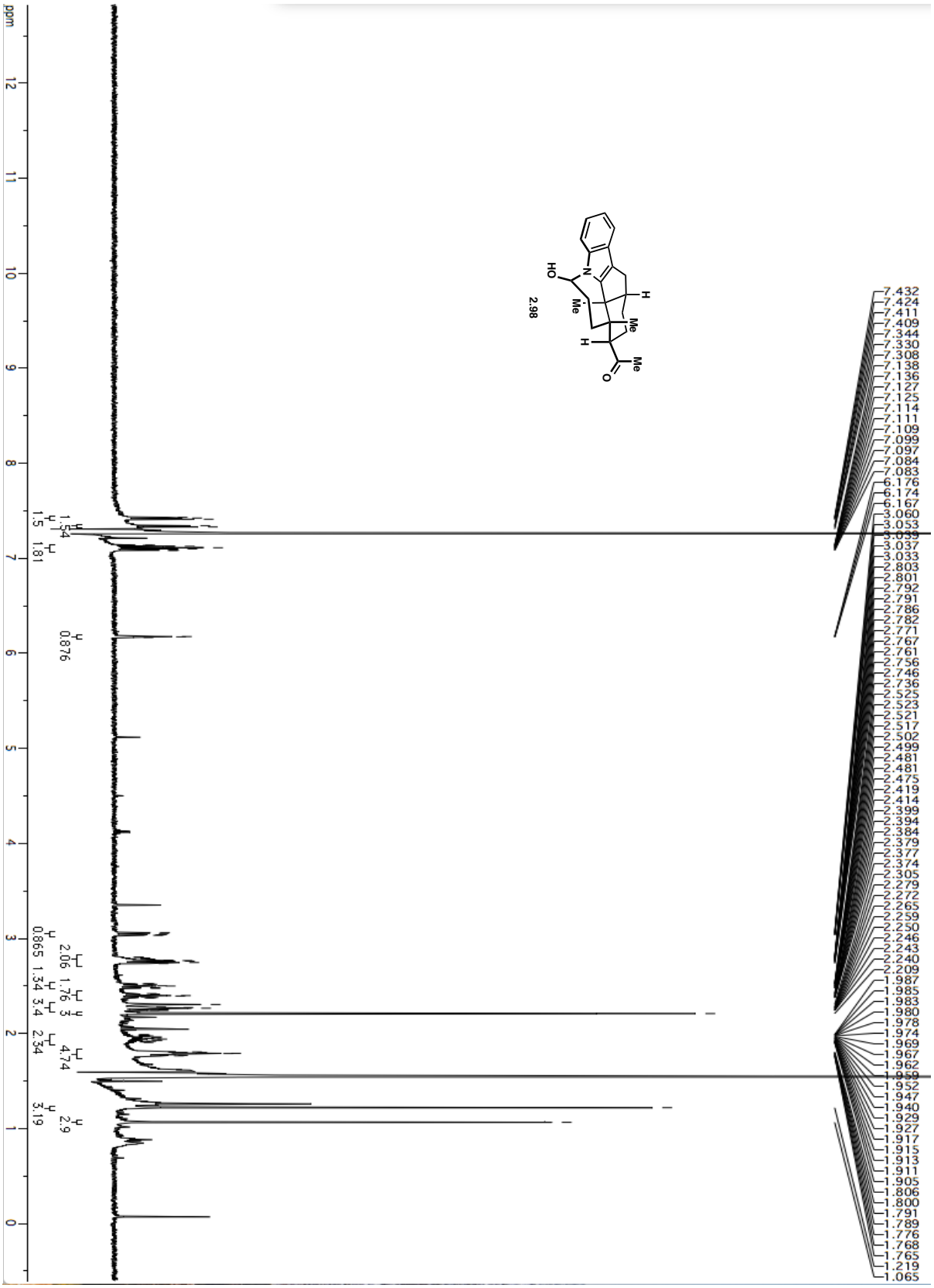
ppm
12
11
10
9
8
7
6
5
4
3
2
1
0
HO
N
Me
H
Me
H
Me
O
2.98
1.5
1.54
1.81
0.876
0.865
2.06
1.34
1.76
3.4
3
2.34
4.74
3.19
2.9
7.432
7.424
7.411
7.409
7.344
7.330
7.308
7.138
7.136
7.127
7.125
7.114
7.111
7.109
7.099
7.097
7.084
7.083
6.176
6.174
6.167
3.060
3.053
3.039
3.037
3.033
2.803
2.801
2.792
2.791
2.786
2.782
2.771
2.767
2.761
2.756
2.746
2.736
2.525
2.523
2.521
2.517
2.502
2.499
2.481
2.481
2.475
2.419
2.414
2.399
2.394
2.384
2.379
2.377
2.374
2.305
2.279
2.272
2.265
2.259
2.250
2.246
2.243
2.240
2.209
1.987
1.985
1.983
1.980
1.978
1.974
1.969
1.967
1.962
1.959
1.952
1.947
1.940
1.929
1.927
1.917
1.915
1.913
1.911
1.905
1.806
1.800
1.791
1.789
1.776
1.768
1.765
1.219
1.065

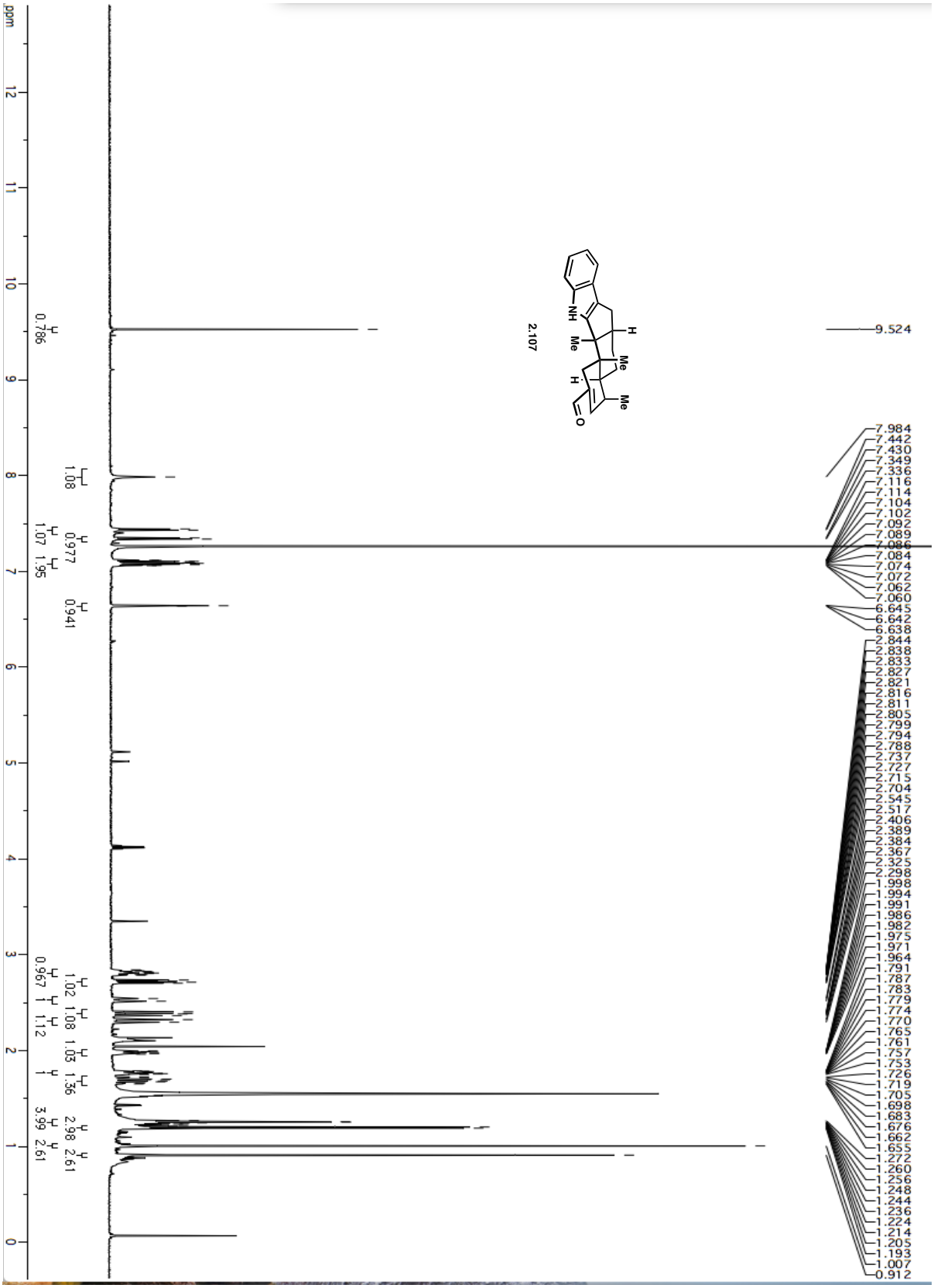
ppm
12
11
10
9
8
7
6
5
4
3
2
1
0
0.786
1.08
0.977
1.07
1.95
0.941
1.02
1.08
0.967
1
1.12
1.03
1.36
1
2.98
3.99
2.61
2.61
2.107
NH
Me
H
Me
H
Me
O
9.524
7.984
7.442
7.430
7.349
7.336
7.116
7.114
7.104
7.102
7.092
7.089
7.086
7.084
7.074
7.072
7.062
7.060
6.645
6.642
6.638
2.844
2.838
2.833
2.827
2.821
2.816
2.811
2.805
2.799
2.794
2.788
2.737
2.727
2.715
2.704
2.545
2.517
2.406
2.389
2.384
2.367
2.325
2.298
1.998
1.994
1.991
1.986
1.982
1.975
1.971
1.964
1.791
1.787
1.783
1.779
1.774
1.770
1.765
1.761
1.757
1.753
1.726
1.719
1.705
1.698
1.683
1.676
1.662
1.655
1.272
1.260
1.256
1.248
1.244
1.236
1.224
1.214
1.205
1.193
1.007
0.912

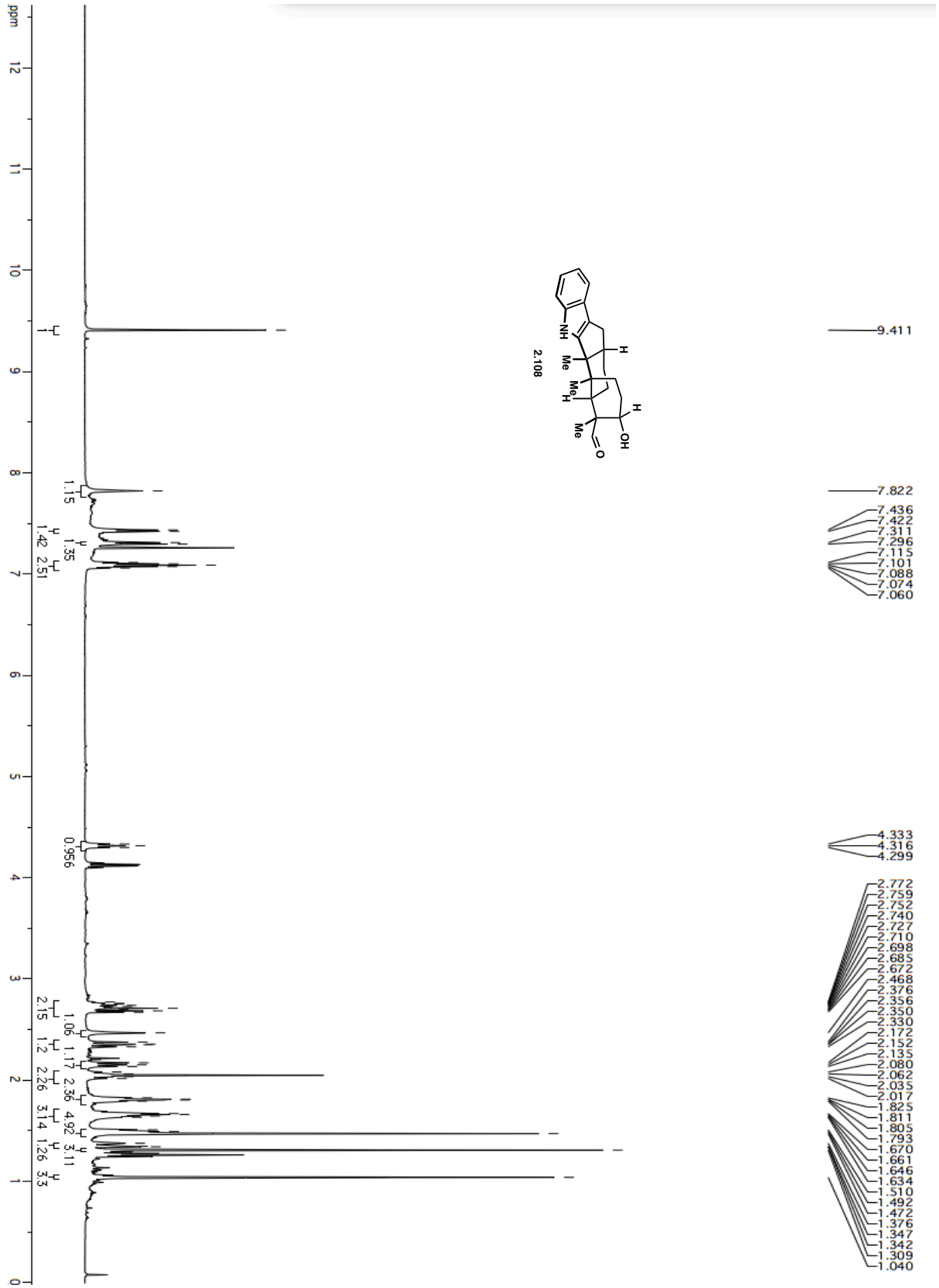
ppm
12
11
10
9
8
7
6
5
4
3
2
1
0
1
1.15
1.42
2.51
1.35
0.956
2.15
1.06
1.2
1.17
2.26
2.36
3.14
4.92
1.26
3.11
3.3
NH
Me
Me
H
H
Me
OH
O
2.108
9.411
7.822
7.436
7.422
7.311
7.296
7.115
7.101
7.088
7.074
7.060
4.333
4.316
4.299
2.772
2.759
2.752
2.740
2.727
2.710
2.698
2.685
2.672
2.468
2.376
2.356
2.350
2.330
2.172
2.152
2.135
2.080
2.062
2.035
2.017
1.825
1.811
1.805
1.793
1.670
1.661
1.646
1.634
1.510
1.492
1.472
1.376
1.347
1.342
1.309
1.040

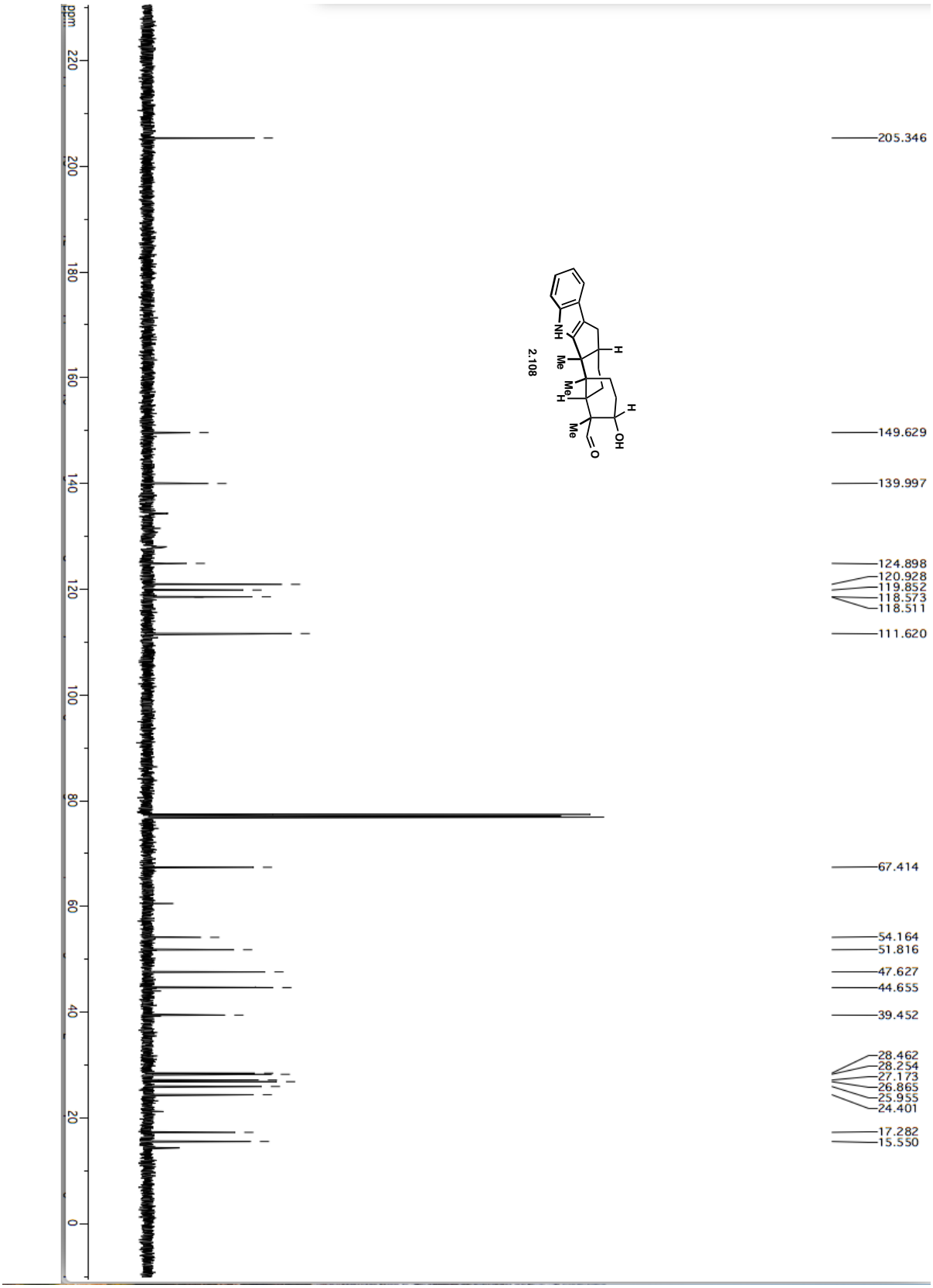
ppm
220
200
180
160
140
120
100
80
60
40
20
0
205.346
149.629
139.997
124.898
120.928
119.852
118.573
118.511
111.620
67.414
54.164
51.816
47.627
44.655
39.452
28.462
28.254
27.173
26.865
25.955
24.401
17.282
15.550
2.108
NH
Me
Me
H
H
OH
Me
O

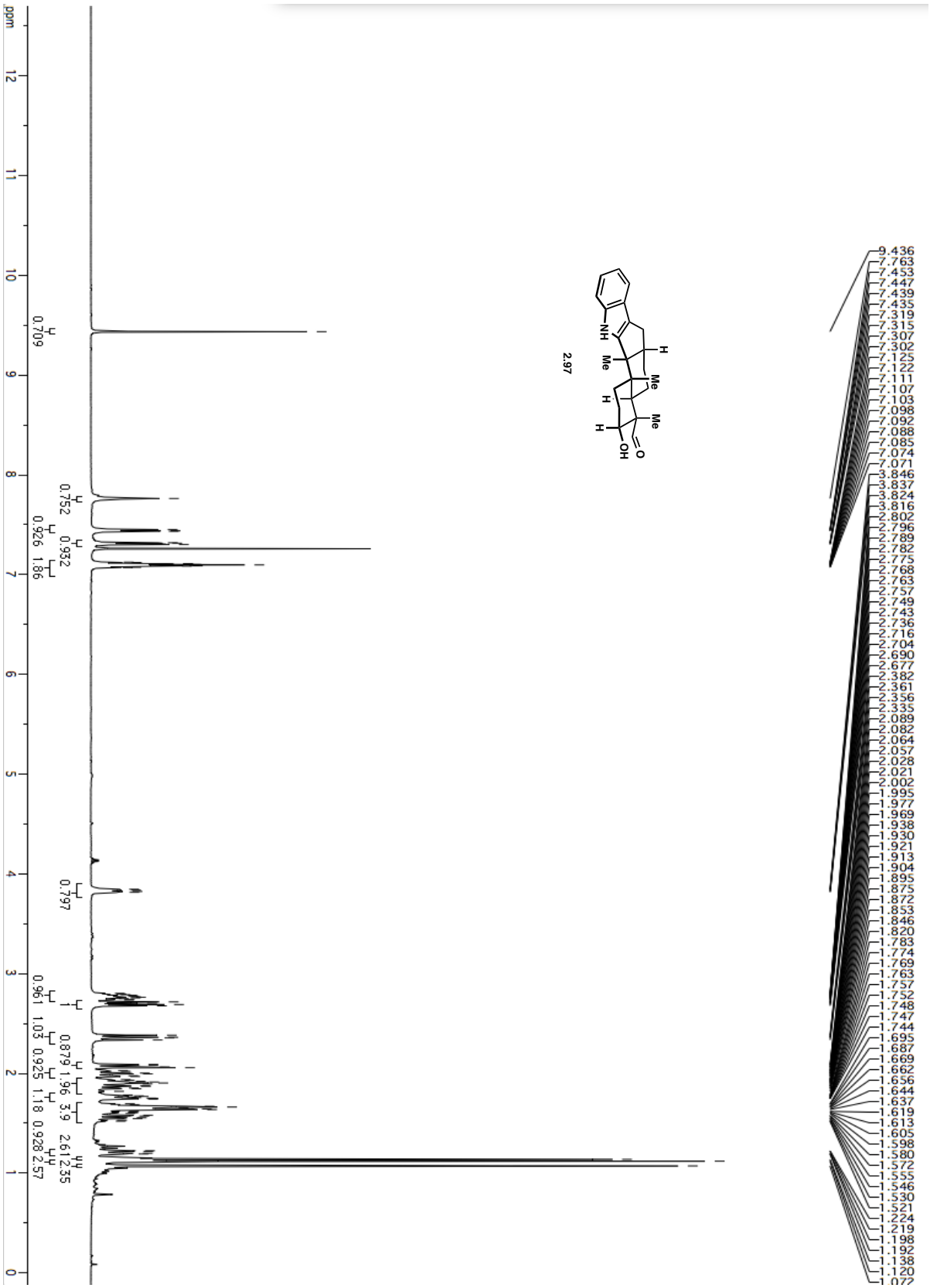
ppm
0.709
0.752
0.932
0.926
1.86
0.797
0.961
1.03
0.879
1.96
0.925
3.9
1.18
0.928
2.61
2.57
2.35
2.97
NH
Me
Me
Me
H
H
H
OH
O
9.436
7.763
7.453
7.447
7.439
7.435
7.319
7.315
7.307
7.302
7.125
7.122
7.111
7.107
7.103
7.098
7.092
7.088
7.085
7.074
7.071
3.846
3.837
3.824
3.816
2.802
2.796
2.789
2.782
2.775
2.768
2.763
2.757
2.749
2.743
2.736
2.716
2.704
2.690
2.677
2.382
2.361
2.356
2.335
2.089
2.082
2.064
2.057
2.028
2.021
2.002
1.995
1.977
1.969
1.938
1.930
1.921
1.913
1.904
1.895
1.875
1.872
1.853
1.846
1.820
1.783
1.774
1.769
1.763
1.757
1.752
1.748
1.747
1.744
1.695
1.687
1.669
1.662
1.656
1.644
1.637
1.619
1.613
1.605
1.598
1.580
1.572
1.555
1.546
1.530
1.521
1.224
1.219
1.198
1.192
1.138
1.120

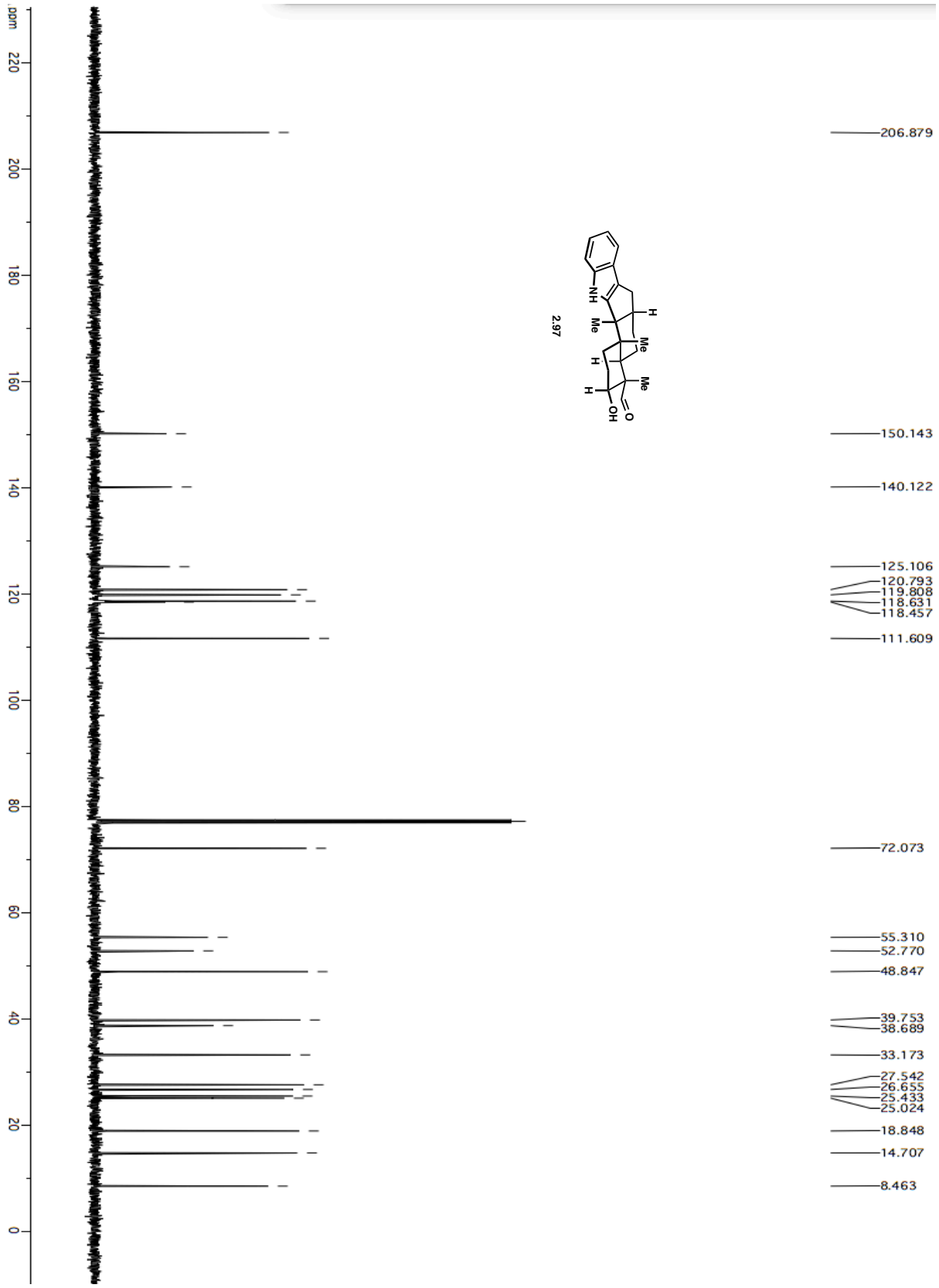
ppm
220
200
180
160
140
120
100
80
60
40
20
0
206.879
150.143
140.122
125.106
120.793
119.808
118.631
118.457
111.609
72.073
55.310
52.770
48.847
39.753
38.689
33.173
27.542
26.655
25.433
25.024
18.848
14.707
8.463
2.97
NH
Me
H
Me
H
Me
H
OH
O

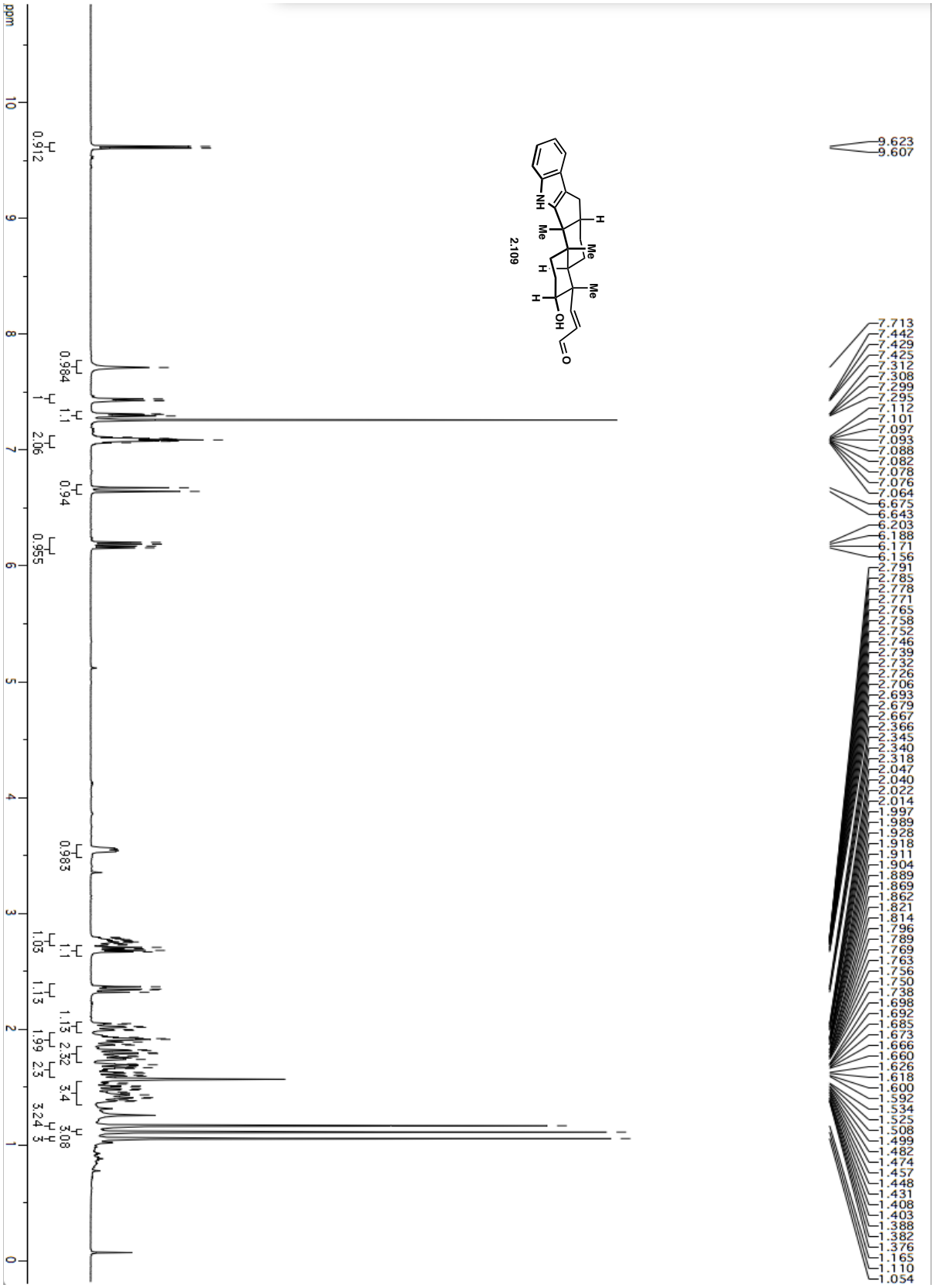
2:109
NH
Me
H
Me
H
Me
H
OH
O
9.623
9.607
7.713
7.442
7.429
7.425
7.312
7.308
7.299
7.295
7.112
7.101
7.097
7.093
7.088
7.082
7.078
7.076
7.064
6.675
6.643
6.203
6.188
6.171
6.156
2.791
2.785
2.778
2.771
2.765
2.758
2.752
2.746
2.739
2.732
2.726
2.706
2.693
2.679
2.667
2.366
2.345
2.340
2.318
2.047
2.040
2.022
2.014
1.997
1.989
1.928
1.918
1.911
1.904
1.889
1.869
1.862
1.821
1.814
1.796
1.789
1.769
1.763
1.756
1.750
1.738
1.698
1.692
1.685
1.673
1.666
1.660
1.626
1.618
1.600
1.592
1.534
1.525
1.508
1.499
1.482
1.474
1.457
1.448
1.431
1.408
1.403
1.388
1.382
1.376
1.165
1.110
1.054
0.912
0.984
1
1.1
2.06
0.94
0.955
0.983
1.1
1.03
1.13
1.13
2.32
1.99
2.3
3.4
3.24
3.08
3
ppm
10
9
8
7
6
5
4
3
2
1
0

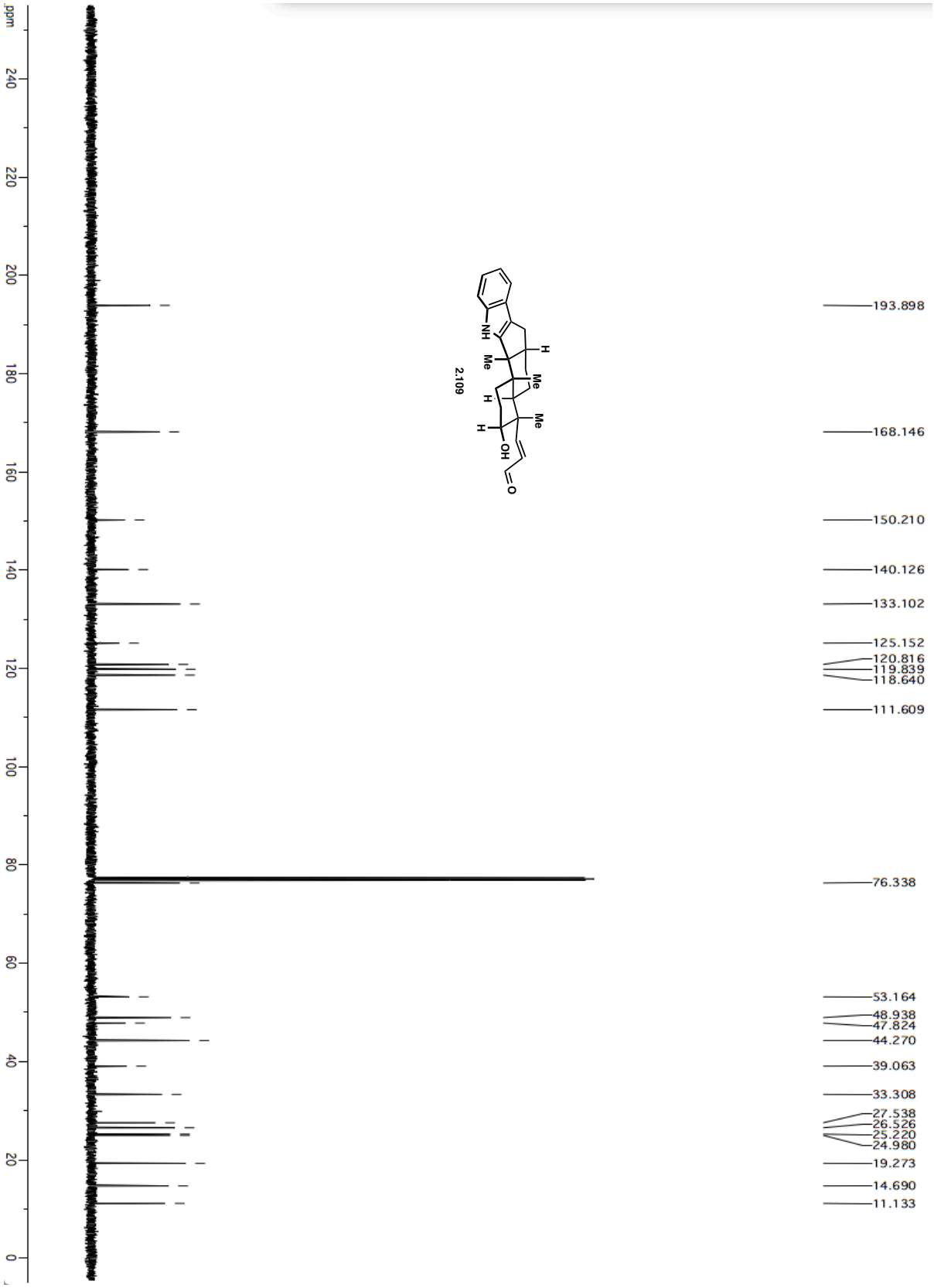
ppm
240
220
200
180
160
140
120
100
80
60
40
20
0
NH
Me
Me
H
Me
H
H
OH
O
2.109
193.898
168.146
150.210
140.126
133.102
125.152
120.816
119.839
118.640
111.609
76.338
53.164
48.938
47.824
44.270
39.063
33.308
27.538
26.526
25.220
24.980
19.273
14.690
11.133

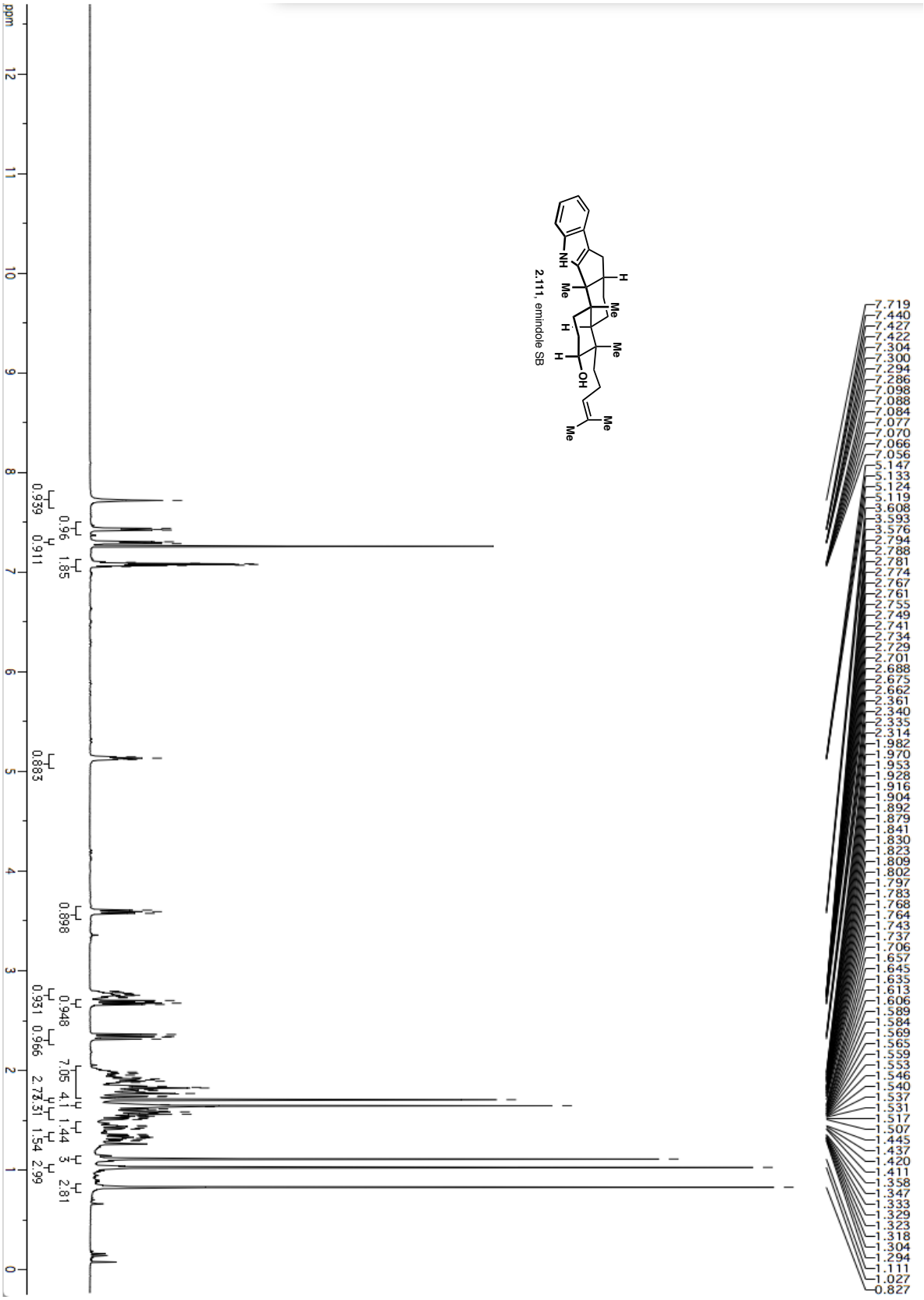
2.111, emindole SB
NH
Me
H
Me
H
Me
H
OH
Me
Me
ppm
0.939
0.911
0.96
1.85
0.883
0.898
0.948
0.931
0.966
7.05
4.1
1.44
2.73
3.31
3
1.54
2.99
2.81
7.719
7.440
7.427
7.422
7.304
7.300
7.294
7.286
7.098
7.088
7.084
7.077
7.070
7.066
7.056
5.147
5.133
5.124
5.119
3.608
3.593
3.576
2.794
2.788
2.781
2.774
2.767
2.761
2.755
2.749
2.741
2.734
2.729
2.701
2.688
2.675
2.662
2.361
2.340
2.335
2.314
1.982
1.970
1.953
1.928
1.916
1.904
1.892
1.879
1.841
1.830
1.823
1.809
1.802
1.797
1.783
1.768
1.764
1.743
1.737
1.706
1.657
1.645
1.635
1.613
1.606
1.589
1.584
1.569
1.565
1.559
1.553
1.546
1.540
1.537
1.531
1.517
1.507
1.445
1.437
1.420
1.411
1.358
1.347
1.333
1.329
1.323
1.318
1.304
1.294
1.111
1.027
0.827

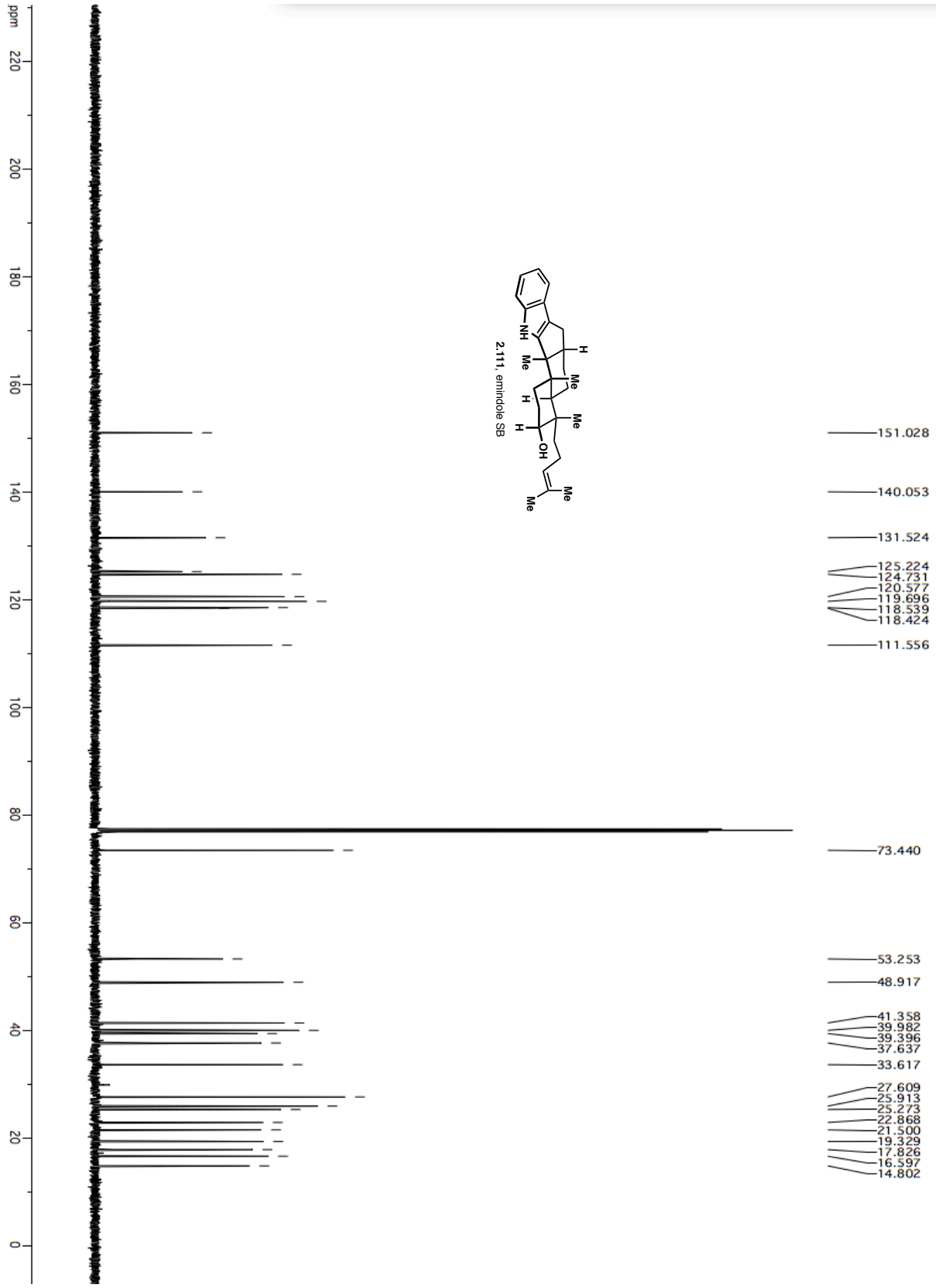
ppm
220
200
180
160
140
120
100
80
60
40
20
0
2.111, emindole SB
NH
Me
H
Me
Me
H
OH
Me
Me
151.028
140.053
131.524
125.224
124.731
120.577
119.696
118.539
118.424
111.556
73.440
53.253
48.917
41.358
39.982
39.396
37.637
33.617
27.609
25.913
25.273
22.868
21.500
19.329
17.826
16.597
14.802

Appendix D: Chapter 3 NMR Spectra

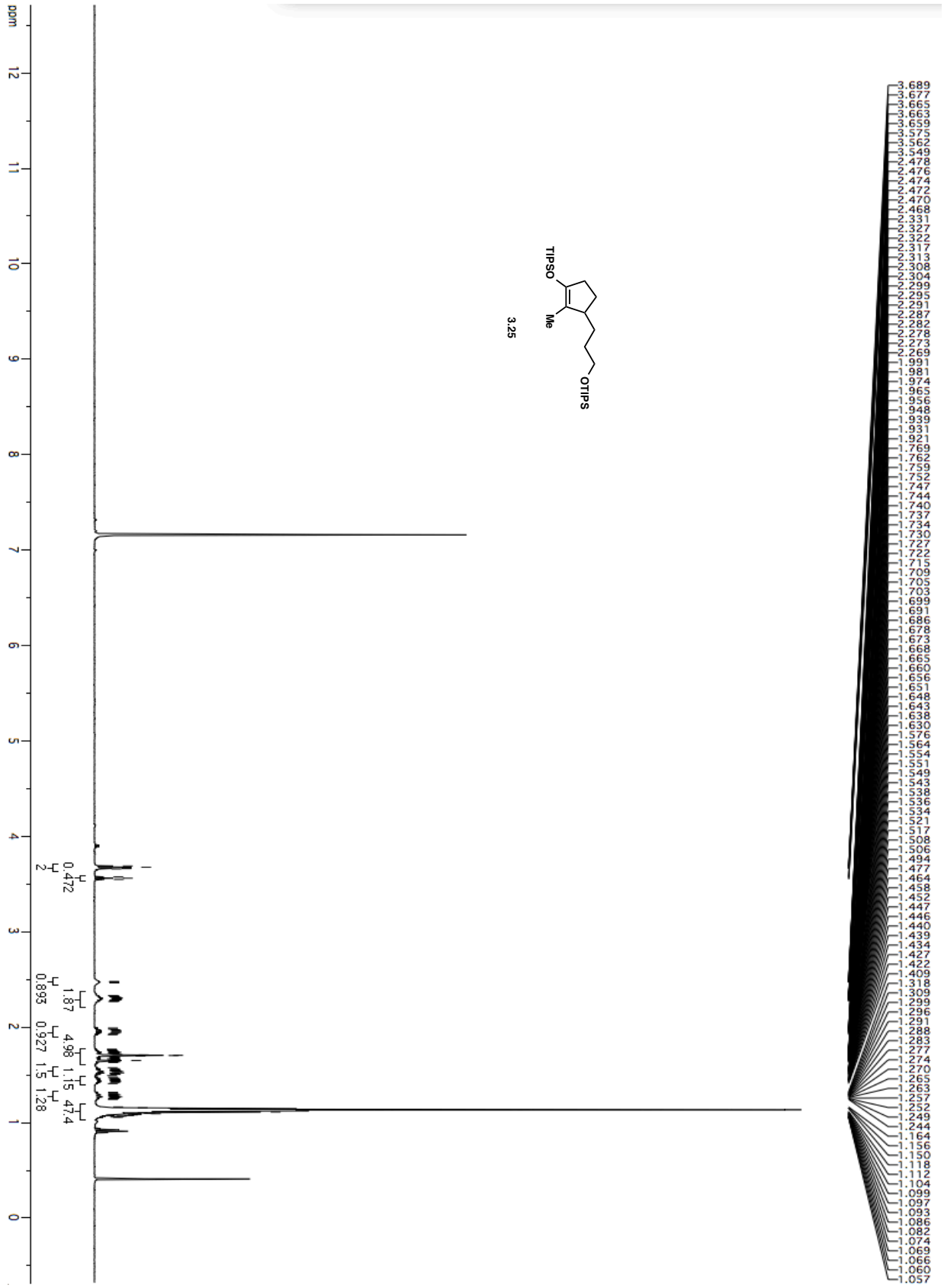
TIPSO
Me
OTIPS
3.25
ppm
0.472
2
1.87
0.893
4.98
0.927
1.15
1.5
47.4
1.28

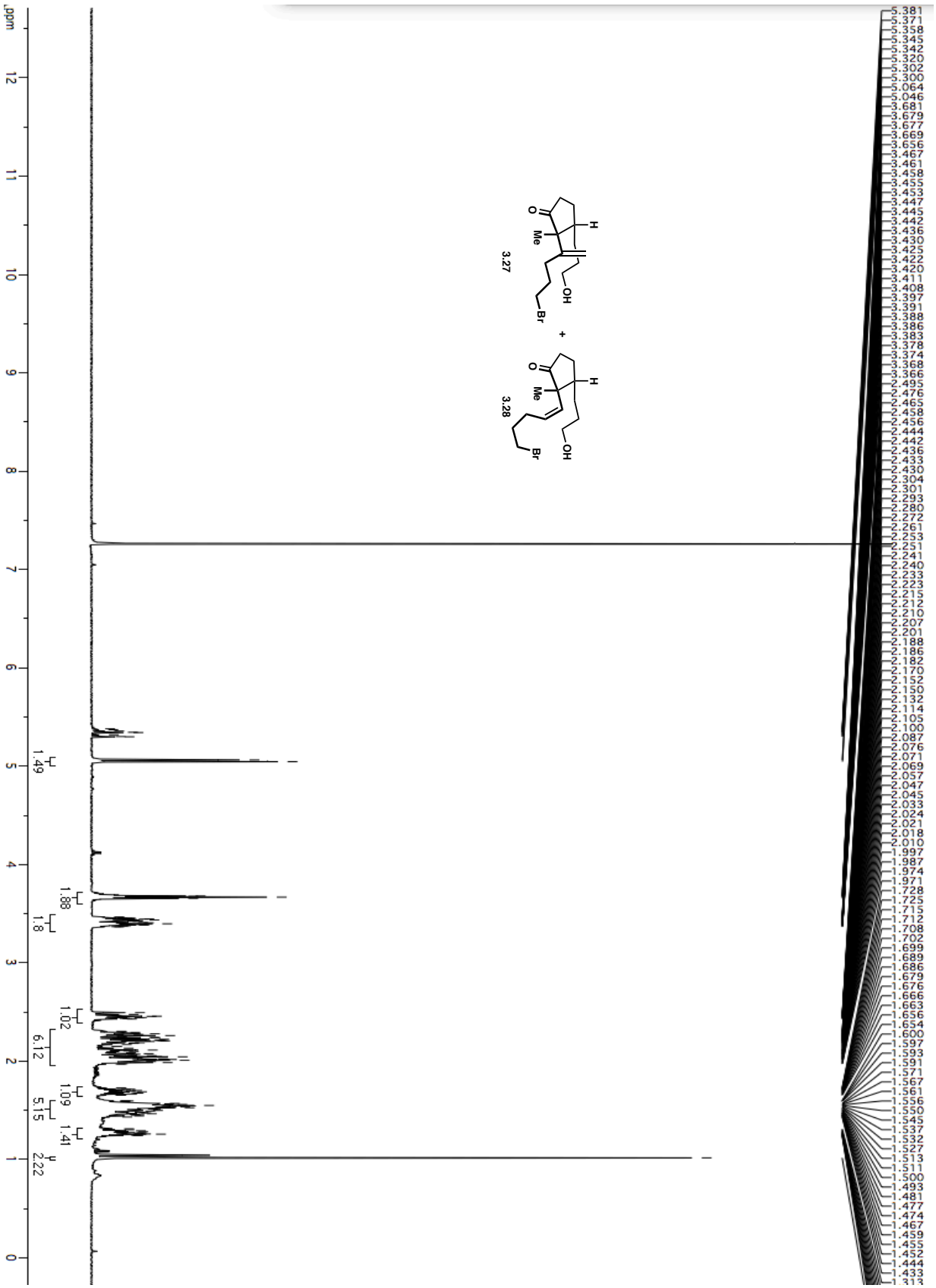
ppm
12
11
10
9
8
7
6
5
4
3
2
1
0
1.49
1.88
1.8
1.02
6.12
1.09
5.15
1.41
2.22
3.27
3.28
O
Me
H
OH
Br
+

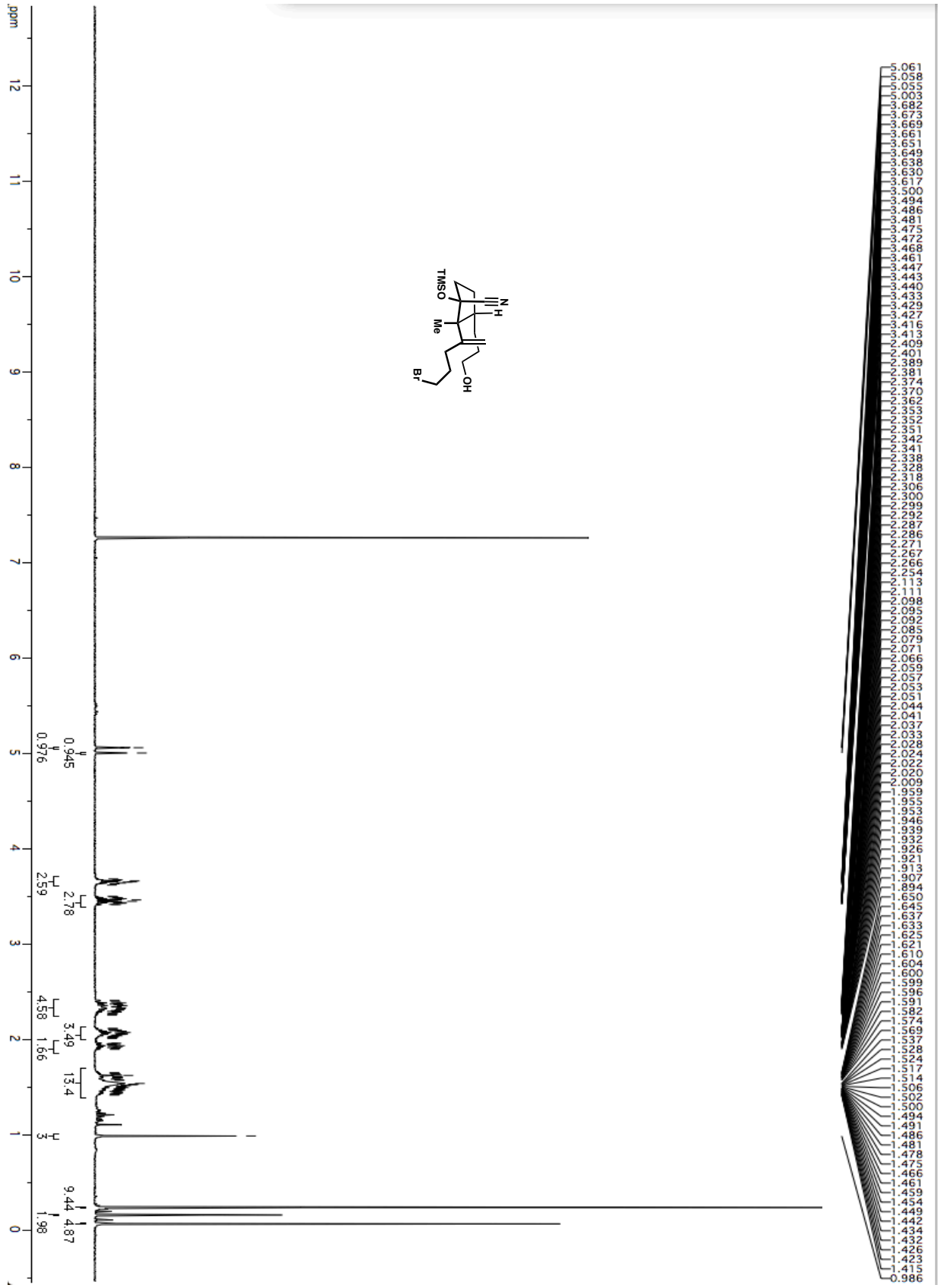
TMSO
Me
N
H
OH
Br
ppm
12
11
10
9
8
7
6
5
4
3
2
1
0
0.976
0.945
2.59
2.78
4.58
3.49
1.66
13.4
3
9.44
4.87
1.98

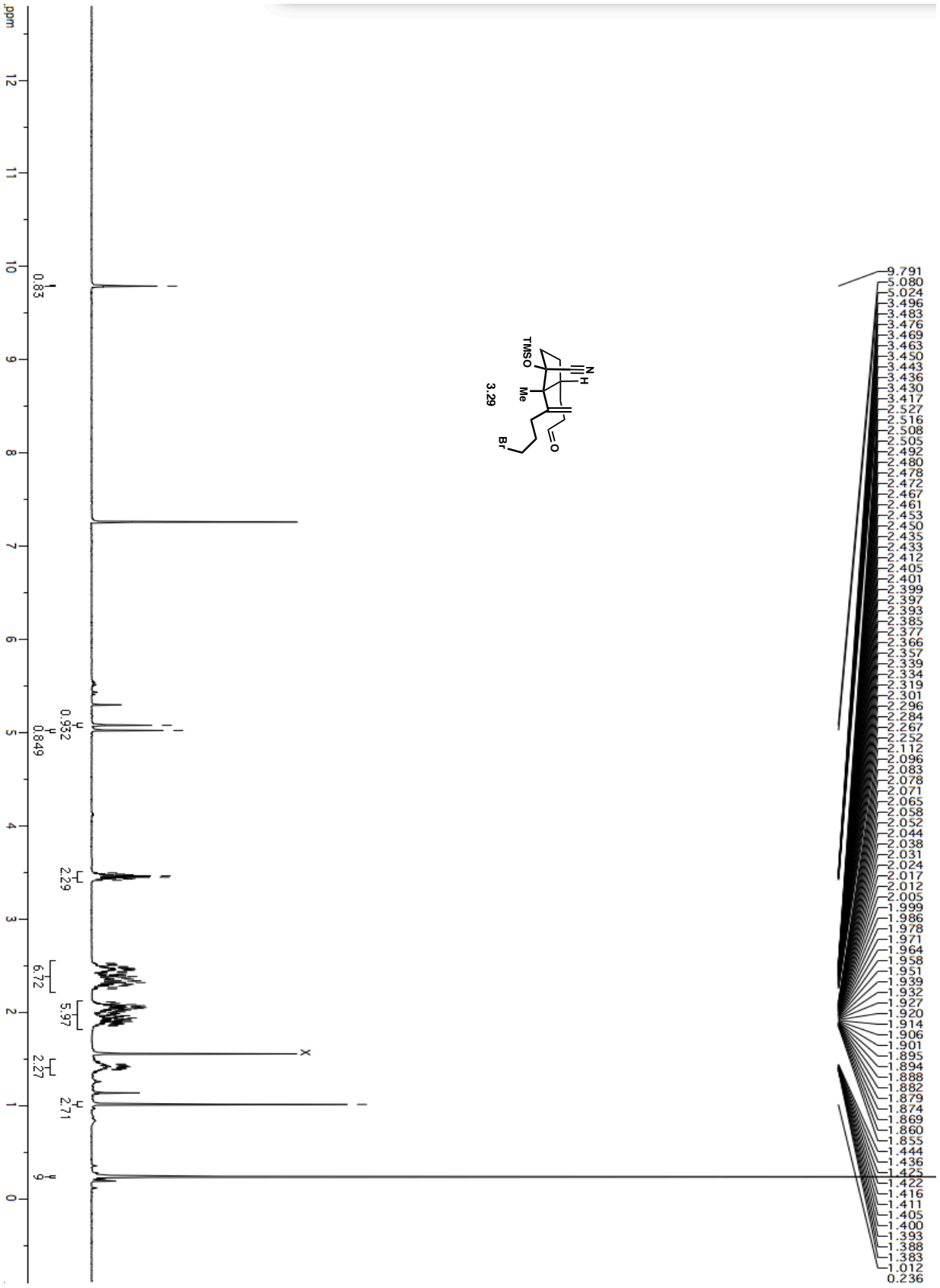
TMSO
Me
3.29
N
H
O
Br
ppm
0.83
0.932
0.849
2.29
6.72
5.97
2.27
2.71
9
9.791
5.080
5.024
3.496
3.483
3.476
3.469
3.463
3.450
3.443
3.436
3.430
3.417
2.527
2.516
2.508
2.505
2.492
2.480
2.478
2.472
2.467
2.461
2.453
2.450
2.435
2.433
2.412
2.405
2.401
2.399
2.397
2.393
2.385
2.377
2.366
2.357
2.339
2.334
2.319
2.301
2.296
2.284
2.267
2.252
2.112
2.096
2.083
2.078
2.071
2.065
2.058
2.052
2.044
2.038
2.031
2.024
2.017
2.012
2.005
1.999
1.986
1.978
1.971
1.964
1.958
1.951
1.939
1.932
1.927
1.920
1.914
1.906
1.901
1.895
1.894
1.888
1.882
1.879
1.874
1.869
1.860
1.855
1.444
1.436
1.425
1.422
1.416
1.411
1.405
1.400
1.393
1.388
1.383
1.012
0.236

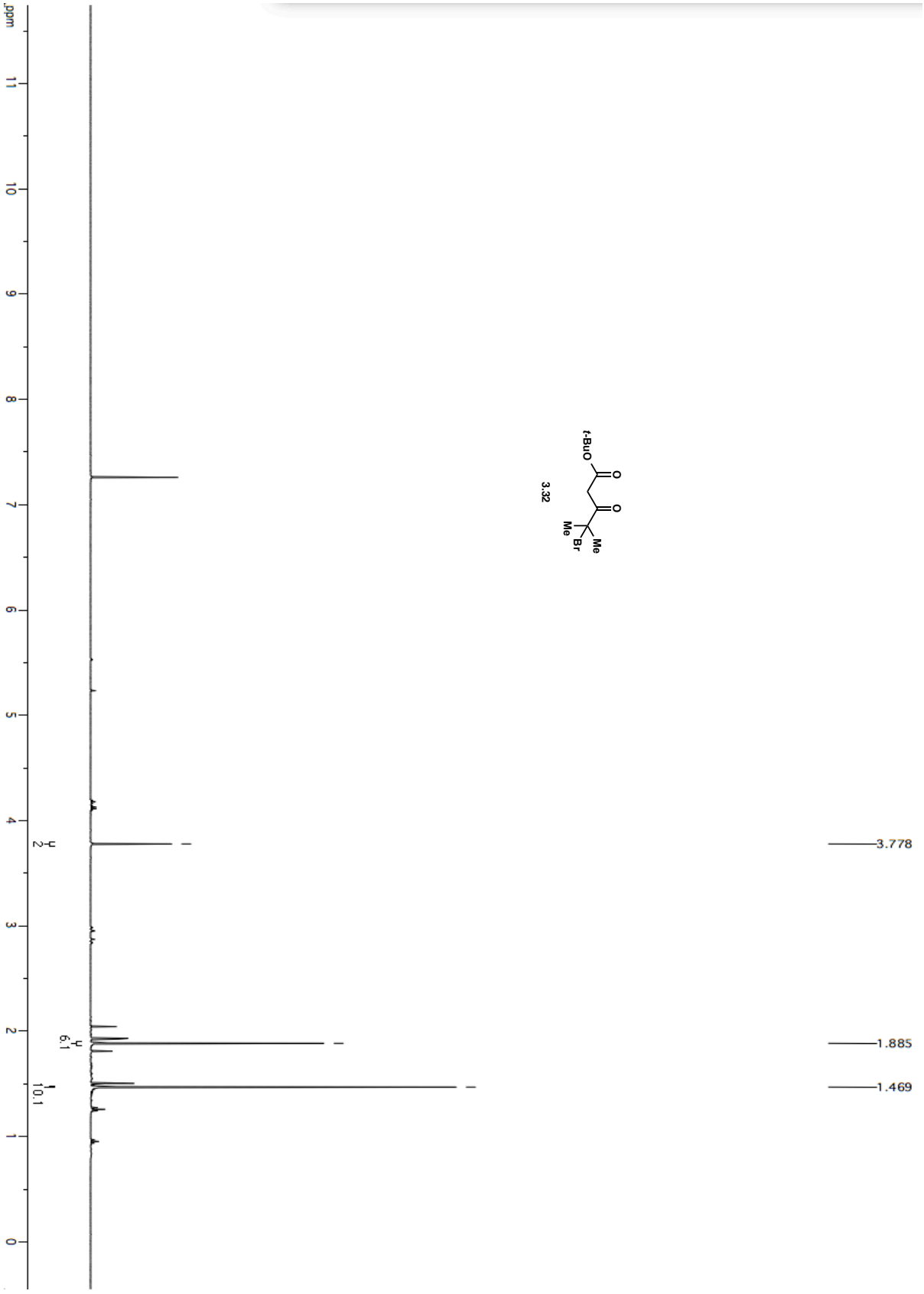
ppm
11
10
9
8
7
6
5
4
3
2
1
0
2
6.1
10.1
3.32
t-BuO
O
O
Me
Br
Me
3.778
1.885
1.469

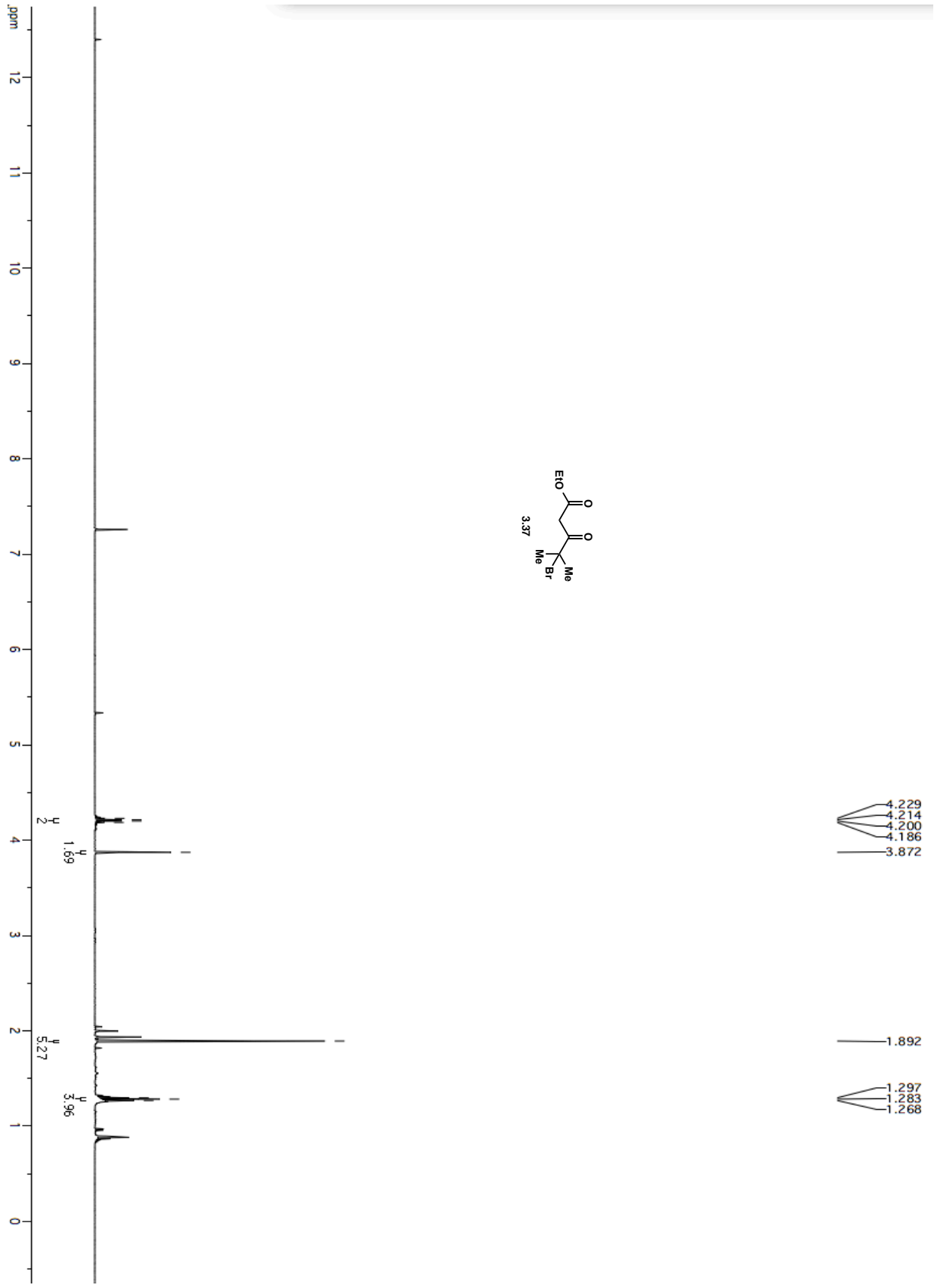
ppm
12
11
10
9
8
7
6
5
4
3
2
1
0
2
1.69
5.27
3.96
EtO
O
O
3.37
Me
Br
Me
4.229
4.214
4.200
4.186
3.872
1.892
1.297
1.283
1.268

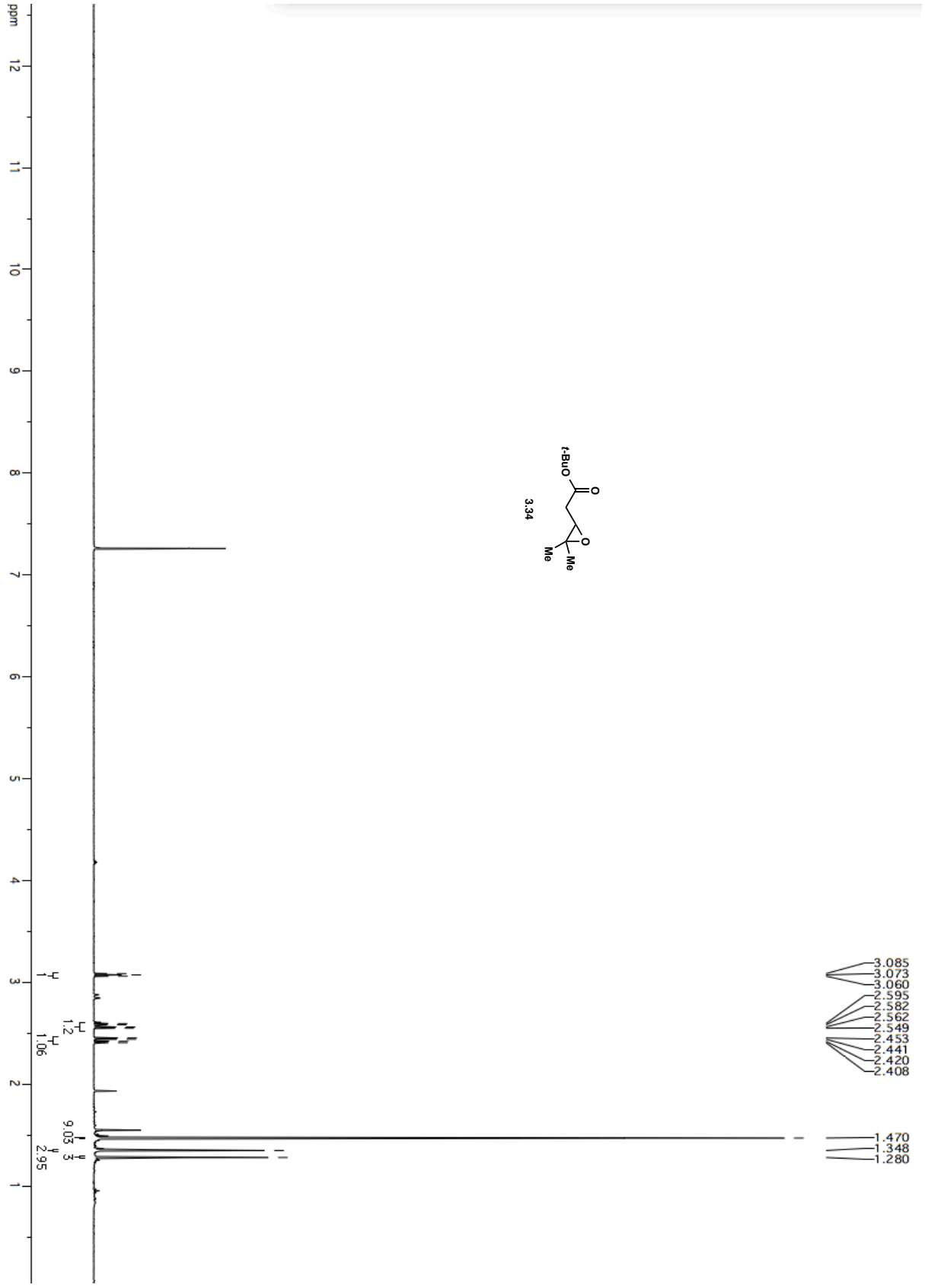
ppm
12
11
10
9
8
7
6
5
4
3
2
1
3.085
3.073
3.060
2.595
2.582
2.562
2.549
2.453
2.441
2.420
2.408
1.470
1.348
1.280
1.06
1.2
9.03
2.95
3.34
t-BuO
O
O
Me
Me

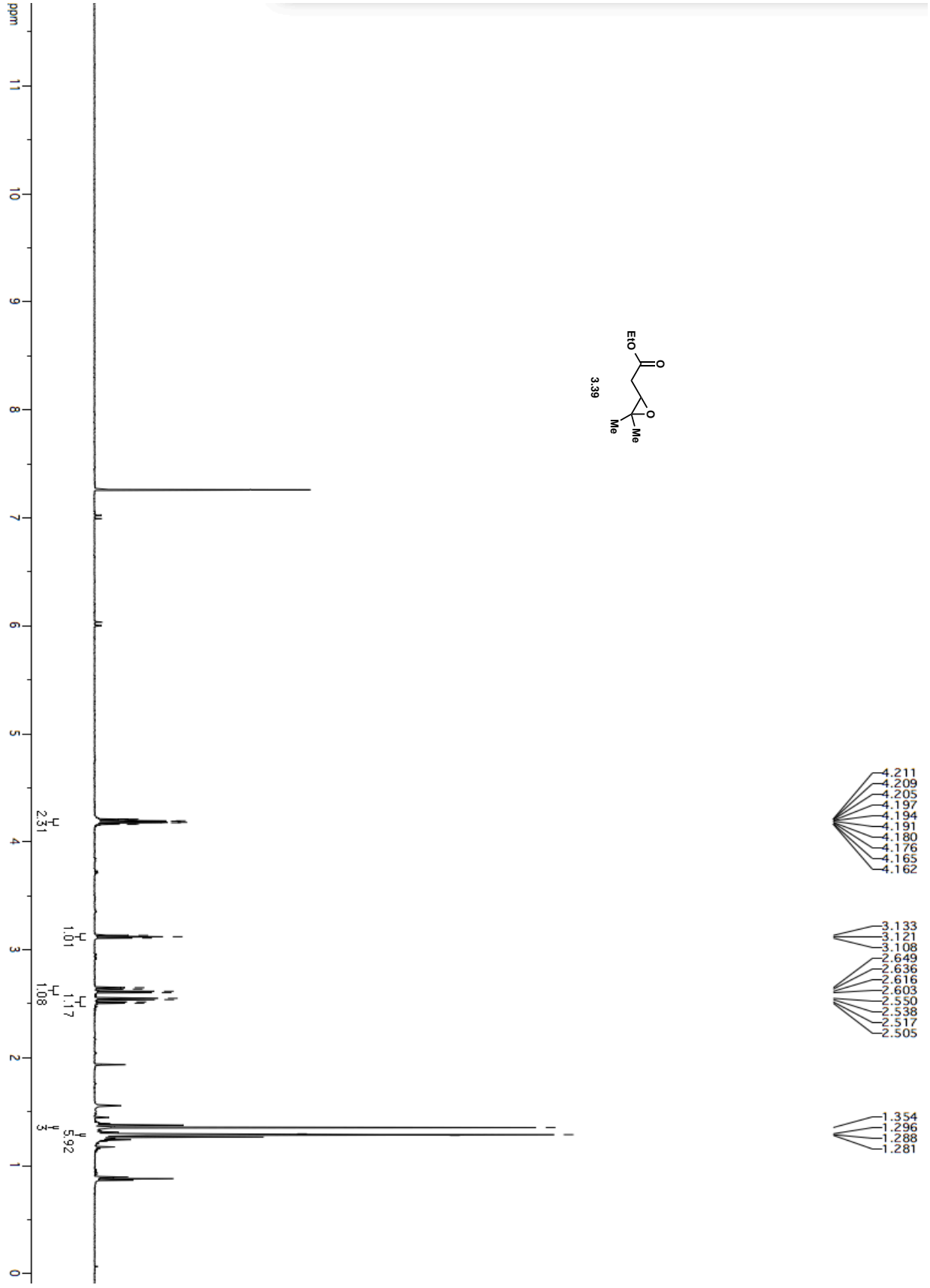
ppm
11
10
9
8
7
6
5
4
3
2
1
0
2.31
1.01
1.17
1.08
5.92
3
3.39
EtO
O
O
Me
Me
4.211
4.209
4.205
4.197
4.194
4.191
4.180
4.176
4.165
4.162
3.133
3.121
3.108
2.649
2.636
2.616
2.603
2.550
2.538
2.517
2.505
1.354
1.296
1.288
1.281

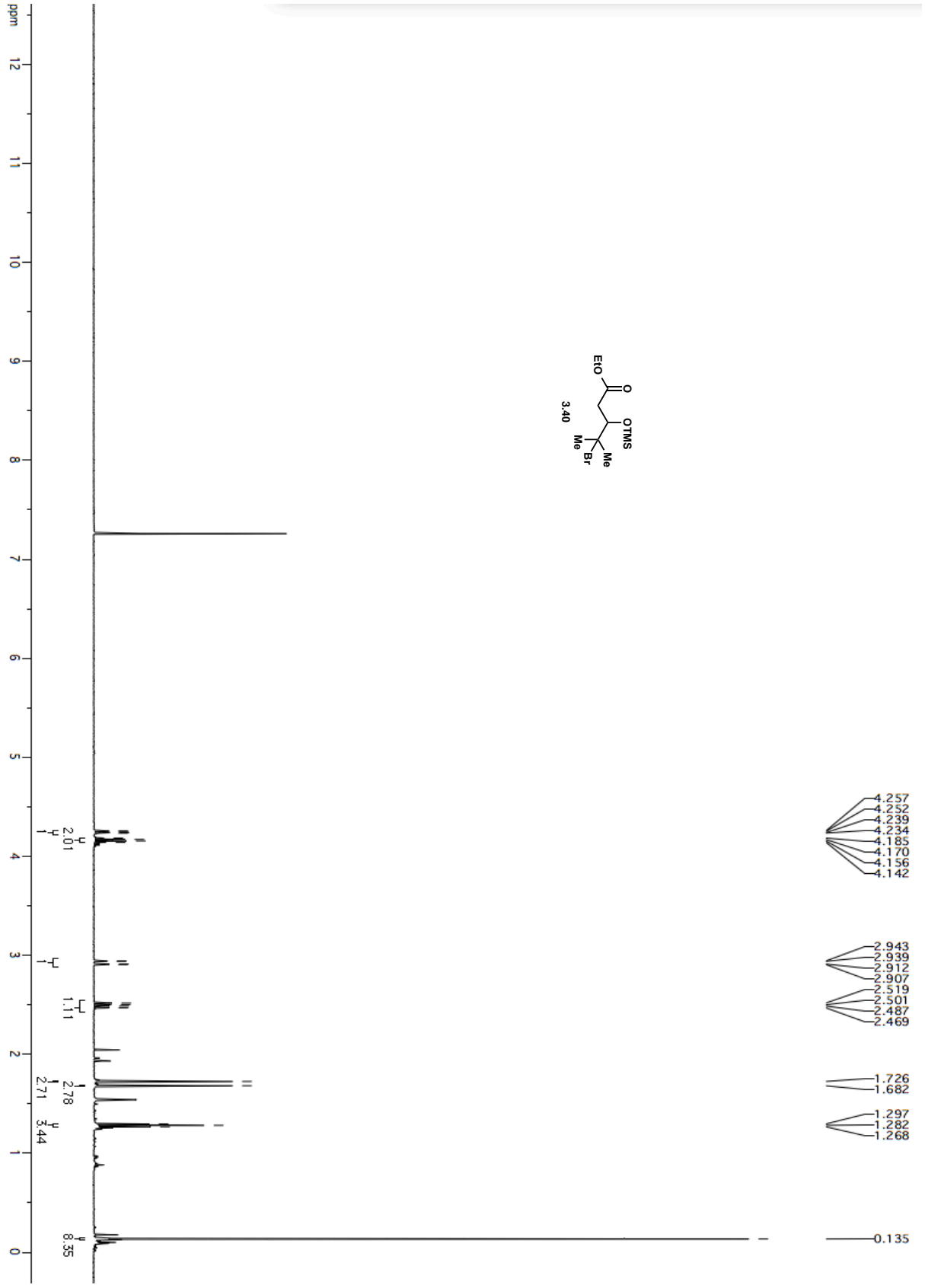
ppm
12
11
10
9
8
7
6
5
4
3
2
1
0
2.01
1.11
2.78
2.71
3.44
8.35
EtO
O
OTMS
3.40
Me
Br
Me
4.257
4.252
4.239
4.234
4.185
4.170
4.156
4.142
2.943
2.939
2.912
2.907
2.519
2.501
2.487
2.469
1.726
1.682
1.297
1.282
1.268
0.135

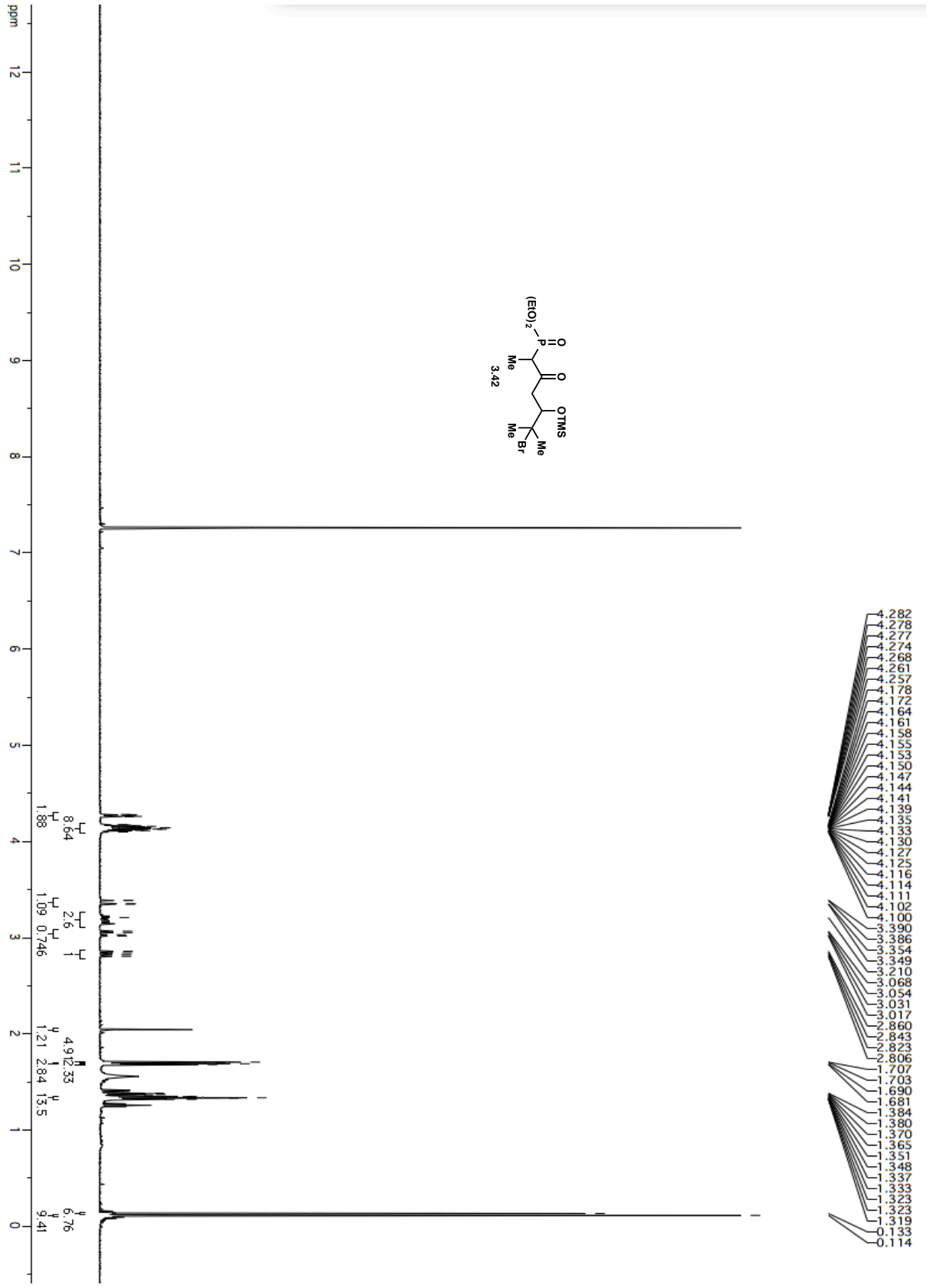
ppm
12
11
10
9
8
7
6
5
4
3
2
1
0
8.64
1.88
2.6
1
1.09
0.746
4.91
2.33
1.21
2.84
13.5
6.76
9.41
(EtO)2
P
O
Me
3.42
O
OTMS
Me
Me
Br
4.282
4.278
4.277
4.274
4.268
4.261
4.257
4.178
4.172
4.164
4.161
4.158
4.155
4.153
4.150
4.147
4.144
4.141
4.139
4.135
4.133
4.130
4.127
4.125
4.116
4.114
4.111
4.102
4.100
3.390
3.386
3.354
3.349
3.210
3.068
3.054
3.031
3.017
2.860
2.843
2.823
2.806
1.707
1.703
1.690
1.681
1.384
1.380
1.370
1.365
1.351
1.348
1.337
1.333
1.323
1.323
1.319
0.133
0.114

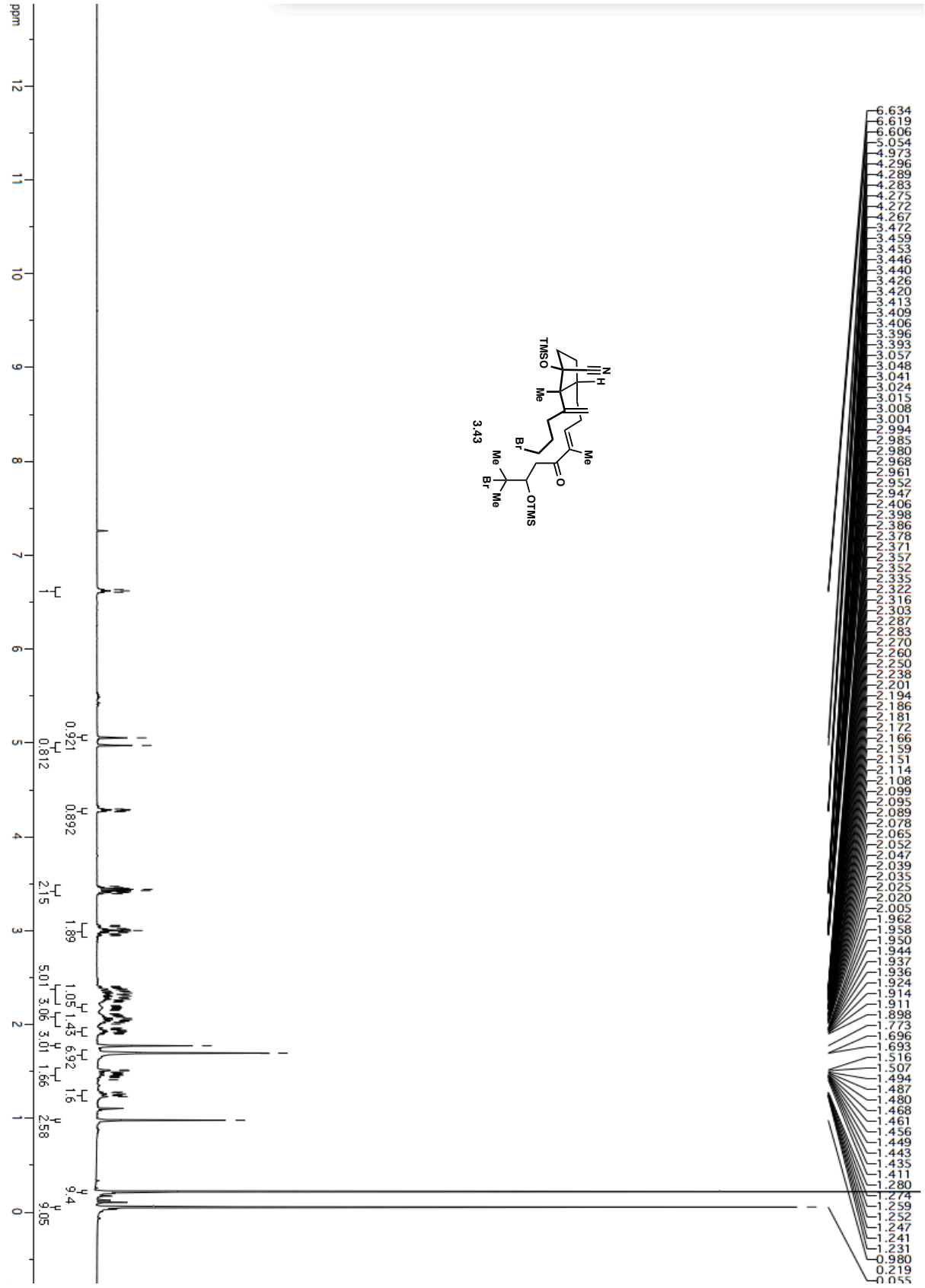
ppm
12
11
10
9
8
7
6
5
4
3
2
1
0
0.921
0.812
0.892
2.15
1.89
5.01
3.06
1.05
1.43
3.01
6.92
1.66
1.6
2.58
9.4
9.05
TMSO
Me
N
H
Br
3.43
Me
O
Me
Br
Me
OTMS
6.634
6.619
6.606
5.054
4.973
4.296
4.289
4.283
4.275
4.272
4.267
3.472
3.459
3.453
3.446
3.440
3.426
3.420
3.413
3.409
3.406
3.396
3.393
3.057
3.048
3.041
3.024
3.015
3.008
3.001
2.994
2.985
2.980
2.968
2.961
2.952
2.947
2.406
2.398
2.386
2.378
2.371
2.357
2.352
2.335
2.322
2.316
2.303
2.287
2.283
2.270
2.260
2.250
2.238
2.201
2.194
2.186
2.181
2.172
2.166
2.159
2.151
2.114
2.108
2.099
2.095
2.089
2.078
2.065
2.052
2.047
2.039
2.035
2.025
2.020
2.005
1.962
1.958
1.950
1.944
1.937
1.936
1.924
1.914
1.911
1.898
1.773
1.696
1.693
1.516
1.507
1.494
1.487
1.480
1.468
1.461
1.456
1.449
1.443
1.435
1.411
1.280
1.274
1.259
1.252
1.247
1.241
1.231
0.980
0.219
0.055

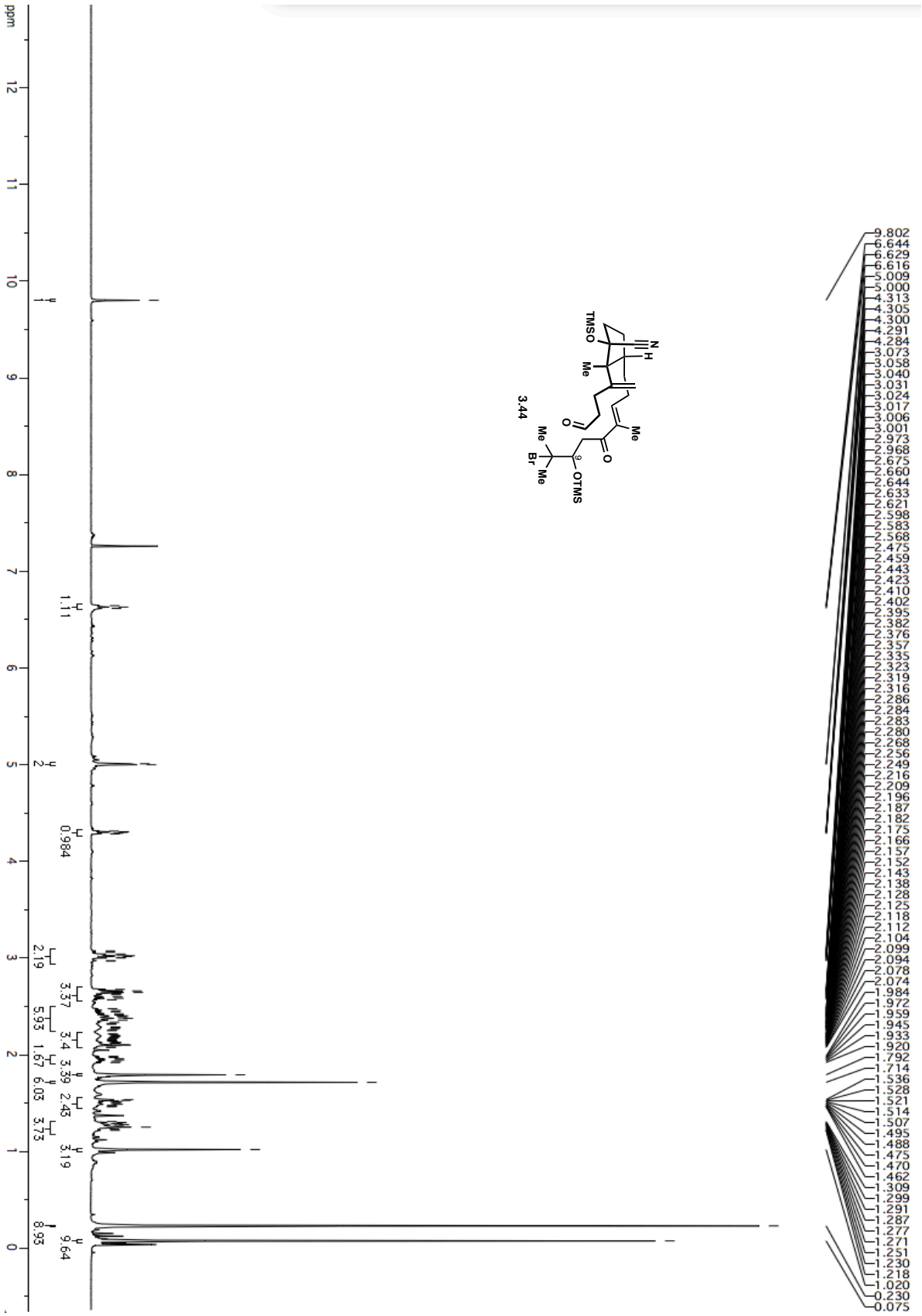
ppm
12
11
10
9
8
7
6
5
4
3
2
1
0
1.11
0.984
2.19
3.37
5.93
3.4
1.67
3.39
6.03
2.43
3.73
3.19
8.93
9.64
TMSO
Me
N
H
Me
O
O
3.44
Me
Br
Me
OTMS
9.802
6.644
6.629
6.616
5.009
5.000
4.313
4.305
4.300
4.291
4.284
3.073
3.058
3.040
3.031
3.024
3.017
3.006
3.001
2.973
2.968
2.675
2.660
2.644
2.633
2.621
2.598
2.583
2.568
2.475
2.459
2.443
2.423
2.410
2.402
2.395
2.382
2.376
2.357
2.335
2.323
2.319
2.316
2.286
2.284
2.283
2.280
2.268
2.256
2.249
2.216
2.209
2.196
2.187
2.182
2.175
2.166
2.157
2.152
2.143
2.138
2.128
2.125
2.118
2.112
2.104
2.099
2.094
2.078
2.074
1.984
1.972
1.959
1.945
1.933
1.920
1.792
1.714
1.536
1.528
1.521
1.514
1.507
1.495
1.488
1.475
1.470
1.462
1.309
1.299
1.291
1.287
1.277
1.271
1.251
1.230
1.218
1.020
0.230
0.075

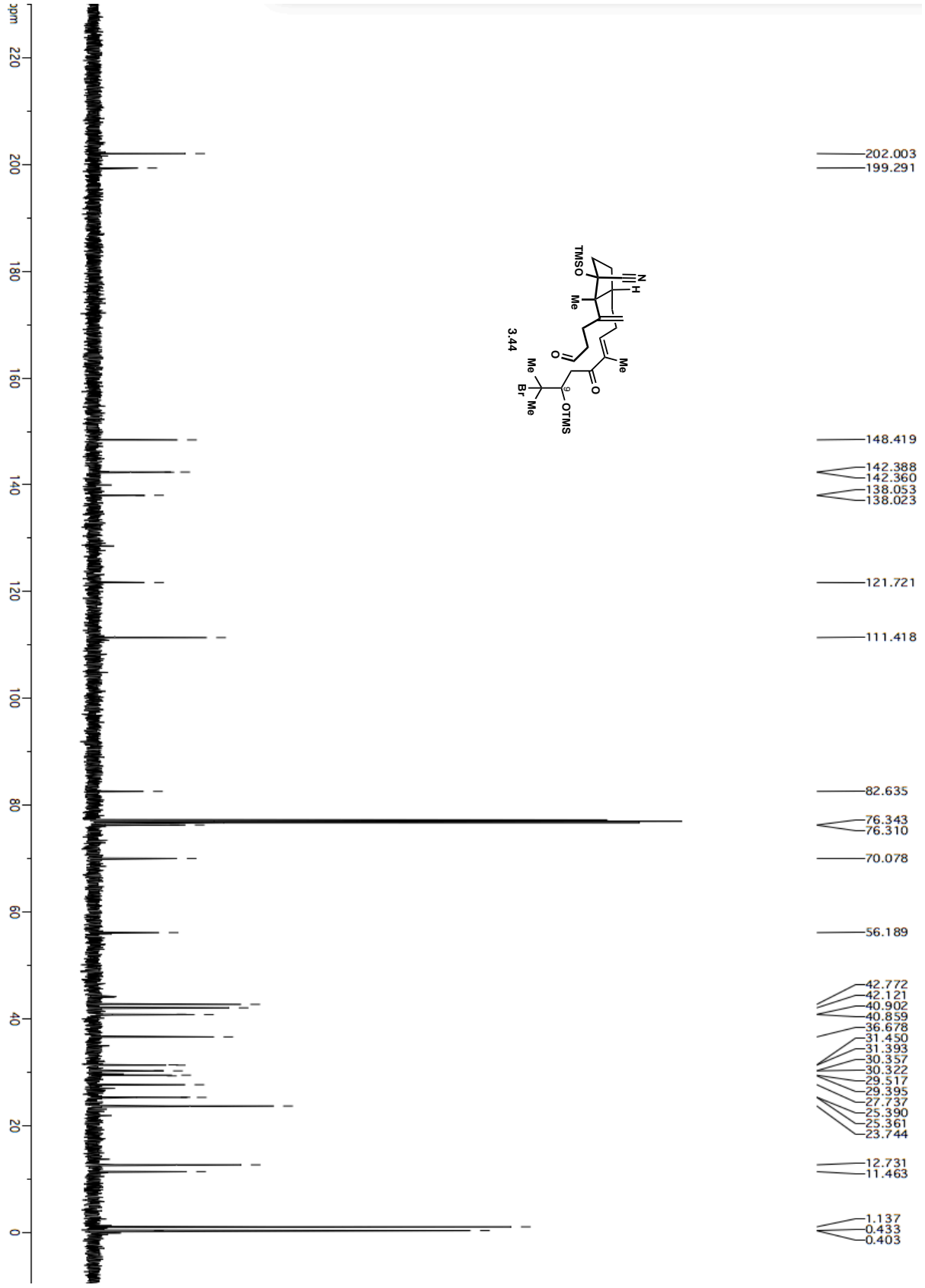
ppm
220
200
180
160
140
120
100
80
60
40
20
0
202.003
199.291
148.419
142.388
142.360
138.053
138.023
121.721
111.418
82.635
76.343
76.310
70.078
56.189
42.772
42.121
40.902
40.859
36.678
31.450
31.393
30.357
30.322
29.517
29.395
27.737
25.390
25.361
23.744
12.731
11.463
1.137
0.433
0.403
TMSO
N
H
Me
O
Me
O
3.44
Me
Br
Me
OTMS

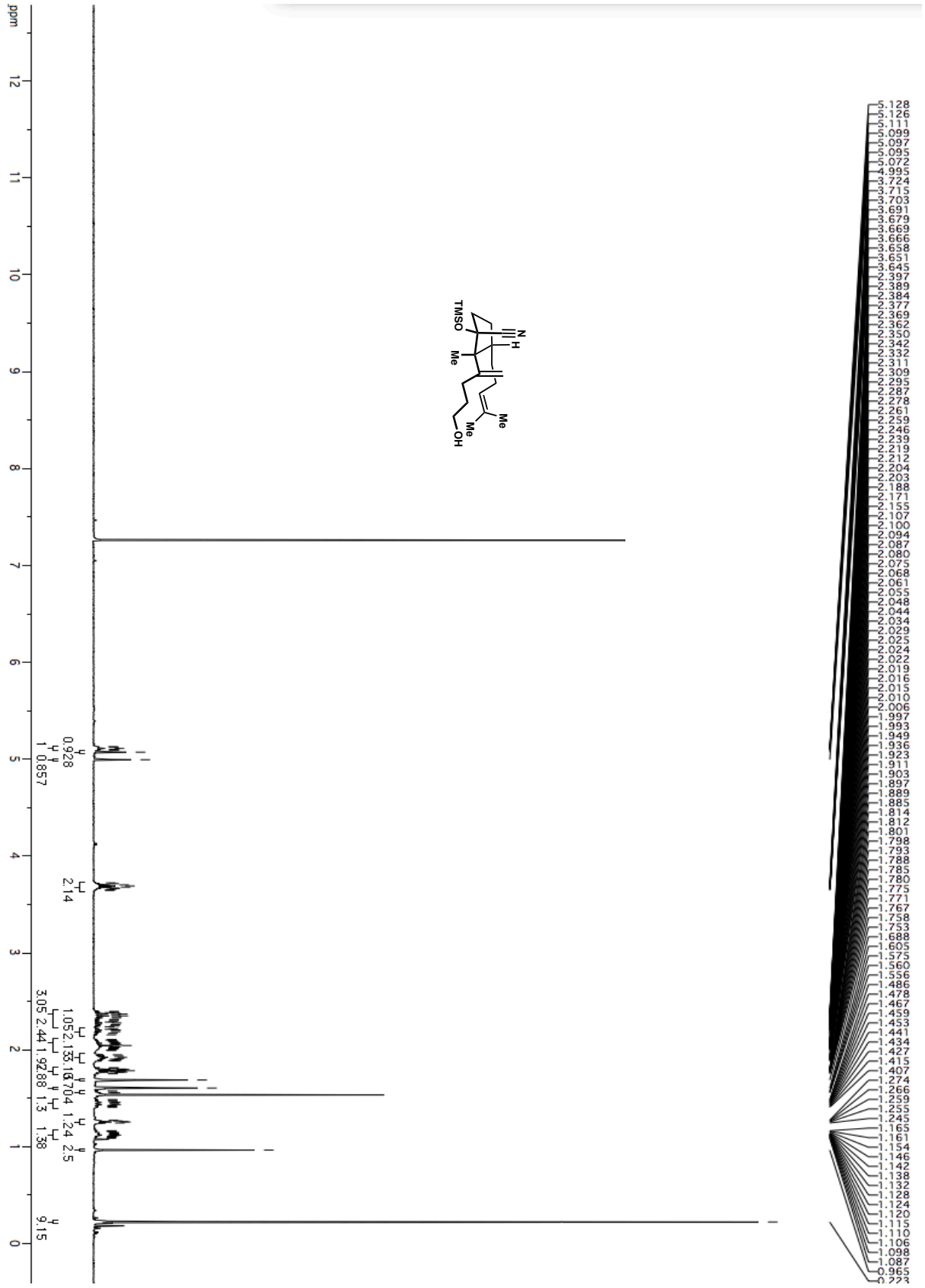
ppm
12
11
10
9
8
7
6
5
4
3
2
1
0
TMSO
Me
N
H
Me
Me
OH
0.928
0.857
2.14
1.05
2.13
3.18
7.04
1.24
2.5
3.05
2.44
1.92
8.88
1.3
1.38
9.15

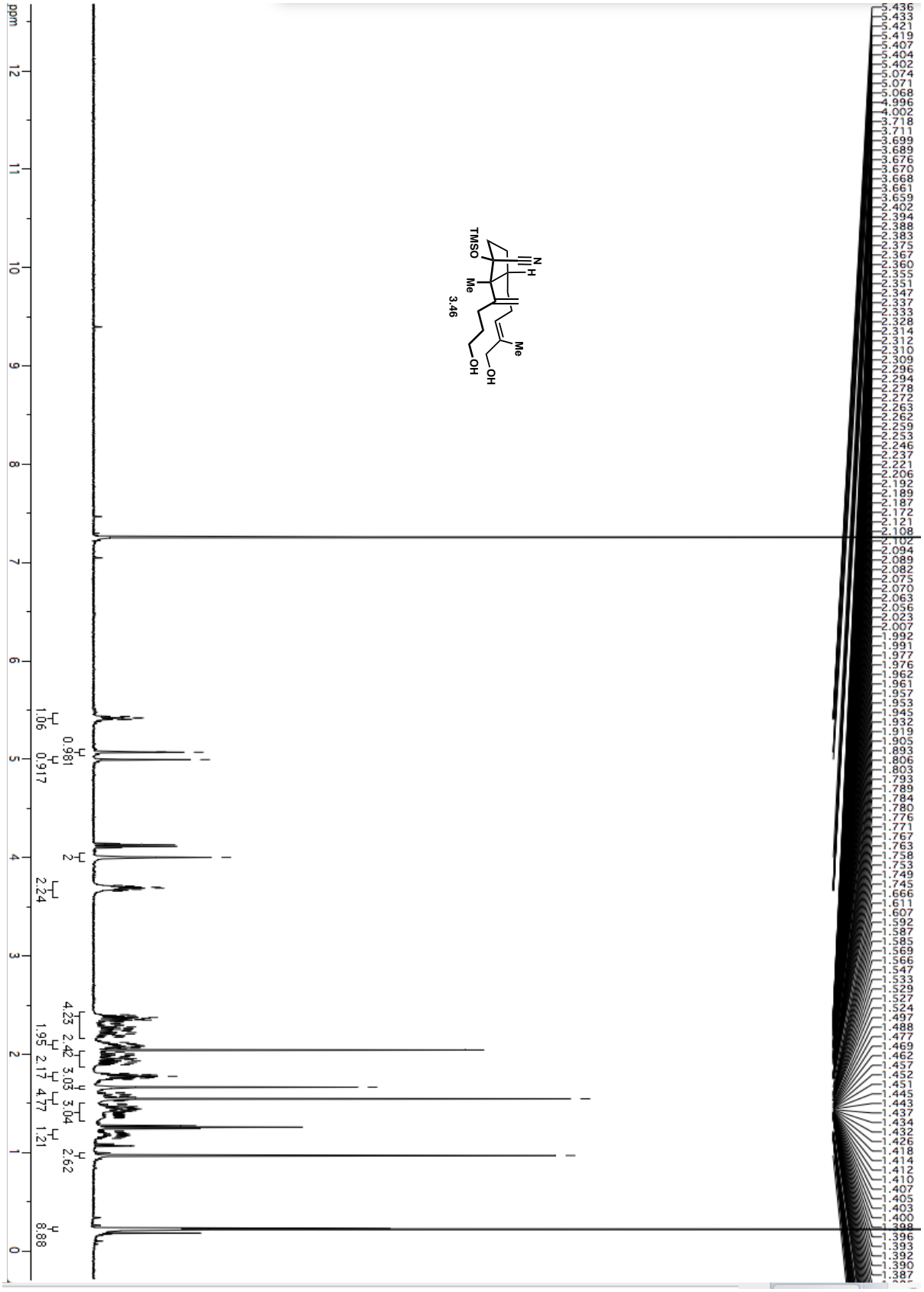
TMSO
Me
N
H
Me
OH
OH
3.46
ppm
0
1
2
3
4
5
6
7
8
9
10
11
12
8.88
2.62
1.21
4.77
3.04
3.03
2.17
2.42
1.95
4.23
2.24
2
0.917
0.981
1.06

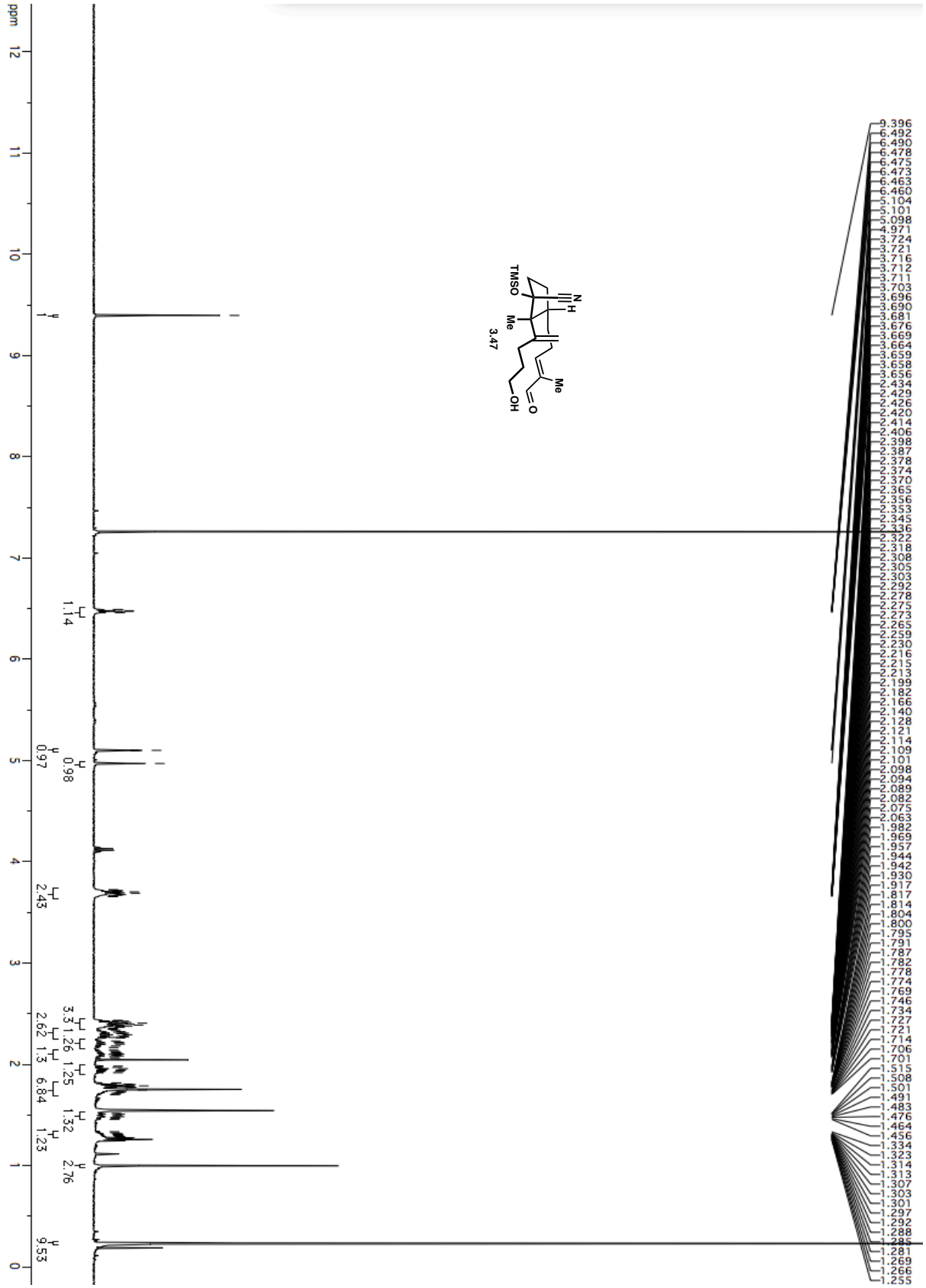
ppm
12
11
10
9
8
7
6
5
4
3
2
1
0
1.14
0.98
0.97
2.43
3.3
1.26
1.25
2.62
1.3
6.84
1.32
1.23
2.76
9.53
TMSO
Me
3.47
N
H
Me
O
OH

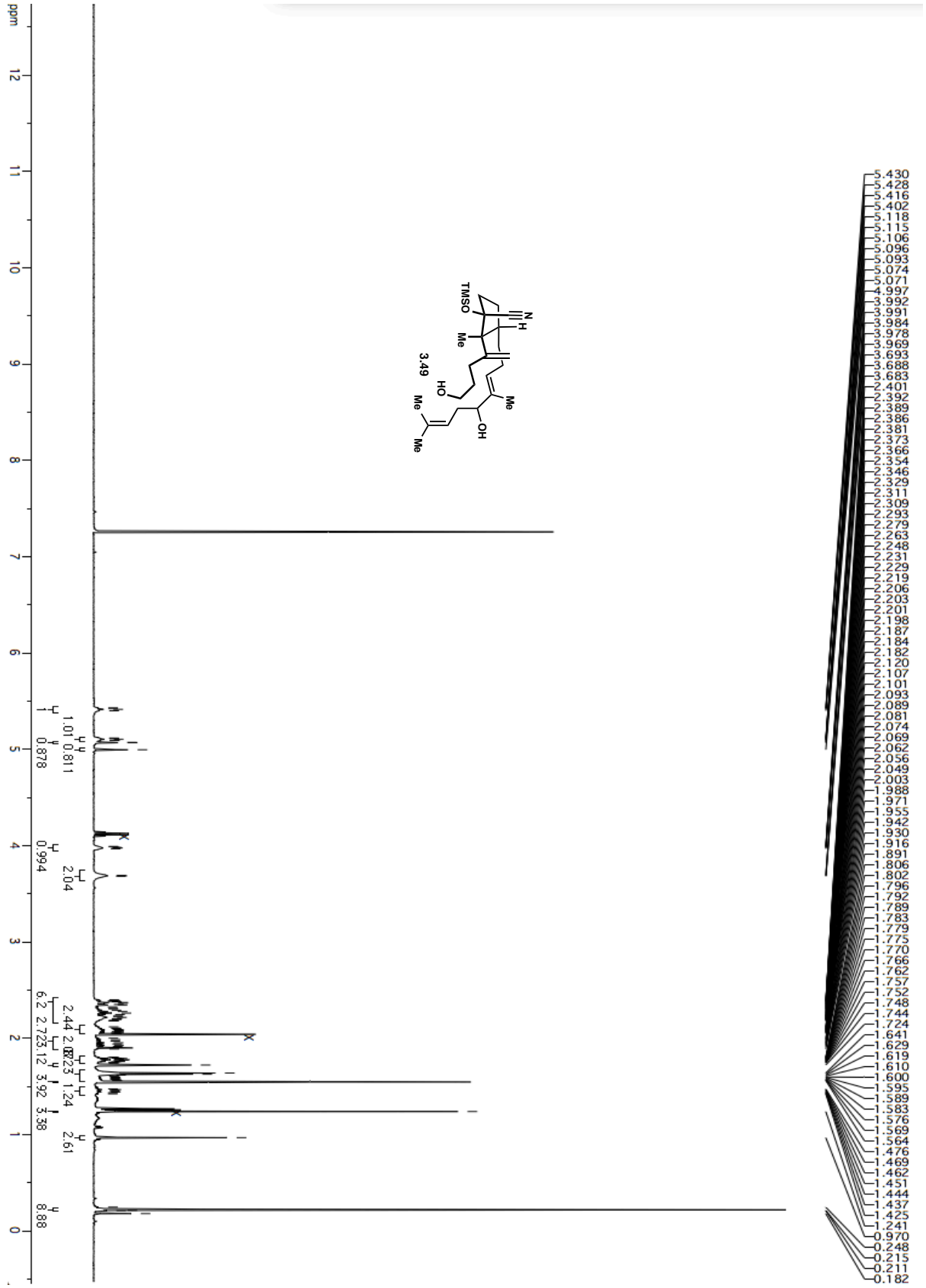
ppm
12
11
10
9
8
7
6
5
4
3
2
1
0
TMSO
Me
N
H
3.49
HO
Me
Me
Me
OH
5.430
5.428
5.416
5.402
5.118
5.115
5.106
5.096
5.093
5.074
5.071
4.997
3.992
3.991
3.984
3.978
3.969
3.693
3.688
3.683
2.401
2.392
2.389
2.386
2.381
2.373
2.366
2.354
2.346
2.329
2.311
2.309
2.293
2.279
2.263
2.248
2.231
2.229
2.219
2.206
2.203
2.201
2.198
2.187
2.184
2.182
2.120
2.107
2.101
2.093
2.089
2.081
2.074
2.069
2.062
2.056
2.049
2.003
1.988
1.971
1.955
1.942
1.930
1.916
1.891
1.806
1.802
1.796
1.792
1.789
1.783
1.779
1.775
1.770
1.766
1.762
1.757
1.752
1.748
1.744
1.724
1.641
1.629
1.619
1.610
1.600
1.595
1.589
1.583
1.576
1.569
1.564
1.476
1.469
1.462
1.451
1.444
1.437
1.425
1.241
0.970
0.248
0.215
0.211
0.182
1.01
0.811
0.878
2.04
0.994
2.44
2.23
1.24
2.61
6.2
2.72
3.12
3.92
3.38
8.88

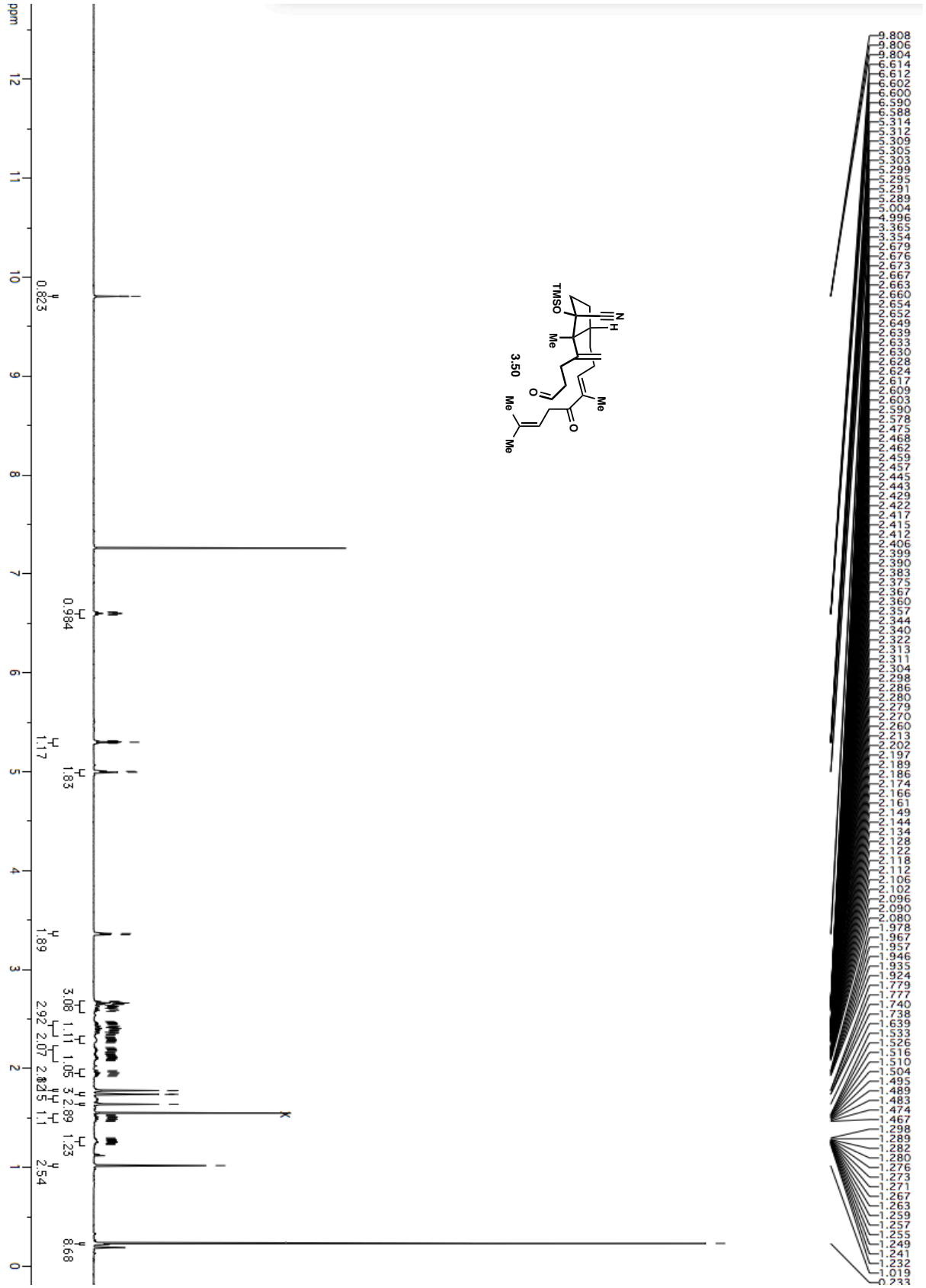
TMSO
N
H
Me
Me
Me
Me
O
O
3.50
ppm
0.823
0.984
1.17
1.83
1.89
3.08
1.11
1.05
3
2.89
1.23
2.92
2.07
2.8
2.5
1.1
2.54
8.68

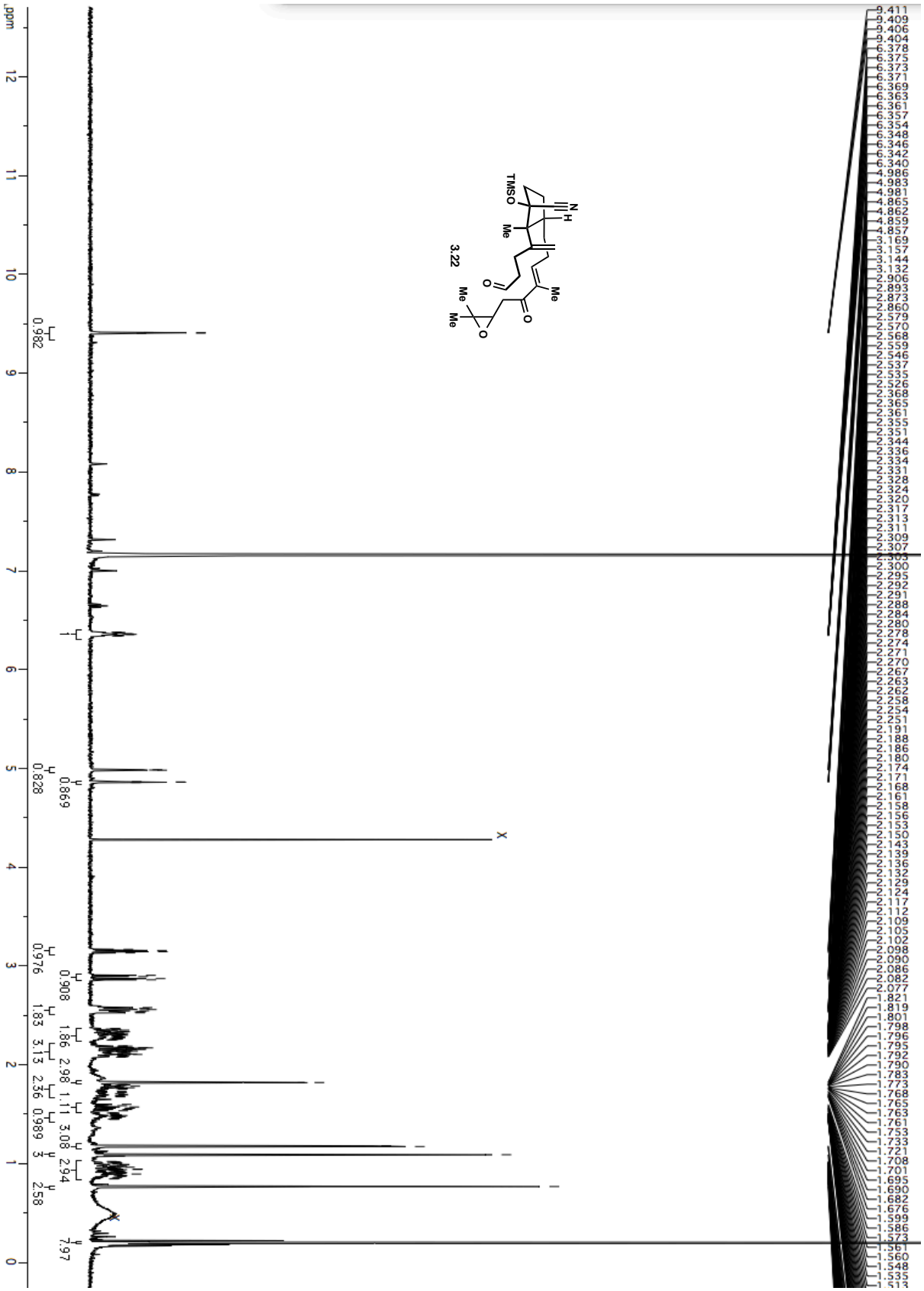
TMSO
Me
N
H
3.22
Me
O
O
Me
Me
O
ppm
0.982
1
0.828
0.869
X
0.976
0.908
1.83
1.86
3.13
2.98
2.36
1.11
0.989
3.08
3
2.94
2.58
7.97

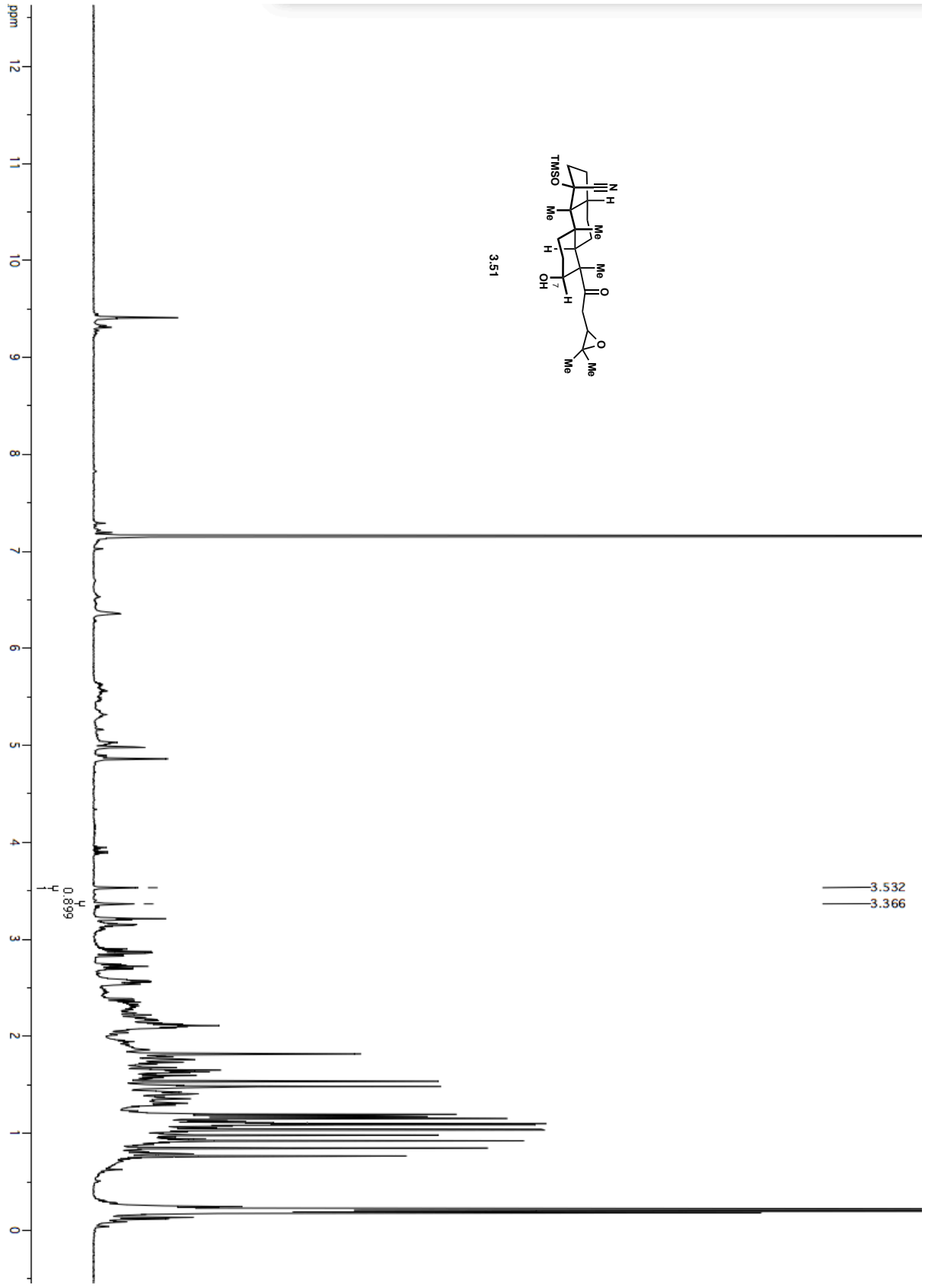
ppm
12
11
10
9
8
7
6
5
4
3
2
1
0
0.869
3.532
3.366
3.51
TMSO
Me
Me
Me
H
OH
H
O
O
Me
Me
N
H

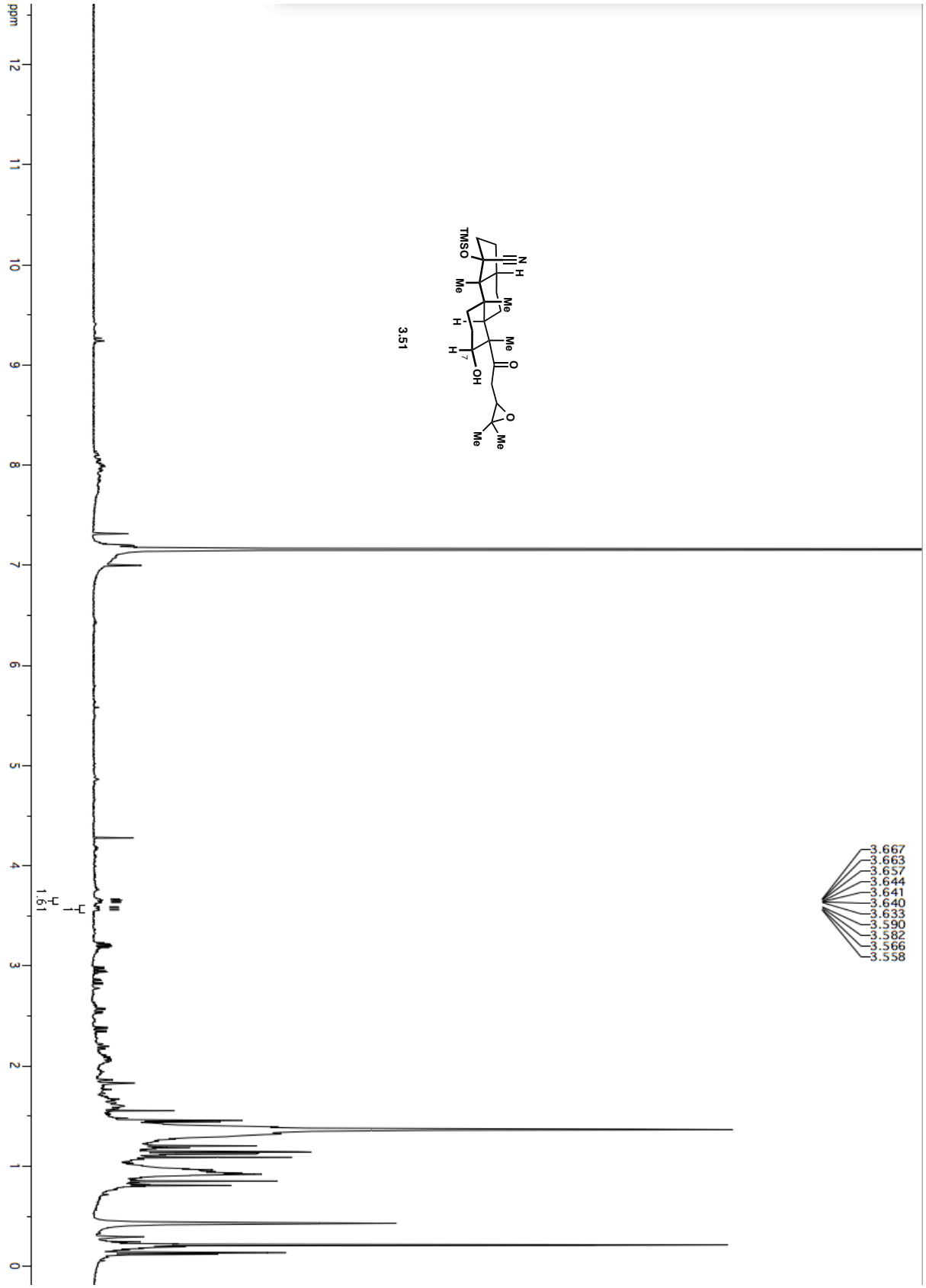
3.667
3.663
3.657
3.644
3.641
3.640
3.633
3.590
3.582
3.566
3.558
3.51
1.61
ppm

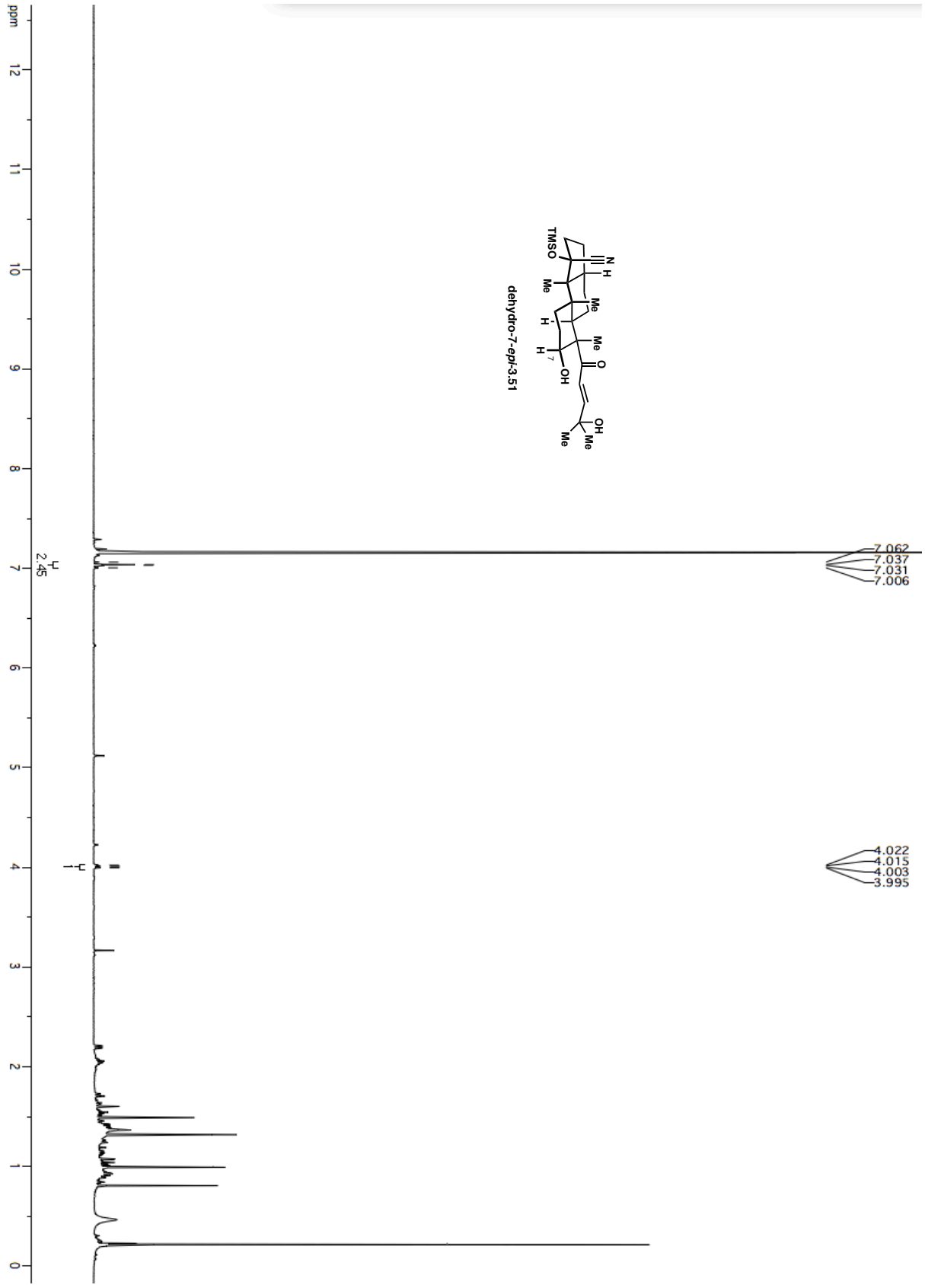
dehydro-7-epi-3.51
7.062
7.037
7.031
7.006
4.022
4.015
4.003
3.995
2.45
1
ppm

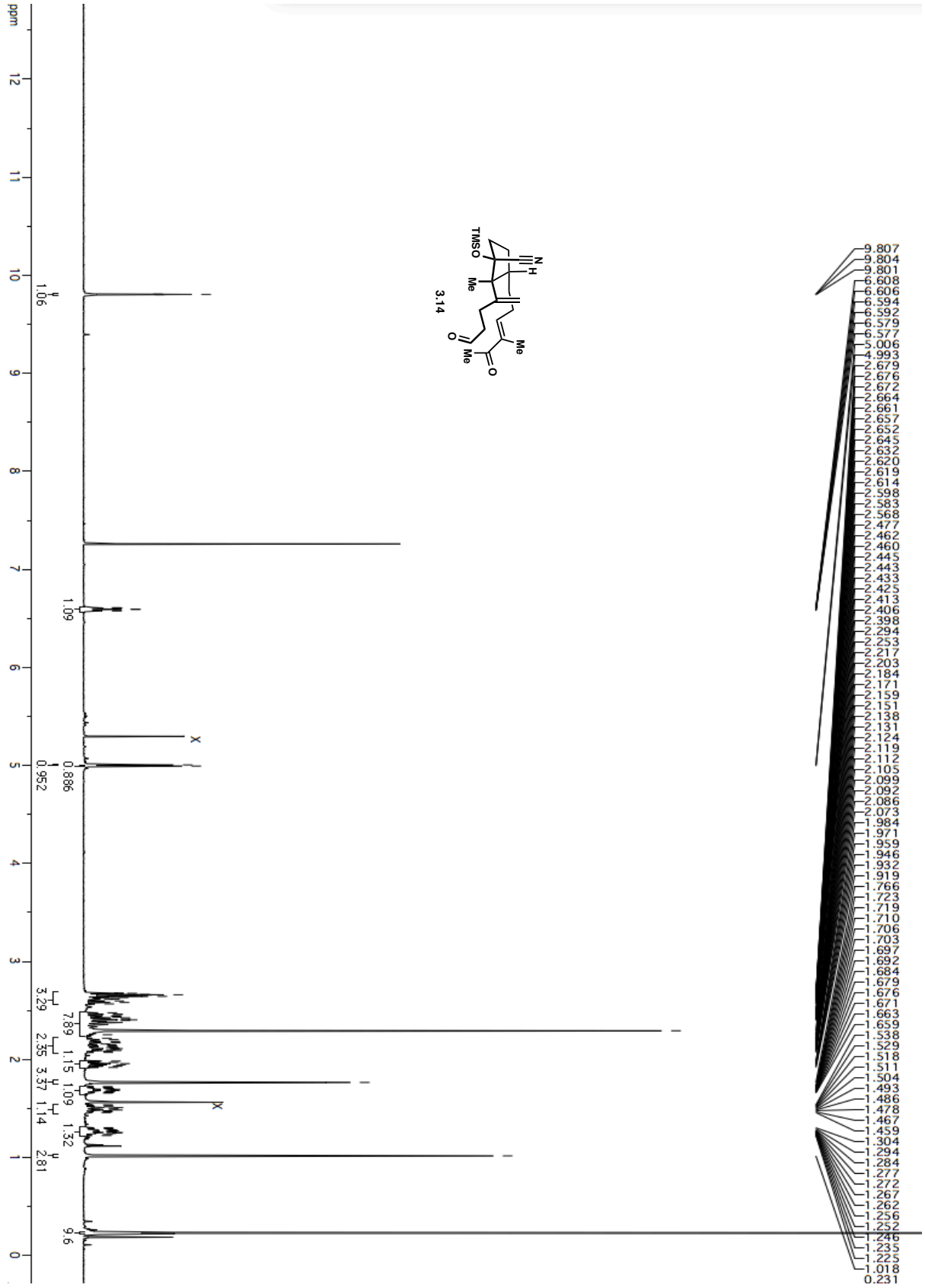
ppm
12
11
10
9
8
7
6
5
4
3
2
1
0
1.06
1.09
0.886
0.952
3.29
7.89
2.35
1.15
3.37
1.09
1.14
1.32
2.81
9.6
3.14
TMSO
Me
N
H
Me
Me
O
O
9.807
9.804
9.801
6.608
6.606
6.594
6.592
6.579
6.577
5.006
4.993
2.679
2.676
2.672
2.664
2.661
2.657
2.652
2.645
2.632
2.620
2.619
2.614
2.598
2.583
2.568
2.477
2.462
2.460
2.445
2.443
2.433
2.425
2.413
2.406
2.398
2.294
2.253
2.217
2.203
2.184
2.171
2.159
2.151
2.138
2.131
2.124
2.119
2.112
2.105
2.099
2.092
2.086
2.073
1.984
1.971
1.959
1.946
1.932
1.919
1.766
1.723
1.719
1.710
1.706
1.703
1.697
1.692
1.684
1.679
1.676
1.671
1.663
1.659
1.538
1.529
1.518
1.511
1.504
1.493
1.486
1.478
1.467
1.459
1.304
1.294
1.284
1.277
1.272
1.267
1.262
1.256
1.252
1.246
1.235
1.225
1.018
0.231

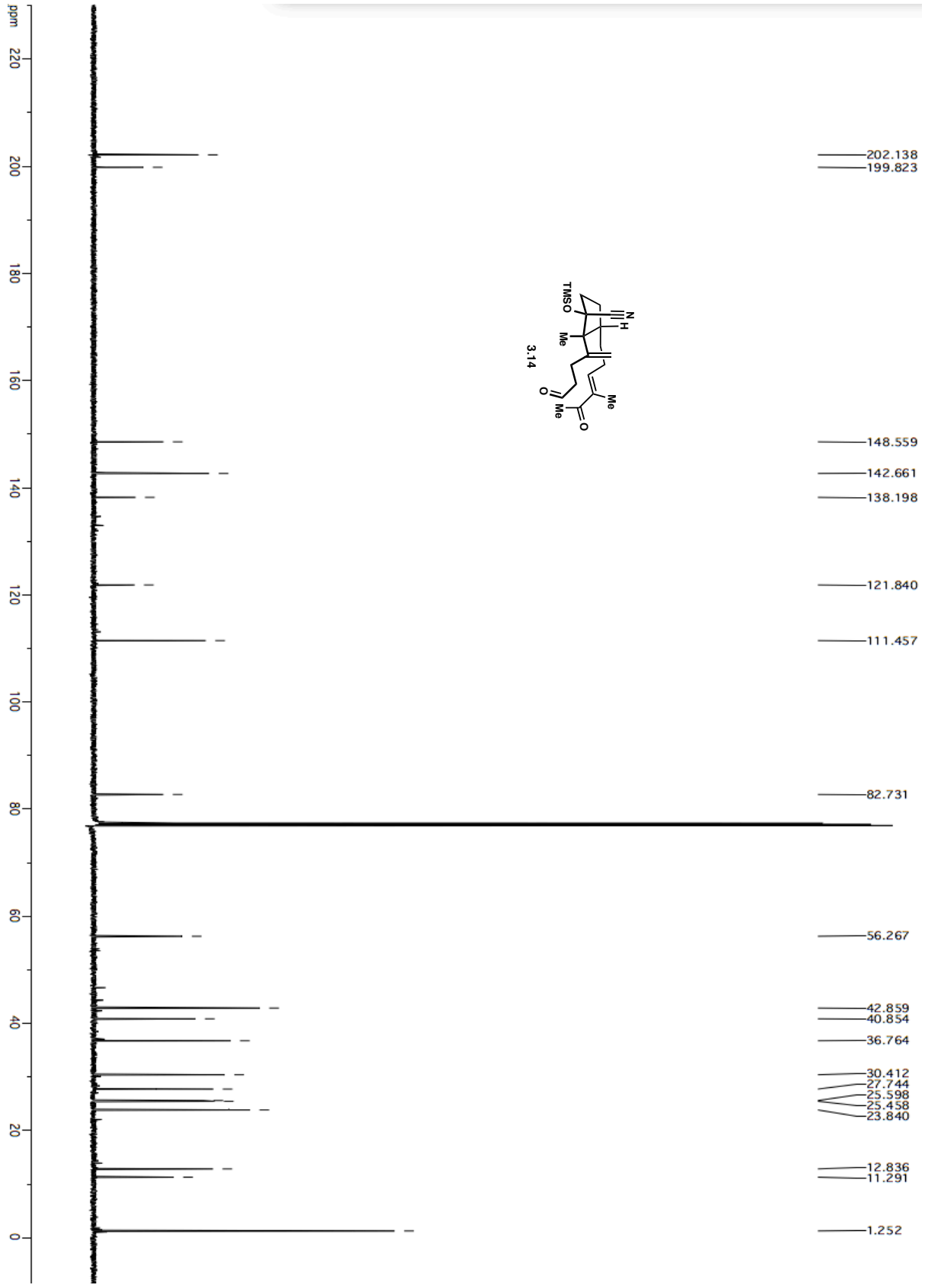
ppm
220
200
180
160
140
120
100
80
60
40
20
0
202.138
199.823
148.559
142.661
138.198
121.840
111.457
82.731
56.267
42.859
40.854
36.764
30.412
27.744
25.598
25.458
23.840
12.836
11.291
1.252
TMSO
Me
N
H
3.14
O
Me
Me
O

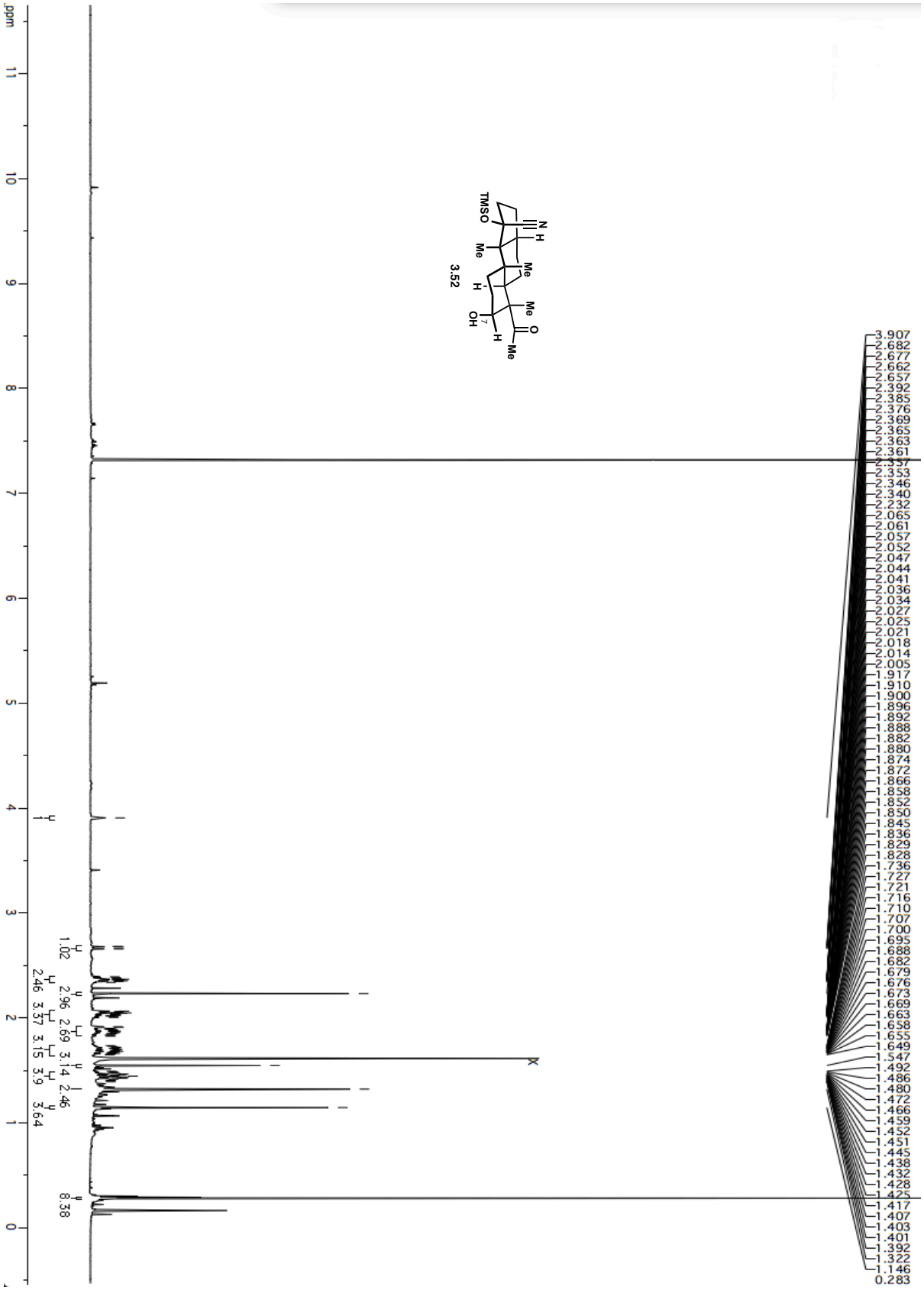
TMSO
N
H
Me
Me
H
3.52
Me
O
OH
H
Me
3.907
2.682
2.677
2.662
2.657
2.392
2.385
2.376
2.369
2.365
2.363
2.361
2.357
2.353
2.346
2.340
2.232
2.065
2.061
2.057
2.052
2.047
2.044
2.041
2.036
2.034
2.027
2.025
2.021
2.018
2.014
2.005
1.917
1.910
1.900
1.896
1.892
1.888
1.882
1.880
1.874
1.872
1.866
1.858
1.852
1.850
1.845
1.836
1.829
1.828
1.736
1.727
1.721
1.716
1.710
1.707
1.700
1.695
1.688
1.682
1.679
1.676
1.673
1.669
1.663
1.658
1.655
1.649
1.547
1.492
1.486
1.480
1.472
1.466
1.459
1.452
1.451
1.445
1.438
1.432
1.428
1.423
1.417
1.407
1.403
1.401
1.392
1.322
1.146
0.283
1.02
2.96
2.69
3.14
2.46
2.46
3.37
3.15
3.9
3.64
8.38
ppm

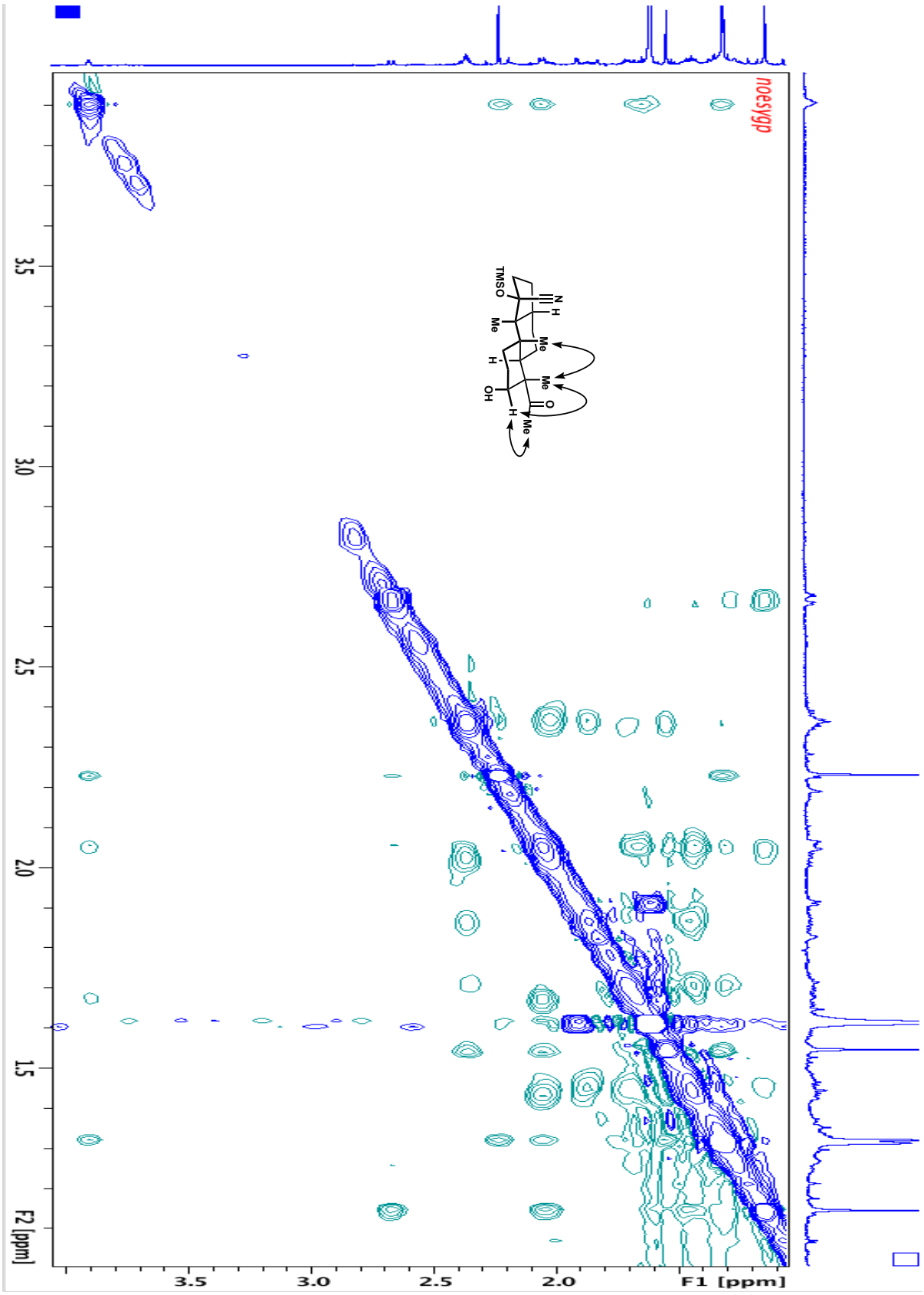
noesygp
TMSO
N
H
Me
Me
H
Me
OH
O
H
Me
3.5
3.0
2.5
2.0
1.5
F2 [ppm]
3.5
3.0
2.5
2.0
F1 [ppm]

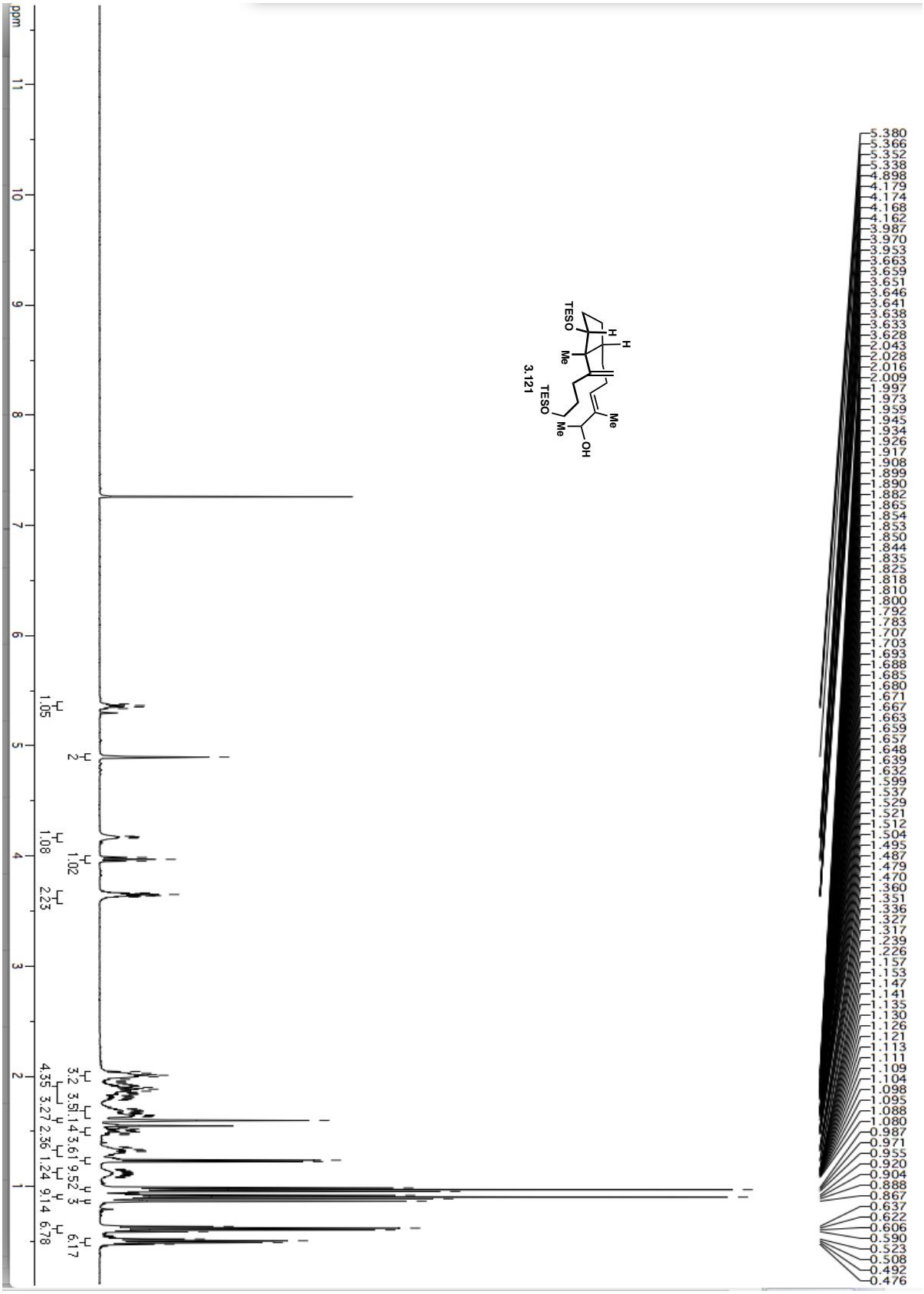
TESO
Me
H
H
TESO
Me
Me
OH
3.121
5.380
5.366
5.352
5.338
4.898
4.179
4.174
4.168
4.162
3.987
3.970
3.953
3.663
3.659
3.651
3.646
3.641
3.638
3.633
3.628
2.043
2.028
2.016
2.009
1.997
1.973
1.959
1.945
1.934
1.926
1.917
1.908
1.899
1.890
1.882
1.865
1.854
1.853
1.850
1.844
1.835
1.825
1.818
1.810
1.800
1.792
1.783
1.707
1.703
1.693
1.688
1.685
1.680
1.671
1.667
1.663
1.659
1.657
1.648
1.639
1.632
1.599
1.537
1.529
1.521
1.512
1.504
1.495
1.487
1.479
1.470
1.360
1.351
1.336
1.327
1.317
1.239
1.226
1.157
1.153
1.147
1.141
1.135
1.130
1.126
1.121
1.113
1.111
1.109
1.104
1.098
1.095
1.088
1.080
0.987
0.971
0.955
0.920
0.904
0.888
0.867
0.637
0.622
0.606
0.590
0.523
0.508
0.492
0.476
ppm
1.05
2
1.02
1.08
2.23
3.2
3.51
4.14
3.61
9.52
3
4.35
3.27
2.36
1.24
9.14
6.78
6.17

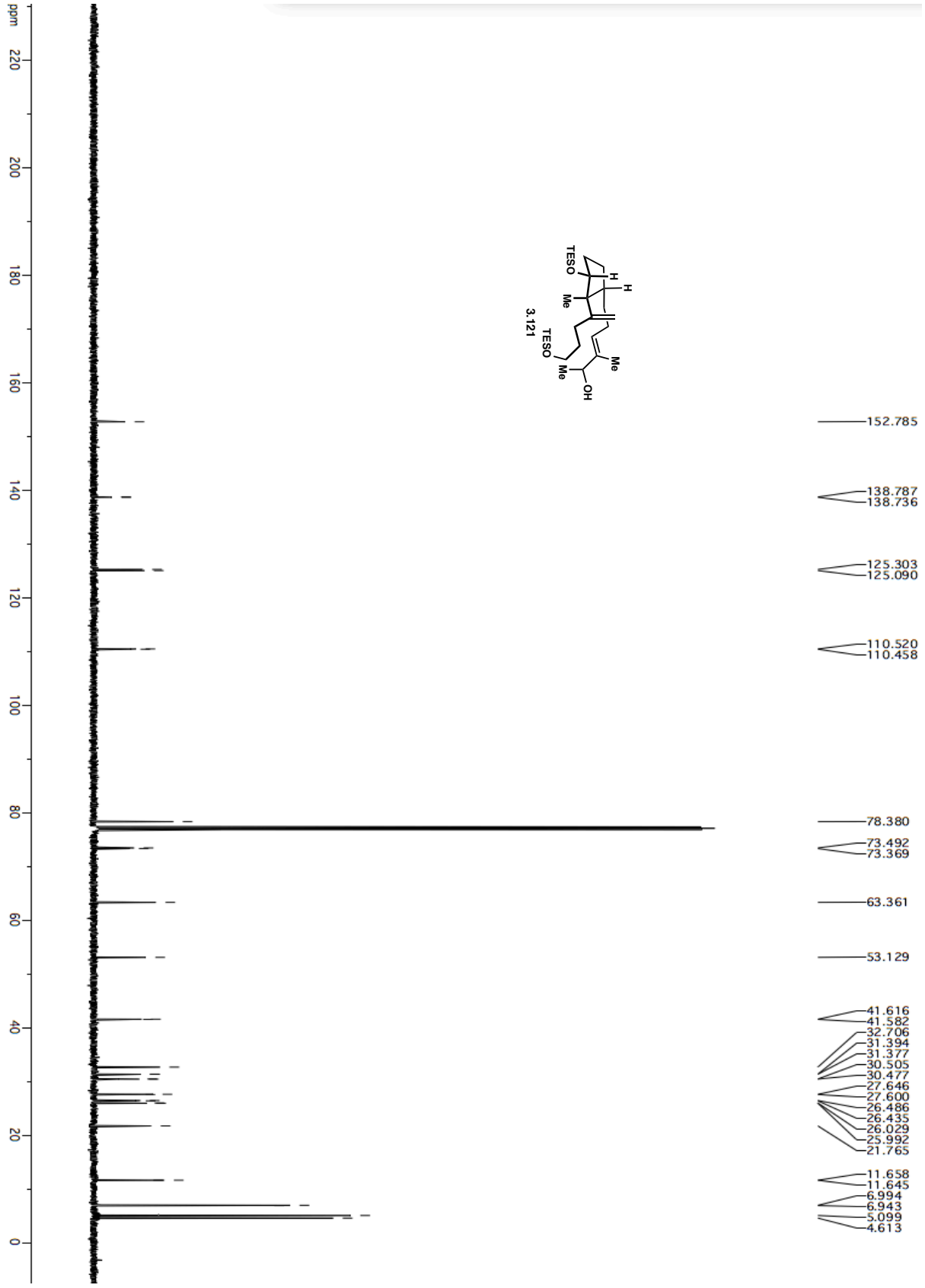
ppm
220
200
180
160
140
120
100
80
60
40
20
0
TESO
H
H
Me
3.121
TESO
Me
Me
OH
152.785
138.787
138.736
125.303
125.090
110.520
110.458
78.380
73.492
73.369
63.361
53.129
41.616
41.582
32.706
31.394
31.377
30.505
30.477
27.646
27.600
26.486
26.435
26.029
25.992
21.765
11.658
11.645
6.994
6.943
5.099
4.613

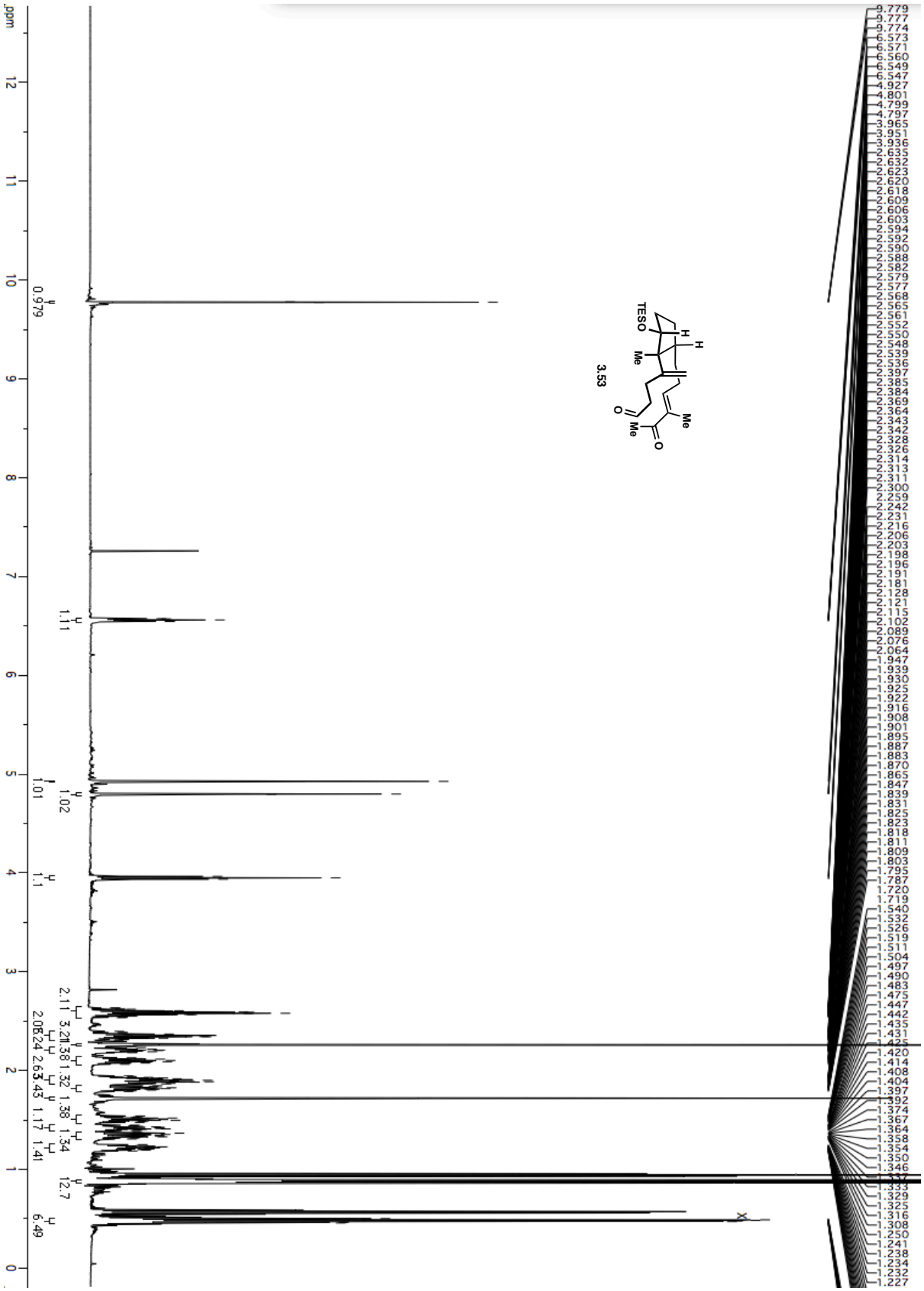
TESO
Me
H
H
Me
Me
O
O
3.53
ppm
0.979
1.11
1.02
1.01
1.1
2.11
3.21
3.38
1.32
1.38
1.34
2.06
2.24
2.63
3.43
1.17
1.41
12.7
6.49

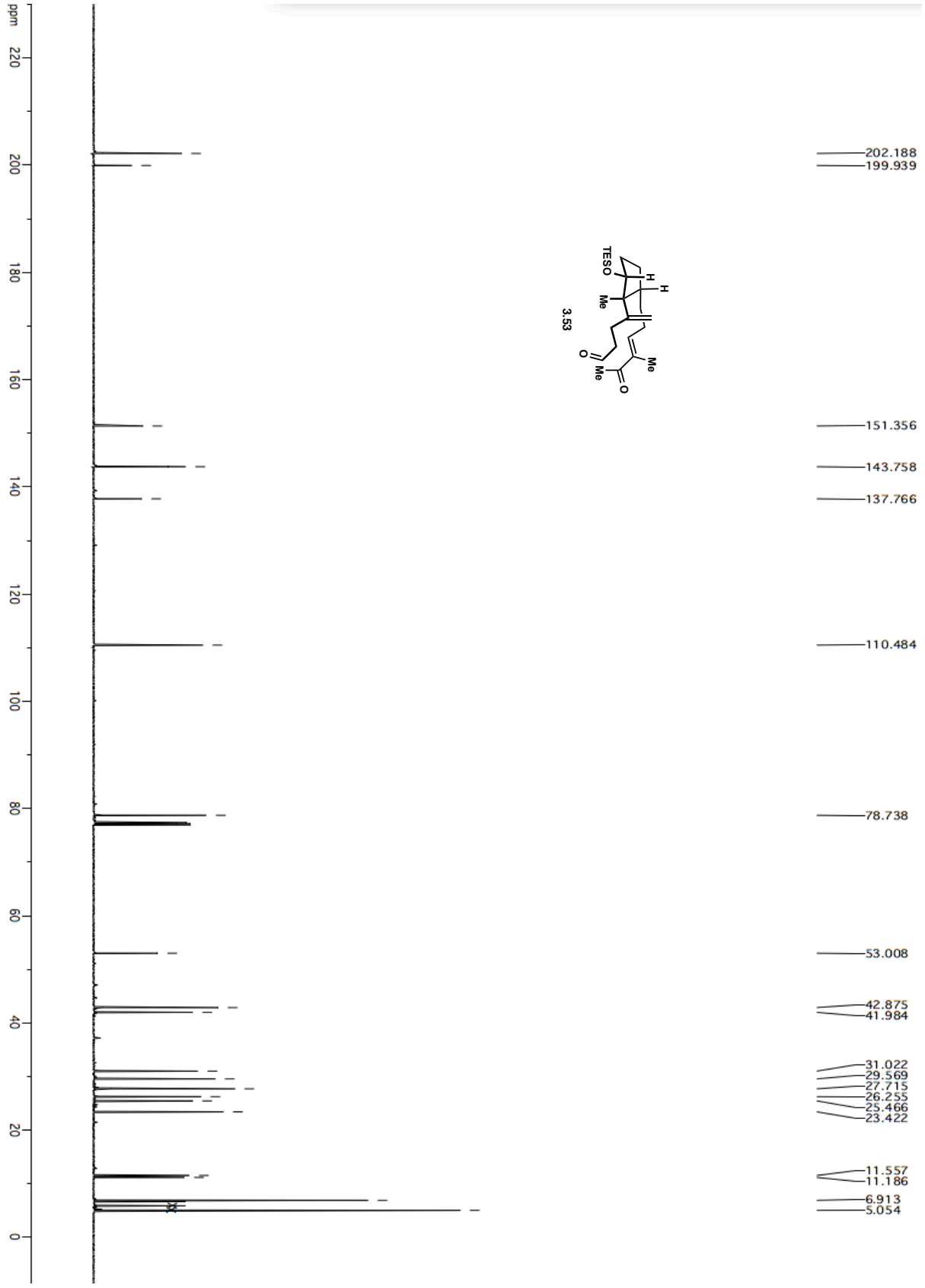
ppm
220
200
180
160
140
120
100
80
60
40
20
0
202.188
199.939
151.356
143.758
137.766
110.484
78.738
53.008
42.875
41.984
31.022
29.569
27.715
26.255
25.466
23.422
11.557
11.186
6.913
5.054
TESO
Me
H
H
3.53
O
Me
Me
O

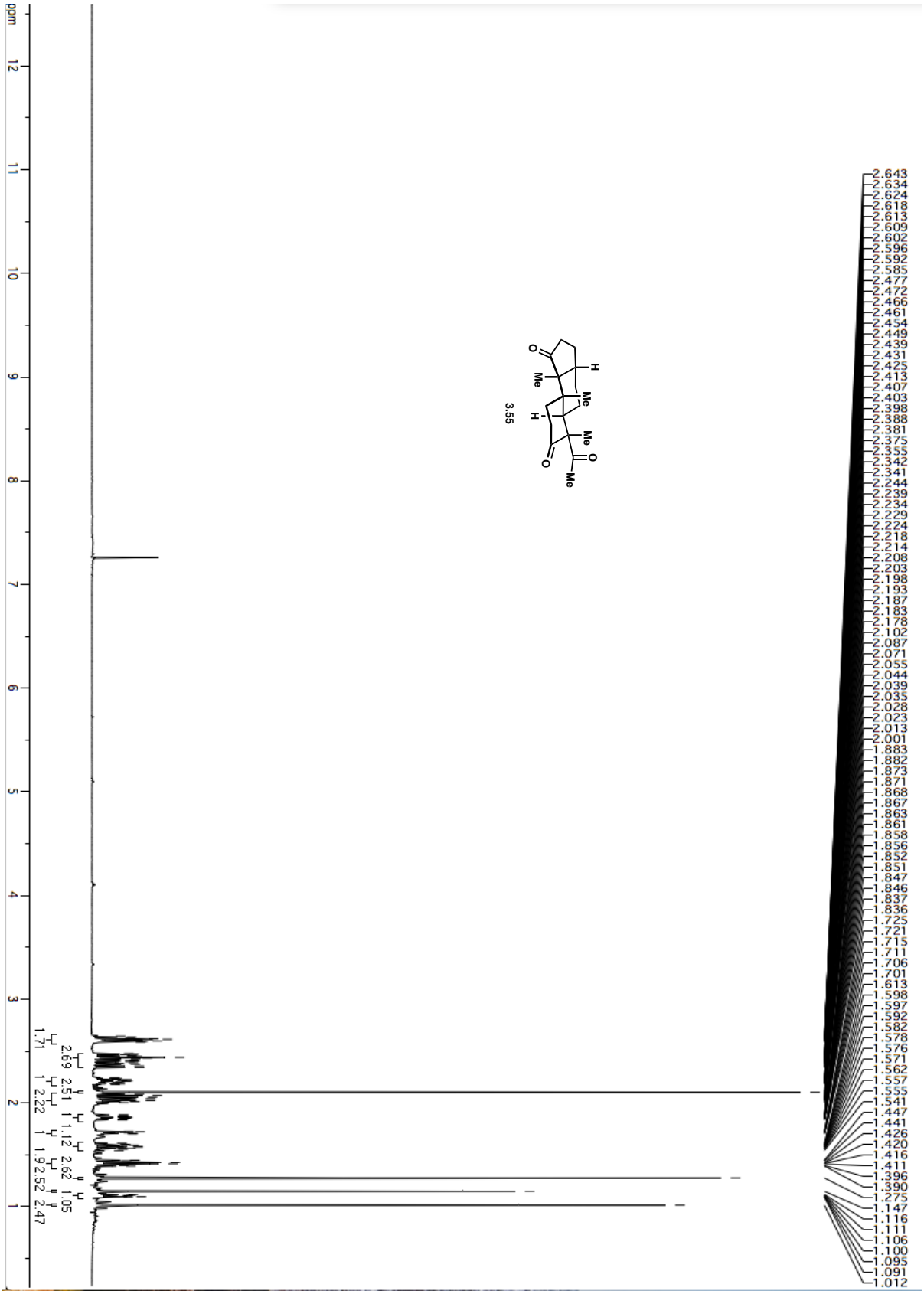
ppm
12
11
10
9
8
7
6
5
4
3
2
1
1.71
2.69
2.51
1.12
2.22
1
1.92
2.62
1.05
2.52
2.47
3.55
O
Me
H
Me
Me
H
O
O
Me
2.643
2.634
2.624
2.618
2.613
2.609
2.602
2.596
2.592
2.585
2.477
2.472
2.466
2.461
2.454
2.449
2.439
2.431
2.425
2.413
2.407
2.403
2.398
2.388
2.381
2.375
2.355
2.342
2.341
2.244
2.239
2.234
2.229
2.224
2.218
2.214
2.208
2.203
2.198
2.193
2.187
2.183
2.178
2.102
2.087
2.071
2.055
2.044
2.039
2.035
2.028
2.023
2.013
2.001
1.883
1.882
1.873
1.871
1.868
1.867
1.863
1.861
1.858
1.856
1.852
1.851
1.847
1.846
1.837
1.836
1.725
1.721
1.715
1.711
1.706
1.701
1.613
1.598
1.597
1.592
1.582
1.578
1.576
1.571
1.562
1.557
1.555
1.541
1.447
1.441
1.426
1.420
1.416
1.411
1.396
1.390
1.275
1.147
1.116
1.111
1.106
1.100
1.095
1.091
1.012

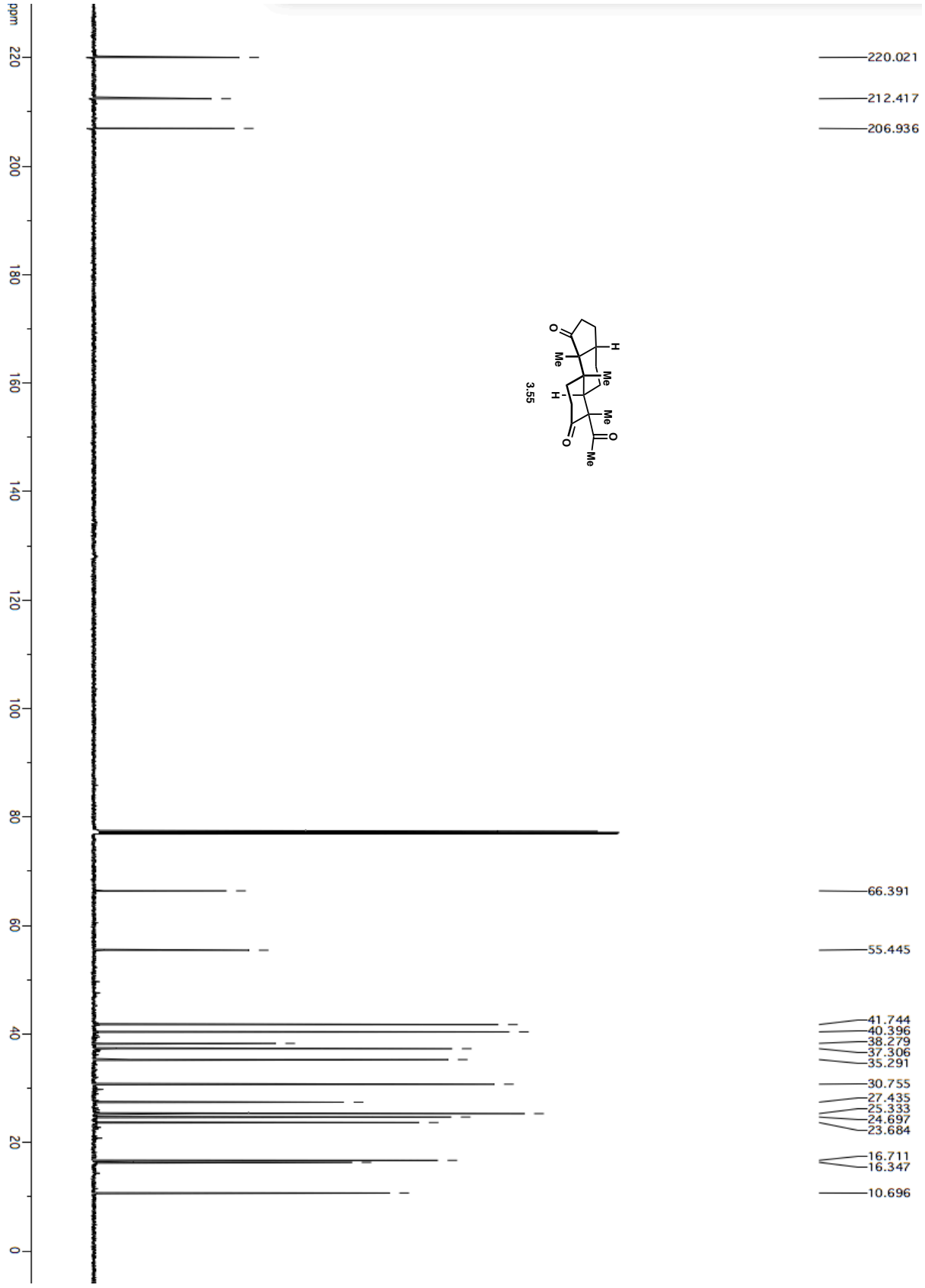
ppm
220
200
180
160
140
120
100
80
60
40
20
0
220.021
212.417
206.936
66.391
55.445
41.744
40.396
38.279
37.306
35.291
30.755
27.435
25.333
24.697
23.684
16.711
16.347
10.696
3.55
O
Me
H
Me
H
Me
O
O
Me

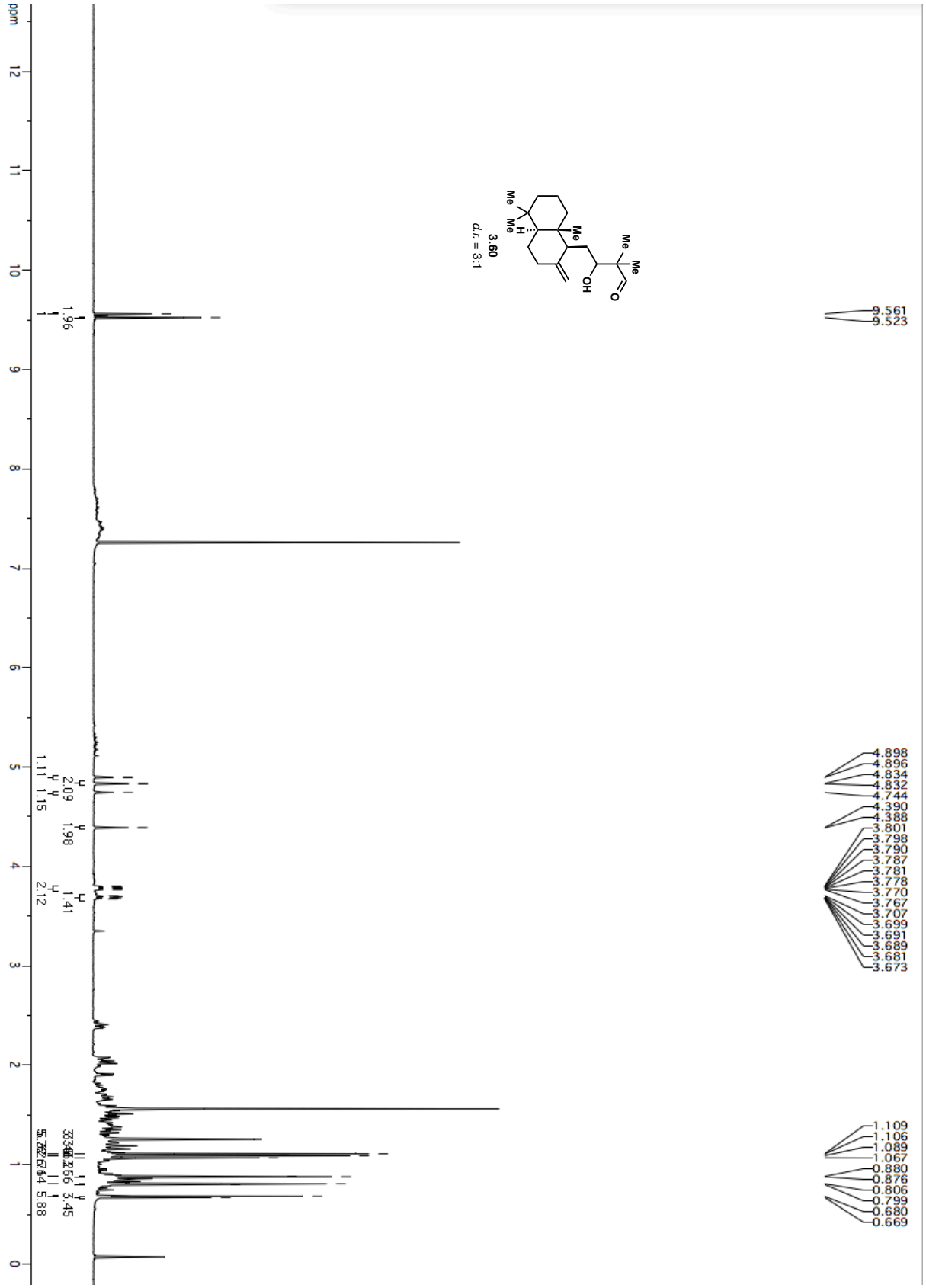
3.60
d.r. = 3:1
9.561
9.523
4.898
4.896
4.834
4.832
4.744
4.390
4.388
3.801
3.798
3.790
3.787
3.781
3.778
3.770
3.767
3.707
3.699
3.691
3.689
3.681
3.673
1.109
1.106
1.089
1.067
0.880
0.876
0.806
0.799
0.680
0.669
1.96
2.09
1.98
1.41
2.12
1.11
1.15
3.45
5.88
ppm

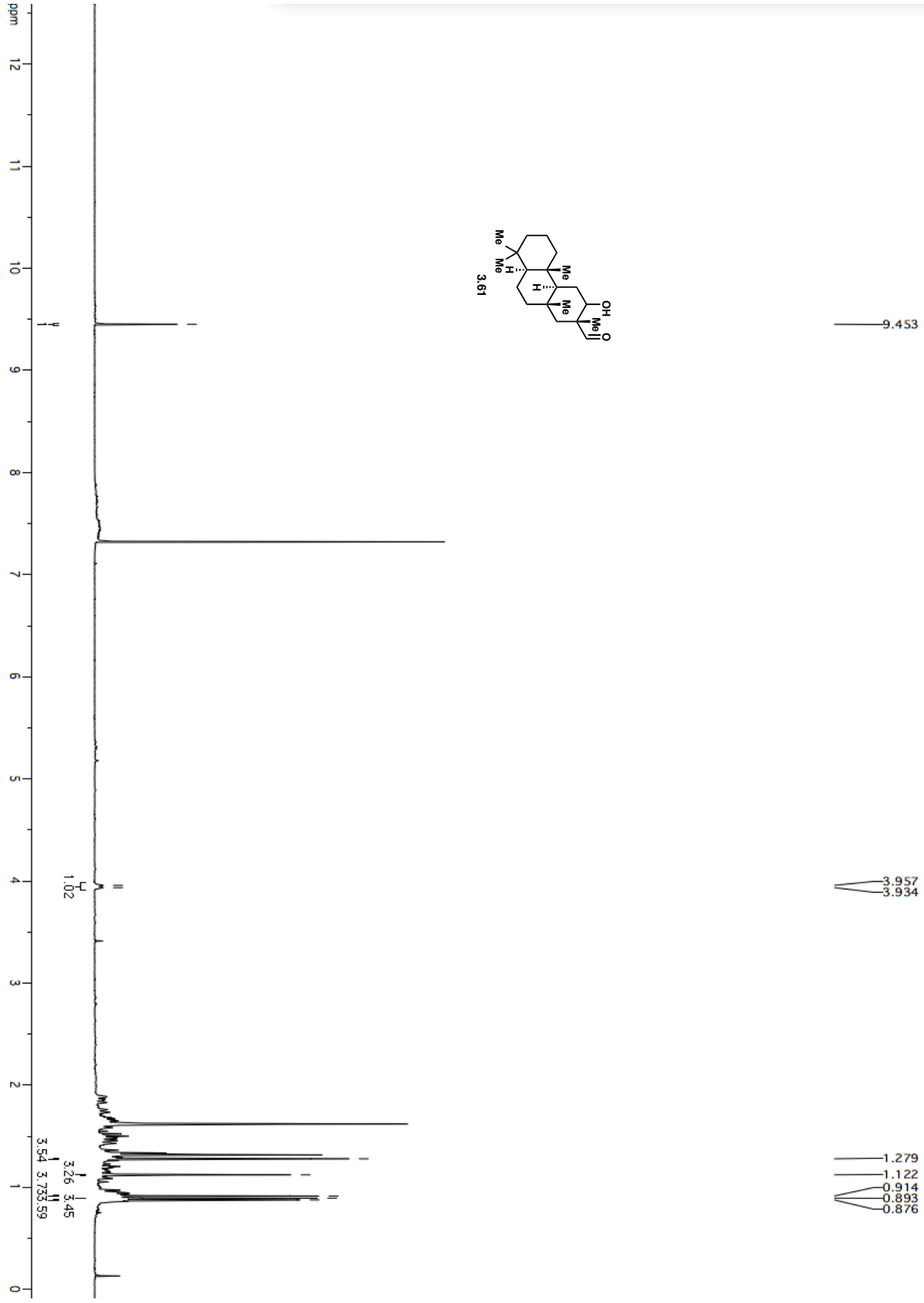
ppm
12
11
10
9
8
7
6
5
4
3
2
1
0
1
1.02
3.54
3.26
3.73
3.59
5.45
Me
Me
H
3.61
Me
H
Me
OH
Me
O
9.453
3.957
3.934
1.279
1.122
0.914
0.893
0.876

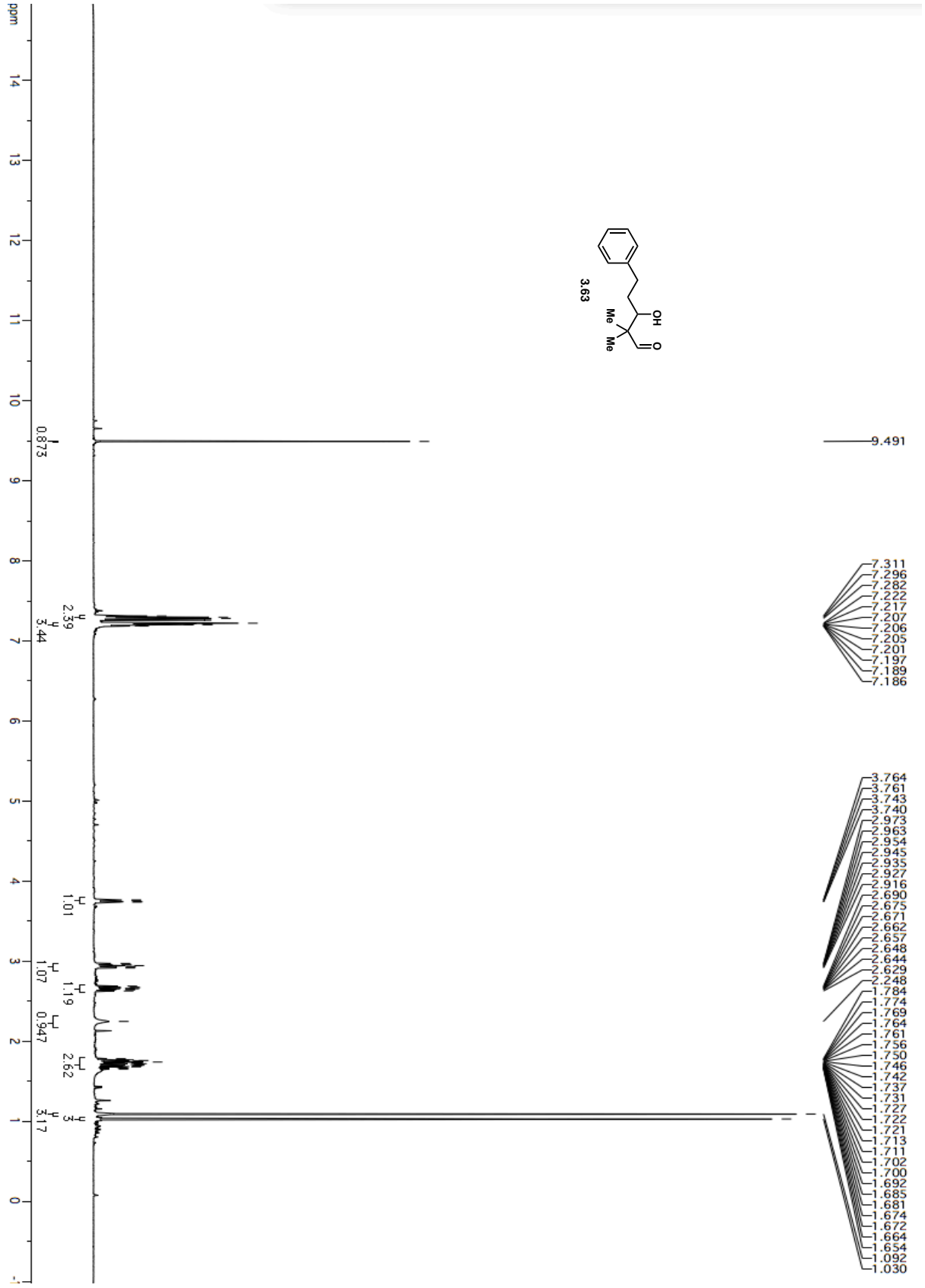
ppm
14
13
12
11
10
9
8
7
6
5
4
3
2
1
0
-1
0.873
2.39
3.44
1.01
1.07
1.19
0.947
2.62
3.17
3.63
Me
Me
OH
O
9.491
7.311
7.296
7.282
7.222
7.217
7.207
7.206
7.205
7.201
7.197
7.189
7.186
3.764
3.761
3.743
3.740
2.973
2.963
2.954
2.945
2.935
2.927
2.916
2.690
2.675
2.671
2.662
2.657
2.648
2.644
2.629
2.248
1.784
1.774
1.769
1.764
1.761
1.756
1.750
1.746
1.742
1.737
1.731
1.727
1.722
1.721
1.713
1.711
1.702
1.700
1.692
1.685
1.681
1.674
1.672
1.664
1.654
1.092
1.030

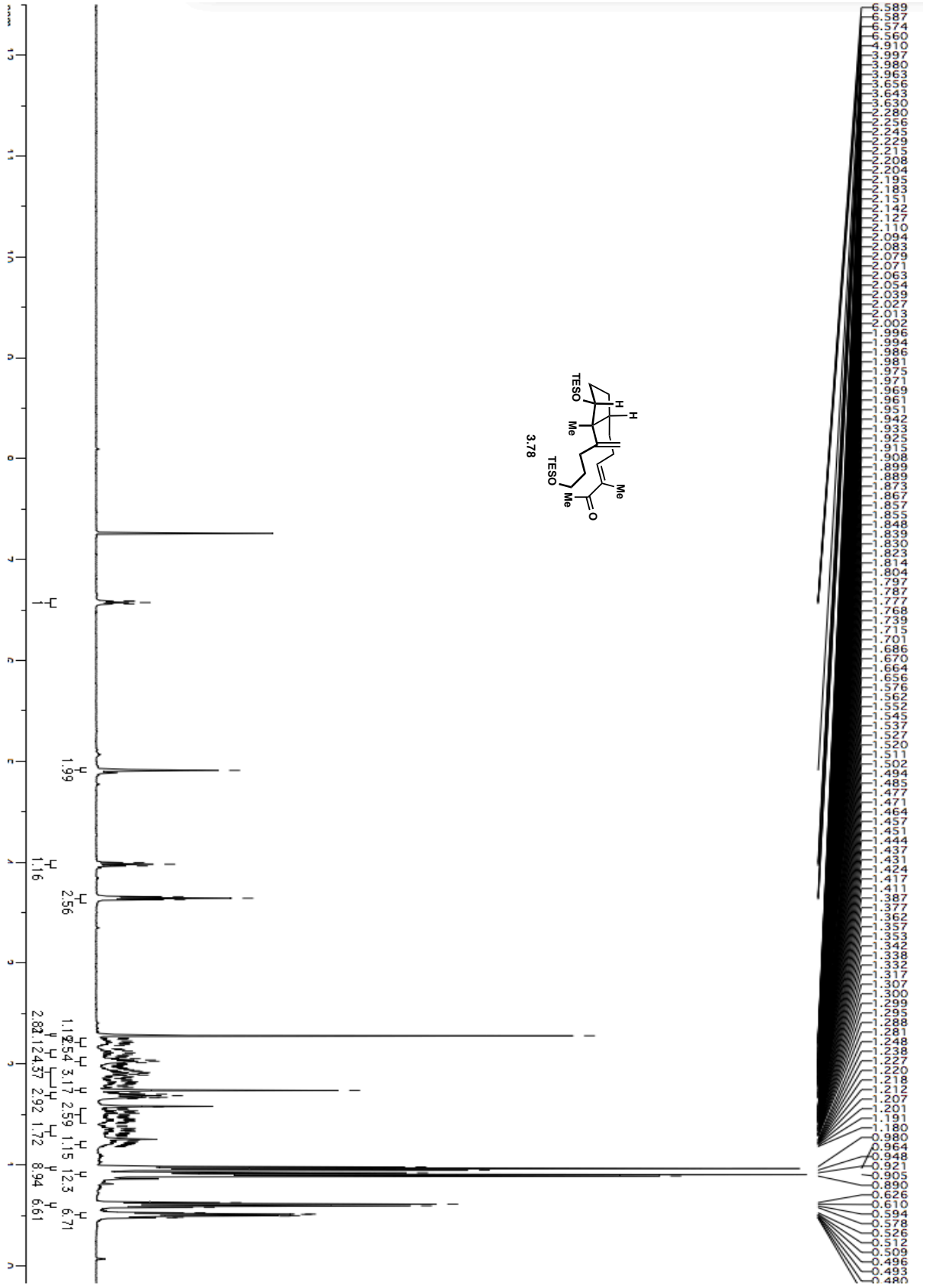
TESO
Me
H
H
Me
TESO
Me
O
3.78

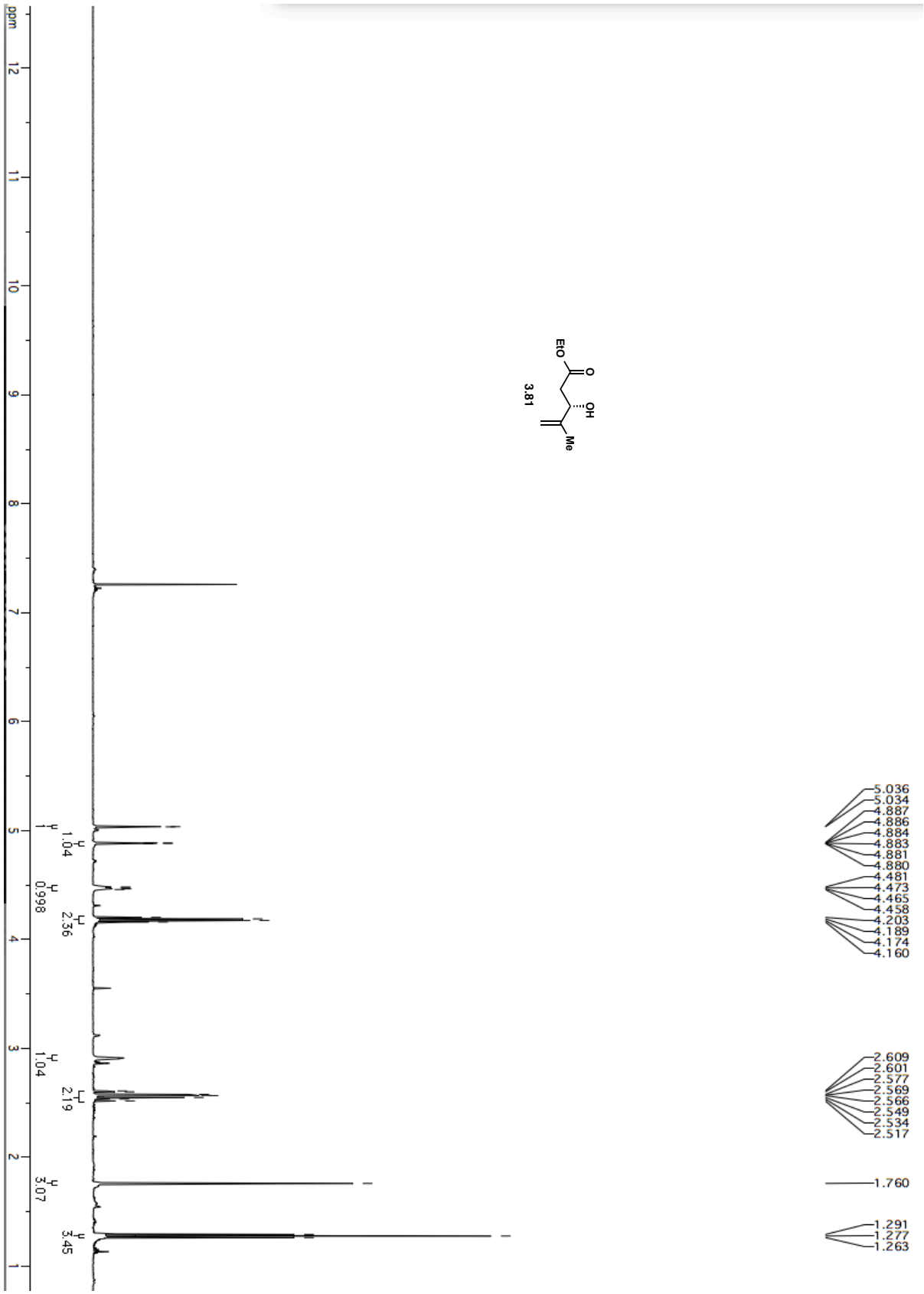
EtO
O
OH
Me
3.81
5.036
5.034
4.887
4.886
4.884
4.883
4.881
4.880
4.481
4.473
4.465
4.458
4.203
4.189
4.174
4.160
2.609
2.601
2.577
2.569
2.566
2.549
2.534
2.517
1.760
1.291
1.277
1.263
1.04
0.998
2.36
1.04
2.19
3.07
3.45
ppm

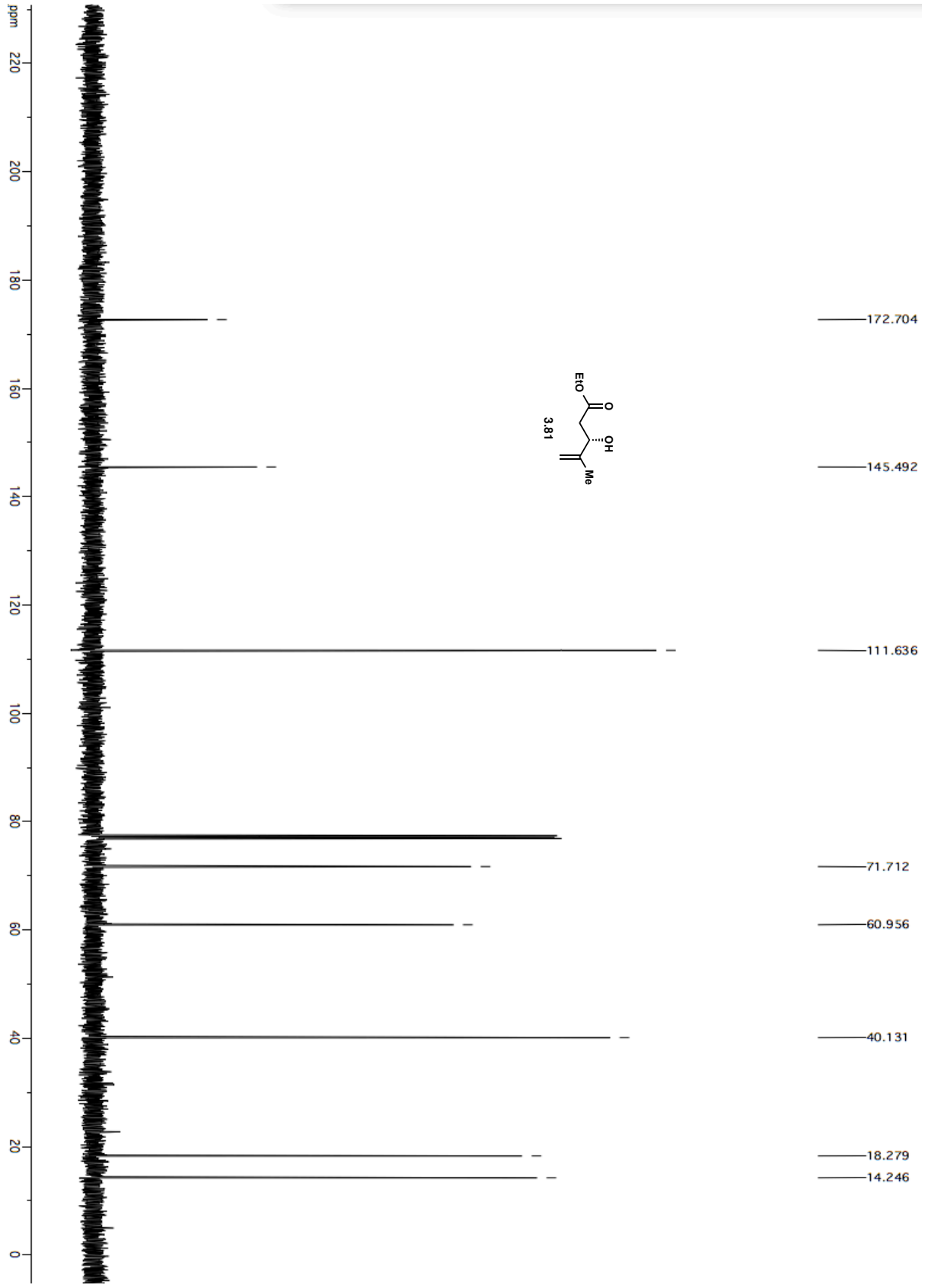
ppm
220
200
180
160
140
120
100
80
60
40
20
0
172.704
145.492
111.636
71.712
60.956
40.131
18.279
14.246
EtO
O
OH
Me
3.81

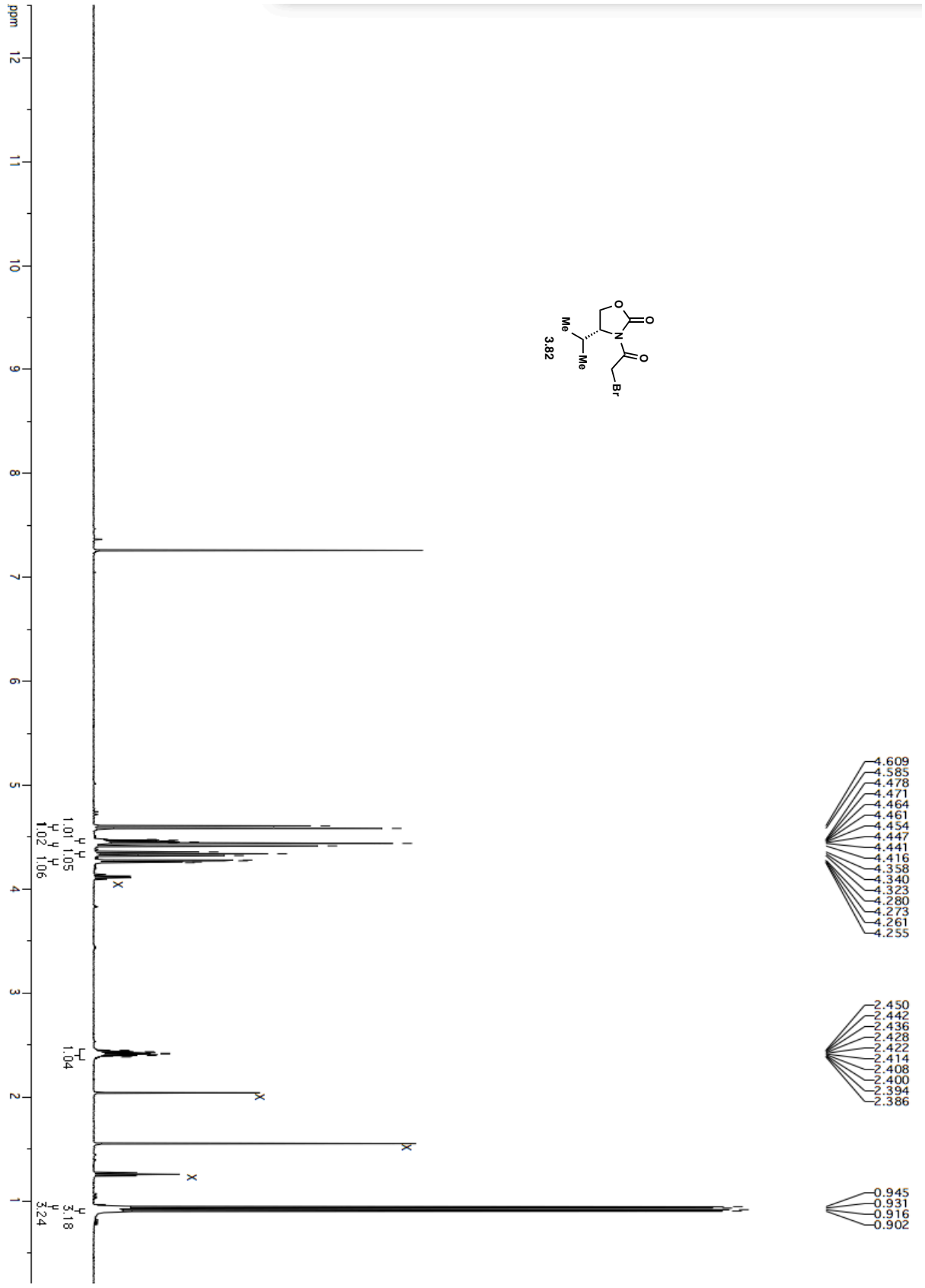
ppm
12
11
10
9
8
7
6
5
4
3
2
1
1.01
1.05
1.02
1.06
1.04
3.18
3.24
3.82
Me
Me
O
O
N
O
O
Br
4.609
4.585
4.478
4.471
4.464
4.461
4.454
4.447
4.441
4.416
4.358
4.340
4.323
4.280
4.273
4.261
4.255
2.450
2.442
2.436
2.428
2.422
2.414
2.408
2.400
2.394
2.386
0.945
0.931
0.916
0.902

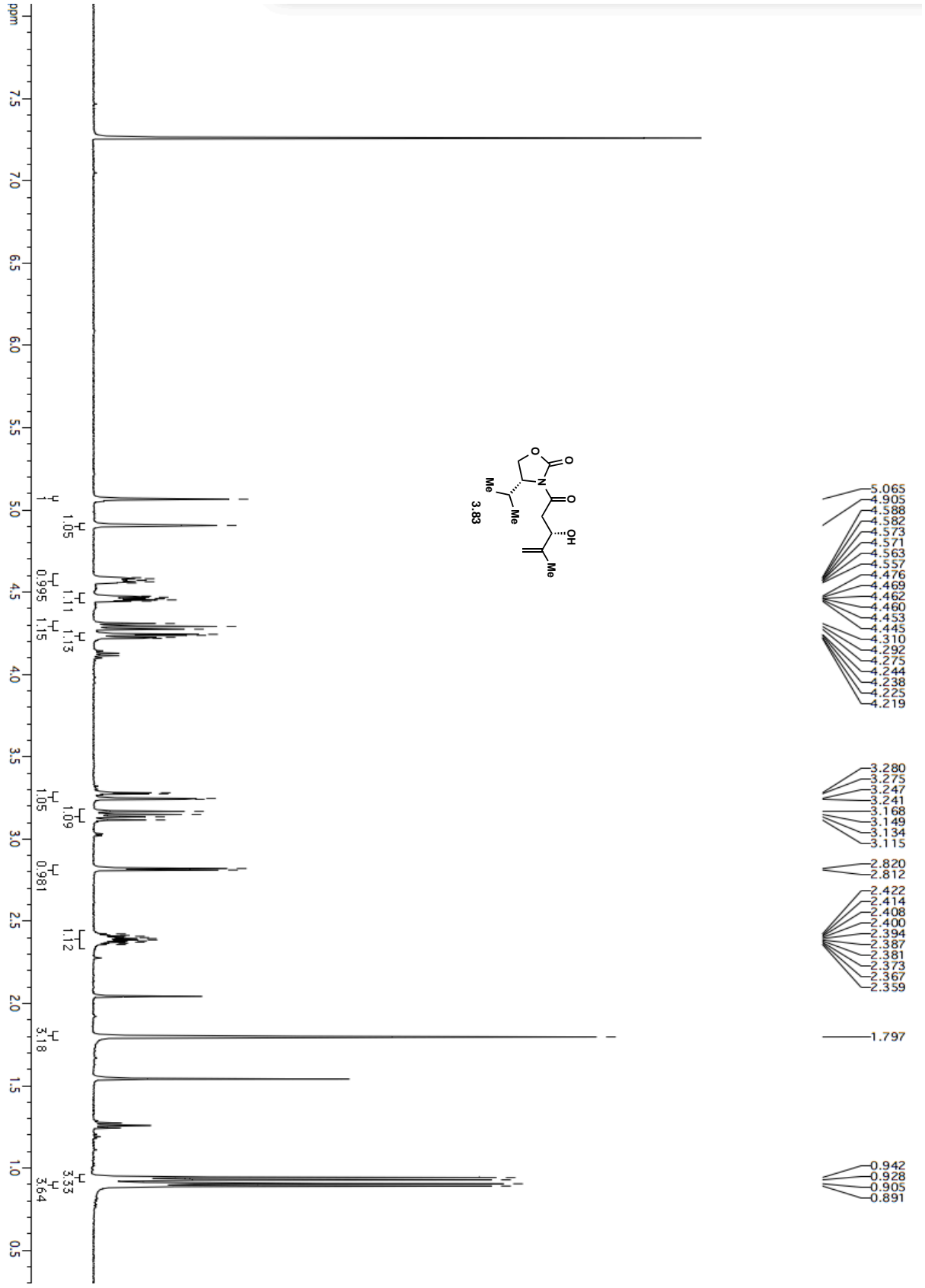
ppm
7.5
7.0
6.5
6.0
5.5
5.0
4.5
4.0
3.5
3.0
2.5
2.0
1.5
1.0
0.5
1.05
0.995
1.11
1.15
1.13
1.05
1.09
0.981
1.12
3.18
3.33
3.64
3.83
Me
Me
O
O
N
O
OH
Me
5.065
4.905
4.588
4.582
4.573
4.571
4.563
4.557
4.476
4.469
4.462
4.460
4.453
4.445
4.310
4.292
4.275
4.244
4.238
4.225
4.219
3.280
3.275
3.247
3.241
3.168
3.149
3.134
3.115
2.820
2.812
2.422
2.414
2.408
2.400
2.394
2.387
2.381
2.373
2.367
2.359
1.797
0.942
0.928
0.905
0.891

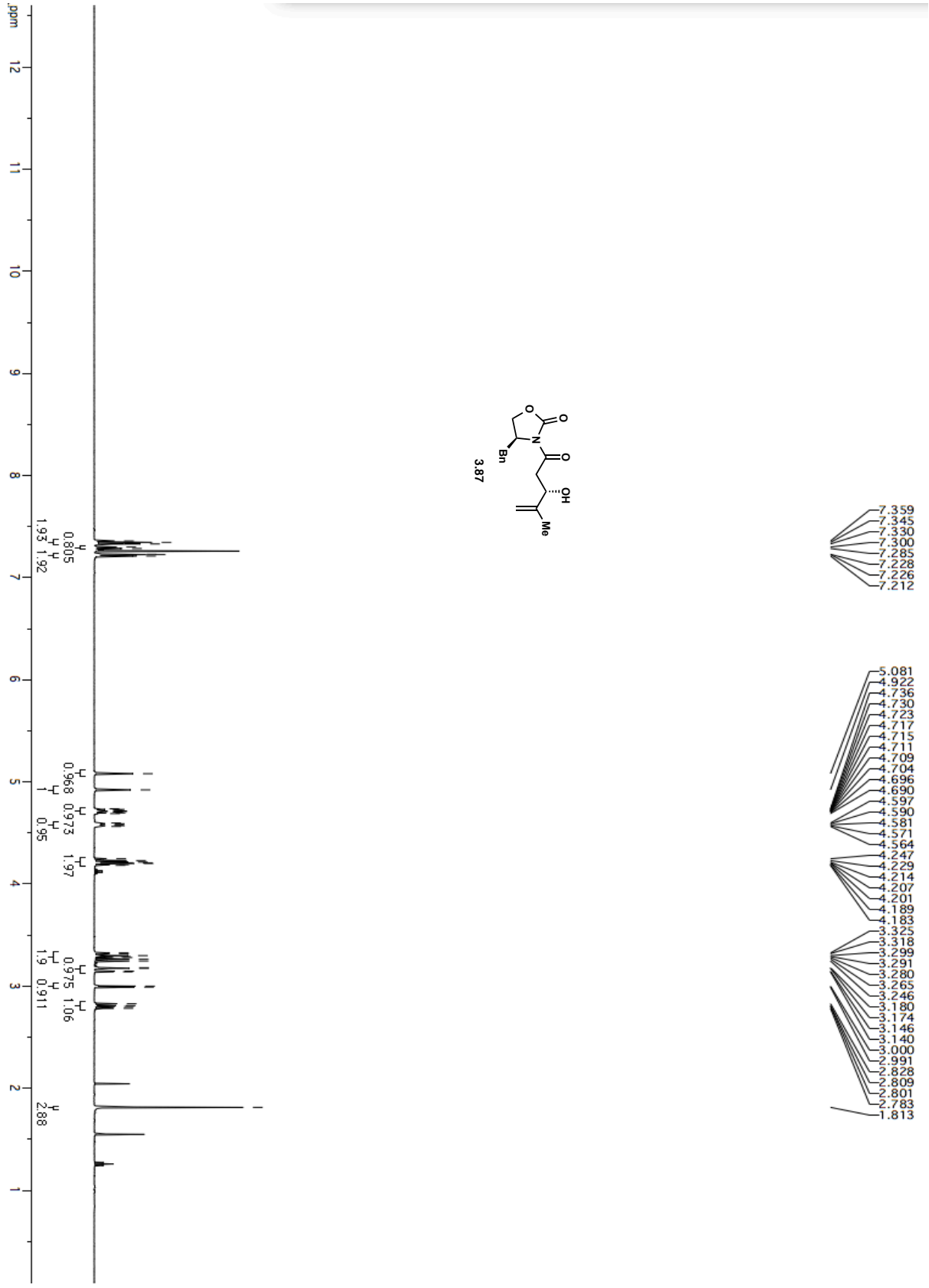
ppm
12
11
10
9
8
7
6
5
4
3
2
1
0.805
1.93
1.92
0.968
1
0.973
0.95
1.97
0.975
1.9
0.911
1.06
2.88
3.87
Bn
OH
Me
7.359
7.345
7.330
7.300
7.285
7.228
7.226
7.212
5.081
4.922
4.736
4.730
4.723
4.717
4.715
4.711
4.709
4.704
4.696
4.690
4.597
4.590
4.581
4.571
4.564
4.247
4.229
4.214
4.207
4.201
4.189
4.183
3.325
3.318
3.299
3.291
3.280
3.265
3.246
3.180
3.174
3.146
3.140
3.000
2.991
2.828
2.809
2.801
2.783
1.813

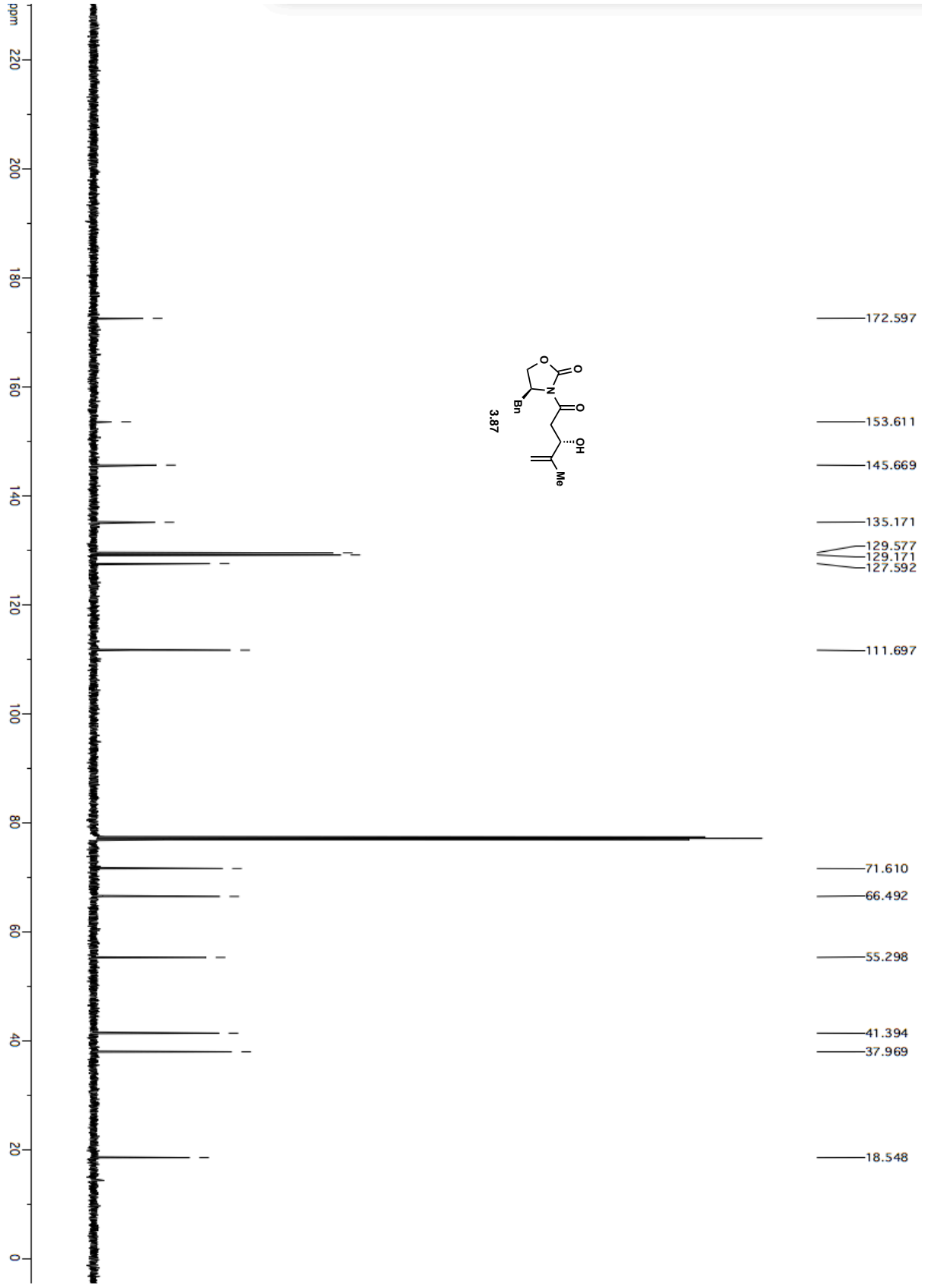
ppm
220
200
180
160
140
120
100
80
60
40
20
0
172.597
153.611
145.669
135.171
129.577
129.171
127.592
111.697
71.610
66.492
55.298
41.394
37.969
18.548
3.87
Bn
OH
Me

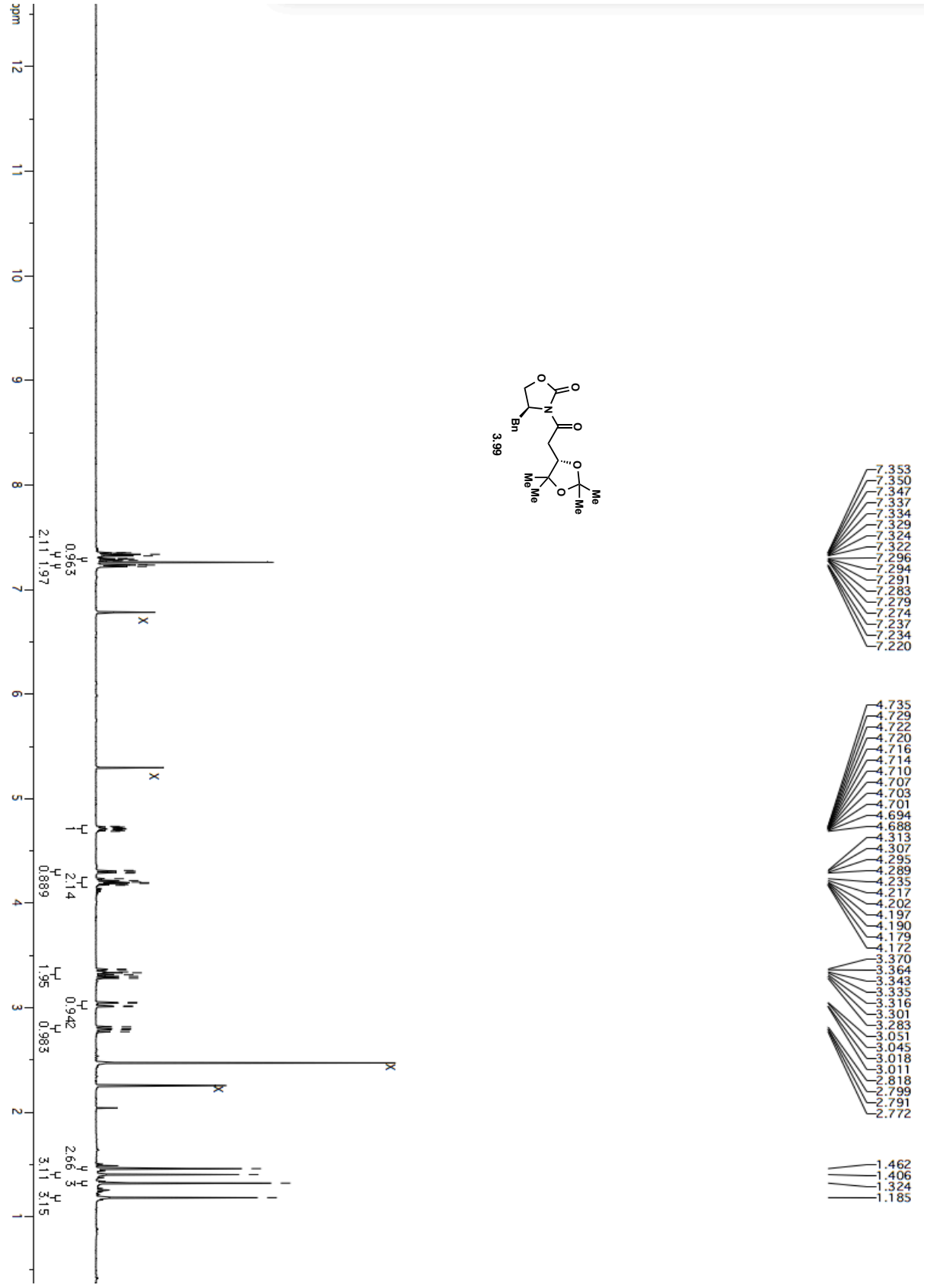
ppm
12
11
10
9
8
7
6
5
4
3
2
1
0.963
2.11
1.97
2.14
0.889
1.95
0.942
0.983
2.66
3.11
3.15
3.99
Bn
Me
Me
Me
Me
7.353
7.350
7.347
7.337
7.334
7.329
7.324
7.322
7.296
7.294
7.291
7.283
7.279
7.274
7.237
7.234
7.220
4.735
4.729
4.722
4.720
4.716
4.714
4.710
4.707
4.703
4.701
4.694
4.688
4.313
4.307
4.295
4.289
4.235
4.217
4.202
4.197
4.190
4.179
4.172
3.370
3.364
3.343
3.335
3.316
3.301
3.283
3.051
3.045
3.018
3.011
2.818
2.799
2.791
2.772
1.462
1.406
1.324
1.185

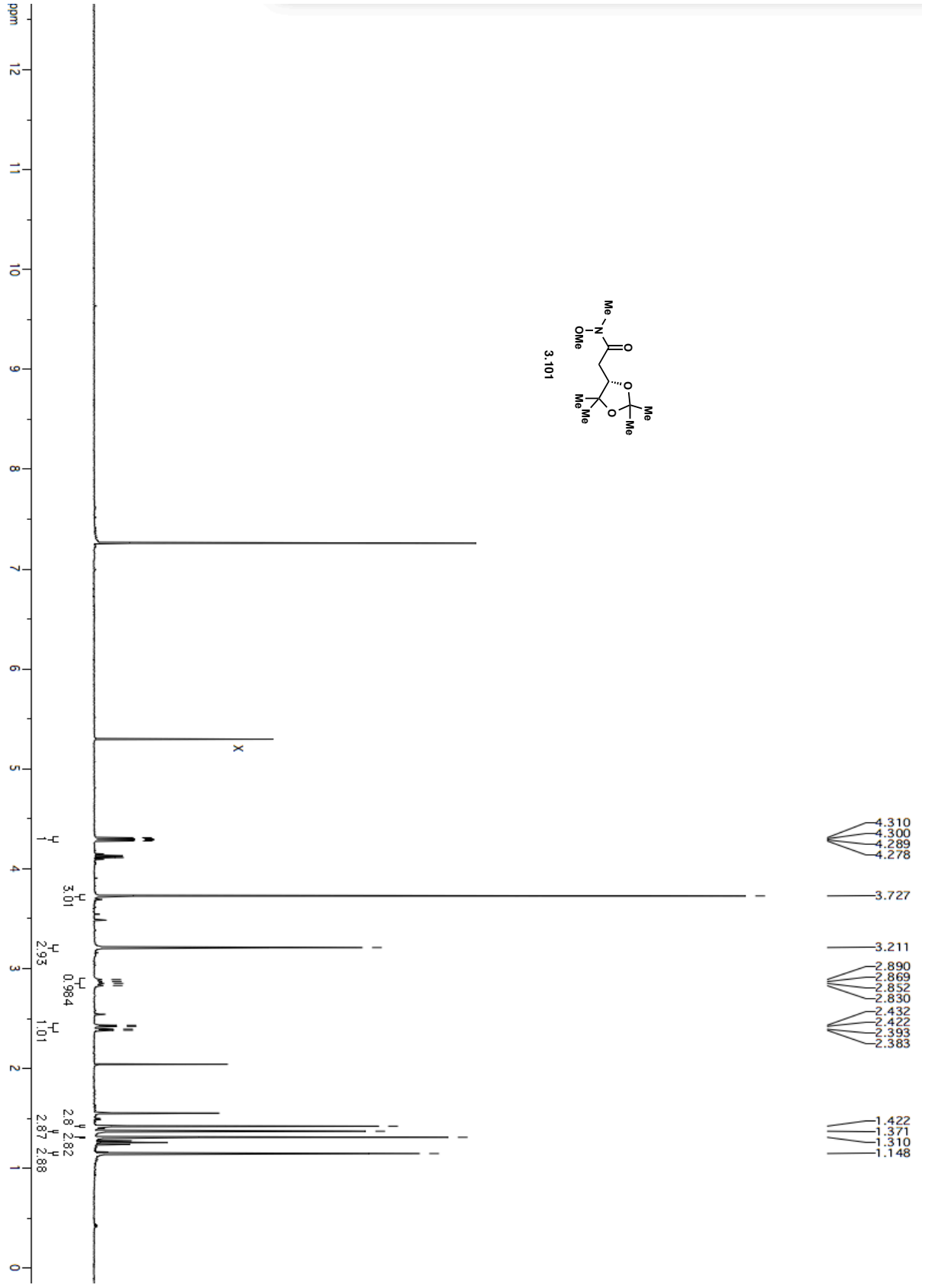
ppm
12
11
10
9
8
7
6
5
4
3
2
1
0
3.101
Me
N
OMe
O
O
Me
Me
Me
O
Me
X
1
3.01
2.93
0.984
1.01
2.8
2.82
2.87
2.88
4.310
4.300
4.289
4.278
3.727
3.211
2.890
2.869
2.852
2.830
2.432
2.422
2.393
2.383
1.422
1.371
1.310
1.148

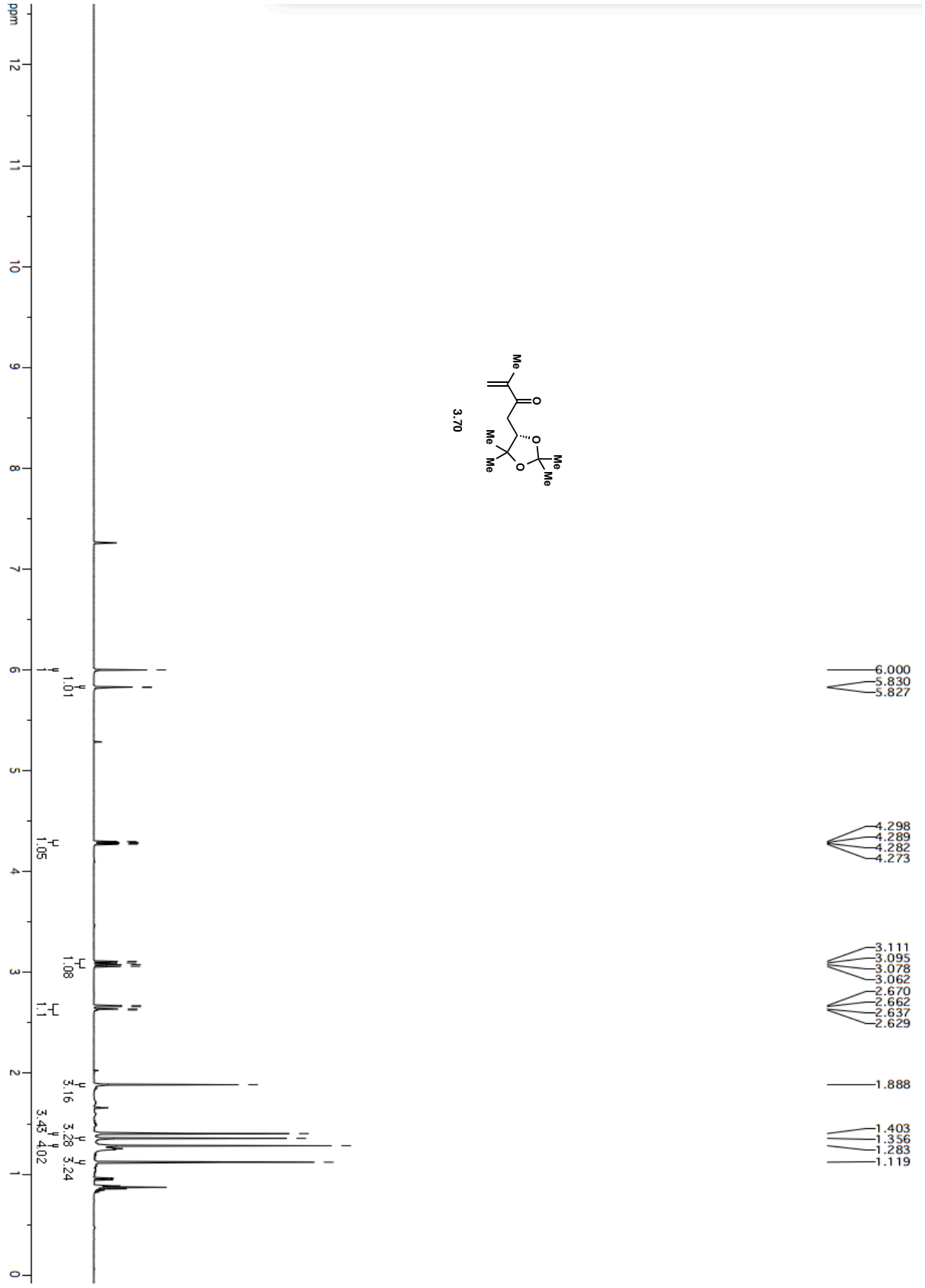
ppm
12
11
10
9
8
7
6
5
4
3
2
1
0
1.01
1.05
1.08
1.1
3.16
3.43
4.02
3.28
3.24
3.70
Me
Me
Me
Me
Me
O
O
O
6.000
5.830
5.827
4.298
4.289
4.282
4.273
3.111
3.095
3.078
3.062
2.670
2.662
2.637
2.629
1.888
1.403
1.356
1.283
1.119

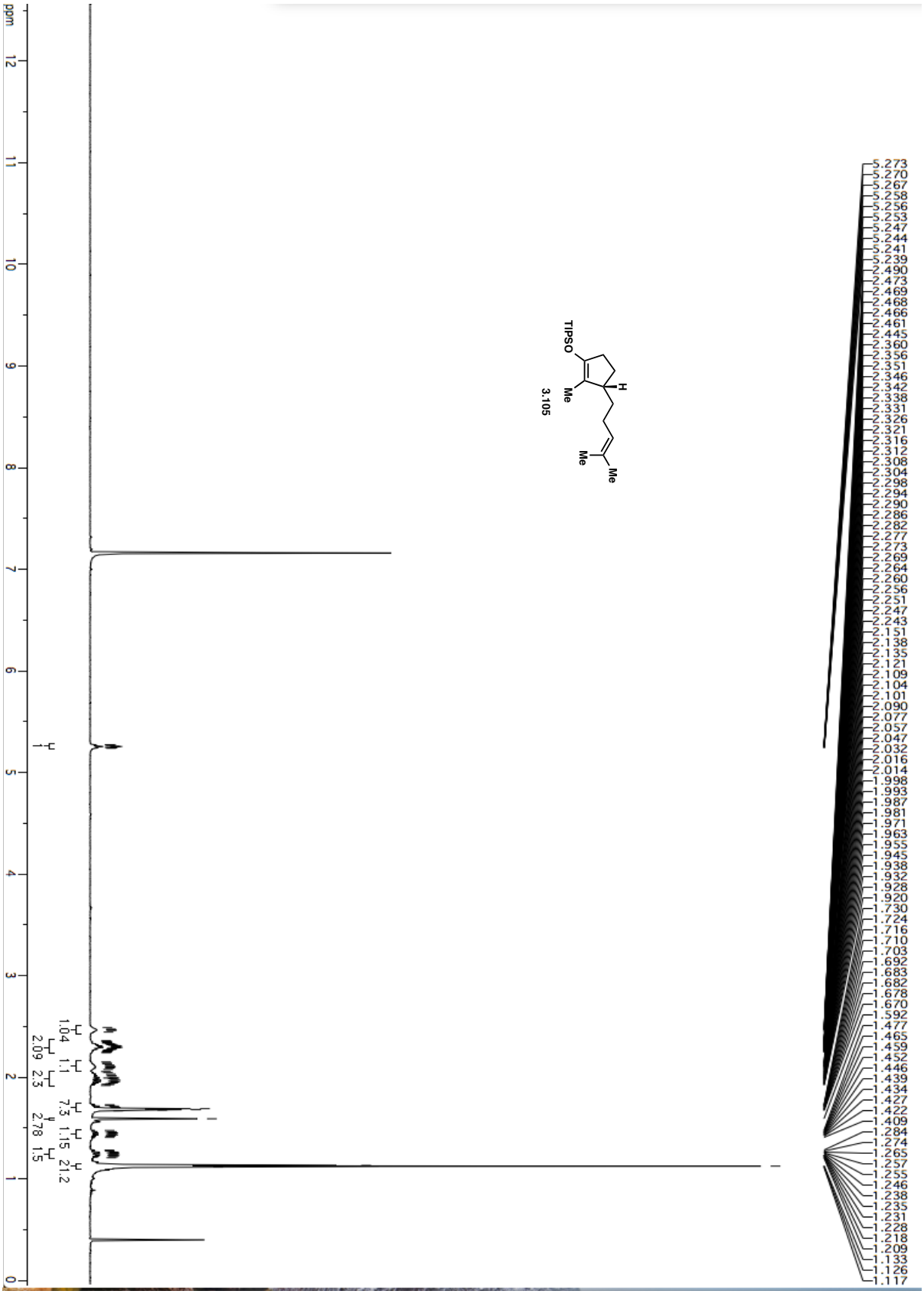
TIPSO
Me
H
Me
Me
3.105
ppm
1.04
1.1
2.09
2.3
7.3
1.15
2.78
1.5
21.2

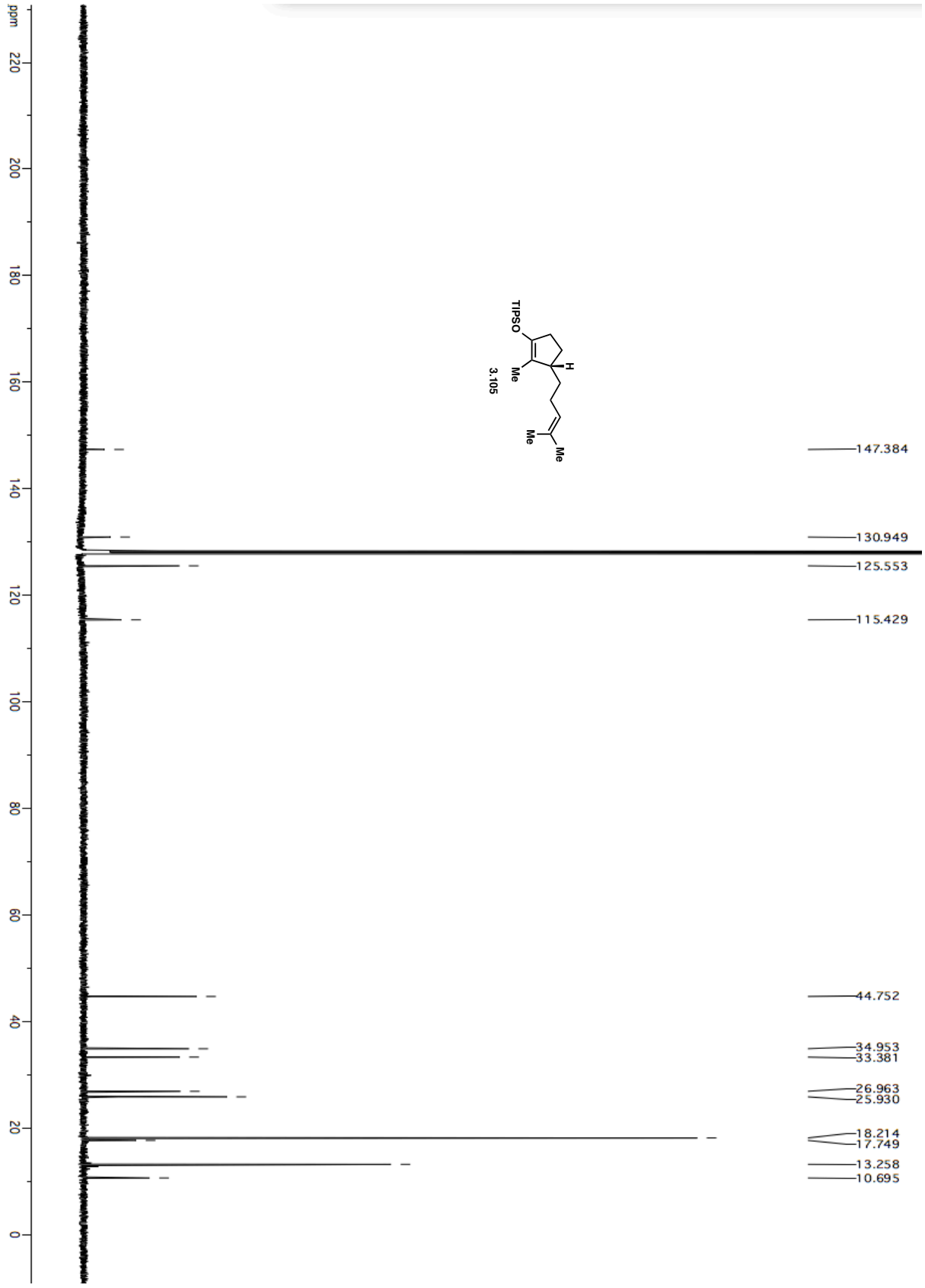
ppm
220
200
180
160
140
120
100
80
60
40
20
0
TIPSO
Me
3.105
H
Me
Me
147.384
130.949
125.553
115.429
44.752
34.953
33.381
26.963
25.930
18.214
17.749
13.258
10.695

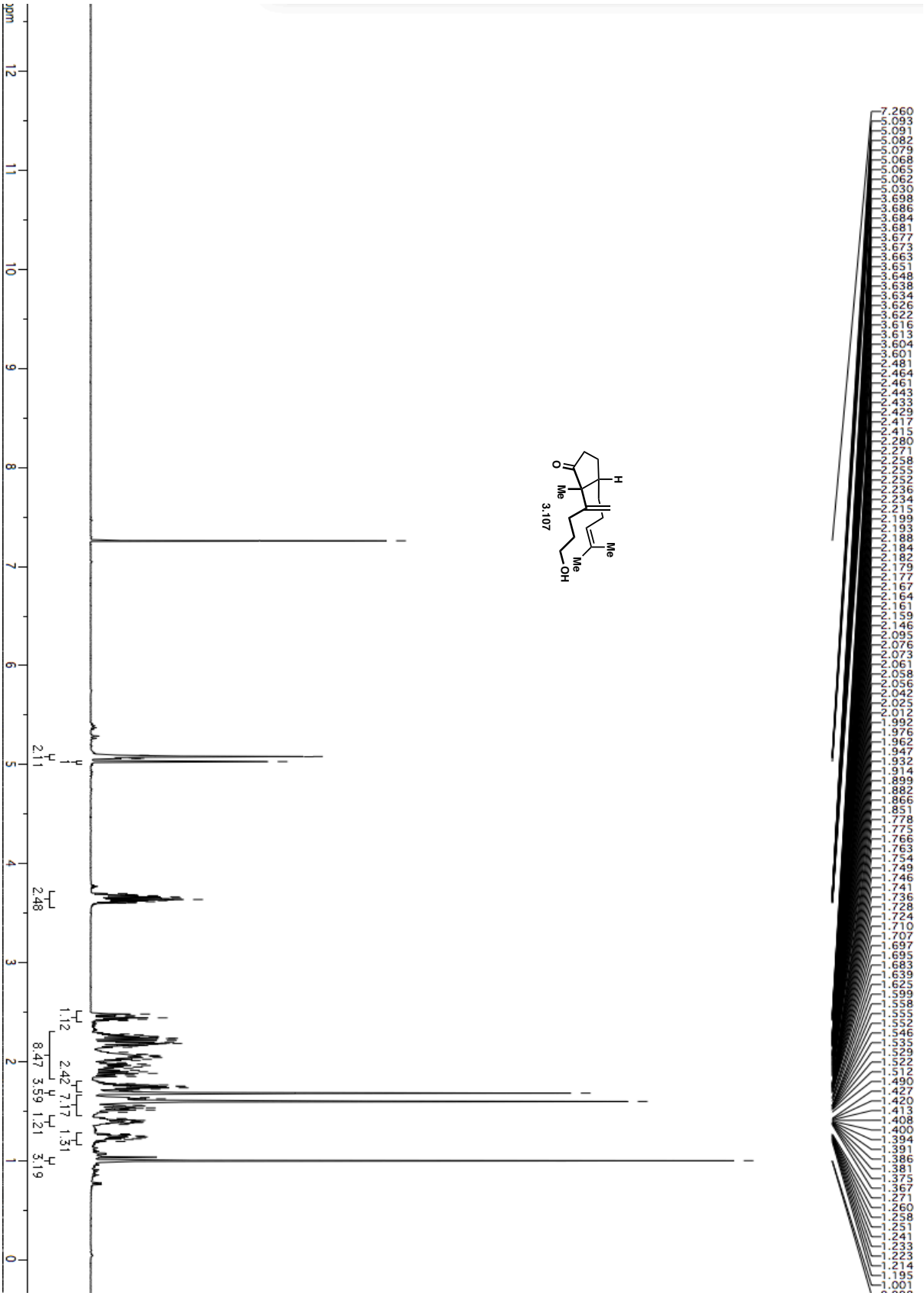
ppm
12
11
10
9
8
7
6
5
4
3
2
1
0
2.11
2.48
1.12
8.47
2.42
7.17
1.31
3.59
1.21
3.19
3.107
O
Me
H
Me
Me
OH
7.260
5.093
5.091
5.082
5.079
5.068
5.065
5.062
5.030
3.698
3.686
3.684
3.681
3.677
3.673
3.663
3.651
3.648
3.638
3.634
3.626
3.622
3.616
3.613
3.604
3.601
2.481
2.464
2.461
2.443
2.433
2.429
2.417
2.415
2.280
2.271
2.258
2.255
2.252
2.236
2.234
2.215
2.199
2.193
2.188
2.184
2.182
2.179
2.177
2.167
2.164
2.161
2.159
2.146
2.095
2.076
2.073
2.061
2.058
2.056
2.042
2.025
2.012
1.992
1.976
1.962
1.947
1.932
1.914
1.899
1.882
1.866
1.851
1.778
1.775
1.766
1.763
1.754
1.749
1.746
1.741
1.736
1.728
1.724
1.710
1.707
1.697
1.695
1.683
1.639
1.625
1.599
1.558
1.555
1.552
1.546
1.535
1.529
1.522
1.512
1.490
1.427
1.420
1.413
1.408
1.400
1.394
1.391
1.386
1.381
1.375
1.367
1.271
1.260
1.258
1.251
1.241
1.233
1.223
1.214
1.195

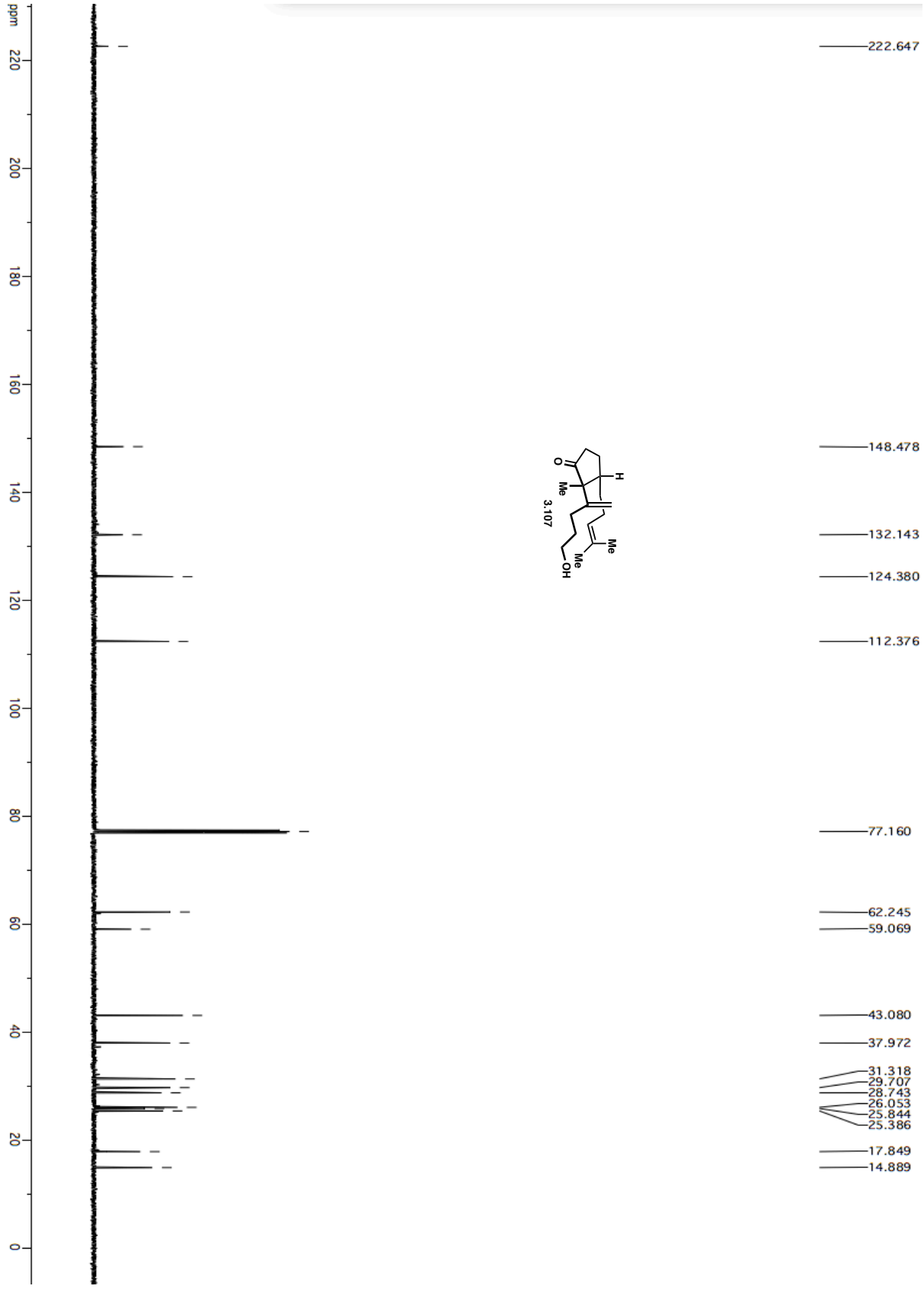
ppm
220
200
180
160
140
120
100
80
60
40
20
0
222.647
148.478
132.143
124.380
112.376
77.160
62.245
59.069
43.080
37.972
31.318
29.707
28.743
26.053
25.844
25.386
17.849
14.889
O
H
Me
3.107
Me
Me
OH

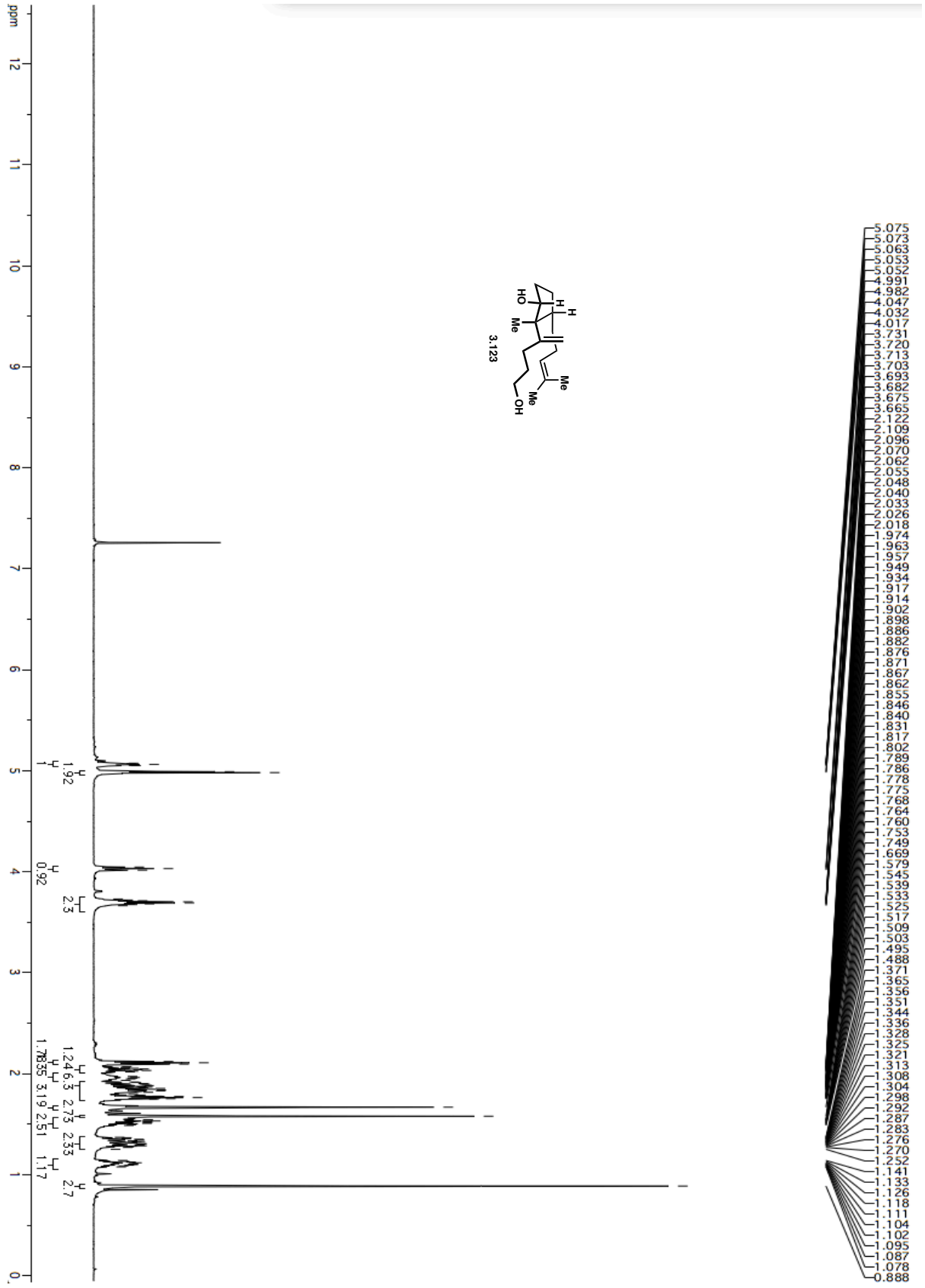
ppm
12
11
10
9
8
7
6
5
4
3
2
1
0
1.92
0.92
2.3
1.24
6.3
2.73
2.33
2.7
1.78
3.35
3.19
2.51
1.17
HO
Me
H
Me
Me
OH
3.123
5.075
5.073
5.063
5.053
5.052
4.991
4.982
4.047
4.032
4.017
3.731
3.720
3.713
3.703
3.693
3.682
3.675
3.665
2.122
2.109
2.096
2.070
2.062
2.055
2.048
2.040
2.033
2.026
2.018
1.974
1.963
1.957
1.949
1.934
1.917
1.914
1.902
1.898
1.886
1.882
1.876
1.871
1.867
1.862
1.855
1.846
1.840
1.831
1.817
1.802
1.789
1.786
1.778
1.775
1.768
1.764
1.760
1.753
1.749
1.669
1.579
1.545
1.539
1.533
1.525
1.517
1.509
1.503
1.495
1.488
1.371
1.365
1.356
1.351
1.344
1.336
1.328
1.325
1.321
1.313
1.308
1.304
1.298
1.292
1.287
1.283
1.276
1.270
1.252
1.141
1.133
1.126
1.118
1.111
1.104
1.102
1.095
1.087
1.078
0.888

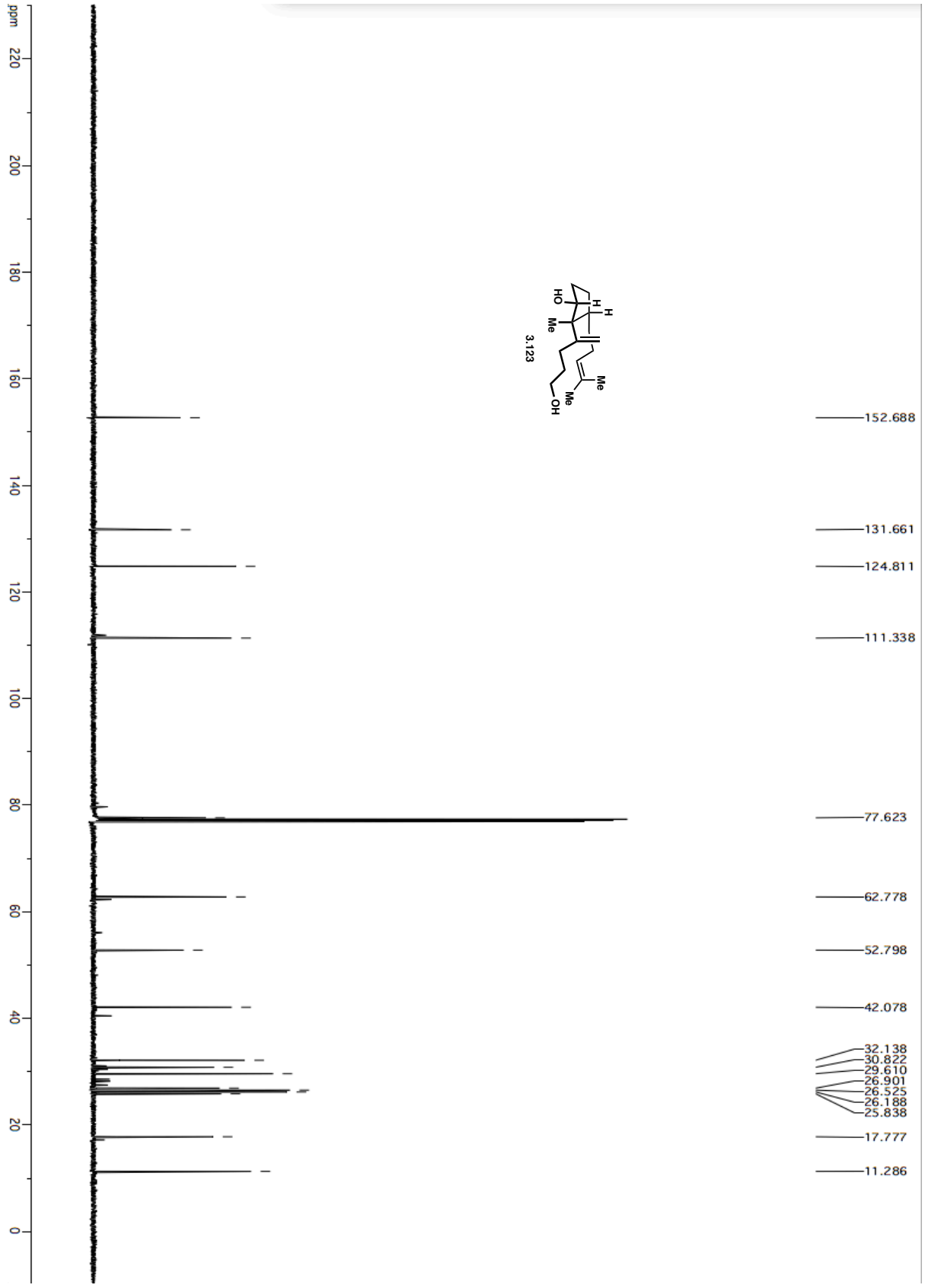
ppm
220
200
180
160
140
120
100
80
60
40
20
0
HO
Me
H
H
Me
Me
OH
3.123
152.688
131.661
124.811
111.338
77.623
62.778
52.798
42.078
32.138
30.822
29.610
26.901
26.525
26.188
25.838
17.777
11.286

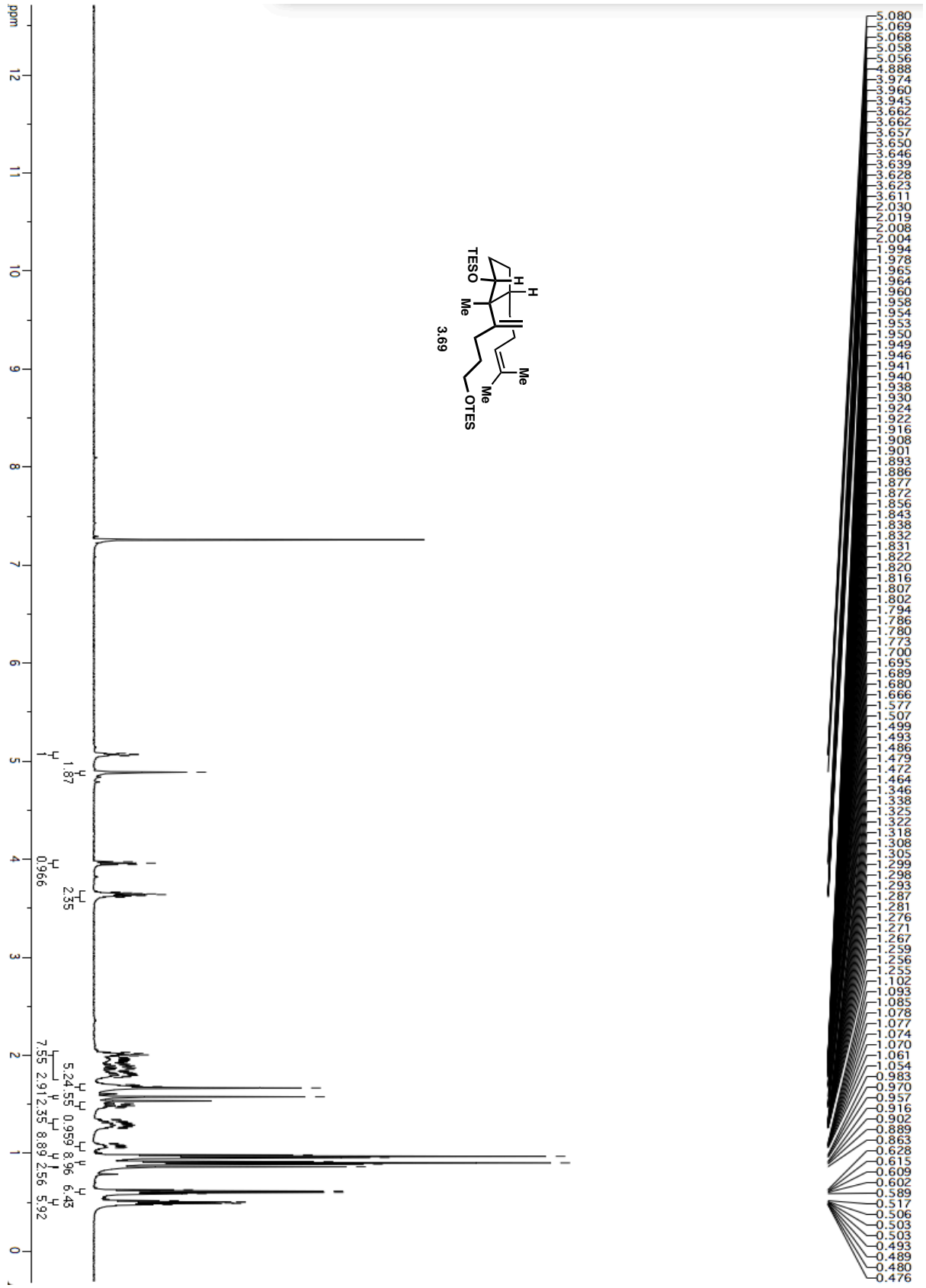
TESO
Me
H
H
Me
Me
OTES
3.69
ppm
1.87
0.966
2.35
5.24
5.55
0.959
8.96
6.43
7.55
2.91
2.35
8.89
2.56
5.92

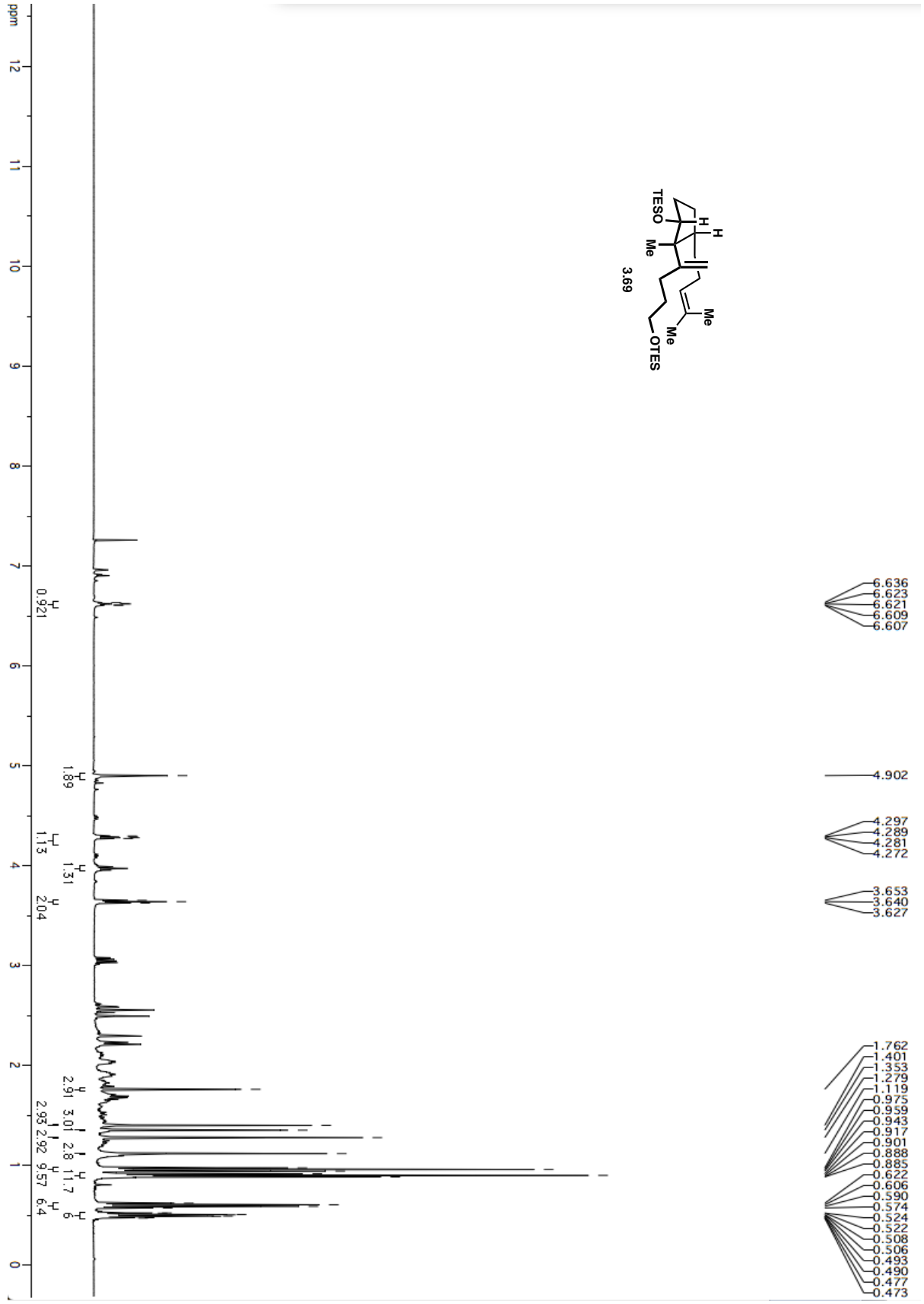
TESO
Me
H
H
Me
Me
OTES
3.69
6.636
6.623
6.621
6.609
6.607
4.902
4.297
4.289
4.281
4.272
3.653
3.640
3.627
1.762
1.401
1.353
1.279
1.119
0.975
0.959
0.943
0.917
0.901
0.888
0.885
0.622
0.606
0.590
0.574
0.524
0.522
0.508
0.506
0.493
0.490
0.477
0.473
0.921
1.89
1.13
1.31
2.04
2.91
3.01
2.93
2.92
2.8
11.7
9.57
6
6.4
ppm

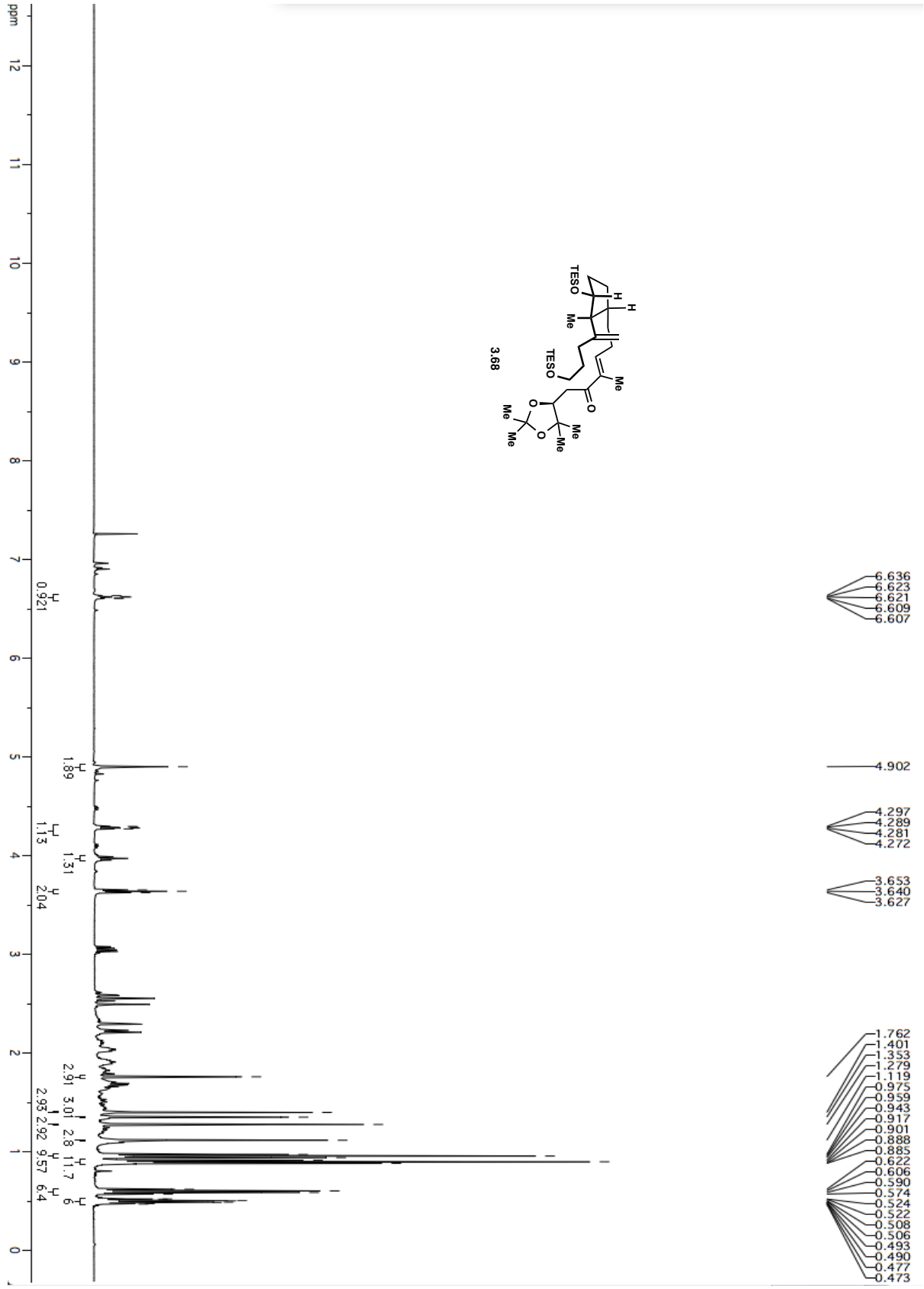
TESO
Me
H
H
TESO
Me
O
O
Me
Me
Me
O
O
Me
Me
3.68
6.636
6.623
6.621
6.609
6.607
4.902
4.297
4.289
4.281
4.272
3.653
3.640
3.627
1.762
1.401
1.353
1.279
1.119
0.975
0.959
0.943
0.917
0.901
0.888
0.885
0.622
0.606
0.590
0.574
0.524
0.522
0.508
0.506
0.493
0.490
0.477
0.473
0.921
1.89
1.13
1.31
2.04
2.91
3.01
2.8
11.7
6
2.93
2.92
9.57
6.4
ppm

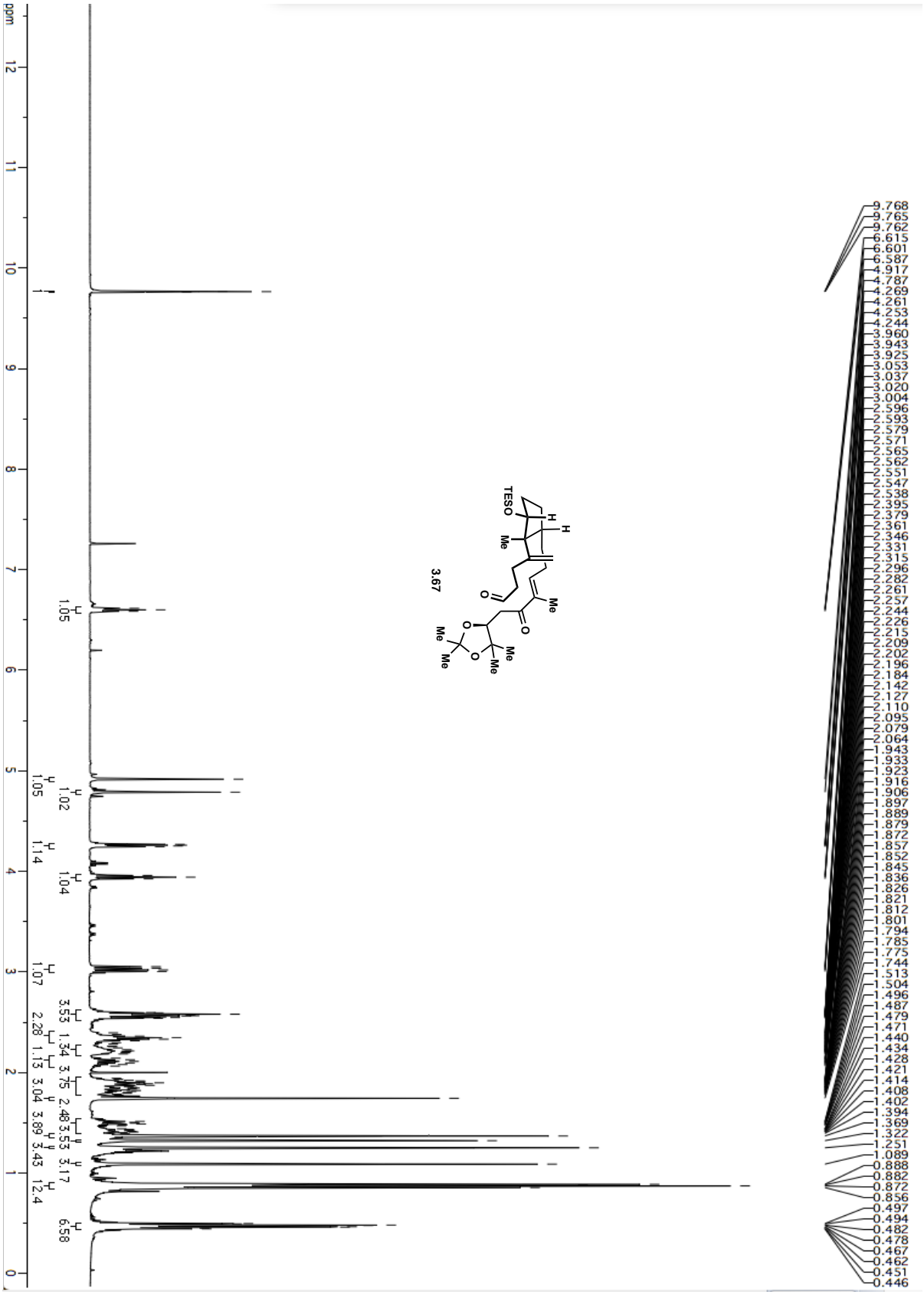
TESO
Me
Me
H
H
Me
O
O
O
O
Me
Me
Me
3.67
9.768
9.765
9.762
6.615
6.601
6.587
4.917
4.787
4.269
4.261
4.253
4.244
3.960
3.943
3.925
3.053
3.037
3.020
3.004
2.596
2.593
2.579
2.571
2.565
2.562
2.551
2.547
2.538
2.395
2.379
2.361
2.346
2.331
2.315
2.296
2.282
2.261
2.257
2.244
2.226
2.215
2.209
2.202
2.196
2.184
2.142
2.127
2.110
2.095
2.079
2.064
1.943
1.933
1.923
1.916
1.906
1.897
1.889
1.879
1.872
1.857
1.852
1.845
1.836
1.826
1.821
1.812
1.801
1.794
1.785
1.775
1.744
1.513
1.504
1.496
1.487
1.479
1.471
1.440
1.434
1.428
1.421
1.414
1.408
1.402
1.394
1.369
1.322
1.251
1.089
0.888
0.882
0.872
0.856
0.497
0.494
0.482
0.478
0.467
0.462
0.451
0.446
ppm
12
11
10
9
8
7
6
5
4
3
2
1
0
1.05
1.02
1.14
1.04
1.07
3.53
1.34
2.28
1.13
3.75
3.04
2.48
3.89
3.53
3.43
3.17
12.4
6.58

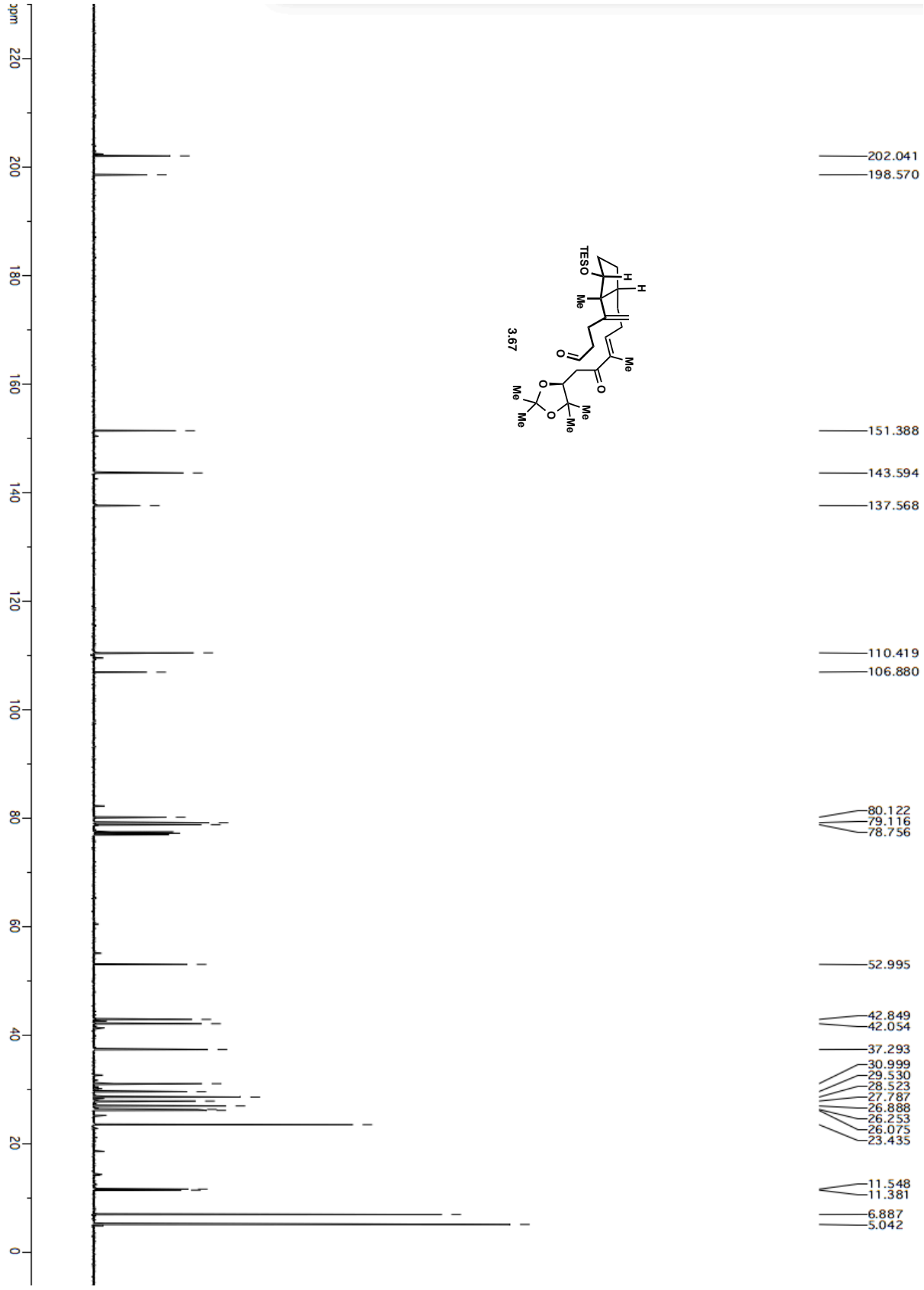
ppm
220
200
180
160
140
120
100
80
60
40
20
0
202.041
198.570
151.388
143.594
137.568
110.419
106.880
80.122
79.116
78.756
52.995
42.849
42.054
37.293
30.999
29.530
28.523
27.787
26.888
26.253
26.075
23.435
11.548
11.381
6.887
5.042
TESO
Me
H
H
O
3.67
Me
O
O
Me
Me
O
Me
Me

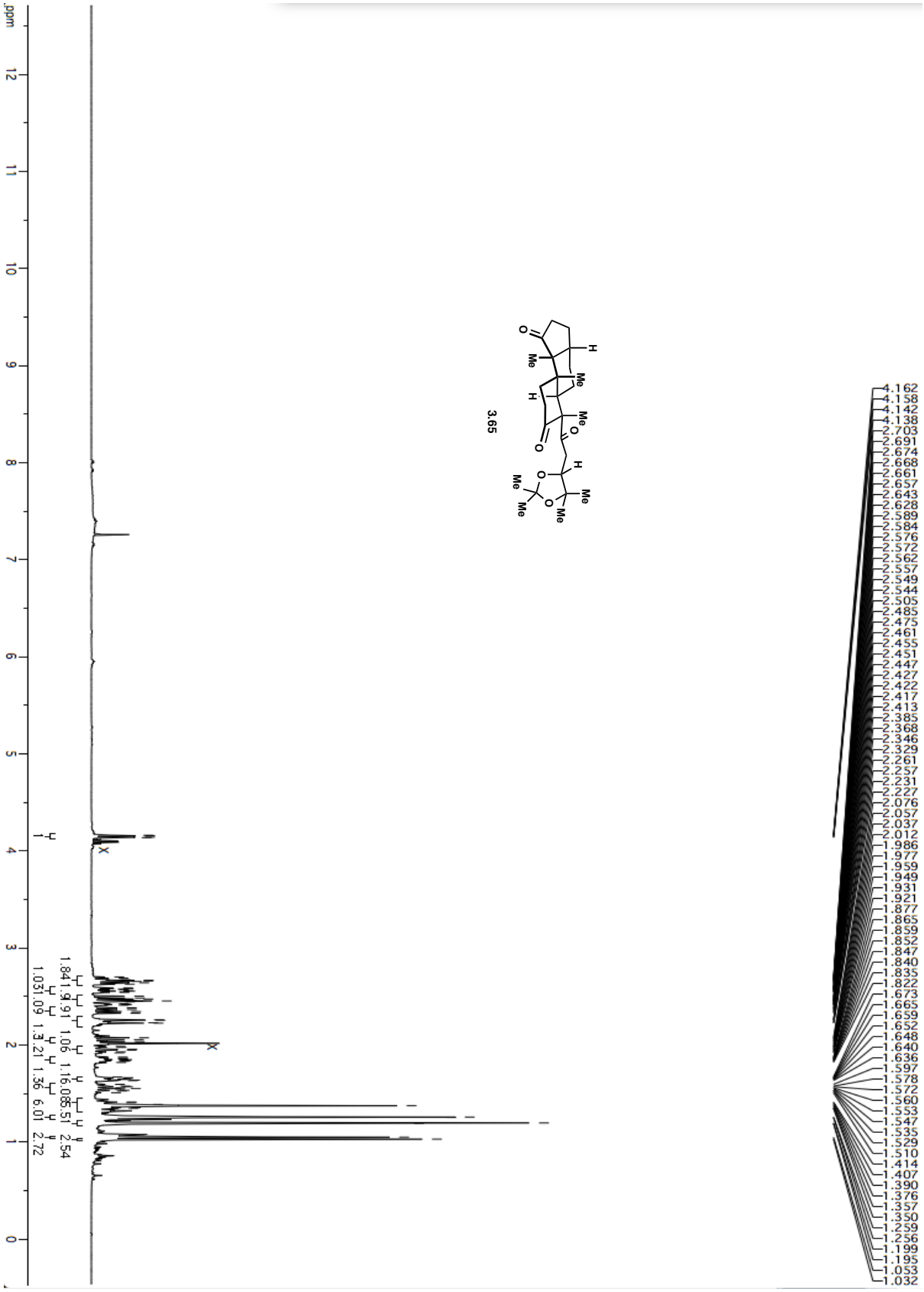
ppm
12
11
10
9
8
7
6
5
4
3
2
1
0
1.00
1.84
1.91
1.06
1.16
0.85
1.51
2.54
1.03
1.09
1.21
1.36
6.01
2.72
3.65
4.162
4.158
4.142
4.138
2.703
2.691
2.674
2.668
2.661
2.657
2.643
2.628
2.589
2.584
2.576
2.572
2.562
2.557
2.549
2.544
2.505
2.485
2.475
2.461
2.455
2.451
2.447
2.427
2.422
2.417
2.413
2.385
2.368
2.346
2.329
2.261
2.257
2.231
2.227
2.076
2.057
2.037
2.012
1.986
1.977
1.959
1.949
1.931
1.921
1.877
1.865
1.859
1.852
1.847
1.840
1.835
1.822
1.673
1.665
1.659
1.652
1.648
1.640
1.636
1.597
1.578
1.572
1.560
1.553
1.547
1.535
1.529
1.510
1.414
1.407
1.390
1.376
1.357
1.350
1.259
1.256
1.199
1.195
1.053
1.032

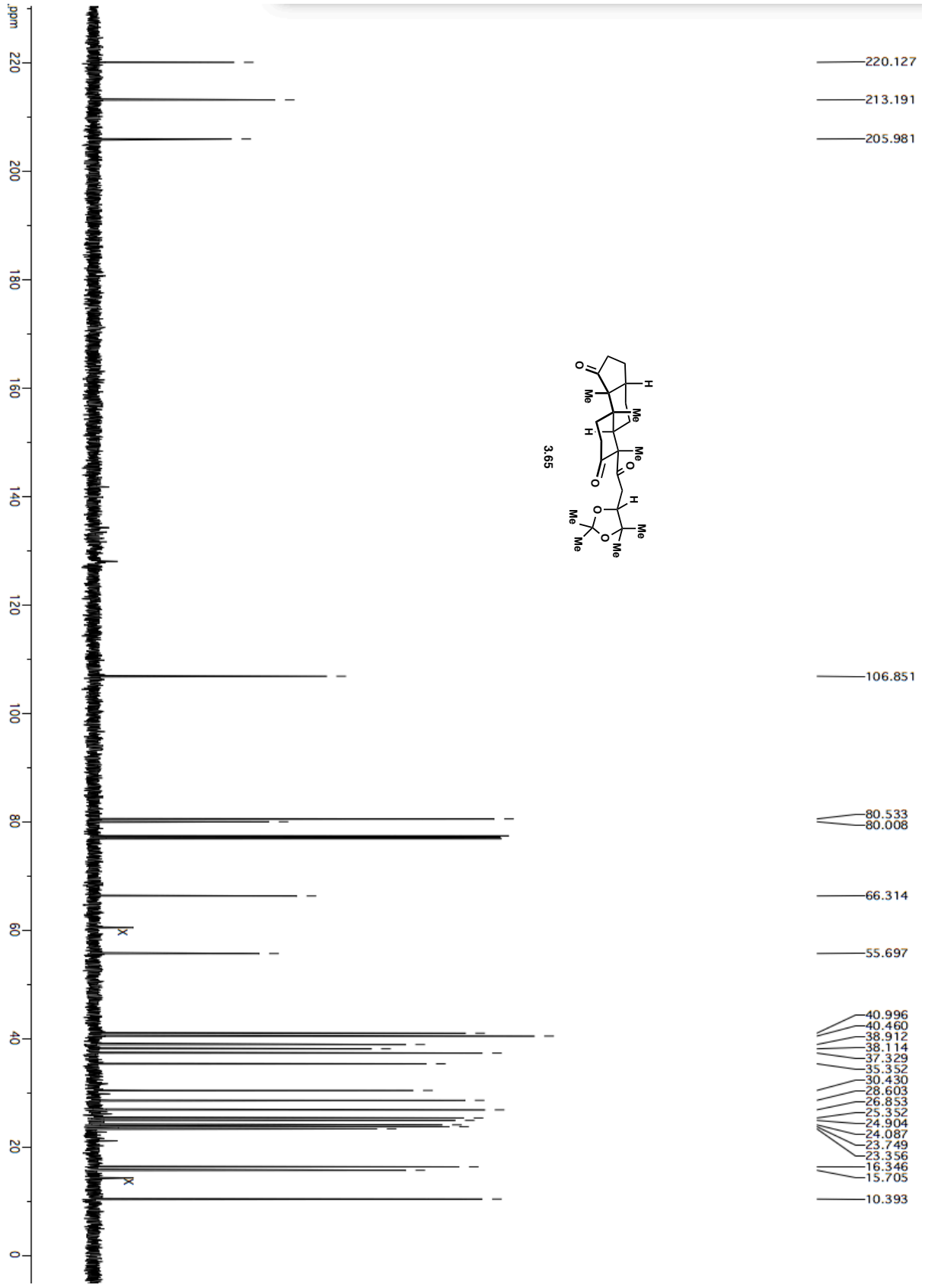
ppm
220
200
180
160
140
120
100
80
60
40
20
0
220.127
213.191
205.981
106.851
80.533
80.008
66.314
55.697
40.996
40.460
38.912
38.114
37.329
35.352
30.430
28.603
26.853
25.352
24.904
24.087
23.749
23.356
16.346
15.705
10.393
3.65
O
Me
H
Me
Me
O
O
H
Me
O
O
Me
Me
Me

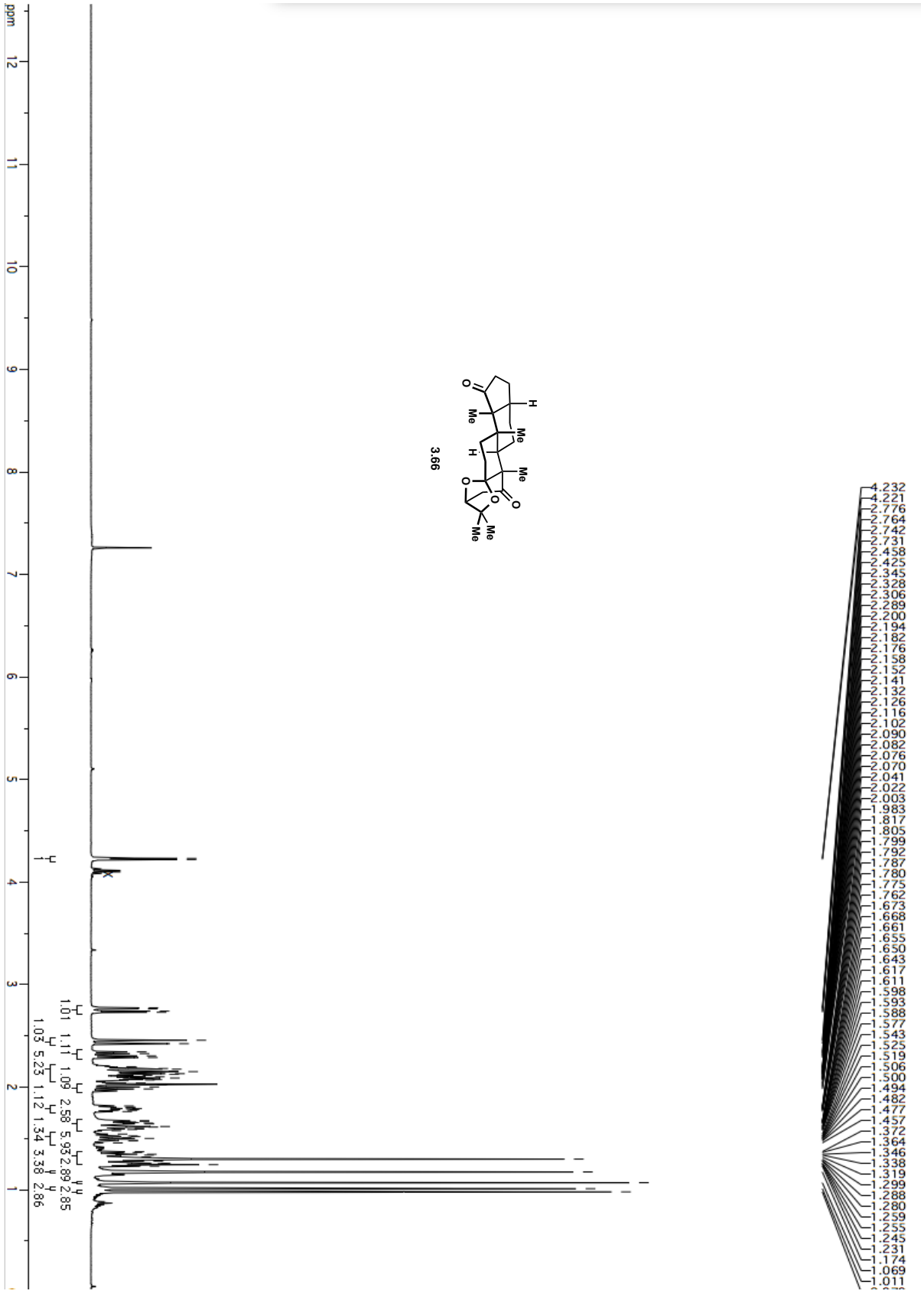
ppm
12
11
10
9
8
7
6
5
4
3
2
1
1.01
1.11
1.09
2.58
5.93
2.89
2.85
1.03
5.23
1.12
1.34
3.38
2.86
3.66
Me
Me
Me
Me
Me
H
H
O
O
O
O
4.232
4.221
2.776
2.764
2.742
2.731
2.458
2.425
2.345
2.328
2.306
2.289
2.200
2.194
2.182
2.176
2.158
2.152
2.141
2.132
2.126
2.116
2.102
2.090
2.082
2.076
2.070
2.041
2.022
2.003
1.983
1.817
1.805
1.799
1.792
1.787
1.780
1.775
1.762
1.673
1.668
1.661
1.655
1.650
1.643
1.617
1.611
1.598
1.593
1.588
1.577
1.543
1.525
1.519
1.506
1.500
1.494
1.482
1.477
1.457
1.372
1.364
1.346
1.338
1.319
1.299
1.288
1.280
1.259
1.255
1.245
1.231
1.174
1.069
1.011

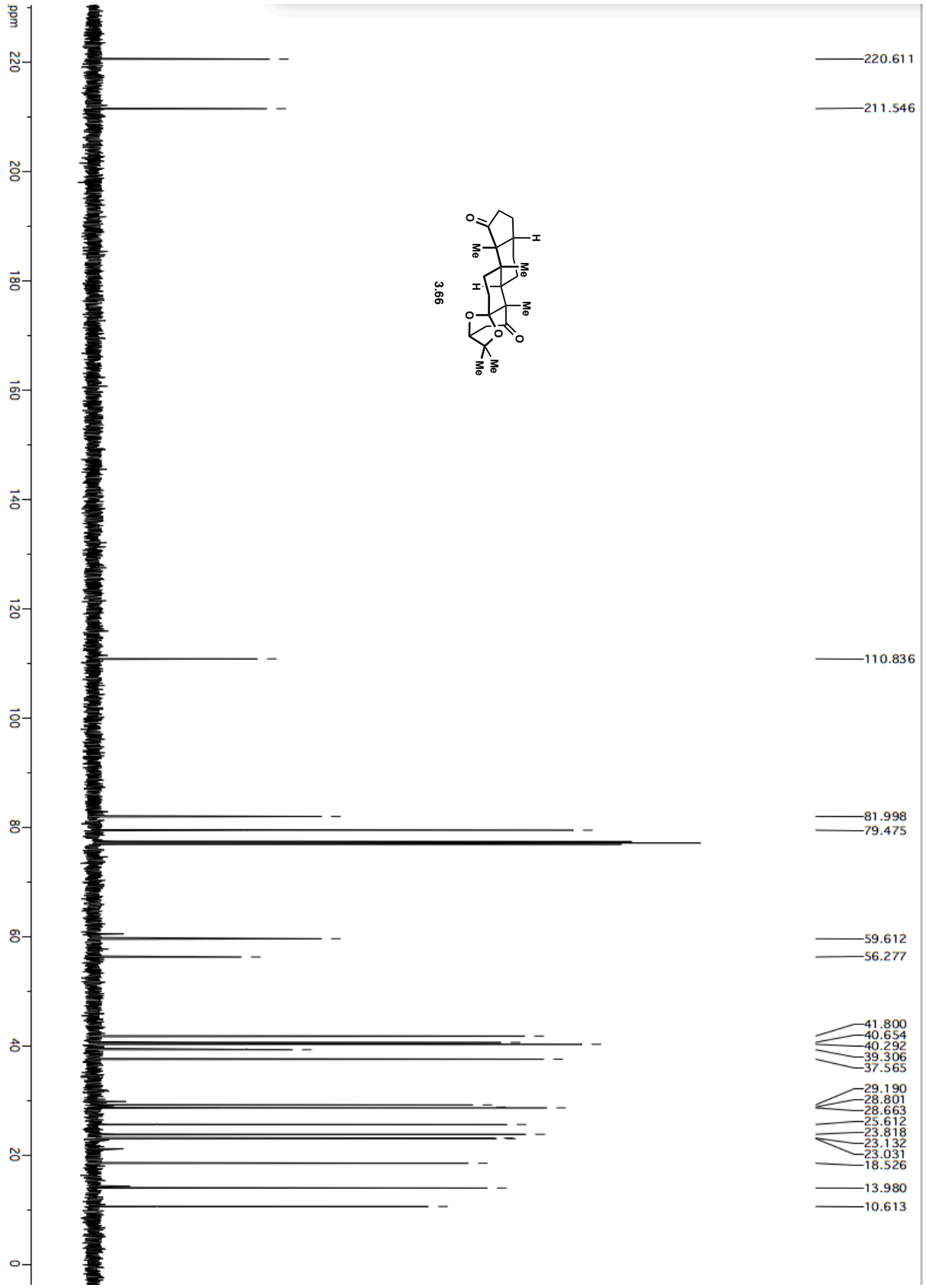
ppm
220
200
180
160
140
120
100
80
60
40
20
0
220.611
211.546
110.836
81.998
79.475
59.612
56.277
41.800
40.654
40.292
39.306
37.565
29.190
28.801
28.663
25.612
23.818
23.132
23.031
18.526
13.980
10.613
3.66
O
Me
H
Me
Me
H
O
O
O
Me
Me

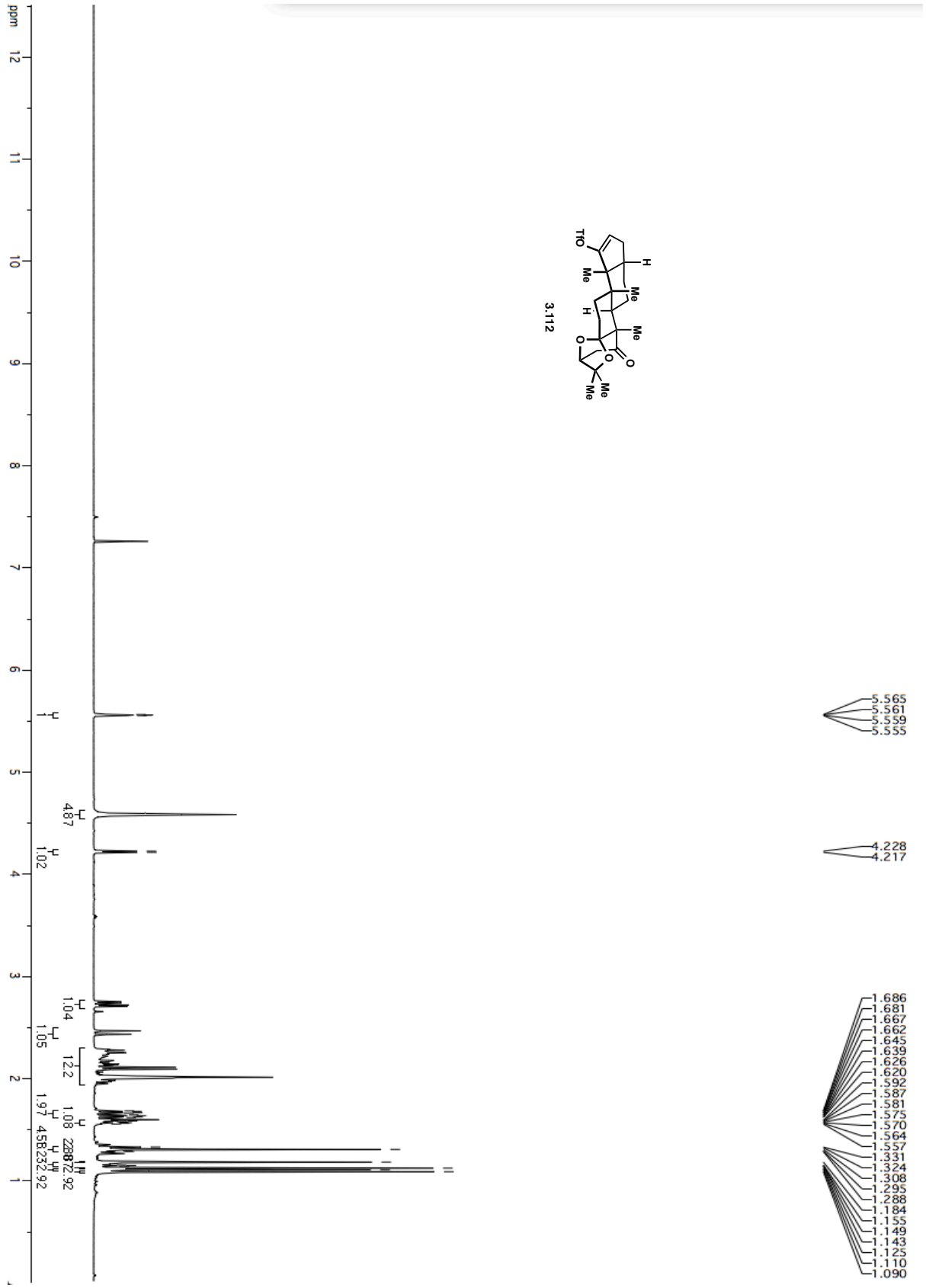
3.112
5.565
5.561
5.559
5.555
4.228
4.217
1.686
1.681
1.667
1.662
1.645
1.639
1.626
1.620
1.592
1.587
1.581
1.575
1.570
1.564
1.557
1.331
1.324
1.308
1.295
1.288
1.184
1.155
1.149
1.143
1.125
1.110
1.090
4.87
1.02
1.04
1.05
12.2
1.08
1.97
4.58
232.92
228.72
232.92

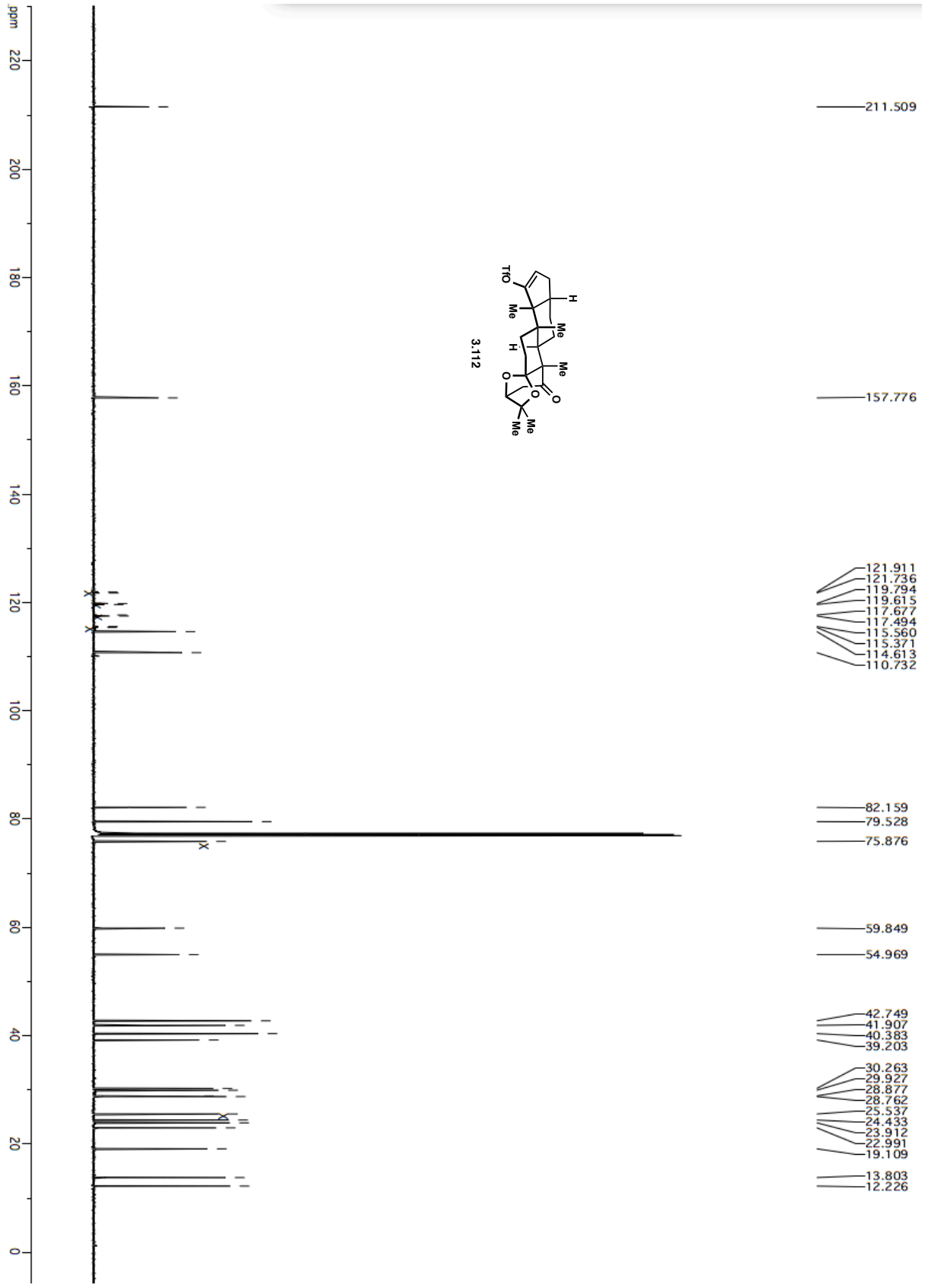
ppm
220
200
180
160
140
120
100
80
60
40
20
0
211.509
157.776
121.911
121.736
119.794
119.615
117.677
117.494
115.560
115.371
114.613
110.732
82.159
79.528
75.876
59.849
54.969
42.749
41.907
40.383
39.203
30.263
29.927
28.877
28.762
25.537
24.433
23.912
22.991
19.109
13.803
12.226
TfO
Me
H
Me
Me
H
O
O
O
Me
Me
3.112

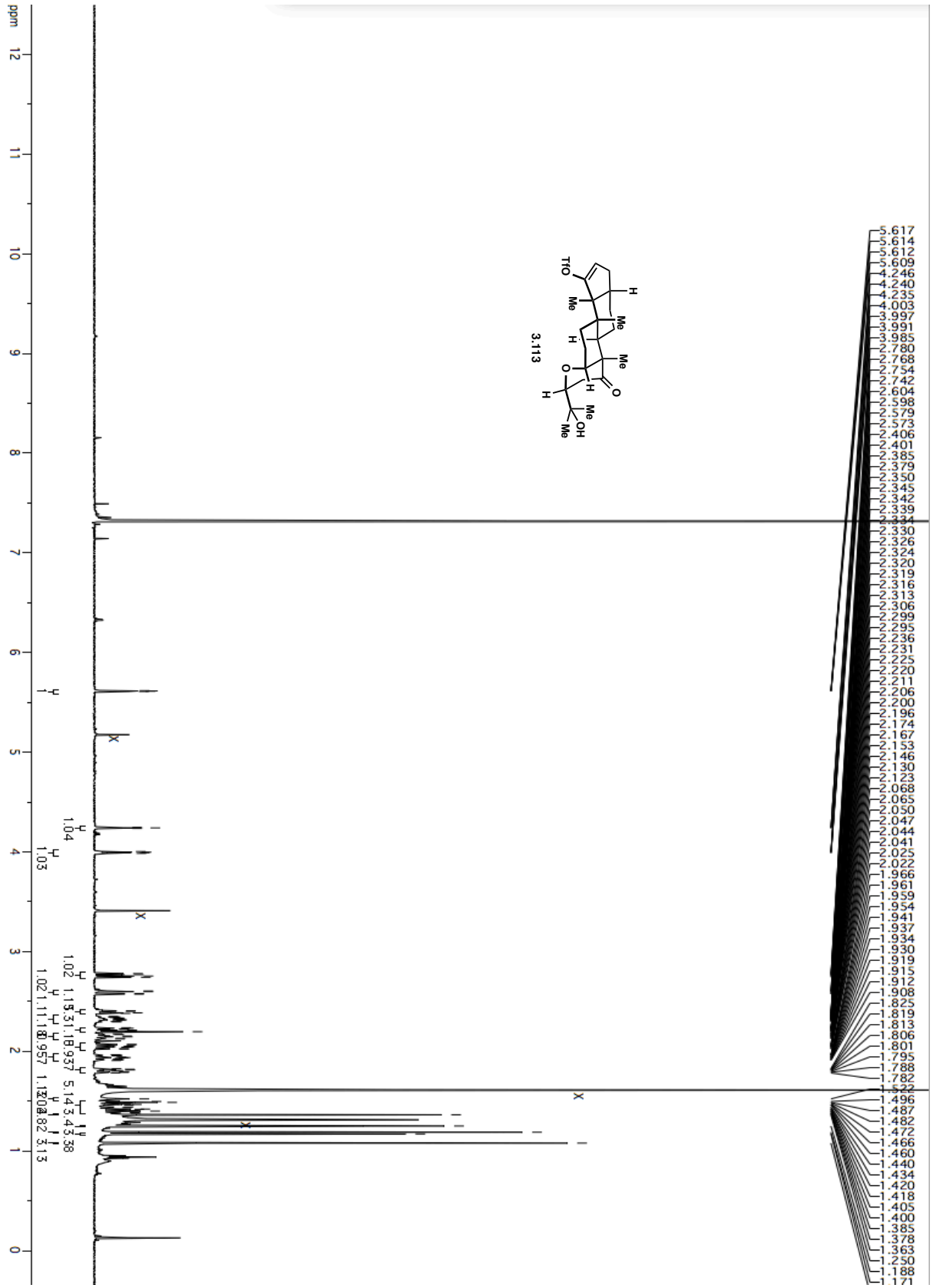
3.113
TfO
Me
H
Me
Me
O
H
Me
OH
Me
ppm
12
11
10
9
8
7
6
5
4
3
2
1
0
1.04
1.03
1.02
1.15
5.31
1.18
9.37
5.14
3.43
3.38
1.02
1.11
1.18
0.95
7
1.12
0.82
3.13

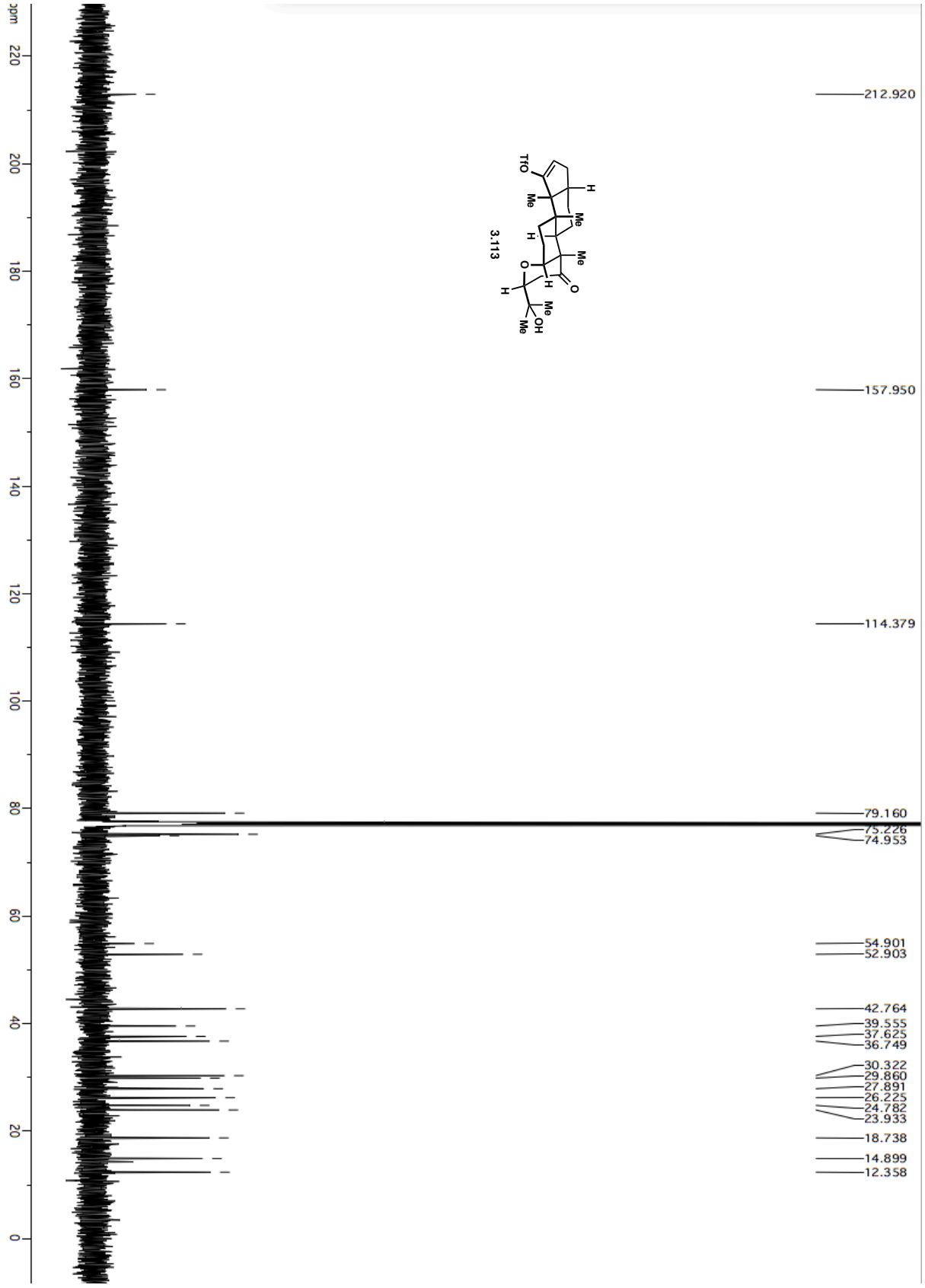
ppm
220
200
180
160
140
120
100
80
60
40
20
0
212.920
157.950
114.379
79.160
75.226
74.953
54.901
52.903
42.764
39.555
37.625
36.749
30.322
29.860
27.891
26.225
24.782
23.933
18.738
14.899
12.358
3.113
TfO
Me
H
Me
H
Me
O
H
O
H
Me
OH
Me

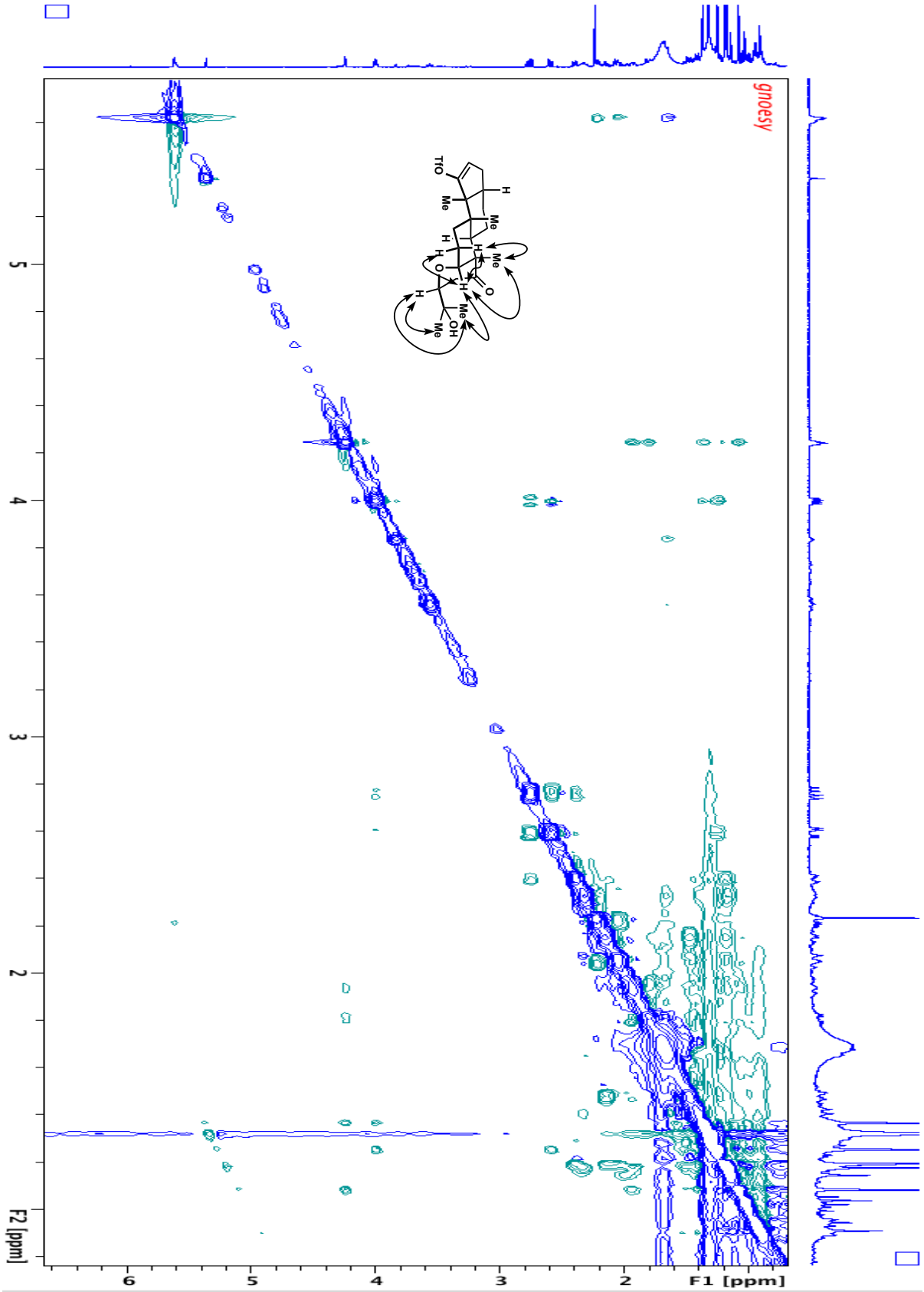
gnoesy
TfO
Me
H
Me
H
H
H
O
H
H
Me
OH
Me
O
F2 [ppm]
F1 [ppm]
6
5
4
3
2

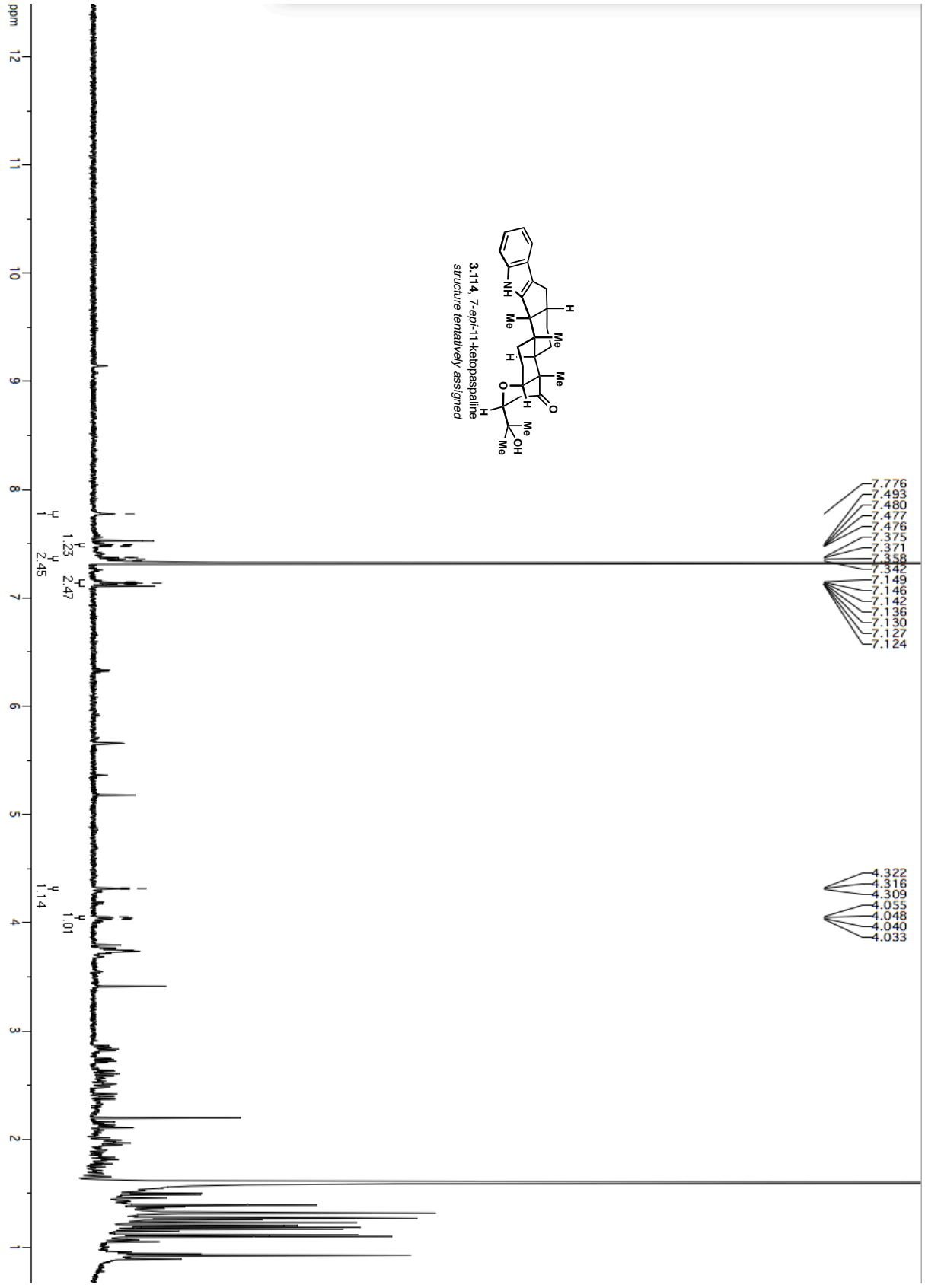
ppm
12
11
10
9
8
7
6
5
4
3
2
1
1.00
1.23
2.45
2.47
1.14
1.01
7.776
7.493
7.480
7.477
7.476
7.375
7.371
7.358
7.342
7.149
7.146
7.142
7.136
7.130
7.127
7.124
4.322
4.316
4.309
4.055
4.048
4.040
4.033
NH
Me
H
Me
Me
O
H
O
H
Me
OH
Me
3.114, 7-epi-11-ketopaspaline
structure tentatively assigned

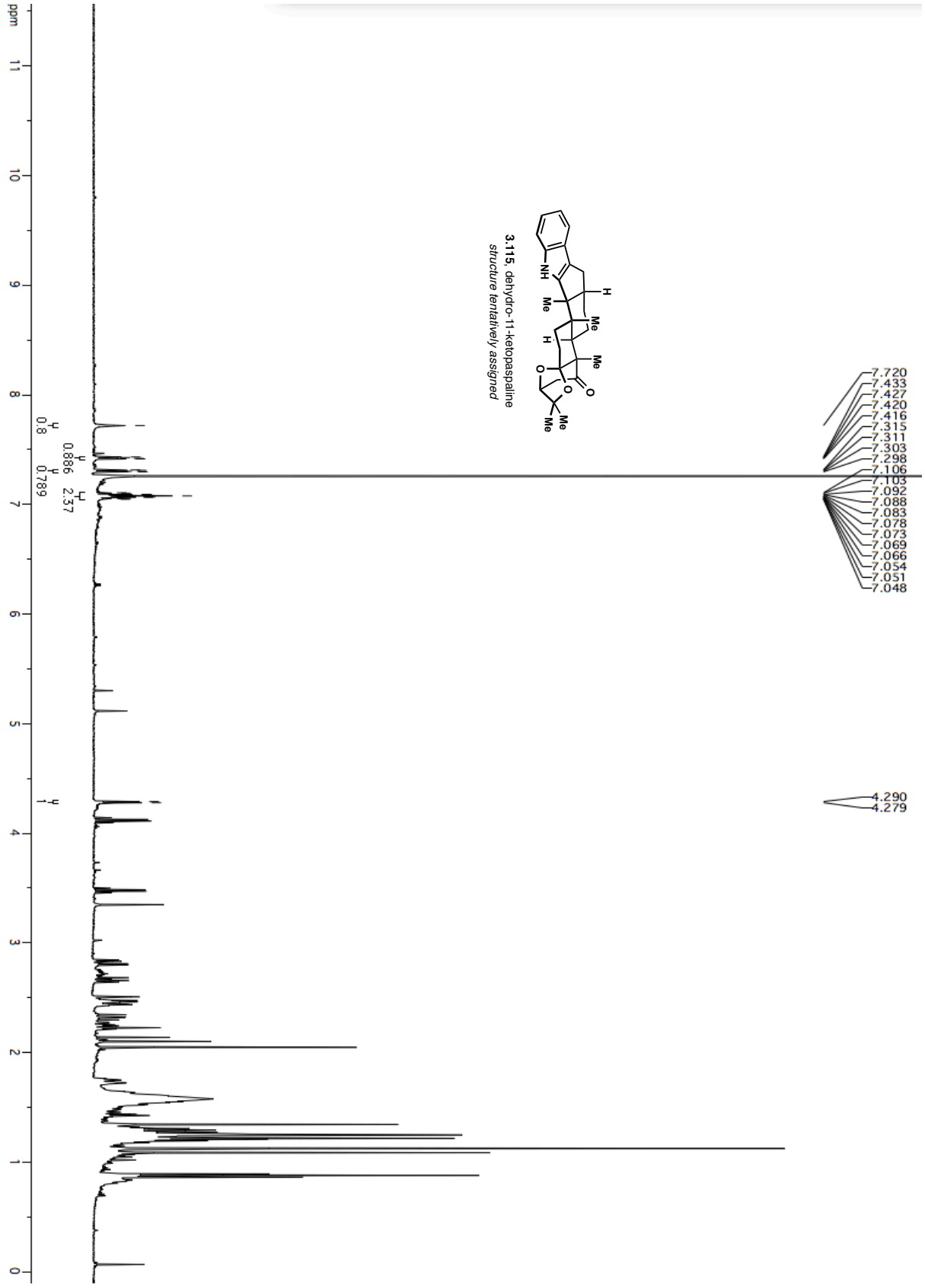

3.115, dehydro-11-ketopaspaline
structure tentatively assigned

Appendix E: Chapter 4 NMR Spectra

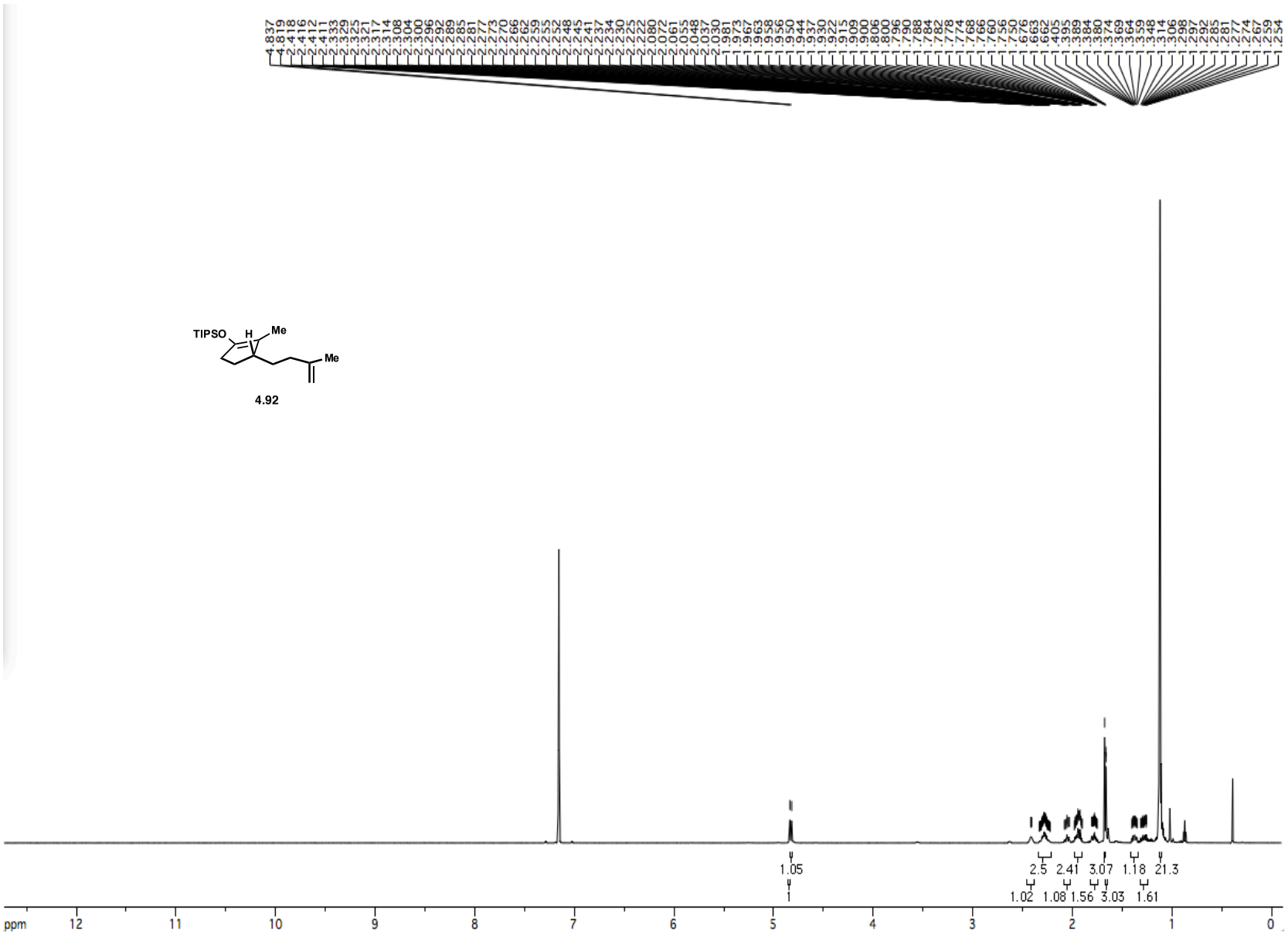
4.837
4.819
2.416
2.412
2.411
2.333
2.329
2.325
2.321
2.317
2.314
2.308
2.304
2.300
2.296
2.292
2.289
2.285
2.281
2.277
2.273
2.270
2.266
2.262
2.259
2.255
2.252
2.248
2.245
2.241
2.237
2.234
2.230
2.225
2.222
2.080
2.072
2.061
2.055
2.048
2.037
2.030
1.981
1.973
1.967
1.963
1.958
1.956
1.950
1.944
1.937
1.930
1.922
1.915
1.909
1.900
1.806
1.800
1.796
1.790
1.788
1.784
1.782
1.778
1.774
1.768
1.766
1.760
1.756
1.750
1.676
1.663
1.662
1.405
1.395
1.389
1.384
1.380
1.374
1.369
1.364
1.359
1.348
1.314
1.306
1.298
1.297
1.292
1.285
1.281
1.277
1.274
1.267
1.259
1.254
TIPSO
H
Me
Me
4.92
1.05
1
2.5
2.41
3.07
1.18
21.3
1.02
1.08
1.56
3.03
1.61
ppm
12
11
10
9
8
7
6
5
4
3
2
1
0

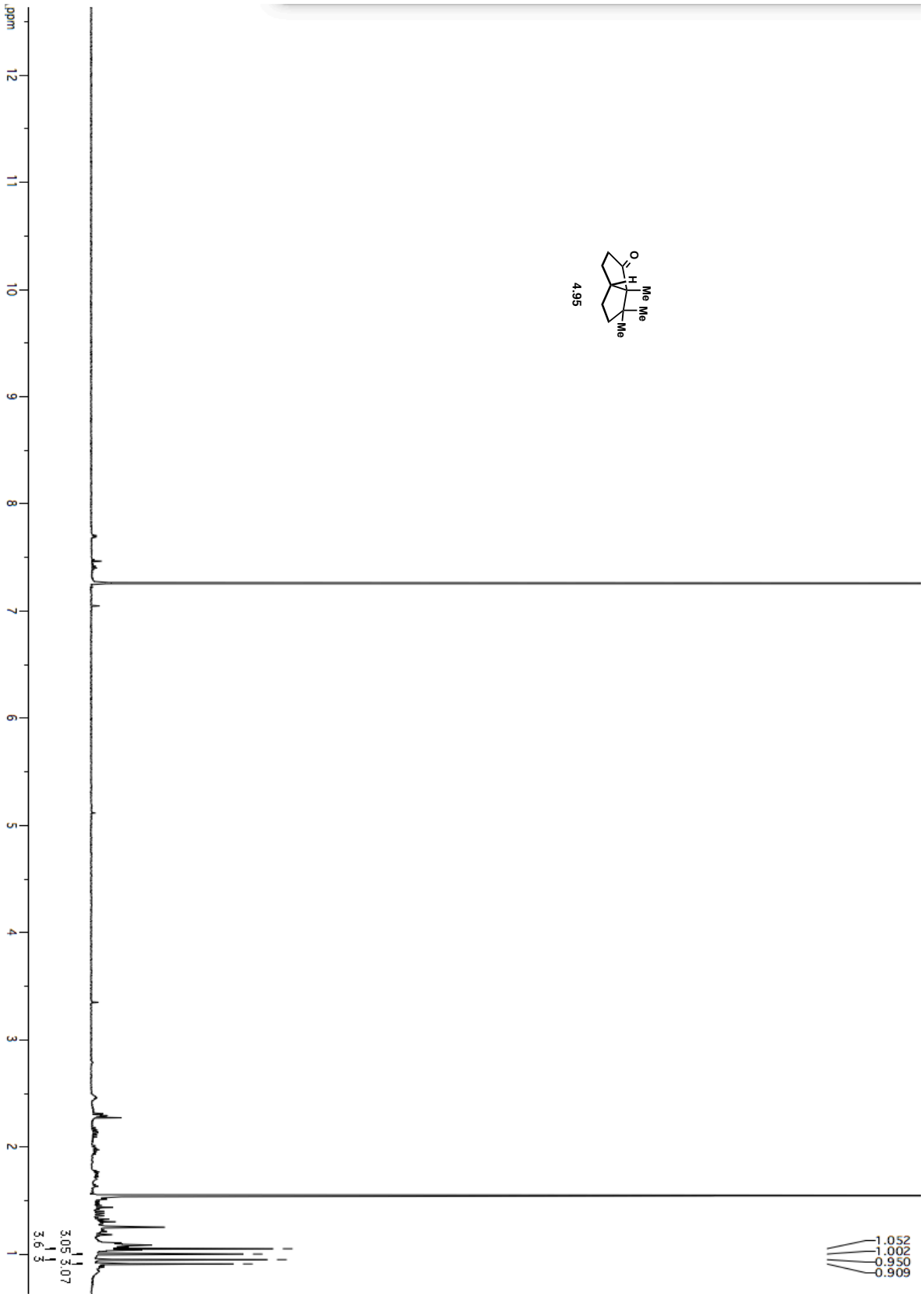
ppm
12
11
10
9
8
7
6
5
4
3
2
1
3.05
3.07
3.6
3
4.95
O
H
Me
Me
Me
1.052
1.002
0.950
0.909

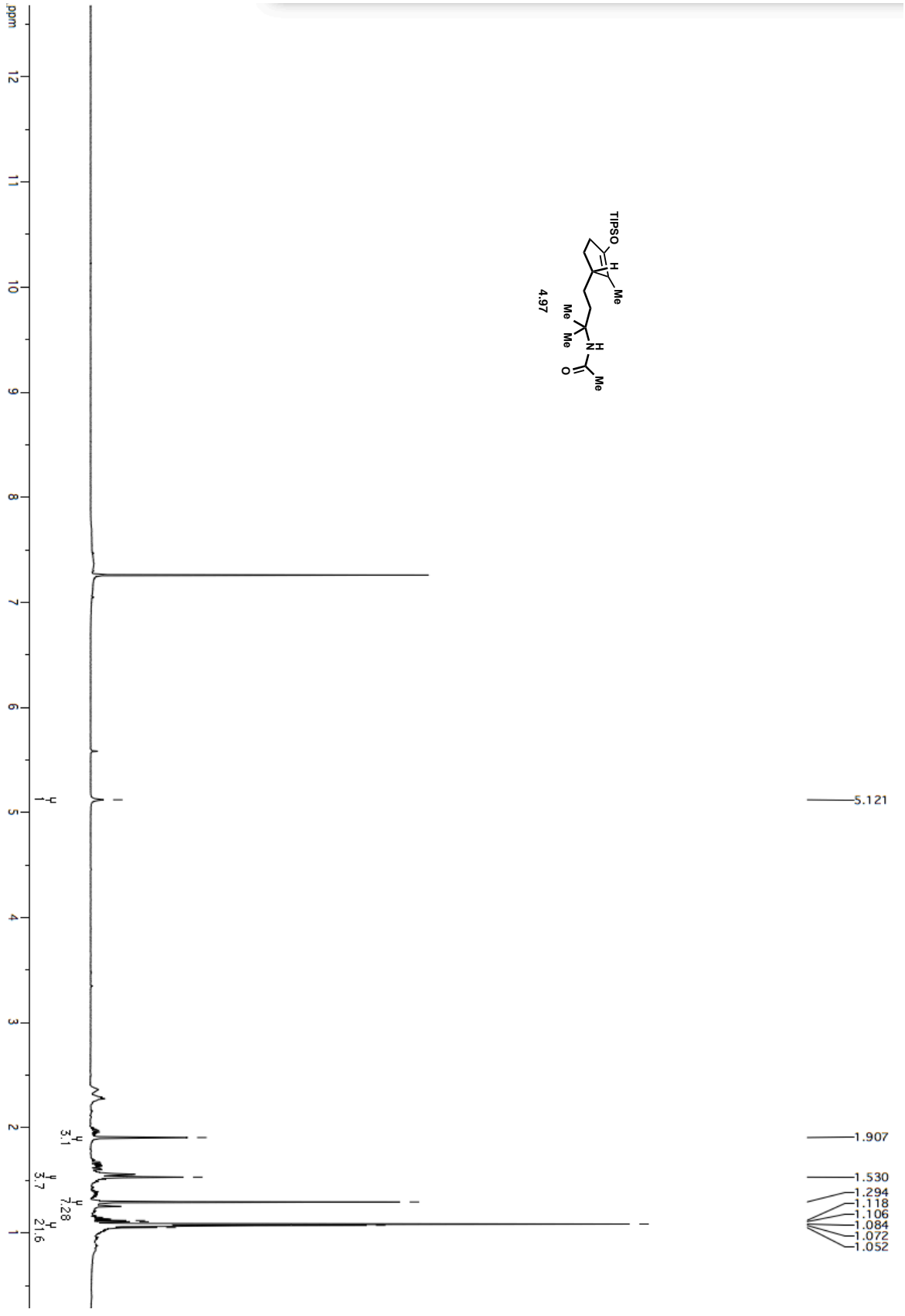
TIPSO
Me
Me
Me
N
H
O
Me
4.97
ppm
12
11
10
9
8
7
6
5
4
3
2
1
1
3.1
3.7
7.28
21.6
5.121
1.907
1.530
1.294
1.118
1.106
1.084
1.072
1.052

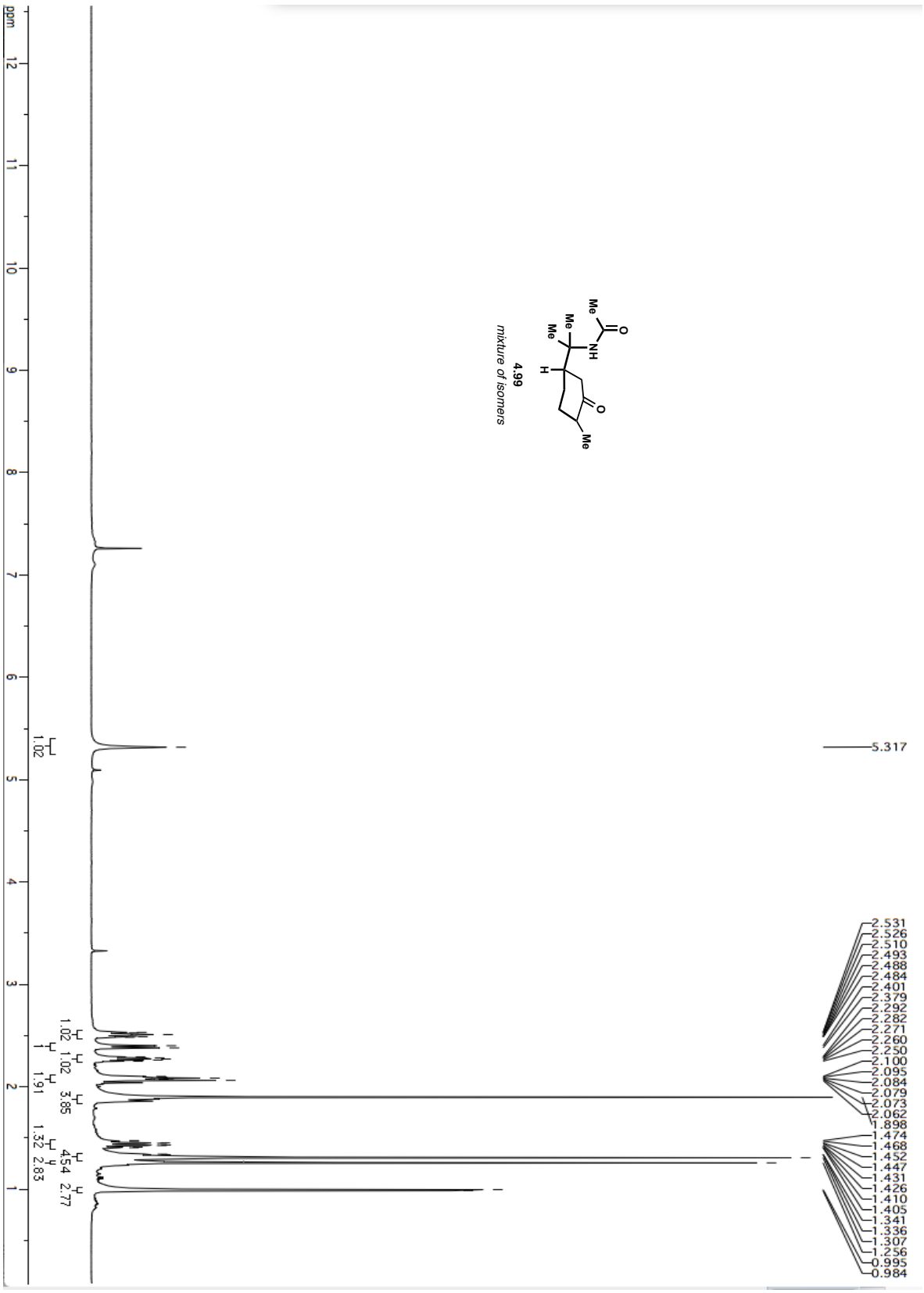
4.99
mixture of isomers
5.317
2.531
2.526
2.510
2.493
2.488
2.484
2.401
2.379
2.292
2.282
2.271
2.260
2.250
2.100
2.095
2.084
2.079
2.073
2.062
1.898
1.474
1.468
1.452
1.447
1.431
1.426
1.410
1.405
1.341
1.336
1.307
1.256
0.995
0.984
1.02
1.02
1.02
3.85
1.91
4.54
1.32
2.77
2.83
ppm

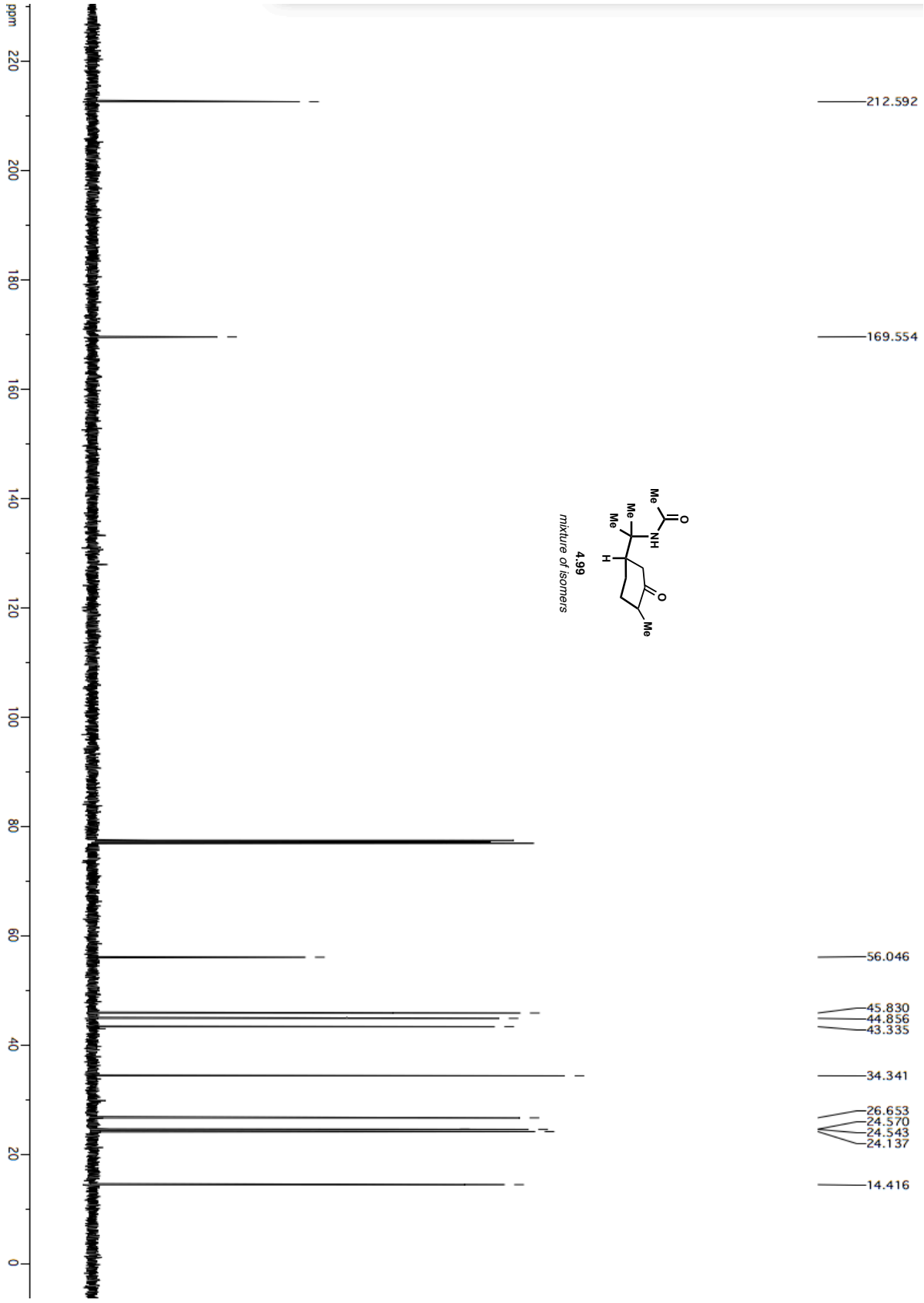
ppm
220
200
180
160
140
120
100
80
60
40
20
0
212.592
169.554
56.046
45.830
44.856
43.335
34.341
26.653
24.570
24.543
24.137
14.416
4.99
mixture of isomers
Me
O
NH
Me
Me
H
O
Me

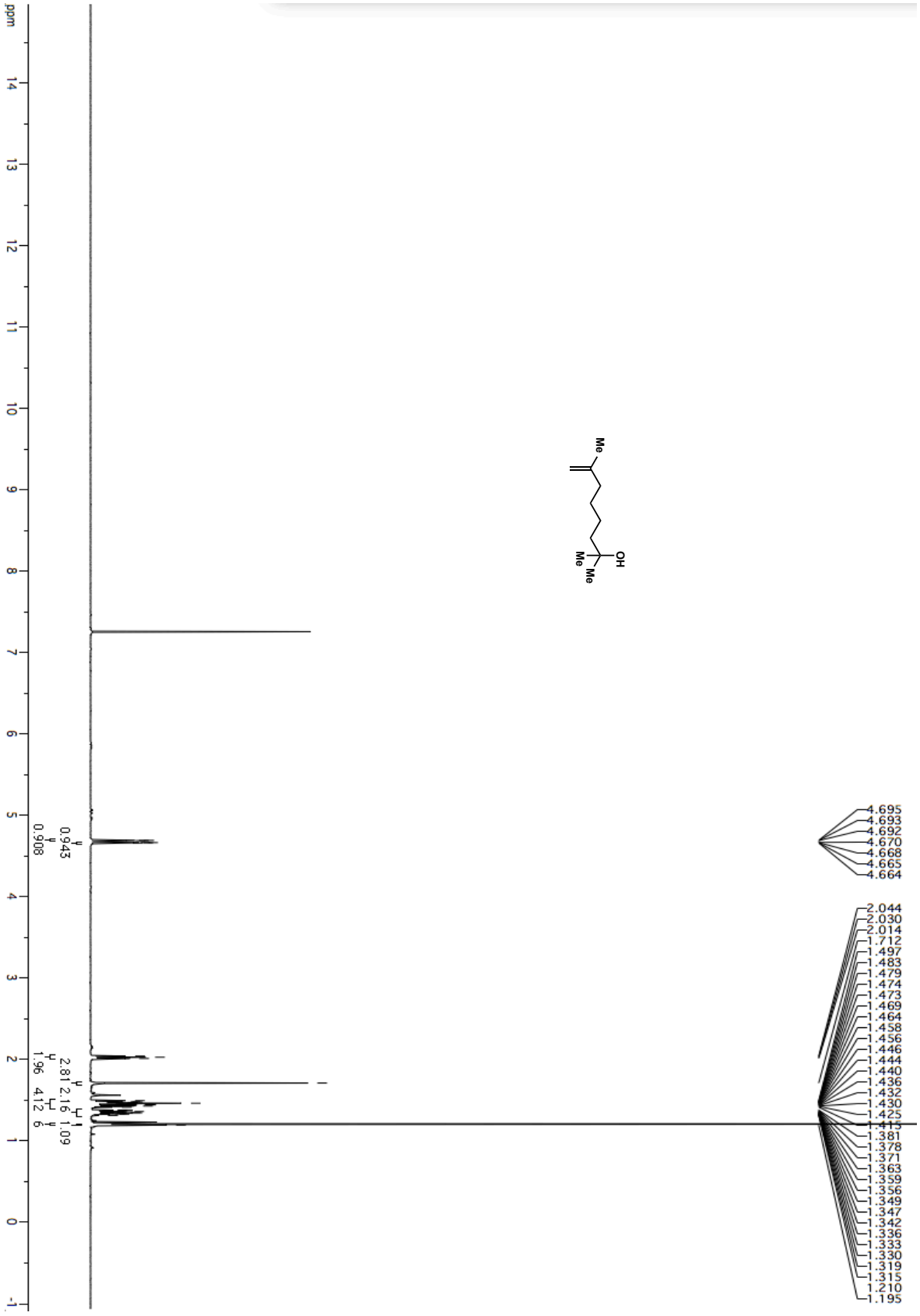
ppm
14
13
12
11
10
9
8
7
6
5
4
3
2
1
0
-1
0.908
0.943
1.96
4.12
6
2.81
2.16
1.09
Me
Me
Me
OH
4.695
4.693
4.692
4.670
4.668
4.665
4.664
2.044
2.030
2.014
1.712
1.497
1.483
1.479
1.474
1.473
1.469
1.464
1.458
1.456
1.446
1.444
1.440
1.436
1.432
1.430
1.425
1.415
1.381
1.378
1.371
1.363
1.359
1.356
1.349
1.347
1.342
1.336
1.333
1.330
1.319
1.315
1.210
1.195

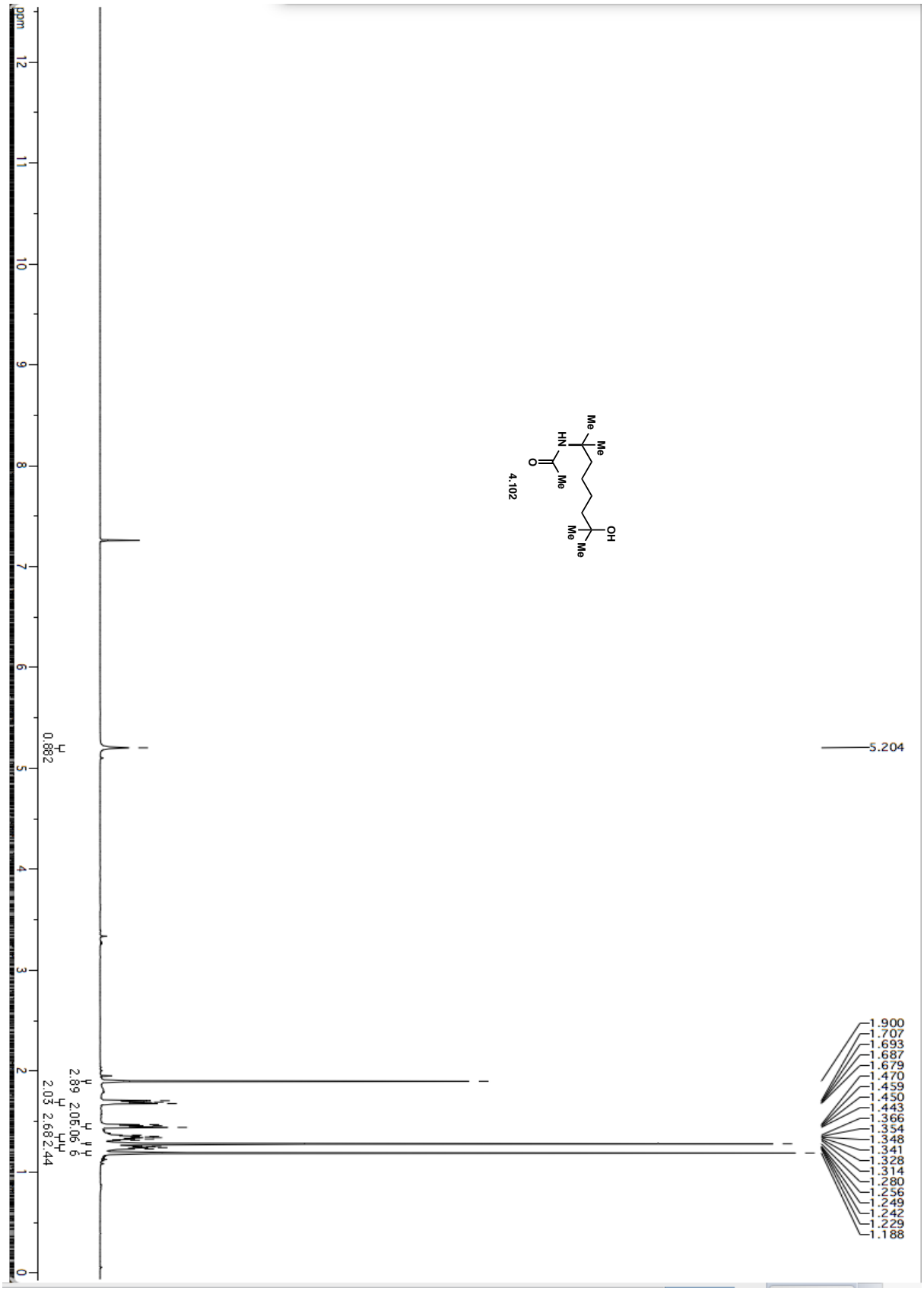
ppm
12
11
10
9
8
7
6
5
4
3
2
1
0
0.882
2.89
2.06
2.06
6
2.03
2.68
2.44
4.102
HN
Me
Me
Me
Me
Me
Me
OH
O
5.204
1.900
1.707
1.693
1.687
1.679
1.470
1.459
1.450
1.443
1.366
1.354
1.348
1.341
1.328
1.314
1.280
1.256
1.249
1.242
1.229
1.188

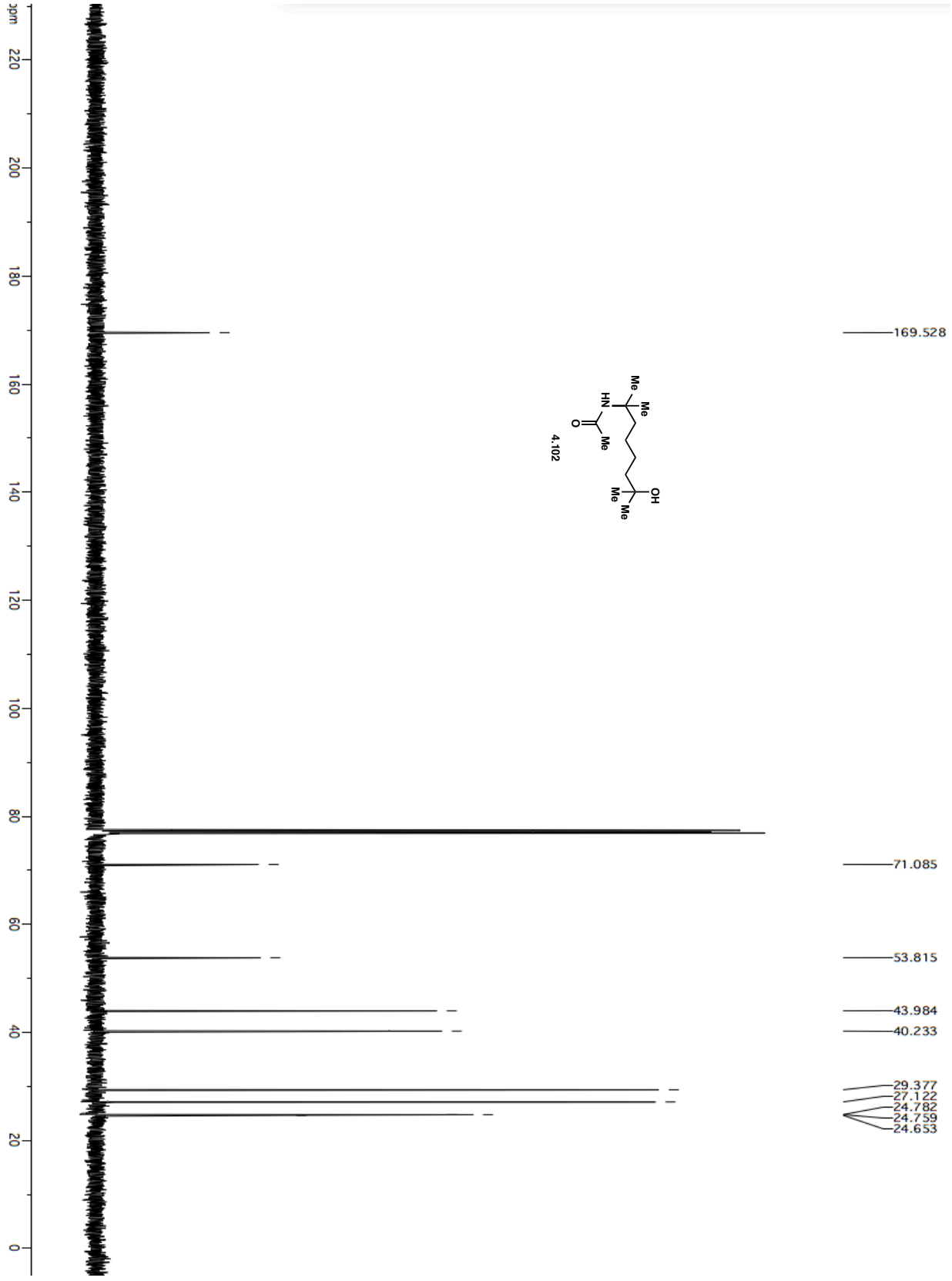
ppm
220
200
180
160
140
120
100
80
60
40
20
0
169.528
71.085
53.815
43.984
40.233
29.377
27.122
24.782
24.759
24.653
4.102
HN
O
Me
Me
Me
Me
Me
OH

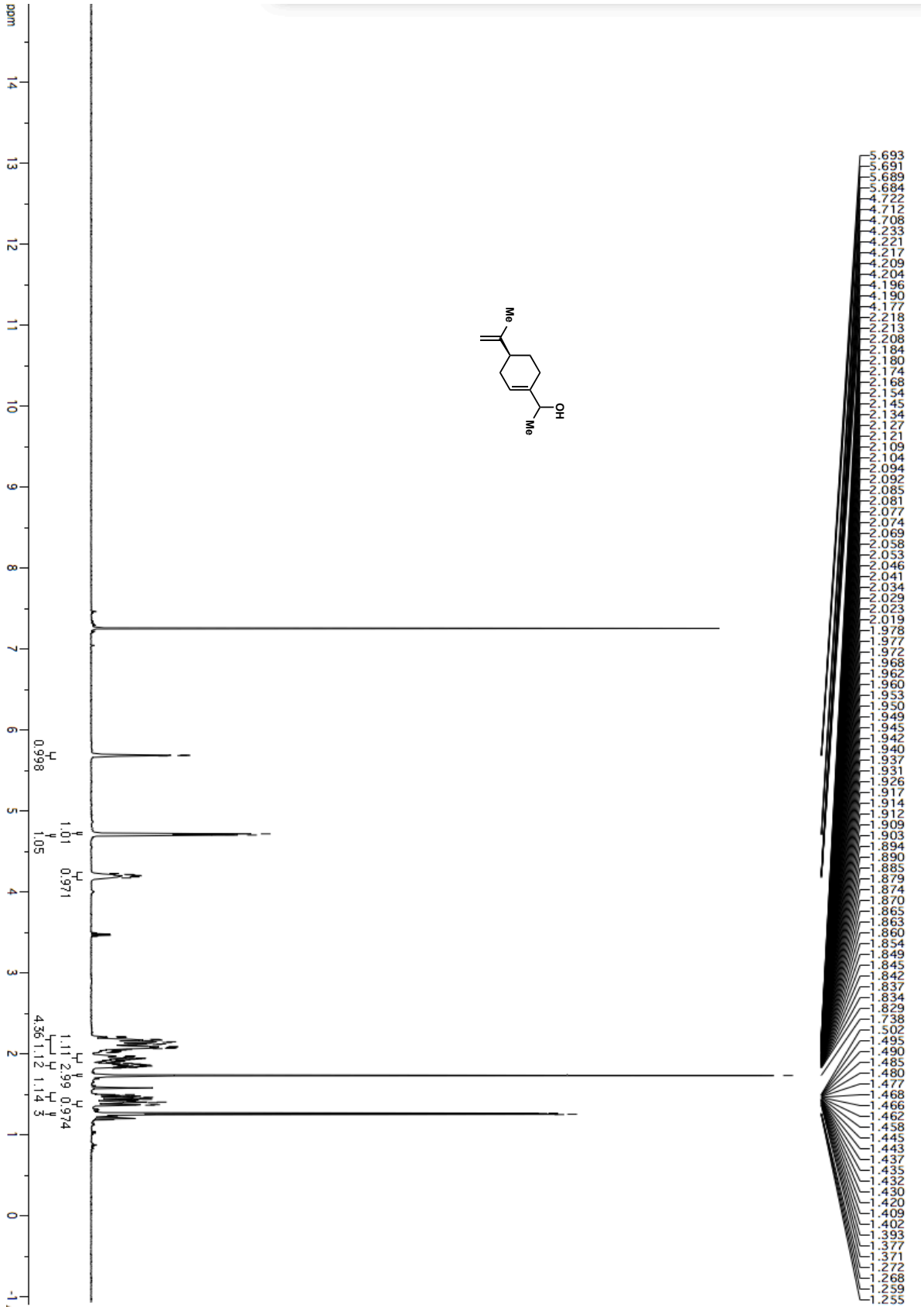
ppm
14
13
12
11
10
9
8
7
6
5
4
3
2
1
0
-1
Me
OH
Me
5.693
5.691
5.689
5.684
4.722
4.712
4.708
4.233
4.221
4.217
4.209
4.204
4.196
4.190
4.177
2.218
2.213
2.208
2.184
2.180
2.174
2.168
2.154
2.145
2.134
2.127
2.121
2.109
2.104
2.094
2.092
2.085
2.081
2.077
2.074
2.069
2.058
2.053
2.046
2.041
2.034
2.029
2.023
2.019
1.978
1.977
1.972
1.968
1.962
1.960
1.953
1.950
1.949
1.945
1.942
1.940
1.937
1.931
1.926
1.917
1.914
1.912
1.909
1.903
1.894
1.890
1.885
1.879
1.874
1.870
1.865
1.863
1.860
1.854
1.849
1.845
1.842
1.837
1.834
1.829
1.738
1.502
1.495
1.490
1.485
1.480
1.477
1.468
1.466
1.462
1.458
1.445
1.443
1.437
1.435
1.432
1.430
1.420
1.409
1.402
1.393
1.377
1.371
1.272
1.268
1.259
1.255
0.998
1.01
1.05
0.971
4.36
1.12
1.11
2.99
1.14
0.974
3

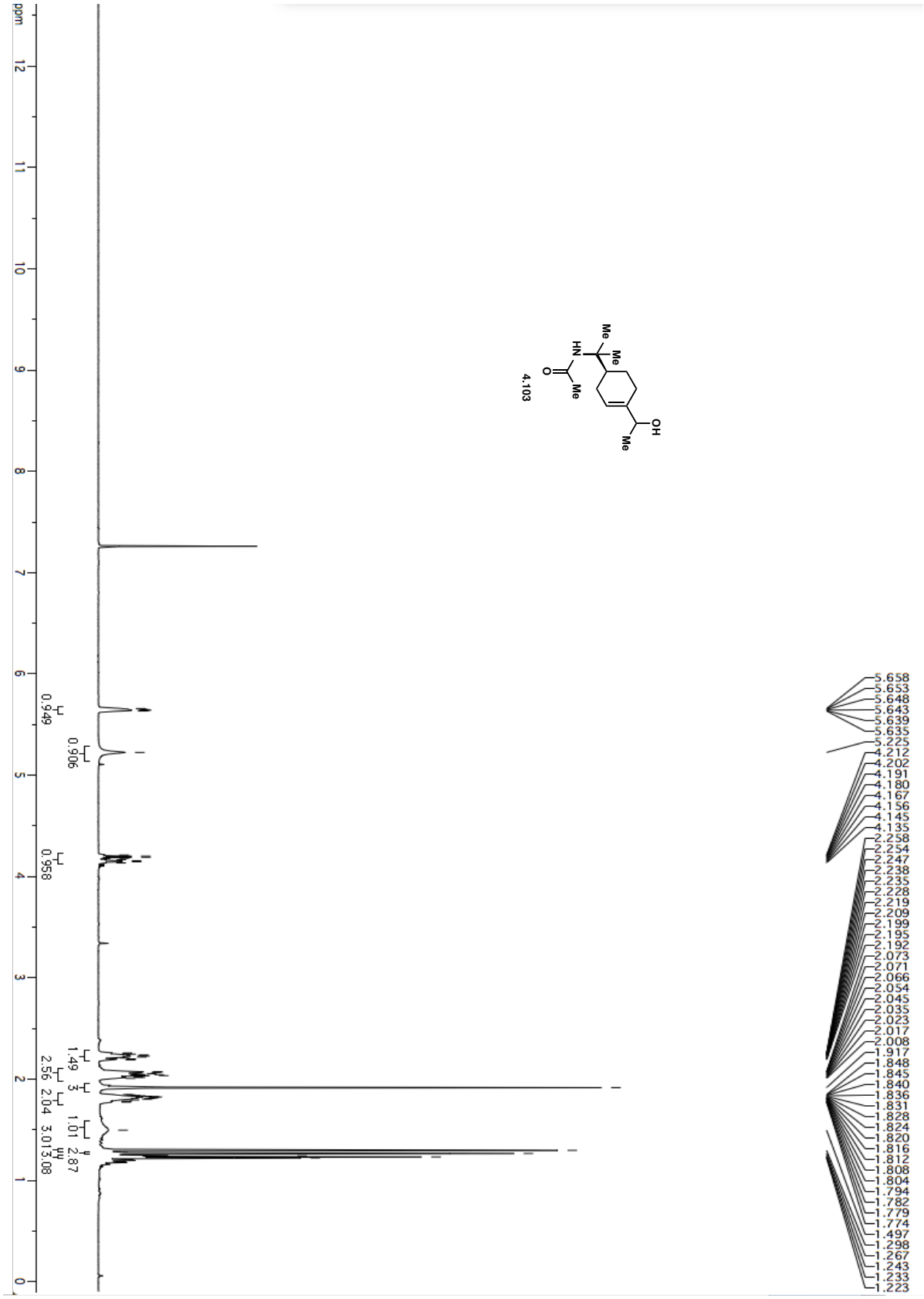
ppm
12
11
10
9
8
7
6
5
4
3
2
1
0
0.949
0.906
0.958
1.49
3
2.56
2.04
1.01
2.87
3.01
3.08
4.103
Me
Me
HN
Me
O
OH
Me
5.658
5.653
5.648
5.643
5.639
5.635
5.225
4.212
4.202
4.191
4.180
4.167
4.156
4.145
4.135
2.258
2.254
2.247
2.238
2.235
2.228
2.219
2.209
2.199
2.195
2.192
2.073
2.071
2.066
2.054
2.045
2.035
2.023
2.017
2.008
1.917
1.848
1.845
1.840
1.836
1.831
1.828
1.824
1.820
1.816
1.812
1.808
1.804
1.794
1.782
1.779
1.774
1.497
1.298
1.267
1.243
1.233
1.223

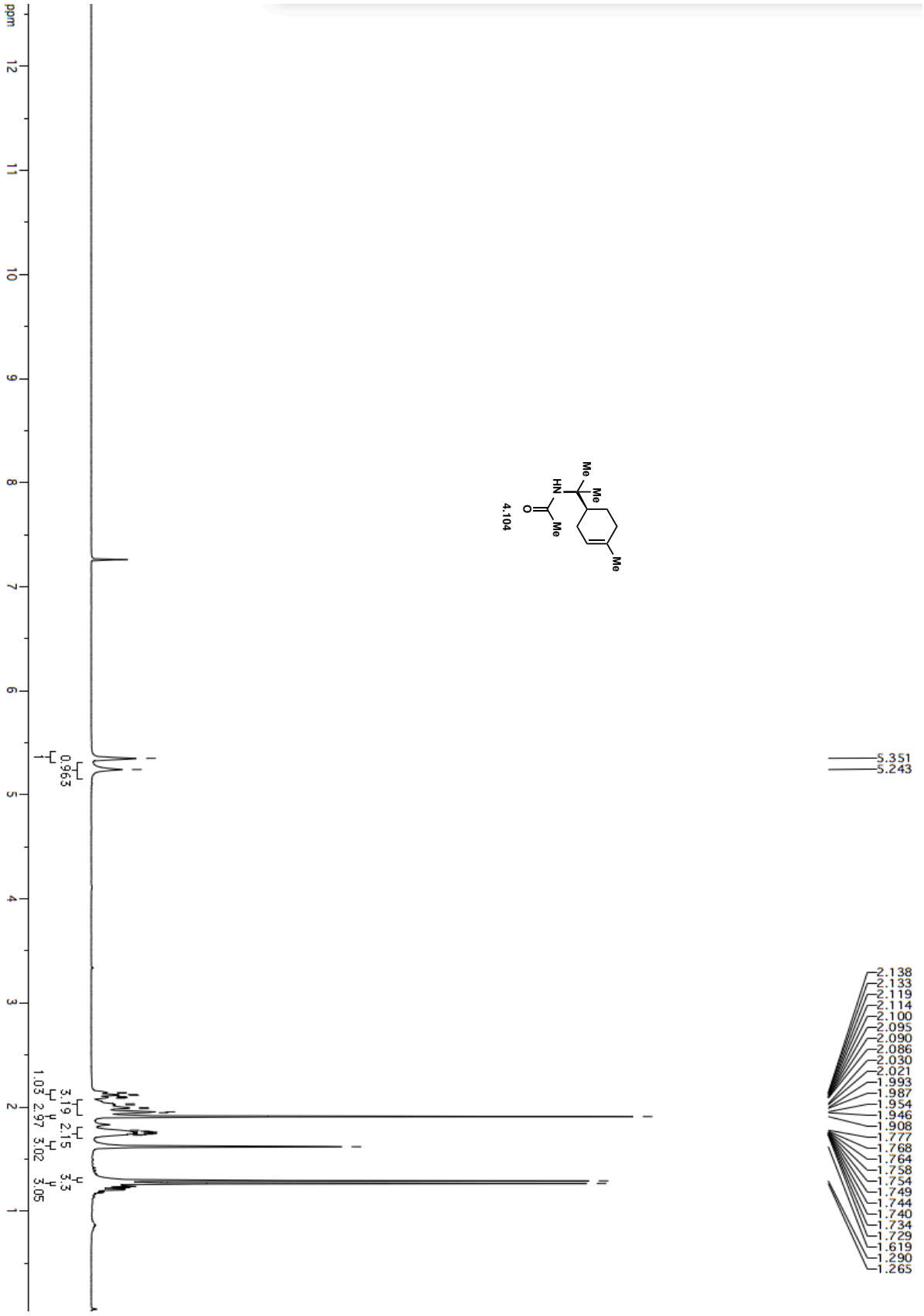
ppm
12
11
10
9
8
7
6
5
4
3
2
1
0.963
3.19
2.15
3.3
1.03
2.97
3.02
3.05
4.104
HN
Me
Me
Me
O
Me
5.351
5.243
2.138
2.133
2.119
2.114
2.100
2.095
2.090
2.086
2.030
2.021
1.993
1.987
1.954
1.946
1.908
1.777
1.768
1.764
1.758
1.754
1.749
1.744
1.740
1.734
1.729
1.619
1.290
1.265

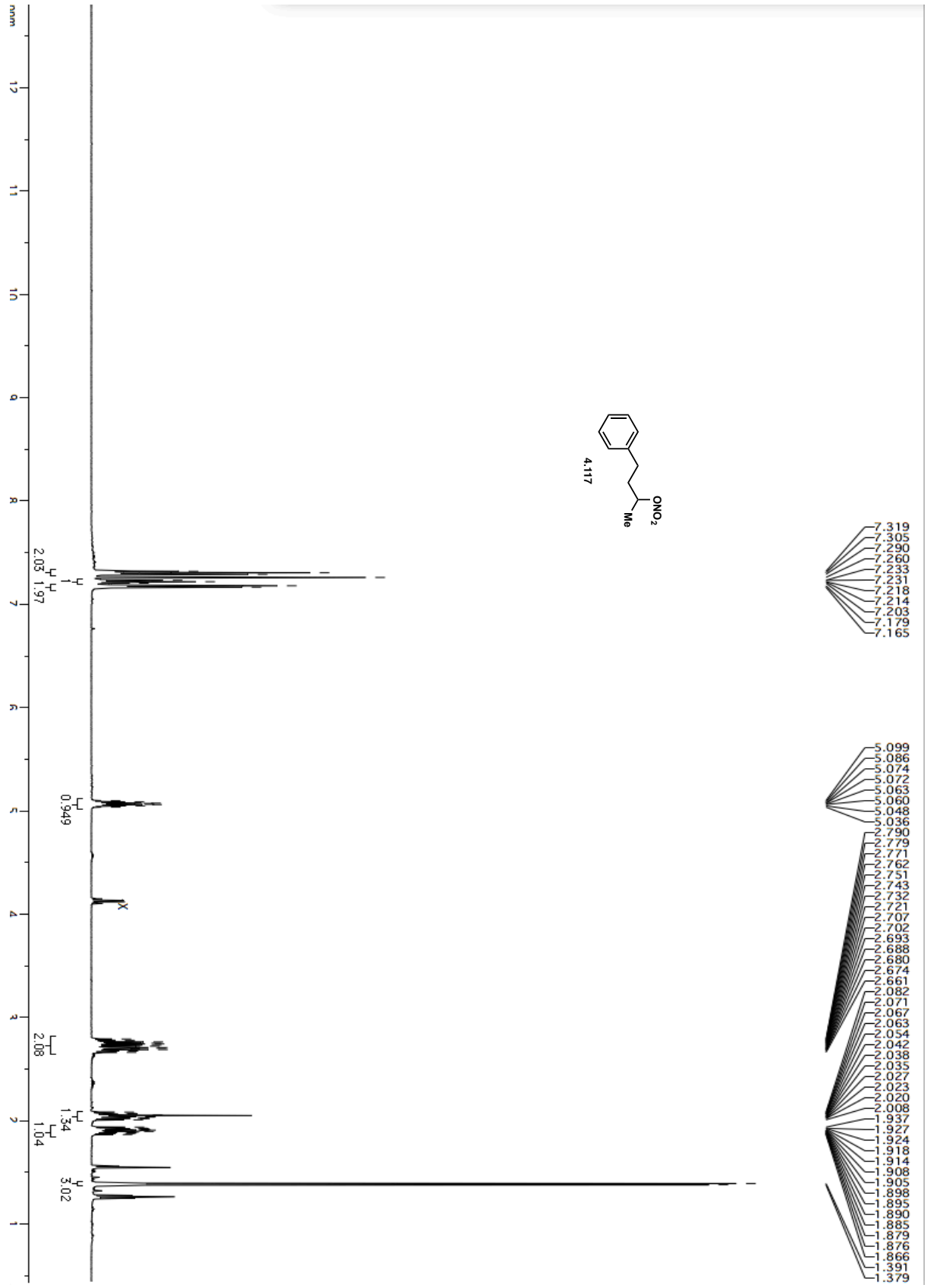
4.117
ONO2
Me
7.319
7.305
7.290
7.260
7.233
7.231
7.218
7.214
7.203
7.179
7.165
5.099
5.086
5.074
5.072
5.063
5.060
5.048
5.036
2.790
2.779
2.771
2.762
2.751
2.743
2.732
2.721
2.707
2.702
2.693
2.688
2.680
2.674
2.661
2.082
2.071
2.067
2.063
2.054
2.042
2.038
2.035
2.027
2.023
2.020
2.008
1.937
1.927
1.924
1.918
1.914
1.908
1.905
1.898
1.895
1.890
1.885
1.879
1.876
1.866
1.391
1.379
2.03
1.97
0.949
2.08
1.34
1.04
3.02

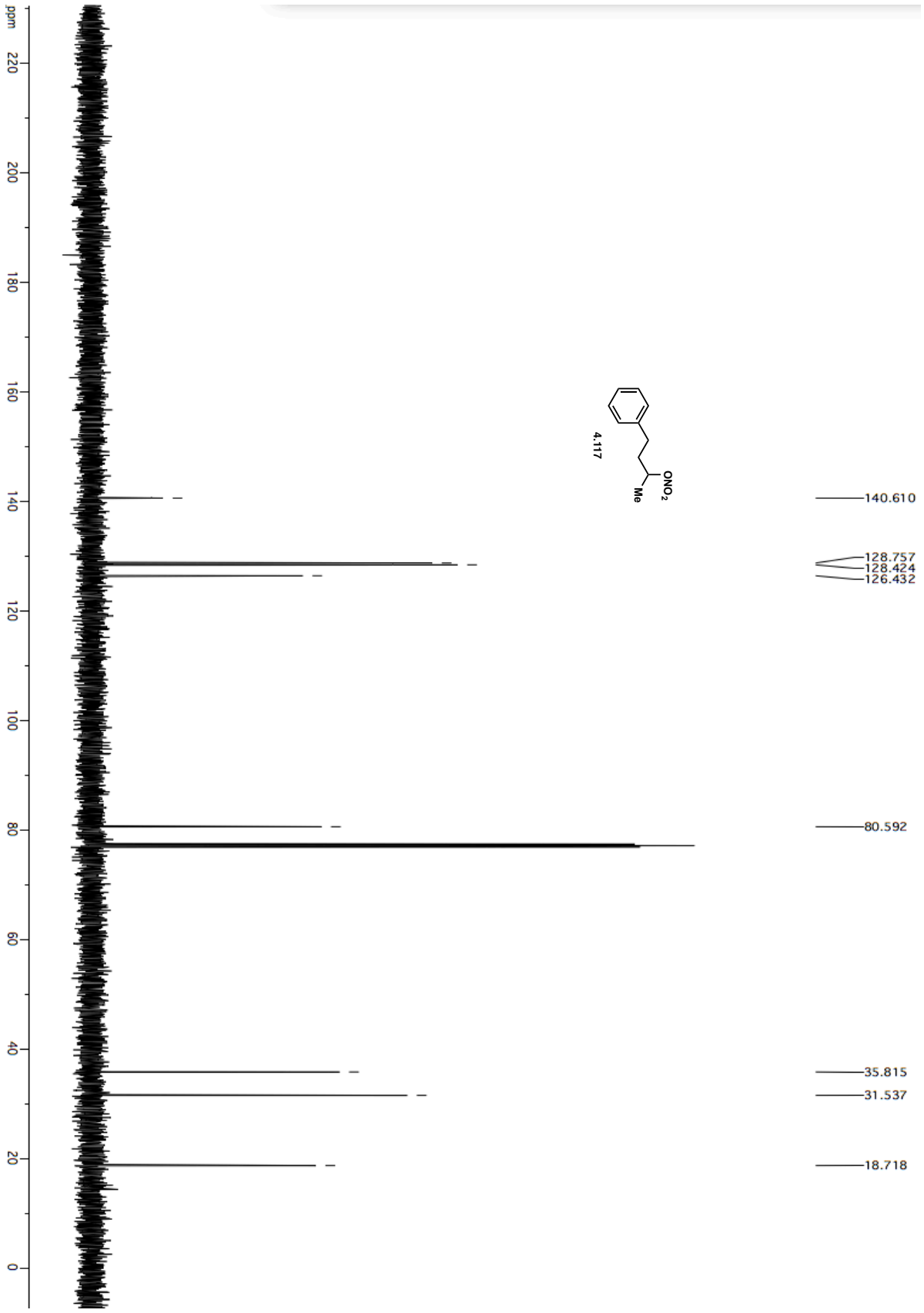
ppm
220
200
180
160
140
120
100
80
60
40
20
0
4.117
ONO2
Me
140.610
128.757
128.424
126.432
80.592
35.815
31.537
18.718

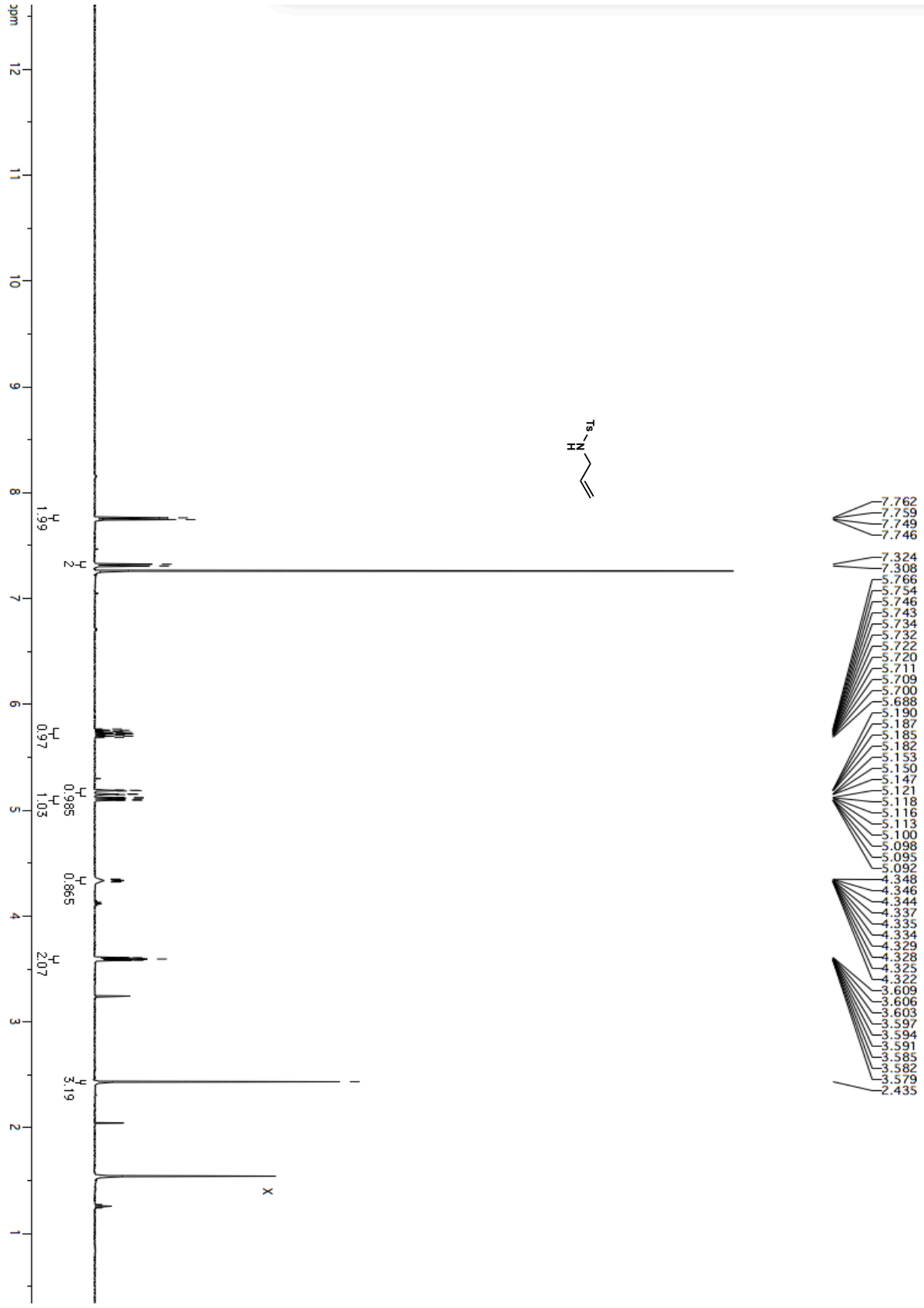
Ts
N
H
7.762
7.759
7.749
7.746
7.324
7.308
5.766
5.754
5.746
5.743
5.734
5.732
5.722
5.720
5.711
5.709
5.700
5.688
5.190
5.187
5.185
5.182
5.153
5.150
5.147
5.121
5.118
5.116
5.113
5.100
5.098
5.095
5.092
4.348
4.346
4.344
4.337
4.335
4.334
4.329
4.328
4.325
4.322
3.609
3.606
3.603
3.597
3.594
3.591
3.585
3.582
3.579
2.435
1.99
2
0.97
0.985
1.03
0.865
2.07
3.19
I
X

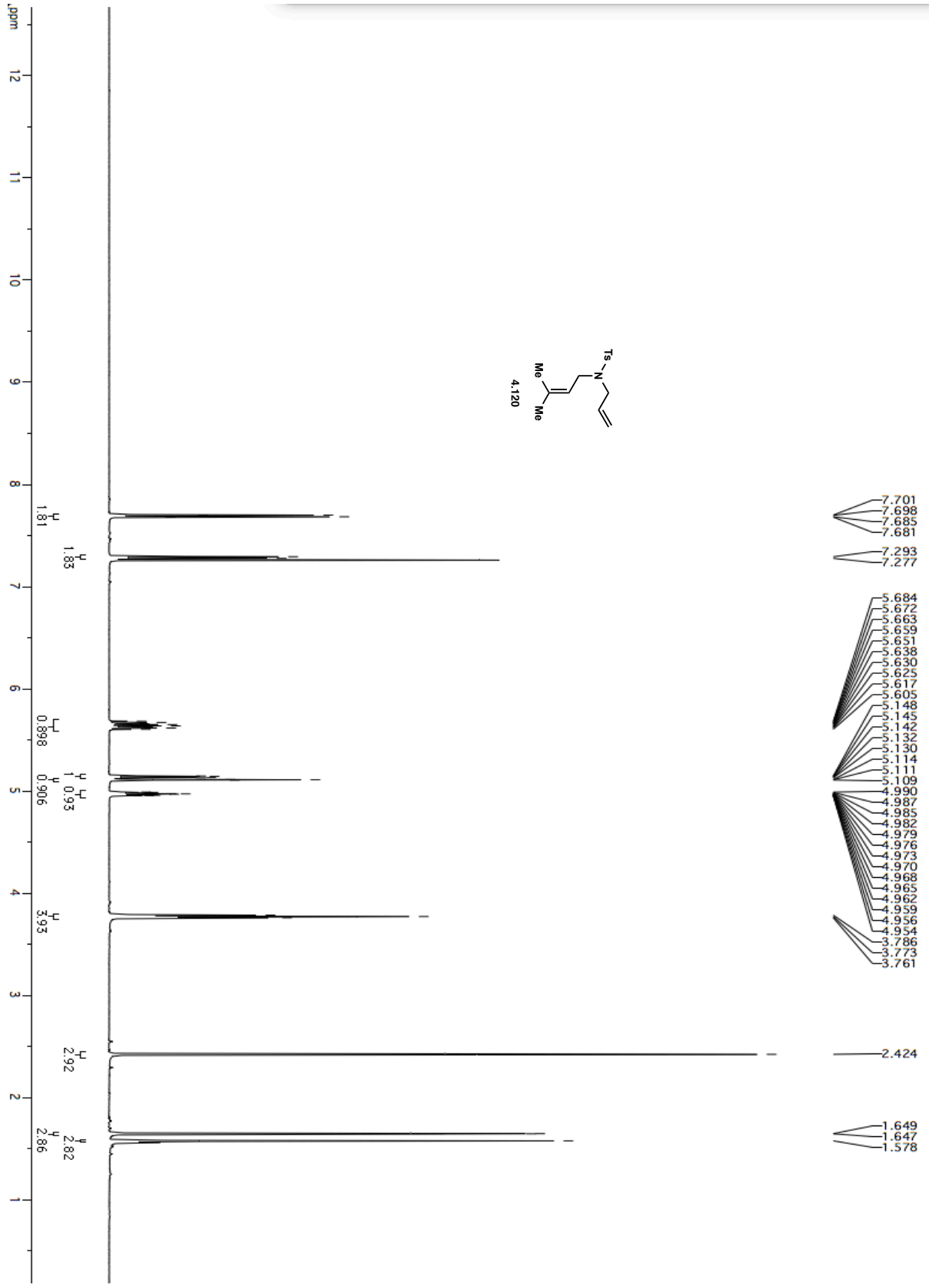
ppm
12
11
10
9
8
7
6
5
4
3
2
1
1.81
1.83
0.898
1
0.93
0.906
3.93
2.92
2.82
2.86
4.120
Me
Me
Ts
N
7.701
7.698
7.685
7.681
7.293
7.277
5.684
5.672
5.663
5.659
5.651
5.638
5.630
5.625
5.617
5.605
5.148
5.145
5.142
5.132
5.130
5.114
5.111
5.109
4.990
4.987
4.985
4.982
4.979
4.976
4.973
4.970
4.968
4.965
4.962
4.959
4.956
4.954
3.786
3.773
3.761
2.424
1.649
1.647
1.578

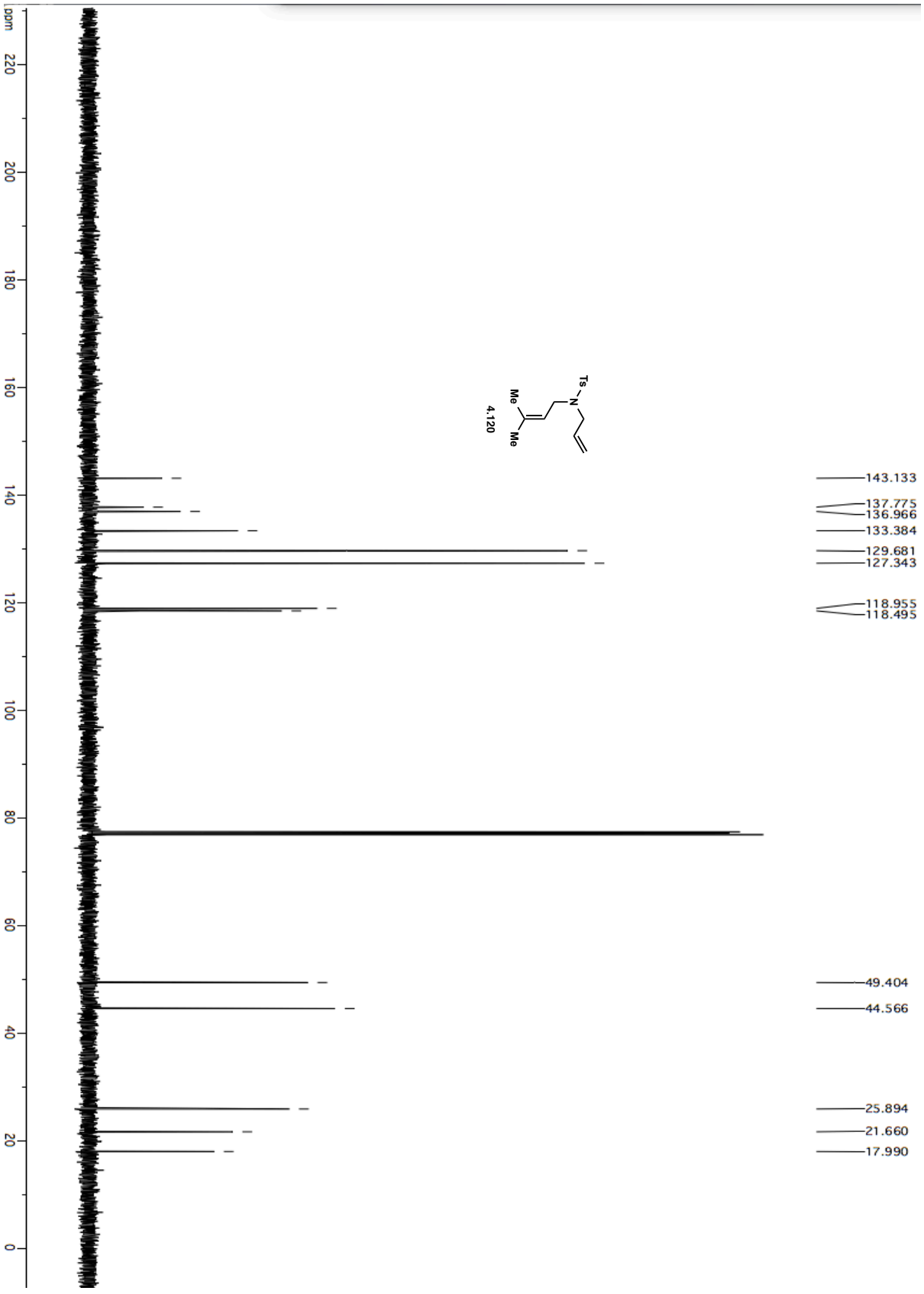
ppm
220
200
180
160
140
120
100
80
60
40
20
0
Ts
N
Me
Me
4.120
143.133
137.775
136.966
133.384
129.681
127.343
118.955
118.495
49.404
44.566
25.894
21.660
17.990

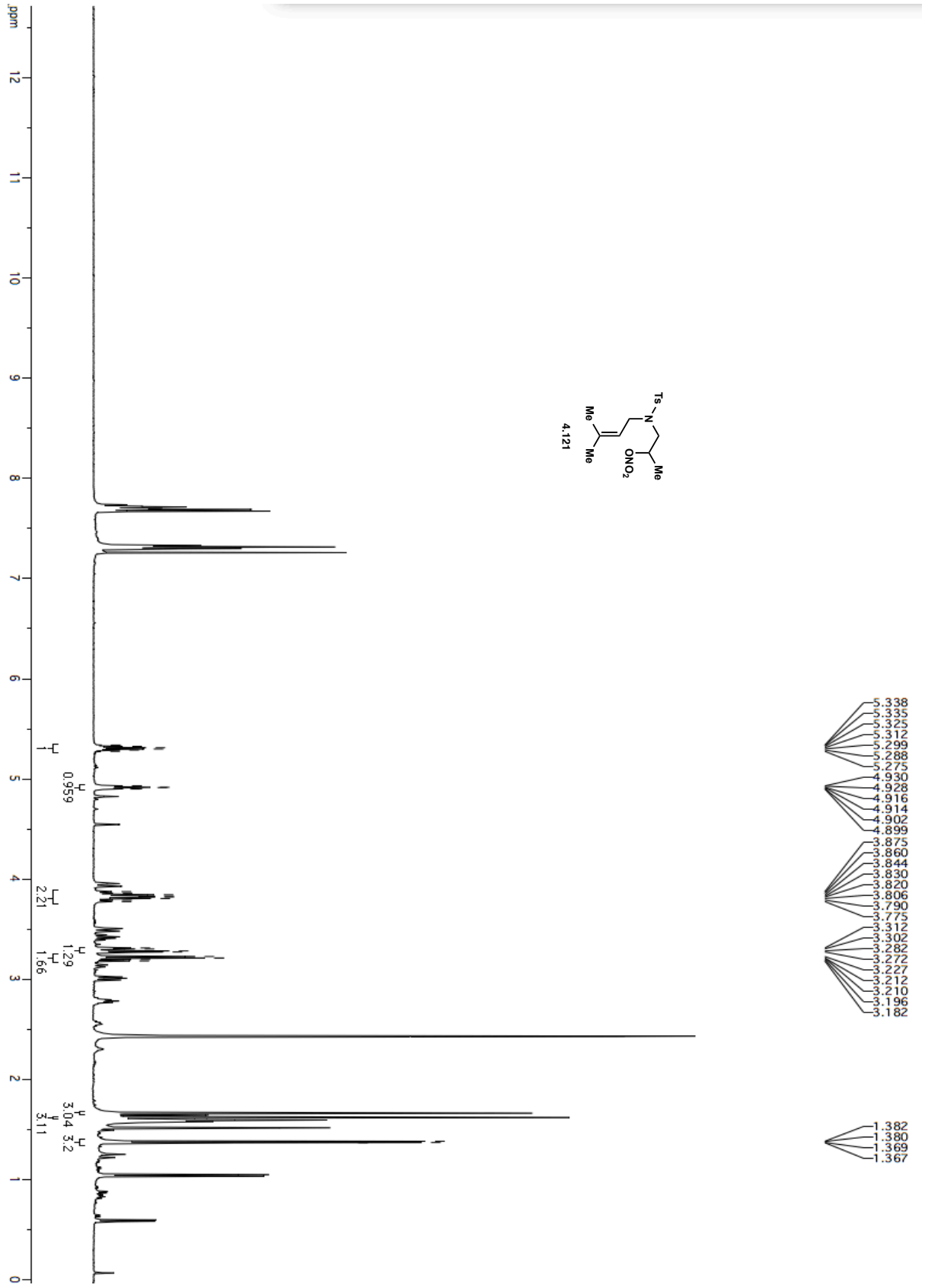
ppm
12
11
10
9
8
7
6
5
4
3
2
1
0
0.959
2.21
1.29
1.66
3.04
3.2
3.11
4.121
Ts
N
Me
Me
ONO2
Me
5.338
5.335
5.325
5.312
5.299
5.288
5.275
4.930
4.928
4.916
4.914
4.902
4.899
3.875
3.860
3.844
3.830
3.820
3.806
3.790
3.775
3.312
3.302
3.282
3.272
3.227
3.212
3.210
3.196
3.182
1.382
1.380
1.369
1.367

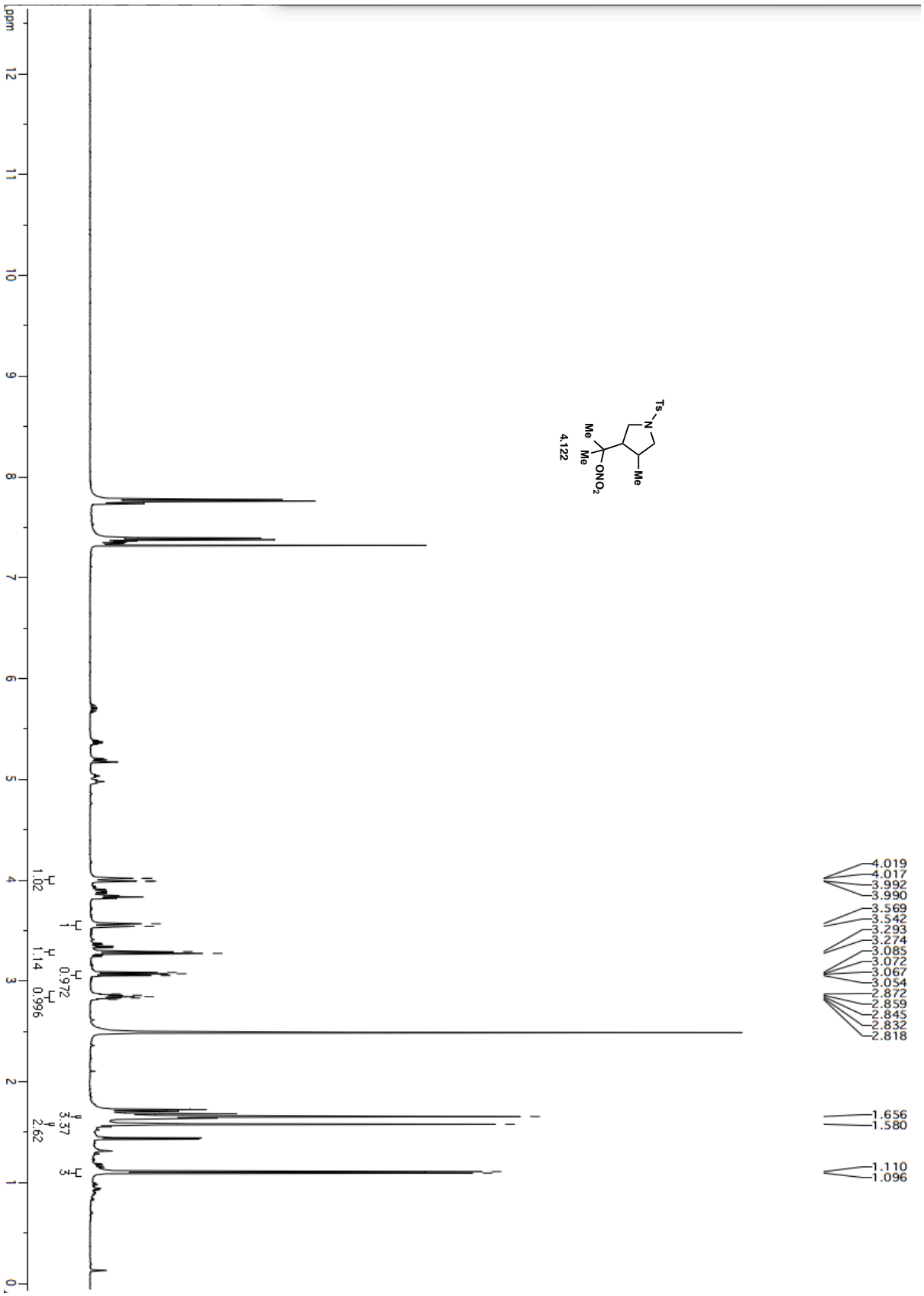
ppm
12
11
10
9
8
7
6
5
4
3
2
1
0
Ts
N
Me
Me
Me
ONO2
4.122
1.02
1
1.14
0.972
0.996
3.37
2.62
3
4.019
4.017
3.992
3.990
3.569
3.542
3.293
3.274
3.085
3.072
3.067
3.054
2.872
2.859
2.845
2.832
2.818
1.656
1.580
1.110
1.096

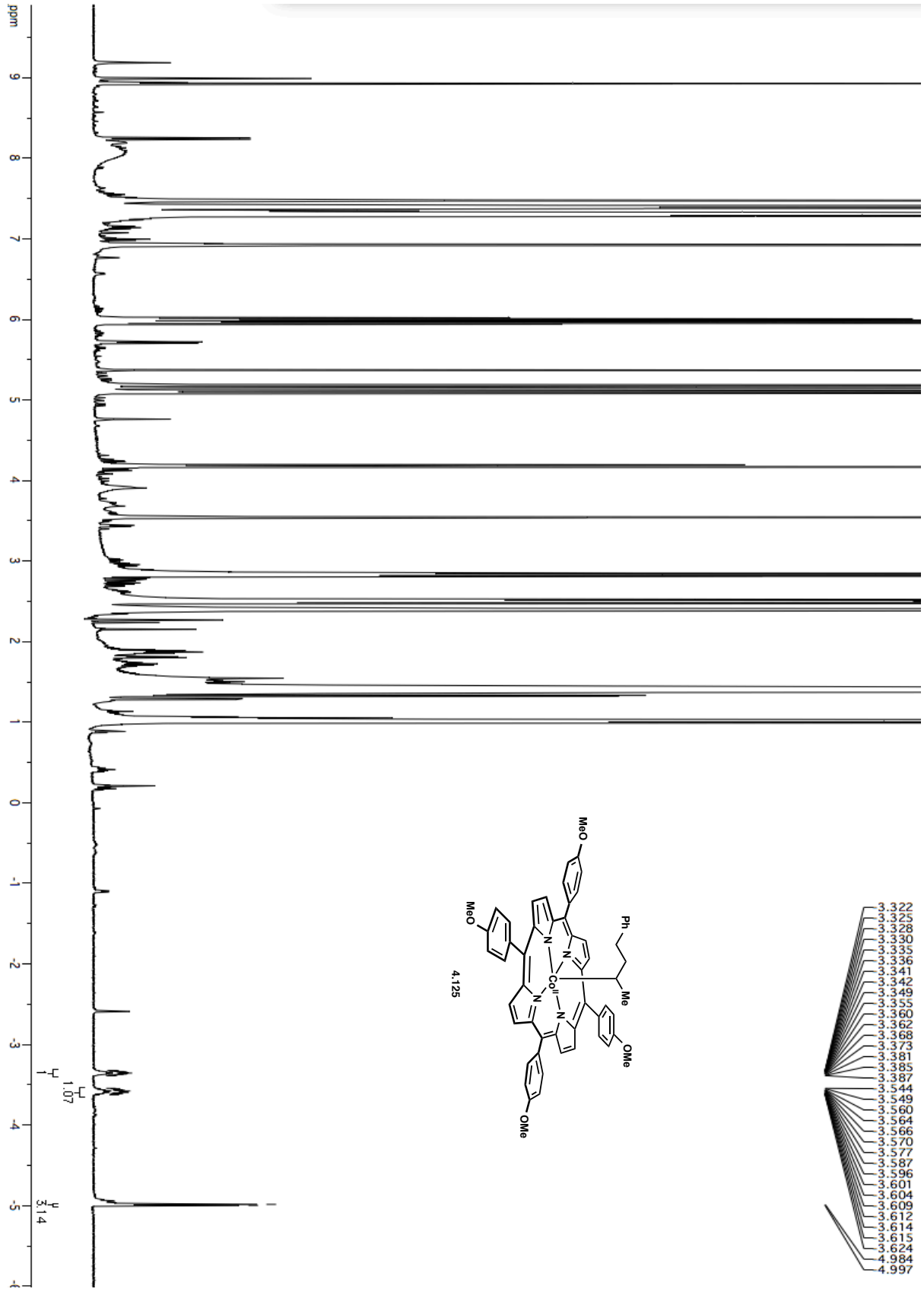
ppm
9
8
7
6
5
4
3
2
1
0
-1
-2
-3
-4
-5
1.07
3.14
MeO
MeO
Ph
Me
OMe
OMe
Co
N
N
N
N
4.125
3.322
3.325
3.328
3.330
3.335
3.336
3.341
3.342
3.349
3.355
3.360
3.362
3.368
3.373
3.381
3.385
3.387
3.544
3.549
3.560
3.564
3.566
3.570
3.577
3.587
3.596
3.601
3.604
3.609
3.612
3.614
3.615
3.624
4.984
4.997

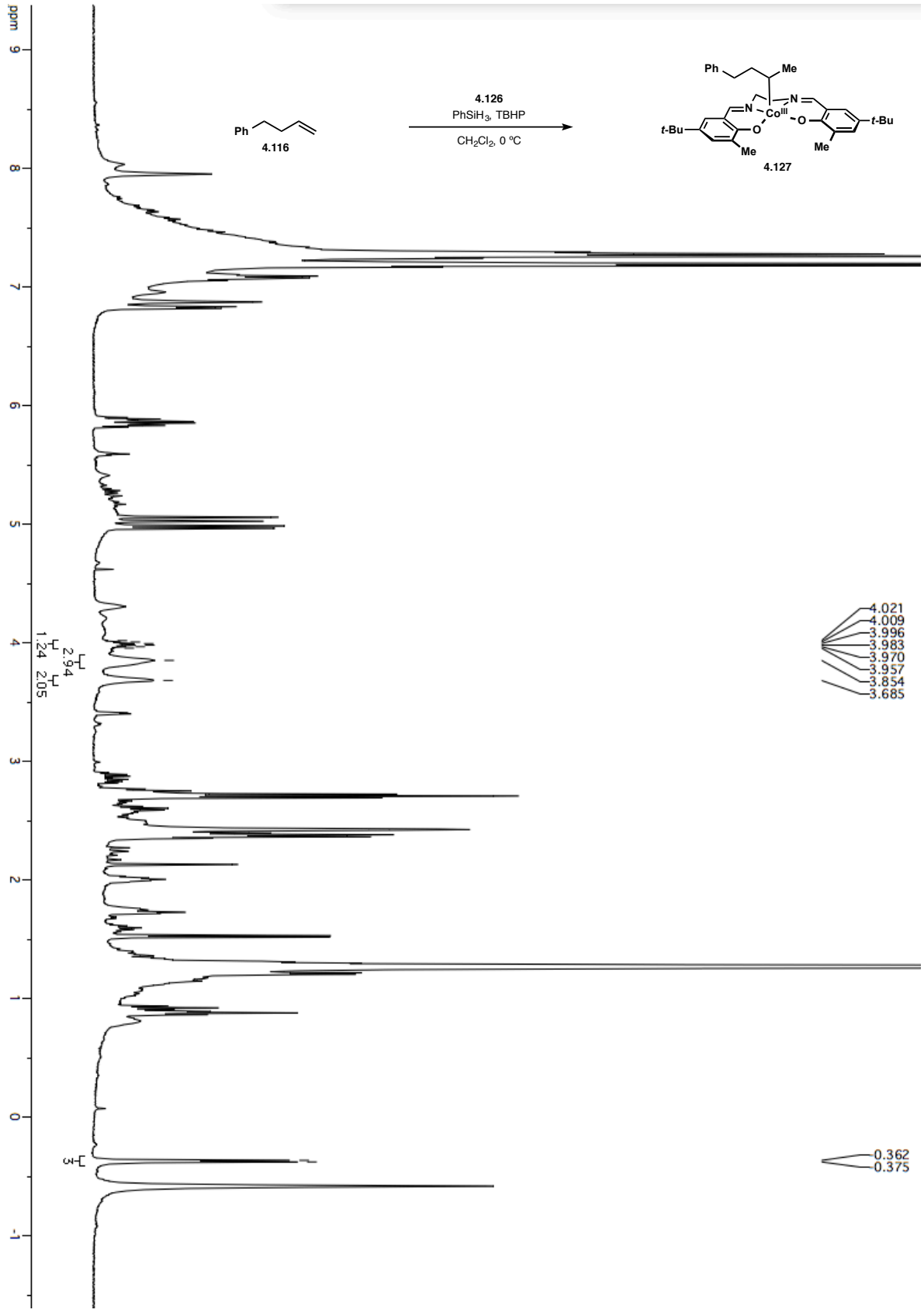
Ph
4.116
4.126
PhSiH3, TBHP
CH2Cl2, 0 °C
Ph
Me
N
N
Co III
O
O
t-Bu
t-Bu
Me
Me
4.127
4.021
4.009
3.996
3.983
3.970
3.957
3.854
3.685
0.362
0.375
1.24
2.94
2.05
3
ppm

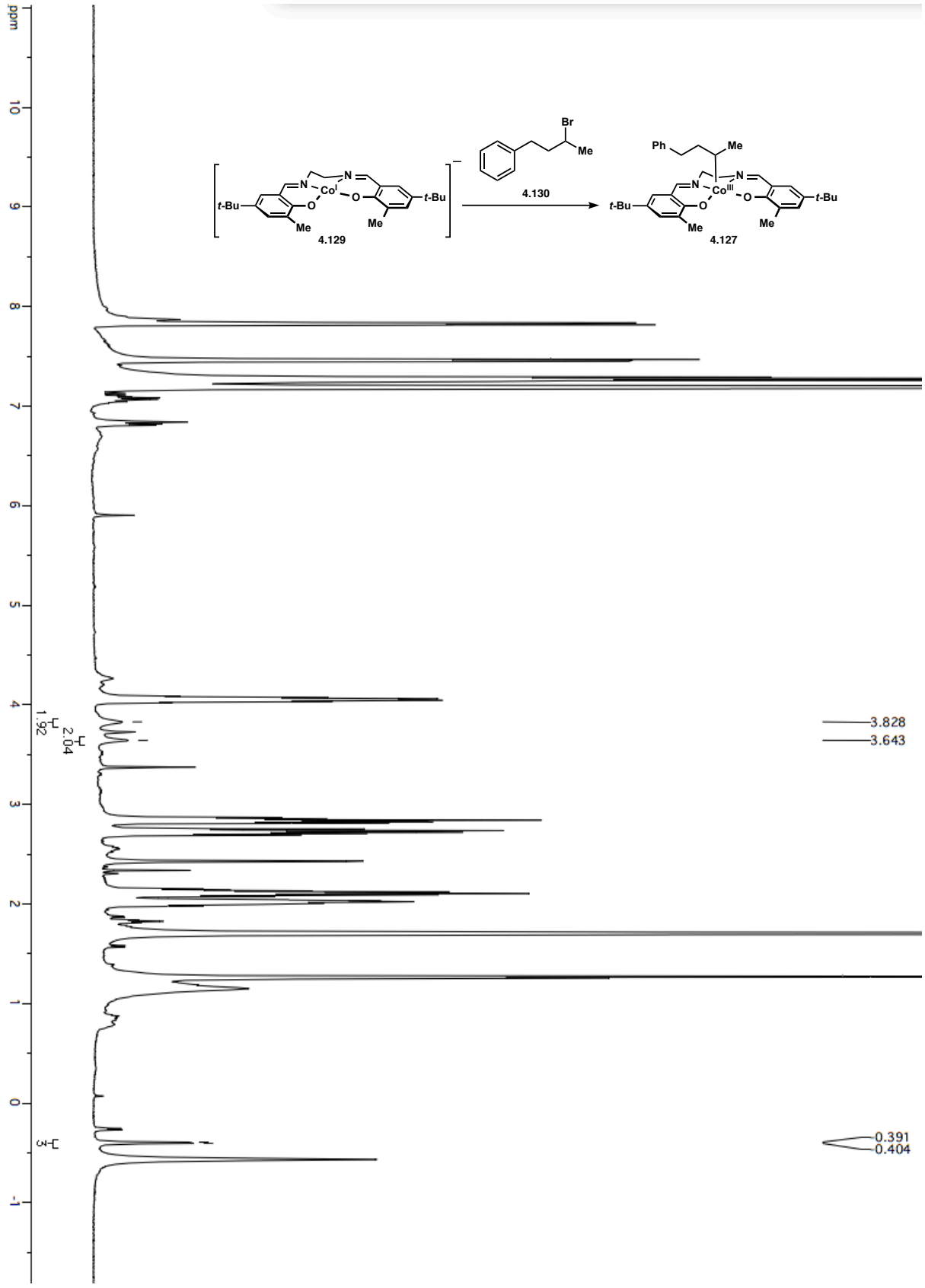
ppm
10
9
8
7
6
5
4
3
2
1
0
-1
1.92
2.04
3
3.828
3.643
0.391
0.404
Br
Me
4.130
Ph
Me
t-Bu
Me
Me
4.129
4.127

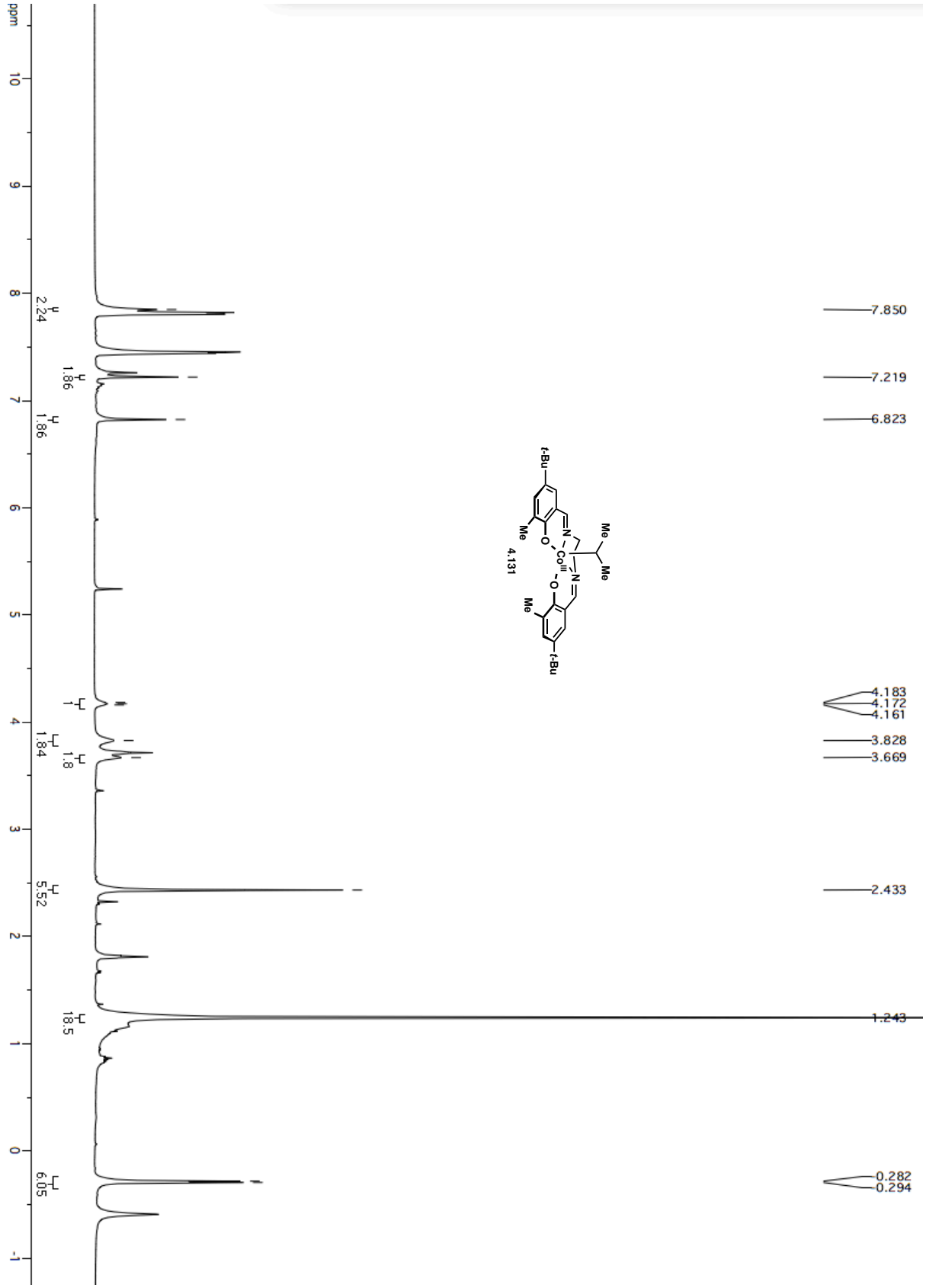
ppm
10
9
8
7
6
5
4
3
2
1
0
-1
2.24
1.86
1.86
1
1.84
1.8
5.52
18.5
6.05
7.850
7.219
6.823
4.183
4.172
4.161
3.828
3.669
2.433
1.243
0.282
0.294
t-Bu
Me
Me
4.131
N
O
Co(III)
O
N
Me
Me
t-Bu

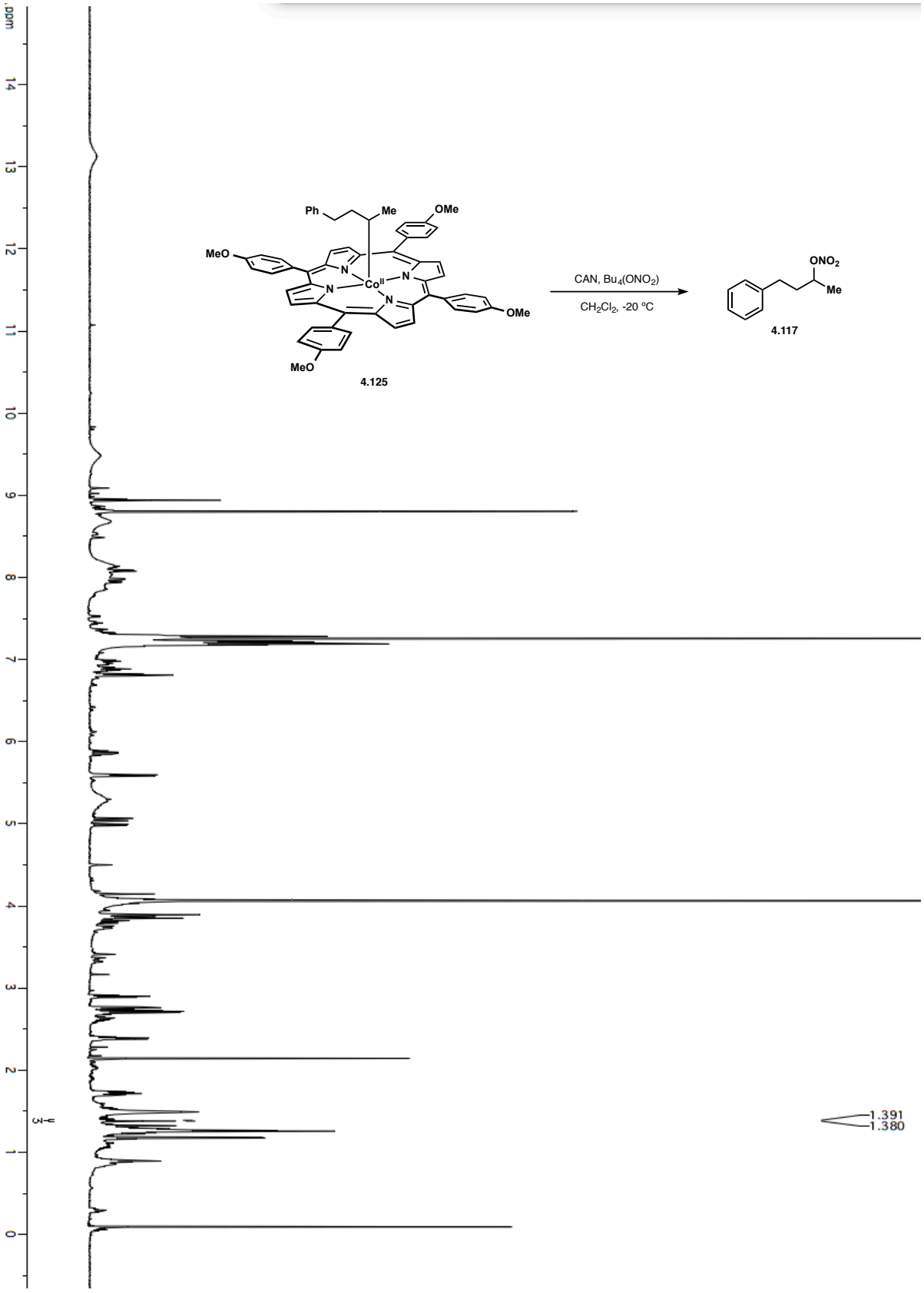
Ph
Me
OMe
MeO
N
Co^II
N
N
N
OMe
MeO
4.125
CAN, Bu4(ONO2)
CH2Cl2, -20 °C
ONO2
Me
4.117
1.391
1.380
ppm

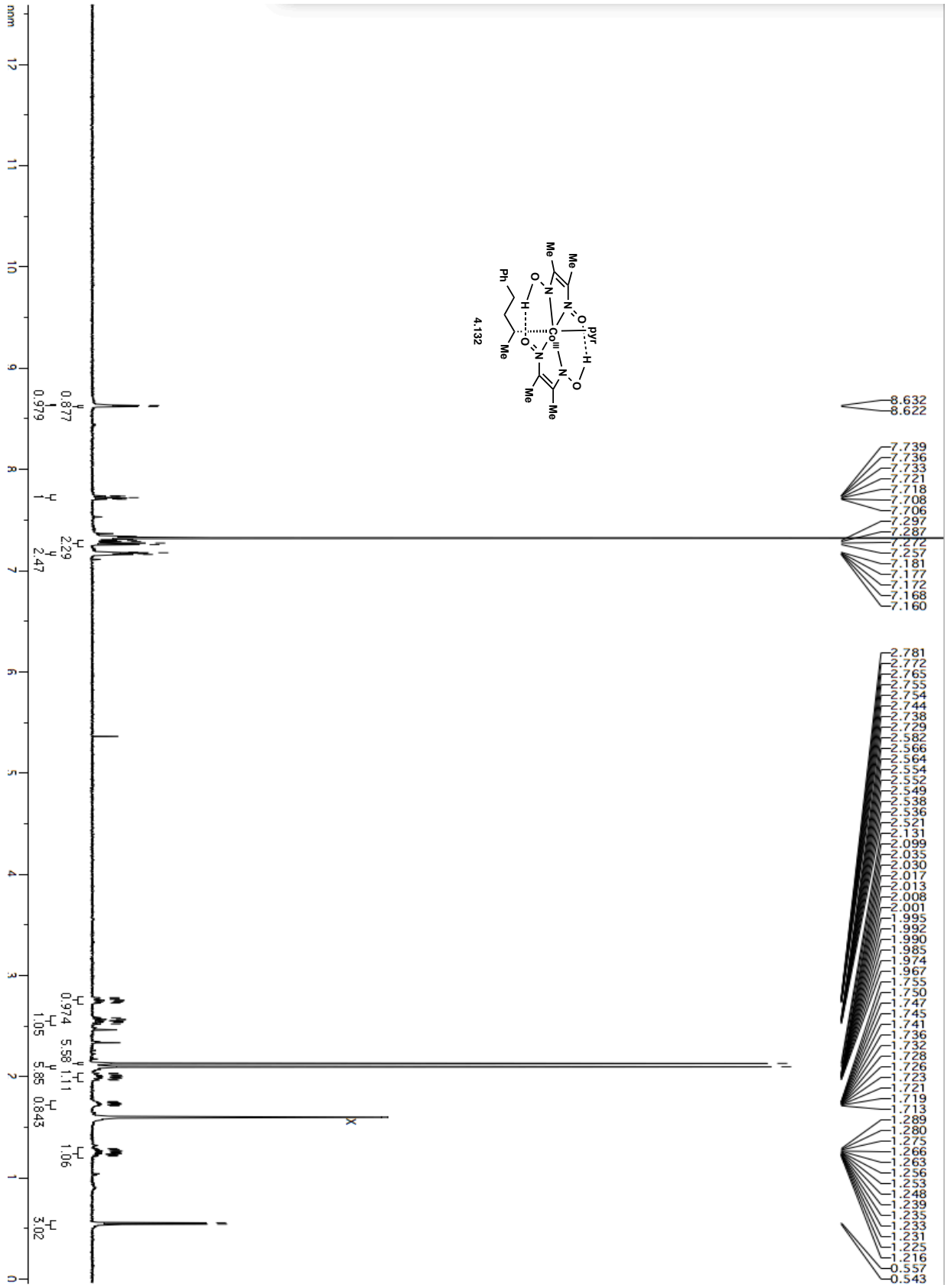
4.132
8.632
8.622
7.739
7.736
7.733
7.721
7.718
7.708
7.706
7.297
7.287
7.272
7.257
7.181
7.177
7.172
7.168
7.160
2.781
2.772
2.765
2.755
2.754
2.744
2.738
2.729
2.582
2.566
2.564
2.554
2.552
2.549
2.538
2.536
2.521
2.131
2.099
2.035
2.030
2.017
2.013
2.008
2.001
1.995
1.992
1.990
1.985
1.974
1.967
1.755
1.750
1.747
1.745
1.741
1.736
1.732
1.728
1.726
1.723
1.721
1.719
1.713
1.289
1.280
1.275
1.266
1.263
1.256
1.253
1.248
1.239
1.235
1.233
1.231
1.225
1.216
0.557
0.543
0.877
0.979
2.29
2.47
0.974
1.05
5.58
1.11
5.85
0.843
1.06
3.02

Appendix F: X-Ray Crystallographic Data for 2.13, 2.57, 2.108, and 3.113

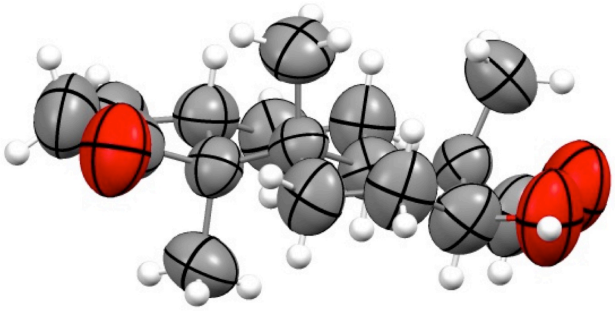

Table 1. Crystal data and structure refinement for **2.13**.

Identification code	svp1 (Sergey Pronin)	
Empirical formula	$C_{17}H_{26}O_3$	
Formula weight	278.38	
Temperature	203(2) K	
Wavelength	0.71073 Å	
Crystal system	Monoclinic	
Space group	$P2_1/n$	
Unit cell dimensions	a = 10.5923(6) Å	a= 90°.
	b = 11.5633(6) Å	b= 98.1413(7)°.
	c = 12.5018(7) Å	g = 90°.
Volume	1515.81(14) $Å^3$	
Z	4	
Density (calculated)	1.220 Mg/m^3	
Absorption coefficient	0.082 mm^{-1}	
F(000)	608	
Crystal color	colorless	
Crystal size	0.390 x 0.128 x 0.109 mm^3	
Theta range for data collection	2.361 to 26.404º	
Index ranges	$-13 \le h \le 13$, $-14 \le k \le 14$, $-15 \le l \le 15$	
Reflections collected	16391	
Independent reflections	3109 [R(int) = 0.0325]	
Completeness to theta = 25.500°	100.0 %	
Absorption correction	Semi-empirical from equivalents	
Max. and min. transmission	0.8620 and 0.8147	
Refinement method	Full-matrix least-squares on F^2	
Data / restraints / parameters	3109 / 0 / 285	
Goodness-of-fit on F^2	1.037	

Final R indices [I>2sigma(I) = 2270 data]	R1 = 0.0424, wR2 = 0.1065
R indices (all data, 0.80Å)	R1 = 0.0632, wR2 = 0.1193
Largest diff. peak and hole	0.261 and -0.135 e.Å^{-3}

Table 2. Atomic coordinates (x 10^4) and equivalent isotropic displacement parameters ($Å^2$ x 10^3) for **2.13**. U(eq) is defined as one third of the trace of the orthogonalized U^{ij} tensor.

	x	y	z	U(eq)
O(1)	7471(1)	3160(1)	7491(1)	56(1)
O(2)	6806(1)	360(1)	6569(1)	60(1)
O(3)	1140(1)	4891(1)	6491(1)	57(1)
C(1)	3420(1)	3239(1)	6297(1)	31(1)
C(2)	4024(2)	4108(1)	7144(2)	41(1)
C(3)	5458(2)	4243(1)	7176(2)	45(1)
C(4)	6118(2)	3084(1)	7393(1)	40(1)
C(5)	5660(1)	2178(1)	6520(1)	34(1)
C(6)	4180(1)	2071(1)	6442(1)	30(1)
C(7)	3623(2)	1127(1)	5650(1)	40(1)
C(8)	2213(2)	898(1)	5706(2)	44(1)
C(9)	1481(2)	2023(1)	5584(1)	39(1)
C(10)	37(2)	2053(2)	5581(2)	52(1)
C(11)	-229(2)	3346(2)	5699(2)	58(1)
C(12)	1007(2)	3883(1)	6232(1)	43(1)
C(13)	2018(1)	2931(1)	6435(1)	35(1)
C(14)	3433(2)	3791(2)	5171(1)	42(1)
C(15)	6172(2)	1034(1)	6993(2)	44(1)
C(16)	6176(2)	2401(2)	5454(2)	45(1)
C(17)	1853(2)	2536(2)	7597(1)	44(1)

Table 3. Bond lengths [Å] and angles [º] for **2.13**.

O(1)-C(4)	1.4239(19)
O(2)-C(15)	1.200(2)
O(3)-C(12)	1.212(2)
C(1)-C(2)	1.533(2)
C(1)-C(14)	1.547(2)
C(1)-C(13)	1.560(2)
C(1)-C(6)	1.5697(19)
C(2)-C(3)	1.521(2)
C(3)-C(4)	1.517(2)
C(4)-C(5)	1.541(2)
C(5)-C(15)	1.518(2)
C(5)-C(16)	1.533(2)
C(5)-C(6)	1.561(2)
C(6)-C(7)	1.535(2)
C(7)-C(8)	1.528(2)
C(8)-C(9)	1.511(2)
C(9)-C(10)	1.529(2)
C(9)-C(13)	1.545(2)
C(10)-C(11)	1.533(3)
C(11)-C(12)	1.516(3)
C(12)-C(13)	1.532(2)
C(13)-C(17)	1.556(2)
C(2)-C(1)-C(14)	107.57(13)
C(2)-C(1)-C(13)	112.58(12)
C(14)-C(1)-C(13)	109.02(12)
C(2)-C(1)-C(6)	109.07(12)
C(14)-C(1)-C(6)	112.92(12)
C(13)-C(1)-C(6)	105.78(11)
C(3)-C(2)-C(1)	113.74(13)
C(4)-C(3)-C(2)	110.31(13)
O(1)-C(4)-C(3)	113.21(14)
O(1)-C(4)-C(5)	108.32(13)
C(3)-C(4)-C(5)	112.52(13)

C(15)-C(5)-C(16)	109.50(13)
C(15)-C(5)-C(4)	104.92(12)
C(16)-C(5)-C(4)	112.71(13)
C(15)-C(5)-C(6)	104.81(12)
C(16)-C(5)-C(6)	115.97(13)
C(4)-C(5)-C(6)	108.08(11)
C(7)-C(6)-C(5)	112.81(11)
C(7)-C(6)-C(1)	113.15(12)
C(5)-C(6)-C(1)	115.67(11)
C(8)-C(7)-C(6)	112.52(13)
C(9)-C(8)-C(7)	109.71(13)
C(8)-C(9)-C(10)	121.20(14)
C(8)-C(9)-C(13)	112.49(13)
C(10)-C(9)-C(13)	104.90(13)
C(9)-C(10)-C(11)	102.67(14)
C(12)-C(11)-C(10)	106.42(15)
O(3)-C(12)-C(11)	124.86(15)
O(3)-C(12)-C(13)	126.51(15)
C(11)-C(12)-C(13)	108.56(14)
C(12)-C(13)-C(9)	101.20(12)
C(12)-C(13)-C(17)	101.36(12)
C(9)-C(13)-C(17)	111.34(13)
C(12)-C(13)-C(1)	118.16(12)
C(9)-C(13)-C(1)	110.02(12)
C(17)-C(13)-C(1)	113.88(13)
O(2)-C(15)-C(5)	125.83(17)

Table 4. Anisotropic displacement parameters ($Å^2 x\ 10^3$) for **2.13**. The anisotropic displacement factor exponent takes the form: $-2p^2[h^2\ a^{*2}U^{11} + ...\ + 2\ h\ k\ a^*\ b^*\ U^{12}]$

	U^{11}	U^{22}	U^{33}	U^{23}	U^{13}	U^{12}
O(1)	39(1)	53(1)	74(1)	-17(1)	-3(1)	-2(1)
O(2)	61(1)	45(1)	73(1)	-10(1)	2(1)	21(1)
O(3)	54(1)	37(1)	80(1)	-3(1)	8(1)	12(1)
C(1)	36(1)	23(1)	35(1)	0(1)	6(1)	0(1)
C(2)	45(1)	27(1)	51(1)	-9(1)	5(1)	4(1)
C(3)	47(1)	31(1)	55(1)	-12(1)	0(1)	-5(1)
C(4)	38(1)	37(1)	44(1)	-7(1)	1(1)	-1(1)
C(5)	37(1)	28(1)	38(1)	-3(1)	5(1)	1(1)
C(6)	38(1)	23(1)	31(1)	-1(1)	6(1)	0(1)
C(7)	45(1)	28(1)	48(1)	-8(1)	7(1)	-1(1)
C(8)	49(1)	32(1)	51(1)	-8(1)	8(1)	-10(1)
C(9)	40(1)	38(1)	40(1)	-1(1)	5(1)	-7(1)
C(10)	41(1)	55(1)	59(1)	0(1)	5(1)	-9(1)
C(11)	40(1)	58(1)	74(1)	5(1)	5(1)	4(1)
C(12)	43(1)	42(1)	47(1)	6(1)	10(1)	6(1)
C(13)	38(1)	28(1)	38(1)	1(1)	7(1)	1(1)
C(14)	44(1)	38(1)	45(1)	12(1)	7(1)	-2(1)
C(15)	41(1)	36(1)	54(1)	-2(1)	1(1)	5(1)
C(16)	44(1)	48(1)	46(1)	-3(1)	13(1)	-2(1)
C(17)	49(1)	46(1)	40(1)	4(1)	15(1)	2(1)

Table 5. Hydrogen coordinates (x 10^4) and isotropic displacement parameters ($Å^2$ x 10^3) for **2.13**.

	x	y	z	U(eq)
H(1)	7690(20)	3780(20)	7767(19)	83(8)
H(2A)	3597(17)	4850(16)	6999(14)	51(5)
H(2B)	3879(16)	3823(15)	7878(15)	48(5)
H(3A)	5682(17)	4578(15)	6511(15)	50(5)
H(3B)	5797(17)	4766(16)	7784(15)	55(5)
H(4A)	5855(15)	2772(15)	8095(14)	45(4)
H(6A)	4047(14)	1804(13)	7189(12)	33(4)
H(7A)	3719(16)	1358(15)	4885(15)	49(5)
H(7B)	4130(15)	403(14)	5840(13)	40(4)
H(8A)	1892(17)	338(16)	5133(15)	55(5)
H(8B)	2134(17)	510(15)	6393(15)	50(5)
H(9A)	1611(15)	2349(14)	4866(14)	42(4)
H(10A)	-216(18)	1621(16)	6211(16)	60(5)
H(10B)	-421(19)	1703(17)	4912(17)	65(6)
H(11A)	-450(20)	3670(20)	4980(20)	91(8)
H(11B)	-900(20)	3522(18)	6116(16)	66(6)
H(14A)	4266(19)	4165(16)	5119(15)	57(5)
H(14B)	2728(19)	4355(16)	4999(15)	56(5)
H(14C)	3301(16)	3206(16)	4556(15)	54(5)
H(15A)	5947(15)	895(14)	7778(14)	44(4)
H(16A)	5992(19)	3163(19)	5192(16)	68(6)
H(16B)	5734(19)	1877(18)	4870(17)	68(6)
H(16C)	7080(20)	2247(18)	5536(17)	75(6)
H(17A)	2102(18)	3183(16)	8134(16)	61(5)
H(17B)	2407(16)	1881(15)	7836(13)	46(5)
H(17C)	940(20)	2351(16)	7618(16)	62(6)

Table 6. Torsion angles [º] for **2.13**.

C(14)-C(1)-C(2)-C(3)	-71.46(17)
C(13)-C(1)-C(2)-C(3)	168.42(14)
C(6)-C(1)-C(2)-C(3)	51.33(18)
C(1)-C(2)-C(3)-C(4)	-57.7(2)
C(2)-C(3)-C(4)-O(1)	-176.82(14)
C(2)-C(3)-C(4)-C(5)	60.0(2)
O(1)-C(4)-C(5)-C(15)	66.81(16)
C(3)-C(4)-C(5)-C(15)	-167.27(14)
O(1)-C(4)-C(5)-C(16)	-52.27(17)
C(3)-C(4)-C(5)-C(16)	73.65(18)
O(1)-C(4)-C(5)-C(6)	178.23(12)
C(3)-C(4)-C(5)-C(6)	-55.85(17)
C(15)-C(5)-C(6)-C(7)	-64.46(16)
C(16)-C(5)-C(6)-C(7)	56.39(17)
C(4)-C(5)-C(6)-C(7)	-175.96(13)
C(15)-C(5)-C(6)-C(1)	163.06(12)
C(16)-C(5)-C(6)-C(1)	-76.09(16)
C(4)-C(5)-C(6)-C(1)	51.56(16)
C(2)-C(1)-C(6)-C(7)	178.22(13)
C(14)-C(1)-C(6)-C(7)	-62.25(17)
C(13)-C(1)-C(6)-C(7)	56.90(15)
C(2)-C(1)-C(6)-C(5)	-49.45(16)
C(14)-C(1)-C(6)-C(5)	70.08(16)
C(13)-C(1)-C(6)-C(5)	-170.77(11)
C(5)-C(6)-C(7)-C(8)	171.15(13)
C(1)-C(6)-C(7)-C(8)	-55.15(18)
C(6)-C(7)-C(8)-C(9)	52.30(19)
C(7)-C(8)-C(9)-C(10)	178.49(15)
C(7)-C(8)-C(9)-C(13)	-56.33(18)
C(8)-C(9)-C(10)-C(11)	167.77(17)
C(13)-C(9)-C(10)-C(11)	39.17(19)
C(9)-C(10)-C(11)-C(12)	-24.0(2)
C(10)-C(11)-C(12)-O(3)	-176.96(18)
C(10)-C(11)-C(12)-C(13)	0.2(2)

O(3)-C(12)-C(13)-C(9)	-159.64(17)
C(11)-C(12)-C(13)-C(9)	23.29(18)
O(3)-C(12)-C(13)-C(17)	85.6(2)
C(11)-C(12)-C(13)-C(17)	-91.43(17)
O(3)-C(12)-C(13)-C(1)	-39.5(2)
C(11)-C(12)-C(13)-C(1)	143.41(15)
C(8)-C(9)-C(13)-C(12)	-172.15(13)
C(10)-C(9)-C(13)-C(12)	-38.49(16)
C(8)-C(9)-C(13)-C(17)	-65.11(17)
C(10)-C(9)-C(13)-C(17)	68.54(17)
C(8)-C(9)-C(13)-C(1)	62.11(16)
C(10)-C(9)-C(13)-C(1)	-164.24(13)
C(2)-C(1)-C(13)-C(12)	66.51(17)
C(14)-C(1)-C(13)-C(12)	-52.76(17)
C(6)-C(1)-C(13)-C(12)	-174.46(13)
C(2)-C(1)-C(13)-C(9)	-178.05(12)
C(14)-C(1)-C(13)-C(9)	62.68(15)
C(6)-C(1)-C(13)-C(9)	-59.02(14)
C(2)-C(1)-C(13)-C(17)	-52.25(17)
C(14)-C(1)-C(13)-C(17)	-171.53(13)
C(6)-C(1)-C(13)-C(17)	66.77(15)
C(16)-C(5)-C(15)-O(2)	-5.1(2)
C(4)-C(5)-C(15)-O(2)	-126.36(18)
C(6)-C(5)-C(15)-O(2)	119.89(18)

Table 7. Hydrogen bonds for **2.13** [Å and º].

D-H...A	d(D-H)	d(H...A)	d(D...A)	<(DHA)
O(1)-H(1)...O(2)#1	0.81(3)	2.05(3)	2.8613(18)	178(3)
C(3)-H(3B)...O(2)#1	1.00(2)	2.643(19)	3.353(2)	128.1(13)
C(11)-H(11A)...O(3)#2	0.97(3)	2.51(3)	3.439(3)	160.1(19)
C(11)-H(11B)...O(1)#3	0.96(2)	2.64(2)	3.542(3)	157.4(17)

Symmetry transformations used to generate equivalent atoms:
#1 -x+3/2,y+1/2,-z+3/2 #2 -x,-y+1,-z+1 #3 x-1,y,z

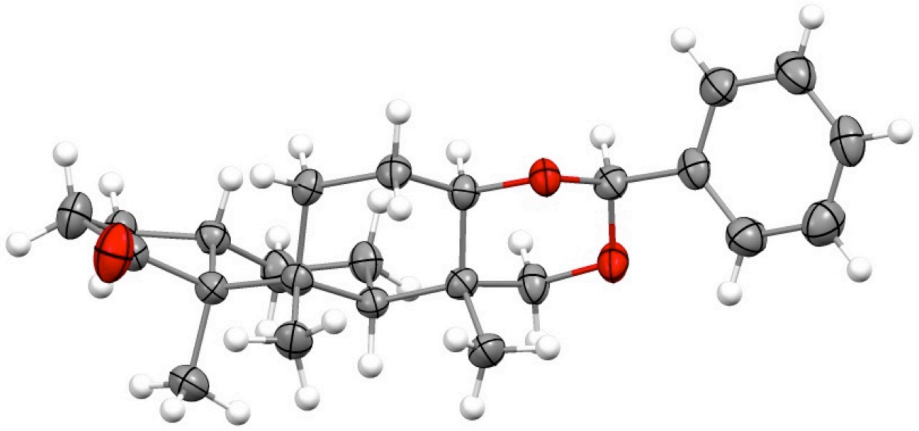

Table 1. Crystal data and structure refinement for **2.57**.

Identification code	svp2 (Eric Kuenstner)	
Empirical formula	$C_{24}H_{32}O_3$	
Formula weight	368.49	
Temperature	88(2) K	
Wavelength	0.71073 Å	
Crystal system	Orthorhombic	
Space group	*Pbca*	
Unit cell dimensions	a = 10.0498(4) Å	a= 90°.
	b = 12.6817(5) Å	b= 90°.
	c = 30.2790(13) Å	g = 90°.
Volume	3859.0(3) $Å^3$	
Z	8	
Density (calculated)	1.269 Mg/m^3	
Absorption coefficient	0.082 mm^{-1}	
F(000)	1600	
Crystal color	colorless	
Crystal size	0.450 x 0.426 x 0.426 mm^3	
Theta range for data collection	2.432 to 29.217º	
Index ranges	$-13 \le h \le 13$, $-17 \le k \le 17$, $-39 \le l \le 40$	
Reflections collected	45527	
Independent reflections	5028 [R(int) = 0.0217]	
Completeness to theta = 25.500°	100.0 %	
Absorption correction	Semi-empirical from equivalents	
Max. and min. transmission	0.8622 and 0.8371	
Refinement method	Full-matrix least-squares on F^2	

Data / restraints / parameters	5028 / 0 / 372
Goodness-of-fit on F^2	1.021
Final R indices [I>2sigma(I) = 4595 data]	R1 = 0.0372, wR2 = 0.0985
R indices (all data, 0.73Å)	R1 = 0.0401, wR2 = 0.1013
Largest diff. peak and hole	0.415 and -0.270 e.$Å^{-3}$

Table 2. Atomic coordinates (x 10^4) and equivalent isotropic displacement parameters ($Å^2$ x 10^3) for **2.57**. U(eq) is defined as one third of the trace of the orthogonalized U^{ij} tensor.

	x	y	z	U(eq)
O(1)	9444(1)	6718(1)	2923(1)	22(1)
O(2)	5845(1)	6654(1)	5314(1)	14(1)
O(3)	8082(1)	6261(1)	5153(1)	11(1)
C(1)	8365(1)	6289(1)	2941(1)	13(1)
C(2)	7908(1)	5429(1)	2620(1)	17(1)
C(3)	6472(1)	5160(1)	2754(1)	15(1)
C(4)	6444(1)	5479(1)	3242(1)	11(1)
C(5)	5130(1)	5558(1)	3483(1)	14(1)
C(6)	5427(1)	5795(1)	3970(1)	13(1)
C(7)	6334(1)	6768(1)	4053(1)	10(1)
C(8)	6663(1)	6889(1)	4558(1)	10(1)
C(9)	5476(1)	6577(1)	4854(1)	13(1)
C(10)	6961(1)	6023(1)	5420(1)	12(1)
C(11)	7764(1)	6106(1)	4693(1)	10(1)
C(12)	9024(1)	6179(1)	4422(1)	12(1)
C(13)	8686(1)	6011(1)	3931(1)	11(1)
C(14)	7631(1)	6800(1)	3756(1)	10(1)
C(15)	7232(1)	6518(1)	3269(1)	11(1)
C(16)	6453(1)	7434(1)	3044(1)	16(1)
C(17)	7012(1)	8039(1)	4683(1)	14(1)
C(18)	8267(1)	7910(1)	3752(1)	14(1)
C(19)	7332(1)	6223(1)	5896(1)	12(1)
C(20)	8094(1)	5479(1)	6122(1)	16(1)
C(21)	8449(1)	5649(1)	6561(1)	19(1)
C(22)	8030(1)	6558(1)	6778(1)	18(1)
C(23)	7270(1)	7300(1)	6554(1)	19(1)
C(24)	6929(1)	7135(1)	6112(1)	17(1)

Table 3. Bond lengths [Å] and angles [º] for **2.57**.

O(1)-C(1)	1.2138(12)
O(2)-C(10)	1.4142(10)
O(2)-C(9)	1.4438(10)
O(3)-C(10)	1.4191(10)
O(3)-C(11)	1.4430(10)
C(1)-C(2)	1.5310(13)
C(1)-C(15)	1.5383(12)
C(2)-C(3)	1.5368(13)
C(3)-C(4)	1.5334(12)
C(4)-C(5)	1.5119(12)
C(4)-C(15)	1.5406(12)
C(5)-C(6)	1.5335(12)
C(6)-C(7)	1.5548(12)
C(7)-C(8)	1.5713(11)
C(7)-C(14)	1.5855(12)
C(8)-C(11)	1.5416(12)
C(8)-C(9)	1.5436(12)
C(8)-C(17)	1.5477(12)
C(10)-C(19)	1.5103(12)
C(11)-C(12)	1.5122(12)
C(12)-C(13)	1.5373(12)
C(13)-C(14)	1.5510(12)
C(14)-C(18)	1.5464(12)
C(14)-C(15)	1.5674(11)
C(15)-C(16)	1.5571(12)
C(19)-C(24)	1.3902(13)
C(19)-C(20)	1.3950(13)
C(20)-C(21)	1.3945(13)
C(21)-C(22)	1.3909(14)
C(22)-C(23)	1.3887(14)
C(23)-C(24)	1.3956(13)
C(10)-O(2)-C(9)	112.59(6)
C(10)-O(3)-C(11)	110.16(6)

O(1)-C(1)-C(2)	123.91(8)
O(1)-C(1)-C(15)	127.28(8)
C(2)-C(1)-C(15)	108.79(7)
C(1)-C(2)-C(3)	105.83(7)
C(4)-C(3)-C(2)	102.29(7)
C(5)-C(4)-C(3)	119.97(7)
C(5)-C(4)-C(15)	111.49(7)
C(3)-C(4)-C(15)	105.45(7)
C(4)-C(5)-C(6)	107.91(7)
C(5)-C(6)-C(7)	115.14(7)
C(6)-C(7)-C(8)	111.00(7)
C(6)-C(7)-C(14)	114.26(7)
C(8)-C(7)-C(14)	112.22(7)
C(11)-C(8)-C(9)	103.67(7)
C(11)-C(8)-C(17)	112.30(7)
C(9)-C(8)-C(17)	105.92(7)
C(11)-C(8)-C(7)	110.19(7)
C(9)-C(8)-C(7)	112.19(7)
C(17)-C(8)-C(7)	112.22(7)
O(2)-C(9)-C(8)	110.12(7)
O(2)-C(10)-O(3)	112.33(7)
O(2)-C(10)-C(19)	108.47(7)
O(3)-C(10)-C(19)	108.14(7)
O(3)-C(11)-C(12)	109.32(7)
O(3)-C(11)-C(8)	109.08(7)
C(12)-C(11)-C(8)	114.74(7)
C(11)-C(12)-C(13)	109.31(7)
C(12)-C(13)-C(14)	113.19(7)
C(18)-C(14)-C(13)	107.92(7)
C(18)-C(14)-C(15)	107.80(7)
C(13)-C(14)-C(15)	110.52(7)
C(18)-C(14)-C(7)	111.57(7)
C(13)-C(14)-C(7)	110.46(7)
C(15)-C(14)-C(7)	108.54(7)
C(1)-C(15)-C(4)	100.66(7)
C(1)-C(15)-C(16)	103.33(7)

C(4)-C(15)-C(16)	110.90(7)
C(1)-C(15)-C(14)	117.38(7)
C(4)-C(15)-C(14)	112.10(7)
C(16)-C(15)-C(14)	111.70(7)
C(24)-C(19)-C(20)	119.41(8)
C(24)-C(19)-C(10)	121.22(8)
C(20)-C(19)-C(10)	119.37(8)
C(21)-C(20)-C(19)	120.30(9)
C(22)-C(21)-C(20)	119.97(9)
C(23)-C(22)-C(21)	119.94(9)
C(22)-C(23)-C(24)	120.02(9)
C(19)-C(24)-C(23)	120.35(9)

Table 4. Anisotropic displacement parameters ($Å^2 x\ 10^3$) for **2.57**. The anisotropic displacement factor exponent takes the form: $-2p^2[h^2\ a^{*2}U^{11} + ...\ + 2\ h\ k\ a^*\ b^*\ U^{12}]$

	U^{11}	U^{22}	U^{33}	U^{23}	U^{13}	U^{12}
O(1)	18(1)	29(1)	19(1)	-6(1)	6(1)	-7(1)
O(2)	11(1)	21(1)	9(1)	-1(1)	0(1)	4(1)
O(3)	10(1)	16(1)	8(1)	0(1)	1(1)	0(1)
C(1)	15(1)	15(1)	10(1)	1(1)	1(1)	1(1)
C(2)	17(1)	21(1)	12(1)	-4(1)	2(1)	-1(1)
C(3)	15(1)	18(1)	11(1)	-2(1)	0(1)	-1(1)
C(4)	12(1)	12(1)	10(1)	0(1)	0(1)	-1(1)
C(5)	12(1)	18(1)	11(1)	-1(1)	-1(1)	-3(1)
C(6)	12(1)	16(1)	10(1)	0(1)	1(1)	-3(1)
C(7)	10(1)	11(1)	10(1)	0(1)	1(1)	0(1)
C(8)	10(1)	10(1)	10(1)	0(1)	0(1)	1(1)
C(9)	10(1)	19(1)	9(1)	0(1)	0(1)	1(1)
C(10)	10(1)	14(1)	11(1)	1(1)	1(1)	0(1)
C(11)	10(1)	11(1)	9(1)	-1(1)	0(1)	0(1)
C(12)	9(1)	15(1)	11(1)	-1(1)	1(1)	1(1)
C(13)	11(1)	13(1)	10(1)	-1(1)	1(1)	1(1)
C(14)	11(1)	9(1)	9(1)	0(1)	1(1)	0(1)
C(15)	12(1)	11(1)	9(1)	1(1)	1(1)	1(1)
C(16)	19(1)	14(1)	14(1)	3(1)	-1(1)	3(1)
C(17)	18(1)	11(1)	14(1)	-2(1)	0(1)	1(1)
C(18)	18(1)	10(1)	15(1)	1(1)	2(1)	-3(1)
C(19)	10(1)	16(1)	10(1)	1(1)	1(1)	-1(1)
C(20)	16(1)	19(1)	14(1)	1(1)	1(1)	4(1)
C(21)	18(1)	24(1)	14(1)	4(1)	-1(1)	4(1)
C(22)	16(1)	26(1)	11(1)	1(1)	-1(1)	-2(1)
C(23)	21(1)	21(1)	16(1)	-4(1)	-3(1)	2(1)
C(24)	18(1)	17(1)	15(1)	-1(1)	-4(1)	3(1)

Table 5. Hydrogen coordinates (x 10^4) and isotropic displacement parameters ($Å^2$ x 10^3) for **2.57**.

	x	y	z	U(eq)
H(2A)	8516(15)	4806(11)	2667(5)	29(4)
H(2B)	8030(14)	5674(12)	2313(5)	29(4)
H(3A)	5828(13)	5572(10)	2581(4)	19(3)
H(3B)	6263(13)	4410(11)	2715(4)	20(3)
H(4A)	6990(12)	4929(10)	3397(4)	14(3)
H(5A)	4629(13)	4909(11)	3461(4)	20(3)
H(5B)	4564(13)	6112(10)	3350(4)	18(3)
H(6A)	5838(13)	5144(10)	4109(4)	17(3)
H(6B)	4578(13)	5919(10)	4128(4)	19(3)
H(7A)	5781(12)	7394(10)	3972(4)	12(3)
H(9A)	4723(12)	7060(10)	4813(4)	14(3)
H(9B)	5196(12)	5833(10)	4798(4)	13(3)
H(10A)	6730(12)	5258(10)	5372(4)	13(3)
H(11A)	7386(12)	5376(10)	4662(4)	12(3)
H(12A)	9650(13)	5624(10)	4525(4)	16(3)
H(12B)	9472(13)	6856(10)	4471(4)	17(3)
H(13A)	8388(12)	5270(10)	3892(4)	13(3)
H(13B)	9524(13)	6095(10)	3755(4)	16(3)
H(16A)	5720(13)	7683(11)	3237(5)	25(3)
H(16B)	6064(13)	7239(11)	2764(4)	21(3)
H(16C)	7049(14)	8044(11)	2986(5)	26(3)
H(17A)	7921(13)	8238(10)	4606(4)	18(3)
H(17B)	6931(13)	8147(11)	5003(4)	20(3)
H(17C)	6406(14)	8510(12)	4540(5)	29(4)
H(18A)	7565(14)	8454(11)	3750(4)	21(3)
H(18B)	8834(13)	7997(10)	3485(4)	19(3)
H(18C)	8834(13)	8048(11)	4015(4)	20(3)
H(20A)	8344(13)	4842(11)	5968(4)	23(3)
H(21A)	8969(15)	5111(12)	6716(5)	29(4)
H(22A)	8291(14)	6683(12)	7082(5)	27(4)

H(23A)	6968(14)	7946(12)	6710(5)	30(4)
H(24A)	6395(14)	7645(11)	5959(5)	26(3)

Table 6. Torsion angles [º] for **2.57**.

O(1)-C(1)-C(2)-C(3)	-177.37(9)
C(15)-C(1)-C(2)-C(3)	1.16(10)
C(1)-C(2)-C(3)-C(4)	-25.00(9)
C(2)-C(3)-C(4)-C(5)	167.28(8)
C(2)-C(3)-C(4)-C(15)	40.55(9)
C(3)-C(4)-C(5)-C(6)	175.22(8)
C(15)-C(4)-C(5)-C(6)	-60.90(9)
C(4)-C(5)-C(6)-C(7)	53.56(10)
C(5)-C(6)-C(7)-C(8)	-175.72(7)
C(5)-C(6)-C(7)-C(14)	-47.61(10)
C(6)-C(7)-C(8)-C(11)	78.79(8)
C(14)-C(7)-C(8)-C(11)	-50.42(9)
C(6)-C(7)-C(8)-C(9)	-36.16(9)
C(14)-C(7)-C(8)-C(9)	-165.37(7)
C(6)-C(7)-C(8)-C(17)	-155.27(7)
C(14)-C(7)-C(8)-C(17)	75.52(9)
C(10)-O(2)-C(9)-C(8)	-57.33(9)
C(11)-C(8)-C(9)-O(2)	58.44(8)
C(17)-C(8)-C(9)-O(2)	-59.95(9)
C(7)-C(8)-C(9)-O(2)	177.30(7)
C(9)-O(2)-C(10)-O(3)	56.12(9)
C(9)-O(2)-C(10)-C(19)	175.60(7)
C(11)-O(3)-C(10)-O(2)	-58.91(9)
C(11)-O(3)-C(10)-C(19)	-178.58(7)
C(10)-O(3)-C(11)-C(12)	-170.26(7)
C(10)-O(3)-C(11)-C(8)	63.54(8)
C(9)-C(8)-C(11)-O(3)	-61.93(8)
C(17)-C(8)-C(11)-O(3)	51.95(9)
C(7)-C(8)-C(11)-O(3)	177.84(6)
C(9)-C(8)-C(11)-C(12)	175.05(7)
C(17)-C(8)-C(11)-C(12)	-71.06(9)
C(7)-C(8)-C(11)-C(12)	54.83(9)
O(3)-C(11)-C(12)-C(13)	179.89(7)
C(8)-C(11)-C(12)-C(13)	-57.23(9)

C(11)-C(12)-C(13)-C(14)	56.68(9)
C(12)-C(13)-C(14)-C(18)	67.80(9)
C(12)-C(13)-C(14)-C(15)	-174.55(7)
C(12)-C(13)-C(14)-C(7)	-54.41(9)
C(6)-C(7)-C(14)-C(18)	163.42(7)
C(8)-C(7)-C(14)-C(18)	-69.09(9)
C(6)-C(7)-C(14)-C(13)	-76.55(9)
C(8)-C(7)-C(14)-C(13)	50.94(9)
C(6)-C(7)-C(14)-C(15)	44.77(9)
C(8)-C(7)-C(14)-C(15)	172.26(7)
O(1)-C(1)-C(15)-C(4)	-158.62(9)
C(2)-C(1)-C(15)-C(4)	22.91(9)
O(1)-C(1)-C(15)-C(16)	86.69(11)
C(2)-C(1)-C(15)-C(16)	-91.77(8)
O(1)-C(1)-C(15)-C(14)	-36.71(13)
C(2)-C(1)-C(15)-C(14)	144.82(8)
C(5)-C(4)-C(15)-C(1)	-170.83(7)
C(3)-C(4)-C(15)-C(1)	-39.08(8)
C(5)-C(4)-C(15)-C(16)	-61.98(9)
C(3)-C(4)-C(15)-C(16)	69.77(9)
C(5)-C(4)-C(15)-C(14)	63.62(9)
C(3)-C(4)-C(15)-C(14)	-164.63(7)
C(18)-C(14)-C(15)-C(1)	70.70(9)
C(13)-C(14)-C(15)-C(1)	-47.02(10)
C(7)-C(14)-C(15)-C(1)	-168.30(7)
C(18)-C(14)-C(15)-C(4)	-173.52(7)
C(13)-C(14)-C(15)-C(4)	68.76(9)
C(7)-C(14)-C(15)-C(4)	-52.52(9)
C(18)-C(14)-C(15)-C(16)	-48.35(9)
C(13)-C(14)-C(15)-C(16)	-166.07(7)
C(7)-C(14)-C(15)-C(16)	72.65(8)
O(2)-C(10)-C(19)-C(24)	-20.63(11)
O(3)-C(10)-C(19)-C(24)	101.44(9)
O(2)-C(10)-C(19)-C(20)	159.47(8)
O(3)-C(10)-C(19)-C(20)	-78.45(10)
C(24)-C(19)-C(20)-C(21)	0.02(14)

C(10)-C(19)-C(20)-C(21)	179.92(8)
C(19)-C(20)-C(21)-C(22)	0.70(15)
C(20)-C(21)-C(22)-C(23)	-0.65(15)
C(21)-C(22)-C(23)-C(24)	-0.11(15)
C(20)-C(19)-C(24)-C(23)	-0.79(14)
C(10)-C(19)-C(24)-C(23)	179.31(9)
C(22)-C(23)-C(24)-C(19)	0.84(15)

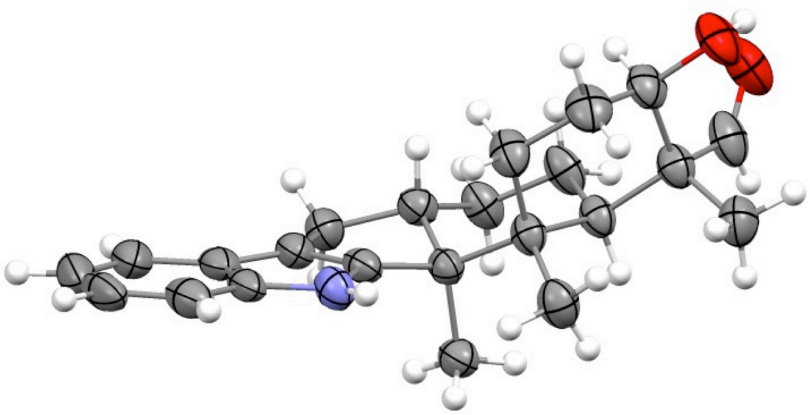

Table 1. Crystal data and structure refinement for **2.108**.

Identification code	svp3 (David George)	
Empirical formula	$C_{23}H_{29}NO_2$	
Formula weight	351.47	
Temperature	133(2) K	
Wavelength	0.71073 Å	
Crystal system	Monoclinic	
Space group	$P2_1/n$	
Unit cell dimensions	a = 15.3662(10) Å	a= 90º.
	b = 13.9849(9) Å	b= 97.3964(8)º.
	c = 17.6635(11) Å	g = 90º.
Volume	3764.2(4) $Å^3$	
Z	8	
Density (calculated)	1.240 Mg/m^3	
Absorption coefficient	0.078 mm^{-1}	
F(000)	1520	
Crystal color	colorless	
Crystal size	0.468 x 0.318 x 0.272 mm^3	
Theta range for data collection	1.654 to 28.761º	
Index ranges	$-20 \le h \le 19$, $-18 \le k \le 18$, $-23 \le l \le 23$	
Reflections collected	44454	
Independent reflections	9214 [R(int) = 0.0266]	
Completeness to theta = 25.500º	99.9 %	
Absorption correction	Semi-empirical from equivalents	
Max. and min. transmission	0.8621 and 0.8187	
Refinement method	Full-matrix least-squares on F^2	

Data / restraints / parameters	9214 / 0 / 490
Goodness-of-fit on F^2	1.032
Final R indices [I>2sigma(I) = 7854 data]	R1 = 0.0441, wR2 = 0.1102
R indices (all data, 0.74 Å)	R1 = 0.0526, wR2 = 0.1163
Largest diff. peak and hole	0.447 and -0.325 e.$Å^{-3}$

Table 2. Atomic coordinates (x 10^4) and equivalent isotropic displacement parameters ($Å^2$x 10^3) for **2.108**. U(eq) is defined as one third of the trace of the orthogonalized U^{ij} tensor.

	x	y	z	U(eq)
O(1)	4010(1)	5089(1)	-103(1)	31(1)
O(2)	3159(1)	6323(1)	846(1)	25(1)
N(1)	3749(1)	780(1)	2045(1)	15(1)
C(1)	3022(1)	2515(1)	2184(1)	13(1)
C(2)	3580(1)	1634(1)	2390(1)	14(1)
C(3)	4249(1)	222(1)	2586(1)	15(1)
C(4)	4605(1)	-684(1)	2505(1)	18(1)
C(5)	5072(1)	-1097(1)	3146(1)	20(1)
C(6)	5190(1)	-615(1)	3850(1)	20(1)
C(7)	4848(1)	292(1)	3927(1)	18(1)
C(8)	4368(1)	728(1)	3289(1)	15(1)
C(9)	3933(1)	1627(1)	3139(1)	14(1)
C(10)	3722(1)	2539(1)	3533(1)	16(1)
C(11)	3478(1)	3181(1)	2823(1)	14(1)
C(12)	2966(1)	4097(1)	2869(1)	16(1)
C(13)	2986(1)	4616(1)	2108(1)	17(1)
C(14)	2669(1)	4026(1)	1380(1)	14(1)
C(15)	2855(1)	4626(1)	660(1)	15(1)
C(16)	3821(1)	4533(1)	545(1)	18(1)
C(17)	4078(1)	3504(1)	438(1)	18(1)
C(18)	3971(1)	2935(1)	1159(1)	16(1)
C(19)	3030(1)	2970(1)	1375(1)	12(1)
C(20)	2073(1)	2277(1)	2333(1)	17(1)
C(21)	2648(1)	5668(1)	809(1)	20(1)
C(22)	2225(1)	4394(1)	-70(1)	21(1)
C(23)	2434(1)	2358(1)	794(1)	18(1)
O(3)	6053(1)	-220(1)	-484(1)	24(1)
O(4)	6788(1)	-1424(1)	691(1)	26(1)
N(2)	6294(1)	4200(1)	1674(1)	17(1)
C(24)	6907(1)	2426(1)	2013(1)	13(1)

C(25)	6392(1)	3347(1)	2065(1)	15(1)
C(26)	5833(1)	4818(1)	2094(1)	18(1)
C(27)	5531(1)	5741(1)	1916(1)	22(1)
C(28)	5092(1)	6209(1)	2447(1)	25(1)
C(29)	4962(1)	5774(1)	3137(1)	25(1)
C(30)	5244(1)	4850(1)	3307(1)	22(1)
C(31)	5679(1)	4348(1)	2776(1)	17(1)
C(32)	6035(1)	3406(1)	2732(1)	16(1)
C(33)	6170(1)	2493(1)	3182(1)	17(1)
C(34)	6389(1)	1811(1)	2544(1)	15(1)
C(35)	6842(1)	869(1)	2737(1)	17(1)
C(36)	6856(1)	329(1)	1984(1)	18(1)
C(37)	7262(1)	881(1)	1350(1)	14(1)
C(38)	7129(1)	265(1)	600(1)	16(1)
C(39)	6184(1)	357(1)	200(1)	18(1)
C(40)	5942(1)	1383(1)	6(1)	20(1)
C(41)	6020(1)	1971(1)	745(1)	18(1)
C(42)	6934(1)	1942(1)	1217(1)	13(1)
C(43)	7849(1)	2625(1)	2407(1)	16(1)
C(44)	7301(1)	-770(1)	831(1)	20(1)
C(45)	7819(1)	461(1)	54(1)	21(1)
C(46)	7573(1)	2521(1)	785(1)	19(1)

Table 3. Bond lengths [Å] and angles [º] for **2.108**.

O(1)-C(16)	1.4436(15)
O(2)-C(21)	1.2035(17)
N(1)-C(2)	1.3798(15)
N(1)-C(3)	1.3863(15)
C(1)-C(2)	1.5185(16)
C(1)-C(20)	1.5504(16)
C(1)-C(11)	1.5593(16)
C(1)-C(19)	1.5650(16)
C(2)-C(9)	1.3639(17)
C(3)-C(4)	1.3957(17)
C(3)-C(8)	1.4212(17)
C(4)-C(5)	1.3860(18)
C(5)-C(6)	1.4051(19)
C(6)-C(7)	1.3862(18)
C(7)-C(8)	1.4038(17)
C(8)-C(9)	1.4321(17)
C(9)-C(10)	1.5080(16)
C(10)-C(11)	1.5484(16)
C(11)-C(12)	1.5110(16)
C(12)-C(13)	1.5318(17)
C(13)-C(14)	1.5522(17)
C(14)-C(19)	1.5785(16)
C(14)-C(15)	1.5819(16)
C(15)-C(21)	1.5218(17)
C(15)-C(16)	1.5300(17)
C(15)-C(22)	1.5440(17)
C(16)-C(17)	1.5103(17)
C(17)-C(18)	1.5285(17)
C(18)-C(19)	1.5429(16)
C(19)-C(23)	1.5435(16)
O(3)-C(39)	1.4441(15)
O(4)-C(44)	1.2114(17)
N(2)-C(25)	1.3776(16)
N(2)-C(26)	1.3912(16)

C(24)-C(25)	1.5198(16)
C(24)-C(43)	1.5480(16)
C(24)-C(34)	1.5635(16)
C(24)-C(42)	1.5653(16)
C(25)-C(32)	1.3655(17)
C(26)-C(27)	1.3937(18)
C(26)-C(31)	1.4199(19)
C(27)-C(28)	1.387(2)
C(28)-C(29)	1.400(2)
C(29)-C(30)	1.383(2)
C(30)-C(31)	1.4071(18)
C(31)-C(32)	1.4319(17)
C(32)-C(33)	1.5037(17)
C(33)-C(34)	1.5466(16)
C(34)-C(35)	1.5085(17)
C(35)-C(36)	1.5313(17)
C(36)-C(37)	1.5554(17)
C(37)-C(38)	1.5721(16)
C(37)-C(42)	1.5740(16)
C(38)-C(44)	1.5180(17)
C(38)-C(39)	1.5361(17)
C(38)-C(45)	1.5469(17)
C(39)-C(40)	1.5100(18)
C(40)-C(41)	1.5345(17)
C(41)-C(42)	1.5399(17)
C(42)-C(46)	1.5472(17)

C(2)-N(1)-C(3)	107.61(10)
C(2)-C(1)-C(20)	107.39(9)
C(2)-C(1)-C(11)	97.09(9)
C(20)-C(1)-C(11)	110.51(10)
C(2)-C(1)-C(19)	118.54(10)
C(20)-C(1)-C(19)	111.17(9)
C(11)-C(1)-C(19)	111.25(9)
C(9)-C(2)-N(1)	110.33(11)
C(9)-C(2)-C(1)	112.40(10)

N(1)-C(2)-C(1)	136.77(11)
N(1)-C(3)-C(4)	129.14(12)
N(1)-C(3)-C(8)	108.63(10)
C(4)-C(3)-C(8)	122.23(11)
C(5)-C(4)-C(3)	117.61(12)
C(4)-C(5)-C(6)	121.18(12)
C(7)-C(6)-C(5)	121.19(12)
C(6)-C(7)-C(8)	119.08(12)
C(7)-C(8)-C(3)	118.71(11)
C(7)-C(8)-C(9)	135.62(12)
C(3)-C(8)-C(9)	105.67(10)
C(2)-C(9)-C(8)	107.72(11)
C(2)-C(9)-C(10)	110.99(10)
C(8)-C(9)-C(10)	141.26(11)
C(9)-C(10)-C(11)	99.29(9)
C(12)-C(11)-C(10)	121.42(10)
C(12)-C(11)-C(1)	110.89(10)
C(10)-C(11)-C(1)	106.18(9)
C(11)-C(12)-C(13)	106.55(10)
C(12)-C(13)-C(14)	115.79(10)
C(13)-C(14)-C(19)	115.44(10)
C(13)-C(14)-C(15)	108.29(9)
C(19)-C(14)-C(15)	113.02(9)
C(21)-C(15)-C(16)	109.49(10)
C(21)-C(15)-C(22)	102.93(10)
C(16)-C(15)-C(22)	112.72(10)
C(21)-C(15)-C(14)	107.71(10)
C(16)-C(15)-C(14)	109.95(10)
C(22)-C(15)-C(14)	113.66(10)
O(1)-C(16)-C(17)	109.36(11)
O(1)-C(16)-C(15)	110.90(10)
C(17)-C(16)-C(15)	111.80(10)
C(16)-C(17)-C(18)	109.48(10)
C(17)-C(18)-C(19)	113.25(10)
C(18)-C(19)-C(23)	108.23(10)
C(18)-C(19)-C(1)	109.36(9)

C(23)-C(19)-C(1)	107.91(9)
C(18)-C(19)-C(14)	111.89(9)
C(23)-C(19)-C(14)	110.10(9)
C(1)-C(19)-C(14)	109.27(9)
O(2)-C(21)-C(15)	126.00(12)
C(25)-N(2)-C(26)	107.53(11)
C(25)-C(24)-C(43)	106.55(9)
C(25)-C(24)-C(34)	96.97(9)
C(43)-C(24)-C(34)	110.36(10)
C(25)-C(24)-C(42)	119.66(10)
C(43)-C(24)-C(42)	110.42(9)
C(34)-C(24)-C(42)	112.01(9)
C(32)-C(25)-N(2)	110.48(11)
C(32)-C(25)-C(24)	111.94(11)
N(2)-C(25)-C(24)	136.71(11)
N(2)-C(26)-C(27)	129.29(13)
N(2)-C(26)-C(31)	108.49(11)
C(27)-C(26)-C(31)	122.21(12)
C(28)-C(27)-C(26)	117.48(13)
C(27)-C(28)-C(29)	121.33(13)
C(30)-C(29)-C(28)	121.26(13)
C(29)-C(30)-C(31)	118.97(13)
C(30)-C(31)-C(26)	118.66(12)
C(30)-C(31)-C(32)	135.49(13)
C(26)-C(31)-C(32)	105.85(11)
C(25)-C(32)-C(31)	107.58(11)
C(25)-C(32)-C(33)	111.13(11)
C(31)-C(32)-C(33)	141.25(12)
C(32)-C(33)-C(34)	99.66(9)
C(35)-C(34)-C(33)	120.77(10)
C(35)-C(34)-C(24)	111.12(10)
C(33)-C(34)-C(24)	105.80(9)
C(34)-C(35)-C(36)	106.93(10)
C(35)-C(36)-C(37)	115.63(10)
C(36)-C(37)-C(38)	108.34(9)
C(36)-C(37)-C(42)	115.12(10)

C(38)-C(37)-C(42)	112.80(9)
C(44)-C(38)-C(39)	108.96(10)
C(44)-C(38)-C(45)	103.18(10)
C(39)-C(38)-C(45)	112.45(10)
C(44)-C(38)-C(37)	107.29(10)
C(39)-C(38)-C(37)	110.70(10)
C(45)-C(38)-C(37)	113.79(10)
O(3)-C(39)-C(40)	109.69(10)
O(3)-C(39)-C(38)	111.05(10)
C(40)-C(39)-C(38)	112.04(10)
C(39)-C(40)-C(41)	109.03(10)
C(40)-C(41)-C(42)	114.41(10)
C(41)-C(42)-C(46)	108.12(10)
C(41)-C(42)-C(24)	110.32(9)
C(46)-C(42)-C(24)	108.02(10)
C(41)-C(42)-C(37)	110.91(10)
C(46)-C(42)-C(37)	110.80(10)
C(24)-C(42)-C(37)	108.63(9)
O(4)-C(44)-C(38)	125.35(12)

Table 4. Anisotropic displacement parameters ($Å^2 x\ 10^3$) for **2.109**. The anisotropic displacement factor exponent takes the form: $-2p^2[h^2a^{*2}U^{11} + ... + 2\ h\ k\ a^*b^*U^{12}]$

	U^{11}	U^{22}	U^{33}	U^{23}	U^{13}	U^{12}
O(1)	28(1)	28(1)	39(1)	19(1)	18(1)	8(1)
O(2)	36(1)	17(1)	25(1)	0(1)	9(1)	-2(1)
N(1)	18(1)	12(1)	14(1)	-1(1)	0(1)	1(1)
C(1)	13(1)	11(1)	14(1)	0(1)	2(1)	-1(1)
C(2)	14(1)	11(1)	16(1)	0(1)	3(1)	-2(1)
C(3)	14(1)	14(1)	17(1)	2(1)	2(1)	-1(1)
C(4)	18(1)	14(1)	22(1)	-1(1)	4(1)	0(1)
C(5)	17(1)	15(1)	28(1)	2(1)	3(1)	2(1)
C(6)	17(1)	20(1)	22(1)	6(1)	0(1)	2(1)
C(7)	18(1)	20(1)	16(1)	1(1)	1(1)	0(1)
C(8)	14(1)	15(1)	17(1)	1(1)	3(1)	-1(1)
C(9)	15(1)	13(1)	15(1)	0(1)	2(1)	-1(1)
C(10)	20(1)	14(1)	13(1)	0(1)	2(1)	1(1)
C(11)	16(1)	13(1)	13(1)	-1(1)	2(1)	0(1)
C(12)	21(1)	14(1)	15(1)	-2(1)	4(1)	1(1)
C(13)	22(1)	12(1)	17(1)	-2(1)	4(1)	1(1)
C(14)	15(1)	12(1)	16(1)	0(1)	3(1)	1(1)
C(15)	16(1)	14(1)	16(1)	2(1)	3(1)	2(1)
C(16)	15(1)	18(1)	19(1)	5(1)	3(1)	0(1)
C(17)	16(1)	20(1)	18(1)	4(1)	6(1)	4(1)
C(18)	15(1)	16(1)	16(1)	2(1)	3(1)	3(1)
C(19)	13(1)	11(1)	13(1)	0(1)	2(1)	1(1)
C(20)	15(1)	17(1)	21(1)	3(1)	4(1)	-1(1)
C(21)	24(1)	18(1)	18(1)	4(1)	4(1)	5(1)
C(22)	18(1)	24(1)	19(1)	4(1)	0(1)	2(1)
C(23)	21(1)	17(1)	17(1)	-2(1)	-1(1)	-2(1)
O(3)	30(1)	24(1)	16(1)	-7(1)	-1(1)	-1(1)
O(4)	41(1)	16(1)	21(1)	-3(1)	4(1)	-2(1)
N(2)	19(1)	12(1)	19(1)	-1(1)	2(1)	2(1)
C(24)	13(1)	11(1)	15(1)	-1(1)	1(1)	1(1)
C(25)	14(1)	12(1)	18(1)	-2(1)	0(1)	-1(1)

C(26)	13(1)	14(1)	25(1)	-6(1)	-2(1)	0(1)
C(27)	18(1)	16(1)	31(1)	-3(1)	-4(1)	0(1)
C(28)	17(1)	15(1)	42(1)	-9(1)	-4(1)	2(1)
C(29)	16(1)	24(1)	36(1)	-15(1)	2(1)	2(1)
C(30)	15(1)	23(1)	27(1)	-9(1)	2(1)	-1(1)
C(31)	12(1)	17(1)	23(1)	-6(1)	-1(1)	-1(1)
C(32)	13(1)	16(1)	19(1)	-4(1)	1(1)	-1(1)
C(33)	17(1)	16(1)	17(1)	-3(1)	4(1)	-1(1)
C(34)	16(1)	14(1)	15(1)	-2(1)	3(1)	-1(1)
C(35)	25(1)	13(1)	14(1)	1(1)	4(1)	0(1)
C(36)	27(1)	11(1)	15(1)	1(1)	2(1)	0(1)
C(37)	17(1)	12(1)	14(1)	-1(1)	0(1)	2(1)
C(38)	19(1)	14(1)	14(1)	-1(1)	1(1)	2(1)
C(39)	21(1)	19(1)	14(1)	-4(1)	0(1)	1(1)
C(40)	20(1)	22(1)	16(1)	-1(1)	-3(1)	5(1)
C(41)	19(1)	18(1)	17(1)	-1(1)	-2(1)	6(1)
C(42)	15(1)	11(1)	14(1)	0(1)	2(1)	2(1)
C(43)	14(1)	15(1)	20(1)	-2(1)	1(1)	0(1)
C(44)	29(1)	17(1)	14(1)	-2(1)	2(1)	5(1)
C(45)	23(1)	21(1)	19(1)	-2(1)	6(1)	3(1)
C(46)	24(1)	15(1)	19(1)	1(1)	6(1)	0(1)

Table 5. Hydrogen coordinates (x 10^4) and isotropic displacement parameters ($Å^2$ x 10^3) for **2.108**.

	x	y	z	U(eq)
H(2)	3942(14)	5612(16)	107(12)	46
H(1)	3651(11)	621(12)	1556(10)	25(4)
H(4A)	4530	-1007	2028	21
H(5A)	5317	-1716	3109	24
H(6A)	5511	-916	4281	24
H(7A)	4936	613	4404	22
H(10A)	4236	2789	3870	19
H(10B)	3222	2456	3829	19
H(11A)	4049	3373	2651	16
H(12A)	3239	4498	3298	20
H(12B)	2354	3955	2950	20
H(13A)	3595	4829	2078	20
H(13B)	2616	5196	2106	20
H(14A)	2016	3974	1353	17
H(16A)	4187	4786	1011	21
H(17A)	4695	3471	334	22
H(17B)	3702	3225	-5	22
H(18A)	4382	3191	1589	19
H(18B)	4133	2260	1081	19
H(20A)	1684	2811	2161	26
H(20B)	2064	2173	2881	26
H(20C)	1872	1697	2052	26
H(21A)	2060	5814	881	24
H(22A)	2389	3779	-278	31
H(22B)	2264	4898	-450	31
H(22C)	1623	4356	54	31
H(23A)	1818	2497	839	28
H(23B)	2551	1678	899	28
H(23C)	2555	2509	276	28
H(4)	6090(15)	-810(17)	-309(13)	53(6)

H(3)	6403(10)	4318(11)	1202(10)	18(4)
H(27A)	5623	6039	1450	26
H(28A)	4874	6837	2339	30
H(29A)	4676	6121	3497	31
H(30A)	5145	4559	3774	26
H(33A)	5631	2295	3393	20
H(33B)	6662	2545	3600	20
H(34A)	5816	1650	2235	18
H(35A)	6520	496	3087	20
H(35B)	7448	978	2988	20
H(36A)	6246	153	1784	21
H(36B)	7189	-272	2092	21
H(37A)	7908	914	1515	17
H(39A)	5780	116	558	22
H(40A)	5333	1415	-257	24
H(40B)	6339	1646	-341	24
H(41A)	5583	1731	1065	22
H(41B)	5871	2644	613	22
H(43A)	8222	2070	2342	25
H(43B)	7834	2740	2952	25
H(43C)	8086	3189	2176	25
H(44A)	7856	-918	1108	24
H(45A)	7670	1054	-229	31
H(45B)	7825	-71	-306	31
H(45C)	8401	526	351	31
H(46A)	8179	2349	979	29
H(46B)	7484	3206	863	29
H(46C)	7460	2374	239	29

Table 6. Torsion angles [º] for **2.108**.

C(3)-N(1)-C(2)-C(9)	-1.82(14)
C(3)-N(1)-C(2)-C(1)	-172.75(13)
C(20)-C(1)-C(2)-C(9)	-89.07(12)
C(11)-C(1)-C(2)-C(9)	25.08(12)
C(19)-C(1)-C(2)-C(9)	143.98(11)
C(20)-C(1)-C(2)-N(1)	81.73(16)
C(11)-C(1)-C(2)-N(1)	-164.12(13)
C(19)-C(1)-C(2)-N(1)	-45.22(19)
C(2)-N(1)-C(3)-C(4)	-177.78(12)
C(2)-N(1)-C(3)-C(8)	1.98(13)
N(1)-C(3)-C(4)-C(5)	-178.89(12)
C(8)-C(3)-C(4)-C(5)	1.37(18)
C(3)-C(4)-C(5)-C(6)	-0.61(19)
C(4)-C(5)-C(6)-C(7)	-0.4(2)
C(5)-C(6)-C(7)-C(8)	0.57(19)
C(6)-C(7)-C(8)-C(3)	0.17(18)
C(6)-C(7)-C(8)-C(9)	-179.21(13)
N(1)-C(3)-C(8)-C(7)	179.04(11)
C(4)-C(3)-C(8)-C(7)	-1.17(18)
N(1)-C(3)-C(8)-C(9)	-1.41(13)
C(4)-C(3)-C(8)-C(9)	178.38(11)
N(1)-C(2)-C(9)-C(8)	0.93(14)
C(1)-C(2)-C(9)-C(8)	174.22(10)
N(1)-C(2)-C(9)-C(10)	-177.60(10)
C(1)-C(2)-C(9)-C(10)	-4.30(14)
C(7)-C(8)-C(9)-C(2)	179.73(14)
C(3)-C(8)-C(9)-C(2)	0.30(13)
C(7)-C(8)-C(9)-C(10)	-2.5(3)
C(3)-C(8)-C(9)-C(10)	178.10(15)
C(2)-C(9)-C(10)-C(11)	-18.91(13)
C(8)-C(9)-C(10)-C(11)	163.34(15)
C(9)-C(10)-C(11)-C(12)	162.33(11)
C(9)-C(10)-C(11)-C(1)	34.58(11)
C(2)-C(1)-C(11)-C(12)	-169.91(9)

C(20)-C(1)-C(11)-C(12)	-58.31(12)
C(19)-C(1)-C(11)-C(12)	65.70(12)
C(2)-C(1)-C(11)-C(10)	-36.15(11)
C(20)-C(1)-C(11)-C(10)	75.46(11)
C(19)-C(1)-C(11)-C(10)	-160.54(9)
C(10)-C(11)-C(12)-C(13)	170.63(10)
C(1)-C(11)-C(12)-C(13)	-63.74(12)
C(11)-C(12)-C(13)-C(14)	53.82(14)
C(12)-C(13)-C(14)-C(19)	-44.68(14)
C(12)-C(13)-C(14)-C(15)	-172.52(10)
C(13)-C(14)-C(15)-C(21)	-39.48(13)
C(19)-C(14)-C(15)-C(21)	-168.68(10)
C(13)-C(14)-C(15)-C(16)	79.77(12)
C(19)-C(14)-C(15)-C(16)	-49.44(13)
C(13)-C(14)-C(15)-C(22)	-152.82(10)
C(19)-C(14)-C(15)-C(22)	77.97(13)
C(21)-C(15)-C(16)-O(1)	-60.87(14)
C(22)-C(15)-C(16)-O(1)	53.05(14)
C(14)-C(15)-C(16)-O(1)	-179.01(10)
C(21)-C(15)-C(16)-C(17)	176.80(10)
C(22)-C(15)-C(16)-C(17)	-69.28(13)
C(14)-C(15)-C(16)-C(17)	58.65(13)
O(1)-C(16)-C(17)-C(18)	174.01(10)
C(15)-C(16)-C(17)-C(18)	-62.78(13)
C(16)-C(17)-C(18)-C(19)	57.88(13)
C(17)-C(18)-C(19)-C(23)	71.93(12)
C(17)-C(18)-C(19)-C(1)	-170.75(10)
C(17)-C(18)-C(19)-C(14)	-49.55(13)
C(2)-C(1)-C(19)-C(18)	-39.17(13)
C(20)-C(1)-C(19)-C(18)	-164.31(10)
C(11)-C(1)-C(19)-C(18)	72.06(12)
C(2)-C(1)-C(19)-C(23)	78.34(12)
C(20)-C(1)-C(19)-C(23)	-46.79(12)
C(11)-C(1)-C(19)-C(23)	-170.42(9)
C(2)-C(1)-C(19)-C(14)	-161.95(10)
C(20)-C(1)-C(19)-C(14)	72.91(11)

C(11)-C(1)-C(19)-C(14)	-50.72(12)
C(13)-C(14)-C(19)-C(18)	-80.18(12)
C(15)-C(14)-C(19)-C(18)	45.25(13)
C(13)-C(14)-C(19)-C(23)	159.43(10)
C(15)-C(14)-C(19)-C(23)	-75.14(12)
C(13)-C(14)-C(19)-C(1)	41.08(13)
C(15)-C(14)-C(19)-C(1)	166.51(9)
C(16)-C(15)-C(21)-O(2)	-1.12(18)
C(22)-C(15)-C(21)-O(2)	-121.22(14)
C(14)-C(15)-C(21)-O(2)	118.42(14)
C(26)-N(2)-C(25)-C(32)	-1.97(14)
C(26)-N(2)-C(25)-C(24)	-170.01(13)
C(43)-C(24)-C(25)-C(32)	-86.84(12)
C(34)-C(24)-C(25)-C(32)	26.86(12)
C(42)-C(24)-C(25)-C(32)	147.14(11)
C(43)-C(24)-C(25)-N(2)	81.08(17)
C(34)-C(24)-C(25)-N(2)	-165.22(14)
C(42)-C(24)-C(25)-N(2)	-44.94(19)
C(25)-N(2)-C(26)-C(27)	-176.08(12)
C(25)-N(2)-C(26)-C(31)	2.69(13)
N(2)-C(26)-C(27)-C(28)	-179.32(12)
C(31)-C(26)-C(27)-C(28)	2.06(18)
C(26)-C(27)-C(28)-C(29)	0.57(19)
C(27)-C(28)-C(29)-C(30)	-2.1(2)
C(28)-C(29)-C(30)-C(31)	0.93(19)
C(29)-C(30)-C(31)-C(26)	1.60(18)
C(29)-C(30)-C(31)-C(32)	-177.94(13)
N(2)-C(26)-C(31)-C(30)	177.95(11)
C(27)-C(26)-C(31)-C(30)	-3.17(18)
N(2)-C(26)-C(31)-C(32)	-2.38(13)
C(27)-C(26)-C(31)-C(32)	176.50(11)
N(2)-C(25)-C(32)-C(31)	0.47(14)
C(24)-C(25)-C(32)-C(31)	171.66(10)
N(2)-C(25)-C(32)-C(33)	-177.64(10)
C(24)-C(25)-C(32)-C(33)	-6.45(14)
C(30)-C(31)-C(32)-C(25)	-179.23(14)

C(26)-C(31)-C(32)-C(25)	1.18(13)
C(30)-C(31)-C(32)-C(33)	-2.1(3)
C(26)-C(31)-C(32)-C(33)	178.36(15)
C(25)-C(32)-C(33)-C(34)	-17.58(13)
C(31)-C(32)-C(33)-C(34)	165.30(15)
C(32)-C(33)-C(34)-C(35)	161.49(11)
C(32)-C(33)-C(34)-C(24)	34.32(11)
C(25)-C(24)-C(34)-C(35)	-169.71(10)
C(43)-C(24)-C(34)-C(35)	-59.14(12)
C(42)-C(24)-C(34)-C(35)	64.33(12)
C(25)-C(24)-C(34)-C(33)	-36.94(11)
C(43)-C(24)-C(34)-C(33)	73.64(12)
C(42)-C(24)-C(34)-C(33)	-162.89(9)
C(33)-C(34)-C(35)-C(36)	173.29(11)
C(24)-C(34)-C(35)-C(36)	-61.99(13)
C(34)-C(35)-C(36)-C(37)	54.09(14)
C(35)-C(36)-C(37)-C(38)	-174.13(10)
C(35)-C(36)-C(37)-C(42)	-46.79(15)
C(36)-C(37)-C(38)-C(44)	-40.54(13)
C(42)-C(37)-C(38)-C(44)	-169.19(10)
C(36)-C(37)-C(38)-C(39)	78.23(12)
C(42)-C(37)-C(38)-C(39)	-50.42(13)
C(36)-C(37)-C(38)-C(45)	-153.99(10)
C(42)-C(37)-C(38)-C(45)	77.36(13)
C(44)-C(38)-C(39)-O(3)	-61.31(13)
C(45)-C(38)-C(39)-O(3)	52.44(14)
C(37)-C(38)-C(39)-O(3)	-179.06(10)
C(44)-C(38)-C(39)-C(40)	175.66(10)
C(45)-C(38)-C(39)-C(40)	-70.60(13)
C(37)-C(38)-C(39)-C(40)	57.91(13)
O(3)-C(39)-C(40)-C(41)	175.88(10)
C(38)-C(39)-C(40)-C(41)	-60.31(14)
C(39)-C(40)-C(41)-C(42)	57.39(14)
C(40)-C(41)-C(42)-C(46)	70.91(13)
C(40)-C(41)-C(42)-C(24)	-171.17(10)
C(40)-C(41)-C(42)-C(37)	-50.77(14)

C(25)-C(24)-C(42)-C(41)	-41.86(14)
C(43)-C(24)-C(42)-C(41)	-166.04(10)
C(34)-C(24)-C(42)-C(41)	70.52(12)
C(25)-C(24)-C(42)-C(46)	76.12(13)
C(43)-C(24)-C(42)-C(46)	-48.05(12)
C(34)-C(24)-C(42)-C(46)	-171.49(10)
C(25)-C(24)-C(42)-C(37)	-163.63(10)
C(43)-C(24)-C(42)-C(37)	72.19(12)
C(34)-C(24)-C(42)-C(37)	-51.24(12)
C(36)-C(37)-C(42)-C(41)	-78.39(13)
C(38)-C(37)-C(42)-C(41)	46.65(13)
C(36)-C(37)-C(42)-C(46)	161.51(10)
C(38)-C(37)-C(42)-C(46)	-73.45(12)
C(36)-C(37)-C(42)-C(24)	43.01(13)
C(38)-C(37)-C(42)-C(24)	168.05(9)
C(39)-C(38)-C(44)-O(4)	3.05(17)
C(45)-C(38)-C(44)-O(4)	-116.62(14)
C(37)-C(38)-C(44)-O(4)	122.94(13)

Table 7. Hydrogen bonds for **2.108** [Å and º].

D-H...A	d(D-H)	d(H...A)	d(D...A)	<(DHA)
O(1)-H(2)...O(2)	0.83(2)	2.13(2)	2.8398(15)	143(2)
N(1)-H(1)...O(3)#1	0.886(18)	2.082(18)	2.9215(14)	157.8(15)
O(3)-H(4)...O(4)	0.88(2)	2.13(2)	2.7948(14)	132.2(19)
N(2)-H(3)...O(1)#2	0.886(17)	2.131(17)	2.9272(16)	149.1(14)

Symmetry transformations used to generate equivalent atoms:
#1 -x+1,-y,-z #2 -x+1,-y+1,-z

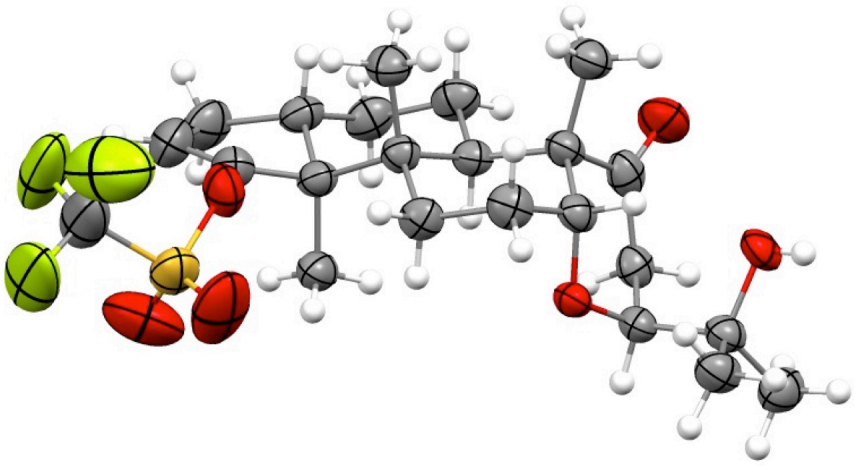

Table 1. Crystal data and structure refinement for **3.113**.

Identification code	svp7 (David George)	
Empirical formula	$C_{23}H_{33}F_3O_6S$	
Formula weight	494.55	
Temperature	153(2) K	
Wavelength	0.71073 Å	
Crystal system	Tetragonal	
Space group	$P4_32_12$	
Unit cell dimensions	a = 8.9857(6) Å	a= 90º.
	b = 8.9857(6) Å	b= 90º.
	c = 57.990(4) Å	g = 90º.
Volume	4682.3(7) $Å^3$	
Z	8	
Density (calculated)	1.403 Mg/m^3	
Absorption coefficient	0.199 mm^{-1}	
F(000)	2096	
Crystal color	colorless	
Crystal size	0.425 x 0.344 x 0.088 mm^3	
Theta range for data collection	1.405 to 27.877º	
Index ranges	$-11 \le h \le 11$, $-11 \le k \le 11$, $-76 \le l \le 75$	
Reflections collected	71941	
Independent reflections	5590 [R(int) = 0.0481]	
Completeness to theta = 25.500º	100.0%	
Absorption correction	Semi-empirical from equivalents	
Max. and min. transmission	0.8015 and 0.7474	

Refinement method	Full-matrix least-squares on F^2
Data / restraints / parameters	5590 / 0 / 307
Goodness-of-fit on F^2	1.085
Final R indices [I>2sigma(I) = 5304 data]	R1 = 0.0357, wR2 = 0.0887
R indices (all data, 0.76 Å)	R1 = 0.0384, wR2 = 0.0901
Absolute structure parameter	0.002(19)
Largest diff. peak and hole	0.375 and -0.321 e.$Å^{-3}$

Table 2. Atomic coordinates (x 10^4) and equivalent isotropic displacement parameters ($Å^2$x 10^3) for **3.113**. U(eq) is defined as one third of the trace of the orthogonalized U^{ij} tensor.

	x	y	z	U(eq)
S(1)	4293(1)	10832(1)	84(1)	27(1)
F(1)	5438(3)	11159(3)	-325(1)	62(1)
F(2)	4046(3)	9246(2)	-289(1)	62(1)
F(3)	3059(2)	11427(2)	-306(1)	58(1)
O(1)	7842(2)	11320(2)	1059(1)	15(1)
O(2)	10243(2)	7754(2)	1250(1)	26(1)
O(3)	10505(2)	11434(2)	1395(1)	18(1)
O(4)	5685(2)	9828(2)	129(1)	24(1)
O(5)	2981(2)	10207(3)	175(1)	48(1)
O(6)	4712(3)	12315(2)	125(1)	46(1)
C(1)	7951(2)	11014(2)	1301(1)	14(1)
C(2)	8224(2)	9347(2)	1337(1)	16(1)
C(3)	9388(2)	8695(2)	1179(1)	17(1)
C(4)	9395(2)	9208(2)	926(1)	15(1)
C(5)	8058(2)	8421(2)	802(1)	14(1)
C(6)	8173(2)	6709(2)	808(1)	19(1)
C(7)	6758(2)	5946(2)	718(1)	20(1)
C(8)	6409(2)	6564(2)	482(1)	17(1)
C(9)	5103(3)	5982(3)	335(1)	25(1)
C(10)	4944(3)	7218(3)	162(1)	25(1)
C(11)	5601(2)	8423(2)	243(1)	19(1)
C(12)	6176(2)	8274(2)	487(1)	16(1)
C(13)	7672(2)	9051(2)	556(1)	14(1)
C(14)	7482(2)	10757(2)	574(1)	17(1)
C(15)	8822(2)	11515(2)	686(1)	18(1)
C(16)	9131(2)	10913(2)	924(1)	15(1)
C(17)	9043(2)	12046(2)	1429(1)	16(1)
C(18)	8955(2)	13624(2)	1335(1)	20(1)
C(19)	8659(3)	12034(3)	1686(1)	22(1)
C(20)	10932(2)	8851(2)	825(1)	22(1)

C(21)	4847(2)	8702(2)	644(1)	19(1)
C(22)	8859(2)	8720(2)	370(1)	20(1)
C(23)	4205(4)	10654(3)	-229(1)	41(1)